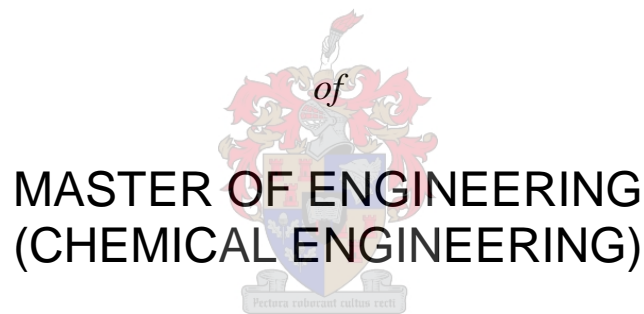


DESIGN, DEVELOPMENT AND OPTIMIZATION OF EDIBLE WAX COATINGS FOR FRESH FRUIT

by

Louise Beatrix Steyn

Thesis presented in partial fulfilment
of the requirements for the Degree



In the Faculty of Engineering
At Stellenbosch University

Supervisor
Prof. J.H. Knoetze

December 2015

Declaration

By submitting this thesis electronically, I declare that the entirety of the work contained therein is my own, original work, that I am the sole author thereof (save to the extent explicitly otherwise stated), that reproduction and publication thereof by Stellenbosch University will not infringe any third party rights and that I have not previously in its entirety or in part submitted it for obtaining any qualification.

Date: **December 2015**

Abstract

The quality of food products has always been a crucial focus point for the food industry. This is even more so for active food products such as fresh fruits, since they have living tissue. Various techniques have been developed over the years to preserve the quality of food products, of which packaging is the ultimate one. With synthetic packaging being unfavourable for active food products, the use of edible films and coatings has been suggested as an alternative. However, the development of new and/or modified edible coatings for fresh fruits have been challenging for the post-harvest industry as a result of differences in the requirements for various fruits and the ever changing United States (US) and European (EU) food regulations.

An edible coating used in the non-processed fruit industry is usually an anionic wax micro-emulsion consisting of a combination of wax, water, a fatty acid and a base. The base ionizes the fatty acid to form a soap, which stabilizes the wax droplets in the water to form a stable emulsion. In order to modify existing wax micro-emulsion edible coating formulations to comply with the US and EU food regulations, an understanding of the manufacturing process, including the significant process parameter(s) and their effects on the final product quality, are required. A better understanding of the process design, the manufacturing processes and the operational manufacturing procedures will thus be of great importance.

In this study, a specific natural wax micro-emulsion coating was investigated by performing experiments on pilot-plant scale. An existing plant-scale semi-batch reactor of *6000 litres*, which is currently employed at an edible coatings manufacturer, was down-scaled to a geometrically similar bench-scale pilot batch reactor with a volume of *6 litres*, which was used in the construction of the bench scale pilot plant. Once a baseline was established for the manufacturing process through literature and commissioning experiments, the significant process parameters were identified and investigated by means of a screening experimental design. The significant process parameters were identified as the *Temperature* [°C], the *High Shear Time Interval* [*min*], the *Stirrer Speed* [*rpm*] and the *High Shear Homogenizer Speed* [*rpm*]. Models that represent the design space were established by performing statistical analyses. The process- and formulation parameters were evaluated according to their effects on the characteristics of the final product and criteria obtained from literature.

Once the main process parameters were identified, the formulation (Carnauba wax, Ammonium Hydroxide, Potassium Hydroxide and Oleic Acid) was established and optimized by

performing a mixture experimental design. The manufacturing process of the optimized Carnauba wax coating was optimized by means of a multifactor response surface methodology (composite experimental design) to decrease the design space to a feasible operating window and yield an optimum quality product. The final formulation- and process parameter setup that was obtained are as follow: *Temperature* [127°C], *High Shear Time* [40 min], *High Shear Speed* [5630 rpm], *Stirrer Speed* [1500 rpm], *Cooling Rate* [1 (coded)], *Inverting Phase Addition Rate* [3 l/h], *%Water* [75.3 %], *%Carnauba Wax* [15.8 %], *%Oleic Acid* [6.3 %], *%Potassium Hydroxide* [0.6 %], *%Ammonium Hydroxide* [2 %].

The final Carnauba wax emulsion formulation- and process parameter setup produced the optimum product obtained throughout this study, which consisted of more than a hundred experiments. The final product has defining characteristics that was compared to commercial data and found to be superior to commercial edible wax emulsions currently being used in the post-harvest industry. A final particle size of $0.472 \mu\text{m}$ were obtained with a narrow particle size distribution. The aims of this study have been met by establishing and validating an optimized edible Carnauba wax emulsion coating and its manufacturing process. The model that has been developed can aid in the advancement of future applications of edible coatings in the food industry.

Opsomming

Die kwaliteit van voedsel produkte was nog altyd a kritieke fokus punt in die voedselbedryf. Dit is veral kritiek vir aktiewe voedsel groepe soos vrugte, aangesien dit uit lewendige weefsel bestaan. Gedurende die afgelope aantal jare is 'n verskeidenheid van tegnieke ontwikkel om die kwaliteit van voedsel produkte te preserveer, waarvan verpakking die mees suksesvolle is. Aangesien sintetiese verpakking ongunstig is vir aktiewe voedsel, word eetbare films en doopmiddels as 'n alternatief vir vars vrugte aanbeveel. Die ontwikkeling van nuwe en/of aangepaste eetbare doopmiddels vir vars vrugte is 'n uitdaging vir die na-oes bedryf as gevolg van die verskillende vereistes vir verskillende vrugte en die veranderende Amerikaanse (VSA) en Europese (EU) voedsel standaarde.

'n Eetbare doopmiddel wat gebruik word in the ongeprosesseerde vrugtebedryf is gewoonlik 'n anioniese was mikro-emulsie wat bestaan uit 'n kombinasie van was, water, 'n vetsuur en 'n basis. Die basis ioniseer die vetsuur om a seep te vorm wat die was druppels stabiliseer in the water om a stabiele emulsie te vorm. Ten einde 'n bestaande eetbare was mikro-emulsie doopmiddel te verander/aan te pas om te voldoen aan die VSA en EU voedsel standaarde, word 'n begrip van die vervaardigingsproses benodig. Dit sluit in die beduidende proses veranderlikes en die effek op die finale produk se kwaliteit. 'n Beter begrip van die proses ontwerp, die vervaardigings prosesse en die operasionele vervaardigings prosedures sal dus van baie waarde wees.

In hierdie studie was 'n spesifieke natuurlike eetbare was mikro-emulsie doopmiddel geondersoek deur eksperimente op loodsaanleg uit te voer. 'n Bestaande industriële vaste maat reaktor met 'n volume van 6000 liter, wat tans operasioneel is by 'n eetbare doopmiddels vervaardiger, is afgeskaal na 'n geometriese soortgelyke laboratorium skaal reaktor met 'n volume van 6 liter. Die afgeskaalde reaktor is geïntegreer in die laboratorium skaal aanleg. Nadat 'n basis vasgestel was vir die vervaardigingsproses deur literatuur en inbedryfstellings eksperimente, is die beduidende proses parameters geïdentifiseer en ondersoek deur middel van 'n siftings eksperimentele ontwerp. Die beduidende proses parameters was geïdentifiseer as die *Temperatuur* [°C], the *Hoë Skeerkrag Tyd Interval* [min], die *Roerder Spoed* [rpm] and the *Hoë Skeerkrag Roerder Spoed* [rpm]. Modelle wat die ontwerp spasie verteenwoordig is ontwikkel deur middel van statistiese analyses. Die proses- en formulاسie parameters is ge-evalueer op grond van die effek wat hulle het op die karaktereenskappe van die finale produk en kriteria wat verkry is vanaf literatuur.

Na die hoof proses parameters geïdentifiseer is, is die formulering (Carnauba wax, Ammoniumhidroksied, Kaliumhidroksied en Oliensuur) bepaal en geoptimeer deur 'n mengsel eksperimentele ontwerp uit te voer. Die vervaardigingsproses van die ge-optimeerde Carnauba was doopmiddel is geoptimeer deur middel van 'n multifaktor reaksie oppervlak metodologie (saamgestelde eksperimentele ontwerp) om die ontwerp spasie na 'n haalbare operasionele bedryfsvenster te verklein en om 'n optimum kwaliteit produk te produseer. Die finale formulering- en proses parameter opset is soos volg: *Temperatuur* [127°C], *Hoë Skeerkrag Tyd Interval* [40 min], *Hoë Skeerkrag Roerder Spoed* [5630 rpm], *Roerder Spoed* [1500 rpm], *Verkoelings Tempo* [1], *Omkeer-Fase Byvoegings Vloeitempo* [3 l/h], *%Water* [75.3 %], *%Carnauba Was* [15.8 %], *%Oliensuur* [6.3 %], *%Kaliumhidroksied* [0.6 %], *%Ammoniumhidroksied* [2 %].

Die finale Carnauba was emulsie formulering- en proses parameter opset het die optimale finale produk vervaardig met die hoogste kwaliteit wat vervaardig is tydens hierdie studie, wat bestaan uit meer as 'n honderd eksperimente. Die finale produk was vergelyk met kommersiële data en dit was gevind dat die finale optimum Carnauba was emulsie produk het uitstaande karaktereienskappe wat hoër geag word as van die kommersiële was emulsies wat tans gebruik word in die na-oes bedryf. Die doel van hierdie studie was om 'n geoptimeerde eetbare Carnauba was emulsie doopmiddel en sy vervaardigings proses vas te stel en te bevestig. Die finale model sal kan bydra tot die ontwikkeling van toekomstige toepassings van eetbare doopmiddels in the voedsel bedryf.

Acknowledgements

I would like to express my sincere gratitude to the following people and institutions for their contribution to the completion of this thesis:

Prof. Hansie Knoetze, my study leader, for all the guidance and knowledge you have provided throughout this research;

Stellenbosch University (Postgraduate Bursary) and the National Research Foundation (NRF), for financial assistance and support;

Mr. Jannie Barnard and Mr. Anton Cordier, Process Engineering Department Workshop, for all the help and support with the building of the pilot plant;

Mrs. Hanlie Botha, head of the analytical laboratory (Process Engineering Department), for all the advice, knowledge and technical assistance;

Mrs. Juliana Steyl, for all the support with the procurement processes;

Staff, friends and fellow postgraduate students at the Department of Process Engineering of Stellenbosch University;

Suandrie McLaren, for all the late night coffee runs, support and encouragement in my many moments of crisis;

Dr. Cato' van Wyk, my grandmother, for all the prayers, unconditional love and support;

Andre', Cato' and Elizabeth, for all the encouragement.

Dedicated to my parents

Chris and Marlette Steyn

For the love and support,
for being my inspiration and for providing me
with every opportunity to persue my goals.

You are my heroes. I love you.

Table of Contents

| | |
|--|------|
| Abstract..... | ii |
| Opsomming..... | iv |
| Acknowledgements | vi |
| Table of Contents..... | viii |
| List of Tables | xi |
| List of Figures | xv |
| Chapter 1: Introduction | 1 |
| 1.1 Background | 1 |
| 1.2 Objectives | 2 |
| 1.3 Mind Map | 3 |
| Chapter 2: Literature Review..... | 4 |
| 2.1 Edible films and coatings | 4 |
| 2.2 Emulsions..... | 13 |
| 2.3 Edible Wax Emulsion Coatings..... | 16 |
| 2.4 Chemistry..... | 63 |
| 2.5 Scaling..... | 69 |
| 2.6 Concluding Remarks | 76 |
| Chapter 3: Research Aims and Objectives..... | 78 |
| Research Aims..... | 78 |
| Aim 1: Design, Build and Commission a Bench Scale Pilot Plant..... | 78 |
| Aim 2: Experimentation, Statistical Modelling and Optimization | 79 |
| Main Objectives | 80 |
| Chapter 4: Equipment Design and Pilot Plant Construction..... | 81 |
| 4.1 Pilot Plant Layout and Process Flow Diagram..... | 81 |
| 4.2 Equipment | 85 |
| 4.3 Control of Process Variables..... | 99 |

| | |
|---|-----|
| Chapter 5: Materials and Methods..... | 101 |
| 5.1 Materials | 101 |
| 5.2 Experimental Procedure | 103 |
| 5.3 Analytical Techniques | 106 |
| Chapter 6: Design of Experiments | 111 |
| 6.1 Assumptions | 112 |
| 6.2 Experimental Designs | 115 |
| Chapter 7: Results and Discussion | 131 |
| 7.1 Screening Experimental Phase | 131 |
| 7.2 Formulation Experimental Phase | 177 |
| 7.3 Composite Experimental Phase | 192 |
| Chapter 8: Comparisons with Commercial Coatings | 217 |
| Chapter 9: Conclusions & Recommendations | 225 |
| References | 230 |
| Appendix A: Commercial Waxes Data Sheets | 241 |
| Appendix B: Pilot Plant Additional Information and Calibrations | 247 |
| Appendix C: Material Safety Data Sheets | 252 |
| Appendix D: Anton Paar Viscometer Procedure | 257 |
| Appendix E: Validation of ANOVA Assumptions..... | 258 |
| Appendix F: Screening Experimental Design Particle Size Results and Discussion..... | 261 |
| Appendix G: Screening Experimental Design Optimization Data | 313 |
| Appendix H: Mixture Experimental Design Particle Size Data Analysis..... | 314 |
| Appendix I: Mixture Experimental Design Roughness Data | 318 |
| Appendix J: Mixture Experimental Design Gloss Data..... | 319 |
| Appendix K: Mixture Experimental Design Optimization Data..... | 320 |
| Appendix L: Composite Experimental Design Data | 321 |
| Appendix M: Composite Experimental Design Optimization Data..... | 322 |
| Appendix N: Comparison with Commercial Coatings..... | 326 |

| | |
|---|-----|
| Appendix O: Screening Experimental Images..... | 334 |
| Appendix P: Mixture Experimental Images | 335 |
| Appendix Q: Composite Experimental Images | 336 |
| Appendix R: Operational Images | 337 |

List of Tables

| | |
|---|-----|
| Table 1 - Edible film and coatings coated foods (Debeaufort et al.,1998) | 5 |
| Table 2 - Active properties of edible films and coatings (Debeaufort et al., 1998)..... | 7 |
| Table 3 - Materials used for edible films and coatings (Han and Gennadios, 2005) | 10 |
| Table 4 - Comparison of oil-in-water emulsions and water-in-oil emulsions (Griffin, 1945) | 14 |
| Table 5 - Characteristics of emulsions (Griffin, 1945)..... | 15 |
| Table 6 - Waxes tested by Hagenmaier et al. | 21 |
| Table 7 - Citrus Coating Composition (Micro-Emulsion and Rosin Solution) (Hagenmaier, 1998) | 23 |
| Table 8 - Components of successful anionic wax micro-emulsions (Hagenmaier, 1998) | 46 |
| Table 9 - The effect of particle size on emulsion and film appearance (Griffin, 1945) | 51 |
| Table 10 - Wax-to-Surfactant Ratio vs. Mean Particle Diameter (um) (Gusman 1947) | 51 |
| Table 11 - Roughness [Ra] measurements of various wax-hydrocolloid coatings (Chen et al., 2000)..... | 54 |
| Table 12 - The effect of lipid content and storage time on the gloss of lipid containing edible biopolymer coatings (Trezza and Krochta, 2000) | 56 |
| Table 13 - Gloss of mesquite based coatings (Bosquez-Molina et al., 2003) | 56 |
| Table 14 - X vs. Weights of Surfactant Components (Gusman 1947)..... | 62 |
| Table 15 - Proportionality constant (K) values (Klein and Lowry) | 71 |
| Table 16 - Pilot Plant Vessel Dimensions | 83 |
| Table 17 - Possible factors and responses..... | 115 |
| Table 18 - Commissioning Experimental Runs Configurations and Formulations..... | 122 |
| Table 19 - Regression statistics - Commissioning Experiments | 123 |
| Table 20 - Screening Experimental Design - Fomulation Parameters Ranges..... | 124 |
| Table 21 - Screening Experimental Design | 125 |
| Table 22 - Mixture Experimental Design - Formulation Parameters Ranges | 127 |
| Table 23 - Mixture Experimental Design | 128 |
| Table 24 - Composite Experimental Design - Process Parameters' Ranges | 129 |
| Table 25 - Composite Experimental Design..... | 130 |
| Table 26 – Mean Particle Sizes (Comparing the Volume-, Area- and Number Distributions) for the Screening Experimental Design..... | 131 |
| Table 27 - Volume Mean Particle Size (Linear Model) ANOVA..... | 134 |
| Table 28 - Volume Mean Particle Size (Reduced Quadratic Model) ANOVA..... | 135 |

| | |
|--|-----|
| Table 29 - Volume Mean Particle Size Model V1 (Screening) - R-Squared Values | 135 |
| Table 30 - Volume Mean Particle Size (Reduced Quadratic Model) ANOVA..... | 144 |
| Table 31 - Volume Mean Particle Size Model V2 (Screening) - R-Squared Values | 145 |
| Table 32 - Comparison of Models' Process- and Formulation Variables..... | 150 |
| Table 33 - Roughness [Ra] Readings for the Screening Experimental Design | 154 |
| Table 34 - Roughness [Ra] measurements of various wax-hydrocolloid coatings (Chen et al., 2001)..... | 155 |
| Table 35 - Roughness (Linear Model) ANOVA | 156 |
| Table 36 - Roughness (Reduced Quadratic Model) ANOVA | 156 |
| Table 37 - Roughness Model - R-Squared Values | 157 |
| Table 38 - Gloss [GU] Readings for the Screening Experimental Design | 160 |
| Table 39 - The effect of lipid content and storage time on the gloss of lipid containing edible biopolymer coatings (Trezza and Krochta, 2000) | 161 |
| Table 40 - Gloss of Mesquite based coatings (Bosquez-Molina et al., 2003)..... | 162 |
| Table 41 - Correlations for the screening experimental responses..... | 163 |
| Table 42 - Gloss (Linear Model) ANOVA | 163 |
| Table 43 - Gloss (Reduced Quadratic Model) ANOVA | 164 |
| Table 44 - Gloss Model - R-Squared Values..... | 164 |
| Table 45 - Viscosity, pH and Density Readings for the Screening Experimental Design | 169 |
| Table 46 - Viscosity, pH and Density (linear Model) ANOVA..... | 170 |
| Table 47 - Viscosity, pH and Density (Reduced Quadratic Model)..... | 171 |
| Table 48 - Optimization Results - Screening Experimental Design..... | 175 |
| Table 49 - Screening Experimental Design - Optimized Process Parameters..... | 175 |
| Table 50 - Screening Experimental Design - Optimized Formulation Parameters | 176 |
| Table 51 - Oleic Acid : Ammonium Hydroxide Ratios | 177 |
| Table 52 - Mixture Experimental Design | 178 |
| Table 53 - Mixture Experimental Design - Formulation Parameter Ranges | 179 |
| Table 54 - Formulation Experimental Design - Process Parameter Settings | 179 |
| Table 55 - Mean- and Median Particle Sizes for the Mixture Experimental Design..... | 180 |
| Table 56 - Area Median Particle Size (Reduce Quadratic Model) ANOVA..... | 181 |
| Table 57 - Area Median Particle Size Model (Mixture) - R-Squared Values | 181 |
| Table 58 - Roughness [Ra] Readings for the Mixture Experimental Design | 186 |
| Table 59 - Gloss [GU] Readings for the Mixture Experimental Design | 188 |
| Table 60 - Optimization Results - Mixture Experimental Design..... | 190 |

| | |
|---|-----|
| Table 61 - Confirmation Run Results | 190 |
| Table 62 - Composite Experimental Design | 192 |
| Table 63 - Composite Experimental Design - Process Parameters' Ranges | 193 |
| Table 64 - Composite Experimental Design - Formulation Settings | 193 |
| Table 65 - Mean- and Median Particle Sizes for the Composite Experimental Design | 194 |
| Table 66 - Number Mean Particle Size Models (Composite) - R-Squared Values | 197 |
| Table 67 - Number Mean Particle Size (Reduced Quadratic Model) ANOVA..... | 197 |
| Table 68 - Number Median Particle Size Models - R-Squared Values | 201 |
| Table 69 - Number Median Particle Size (Reduced Quadratic Model) ANOVA..... | 201 |
| Table 70 - Area Median Particle Size (Reduced Quadratic Model) ANOVA | 203 |
| Table 71 - Area Median Particle Size Model (Composite) - R-Squared Values..... | 204 |
| Table 72 - Roughness [Ra] Readings for the Composite Experimental Design..... | 205 |
| Table 73 - Comparison of the Average Roughness (Screening-, Formulation- and Composite Experimental Designs) | 206 |
| Table 74 - Gloss [GU] Readings for the Composite Experimental Design | 208 |
| Table 75 - Gloss (Reduced Quadratic Model) ANOVA - Composite Experimental Design | 209 |
| Table 76 - Gloss Model (Composite) - R-Squared Values | 209 |
| Table 77 - Composite Experimental Design Optimization Results | 211 |
| Table 78 - Composite Experimental Design - Confirmation Runs Results | 211 |
| Table 79 - Correlations for the composite experimental data | 212 |
| Table 80 - pH and Density Readings for the Composite Experimental Design | 215 |
| Table 81 - Final Optimized Formulation- and Process Parameter Settings | 215 |
| Table 82 - Volume Median Particle Size (Linear Model) ANOVA..... | 261 |
| Table 83 - Volume Median Particle Size (Reduced Quadratic Model) ANOVA..... | 262 |
| Table 84 - Volume Median Particle Size (Reduced Quadratic Model) ANOVA..... | 268 |
| Table 85 - Area Mean Particle Size (Linear Model) ANOVA | 271 |
| Table 86 - Area Mean Particle Size (Reduced Quadratic Model) ANOVA | 271 |
| Table 87 - Area Mean Particle Size (Reduced Quadratic Model) ANOVA | 278 |
| Table 88 - Area Median Particle Size (Linear Model) ANOVA..... | 279 |
| Table 89 - Area Median Particle Size (Reduced Quadratic Model) ANOVA | 279 |
| Table 90 - Area Median Particle Size (Reduced Quadratic Model) | 284 |
| Table 91 - Number Mean Particle Size (Linear Model) ANOVA..... | 293 |
| Table 92 - Number Mean Particle Size (Reduced Quadratic Model) ANOVA..... | 293 |
| Table 93 - Number Mean Particle Size (Reduced Quadratic Model) ANOVA..... | 297 |

| | |
|---|-----|
| Table 94 - Number Median Particle Size (Linear Model) ANOVA..... | 304 |
| Table 95 - Number Median Particle Size (Reduced Quadratic Model) ANOVA..... | 304 |
| Table 96 - Number Mean Particle Size (Reduced Quadratic Model) ANOVA..... | 306 |

List of Figures

| | |
|---|----|
| Figure 1 - Selective functions of edible films and coatings (redrawn from Debeaufort et al. (1998)) | 7 |
| Figure 2 - Various ways for modifying the characteristics of edible films and coatings (redrawn from Han and Gennadios, 2005)..... | 12 |
| Figure 3 - Typical Wax Emulsification Plant – redrawn from Rhe America (2014)..... | 17 |
| Figure 4 - The effect of Wax-to-Surfactant Ratio on the Particle Size [S. Gusman, 1947] | 52 |
| Figure 5 - The effect of the Oil-to-Surfactant Ratio on the Particle Size [N. Sudurni et al., 2005] | 52 |
| Figure 6 - Schematic illustration of both Catastrophic and Transitional phase inversion for the preparation of micro-emulsions (Redrawn from Fernandez et al., 2004)..... | 65 |
| Figure 7 - The wax coating formation process (Pressure Method) – redrawn from Western Asphalt Products (2013) | 67 |
| Figure 8 - Formation of an Anionic Emulsifier – redrawn from Western Asphalt Products (2013) | 68 |
| Figure 9 - Electrostatically stabilized wax droplet – redrawn from Western Asphalt Products (2013)..... | 68 |
| Figure 10 – The chemical structure of Ammonium Oleate | 69 |
| Figure 11 – Basic layout of a commercial edible wax emulsion plant..... | 81 |
| Figure 12 - Process Flow Diagram showing the Pilot Plant layout | 82 |
| Figure 13 - Schematic diagram of the pressure vessel | 83 |
| Figure 14 - Schematic diagram of the Pressure Vessel (Top dome, Middle Section and Bottom dome)..... | 86 |
| Figure 15 - Schematic of the Pressure Vessel with the heating coil..... | 87 |
| Figure 16 - Top dome..... | 88 |
| Figure 17 - Initial Mechanical Seal Housing Design | 88 |
| Figure 18 - Mechanical seal spring-loaded static carbon part [Eagle Burgmann©]..... | 89 |
| Figure 19 - Basic schematic of final Mechanical Seal Housing | 90 |
| Figure 20 - Final Mechanical Seal Housing Design..... | 90 |
| Figure 21 - Top Dome with the Mechanical Seal Housings | 91 |
| Figure 22 - Mechanical seal housings installed on the top dome of the pressure vessel..... | 91 |
| Figure 23 - Stirrer Blade Design | 92 |
| Figure 24 - Stirrer axle with blades..... | 92 |

| | |
|--|-----|
| Figure 25 - High shear homogenizer shear plate..... | 93 |
| Figure 26 - Shearing section of the high shear homogenizer | 93 |
| Figure 27 - High shear homogenizer's bearing support and bearing support with bearing cover (Stator)..... | 94 |
| Figure 28 - High shear homogenizer impeller (Rotor) | 94 |
| Figure 29 - High shear homogenizer..... | 95 |
| Figure 30 - Complete top dome..... | 95 |
| Figure 31 - P&ID including the data logging and temperature control capabilities | 97 |
| Figure 32 - Pilot Plant Setup | 103 |
| Figure 33 - Scattering of light from small and large particles – Laser Diffraction | 106 |
| Figure 34 – Commissioning Experiment - Temperature vs. Pressure..... | 121 |
| Figure 35 - Relative contribution of the process- and formulation parameters to the volume mean particle size | 123 |
| Figure 36 - Screening experimental design: Five formulation blends at nine process combinations | 125 |
| Figure 37 - Mixture experimental design: Seven blends | 127 |
| Figure 38 - Central Composite Design for three factors..... | 129 |
| Figure 39 - EXP S1: Volume, Area and Number Cumulative Frequency vs. Particle Diameter. 132 | |
| Figure 40 - EXP S1: Volume, Area and Number Frequency vs. Particle Diameter (0 – 20 µm) 133 | |
| Figure 41 - Volume Mean Particle Size Model V1 (Screening Experimental Design) – Particle Size vs. Wax-to-Surfactant Ratio vs. Stirring Speed..... | 137 |
| Figure 42 - Volume Mean Particle Size Model V1 (Screening Experimental Design) – Particle Size vs. Wax-to-Surfactant Ratio..... | 138 |
| Figure 43 - The effect of Wax-to-Surfactant Ratio on the Particle Size Distribution (Screening Experimental Design)..... | 139 |
| Figure 44 - Volume Mean Particle Size Model V1 (Screening Experimental Design) – Particle Size vs. Wax-to-Surfactant Ratio vs. HS Time Interval - 1..... | 139 |
| Figure 45 - Volume Mean Particle Size Model V1 (Screening Experimental Design) - Particle Size vs. Wax-to-Surfactant Ratio vs. HS Time Interval - 2..... | 140 |
| Figure 46 - Volume Mean Particle Size Model V1 (Screening Experimental Design) – Particle Size vs. Wax-to-Surfactant Ratio vs. Cooling Rate - 1..... | 141 |
| Figure 47 - Volume Mean Particle Size Model V1 (Screening Experimental Design) - Particle Size vs. Wax-to-Surfactant Ratio vs. Cooling Rate - 2..... | 142 |

Figure 48 - Volume Mean Particle Size Model V1 (Screening Experimental Design) - Particle Size vs. Wax-to-Surfactant Ratio vs. Inverting Phase Addition Rate 142

Figure 49 - Volume Mean Particle Size Model V1 (Screening Experimental Design) - Predicted vs. Actual..... 143

Figure 50 - Actual measured response vs. model predicted value..... 146

Figure 51 - Relative contribution of the volume mean particle size model factors to the volume mean particle size 146

Figure 52 - Volume Mean Particle Size Model V2 (Screening Experimental Design) - Particle Size vs. Wax-to-Surfactant Ratio vs. HS Time Interval..... 147

Figure 53 - Volume Mean Particle Size Model V2 (Screening Experimental Design) - Predicted vs. Actual..... 147

Figure 54 - Area- vs. Number- vs. Volume Mean Particle Size Data Comparison 150

Figure 55 - Area- vs. Number- vs. Volume Median Particle Size Data Comparison 151

Figure 56 - Comparison of EXP S4 vs. EXP S20..... 151

Figure 57 - Mean vs. Median Comparison for the Volume-, Area and Number Particle Size Distributions 152

Figure 58 - EXP S4 Volume-, Area- and Number Particle Size Data Sets Comparison 153

Figure 59 - Roughness Specimens for EXP S15 and S16 (top and bottom, respectively) 155

Figure 60 - Actual measured response vs. model predicted value..... 157

Figure 61 - Relative contribution of factors to the roughness 158

Figure 62 - Volume Mean Particle Size Model V2 (Screening Experimental Design) - Roughness vs. Wax-to-Surfactant Ratio vs. Temperature 158

Figure 63 - Volume Mean Particle Size Model V2 (Screening Experimental Design) - Roughness vs. Wax-to-Surfactant Ratio vs. Stirring Speed 159

Figure 64 - Roughness Data vs. Volume Distribution Particle Size Data Comparison 160

Figure 65 - Actual measured response vs. model predicted value..... 165

Figure 66 - Relative contribution of the factors to the gloss..... 165

Figure 67 - Volume Mean Particle Size Model V2 (Screening Experimental Design) - Gloss vs. Wax-to-Surfactant Ratio vs. High Shear Homogenizing Speed 166

Figure 68 - Volume Mean Particle Size Model V2 (Screening Experimental Design) 0 Gloss vs. Wax-to-Surfactant Ratio vs HS Time Interval 167

Figure 69 - Gloss Data vs. Volume Distribution Particle Size Data Comparison 167

Figure 70 - Gloss Data vs. Roughness Data Comparison 168

Figure 71 - Temperature and Pressure Curve - EXP S27..... 172

| | |
|---|-----|
| Figure 72 - Target Response Output..... | 174 |
| Figure 73 - Minimizing Response Output | 174 |
| Figure 74 - Step Response Output..... | 174 |
| Figure 75 - EXP M11: Volume, Area and Number Frequency vs. Particle Diameter | 180 |
| Figure 76 - Actual measured response vs. model predicted value..... | 182 |
| Figure 77 - Relative contribution of the area median particle size model factors to the area median particle size..... | 183 |
| Figure 78 - Area Median Particle Size Model (Mixture Experimental Design) - Particle Size vs. %Wax vs. %Oleic Acid vs. %OAmmonium Hydroxide..... | 183 |
| Figure 79 - Area Median Particle Size Model (Mixture Experimental Design) - Particle Size vs. Wax-to-Surfactant Ratio | 184 |
| Figure 80 - Area Median Particle Size Model (Mixture Experimental Design) - Predicted vs. Actual..... | 185 |
| Figure 81 - Cracked dried Carnauba wax coating (EXP M8, EXP M12 and EXP M15)..... | 187 |
| Figure 82 - Uniform dried Carnauba wax coating (EXP M3)..... | 187 |
| Figure 83 - Temperature and Pressure Curve - EXP M11 | 189 |
| Figure 84 - Area Median Particle Size Model (Mixture Experimental Design) - Particle Size vs. Wax-to-Surfactant Ratio | 191 |
| Figure 85 - EXP F17: Volume, Are and Number Frequency vs. Particle Diameter..... | 195 |
| Figure 86 - Comparison of Screening-, Mixture and Composite Experimental Design Volume Particle Size Distribution [Range=0-100 μm]..... | 195 |
| Figure 87 - Comparison of Screening-, Mixture and Composite Experimental Design Volume Particle Size Distribution [Range=0-10 μm]..... | 196 |
| Figure 88 - Actual measured response vs. model predicted value..... | 198 |
| Figure 89 - Relative contribution of the Number Mean Particle Size Model factors to the number mean particle size | 199 |
| Figure 90 - Number Mean Particle Size Model (Composite Experimental Design) - Particle Size vs. Temperature vs. Stirring Speed..... | 199 |
| Figure 91 - Number Mean Particle Size Model (Composite Experimental Design) - Particle Size vs. Temperature vs. HS Time Interval..... | 200 |
| Figure 92 - Actual measured response vs. model predicted value..... | 202 |
| Figure 93 - Relative contribution of the Number Median Particle Size Model facotrs to the number median particle size | 203 |
| Figure 94 - Actual measured response vs. model predicted value..... | 204 |

| | |
|---|-----|
| Figure 95 - EXP F8: Dried Coating | 206 |
| Figure 96 - Uniform dried Carnauba wax coating (EXP F1)..... | 207 |
| Figure 97 - Temperature and Pressure Curve - EXP F1..... | 210 |
| Figure 98 - Number Mean Particle Size Model (Composite Experimental Design) - Particle Size vs. Temperature..... | 212 |
| Figure 99 - Number Median Particle Size Model (Composite Experimental Design) - Particle Size vs. Temperature | 213 |
| Figure 100 - Area Median Particle Size Model (Composite Experimental Design) - Particle Size vs. Temperature..... | 213 |
| Figure 101 - Number Median Model - Mean- and Median Particle Sizes | 214 |
| Figure 102 – Comparison of Number Median Model (Composite) and Commercial Waxes ... | 217 |
| Figure 103 – Comparison of Number Median Model (Composite) and Commercial Waxes – Number Distribution (logarithmic scale) | 218 |
| Figure 104 – Comparison of Number Median Model (Composite) and Commercial Waxes – Volume Distribution (logarithmic scale)..... | 219 |
| Figure 105 – Comparison of Number Median Model (Composite) and Commercial Waxes - Area Distribution (logarithmic scale)..... | 219 |
| Figure 106 – Volume-, Area- and Number Particle Size Data – TR Coating..... | 220 |
| Figure 107 – Volume-, Area- and Number Particle Size Data - Number Median Model (Composite) | 220 |
| Figure 108 - Comparison of Number Median Model (Composite) and Commercial Waxes.... | 221 |
| Figure 109 - Comparison of Number Median Model (Composite) and Commercial Waxes – Number Distribution (logarithmic scale) | 222 |
| Figure 110 – Comparison of Number Median Model (Composite) and Commercial Waxes - Volume Distribution (logarithmic scale)..... | 222 |
| Figure 111 – Comparison of Number Median Model (Composite) and Commercial Waxes - Area Distribution (logarithmic scale)..... | 223 |
| Figure 112 - Volume-, Area- and Number Particle Size Data - Commercial Wax F | 223 |
| Figure 113 - Top dome area showing the safety glass and fan-belt cover | 247 |
| Figure 114 - Schematic of the pilot plant frame..... | 248 |
| Figure 115 - Completed Pilot Plant..... | 248 |
| Figure 116 – Hot Water Pump [E-102] Calibration..... | 249 |
| Figure 117 - Stirrer motor [M-101] calibration..... | 250 |
| Figure 118 - High shear homogenizer motor [M-102] calibration | 250 |

Figure 119 – Screening Experimental Design Particle Size Data - Residuals vs. Run..... 258

Figure 120 - Screening Experimental Design Particle Size Data - Normal Plot of Residuals..... 259

Figure 121 - Screening Experimental Design Particle Size Data - Residuals vs. Predicted 260

Figure 122 - Volume Median Particle Size Model V1 (Screening Experimental Design) - Particle Size vs. Wax-to-Surfactant Ratio vs. Stirring Speed..... 263

Figure 123 - Volume Median Particle Size Model V1 (Screening Experimental Design) - Particle Size vs. Wax-to-Surfactant Ratio..... 264

Figure 124 - Volume Median Particle Size Model V1 (Screening Experimental Design) - Particle Size vs. Wax-to-Surfactant Ratio vs. Cooling Rate 265

Figure 125 - Volume Median Particle Size Model V1 (Screening Experimental Design) - Particle Size vs. Wax-to-Surfactant Ratio vs. Inverting Phase Addition Rate 266

Figure 126 - Volume Median Particle Size Model V1 (Screening Experimental Design) - Predicted vs. Actual 267

Figure 127 - Volume Median Particle Size Model V2 (Screening Experimental Design) - Particle Size vs. Wax-to-Surfactant Ratio vs. Cooling Rate 269

Figure 128 - Volume Median Particle Size Model V2 (Screening Experimental Design) - Predicted vs. Actual 270

Figure 129 - Area Mean Particle Size Model V1 (Screening Experimental Design) - Particle Size vs. Wax-to-Surfactant Ratio vs. Stirring Speed 273

Figure 130 - Area Mean Particle Size Model V1 (Screening Experimental Design) - Particle Size vs. Wax-to-Surfactant Ratio..... 274

Figure 131 - Area Mean Particle Size Model V1 (Screening Experimental Design) - Particle Size vs. Wax-to-Surfactant Ratio vs. Cooling Rate 275

Figure 132 - Area Mean Particle Size Model V1 (Screening Experimental Design) - Particle Size vs. Wax-to-Surfactant Ratio vs. Inverting Phase Addition Rate..... 276

Figure 133 - Area Mean Particle Size Model V1 (Screening Experimental Design) - Predicted vs. Actual..... 277

Figure 134 - Area Median Particle Size Model V1 (Screening Experimental Design) - Particle Size vs. Wax-to-Surfactant Ratio vs. High Shear Homogenizing Speed 280

Figure 135 - Area Median Particle Size Model V1 (Screening Experimental Design) - Particle Size vs. Wax-to-Surfactant Ratio..... 281

Figure 136 - Area Median Particle Size Model V1 (Screening Experimental Design) - Particle Size vs. Wax-to-Surfactant Ratio vs. Inverting Phase Addition Rate 282

| | |
|---|-----|
| Figure 137 - Area Median Particle Size Model V1 (Screening Experimental Design) - Predicted vs. Actual..... | 283 |
| Figure 138 - Area Median Particle Size Model V2 (Screening Experimental Design) - Particle Size vs. Wax-to-Surfactant Ratio vs. HS Time Interval..... | 286 |
| Figure 139 - Area Median Particle Size Model V2 (Screening Experimental Design) - Particle Size vs. Wax-to-Surfactant Ratio vs. High Shear Homogenizing Speed..... | 287 |
| Figure 140 - Area Median Particle Size Model V2 (Screening Experimental Design) - Particle Size vs. Wax-to-Surfactant Ratio vs. HS Time Interval..... | 288 |
| Figure 141 - Area Median Particle Size Model V2 (Screening Experimental Design) - Particle Size vs. Wax-to-Surfactant Ratio vs. Inverting Phase Addition Rate | 289 |
| Figure 142 - Area Median Particle Size Model V2 (Screening Experimental Design) - Particle Size vs. Wax-to-Surfactant Ratio vs. Temperature | 290 |
| Figure 143 - Area Median Particle Size Model V2 (Screening Experimental Design) - Predicted vs. Actual..... | 291 |
| Figure 144 - Particle Size compared to Literature Data..... | 292 |
| Figure 145 - Number Mean Particle Size Model V1 (Screening Experimental Design) - Particle Size vs. Wax-to-Surfactant Ratio vs. Temperature | 295 |
| Figure 146 - Number Mean Particle Size Model V1 (Screening Experimental Design) - Particle Size vs. Wax-to-Surfactant Ratio..... | 295 |
| Figure 147 - Number Mean Particle Size Model V1 (Screening Experimental Design) – Predicted vs. Actual..... | 296 |
| Figure 148 - Number Mean Particle Size Model V2 (Screening Experimental Design) - Particle Size vs. Wax-to-Surfactant Ratio vs. High Shear Homogenizing Speed..... | 299 |
| Figure 149 - Number Mean Particle Size Model V2 (Screening Experimental Design) - Particle Size vs. Wax-to-Surfactant Ratio vs. Cooling Rate | 300 |
| Figure 150 - Number Mean Particle Size Model V2 (Screening Experimental Design) - Particle Size vs. Wax-to-Surfactant Ratio vs. HS Time Interval..... | 300 |
| Figure 151 - Number Mean Particle Size Model V2 (Screening Experimental Design) - Particle Size vs. Wax-to-Surfactant Ratio vs. Inverting Phase Addition Rate | 301 |
| Figure 152 - Number Mean Particle Size (Screening Experimental Design) - Particle Size vs. Wax-to-Surfactant Ratio vs. Temperature..... | 302 |
| Figure 153 - Number Mean Particle Size Model V2 (Screening Experimental Design) - Predicted vs. Actual..... | 303 |

| | |
|---|-----|
| Figure 154 - Number Median Particle Size Model V1 (Screening Experimental Design) - Predicted vs. Actual | 305 |
| Figure 155 - Number Median Particle Size Model V2 (Screening Experimental Design) - Particle Size vs. Wax-to-Surfactant Ratio vs. High Shear Homogenizing Speed | 308 |
| Figure 156 - Number Median Particle Size Model V2 (Screening Experimental Design) - Particle Size vs. Wax-to-Surfactant Ratio vs. Cooling Rate | 309 |
| Figure 157 - Number Median Particle Size Model V2 (Screening Experimental Design) - Particle Size vs. Wax-to-Surfactant Ratio vs. HS Time Interval..... | 310 |
| Figure 158 - Number Median Particle Size Model V2 (Screening Experimental Design) - Particle Size vs. Wax-to-Surfactant Ratio vs. Inverting Phase Addition Rate | 311 |
| Figure 159 - Number Median Particle Size Model V2 (Screening Experimental Design) - Particle Size vs. Wax-to-Surfactant Ratio vs. Temperature | 311 |
| Figure 160 - Number Median Particle Size Model V2 (Screening Experimental Design) - Predicted vs. Actual | 312 |
| Figure 161 – Number Median Particle Size Distribution Data vs. Roughness- and Gloss Data Comparison..... | 325 |
| Figure 162 – Number Median Particle Size Distribution Data vs. Gloss Data Comparison | 325 |

Chapter 1: Introduction

1.1 Background

The need to protect food products from physical, chemical and biological deterioration has always been a crucial objective for the food industry. Various techniques have been developed over the years to preserve the quality of food products, of which packaging is the ultimate one. When it comes to fresh fruit, synthetic packaging is not favoured since fruits, having living tissue, are considered active foods. The use of edible films and coatings have been suggested as an alternative packaging for these active foods, resulting in the development of new and/or modified edible coatings. However, improving the functionality and performance of these edible coatings has been one of the challenges of the post-harvest industry.

This development has been problematical due to the difference in requirements of certain fruits demanding the development of both natural and polyethylene coatings, in addition to having to comply with the ever changing United States (US) and European (EU) food regulations. One such edible coating used in the non-processed fruit industry is an anionic wax micro-emulsion consisting of a combination of wax, water, a fatty acid and a base. The base ionizes the fatty acid to form a soap, which stabilizes the wax droplets in the water to form an emulsion. The performance of any specific wax as a coating depends largely on the quality of the emulsion (Hagenmaier, Baker 1994). The characteristics of emulsions are built into them during the manufacturing process and are not necessarily related to the properties and characteristics of the major ingredients (Griffin 1945). These characteristics include; appearance, viscosity, dispersibility, stability, wetting- and spreading capabilities and its particle size (Griffin 1945).

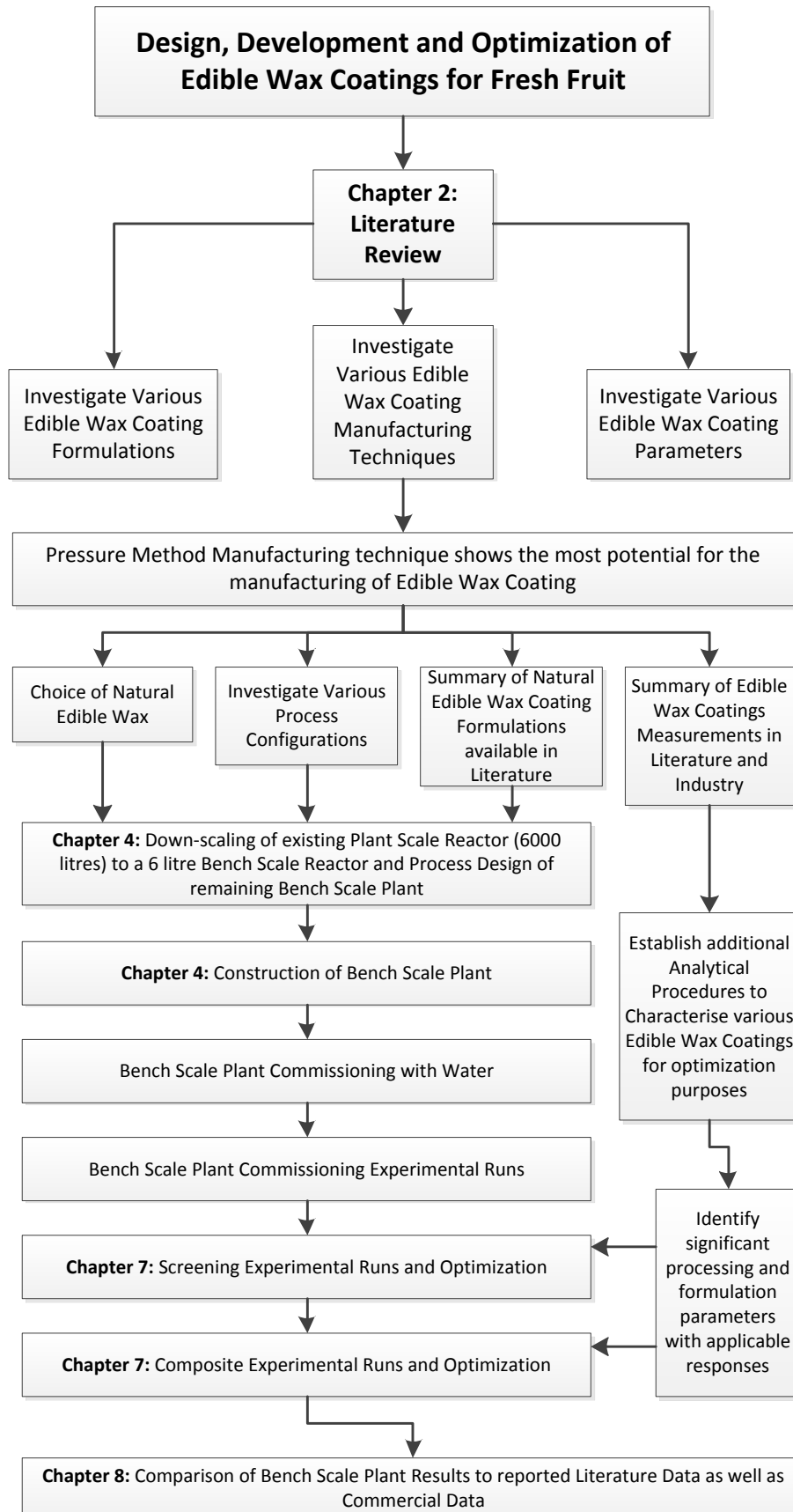
1.2 Objectives

In order to investigate newly modified wax micro-emulsion formulations that comply with the US and EU food regulations, it is required that a more in-depth understanding of the overall manufacturing process, including the process parameters and their effects on the quality of the final product, is gained. The main objective of this study is focussed on gaining a better understanding of the process design, the manufacturing processes and the operational manufacturing procedures of these wax micro-emulsions. To gain this understanding, the first objective of this study will be to down-scale an existing plant-scale batch reactor of *6000 litres*, which is currently employed at an edible coatings manufacturer, to a geometrically similar bench-scale batch reactor with a volume of *6 litres*. The bench scale reactor will then be implemented in a pilot plant setup.

Once the bench scale pilot plant has been commissioned, the second objective of this study will involve investigating a specific natural micro-emulsion coating by performing experimental runs. Screening experimental runs will initially be performed to identify the main process/formulation parameter/s. The results of these experimental runs will be optimised by means of statistical analysis software (Design Expert©). The models obtained during the optimisation of the screening experimental design will further be used to set up a composite experimental design. The final composite experimental design results will be optimised to obtain the optimum process- and formulation parameter settings to yield a favourable product evaluated according to literature.

The third and final objective will be to compare the final optimized results with existing commercial wax coatings currently being used in the industry. No tests or analyses will be performed with the wax coatings on fruit.

1.3 Mind Map



Chapter 2: Literature Review

2.1 Edible films and coatings

2.1.1 What are natural films and coatings?

There has always been a need to enhance the quality of food products by protecting them from physical, chemical and biological deterioration. The quality of food products depends on hygienic, nutritional and organoleptic characteristics (Debeaufort, Quezada-Gallo & Voilley 1998). Unfortunately, during storage and commercialization these characteristics evolve and change (Debeaufort, Quezada-Gallo & Voilley 1998). Various techniques (physical and chemical processes) have been developed to preserve these characteristics, namely sterilization, high pressure, radiation or active agents (Debeaufort, Quezada-Gallo & Voilley 1998). Nevertheless, the use of packaging is still the ultimate step of the food preservation process (Debeaufort, Quezada-Gallo & Voilley 1998). Synthetic packaging (e.g. resin-, composite-, cellulosic-, plastic-films etc.) is widely used due to its efficiency to reduce mass-, gas- and solute- transfer between food and its storage medium (Debeaufort, Quezada-Gallo & Voilley 1998). Since synthetic packaging materials do not offer edibility and biodegradability, the use of edible films and coatings have been suggested as an alternative food packaging for active foods (Han, Aristippos 2005).

In order to define edible films and coatings, it is necessary to understand the difference between films and coatings. Films are generally defined as stand-alone thin layers of materials, while coatings are a particular form of film applied directly on the surface of materials (Han, Aristippos 2005). Sheets are another form of film that consists of thick films (Han, Aristippos 2005). Films are usually comprised of polymers able to provide mechanical strength to a stand-alone structure (Han, Aristippos 2005). Due to coatings being applied directly to the surface of materials, it forms part of the final product making it difficult to remove (Han, Aristippos 2005). According to Debeaufort et al., when a packaging like a film, a sheet, a thin layer or a coating is an integral part of a food and is eaten with the food, then it is qualified as “edible packaging” (Debeaufort, Quezada-Gallo & Voilley 1998).

2.1.2 History

The use of edible films and coatings, to prolong the shelf life and quality of food, has been existed for many years. Since the twelfth and thirteenth centuries wax has been used to delay the dehydration of citrus fruit in China (Debeaufort, Quezada-Gallo & Voilley 1998). In Asia the appearance and preservation of foods have been improved by the application of a proteic edible film obtained from the skin of boiled soy milk, since the fifteenth century (Debeaufort, Quezada-Gallo & Voilley 1998). Although it's not the earliest use of edible coatings, the coating of meat with fat to prevent shrinkage has been the usual practice since at least the sixteenth century, according to Kester and Biquet (1986) (Debeaufort, Quezada-Gallo & Voilley 1998). In the last century nuts, almonds and hazelnuts have initially been coated with sucrose as an edible protective coating to prevent oxidation and rancidness during storage (Debeaufort, Quezada-Gallo & Voilley 1998). **Table 1** lists some of the foods that have been coated with edible films and coatings.

Table 1 - Edible film and coatings coated foods (Debeaufort et al.,1998)

| Coated Foods |
|--|
| Meat |
| Poultry |
| Seafood |
| Fruits |
| Vegetables |
| Grains |
| Candies |
| Heterogeneous and Complex Foods |
| Fresh, Cured, Freezed and Processed Foods |

Currently, the application of edible films and coatings concerns the use of emulsion made from waxes and oils coated on to fruits to improve their characteristics e.g. appearance (e.g. shininess, colour, softening etc.), in order to prevent the onset of mealiness, carriage of fungicides, decreasing the ripening rate and the rate of water loss (Debeaufort, Quezada-Gallo & Voilley 1998).

2.1.3 Functions and advantages of edible films and coatings

The most advantageous characteristic of edible films and coatings are their **edibility** and inherent **biodegradability** (Han, Aristippos 2005, Guilbert, Gontard & Gorris 1996). To ensure that the resultant film or coating is fully edible, all the film components (including biopolymers, plasticizers and other additives) should be food-grade (FDA approved) quality (Guilbert, Gontard & Gorris 1996). Furthermore, all the process facilities should be suitable for food processing (Guilbert, Gontard & Gorris 1996). Edible packaging can be considered as food ingredients or food additives, depending on the application (Debeaufort, Quezada-Gallo & Voilley 1998). Generally edible packaging does not provide significant nutritional value to the coated food, therefore they should rather be considered as an additive rather than an ingredient (Debeaufort, Quezada-Gallo & Voilley 1998). Overall, it all depends on the application of the edible film or coating. Because edible films and coatings are both a packaging and a food component, they have to fulfil certain requirements as mentioned by Debeaufort et al. (Debeaufort, Quezada-Gallo & Voilley 1998):

- They require good sensory qualities e.g. if the edible film or coating is used as a food component, it usually has to be tasteless to be undetected during consumption.
- High barrier and mechanical efficiencies are required.
- Enough biochemical, physicochemical and microbial stability is essential for the quality and stability of some fresh, treated, or frozen food products.
- Free of toxins in order to be safe for human consumption.
- Simple technology is required to make the manufacturing process easy.
- In order to be biodegradable, non-polluting raw materials should be used in the formulation.
- The cost of raw materials and the manufacturing process should be low.

From the above mentioned requirements, it is noted that edible packaging must have some functional- and specific properties (Debeaufort, Quezada-Gallo & Voilley 1998). In addition Baker and Hagenmaier (1997) states that when it comes to sensory properties, a successful coating should contribute no unpleasant mouth feel or flavour to the coated food (Baker, Hagenmaier 1997). Thus films and coatings should not lead to the generation of off-flavours in the applied food during storage, as a result of alterations to coated food's metabolism (Baker, Hagenmaier 1997). The basic property edible films and coatings should have, is to be selective towards mass transfer (e.g. gas, vapours, solute or water) (Debeaufort, Quezada-Gallo & Voilley 1998). **Figure 1** represents the selective functions of edible films and coatings (Debeaufort, Quezada-Gallo & Voilley 1998).

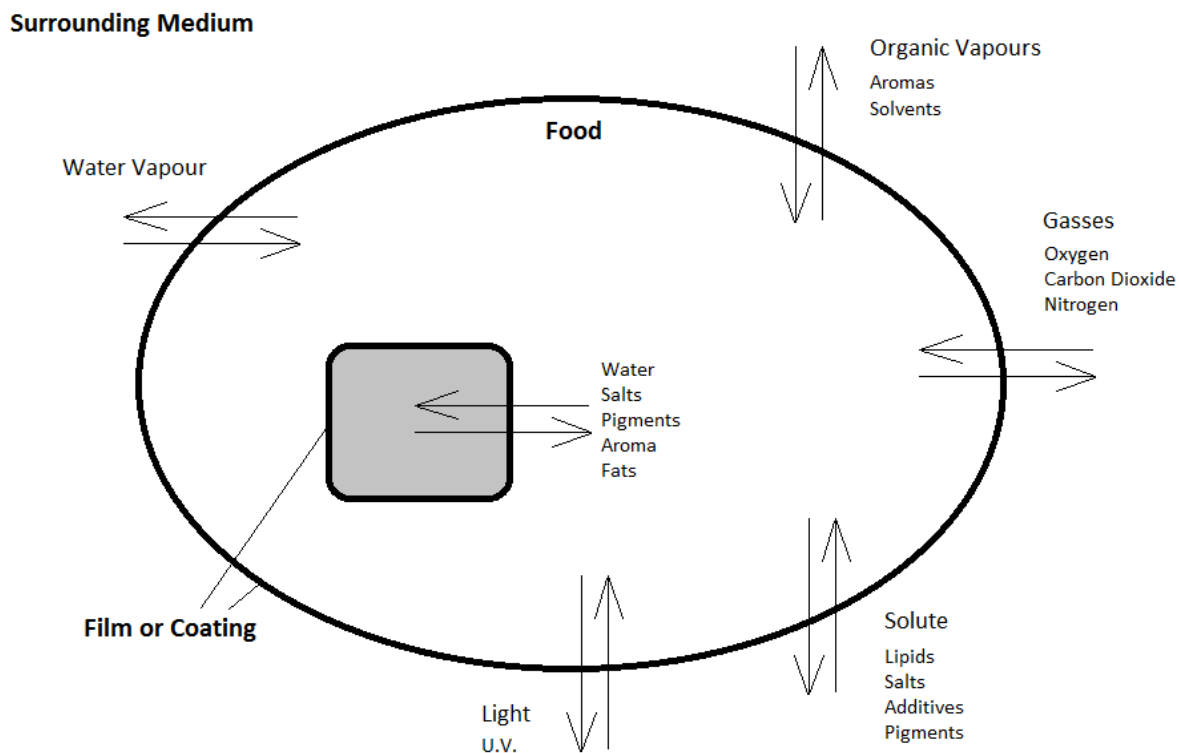


Figure 1 - Selective functions of edible films and coatings (redrawn from Debeaufort et al. (1998))

Edible packaging can also have active properties or a combination of both selective and active properties (Debeaufort, Quezada-Gallo & Voilley 1998). Some of the active properties that edible packaging can possess are summarized by Debeaufort et al. in **Table 2**.

Table 2 - Active properties of edible films and coatings (Debeaufort et al., 1998)

| Active Properties | |
|--|-----------------------------------|
| Encapsulation or carriage | |
| Flavours, spices | Antimicrobial, antioxidant agents |
| Pigments, light absorbers | Salts |
| Other food additives | |
| Improvement of mechanical resistance | |
| Improvement of appearance | |
| Colour | Shininess |
| Transparency | Roughness |
| Sticking | |
| Individual protection of small pieces of food | |
| Separation of food by individual portion | |
| Soluble package for pre-dosed food ingredients or additives | |

Edible films and coatings can, to an extent, provide **physical- and mechanical protection** against physical damage, e.g. mechanical impact, pressure, vibrations etc., to the coated food products (Han, Aristippos 2005). Various standardized tests are performed in order to determine the extent to which the films or coatings can provide this physical- and mechanical protection (Han, Aristippos 2005). These standardized tests include tensile strength-, elongation-at-break-, elastic modulus-, compression strength-, puncture strength-, stiffness-, tearing strength-, burst strength-, abrasion resistance-, adhesion force- and the folding endurance test (Han, Aristippos 2005).

There are numerous variables that affect the physical and mechanical properties of edible films and coatings. Of all the variables, edible films and coatings are the most sensitive to moisture (humidity) and temperature (Han, Aristippos 2005, Guilbert, Gontard & Gorris 1996). In connection with the moisture, at higher relative humidity conditions, edible films and coatings' physical strength is lower than that at lower relative humidity (Han, Aristippos 2005). This is due to the absorbed moisture acting as a plasticizer (Han, Aristippos 2005). Plasticizers are low molecular weight agents that decrease the glass transition temperature of polymers (Han, Aristippos 2005). Furthermore, in connection with the temperature, the physical strength of film-forming materials decreases greatly when the temperature increases above the glass transition temperature (Han, Aristippos 2005, Guilbert, Gontard & Gorris 1996). Thus a high relative humidity (and large amount of plasticizers) lowers the glass transition temperature of film-forming materials (Guilbert, Gontard & Gorris 1996).

As previously mentioned, the main cause of the deterioration of a food product quality is due to exchanges (mass transfer) between the foods and their surroundings (Debeaufort, Quezada-Gallo & Voilley 1998). This includes moisture absorption, oxygen invasion, flavour loss, undesirable odour absorption and the migration of packaging components into the food (Debeaufort, Quezada-Gallo & Voilley 1998, Han, Aristippos 2005). By wrapping these food products (or heterogeneous parts in the food products) with edible films or coatings, these exchanges can be prevented in order to preserve the quality of the food (Han, Aristippos 2005, Guilbert, Gontard & Gorris 1996). For instance, penetrated oxygen causes the oxidation of food ingredients (Guilbert, Gontard & Gorris 1996). Therefore by preventing oxygen invasion (decreasing the oxygen permeability of the film or coating), the oxidation of the food products can be prevented, thus increasing the quality (Han, Aristippos 2005).

The **barrier properties** of edible films and coatings are significantly affected by the type of film-forming materials used and the environmental conditions (e.g. relative humidity and temperature) (Han, Aristippos 2005). Oxygen permeability is especially sensitive to the relative humidity of the surrounding medium (Guilbert, Cuq & Gontard 1997). The oxygen permeability

increases significantly at higher relative humidity conditions (Guilbert, Cuq & Gontard 1997). In other words, it is crucial to maintain a relatively low humidity environment in order to maximize the effectiveness of the edible films and coatings as gas barriers (Han, Aristippos 2005, Guilbert, Cuq & Gontard 1997). Temperature is also a crucial variable when it comes to barrier properties. An increase in the temperature of the environment provides more kinetic energy to the migrating substances, which increases the permeability (Han, Aristippos 2005).

Edible films and coatings can greatly improve the quality of food products. An improvement in the quality of food products is directly related to the ***shelf-life extension and safety enhancement*** (Han, Aristippos 2005). As a result, the possibility of contamination by foreign matter is reduced (Han, Aristippos 2005). In addition the minimally processed food industry has increased significantly in the past decade (Hyun Jin 1999). Minimally processed foods are food products that preserve their nutritional value, retain a natural and fresh colour, flavour and texture with little processing required, e.g. contain few additives (preservatives) (Allende, Tomás-Barberán & Gil 2006). For this reason, there is a requirement to secure the safety and to increase the shelf-life of the food-products involved, thus opening up a market for edible films and coatings (Hyun Jin 1999).

2.1.4 The efficiency of edible films and coatings

The efficiency of edible packaging is strongly dependant on the nature of the components, the composition and structure of the film or coating (Debeaufort, Quezada-Gallo & Voilley 1998). For example, films or coatings made from lipids or hydrophobic substances such as resins, waxes or some non-soluble proteins are the most effective for the retardation of moisture transfer (Hagenmaier, Baker 1994). **Table 3** summarizes the various materials used for edible films and coatings (Han, Aristippos 2005).

Table 3 - Materials used for edible films and coatings (Han and Gennadios, 2005)

| Materials | |
|-------------------------|---|
| Functional Compositions | Materials |
| Film-forming materials | Proteins collagen, gelatin, casein, whey protein, corn zein, wheat gluten, soy protein, egg white protein, fish myofibrillar protein, sorghum protein, pea protein, rice bran protein, cottonseed protein, peanut protein, keratin |
| | Polysaccharides starch, modified starch, modified cellulose (CMC, MC, HPC, HPMMC), alginate, carrageenan, pectin, pullulan, chitosan, gellan gum, xanthan gum |
| | Lipids waxes (beeswax, paraffin, canauba wax, candelilla wax, rice bran wax), resins (shellac, terpene), acetoglycerides |
| Plasticizers | glycerine, propylene glycol, sorbitol, sucrose, polyethylene glycol, corn syrup, water |
| Other additives | emulsifiers (lecithin, Tweens, Spans), lipid emulsions (edible waxes, fatty acids) |

Debeaufort et al. states that film-forming materials are able to form a continuous structure by settling the interactions between molecules under the action of a chemical or a physical treatment (Debeaufort, Quezada-Gallo & Voilley 1998). The film formation of these substances involves one of the following processes (Debeaufort, Quezada-Gallo & Voilley 1998):

- Melting and solidification of solid fats, waxes and resins.
- Removal of the solvent out of a hydrocolloid dispersed in an aqueous solution in order to cause it to precipitate or to gel.
- Combining two hydrocolloid solutions with opposite charges to induce interactions and precipitation of the polymer mixture.

- Thermal gelation or coagulation by the heating of the macromolecule solution. This process involves denaturation, jellification, precipitation or rapid cooling of a hydrocolloid solution.

The basic film-forming mechanisms include intermolecular forces such as covalent bonds (e.g. disulphide bonds and cross linking) and/or electrostatic, hydrophobic or ionic interactions (Han, Aristippos 2005). During fabrication, these film-forming mechanisms will be initiated (Han, Aristippos 2005). To ensure that the resulting film or coating is edible, the mechanisms involved in the fabrication process, should be appropriate for food processes, namely: pH modification, salt addition, heating, enzymatic modification, drying, use of food-grade solvent where applicable and the addition of other food-grade chemicals (Food and Drug Association (FDA) approved) (Han, Aristippos 2005). It is essential to control the process conditions during fabrication, since changes in treatment conditions can alter the kinetic- and reaction mechanisms (Guilbert, Gontard & Gorris 1996).

Additional materials such as plasticizers and other additives are also used in edible films and coatings (as indicated in **Table 3**). Plasticizers are low molecular weight agents that decrease the glass transition temperature of the polymers, by being incorporated into the film-forming materials (Han, Aristippos 2005). The plasticizers position them between the polymer molecules and interfere with the polymer-polymer interaction to enhance the flexibility and processability of the final polymer (Guilbert, Cuq & Gontard 1997). Other additives such as active agents can be carried by edible films and coatings. These active agents (including emulsifiers, antioxidants, antimicrobials, nutraceuticals, flavours and colorants) can enhance the quality and safety of the food, up to the level where they interfere with the mechanical- and physical properties of the films (Guilbert, Gontard & Gorris 1996).

2.1.5 The basic film-forming mechanism of edible films and coatings

According to Han and Gennadios (2005), an edible film is essentially a dried and extensively interacting polymer network of a three-dimensional gel structure (Han, Aristippos 2005). These interactions include intermolecular forces such as covalent bonds (e.g. disulphide bonds and cross linking) and/or electrostatic, hydrophobic or ionic interactions (Han, Aristippos 2005). There are two types of main film-forming processes namely wet casting or dry casting (Han, Aristippos 2005). Despite which process is used, the film-forming materials should form a specially rearranged gel structure with all the incorporated film-forming agents (e.g. biopolymers, plasticizers, solvents etc.) (Han, Aristippos 2005). The initial stage in the film-forming process is the wet-gelation mechanism (Han, Aristippos 2005). However, the film-forming during the drying process may differ from the wet-gelation mechanism (Han, Aristippos 2005). A critical stage of transition from a wet gel to a dry film exists, which relates to a phase transition from a polymer-in-water (or other solvents) system to a water-in-polymer system (Han, Aristippos 2005). Potential chemical and physical approaches to the modification of film-forming mechanisms by altering film-forming raw materials, varying film-forming processing conditions and applying treatment on formed films, are described in **Figure 2** (Han, Aristippos 2005).

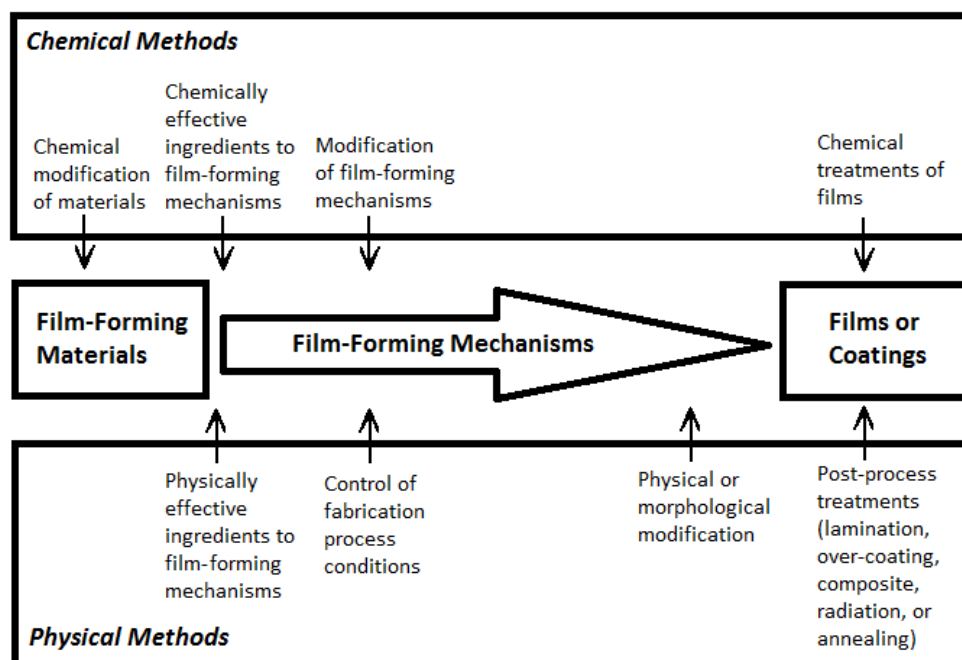


Figure 2 - Various ways for modifying the characteristics of edible films and coatings (redrawn from Han and Gennadios, 2005)

2.2 Emulsions

2.2.1 What is an emulsion?

An emulsion is defined as a mixture of two or more immiscible liquids, one being present in the other in the form of droplets (Griffin 1945). Berkman and Egloff define it in a simpler term as a liquid/liquid dispersion system (Berkman, Egloff 1941). Micro-emulsions are a type of emulsion with the discontinuous phase having an average droplet diameter of less than $0.2 \mu\text{m}$ (Hagenmaier, Baker 1997). Emulsions are found in nature of which milk and rubber latex is the two principal examples (Griffin 1945). Both these examples are stabilized by natural emulsifying agents, unlike commercial emulsions which require additional emulsifying agents (Griffin 1945). The risk of deterioration during storage is much greater for emulsions than with a non-emulsified product, since emulsions are inherently unstable systems (Griffin 1945). Currently emulsions are used in a variety of fields including textiles, leather- and metal treatment, foods, cosmetics, pharmaceuticals, paints, agricultural chemicals, polymerizations, cleaning and polishing and ore- and petroleum recovery (Griffin 1945, Hagenmaier 1998, Gutiérrez et al. 2008, Mehvar et al. 2012, Yang et al. 2000).

Technically, a mixture of a solid dispersed in a liquid is defined as a suspension or dispersion (Griffin 1945). An example of such an emulsion is molten waxes that are emulsified to form wax emulsions, which is in fact a suspension or dispersion at room temperature (Griffin 1945). Emulsions can either be an oil-in-water (wax-in-water) emulsion or a water-in-oil (water-in-wax) emulsion (also defined as an inverse emulsion) (Griffin 1945). In the case of a wax-in-water emulsion, the wax is known as the dispersed phase while the water is the continuous phase and vice-versa for the water-in-wax emulsion (Berkman, Egloff 1941). A key factor in emulsion formulation and design is the understanding of the type of emulsion which is at hand, since the emulsion characteristically assumes the properties of the continuous phase (external phase) (Griffin 1945). Take the case of edible wax coatings, a wax-in-water emulsion can be diluted with water or dried by evaporation leaving the wax as a film (Griffin 1945). Oil-in-water emulsions generally conduct electricity and can be diluted with water (Griffin 1945). In contrast, water-in-oil emulsions conduct electricity poorly if at all and can be diluted with oil or solvents (Griffin 1945). A basic comparison of the two types of emulsions is presented in **Table 4**.

Table 4 - Comparison of oil-in-water emulsions and water-in-oil emulsions (Griffin, 1945)

| Comparison | |
|---|---|
| Oil-in-Water Emulsions | Water-in-Oil Emulsions |
| Conducts electricity | Poor conductor of electricity |
| Dilutable with water | Dilutable with oil |
| Feels like water | Feels more like oil |
| Dries rapidly (loses water) | Resist drying or loss of water (although they do lose a volatile solvent readily) |
| Can be washed away | Difficult to wash away |
| Are more corrosive | Less corrosive |
| Exhibits the aqueous properties of the continuous phase | Exhibits the properties of the continuous oil phase |

When two immiscible liquids are mixed an interface is formed. If the formed interface is stable the Gibbs free energy of the formation is positive, thus the formation of emulsions is nonspontaneous and they are thermodynamically unstable (Wagner 1976, Tadros et al. 2004). The instability is explained by means of the Gibbs free energy of the system. A decrease in the area between the different phases results in a decrease in the Gibbs free energy of the system (Wagner 1976, Tadros et al. 2004). A surfactant decreases the interfacial tension resulting in a stable emulsion (Wagner 1976, Tadros et al. 2004). Surfactants accumulate at the oil-water interface by means of adsorption, with the hydrophobic portion oriented towards the hydrophobic phase (the oil) and the hydrophilic portion oriented towards the hydrophilic phase (the water) (Tadros et al. 2004). The surface tension of the water and the oil-water interface is reduced due to the adsorption resulting in more stable system (a lower Gibbs free energy) (Tadros et al. 2004).

2.2.2 Characteristics of Emulsions

Emulsions can be characterised according to various aspects, namely appearance, viscosity, dispersibility, ease of preparation, stability, wetting and spreading ability and its particle size (Griffin 1945). When it comes to the particle/globule size of the phase distributed in the medium of an emulsion, it draws a distinction between molecular- and coarse systems (Berkman, Egloff 1941). Molecular systems are composed of molecules or aggregates of molecules (colloidal systems), while coarse systems consist of particles that are visible under a microscope (Berkman, Egloff 1941). The characteristics of emulsions are not necessarily related to the properties and characteristics of the major ingredients, but built into the emulsion during formulation and can often be prepared to suit specific application requirements (Griffin 1945). The characteristics of emulsions and where they originate from are summarized in **Table 5**, as stated by Griffin (1945) (Griffin 1945).

Table 5 - Characteristics of emulsions (Griffin, 1945)

| Emulsion Characteristics | |
|-------------------------------|--|
| Characteristics | Reason |
| Appearance: | |
| Clarity | |
| <i>Clear</i> | Small particle size; Matched refractive indexes |
| <i>Translucent</i> | Medium particle size |
| <i>Opaque</i> | Large particle size; Unmatched refractive indexes |
| Colour | |
| <i>White</i> | Large particle size; Unmatched refractive indexes |
| <i>Grey</i> | Medium-small particle size; Unmatched refractive indexes |
| <i>Colours</i> | Colours in continuous phase |
| Viscosity: | |
| High | High internal phase (HIP) emulsion; Small particle size; Thickeners in outside phase |
| Thin | Low internal phase (LIP) emulsion with no thickener |
| Dispersibility: | |
| In water | Oil-in-Water |
| In oil | Water-in-Oil |
| Ease of preparation: | |
| High, easy | Emulsifier, Solution level; Low viscosity concentrate |
| Low, difficulties | Low emulsifier level |
| Re-emulsification | Emulsifier selection; Emulsifier level |
| Stability: | |
| High, good | Emulsifier selection; Emulsifier moderately high |
| Low, poor | Low emulsifier levels; Emulsifier selected for other property |
| Stable to electrolytes | Emulsifier selection |
| On evaporation (Oil-in-Water) | Emulsifier selection; Emulsifier level |
| Spoilage | Preservative selection; Sterile packaging |
| Wetting-Spreading: | |
| High | Emulsion type; Emulsifier selection |
| Low | Emulsifier selection |
| Particle size: | |
| Small | Emulsifier selection; Emulsifier level |
| Large | Emulsifier level |

2.3 Edible Wax Emulsion Coatings

According to Griffin (1945), a good manufacturing process for emulsions is based on a properly developed laboratory procedure. That said, the scale-up of the process introduces various problems of agitation, incorporation of air, surface-volume ratios, addition rates of ingredients (especially at inversion points), cooling rates and raw material control (Griffin 1945).

2.3.1 Equipment

Various small scale pilot-plant models of planetary mixers, motor-driven propellers, turbines, colloid mills and homogenizers are available. However, agitation is usually much more vigorous and efficient than that in plant-scale equipment which is crucial when applying results from one to another to up-scale (Griffin 1945). Griffin (1945) stated that the surface-to-volume ratios, peripheral speeds of agitation, tendencies to maelstrom and foam production and heating and cooling rates differ in equipment scale-up. Plant conditions should be duplicated as far as possible during laboratory preparations, to the side of too little energy input if possible (Griffin 1945). Another serious problem in the laboratory occurs when emulsions are heated and then cooled during preparation. In the laboratory (e.g. a scale of 6 litres), cooling takes a few minutes, while on a larger scale (6000 litres) cooling takes much longer (Griffin 1945). This is especially crucial in the production of emulsions containing wax components (e.g. edible wax emulsions), due to the rate of cooling through the melting range being very important, as reported by Griffin (1945).

Similarly, in the case of emulsions formulated to produce small particle size through the emulsion inversion point method requires particular attention at the inversion point (to be discussed in **Section 2.4.2 – Inversion Point**) (Griffin 1945, Fernandez et al. 2004, Li et al. 2010). The inversion point will be discussed in more detail in **Section 2.4.2 – The Inversion Point**. A smooth and complete inversion produces the smallest particle size (Griffin 1945, Li et al. 2010). **The major factors that control the inversion point include temperatures and the addition rate of the inverting phase** (e.g. the final continuous phase) (Griffin 1945). Generally the slow addition of the inverting phase is desired to achieve the finest particle size (Griffin 1945, Gutiérrez et al. 2008, Pey et al. 2006, Wang et al. 2007, Lashmar, Richardson & Erbod 1995, Lashmar, Beesley 1993). Additionally Griffin (1945) states that the cycle time is also a very important factor affecting the progression of the emulsion inversion point method.

When it comes to raw materials it is necessary to select high quality and consistent materials for laboratory use, since it will determine the raw materials used on plant scale. Especially in the case of natural products e.g. waxes, the laboratory preparation of the emulsion should be made with similar raw materials and tested for critical properties (Griffin 1945). Another critical factor is the quality of the water. Variations in water (e.g. metal ion and bacterial content) can produce disturbing effects that are frequently blamed on other ingredients. Other factors such as the weather (e.g. ambient temperature, wind etc.) can also result in the quality and composition of the water being different in the laboratory than at the plant. To prevent any disturbances due to the water quality, a standard should be established for both the laboratory and the plant (Griffin 1945).

Emulsions can either be produced by batch- or continuous processes. The plant scale process should be based on the laboratory (pilot-plant) tests from which a detailed procedure should be established for preparing the specific emulsion (Griffin 1945). A typical wax emulsification plant is presented in **Figure 3** (Rhe America 2014, Rhe America 2014).

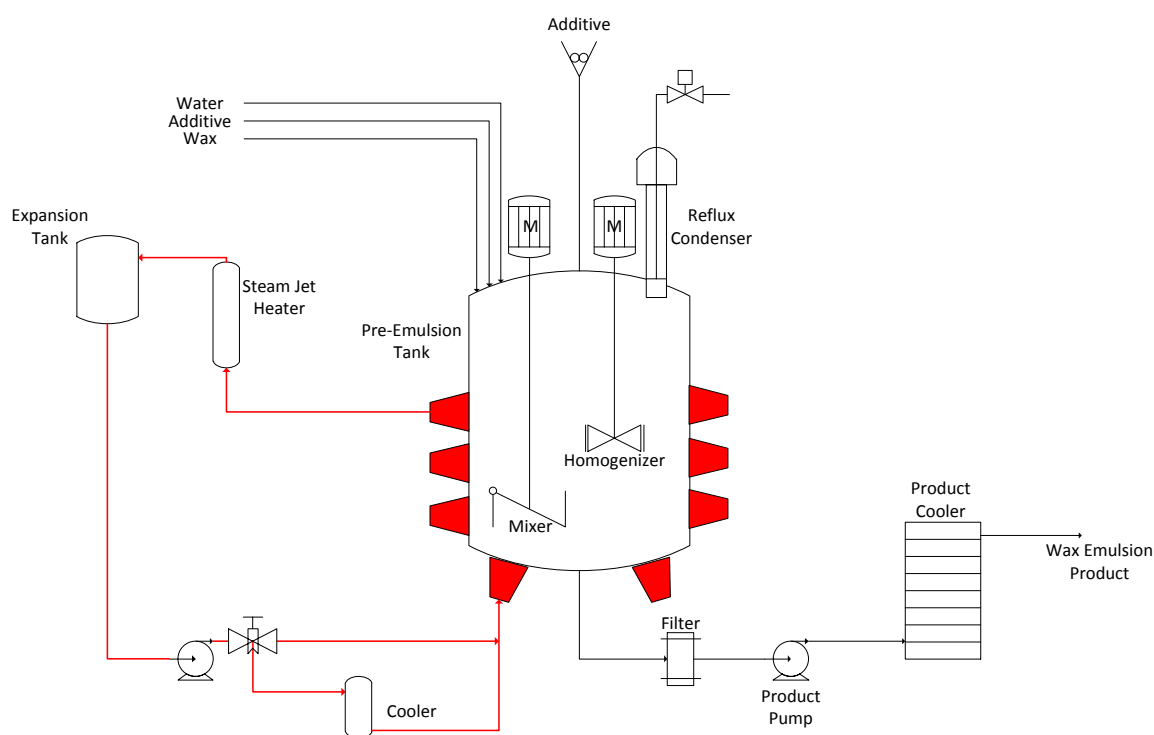


Figure 3 - Typical Wax Emulsification Plant – redrawn from Rhe America (2014)

The rate at which the ingredients are added and the temperature are two very important factors in the emulsion production process (Griffin 1945). *Addition of Ingredients:* In the case where wax micro-emulsions are prepared according to the emulsion inversion point (EIP) method (to be discussed in **Section 2.4**), specific procedures should be worked out in order to ensure that the appropriate amount of water is added at the right moment (Griffin 1945, Gutiérrez et al. 2008, Li et

al. 2010, Pey et al. 2006, Wang et al. 2007, Wang et al. 2007, Lashmar, Richardson & Erbod 1995, Lashmar, Beesley 1993). Generally, the water is slowly added to the molten wax mixture, until the inversion point is reached (at which point the viscosity suddenly decreases) (Griffin 1945, Gutiérrez et al. 2008, Li et al. 2010, Lashmar, Richardson & Erbod 1995, Lashmar, Beesley 1993). The rest of the water may then be added rapidly (Griffin 1945). *Temperature*: Heating is crucial in wax emulsions (Griffin 1945, Lashmar, Richardson & Erbod 1995, Danghui, Fengyan & Tianbo 2012, Jass 1967). It is required that the wax is heated to about 10 – 20°C above its melting point (Hagenmaier, Baker 1994, Griffin 1945, Hagenmaier, Baker 1997, Hagenmaier 1998, Hagenmaier 2004, Hagenmaier 2000). Shocking the wax by cooling it too quickly must be avoided (Griffin 1945). Thus, the cooling rate of wax emulsions is critical, especially at the melting point of the wax (Griffin 1945, Lashmar, Richardson & Erbod 1995, Danghui, Fengyan & Tianbo 2012). The best cooling rate should be determined for each emulsion (Griffin 1945).

The equipment used to prepare the emulsion has to be able to break up or disperse the internal phase in the external phase, so that the particle size of the resultant emulsion is sufficiently small to ensure stability (Griffin 1945, Lashmar, Richardson & Erbod 1995, Danghui, Fengyan & Tianbo 2012). There are a few major concerns when choosing emulsifying equipment, including the apparent viscosity during all stages of manufacturing, the amount of mechanical energy input required and the heat exchange demand (Griffin 1945). One of the main factors that affect the preparation process of emulsions is the type of agitation (Griffin 1945). Mechanical mixing is widely used in chemical processing for both single-phase and multi-phase systems (Kamienski 1986). In multi-phase systems, mixing enhances mass exchange between the phases to an extent which depends mainly on the interfacial area and the hydrodynamic conditions (Kamienski 1986). **Propeller agitators** are a popular type of equipment used for agitation, which consists of one or more propellers mounted on a common shaft in a mixing vessel (or pressure vessel) (Griffin 1945). The equipment can be modified by changing the propeller spacing, adding a variable speed controller or by using two or more propeller shafts and custom propeller blades (Griffin 1945). Bouchama et al. (2003) used geometrically similar vessel with a three blade impeller (radius 2.5 cm) connected to a stirrer motor with a variable speed controller to ensure a constant stirring rate, during their study on the mechanism of catastrophic phase inversion in emulsions (Bouchama et al. 2003). The variable speed drive was installed to ensure a constant stirring rate, independent of the viscosity of the emulsion, since a strong change in viscosity occurs during the phase inversion (Bouchama et al. 2003).

Daglas and Stamatoudis (2000) conducted a study on the effect of the impeller vertical position on drop sizes in agitated dispersions, in which the effect of impeller height relative to the vessel bottom was studied by measuring the drop size distribution of kerosene dispersions in water at two positions inside a stirred tank (Daglas, Stamatoudis 2000). Measurements were taken at various heights (1/3, 1/2 and 2/3 of the total vessel height) for different rotational speeds (250, 300, 350 and 400 RPM) and for hold-up fractions of 0.02 and 0.04 (Daglas, Stamatoudis 2000). They concluded that the height of the impeller affects the drop size and that this height is dependent on operating conditions (Daglas, Stamatoudis 2000). In a study conducted on the prediction of particle size in agitated dispersions, Shinnar and Church (1960) found that the behaviour of turbulent flow and the particle size distribution in stirred tanks can be predicted by using the concepts of local isotropy (Shinnar, Church 1960).

Another device used for mixing is **high shear devices**. These devices are commonly used in the chemical process industries to accomplish the most demanding mixing tasks, including the food, cosmetics, pharmaceuticals and consumer industries (Myers et al. 1999). High shearing devices are suitable for blending miscible liquids of dramatically different viscosities to uniformity, incorporating and dispersing fine solids into viscous liquids or forming emulsions of immiscible liquids (Myers et al. 1999). A high shearing device can be designed and operated in such a way that its power input is used to maximize flow with minimal shear, maximize shear with minimal flow or a balance between the two (Myers et al. 1999). Various types of high shear mixers exist, including homogenizers, pipeline mixers, colloid mills and specialized high shear mixers (Myers et al. 1999). Myers et al. (1999) states in their study on high-shear mixing that a combination of high-shear devices or a combination of a high-shear mixer and an agitator or static mixer may provide optimal performance (Myers et al. 1999). With the addition of an agitator or static mixer, it ensures that all the material will pass through the high-shear region (Myers et al. 1999). Myers et al. derived a relationship that relates the shear produced by a rotor with the rotor rotational speed and diameter (Myers et al. 1999). This relationship is represented by **Equation 1**.

$$\text{Shear} \propto N^2 D^2$$

Equation 1

(Myers et al. 1999)

N – Rotor rotation speed [rpm]

D – Rotor diameter [m]

From **Equation 1** it is noted that shear can be maximized relative to flow by operating a small-diameter impeller at a high speed (Myers et al. 1999). A common high-shear blade (rotor) used in

industries is 0.1 m in diameter and revolves at 3550 rpm (motor speed) (Myers et al. 1999). Due to high-shear mixers running at a very high speed, their torques are sufficiently low so that they can be driven directly by a motor (Myers et al. 1999). Myers et al. (1999) explains that a large homogenizer transmits a torque of only 200 Nm, while a large agitator delivers 85 000 Nm (Myers et al. 1999). They concluded that the forces resulting from high shear are responsible for droplet and agglomerate breakup and especially effective when the fluid is rapidly accelerated, when working with two immiscible fluids (Myers et al. 1999). In addition, trials also revealed that by adding a variable-speed controller, the particle size and distribution could be controlled and made to specifications when working with emulsions (Myers et al. 1999).

2.3.2 Formulations and manufacturing methods

Non-water-soluble film-forming substances such as oils, fats and waxes are applied on foods as emulsions, micro-emulsions in water or as solutions in organic solvents (Hagenmaier 1998). In addition, emulsion based edible packaging only requires one operation in its preparation, thus having the advantage of being economically favourable above other films and coatings (Debeaufort, Quezada-Gallo & Voilley 1998). Edible coatings made of wax are largely used as coatings on fruits (e.g. oranges, lemons, grapefruits, apples, pears etc.) (Debeaufort, Quezada-Gallo & Voilley 1998). These waxes include: mineral oils, paraffin, carnauba, candellilla, beeswax, polyethylene, shellac etc.

In recent years Robert D. Hagenmaier et al. has evaluated the performance of more than 600 wax micro-emulsions as food and fruit coatings (Hagenmaier, Baker 1994). This was carried out as a result of there being little information on wax micro-emulsions available in literature (Hagenmaier 1998, Bennett 1975). Hagenmaier et al. (1998) found that much trial and error is involved in arriving at suitable formulations, especially formulations where ingredients are restricted to those approved for use in foods (FDA approved) (Hagenmaier 1998). Micro-emulsions are defined as a mixture of two immiscible liquid phases with the discontinuous phase having a drop diameter of less than 0.2 μm (Hagenmaier, Baker 1994). It was evident in the course of their work that the performance of any specific wax as a coating, depended considerably on the quality of the emulsions and also the presence of minor ingredients in the formulation (Hagenmaier, Baker 1994). All the waxes and additives used in Hagenmaier et al.'s study are listed in **Table 6** (Hagenmaier 1998).

Table 6 - Waxes tested by Hagenmaier et al.

| Waxes, Resins and Additives | |
|--|------------------------------------|
| Waxes and Resins | Additives |
| Polyethylene waxes <i>E10</i> and <i>E20</i> | Oleic acid |
| Licowax PED121 | Myristic acid |
| Oxidized Polyethylene wax | Mineral oil |
| Candelilla wax | Petroleum jelly |
| Beeswax | Sorbitan monostearate (surfactant) |
| Rice bran wax | Glycerol mono/di-oleate |
| Carnauba wax | |
| Petroleum wax | |
| Paraffin wax | |
| Rosin modified maleic wood resin | |
| Hydrogenated wood rosin | |
| Montan wax | |
| Hydrocarbon waxes <i>Polywax 500</i> and <i>BeSquare 195</i> | |

Three different methods were used to manufacture the micro-emulsions, the **Non-Pressure Method** (consisting of the **Water-to-Wax Method** and the **Wax-to-Water Method**) the **Semi-Pressure Method** and the **Pressure Method** (Hagenmaier, Baker 1994, Baker, Hagenmaier 1997, Hagenmaier, Baker 1997, Hagenmaier 1998, Hagenmaier 2004, Hagenmaier, Shaw 2002). Each of the methods are discussed below:

Non-Pressure Method (Water-to-Wax Method)

For the Non-Pressure (Water-to-Wax method), the wax and other ingredients, except the water, are heated to 10 – 20°C above the melting point of the wax (Hagenmaier 1998). Hot water at a temperature of between 90 – 100°C is slowly added while stirring (Hagenmaier 1998). The mixture is then cooled to 50°C in a water bath while stirring continuously (Hagenmaier 1998). Special precautions should be taken to deal with Ammonia volatility (Hagenmaier 2004).

Non-Pressure Method (Wax-to-Water Method)

The Non-Pressure (Wax-to-Water) method is essentially the opposite of the Non-Pressure (Water-to-Wax) method (Hagenmaier 1998). The molten wax mixture, as described above, is poured into a vortex of hot water that is rapidly stirred (Hagenmaier 1998). Once the molten wax mixture is added, the mixture is cooled to 50°C in a water bath while stirring continuously (Hagenmaier 1998).

Semi-Pressure Method

The Semi-Pressure method requires that the wax, water (in a weight ratio of 1:2), fatty acid and ammonia is heated above the melting point of the wax in a pressure vessel and mixed for 20 mins (Hagenmaier 2004). The pressure vessel is then cooled to about 95°C and opened to the atmosphere (Hagenmaier 2004). Water (90 – 100°C) is then added to invert and dilute the micro-emulsion to produce a final emulsion consisting of between 60 – 80% water (Hagenmaier 2004).

Pressure Method

The previously discussed methods were used for waxes having melting points above that of Carnauba wax (85°C) (Hagenmaier 2004). The Pressure method is useful for all types of waxes, especially Carnauba wax and is similar to the Water-in-Wax method (Hagenmaier 2004). The unmelted wax, together with part of the water (also known as the initial water) is placed in a pressure vessel. The mixture is then heated to 10 – 30°C above the melting point of the wax, while continuously stirring (faster than 500 rpm) (Hagenmaier, Baker 1994, Hagenmaier, Baker 1997, Hagenmaier 1998, Hagenmaier 2004). Hot water at a temperature of 90 – 100°C is then forced into the cell by means of a pump, keeping the pressure constant inside of the vessel. The mixture is then cooled in a water bath to 50°C while still stirring. Hagenmaier et al. states that the Pressure method is preferred for ammonia-based wax emulsions (Hagenmaier 1998).

The final micro-emulsions manufactured by all three methods, contained 60 – 80% water (Hagenmaier 1998). In order to evaluate the quality of the emulsions, the appearance and performance of each emulsion was tested (Hagenmaier 1998). The appearance was primarily evaluated by measuring the turbidity with a *Ratio/XR turbidimeter* (Hagenmaier 1998). A turbidity measurement range of 0 – 2000 nephelometric turbidity units (*NTU*) was used (Hagenmaier 1998). The amount of cream that separated by gravity was also observed after storage at about 25°C for at least one week (Hagenmaier 1998).

In addition, the 'gloss' and the 'fracture' was also determined (Hagenmaier 1998). The gloss was determined by drying each emulsion on a polystyrene weigh boat (0.5 g on an area of 25 cm²) or applying the emulsions to apples or citrus (0.5 ml per fruit). The applied emulsions' gloss were then either measured with a *reflectance meter* (gloss units (*GU*)) or it was evaluated by a panel of evaluators (Hagenmaier 1998). Each emulsion's tendency to fracture was determined subjectively after hitting and rubbing together two pieces of fruit, wiping of the contacted areas with a black cloth and then rating the amount of coating found on the cloth according to the following scale: 1 =

none; 2 = minimal; 3 = significant but acceptable; 4 = heavy and unacceptable; and 5 = virtually all coating removed (Hagenmaier 1998) .

The internal gases and air flux of five coatings, which were applied to citrus fruit, were measured (Hagenmaier 1998). Air flux is the amount of air passing through the peel at an applied pressure of 0.08 *atm* (Baker, Hagenmaier 1997, Hagenmaier 1998). The five coatings that were used consisted of a 0, 5, 15, 30 and 100% of a rosin solution and the balance wax micro-emulsion (Hagenmaier 1998). Both the micro-emulsion and rosin compositions are presented in **Table 7** (Hagenmaier 1998).

Table 7 - Citrus Coating Composition (Micro-Emulsion and Rosin Solution) (Hagenmaier, 1998)

| Citrus Coating | | | |
|---------------------------------|-------|-------------------|-------|
| Micro-Emulsion for Citrus Fruit | | Rosin Solution | |
| Carnauba | 7.6% | Resinall | 16.4% |
| Polyethylene Wax E20 | 8.2% | Oleic Acid | 4.6% |
| Foral AX | 0.8% | Morpholine | 8.8% |
| Morpholine | 4.5% | Water | 70.2% |
| Water | 78.9% | | |

The coated citrus fruits were stored for 7 days at 21°C after which the internal gasses and air flux were measured on 10 fruit of each coating (Hagenmaier, Baker 1994, Baker, Hagenmaier 1997, Hagenmaier, Baker 1997, Hagenmaier 1998). Internal gas samples were withdrawn from the fruit by means of a syringe (Hagenmaier, Baker 1994, Baker, Hagenmaier 1997, Hagenmaier 1998, Hagenmaier 1998, Hagenmaier, Shaw 1991). The CO_2 concentration was measured with a *Hewlett Packard 5859* gas chromatograph fitted with a GSQ column (30 mm × 0.53 mm i.d.) while the O_2 concentration was measured with a *Model 507* analyser (Hagenmaier 1998).

According to Hagenmaier (1998), experience has shown that a necessary condition for having a good wax coating is that the wax be prepared as a micro-emulsion, so that when the water evaporates, the emulsion will have a smooth surface (Hagenmaier, Baker 1994, Hagenmaier, Baker 1997, Hagenmaier 1998, Hagenmaier 2004, Hagenmaier 2000). Thus, the wax emulsion should have a sufficiently small drop size of less than 0.2 μm , that it appears transparent to translucent and not milky white, as stated by Prince (1977) (Hagenmaier, Baker 1994, Hagenmaier, Baker 1997, Hagenmaier 1998, Hagenmaier 2004, Hagenmaier, Shaw 2002, Bai, Baldwin & Hagenmaier 2002). Hagenmaier (1998) considered that if the drop size was sufficiently small (a turbidity of less than 1500 *NTU* and a cream formation by gravity separation made up of less than 7% of the volume), it means that the wax was successfully emulsified (Hagenmaier 1998). However, these

criteria may be too strict, since some of the micro-emulsions with a turbidity of higher than 2000 *NTU* had no cream formation and may have been suitable for use as a coating (Hagenmaier 1998). These micro-emulsions were made with high-melting polyethylene (Hagenmaier 1998).

As previously mentioned, Hagenmaier et al. has tested more than 600 wax micro-emulsions formulations that are used as food- and fruit coatings (Hagenmaier, Baker 1994, Hagenmaier, Baker 1997, Hagenmaier 1998, Hagenmaier 2004, Hagenmaier 2000, Hagenmaier, Shaw 1991). Of all the formulation that were produced, only about 200 were suitable anionic wax micro-emulsions (formulations that meet the criteria mentioned above) (Hagenmaier 1998). All the formulations are made with FDA approved ingredients for the use in food and/or fruit coatings (Hagenmaier 1998). The basic formulation of all these coatings consists of water, wax, fatty acids (Oleic-, Myristic- or Palmitic acid) and a base which is either morpholine or ammonia (sometimes supplemented with Potassium Hydroxide) (Hagenmaier 1998). Formulations for these coatings are summarized in **Table 8** (Hagenmaier 1998).

Table 8 - Components of successful anionic wax micro-emulsions (Hagenmaier, 1998)

| Components of Anionic Wax Micro-Emulsions (Turbidity < 1500 NTU (g/100g wax) and less than 10% cream layer) (Hagenmaier, 1998) | | | | | | |
|--|---------------------------|---|--|---|------------|------------------------|
| Type Wax | Fatty Acids (g/100 g wax) | | Emulsification Technique | Morpholine, NH ₃ , KOH (moles/100 g wax) | pH | Lowest Turbidity (NTU) |
| | Oleic Acid | Total | | | | |
| Carnauba wax No.3 | 14 – 20 | 14 – 20 | Water-to-Wax | 0.1 – 0.2 Morpholine + <0.01 KOH | 9.1 – 9.3 | 400 |
| | 6 – 20 | 8 – 24 | Pressure Cell (initial water of 70-110g/100g wax) | 0.14 – 0.26 NH ₃ + 0.01 KOH | 9.2 – 10.6 | 325 |
| Carnauba wax No.1 | 12 – 15 | 20 (with balance oleic- or myristic acid) | Water-to-Wax | 0.14 – 0.21 NH ₃ | 9.2 – 9.6 | 423 |
| | 20 | 20 | Water-to-Wax | 0.23 Morpholine | 8.8 | 462 |
| 75% Carnauba wax No.3, 25% Rice bran wax | 25 | 25 | Water-to-Wax | 0.17 Morpholine | NV | NV |
| 50% Carnauba wax No.3, 50% Candelilla wax | 7 – 8 | 20 (with balance oleic- or myristic acid) | Water-to-Wax or Pressure Cell (initial water of 50g/ 100g wax) | 0.25 NH ₃ | 9.5 – 10.1 | 280 |
| 20-50% Carnauba wax No.3, balance Candelilla wax | 7 – 11 | 20 | Wax-to-Water or Water-to-Wax | 0.15 Morpholine | 8.7 – 9.0 | 230 |
| Candelilla wax | 8 – 15 | 8 – 20 (with balance myristic- or palmitic acid) | Water-to-Wax | 0.07 – 0.18 Morpholine | 8.6 – 9.1 | 175 |
| | 5 – 15 | 12 – 24 (with balance myristic- or palmitic acid) | Water-to-Wax or Pressure Cell (initial water of 48-100g/ 100g wax) | 0.21 – 0.26 NH ₃ | 9.2 – 10.1 | 166 |
| | 0 – 12 | 6 – 16 (with balance myristic- or palmitic acid) | Water-to-Wax | 0.08 Morpholine + 0.13 NH ₃ | 8.7 – 9.2 | 339 |
| 60 – 80% AC316, with balance Candelilla wax | 18 – 20 | 23 – 25 (with balance oleic- or myristic acid) | Pressure Cell (initial water of 50-150g/ 100g wax) | 0.3 NH ₃ + 0 – 0.14 Morpholine | 9.6 – 10.1 | 482 |
| 50 – 80% AC673, with | 14 – 25 | 19 – 25 (with balance oleic- or myristic acid) | Pressure Cell (initial water | 0.32 NH ₃ | 9.8 – | 58 |

| | | | | | | |
|--|---------|--|---|--|-----------|------|
| balance Candelilla wax | | | of 50-100g/ 100g wax) | | 10.0 | |
| 50 – 90% AC673, AC680 or E20, with balance Candelilla wax | 18 – 20 | 18 – 28 | Wax-to-Water | 0.17 – 0.23 Morpholine | 8.6 – 9.0 | 178 |
| AC629 (Polyethylene wax) or E10 (Polyethylene wax) | 0 – 20 | 12 – 20 | Wax-to-Water | 0.11 – 0.2 Morpholine | 8.7 – 8.9 | 330 |
| AC680 (Polyethylene wax) or E20 (Polyethylene wax) | 0 – 13 | 18 – 20 (with balance oleic- or myristic acid) | Pressure Cell (initial water of 50g/ 100g wax) | 0.26 NH ₃ | 9.5 – 9.9 | 233 |
| | 0 – 28 | 12 – 28 (with balance oleic- or myristic acid) | Wax-to-Water | 0.17 – 0.21 Morpholine | 8.5 – 8.8 | 204 |
| AC673 (Polyethylene wax) | 18 – 20 | 18 – 20 | Wax-to-Water or Pressure Cell (initial water of 160g/ 100g wax) | 0.22 Morpholine | 9.3 | 577 |
| 50% E20 (Polyethylene wax), 50% Petroleum wax or BeSquare | 0 – 18 | 18 | Wax-to-Water | 0.2 Morpholine | 8.9 – 9.1 | 857 |
| 88% Candelilla wax, 12% Paraffin wax | 12 | 15 (with balance oleic- or myristic acid) | Pressure Cell (initial water of 50g/ 100g wax) | 0.21 NH ₃ + 0.03 Morpholine | 9.3 | 540 |
| 50 – 67% Beeswax, with balance Candelilla wax | 0 – 11 | 22 (with balance myristic- or palmitic acid) | Water-to-Wax or Pressure Cell (initial water of 50g/ 100g wax) | 0.25 NH ₃ | 9.4 | 351 |
| 50% Beeswax, 50% Carnauba wax No.3 | 11 – 12 | 22 – 24 | Water-to-Wax | 0.18 Morpholine | 8.7 | 1250 |
| 40 – 60% Carnauba No.3, with balance W20 or AC673 (Polyethylene wax) | 18 – 31 | 18 – 31 | Water-to-Wax | 0.17 – 0.22 Morpholine | 8.5 – 8.9 | 200 |
| Montan wax | 12 – 15 | 12 – 15 | Water-to-Wax | 0.18 Morpholine | 8.8 | 480 |
| 82% AC680, 18% Paraffin wax | 13 | 17 (with balance oleic- or myristic acid) | Water-to-Wax | 0.17 Morpholine | 8.9 | 660 |

Only the successful anionic micro-emulsion formulations and their component ranges from Hagenmaier and Baker's study are presented in **Table 8** (Hagenmaier, Baker 1994, Hagenmaier 1998). Hagenmaier et al. found that the Carnauba wax formulations made with the Pressure Method had a lower turbidity and percentage cream formation than the formulations made with the Water-to-Wax or Wax-to-Water methods (Hagenmaier, Baker 1994, Hagenmaier 1998). Burns and Strauss (1965) confirmed this occurrence and it was found to be true for some of the other wax micro-emulsion formulations as well (Hagenmaier, Baker 1994, Hagenmaier 1998). For instance, in the case of emulsions containing aqueous ammonia, the best results were obtained by heating the wax, initial water, fatty acid and ammonia to 120°C, followed by adding enough hot water to have a resultant total solids of 25% (Hagenmaier 1998). Hagenmaier (1998) adds that the addition of KOH to some of the wax micro-emulsions resulted in an improved gloss in the coatings (Hagenmaier 1998). It was also found that Candelilla and Carnauba wax coatings had higher gloss when the micro-emulsions were rapidly cooled (Hagenmaier 1998).

Baker and Hagenmaier (1997) conducted a study on the reduction of fluid loss from grapefruit segments with wax micro-emulsion coatings in which polyethylene, candelilla and carnauba waxes were used to prevent weight loss (Baker, Hagenmaier 1997). It was concluded in their study that polyethylene and carnauba wax micro-emulsion coatings can provide a potential means to control fluid leakage from fresh grapefruit segments (Baker, Hagenmaier 1997). Furthermore Debeaufort et al. also states that emulsion coatings consisting of waxes and oils are really efficient barriers to water and can prevent weight loss of fruits (Debeaufort, Quezada-Gallo & Voilley 1998). However, applying a thicker layer of wax/oil emulsion coating to the fruit can alter the rate of oxygen and carbon dioxide exchange, consequently affecting the ripening process (Debeaufort, Quezada-Gallo & Voilley 1998). Guilbert et al. (1997) highlights that moisture loss is the most critical quality degradation factor of fresh produce and that moisture-barrier properties of edible films and coatings can protect fresh fruits and vegetables from dehydration (Guilbert, Cuq & Gontard 1997).

2.3.3 Characterization of Edible Wax Emulsions

2.3.3.1 Particle size and distribution

In Guitierrez's study on nano-emulsions, she states that optimization is generally directed to obtain a minimum particle size (droplet size) and/or minimum polydispersity (Gutiérrez et al. 2008). Hagenmaier (2004) concluded in his study on fruit coatings containing ammonia instead of morpholine, that although a higher gloss was obtained with more turbid experimental coatings, that it does not contradict the conventional wisdom that low turbidity (which indicates a small particle (droplet) size) is better, as confirmed by Prince (1977) (Hagenmaier 2004). Berkman and Egloff stated that the stability of an emulsion is indicated, among other factors, by the presence of small globules (Berkman, Egloff 1941). The larger the particle size, the greater is the tendency to coalescence and increase in particle size (Griffin 1945). Another phenomena that causes instability in emulsions is Ostwald ripening, whereby small solution particles dissolve and redeposit into larger solution particles (Taylor 1998, Kabalnov, Shchukin 1992). This leads to the coarsening of the dispersed phase (Meinders, Kloek & van Vliet 2001). Coalescence can be retarded by increasing the viscosity of the continuous phase or by the addition of an emulsifier or gum which provides a protective colloid action (Griffin 1945). The particle/globule size of a liquid emulsion is related to various factors, namely the method of preparation, the energy input, the viscosity difference between the phases and the type and amount of surfactant used (Griffin 1945).

In connection with small particle size formation there are two types of emulsions, namely low emulsifier formulas and high emulsifier formulas (Griffin 1945). Low emulsifier formulas require a substantial amount of mechanical energy (e.g. stirring energy), while high emulsifier formulas require only moderate mechanical effort (Griffin 1945). A very important variable which determines the particle size of an emulsion is the energy input (Griffin 1945). The general tendency is that the particle size decreases with vigorous agitation (high energy input), smaller viscosity difference between the two phases and the use of a larger amount of the proper surfactant (e.g. emulsifier) (Griffin 1945, Li et al. 2010, Pey et al. 2006, Lashmar, Richardson & Erbod 1995, Danghui, Fengyan & Tianbo 2012). In some instances, a fine particle size may be achieved by the Emulsion Inversion Point (EIP) method, as will be described in **Section 2.4.2 – The Inversion Point** (Griffin 1945, Fernandez et al. 2004, Li et al. 2010, Bouchama et al. 2003, Ee et al. 2008, Liu et al. 2006, Sajjadi 2006).

The average particle size of an emulsion may be used as a product specification, due to the stability of the emulsion being dependent on it. The particle size of emulsions is best determined by photomicroscope techniques, namely particle counting and a particle size distribution curve or profile (Griffin 1945). In Lin Ee et al.'s (2008) study on the droplet size and stability of nano-emulsions produced by the PIT method, the mean droplet size and dispersibility of the emulsions were determined by dynamic light scattering (DLS) technique (Ee et al. 2008). A *Malvern® Zetasizer Nano*, series *ZEN 3600*, with a 532 nm green laser and a scattering angle of 173°, was used (Ee et al. 2008). In addition, the stability of the nano-emulsions produced was assessed by measuring the variation of the droplet sizes as a function of the storage time at a fixed temperature (Ee et al. 2008). Akay (1997) used optical and electron microscopy to determine the particle size and distribution during his study on the flow-induced phase inversion in the intensive processing of concentrated emulsions (Akay 1998).

Daglas and Stamatoudis (2000) conducted a study on the effect of impeller vertical position on drop sizes in agitated dispersions, in which they used photo-micrographic techniques to determine the drop size distribution of the emulsions (Daglas, Stamatoudis 2000). Pictures were taken at a distance of 0.5 cm from a glass wall, at two positions *A* and *B* ($A = 4\text{ cm}$ and $B = 1\text{ cm}$ below the top of the vessel) (Daglas, Stamatoudis 2000). In addition, photographs were taken through a *Sz-Tr Olympus Zoom Stereo* microscope by a camera attached to it (Daglas, Stamatoudis 2000). Scanning electron microscopy (SEM) imaging is also a popular technique for determining the particle size of emulsions (Hautala).

Trezza and Krochta (2000) conducted dispersion particle size analysis by using a *Malvern® MS 20* particle size analyser (Trezza, Krochta 2001). A lens focal length of 45 mm and an obscuration value maintained in the range of 0.14 – 0.30, were the parameters that were chosen for the analysis (Trezza, Krochta 2001). Vargas et al. (2009) also used a laser diffractometer (Mastersize 2000, Malvern Instruments) in their study on chitosan-oleic acid composite films (Vargas et al. 2009). Fernanadex et al. (2004) measured the oil droplet size distribution by means of laser light scattering (HORIBA La-900) in his study on nano-emulsion formation by emulsion phase inversion (Fernandez et al. 2004). Due to particle sizing techniques generally being complex and time-consuming, the particle size of emulsions is often estimated by the appearance (light scattering) of the film that forms once the emulsion has dried (Griffin 1945). The relationship of the particle size to the appearance of the emulsion and film is described in **Table 9** (Griffin 1945).

Table 9 - The effect of particle size on emulsion and film appearance (Griffin, 1945)

| Emulsion and Film Appearance | |
|--|--|
| Particle Size | Appearance |
| Macro globules | The two phases may be distinguishable |
| > 1 μm | Milky-white emulsion |
| 1 – 0.1 μm | Blue-white emulsion, especially a thin layer |
| 0.1 – 0.05 μm | Grey semi-transparent, dries bright (high gloss) |
| 0.05 μm and smaller | Transparent, dries bright (high gloss) |

Li et al. determined the droplet size distribution of paraffin wax emulsions by means of laser diffraction ($\lambda = 750 \text{ nm}$) using an LS 230 Particle Size (Coulter, USA) with a measuring range of 0.04 – 2000 μm (Li et al. 2010).

In a study conducted by Trezza and Krochta (2000) on the gloss of edible coatings as affected by surfactants, lipids, relative humidity and time, the authors concluded that the gloss of edible coatings was high when the particle size of the emulsion was low (Trezza, Krochta 2000). In addition the particle size distribution also influences the gloss of the edible coatings. The more uniform distribution resulted in higher gloss values (Trezza, Krochta 2000). Trezza and Krochta (2000) also found that a small Sauter Mean Diameter (SMD) of 0.39 μm created a stable dispersion (Trezza, Krochta 2000).

The effect of wax-to-surfactant ratio on particle size

In Samuel Gusman's study on Carnauba wax emulsions, he concluded that an increase in the ratio of emulsifying agent to Carnauba wax lowers the mean particle size of the dispersed phase particles (Gusman 1947). One of the assumptions he made in order to complete his study was that the emulsion particles are composed solely of Carnauba wax (Gusman 1947). The particle sizes are represented in **Table 10**.

Table 10 - Wax-to-Surfactant Ratio vs. Mean Particle Diameter (μm) (Gusman 1947)

| Wax-to-Surfactant Ratio | Mean Particle Diameter (μm) |
|--------------------------------|--|
| 4.88 | 0.703 |
| 4.27 | 0.623 |
| 3.79 | 0.590 |
| 3.79 | 0.605 |
| 3.41 | 0.552 |
| 3.10 | 0.522 |
| 3.10 | 0.516 |
| 2.84 | 0.514 |
| 2.44 | 0.453 |
| 1.90 | 0.412 |
| 1.90 | 0.421 |

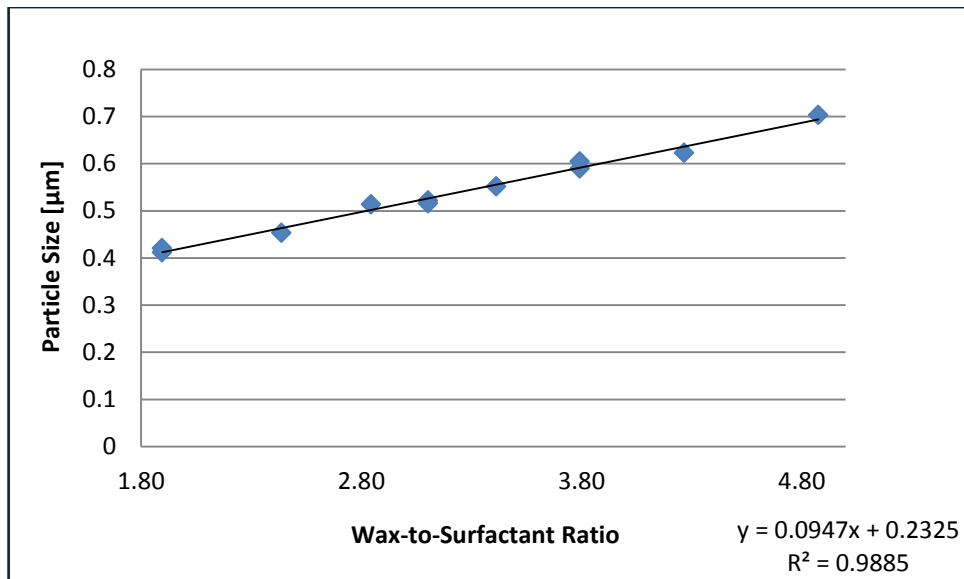


Figure 4 - The effect of Wax-to-Surfactant Ratio on the Particle Size [S. Gusman, 1947]

When examining the visual representation (**Figure 4**) of the effect of the wax-to-surfactant ratio on the particle size, it is possible to see that a linear relationship exists ($R^2 = 0.9885$). This relationship can be seen in various literature sources (Pey et al. 2006, Liu et al. , McClements 2010). Sadurni et al. found that the droplet size of oil in water nano-emulsions increases with an increase in the oil-to-surfactant ratio (**Figure 5**) (Sadurní et al. 2005). However, Sadurni et al.'s data has an exponential trend ($R^2 = 0.9999$).

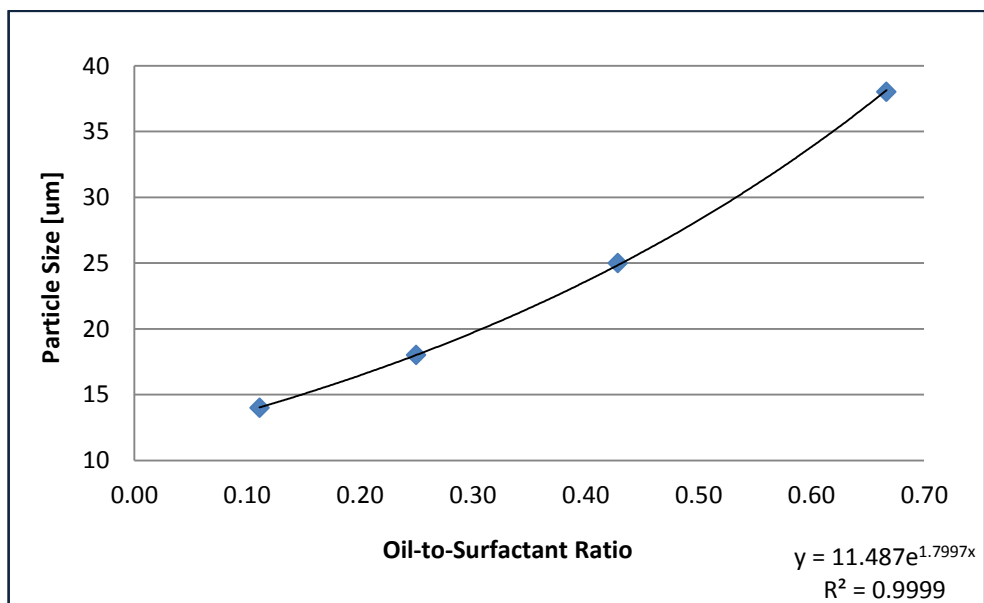


Figure 5 - The effect of the Oil-to-Surfactant Ratio on the Particle Size [N. Sudurni et al., 2005]

The effect of the Inverting phase addition rate on the particle size

Guitierrez et al. concluded that with the slow addition of water to a lamellar liquid crystalline phase small particle sized emulsions (nano-emulsions) can be obtained, while larger particle sized emulsions are obtained by rapid dilution (Gutiérrez et al. 2008). The liquid crystalline phase (gel phase), or in this case the lyotropic liquid crystalline phase, are formed by the solvent action/interaction of three components which are usually water, oil (or wax) and a surfactant (Klein 2008).

The effect of emulsification temperature on the particle size

Lashmar et al. (1995) concluded in his study on the correlation of physical parameters of an oil in water emulsion with manufacturing procedures and stability, that an increase in the homogenization time and speed produced emulsions with a smaller than average number of large droplets as did the high shear homogenizing temperature (Lashmar, Richardson & Erbod 1995). He also confirmed Becker's (1966) findings that phase inversion during the manufacturing of emulsions plays a crucial role in the uniformity of the droplets that will be obtained (Lashmar, Richardson & Erbod 1995).

The effect of high shear homogenizing speed on the particle size

Lashmar et al. concluded that the high shear homogenizing speed is one of the process parameters that had the greatest impact on the final quality of the emulsion that was investigated (Lashmar, Richardson & Erbod 1995). This suggested that the mixing efficiency of an emulsification vessel will have a significant effect on the final product quality (Lashmar, Richardson & Erbod 1995). Lashmar et al. supports Eccleston and Beattie's (1988) findings who stated that with an increase in homogenization speed, the higher shearing forces disrupt the hydrocarbon chains of the oil and wax droplets exposing the surfactant chains to the water which results in the formation of an additional gel phase (Lashmar, Richardson & Erbod 1995).

2.3.3.2 Roughness

Chen and Nussinovitch (2000) found in their study on the permeability and roughness determinations of wax-hydrocolloid coatings, and their limitations in determining citrus fruit overall quality, that the average roughness of the wax-hydrocolloid coatings were slightly (but not statistically) higher than that of the commercial citrus coatings (Chen, Nussinovitch 2001). They measured the roughness of the dried coatings with a portable surface roughness tester (Surftest-301, Mitutoyo©) (Chen, Nussinovitch 2001). Twenty roughness average (*Ra*) readings were taken for each formulation (Chen, Nussinovitch 2001). The *Ra* value is defined as the arithmetic mean deviation of the roughness profile (Chen, Nussinovitch 2001). The roughness values measured during Chen and Nussinovitch (2000) are presented in **Table 11**.

Table 11 - Roughness [*Ra*] measurements of various wax-hydrocolloid coatings (Chen et al., 2000)

| Coating | Ra |
|----------------------------------|------|
| Wax coating* with Xanthan | 0.86 |
| Wax coating* with Guar | 0.82 |
| Wax coating* with Locus Bean Gum | 0.89 |
| Wax coating* | 0.84 |
| Commercial | 0.78 |
| Control | 0.7 |

* The wax coating consisted of a wax emulsion prepared with 10% Carnauba wax, 2% Shellac, 1.8% Oleic acid and 2.4% Morpholine

In a study on specular reflection, gloss, roughness and surface heterogeneity of biopolymer coatings, Trezza and Krochta (2001) concluded that the particle size distribution of a wax emulsion determines the uniformity of the surface and thus determines both the roughness and gloss of the dried surface (Trezza, Krochta 2001). Large dispersed particles may create a heterogeneous and rough surface that influences the coating's gloss (Trezza, Krochta 2000).

2.3.3.3 Gloss

In the consumer industry appearance plays a vital role. How attractive a product looks may determine whether or not it will sell. One of the factors on which appearance is judged by is gloss (Trezza, Krochta 2001). Attributes such as gloss, influence the judgement of colour differences (Suslick 1998). According to the FDA Consumer report of February 1982, products such as apples, citrus fruits, vegetables, and confectionary products (e.g. chocolate) are coated with waxes and glazes to provide a high gloss (Trezza, Krochta 2001). In a study on the specular reflection, gloss,

roughness and surface heterogeneity of biopolymer coatings, Trezza and Krochta (2000) highlights that little data are available in literature on the gloss properties of edible coatings (Trezza, Krochta 2001). With this in mind, they stated that a greater understanding of these attributes (e.g. gloss) will allow food product formulators to optimize the gloss of the coatings and indirectly the gloss of the coated product (Trezza, Krochta 2001).

Gloss is defined as the ability or capacity of a surface to direct reflected light (Trezza, Krochta 2001). There are six types of gloss that are distinguished (Suslick 1998):

1. Specular gloss
2. Sheen
3. Contrast gloss / lustre
4. Absence-of-bloom gloss
5. Distinctness-of-image gloss
6. Surface uniformity gloss

Hence, gloss is not a single parameter, but a number of surface phenomena that comprises the light-reflecting properties of a surface (Trezza, Krochta 2001). Specular gloss is the type of gloss that gives the perception of a “shiny surface” and will be the one that will be focussed on in this thesis (Trezza, Krochta 2001). Various factors can reduce gloss, including physical effects such as rough or chemically heterogeneous surfaces (Trezza, Krochta 2001). In the case of coatings containing dispersed particles (e.g. edible wax coatings), the shape and size distributions of the particles also influence gloss (Trezza, Krochta 2001).

In a study conducted by Trezza and Krochta (2000) on the gloss of edible coatings as affected by surfactants, lipids, relative humidity and time, they concluded that the gloss of edible coatings was high when the particle size distribution of the emulsion was low (Trezza, Krochta 2000). In addition the particle size and particle size distribution also influences the gloss of the edible coatings. The more uniform distribution resulted in higher gloss values (Trezza, Krochta 2000). Trezza and Krochta (2000) also found that a small Sauter Mean Diameter (SMD) of $0.39 \mu\text{m}$ created stable dispersion (Trezza, Krochta 2000). This phenomena is known as the Ouzo effect, whereby the dispersed phase disperses into nano-size droplets within the outer phase without the use of surfactants, dispersing agents (Vitale, Katz 2003). The gloss values (*GU*) obtained during their study are presented in **Table 12**.

Table 12 - The effect of lipid content and storage time on the gloss of lipid containing edible biopolymer coatings (Trezza and Krochta, 2000)

| Coating | Number of Samples | Mean Gloss [GU] |
|-------------------------------|-------------------|-----------------|
| Shellac | 9 | 93 |
| Zein | 3 | 92 |
| Whey Protein Isolate | 13 | 91 |
| Dextrin | 4 | 84 |
| Hydroxypropyl methylcellulose | 4 | 64 |

Hagenmaier and Baker (1997) determined the gloss of 19 Morpholine-free wax emulsions (Hagenmaier, Baker 1997). These edible wax emulsions included various combinations of Candelilla wax, beeswax, Carnuba wax, Polyethylene wax and petroleum wax (Hagenmaier, Baker 1997). The gloss measurements were measured with a TRI-gloss (BYK Gardner Inc.) gloss meter (Baker, Hagenmaier 1997, Hagenmaier, Baker 1997). Ten measurements were taken for each sample at a reflectance angle of 20° (Hagenmaier, Baker 1997). Hagenmaier and Baker (1997) concluded in their study that polyethylene and Carnuba wax coatings had the best gloss, but were also the most brittle (Hagenmaier, Baker 1997). They also found that preliminary observations indicated that the turbidity was high for Ammonia-based wax micro-emulsions used in conjunction with Oleic acid as the sole source of fatty acid (Hagenmaier, Baker 1997).

In a study on the moisture barrier properties of mesquite gum-candelilla wax based edible emulsion coatings, Bosquez-Molina et al. (2003) measured their gloss with a Novo-Gloss (Rhopoint Instrumentation Ltd.) gloss meter at a reflective angle of 60° (Bosquez-Molina, Guerrero-Legarreta & Vernon-Carter 2003). Three measurements were made for each sample (Bosquez-Molina, Guerrero-Legarreta & Vernon-Carter 2003). The results obtained during their study are represented in **Table 13**.

Table 13 - Gloss of mesquite based coatings (Bosquez-Molina et al., 2003)

| Coating | Gloss [GU] |
|---------------------------------|------------|
| Mesquite-Candelilla:Mineral oil | 52.1 |
| | 51.6 |
| | 52.2 |
| | 54.3 |
| | 45.7 |
| Mesquite-Candelilla | 43.5 |
| | 41.6 |
| | 45.7 |
| | 22.1 |

| Coating | Gloss [GU] |
|--------------------------------|------------|
| Mesquite-Candelilla:Oleic acid | 31.6 |
| | 32.2 |
| | 22.3 |
| | 38.9 |
| Mesquite-Candelilla:Beeswax | 44.4 |
| | 43.3 |
| | 43.8 |

Lin and Zhao (2007) states in their research on innovations in the development and application of edible coatings, that testing the gloss with a gloss meter at 20°, 60° or 85° is in accordance (Lin, Zhao 2007)(Lin, Zhao 2007)(Lin, Zhao 2007) with the American Society for Testing and Materials method D523.11 (Lin, Zhao 2007).

2.3.3.4 Viscosity, pH and Density

Due to the limited research on edible Carnauba wax emulsions, there are little to none literature sources providing the characteristics of these coatings. Hagenmaier (1998) stated in his study on micro-emulsion formulations that the pH of Carnauba wax emulsions manufactured with the pressure cell method should be between 9.2 – 10.6 (Hagenmaier 1998).

Vargas et al. (2009) stated certain characteristics in their study on chitosan-oleic acid composite films (Vargas et al. 2009). The density of the film-forming dispersions were measured by means of a digital densitometer DA-110M (Mettler Toledo, Spain) (Vargas et al. 2009). The pH was measured with a pH-meter C831 (Consort, Belgium) that takes into account the effect of temperature (Vargas et al. 2009). Rheological properties of the film-forming dispersions were measured by means of a rotational rheometer with a type Z34DIN Ti sensor system of coaxial cylinders (HAAKE Rheostress 1, Thermo Electric Corporation) (Vargas et al. 2009). The measurements were performed at a temperature of 25°C (Vargas et al. 2009).

A few commercial edible Carnauba wax emulsions are available to the post-harvest industry. However these commercial coatings still contain Morpholine. Citrosol© has a pH of 9.9 – 10.9 and a density of 995 – 1010 kg/m^3 . An alternative product from Citrosol© containing polyethylene wax has a pH of 8.5 – 10.1 and a density of 1000 – 1014 kg/m^3 (Documentation can be viewed in **Appendix A**).

2.3.4 Carnauba wax emulsions

Robert D. Hagenmaier has contributed significantly to the literature on edible wax coatings for the post-harvest industry, as seen in previous sections. In one of his studies on fruit coatings containing Ammonia instead of Morpholine (2004), he mentions that Carnauba wax coatings are widely used for both apples and citrus fruit (Hagenmaier 2004). Of the various ammonia-based anionic micro-emulsions he studied (including Beeswax, Candelilla wax, Carnauba wax, Polyethylene wax, Shellac, Wood rosin), Carnauba wax coatings allowed for optimum exchange of gasses on pomelo fruit and was successfully tested on apples and oranges as well (Hagenmaier 2004). It was also found that coatings made from waxes such as Carnauba wax or Polyethylene wax had lower CO_2 levels and higher internal O_2 than coatings composed primarily of Shellac and Wood rosin (Hagenmaier, Shaw 2002). These conditions are favoured since internal O_2 is required for aerobic respiration, which prevents the production of ethanol, acetaldehyde and other off-flavour components (Hagenmaier, Shaw 2002). Citrus fruits coated with Carnauba wax coatings also give better protection against weight loss than Shellac or Polyethylene wax; hence Carnauba has a higher resistance to water vapour (Hagenmaier, Baker 1994).

Bai et al. states in their study on coatings for fresh fruit that Carnauba wax does not discolour over time and has been used commercially to coat apples (Bai, Baldwin & Hagenmaier 2002). In addition, Carnauba wax coatings modify the internal atmosphere in the coated fruit less than Shellac coatings or synthetic coatings (Bai, Baldwin & Hagenmaier 2002). Hagenmaier (2002) states that the most useful wax formulation accepted for fruit coatings is a anionic micro-emulsion that consists of water, wax and soap (a fatty acid anion and an appropriate (base) cation) (Hagenmaier 2004). Thus, by careful consideration of the literature available on edible wax coatings for fresh fruit and taking into account the cost and availability associated with natural waxes, Carnauba wax anionic micro-emulsions will be researched in this study.

Carnauba wax, also known as the “Queen of Wax”, is found as a thin layer on the fruit, leaves and blossoms of the Carnauba palm (*Corypha Cerifera*) (Gusman 1947). It consists of 75 – 85% aliphatic and aromatic (cinnamic acid base) mono- and di-esters, 3 – 6% free wax acids, 10 – 15% free wax alcohols, 2 – 3% lactides, 1 – 2% hydrocarbons and 4 – 6% resins (Endlein E. 2011). The Carnauba palm originates in the shoulder of Brazil in Ceara and Piauhy (Gusman 1947). Brazil’s tropical climate is suitable for the growth of the Carnauba palms, due to its semi-arid climate with heavy rainfall during the first few months of the year (Gusman 1947). During the dry seasons, the wax film that coats the exposed surfaces of the palm, prevents evaporation of water (Gusman 1947).

Carnauba wax is harvested during the dry seasons (August – December) in a crude manner (Gusman 1947, Bengsten 2011, Bengsten 2011). Most of the production is accomplished by cheap native labour (Gusman 1947, Bengsten 2011, Bengsten 2011). The production process is as follows (Gusman 1947, Bengsten 2011, Bengsten 2011):

In the **Fields**:

1. The leaves are cut from the Carnauba palm
2. The leaves are then carried from the trees to a drying place in the sun
3. The leaves are turned while drying in the sun
4. The leaves are then beaten (manually or by machine) to separate the wax from the leaves

On the **Farms**:

1. The wax powder (beaten from the leaves) is boiled with water and cooled
2. The cooled crude wax is hammered into small pieces

In the **Factories**:

1. The crude wax is purified by heating, filtering and cooling to form flakes
2. The purified Carnauba wax flakes are then exported

Although 22 409 *tons* of Carnauba wax was produced in 2006 in Brazil, the yearly yield per tree is only about 100 – 150 *grams* (Gusman 1947, Bengsten 2011, Bengsten 2011). Carnauba wax is used for various products in the cosmetics-, food product- and polish- industries (Bengsten 2011, Bengsten 2011). These products include candies/sweets, chewing gums, chocolates, fruit coatings, polishing wax, food packaging, medicine/capsules, paints, cosmetics, bullet coatings, bar codes, computer chips, just to name a few (Bengsten 2011, Bengsten 2011).

Carnauba wax has a much higher melting point (82 – 86°C) than other natural waxes and is also a very hard wax (Bengsten 2011, Bengsten 2011). One of the advantages of Carnauba wax is that once it is applied to a surface, it will not flake off with time, thus making it favourable for applications in which a flaking finish would look unsightly, for example fruit coating applications (Bengsten 2011, Bengsten 2011).

Of the three preparation methods studied by Hagenmaier (1991-2004) (the Pressure method, Semi-Pressure method and the Non-Pressure method) (**Section 2.3.2 – Formulations and**

Manufacturing Methods), the Pressure method is most appropriate for Carnauba wax micro-emulsion formulations (Hagenmaier 2004). It is also a commonly used industrial procedure used for manufacturing micro-emulsions (Hagenmaier, Baker 1994). Due to very limited literature available on edible Carnauba wax anionic micro-emulsion coatings, Hagenmaier (2004) used a trial-and-error process to establish over 150 different formulations (Hagenmaier 2004). Although full formulations are not published, basic formulations are stated in some literature sources. They are as follow:

- **Formulation 1:** 15 wt% Carnauba wax, 3 wt% fatty acid (combination of Oleic-, Myristic- and/or Lauric acid), 1.8 wt% 30% Ammonium hydroxide and 40 wt% water is heated (to about 10 – 30°C above the melting point of the wax) in a pressure vessel (1l) with agitation (200 rpm) for about 15 mins. Hot water (95 – 100°C) is gradually added in increments to attain an emulsion with a water content of 70 – 80% (Hagenmaier, Baker 1994). The emulsion is then cooled to 50°C. Thus *Formulation 1* is made according to the Pressure method.

Due to some observations suggesting that it improved the gloss of the coatings, a small amount (0.7 wt%) of Potassium hydroxide was added to all the Carnauba wax emulsions (Hagenmaier 1998).

- **Formulation 2:** *Formulation 2* is made by means of the Pressure method and the basic composition is as follow; 15 wt% wax, 3 wt% fatty acid, 0.1 wt% antifoam, 2 wt% 30% Ammonium hydroxide and 7.6 wt% water is heated in a pressure vessel (27 cm X 5 cm) to about 20°C above the melting point of the wax with agitation (500 rpm). Hot water (95 – 100°C) is gradually added at intervals of 1 min in 3 increments of 10 wt%, 10 wt% and 51 wt%. The emulsion is then cooled while stirring continuously until the temperature reaches 50°C (Hagenmaier, Baker 1997).
- **Formulation 3:** *Formulation 3* is also manufactured according to the Pressure method and although the procedure is not specified, the weight percentages are given and are as follow; 16.7 wt% Carnauba wax, 3.3 wt% Oleic acid, 2.5 wt% Morpholine and the balance (77.5 wt%) water (Hagenmaier 2005).
- **Formulation 4:** With one of the formulations stated in Hagenmaier's study on wax micro-emulsion formulations for the use as fruit coatings (1998), the Pressure method is used to produce a Carnauba wax micro-emulsion. The basic composition is given and is as follow: (6 – 20 g)/100 g wax Oleic acid, (70 – 110g)/100g wax initial water, (2.38 –

4.43 g)/100 g wax Ammonia and (0.56 g)/100 g wax Potassium hydroxide. A balance of water is added to achieve an emulsion consisting of about 20 – 30 % solids (Hagenmaier 1998). Hagenmaier mentions that good emulsions were made with the Pressure method by heating the wax mixture to 100 – 130°C before adding the balance of water (Hagenmaier 1998).

- **Formulation 5:** In Samuel Gusman's study of Carnauba wax emulsions (1946), he used a method of preparation that was essentially used commercially by the S.C. Johnson and Son Company© (a global manufacturer of household cleaning supplies and other consumer chemicals) (Gusman 1947). Carnauba wax (20 g), Triethanolamine (3.0x g), Oleic acid (2.5x g) and Sodium hydroxide (0.36x g or 2x ml of 18% by volume solution) is melted together. x is a constant depending on the ratio of wax to surfactant that is required, where the surfactant consists of Triethanolamine, Oleic acid and Sodium hydroxide. Gusman (1946) examined the weight ratios (x) 3 to 2.5 to 0.36 (Gusman 1947). The commercial wax emulsions, manufactured by the S.C. Johnson and Son Company©, were manufactured with a value of $x = 1$ (Gusman 1947).

The four components mentioned above are well mixed and kept at a temperature between 110 – 125°C for 15 mins. The melted mixture is then poured in a steady stream into 180 ml of boiling water (a temperature of 95 – 100°C) while stirring vigorously. The emulsion is cooled and cold distilled water is added to the cooled emulsion to make a final volume of 210 ml (Gusman 1947). Hence, Gusman (1946) used the Wax-to-Water (Non-Pressure) method. Values for x , with the corresponding weights of the surfactant components (Triethanolamine, Oleic acid and Sodium hydroxide), are presented in **Table 14** as published by Gusman (1947) (Gusman 1947).

Table 14 - X vs. Weights of Surfactant Components (Gusman 1947)

| Wax-to-Surfactant Ratio (x) | Carnauba Wax (g) | Triethanolamine (g) | Oleic Acid (g) | Sodium Hydroxide (g) |
|------------------------------------|-------------------------|----------------------------|-----------------------|-----------------------------|
| 0.5 | 20 | 1.5 | 1.25 | 0.18 |
| 0.6 | 20 | 1.8 | 1.5 | 0.216 |
| 0.7 | 20 | 2.1 | 1.75 | 0.252 |
| 0.8 | 20 | 2.4 | 2 | 0.288 |
| 0.9 | 20 | 2.7 | 2.25 | 0.324 |
| 1 | 20 | 3 | 2.5 | 0.36 |
| 1.1 | 20 | 3.3 | 2.75 | 0.396 |
| 1.2 | 20 | 3.6 | 3 | 0.432 |
| 1.3 | 20 | 3.9 | 3.25 | 0.468 |
| 1.4 | 20 | 4.2 | 3.5 | 0.504 |
| 1.5 | 20 | 4.5 | 3.75 | 0.54 |
| 1.8 | 20 | 5.2 | 4.5 | 0.648 |

Of the many ammonia-based Carnauba wax coating formulations that were tested, Hagenmaier (2004) stated that the best gloss was obtained when the total fatty acid content was about 14g/100g of Carnauba wax (Hagenmaier 2004). The fatty acid consisted of Lauric acid and Myristic acid in a ratio of about 2.7: 1 (Hagenmaier 2004). In addition, a formulation that produced a coating that resulted in minimum weight loss in citrus fruit, had a fatty acid content made up of Oleic-, Lauric- and Myristic acid in the ratio of 6.2: 5.7: 2.1 (Hagenmaier 2004).

2.4 Chemistry

2.4.1 Morpholine or Ammonia?

Morpholine has been used for more than 50 years as a base to ionize fatty acids, which is a required step in the manufacturing of anionic wax micro-emulsions, as stated by Eaton and Hughes (1950) and Treffler (1952) (Hagenmaier 2004). The FDA requires that if morpholine is used as a component of a protective coating for fruits and vegetables, it is required to be used as the salt(s) of one or more of the fatty acids (FDA, 21CFR.172.235) (Hagenmaier 2004). It is thus implied that the morpholine and fatty acids should be present in equimolar levels (Hagenmaier 2004). However, with the fatty acid content being much less than the current average content of morpholine in edible wax coatings, it seems possible that some reduction in morpholine usage might be on the books (Hagenmaier 2004). That said, morpholine does have an advantage with its low volatility, which makes it easy to store the micro-emulsion coatings in inexpensive containers (Hagenmaier 2004). For these reasons, Hagenmaier (2004) investigated the use of ammonia as an alternative to morpholine in fruit coatings (Hagenmaier 2004). [Further discussed in **Section 2.4.3 – The Stabilizing Process**]

2.4.2 The inversion Point

The droplet size (particle size) plays a very important role in the quality (stability and characteristics) of an emulsion. Due to micro-emulsions being ideal for edible films and coatings, it is required that a stable micro-emulsion (particle size $< 0.2 \mu\text{m}$) be formulated. Fernandez et al. (2004) states that depending on the preparation method, different particle size distributions might be achieved, explaining why the route of preparation can have an influence on the emulsion stability (Fernandez et al. 2004). Micro-emulsions with particle sizes in the submicronmeter-range can be prepared mechanically using a high energy input (Fernandez et al. 2004). The high energy input is generally achieved by high-shear stirring, high-pressure homogenizers or ultra-sound generators (Fernandez et al. 2004). High energy input leads to deforming forces that are able to break the droplets into smaller ones (Fernandez et al. 2004). Thus, the smaller the particle size, the more energy and/or surfactant is required, making this preparation route unfavourable for industrial applications when very small particles are desired (Fernandez et al. 2004). Surfactants are molecules that contain both a polar group (soluble in water) and an aliphatic tail (soluble in oil) (De Gennes, Taupin 1982). Nevertheless, micro-emulsions can also be prepared by using the physicochemical

properties of the system, also referred to as low-energy emulsification methods (Fernandez et al. 2004).

Low-energy emulsification methods make use of changing the spontaneous curvature of the surfactant (Fernandez et al. 2004). In the case of non-ionic surfactants, this can be achieved by changing the temperature of the system, forcing the transition from an oil-in-water emulsion at low temperatures to a water-in oil emulsion at high temperatures (Fernandez et al. 2004). This method is referred to as the **Phase Inversion Temperature (PIT) method** (indicated on **Figure 6**) (Fernandez et al. 2004, Lin, Kurihara & Ohta 1975). Alternatively, other parameters such as salt concentration or pH value may be considered as well, generalized by considering the surfactant affinity difference instead of the temperature alone (Fernandez et al. 2004).

Another method to obtain a transition in the spontaneous radius of curvature is by changing the water volume fraction (Fernandez et al. 2004). This is known as the **Emulsion Inversion Point (EIP) method** (Fernandez et al. 2004). Initially water droplets are formed in a continuous phase by successively adding water into oil (Fernandez et al. 2004). By increasing the volume fraction, the spontaneous curvature of the surfactant is changed from initially stabilizing a water-in-oil emulsion to an oil-in-water emulsion at the inversion locus (Fernandez et al. 2004). According to Griffin (1945), the phase volume ratio at the point of inversion was found to be equal to the square root of the ratio of the viscosities of the two components (Griffin 1945). The EIP method is well known for short-chain surfactants which form flexible monolayers at the oil-water interface, which results in a bi-continuous micro-emulsion at the inversion point (Fernandez et al. 2004). This transition, also known as catastrophic phase inversion (indicated on **Figure 6**), is where minimal interfacial tension is achieved and reported to facilitate the formation of fine droplets (Fernandez et al. 2004, Bouchama et al. 2003, Akay 1998, De Gennes, Taupin 1982, Lin, Kurihara & Ohta 1975).

The term catastrophic phase inversion was first introduced by Salager (1988) (Bouchama et al. 2003, Salager 1988). He stated that it describes the inversion in emulsions induced by changes in the emulsion water-to-oil ratio, as opposed to transitional inversion introduced by changing the surfactant affinity for the two phases of an emulsion (Salager 1988). Baciú et al. defines the phase inversion as a phenomenon where the continuous and dispersed phase spontaneously inverts with a small change in the operational conditions (Baciú, Moşescu & Nan 2008). **Figure 6** is a schematic illustration of both the Catastrophic and Transitional phase inversion for the preparation of micro-emulsions (Fernandez et al. 2004).

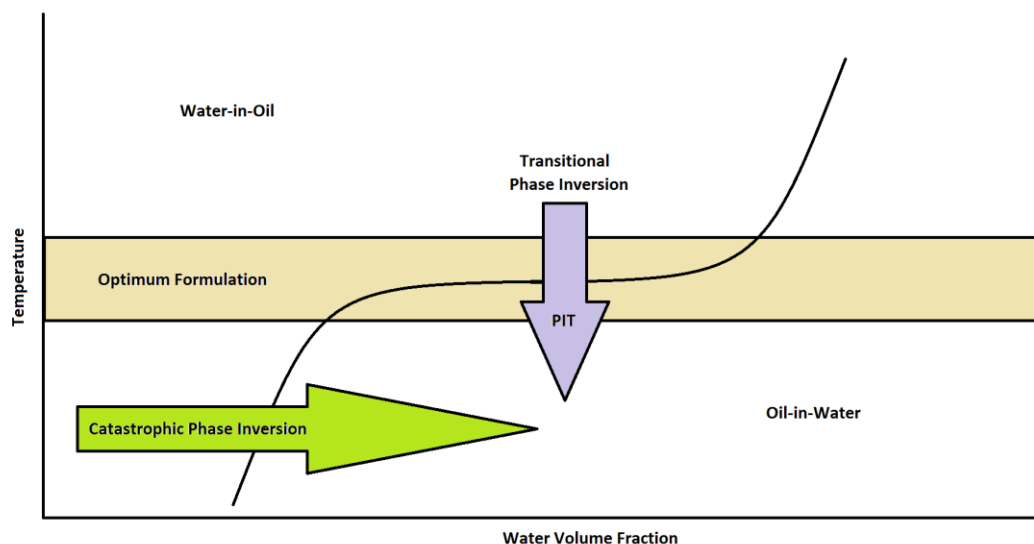


Figure 6 - Schematic illustration of both Catastrophic and Transitional phase inversion for the preparation of micro-emulsions (Redrawn from Fernandez et al., 2004)

In Fernandez et al.'s (2004) study on the nano-emulsion formation by emulsion phase inversion, it was concluded that a critical surfactant concentration is necessary for emulsification via the EIP method (Fernandez et al. 2004). Hence, the surfactant-to-oil weight ratio is of importance rather than the amount of water for spontaneous emulsification by phase inversion (Fernandez et al. 2004). That said, when emulsifying via emulsion phase inversion (EIP), finely dispersed oil droplets can be achieved, much smaller than by mechanical emulsification solely (Fernandez et al. 2004). Griffin (1945) states that a smooth and complete inversion produces the smallest particle size and that overall the particle (drop) size of an emulsion may be reduced by:

- 1.1) Increasing the amount of emulsifier/surfactant
- 1.2) Improving its hydrophilic-lipophilic balance (HLB)
- 1.3) Preparing the emulsion by phase inversion to provide an extended internal phase at the time of inversion to the final emulsion type and
- 1.4) Improve agitation

In their study on the determination of the phase inversion point, Baciú et al. states that in many applications it is practically impossible to predict the conditions for phase inversion (Baciú, Moşescu & Nan 2008). That said, at the phase inversion point in all cases, both liquids must be at intimate contact and the pressure drop peak (associated with phase inversion) can be evaluated with emulsion viscosity models (Baciú, Moşescu & Nan 2008). In addition it is also stated that near the phase inversion, the rheological characteristics of the dispersion and the associated pressure drop changes abruptly and significantly (Baciú, Moşescu & Nan 2008). Hagenmaier (1994) confirms

this finding by stating that as the continuous phase (water) is added to the wax and surfactant mixture during the Pressure method, the viscosity gradually increases, then decreases as the inversion point is passed (Hagenmaier, Baker 1994).

2.4.3 The stabilizing process

Hagenmaier et al. (1998) stated that edible wax micro-emulsion formulations made with aqueous ammonia as an ingredient are more acceptable with foods, since it is approved by the FDA (Hagenmaier 1998). The use of morpholine as an ingredient in edible coatings is limited to fruit coatings only (Hagenmaier 1998). Kielhorn and Rosner (1996) also stated that morpholine can react to form carcinogens namely N-nitrosomorpholine (Kielhorn, Rosner 1996). Because of its low boiling point (-37°C), aqueous ammonia cannot be used to make wax emulsions containing relative high melting point waxes (e.g. 85°C and higher) with the Water-to-Wax method, since it boils off too quickly (Hagenmaier 1998). This is due to the emulsification temperature required to be higher than the melting point of the wax that is used (Hagenmaier 1998). However, the Pressure method is sufficient with ammonia containing wax micro-emulsion formulations (Hagenmaier 2004). So why use Ammonia instead of morpholine?

The most useful wax formulations for fruit coatings are anionic micro-emulsions that consist of water, wax and 'soap' (anionic emulsifier) (Hagenmaier 2004). This anionic emulsifier consists of a fatty acid anion plus an appropriate base (cation) (Hagenmaier 2004). Once the micro-emulsion is applied to the fruit, the cation evaporates to form a homogenous even wax coating (Hagenmaier 2004). If the cationic moiety consists of inorganic cations like potassium or sodium, the coating would consist largely of water-dispersible soap (Hagenmaier 2004). Thus, in order for the coating to be water resistant, it is preferred that ammonia or an amine is used, which acts as a cation in aqueous solution, but evaporates as the coating dries (Hagenmaier 2004). Ammonia meets these chemical demands, thus making it a suitable and safer alternative to morpholine (Hagenmaier 2004). The wax emulsion stabilizing and coating formation process is illustrated in **Figure 7**.

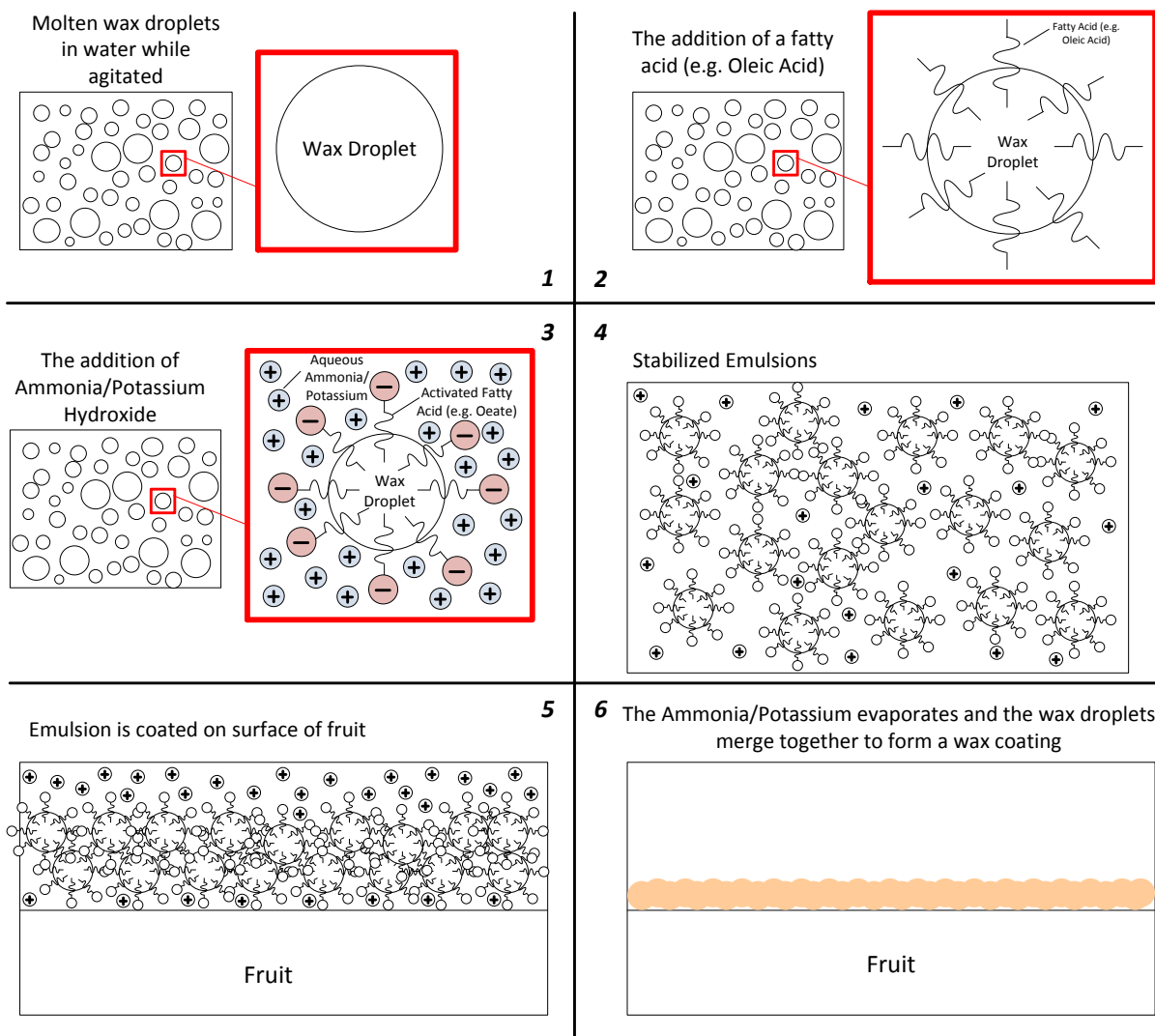


Figure 7 - The wax coating formation process (Pressure Method) – redrawn from Western Asphalt Products (2013)

Initially, the molten wax is mixed (by means of agitation) with the initial water at which point the wax emulsion is a water-in-wax emulsion. Once the additional hot water is added, the emulsion inverts from a water-in-wax emulsion to a wax-in-water emulsion. This point is also known as the phase inversion point (as described in **Section 2.4.2 – The Inversion Point**) (Fernandez et al. 2004). During the first stage presented in **Figure 7**, the molten wax and water is continuously stirred by means of an agitator and high shear homogenizer in the pressure vessel, while heating the mixture to a temperature above the melting point of the wax. Due to the wax being hydrophobic, the water and the wax is immiscible and will not form a homogenous medium. Thus when the agitation stops at this point in the process, the mixture will split into two phases. In the second stage, the fatty acid (in this thesis oleic acid will be used) is added.

During the third stage an appropriate base (in this thesis ammonium- and/or potassium hydroxide will be used) is added in order to activate/charge the fatty acid (Western Asphalt Products

2013). The ammonium- and/or potassium hydroxide activates/charges the oleic acid and forms oleates (polyelectrolytes) which has a negatively charged “head”-group and a hydrocarbon “tail”-group as represented by **Figure 8** (Western Asphalt Products 2013).

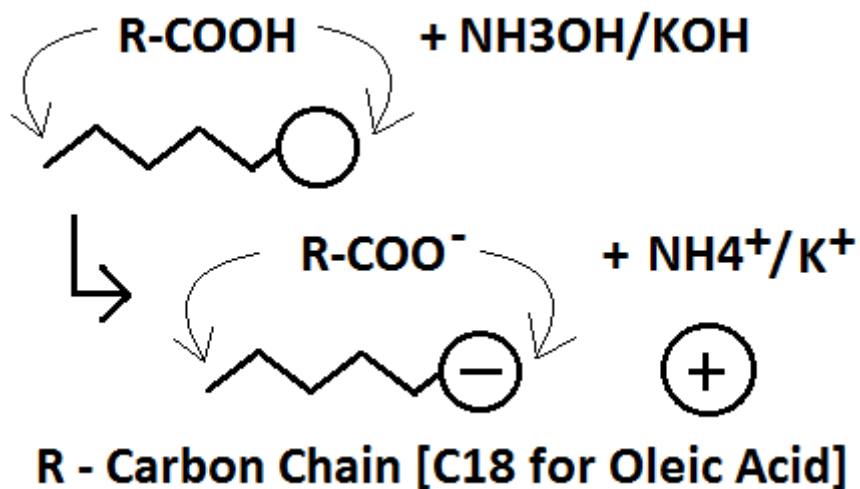


Figure 8 - Formation of an Anionic Emulsifier – redrawn from Western Asphalt Products (2013)

The hydrocarbon “tail”-group buries itself in the wax droplets while upholding charge-polarized portions in the continuous/water phase (Western Asphalt Products 2013). The charged “head”-groups produce a sphere of charge about the wax droplets, thus stabilizing the wax droplets by means of electrostatic repulsion as seen in **Figure 9** (Western Asphalt Products 2013).

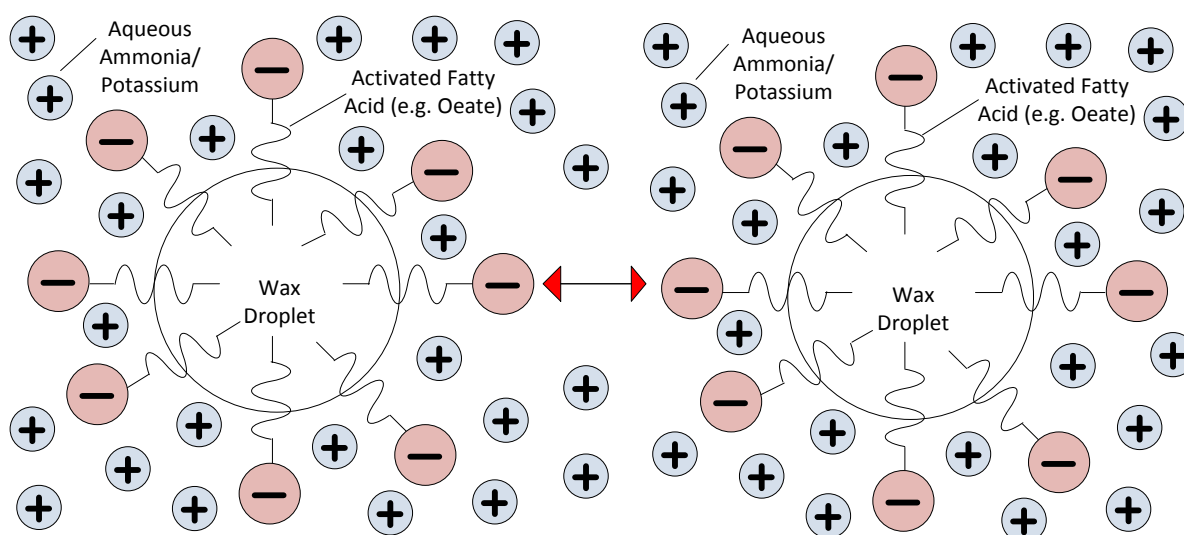


Figure 9 - Electrostatically stabilized wax droplet – redrawn from Western Asphalt Products (2013)

Once the wax micro-emulsion is applied to fruit the water and ammonia evaporates, leaving the resin of fatty acid in its original waterproof state (Olson 1943, Flint, Sharp 1942). Adjacent wax

droplets are merged together forming an evenly distributed continuous wax coating (as represented in step 5 and step 6 in **Figure 7**) (Western Asphalt Products 2013). The chemical structure for aqueous ammonium oleate is represented in **Figure 10**.

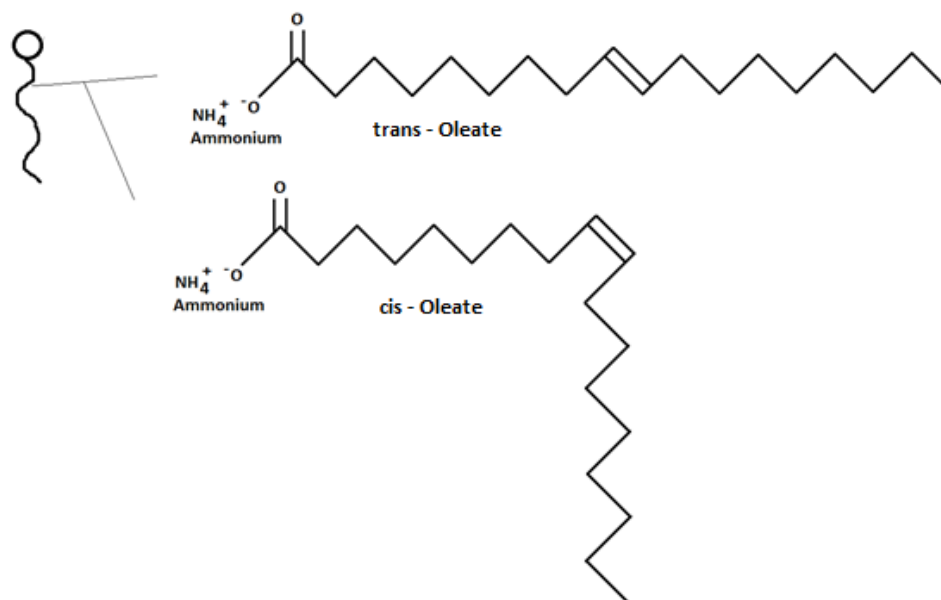


Figure 10 – The chemical structure of Ammonium Oleate

2.5 Scaling

2.5.1 Scaling of agitators

Stirred tanks represent the most popular reactors and mixers in the chemical industry, especially for the use in liquid-liquid dispersions (Podgórska, Baldyga 2001). During the literature review it was established that the droplet size and -distribution are very important when manufacturing emulsions, since it determines various characteristics (e.g. stability, gloss etc.) of the final product (Podgórska, Baldyga 2001). It is well known that the geometry and scale of the vessel and impeller, agitation rate as well as the physical properties of the mixed phases, determine the breakage- and coalescence rates and resulting drop size distribution (Podgórska, Baldyga 2001). Two methods are commonly used for the scaling up of stirred reactors from the pilot plant to commercial scale. The one uses constant energy per unit mass and the other uses dimensional analysis (Shinnar, Church 1960). With the energy input method, the main difficulty is the lack of theoretical derivation to explain its limited applicability (Shinnar, Church 1960). With the dimensional analysis method, the

difficulty is when dispersions of small drops or particles are involved and only pilot plant data are available (Shinnar, Church 1960).

When two immiscible liquids are dispersed by turbulent agitation, the breakup and coalescence of droplets occurs continuously (Shinnar, Church 1960). The breakup of droplets may be caused by either viscous shear or by turbulent pressure fluctuations (Shinnar, Church 1960). When a droplet breaks up as a result of viscous shear, the droplet is first elongated into a cylindrical thread which then breaks into a number of smaller droplets (Shinnar, Church 1960, Tolosa et al. 2006). In the case of turbulent pressure fluctuations, the droplet is exposed to local pressure fluctuation, causing the droplet to oscillate (Shinnar, Church 1960)(Tolosa et al. 2006). If the kinetic energy is sufficient to make up for the difference in the surface energy between the single drop and two smaller droplets, the oscillating drop becomes unstable and splits into two or more smaller droplets (Shinnar, Church 1960). A relationship between this kinetic energy, the droplet size and the surface tension was derived and is represented by **Equation 2** (Shinnar, Church 1960).

Equation 2

$$E_k / \sigma d^2 = \text{Constant} \sim 0.24$$

(Shinnar, Church 1960)

E_k – Kinetic energy
 σ – Surface tension
 d – Diameter of droplet

Shinnar and Church (1960) concluded that for geometrically similar systems, equal drop size can be obtained if the energy input per unit mass is kept constant (Shinnar, Church 1960).

Andrew Klein and Vern Lowry conducted a study on mixing scale-up considerations for emulsion polymerization (Klein, Lowry 1996). Emulsion polymerization starts with an emulsion incorporating water, monomer and surfactant (Arshady 1992). The most common type of emulsion polymerization is an oil-in-water emulsion, in which droplets of monomer (oil) is emulsified in water (the continuous phase) (Arshady 1992). Klein and Lowry states that one possible approach to scale-up a mixing process, is to break the process down into individual, but interrelated steps (Klein, Lowry 1996). In their study they consider the effect of mixing on the microscopic heterogeneity of the continuous phase, fluid shear rates and heat transfer separately (Klein, Lowry 1996). An energy balance approach was used to analyse the fluid motion in an agitated reactor in order to develop scaling relationships (Klein, Lowry 1996). The power input P (ft.lb./sec.) was thought to depend on linear dimensions e.g. the impeller diameter D (ft.), the tank diameter T (ft.), the liquid depth in the reactor H (ft.), the height of the impeller off the reactor bottom C (ft.), the pitch of the impeller S , the length of the impeller blades L (ft.), the width of the impeller blades W (ft.), the width of baffles J

(ft.) and fluid properties e.g. density ρ (lb. mass/cu.ft.), kinematic viscosity ν (squ.ft./sec.), the gravitational constant g (ft./sec²) and the rotational speed of the impeller N (rps) (Klein, Lowry 1996). After applying dimensional analysis to the functional relationship of the variables mentioned above, the following dimensionless groups were produced (Klein, Lowry 1996).

Reynolds Number

$$Re = D^2 N / \nu$$

Froude Number

$$Fr = DN^2 / g$$

Power Number

$$P = Pg / \rho N^3 D^5$$

The force of viscosity and the gravity is characterized by the Reynolds and Froude number, while the Power number characterizes the basic flow pattern (Klein, Lowry 1996). The conditions for geometrical similarity were derived from the dimensionless groups and it is represented by **Equation 3** (Klein, Lowry 1996).

Equation 3

$$P \cdot Fr^h = K \cdot Re^m$$

(Klein, Lowry 1996)

K – Proportionality constant

h – Distance impeller is located from bottom of reactor

In the case of baffled reactor systems, the Froude number equals 1, indicating the lack of gravitational effects, yielding the following equation (Klein, Lowry 1996):

$$P = K \cdot Re^m$$

(Klein, Lowry 1996)

$m = 0$ (Turbulent flow)

$m = -1$ (Laminar flow)

Typical values for the proportionality constant K can be seen in **Table 15** (Klein, Lowry 1996).

Table 15 - Proportionality constant (K) values (Klein and Lowry)

| Typical values for the Proportionality Constant, K (Klein and Lowry) | | |
|--|----------------|--------------|
| | Turbulent Flow | Laminar Flow |
| Propeller (3 blades) | 0.32 | 41 |
| Turbine (4 flat blades) | 4.5 | 70 |
| Paddles (4 flat blades) | 2.75 | 49 |

Klein and Lowry also investigated the minimum rotational speed of an impeller (N_{min}) required to disperse a liquid-liquid system (Klein, Lowry 1996). In order to have derived an equation useful as a scale up criteria for the rotational speed, the assumption was made that the fluid parameters are constant and that geometric similarity exist, resulting in the following equation (Klein, Lowry 1996):

$$D_i^{0.765} N_{min} = \text{Constant}$$

Equation 4

D_i – Impeller diameter

Thus, **Equation 4** can be used to scale the rotational speed of a geometrically similar reactor.

Podgorska and Baldyga (2001) conducted a study on the scale-up effects on the drop size distribution of liquid-liquid dispersions in agitations in agitates vessels, in which four methods for scaling-up agitated vessels were tested against a predicted model (Podgórska, Baldyga 2001). The four different scale-up criteria that were considered were as follow:

I) Equal power input per unit mass and geometrical similarity

$$\left(\frac{\text{Power input}}{\text{Unit mass}} = \text{Constant}, \frac{\text{Diameter}}{\text{Tank Diameter}} = \text{Constant} \right)$$

$$\tau_{c,i} / \tau_{c,1} = \left(D_i / D_1 \right)^{2/3}, i = 2,3,4$$

Equation 5

(Podgórska, Baldyga 2001)

τ_c – Circulation time (seconds)
 D – Impeller diameter (meter)

Equation 6

$$N_i / N_1 = \left(D_{a1} / D_{ai} \right)^{2/3}$$

(McCabe, Smith & Harriott 1985)

N – Impeller rotation speed (rpm)

II) Equal average circulation time and geometrical similarity

$$\left(\tau_c = \text{Constant}, \frac{\text{Impeller Diameter}}{\text{Tank Diameter}} = \text{Constant} \right)$$

$$\overline{\langle \varepsilon \rangle}_i / \overline{\langle \varepsilon \rangle}_1 = \left(D_i / D_1 \right)^2, i = 2,3,4$$

Equation 7

(Podgórska, Baldyga 2001)

$\overline{\langle \varepsilon \rangle}$ – Power input per unit mass

III) Equal power input per unit mass, equal average circulation time and no geometrical similarity

$$\left(\overline{\varepsilon}\right) = \text{Constant}, \text{Diameter}/\text{Tank Diameter} \neq \text{Constant}$$

Equation 8

$$D_i/D_1 = \left(T_i/T_1\right)^{3/2} \left(N_{Q1}/N_{Qi}\right)^{3/4}, i = 2,3,4$$

(Podgórska, Baldyga 2001)

Equation 9

$$N_i/N_1 = \left(T_1/T_i\right)^{3/2} \left(N_{Qi}/N_{Q1}\right)^{5/4}, i = 2,3,4$$

(Podgórska, Baldyga 2001)

T – Tank diameter (meter)

N_Q – Pumping number

IV) Equal impeller tip speed and geometrical similarity

$$(ND = \text{Constant}, D/T = \text{Constant})$$

Equation 10

$$\overline{\varepsilon}_i/\overline{\varepsilon}_1 = D_1/D_i, i = 2,3,4$$

(Podgórska, Baldyga 2001)

Equation 11

$$\tau_{Ci}/\tau_{C1} = D_i/D_1, i = 2,3,4$$

(Podgórska, Baldyga 2001)

Podgórska and Baldyga (2001) found that **Criterion I** results in producing larger drops in larger scale systems, which is a result of faster break-up in larger tanks due to intermittency (Podgórska, Baldyga 2001). **Criterion II** yielded much smaller drops in larger tanks as a result of the increased power input per unit mass and breakage rate (Podgórska, Baldyga 2001). **Equation 8** and **Equation 9** predict the impeller diameter larger for larger scale systems, making **Criterion III** limited to certain cases (Podgórska, Baldyga 2001). The final criterion, **Criterion IV**, resulted in a significant larger drop size when scaling up due to combined effects of increased circulation time and a decrease in the power input per unit mass (Podgórska, Baldyga 2001). Overall, it was concluded that there is no simple scaling-up method valid for both fast and slow coalescing systems (Podgórska, Baldyga 2001).

2.5.2 Scaling of high shear devices

Scale-up of high shear mixers is a particular challenging issue, since many of the variables typically observed with low speed agitators do not apply (Beaudette 2001). According to Rahmanian et al. (2008), the mechanics of particle interactions and the prevailing level of compressive stresses and shear strains are affected by the scale of operation, which in return affects the final product properties (Rahmanian et al. 2008). As for the case with scaling-up of agitators, the ultimate goal in scaling-up of high shear devices is to keep the product properties constant (Hautala , Rahmanian et al. 2008).

In their study on the scale-up of high-shear mixer granulators, Rahmanian et al. (2008) states that their literature survey showed that two scaling rules have been used most frequently i.e. constant tip speed and constant Froude number, and more recently Tardos et al. (2004) proposed a new rule based on constant shear stress (Rahmanian et al. 2008, Tardos, Khan & Mort 1997, Tardos et al. 2004). Tardos et al. (2004) considered the conditions for granular growth to coalescence and granule breakage under shear deformation and related them to a critical level of prevailing shear stress which was quantified by experimental work (Rahmanian et al. 2008, Tardos et al. 2004). During Rahmanian et al. (2008)'s study, the effects of impeller speeds at different scales of a high-shear granulator were investigated, by following the previously mentioned three scaling rules on the mechanical strength of granules (Rahmanian et al. 2008):

- Constant tip speed ($n = 1$)
- Constant shear stress ($n = 0.8$)
- Constant Froude number ($n = 0.5$)

These three scaling rules can be summarized by **Equation 12** (Rahmanian et al. 2008):

$$N_x/N_y = \left(D_y/D_x \right)^n$$

Equation 12

(Rahmanian et al. 2008)

N – Impeller rotational speed (rpm)

D – Blade diameter (m)

x, y – Different scales of high – shear mixers

n – Constant depending on the rule

It was concluded by Rahmanian et al (2008) that the constant Froude number and constant shear stress scaling rules are unsuitable for the scale-up of high-shear granulators (Rahmanian et al.

2008). Furthermore, it was concluded that the constant tip speed rule produced agglomerates of comparable mechanical strength, making this the favourable scaling rule (Rahmanian et al. 2008). That said, Beaudette (2001) states that tip speed only consider the speed of the mixer and the rotor diameter, and not the impact of viscosity, volume and specific gravity on fluid behaviour (Beaudette 2001). For this reason tip speed is a useful tool, but is not sufficient enough by itself to insure 100% scale-up success (Beaudette 2001).

2.5.3 Scaling of reactors

Hu (2004) conducted a study on the scaling-up and scaling-down of bioreactors in which he states that in scaling up different processes, it is crucial to keep the most important variable(s) constant or at least above the critical value (Hu 2004). It was assumed during his (Hu (2004)) study that the scale change will maintain geometrical similarity of reactors (Hu 2004). In other words, the effect of different reactor sizes can be compared using a characteristic length (tank inside diameter) (Hu 2004). As a result, if the tank diameter increases by tenfold, all the other length scale (tank height, impeller diameter, etc.) all increase proportionally by tenfold (Hu 2004). This type of scaling also relates to the use of a constant length-to-inside diameter as a scaling factor.

2.6 Concluding Remarks

The important application of edible films and coatings currently concerns the use of emulsions made of waxes and oils coated on fruits. It is thus proposed that a natural edible wax emulsion coating for fruits is investigated. An existing plant-scale reactor will be down-scaled to a bench scale reactor and incorporated into a pilot plant, in order to investigate a specific natural edible wax coating formulation. It is proposed that the agitator be scaled by using the scaling criterion of equal power input per unit mass and geometrical similarity, while the constant Froude number criterion is used to scale the high shear homogenizer. In order to down-scale the existing plant scale reactor and ensure geometric similarity, it is proposed that a constant length-to-inside diameter will be used as a scaling factor for all the reactor dimensions.

It was stated that the particle size of an emulsion is one of the main factors that determines the characteristics of the final emulsion product (Hagenmaier, Baker 1994, Griffin 1945, Hagenmaier 1998, Ee et al. 2008). In addition, it was also indicated that a smooth and complete phase inversion is required in order to produce the smallest particles in emulsions, which is very favourable in edible wax coatings for fresh fruit (Hagenmaier, Baker 1994, Guilbert, Gontard & Gorris 1996, Hagenmaier 1998, Hagenmaier 1998, Hagenmaier 2004, Hagenmaier 2000)(Griffin 1945). With the major factors controlling the inversion point being temperature and the addition rate of the inverting phase (Griffin 1945), it is proposed that the following process parameters are investigated:

- Temperature (Lashmar, Richardson & Erbod 1995, Lashmar, Beesley 1993, Danghui, Fengyan & Tianbo 2012, Danghui, Fengyan & Tianbo 2012, Adler-Nissen, Mason & Jacobsen 2004, Bornfriend 1978)
- High shear homogenizer speed (Griffin 1945, Lashmar, Richardson & Erbod 1995, Lashmar, Beesley 1993, Danghui, Fengyan & Tianbo 2012, Myers et al. 1999, Milanovic et al. 2011)
- Mixer speed / Homogenizer speed (Griffin 1945, Lashmar, Richardson & Erbod 1995, Lashmar, Beesley 1993, Danghui, Fengyan & Tianbo 2012, Myers et al. 1999, Milanovic et al. 2011)
- Emulsification time / High shear homogenizing time (Griffin 1945, Lashmar, Richardson & Erbod 1995, Lashmar, Beesley 1993, Danghui, Fengyan & Tianbo 2012)
- Inverting phase addition rate (Fernandez et al. 2004, Lashmar, Richardson & Erbod 1995, Lashmar, Beesley 1993)

- Final product cooling rate (Griffin 1945, Lashmar, Richardson & Erbod 1995, Lashmar, Beesley 1993)
- Wax-to-Surfactant Ratio (Gusman 1947, McClements 2010, Sadurní et al. 2005)

By determining the following measurements:

- Particle size and distribution (Griffin 1945, Danghui, Fengyan & Tianbo 2012, Trezza, Krochta 2001)
- Surface roughness (Lashmar, Richardson & Erbod 1995, Lashmar, Beesley 1993, Trezza, Krochta 2001, McClements 2010)
- Density (Vargas et al. 2009)
- Viscosity (Vargas et al. 2009)
- Gloss (Bai, Baldwin & Hagenmaier 2002, Trezza, Krochta 2001, Vargas et al. 2009)
- Acidity [pH] (Vargas et al. 2009)

To analyse the data, which will be obtained through design of experiments (DOE), it is proposed that a statistical analysis program is used in order to determine the key factors that determine the quality and stability of the newly developed natural wax coating. Design Expert© will be used to perform the statistical analysis and optimization. Due to the amount of possible factors, it is proposed that a fractional factorial is performed for screening purposes, with a high and low level for each of the factors. After the screening experimental runs are completed the data will then be interpreted and the key factor(s) identified. The runs can then be repeated with a composite design examining more levels. The process will then be optimized by means of further statistical analysis.

Chapter 3: Research Aims and Objectives

In answer to *Chapter 1* the main focus of this study is to design, build and commission a pilot plant that can be used to establish and optimize a specific natural edible wax emulsion coating. The first part of the study will focus on the designing, building and commissioning of a bench scale pilot plant, while the second part will focus more on experiments, statistical modelling and optimization. For the experimental work to commence, a basic formulation will have to be established once the bench scale pilot plant is operational.

Research Aims

Aim 1: Design, Build and Commission a Bench Scale Pilot Plant

Bench Scale Pilot Plant Design and Construction

An existing commercial size pressure vessel of 6000 l, which is currently operational, will be down-scaled to a 6 l bench scale semi-batch pressure vessel. The pressure vessel will include a high shear homogenizer and stirrer, amongst other things (similar to a typical emulsification plant presented in the literature study *Chapter 2*) (Rhe America 2014). In order to have two axels (the high shear homogenizer and stirrer) rotating at a certain speed while maintaining the pressure inside the pressure vessel, seal-housings will have to be designed and manufactured. The 6 l pressure vessel will be incorporated into a complete bench scale pilot plant.

Pilot Plant Commissioning

Once the bench scale pilot plant is complete it will be commissioned by running the process with water while ensuring that there are no leaks in the system. This will also ensure that the heating and cooling capabilities of the pressure vessel are sufficient enough. Once the bench scale pilot plant is fully operational, commissioning runs will be performed with basic formulations obtained from literature. These formulations will serve as a baseline in order to establish a natural wax edible coating formulation.

Aim 2: Experimentation, Statistical Modelling and Optimization

Pilot Plant Experiments

The primary focus of the experiments will be to obtain an optimum product with favourable properties evaluated according to literature. The initial experiments performed on the pilot plant will be used to establish a baseline formulation from basic formulations that have been published. Once a baseline formulation is established a preliminary investigation will be performed to identify the main process parameters by means of screening experiments. With the main process parameters identified, composite design experiments can be performed to optimize the process in order to yield a favourable final product.

Statistical Modelling and Optimization

Additional objectives of this study, which are entwined with the pilot plant experiments objectives, are statistical modelling and optimization. Once the screening experiments have been completed, statistical models will be fitted to the response data. The models will then be optimized in order to obtain the factors and ranges of the experimental set that will follow. Once the response data of the final experimental set is statistically analysed and models have been fitted, the final optimized natural edible wax emulsion formulation will be established.

Commercial Data Comparison

Once the optimized natural edible wax emulsion formulation has been established, the data will be compared to commercial data. Four commercial wax companies' products will be compared on equal bases to establish how the optimized final product compares.

Main Objectives

The main objectives of this study are as follow:

- 1) Design, build and commission a bench scale pilot plant (including a bench-scale reactor [6 l]), by scaling down an existing commercial plant's reactor [6000 l] that is currently manufacturing natural wax coatings.
- 2) Establish a baseline Carnauba wax emulsion formulation and manufacturing procedures for the bench scale pilot plant. In addition establish analytical procedures to characterise the Carnauba wax emulsion coatings (formulations).
- 3) Identify and manipulate the significant process- and formulation parameter(s) during the optimization of the baseline Carnauba wax emulsion formulation e.g. stirring and shearing rates, stirring configurations, temperature etc.
- 4) Set up a Design of Experiments (statistical analysis) to conduct experimental procedures, keeping in mind the limitations of raw product availability and cost.
- 5) Determine the main process- and formulation parameter(s) affecting the quality (e.g. particle size, high gloss etc.) of the Carnauba wax emulsions, in order to optimize the manufacturing process and formulation (determine the optimum setting for each significant process parameter/s).
- 6) Optimize the process- and formulation parameter(s) to yield a favourable final product by examining important characteristics identified throughout the literature review, e.g. particle size, viscosity, turbidity, gloss etc.
- 7) Compare the final optimized results with reported literature data as well as commercial data.

Chapter 4: Equipment Design and Pilot Plant Construction

This section will focus on the design of the equipment and construction of the pilot plant. The initial down-scaling of the existing 6000 l commercial pressure vessel to a 6 l bench-scale pressure vessel will be discussed. A detailed discussion about the mechanical seal housing designs and setup are presented in this section. Additional safety features that were installed on the pilot plant as well as the heating, cooling and data logging capabilities of the pilot plant will be discussed. Any problems that arose throughout the construction and initial commissioning phases will be included throughout this section.

4.1 Pilot Plant Layout and Process Flow Diagram

4.1.1 Basic Plant Layout

The basic layout of the typical commercial plant that is currently manufacturing edible wax emulsion coatings for the post-harvest industry is represented in **Figure 11**.

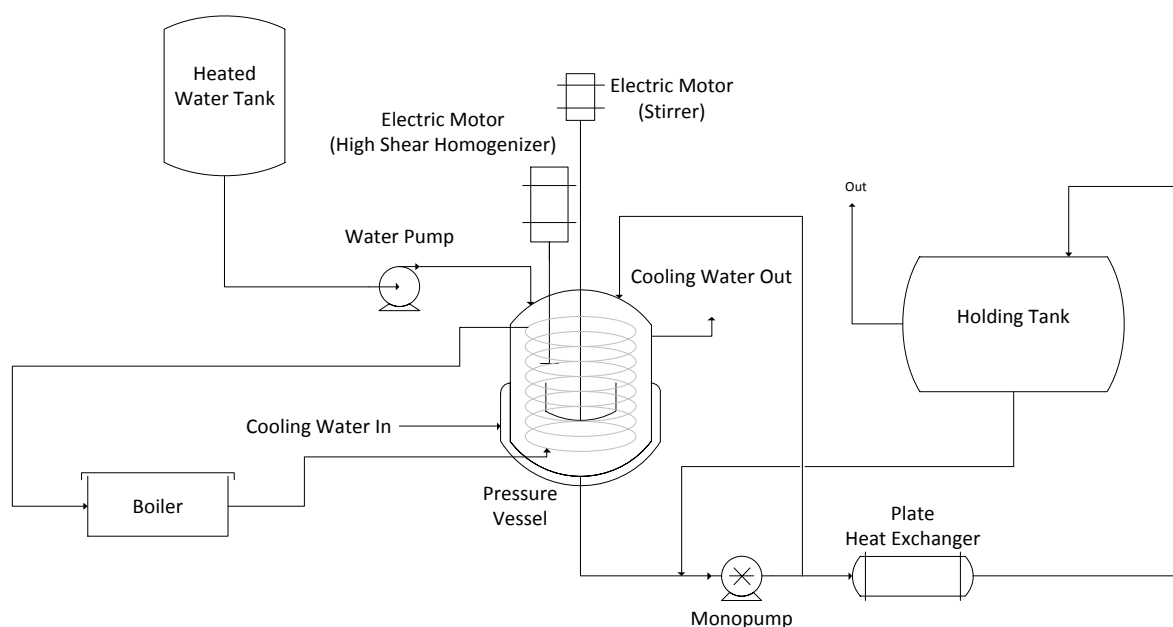


Figure 11 – Basic layout of a commercial edible wax emulsion plant

4.1.3 Scaling

The ratio between the reactor length and the inside diameter of the commercial plants' vessel was used to obtain the corresponding length and inside diameter of the pilot plant vessel. A constant length-to-inside diameter was used as scaling factor for all the pilot plant dimensions.

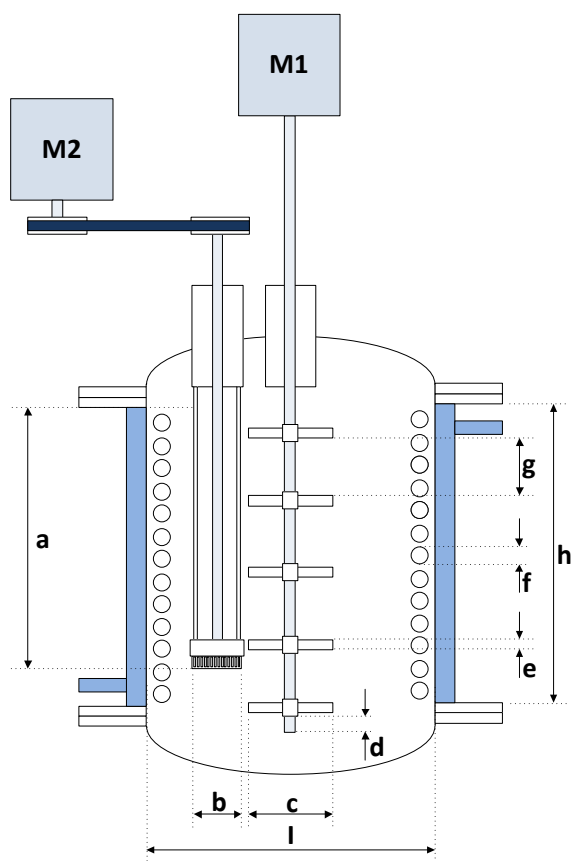


Figure 13 - Schematic diagram of the pressure vessel

The dimensions of the pilot plant vessel (as seen in **Figure 13**) were calculated by means of the scaling factor as presented in **Table 16**.

Table 16 - Pilot Plant Vessel Dimensions

| Symbols | Dimensions [mm] | Scaling Method |
|---------|-----------------|------------------------------------|
| a | 213 | Constant Length-to-Inside Diameter |
| b | 23 | Constant Length-to-Inside Diameter |
| c | 80 | Constant Length-to-Inside Diameter |
| d | 10 | Constant Length-to-Inside Diameter |
| e | 10 | Constant Length-to-Inside Diameter |
| f | 6.2 | Constant Length-to-Inside Diameter |
| g | 45 | Constant Length-to-Inside Diameter |
| h | 250 | Constant Length-to-Inside Diameter |
| i | 181 | Constant Length-to-Inside Diameter |

For example the blade length (**c**) was calculated as follow (Hu 2004):

$$\left(\frac{c}{I}\right)_{Pilot\ Plant} = \left(\frac{c}{I}\right)_{Commercial\ Plant}$$

The speed of the stirrer (**Motor M1**) and the high shear homogenizer was scaled according to the criterion of equal power input per unit mass and geometrical similarity and the constant Froude number criterion for the high shear homogenizer. The equal power input per unit mass and geometrical similarity criterion that was used to scale the speed of the stirrer were proposed by McCabe et al. (1985) (McCabe, Smith & Harriott 1985). The equation is as follow:

$$N_i/N_1 = \left(D_{a1}/D_{ai}\right)^{2/3} \quad (\text{McCabe, Smith \& Harriott 1985})$$

N – Impeller rotation speed (rpm)

D – Impeller diameter (meter)

The high shear homogenizer speed (**Motor M2**) was scaled with the following equation published by Rahmanian et al. (2008) with the constant Froude number rule [$n = 0.5$]:

$$N_x/N_y = \left(D_y/D_x\right)^n \quad (\text{Rahmanian et al. 2008})$$

N – Impeller rotational speed (rpm)

D – Blade diameter (m)

x, y – Different scales of high – shear mixers

n – Constant depending on the rule

The high shear homogenizer's pulley ratio of 2 was taken into account to scale the speed of the high shear homogenizer's impeller speed. Both the scaled stirrer- and high shear homogenizer speed was used as a starting point for the experimental runs.

4.2 Equipment

In this subsection the main process units will be discussed. The focus will be on the design and manufacturing of the units. To minimize the cost of the pilot plant, various process units from a decommissioned pilot plant facility was used in the proposed pilot plant. A list of the process units used from the decommissioned pilot plant facility is presented below:

- Two electric motors:
E.M.L© [IEC 34-1]
0.55 kW
- Two frequency inverters (Variable Speed Drives):
Yaskawa© VS mini J7
0.55 kW / 200 V single phase
- Electric motor with installed gearbox:
Gearedmotors of South Africa©
0.25 kW
- Hydraulic gear pump:
Omax© KRP4 – 14A
- Circulator (heating pump):
Haake DL-3
- Positive displacement pump:
Fluid Metering Instrumentation (F.M.I)© [RHV-1]
- Positive displacement pump controller:
F.M.I© Stroke rate controller V200

4.2.1 Pressure Vessel

The pressure vessel used in the commercial plant is a 6000 l semi-batch pressure vessel with a heating coil, cooling jacket, stirrer and high shear homogenizer. The size of the pressure vessel is critical, due to size limitations during the manufacturing of the vessel components and due to operating costs. If the dimensions of the pressure vessel are too small, the manufacturing of the small components e.g. the high shear, homogenizer would have been difficult and problematic. If the dimensions were too large the operating cost of the pilot plant would have been unnecessarily high. The down-scaled size of the pressure vessel was determined by the size of the domes that toolery was available for. The final bench scale pressure vessel size was 6 l. **Figure 14** shows a

schematic diagram (quarter section view) of the pressure vessel with the top dome, middle section and bottom dome clearly visible.

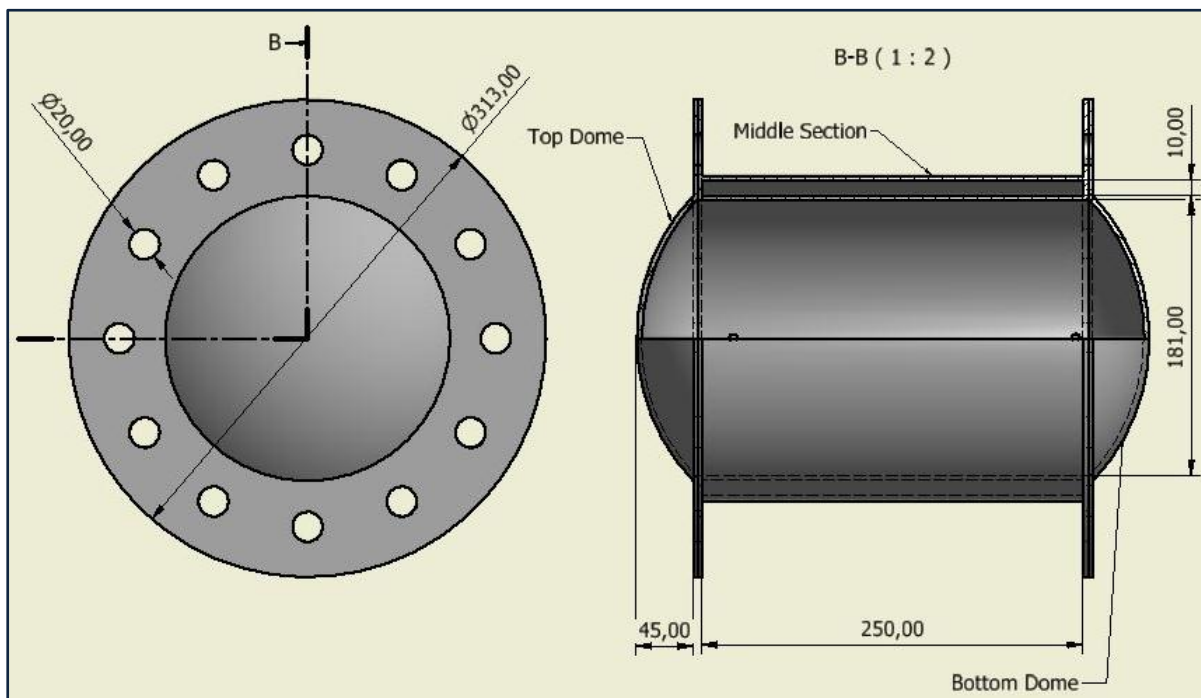


Figure 14 - Schematic diagram of the Pressure Vessel (Top dome, Middle Section and Bottom dome)

The pressure vessel was manufactured from 316 stainless steel. Four 6 mm thick stainless steel flanges were laser cut. The two domes were welded onto two of the flanges which formed the top and bottom domes. For the middle section two stainless steel pipes with a diameter of 181 mm and 207 mm respectively, were welded onto the additional two flanges to form the middle section with a cooling jacket. The heating coil (21 coils) was formed with 6 mm stainless steel tubing. Four 2 mm thick stainless steel strips were spot welded onto the coil to ensure that the coil's pitch is set at 10 mm, as seen in **Figure 15**.

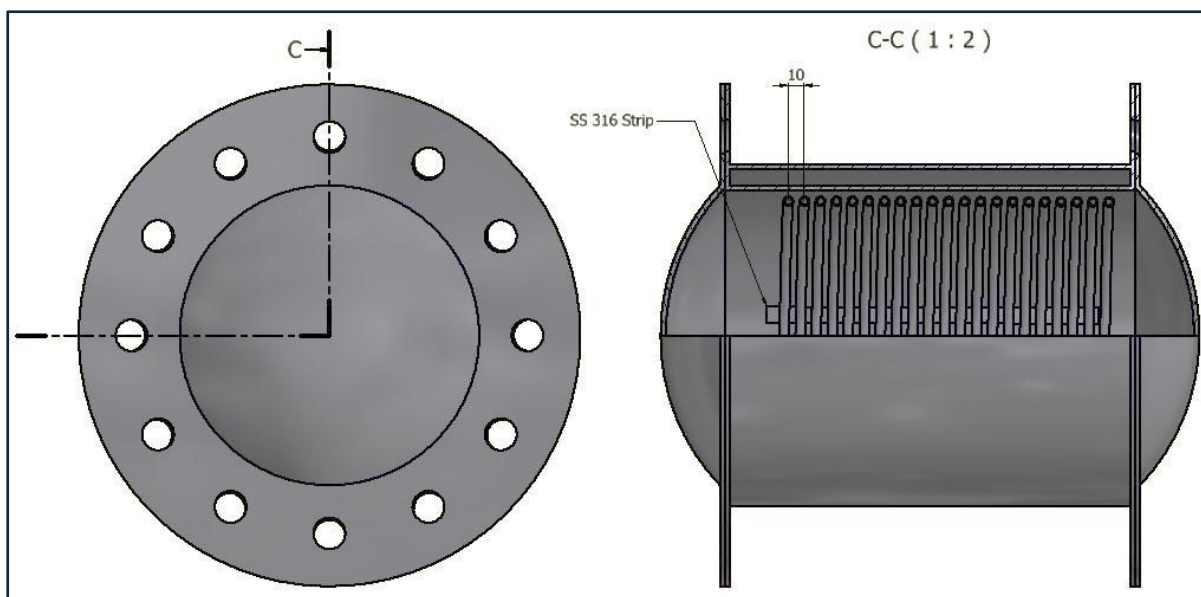


Figure 15 - Schematic of the Pressure Vessel with the heating coil

The coil was kept inside of the pressure vessel with two stainless steel compression fittings (6mm to 8mm) that penetrates the cooling jacket. The two compression fittings were also the inlet and outlet for the heating oil that flows from the bottom to the top of the coil. To ensure that the three parts of the pressure vessel could be securely assembled, 24 stainless steel bolts and nuts were used to fasten the top- and bottom dome onto the middle section. Cork packing was glued to each dome's flange to ensure that the assembled pressure vessel was airtight. A sampling valve [V-2] was placed at the bottom dome of the pressure vessel. The sampling valve was also used for cleaning purposes. An additional compression fitting was welded into the bottom dome in which a temperature probe could fit.

The top dome was customized to accommodate two mechanical seal housings (two mounts), two manholes and two quarter inch stainless steel sockets, as seen in **Figure 16**. One of the manholes housed a sight glass through which a light shined to ensure visibility inside the pressure vessel during an experimental run. The second manhole was used as an inlet to the pressure vessel as well as a sight hole. The inlet was sealed with a silicone sealed sight glass bolted with a 316 stainless steel flange [V-1]. One of the quarter inch sockets housed a pressure transducer and pressure gauge, while the other socket accommodated a stainless steel T-piece which was connected to the hot water inlet and air inlet respectively. The hot water inlet was controlled with V-3, while the airflow was controlled with V-5.

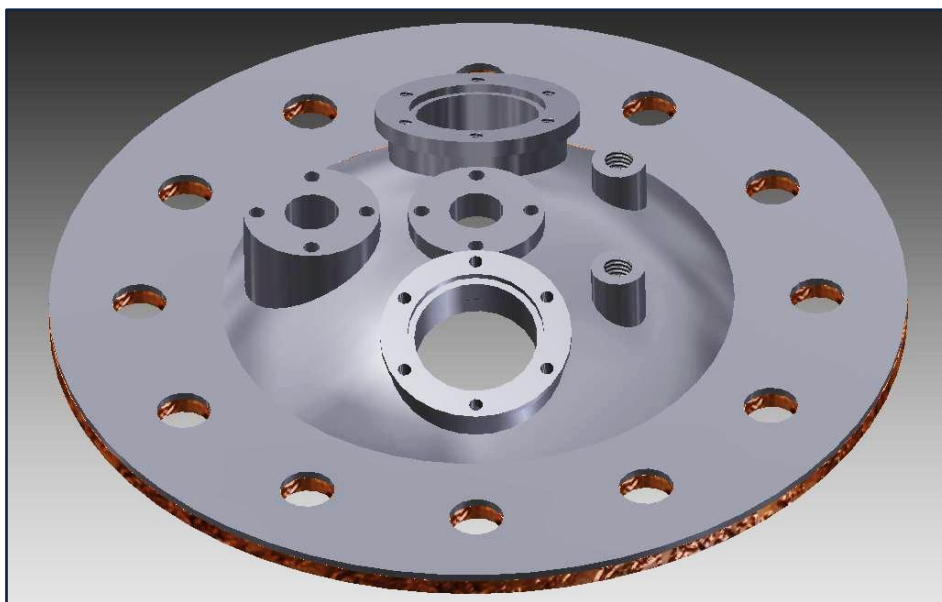


Figure 16 - Top dome

4.2.2 Mechanical Seal Housing

In order to have two axles rotate at a speed of between 5000 – 8000 *rpm* and 500 – 1800 *rpm* respectively while maintaining a certain pressure of between 1 – 3 *bar (abs)*, mechanical seals had to be used. The initial mechanical seal housing (MSH) design was based on mechanical seals used in swimming pool pumps in order to minimize the cost of the pilot plant. The initial design for both the stirrer- and high shear homogenizer's MSH are presented in **Figure 17**.

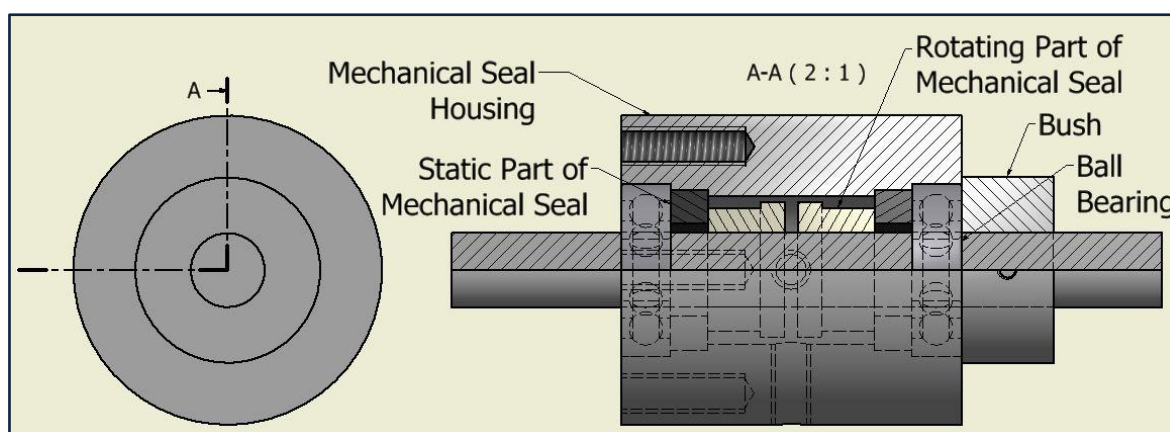


Figure 17 - Initial Mechanical Seal Housing Design

A back-to-back double mechanical seal configuration was used, as seen in **Figure 17**. The spring-loaded rotating parts were faced back-to-back and sealed onto the axle by means of an O-ring. The static parts were kept in place by means of a top rubber part and two ball bearings. An additional bush, kept in place by means of a grub screw, secured the ball bearing at the top of the

MSH. Two quarter inch threaded holes were placed in the middle of the housings in which two hose tails were screwed. Water pipes were connected to the hose tails in order to supply the mechanical seals with water (seal water), to prevent the seals from running dry. The MSHs were machined from 316 stainless steel. The mechanical seals' static part consists of ceramic, while the rotating part consists of carbon.

Once the initial MSHs were manufactured, they were installed onto the top dome. The pressure vessel was commissioned with water to check for any leaks while both the stirrer- and high shear homogenizer's motors were running at the required speed ranges. It was found that the inexpensive swimming pool pump mechanical seals were not sufficient enough. The mechanical seals leaked through the seal water pipes. In addition it was also noted that the stirrer's axle, being longer than that of the high shear homogenizer's axle, warped considerably which indicated that the axle was not stabilized correctly. As a result, the MSH had to be re-designed with suitable mechanical seals and an appropriate stabilizing setup.

Customized industrial mechanical seals [Eagle Burgmann©] which are manufactured for high axle speeds and a pressure of between 6 – 8 bar (*abs*), were imported from Germany. A similar back-to-back double seal configuration was used in the final MSH design. In the case of the imported mechanical seals, the spring-loaded static carbon parts (**Figure 18**) sealed with O-rings on the MSHs while the tungsten rotating part sealed with an O-ring and lock pin on the axle.



Figure 18 - Mechanical seal spring-loaded static carbon part [Eagle Burgmann©]

Due to the MSH mount on the top dome's dimensions being fixed, there was a size limitation for the newly designed MSHs. The base of the MSH had to be the same dimensions as that of the initial MSHs. The basic final MSH design is presented in **Figure 19**.

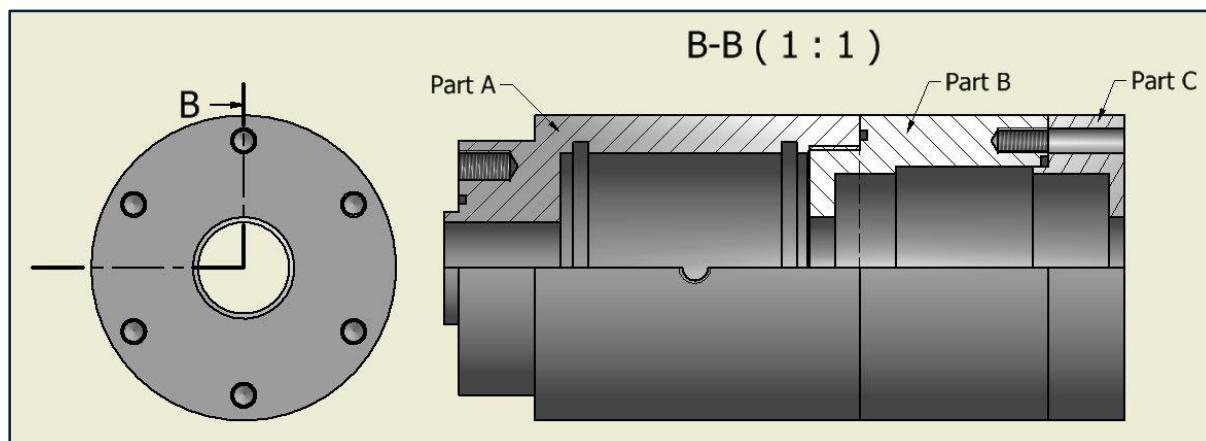


Figure 19 - Basic schematic of final Mechanical Seal Housing

The final MSH design consists of three parts namely *Part A*, *Part B* and *Part C*. *Part A* screws onto the top dome of the pressure vessel and contains the mechanical seals. *Part B* screws into *Part A* and contains the bottom ball bearings. Finally, *Part C* screws onto *Part B* and contains the top ball bearing. All three parts seal with a Viton O-ring onto the next part. The final MSH design including the mechanical seals and ball bearings are presented in **Figure 20**.

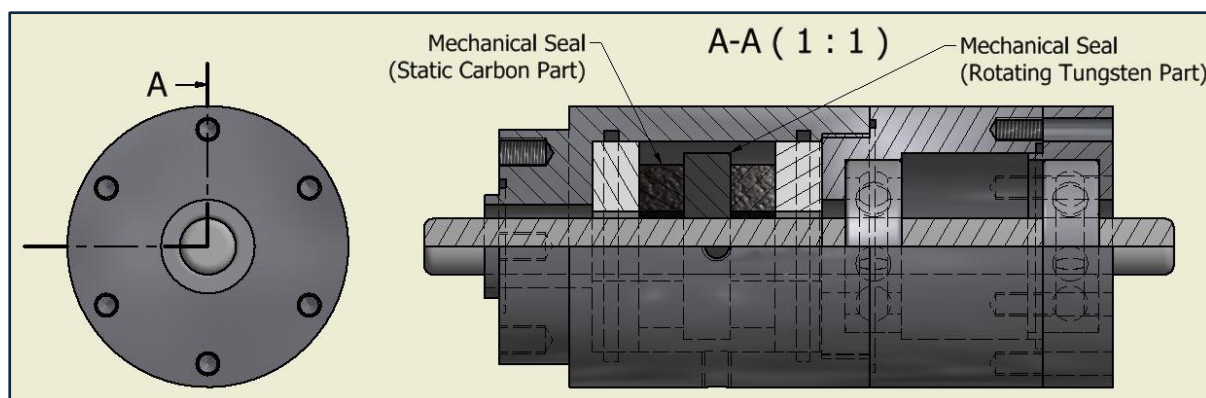


Figure 20 - Final Mechanical Seal Housing Design

From **Figure 20** it is possible to see that the ball bearings are placed above the mechanical seals and further apart (from the right of **Figure 20**). This ball bearing configuration made the stirrer axle more stable, especially at the high speed settings. Moving further left in **Figure 20** (*Part A*) the static carbon part, the rotating tungsten part and second static carbon part are visible. It is also possible to see the quarter inch threaded holes in *Part A* for the hose tails supplying seal water to

the mechanical seals that prevents them from running dry. **Figure 21** shows the top dome with the stirrer and high shear homogenizer MSHs.

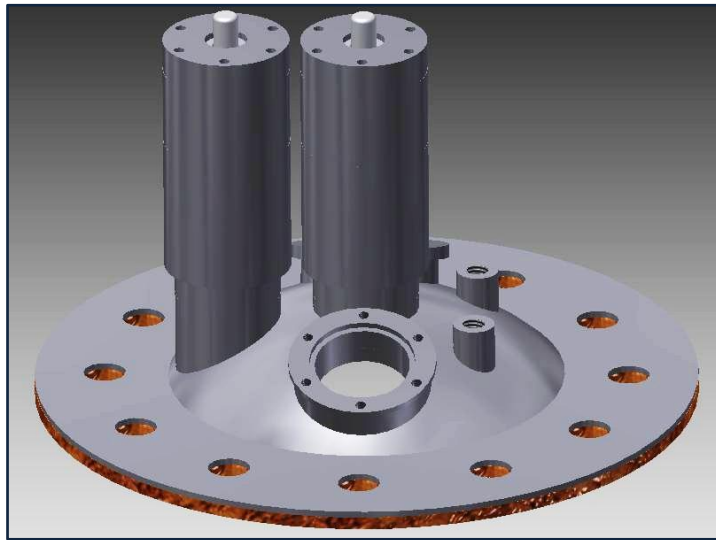


Figure 21 - Top Dome with the Mechanical Seal Housings

The redesigned MSHs were commissioned with water to ensure that there were no leaks. It was found that the newly designed mechanical seal housings worked much better than the initial design. The imported mechanical seals were sufficient enough to maintain the required pressures, even at high axle speeds. **Figure 22** presents the installed MSHs on the top dome of the pressure vessel.



Figure 22 - Mechanical seal housings installed on the top dome of the pressure vessel

4.2.3 Stirrer

Once the MSHs were installed, the stirrer's axle configuration could be manufactured and installed. The stirrer's axle is in the middle of the pressure vessel, while the high shear homogenizer's axle is to the side on the left (**Figure 21**). The dimensions of the stirrer's blades were determined by means of the scaling factor.

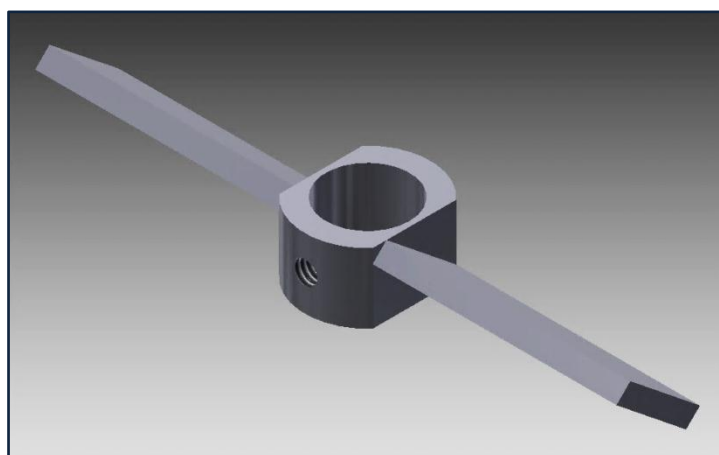


Figure 23 - Stirrer Blade Design

Figure 23 presents the blade design for the stirrer. The blades were machined from 316 stainless steel and have a total blade length of 80 mm and a blade pitch of 45°. The blades are kept secured on the 12 mm stirrer axle by means of grub screws. A five blade flat configuration was used for the stirrer axle as presented in **Figure 24**. The first blade was placed 10 mm from the bottom. Moving upwards along the axle, each blade was placed 45 mm from each other.

One of the motors [E.M.L©] [**M-101**] from the decommissioned pilot plant was used to drive the stirrer. The stirrer motor was also equipped with a variable speed controller (frequency inverter) [Yaskawa©] (also obtained from the decommissioned pilot plant) to ensure a constant stirring rate, independent of the viscosity of the emulsion. A significant change in the viscosity was expected, especially when the phase inversion point was approached, as stated by Bouchama et al. (Bouchama et al. 2003).

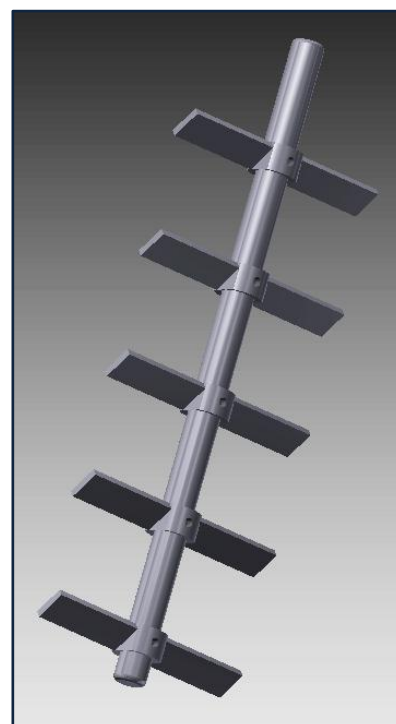


Figure 24 - Stirrer axle with blades

4.2.4 High Shear Homogenizer (Rotor and Stator)

Myers et al. (1999) states in their study on high-shear mixing that a combination of high-shear devices or a combination of a high-shear mixer and an agitator or static mixer may provide optimal performance (Myers et al. 1999). With the addition of an agitator or static mixer, it ensures that all the material will pass through the high-shear region (Myers et al. 1999). This is a clear indication that a high shear homogenizer is required. The high shear homogenizer was also one of the main obstacles during the designing and construction of the pilot plant. Due to the size of the proposed pilot plant (6 l), the size of the high shear homogenizer's dimensions (down scaled with the scaling factor) became very small which resulted in the machining of the parts being problematic. One such problematic part was the high shear homogenizer shearing plate. A basic schematic of the plate as it should have been machined is presented in **Figure 25**.

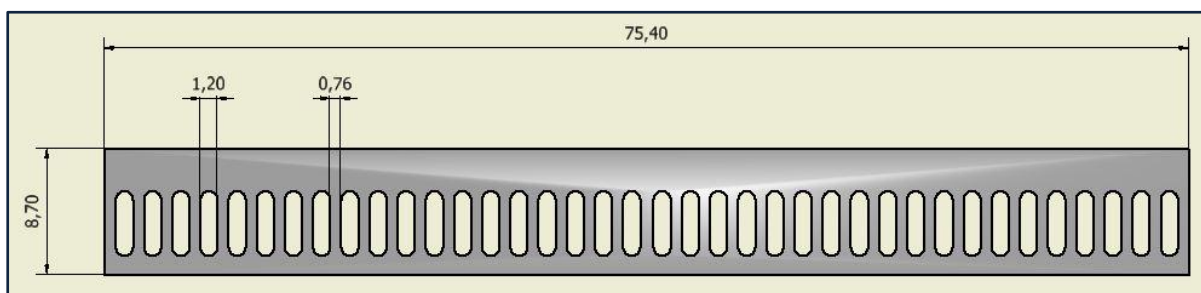


Figure 25 - High shear homogenizer shear plate

The dimensions of the high shear homogenizer shear plate were determined by means of the scaling factor. With the dimensions too small to mill or drill with the basic machining tools that were available, an alternative method had to be found. Various methods were considered of which laser cutting was chosen, due to it being the most accurate and cost effective method of cutting compared to the other methods considered (e.g. water jet cutting). Once the shear plate was laser cut from 316 stainless steel, it was carefully rolled to form the shearing section of the high shear homogenizer as seen in **Figure 26**.



Figure 26 - Shearing section of the high shear homogenizer

The shearing section was spot welded onto the bearing support to form the impeller housing. The bearing support was machined from 316 stainless steel and houses a bearing which supports the high shear homogenizer axle, as seen in the image to the left in **Figure 27**. A bearing cover, which was also machined from 316 stainless steel, was screwed onto the bearing support to keep the bearing in place. The bearing cover also contains four holes which supports four support rods. The image on the right in **Figure 27** shows the bearing cover and the support rod holes.

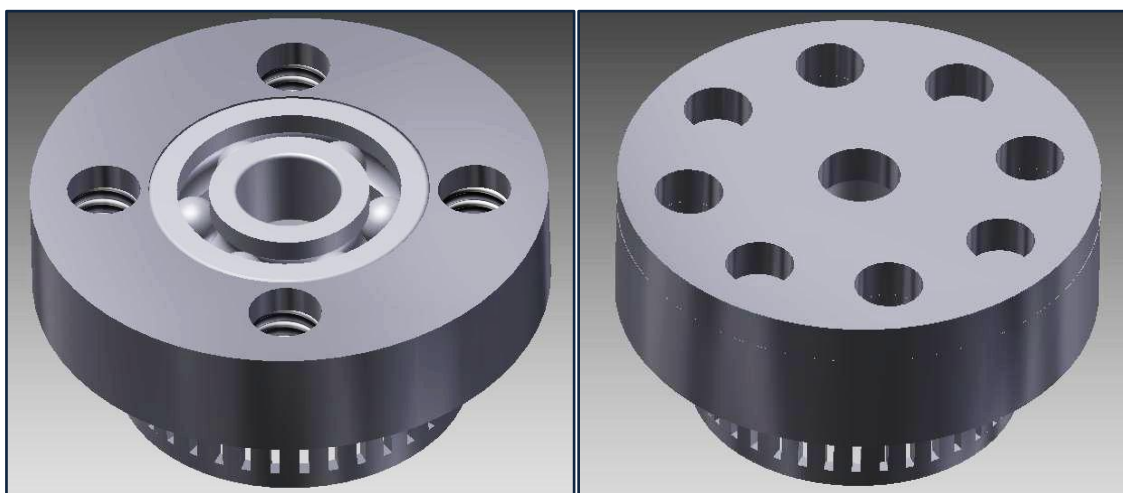


Figure 27 - High shear homogenizer's bearing support and bearing support with bearing cover (Stator)

Another part that was problematic to manufacture was the high shear homogenizer impeller. The impeller consists of four small blades with a blade pitch of 90°. The blades were manufactured from 316 stainless steel and were spot welded onto an impeller base to form the impeller, as seen in **Figure 28**.

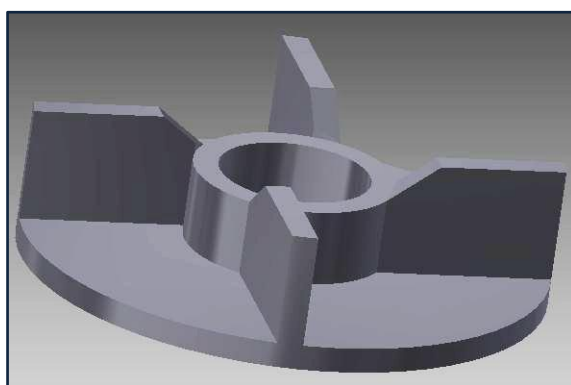


Figure 28 - High shear homogenizer impeller (Rotor)

A similar stabilizing plate was machined out from 316 stainless steel to stabilize the four stabilizing rods. The high shear homogenizer was screwed onto the top dome through the stabilizing

plate. Once all the parts were manufactured the high shear homogenizer was assembled and installed onto the top dome. The complete high shear homogenizer is presented in **Figure 29**.

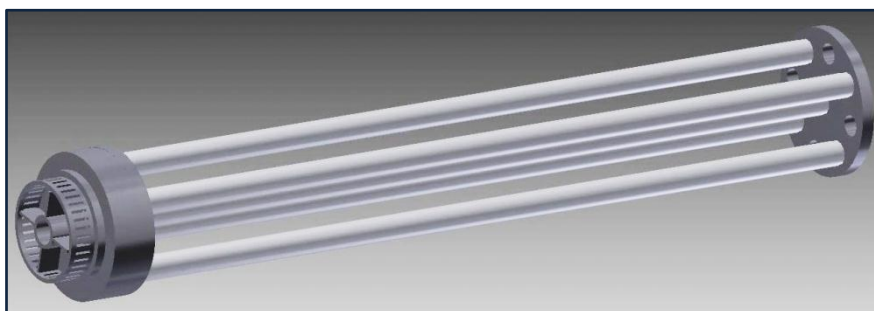


Figure 29 - High shear homogenizer

The high shear homogenizer's axle was driven by the second motor [E.M.L©] [**M-102**] obtained from the decommissioned pilot plant. The high shear homogenizer's axle and **M-102** were both equipped with a pulley. The pulley ratio of **M-102** to the high shear homogenizer's pulley was 2. Thus, the speed of the high shear homogenizer's axle was doubled in terms of the speed of **M-102**. In the case of the high shear homogenizer, the motor was also equipped with a variable speed controller (frequency inverter) [Yaskawa©] (also obtained from the decommissioned pilot plant). The variable speed controller ensured that a constant high shear rate was maintained, independent of any change in the viscosity of the emulsion (Bouchama et al. 2003). The high shear homogenizer's axle was stepped up from a diameter of 6 mm to an 12 mm axle which was the size of the motor's axle socket. **Figure 30** shows the top dome with the MSHs, high shear homogenizer and the stirrer installed.



Figure 30 - Complete top dome

4.2.5 Additional Equipment

In order to complete the pilot plant, a few additional equipment units had to be designed, manufactured and installed. A brief discussion on these units follows:

4.2.5.1 Heating Oil Bath [H-101]

A heating oil bath had to be manufactured to supply hot oil to the heating coil situated inside the pressure vessel. A basic oil bath was manufactured out of 3 mm 316 stainless steel sheets. A cover was also manufactured for safety and to prevent the oil from becoming contaminated. The circulator [HAAKE©] [E-103] obtained from the decommissioned pilot plant, was installed inside of the oil bath. E-103 circulated the oil through an element to ensure that the oil's temperature was kept at the set temperature. A hydraulic gear pump [E-101] pumped the oil from the heating oil bath through the heating coil and back to the heating oil bath. E-101 was driven by an electric motor with an installed gearbox [M-103] [Gearedmotors of South Africa©]. Both E-101 and M-103 were obtained from the decommissioned pilot plant. The heating oil had a constant flow rate, due to the gearbox, that was sufficient enough for the heating of the pressure vessel.

In case a problem occurred with the hydraulic gear pump, two valves [V-6 and V-7] were placed on either side of the pump. This makes it possible to isolate the pump, simplifying either the repairing or the replacing of the pump. Castrol© Perfecto HT-5 heat transfer oil was used as the heating oil.

4.2.5.2 Hot Water Tank

In order to supply the pressure vessel (while under pressure) with water at a temperature of between 90 – 100°C, a hot water tank had to be manufactured. A basic water tank was designed that could accommodate an electrical heating element. The heating element had a thermostat controlled by a temperature probe that was placed through a compression fitting welded into the bottom of the hot water tank. An additional two sockets were also welded into the bottom and top of the hot water tank into which a nipple was screwed followed by a valve in each [V-4 in the bottom and V-8 in the top]. Teflon tubing ran from V-4 to the positive displacement pump [F.M.I©] [E-102] obtained from the decommissioned pilot plant. E-102 pumped the hot water from the hot water tank to the pressure vessel through V-3. A stroke rate controller [F.M.I©] was connected to E-102 in order to control the flow rate of hot water into the pressure vessel.

4.2.5.3 Data Logging, Temperature Control and additional Safety features

It was crucial to have a proper data logging- and temperature control system since one of the two main factors affecting the emulsification process is temperature and pressure. In addition, safety was very important and a few precautionary modifications were made to the pilot plant to ensure that it can be operated safely. A final piping and instrumentation diagram (P&ID) is presented in **Figure 31**.

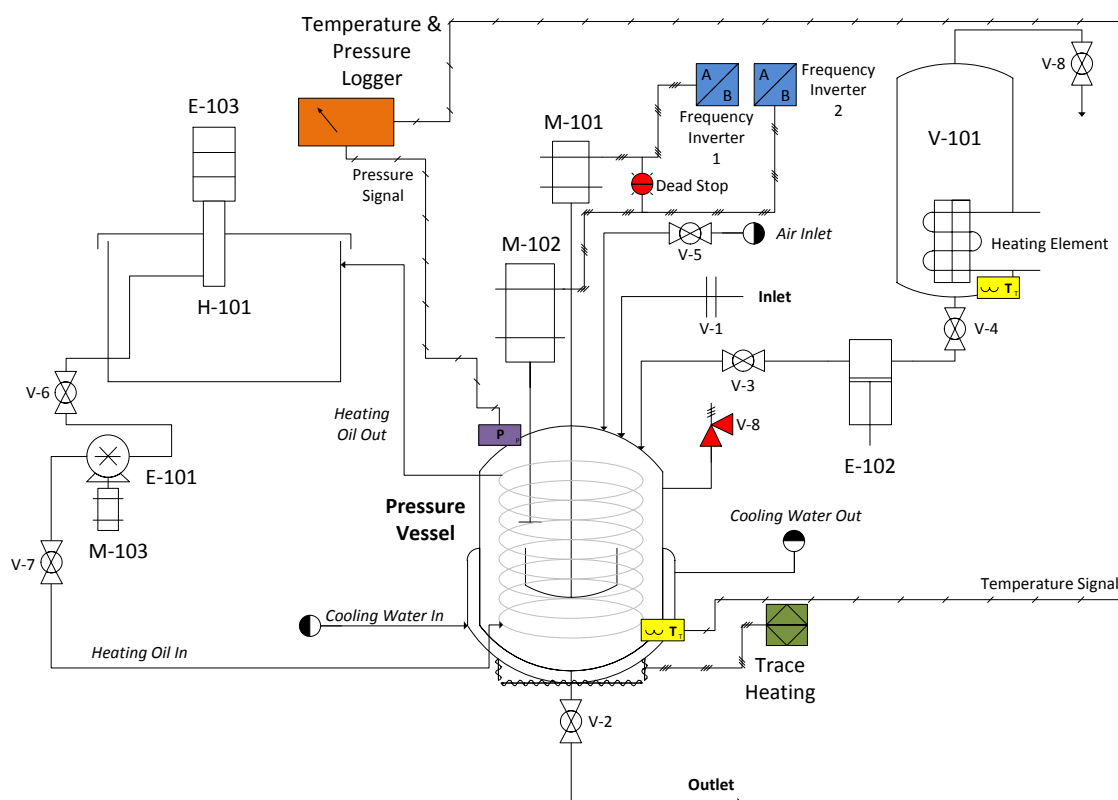


Figure 31 - P&ID including the data logging and temperature control capabilities

Reference will be made to the tags in the P&ID presented in **Figure 31**. As mentioned in **Section 4.2.1 – Pressure Vessel** a temperature probe (yellow icon at the bottom of the pressure vessel) was placed in a compression fitting welded into the bottom dome of the pressure vessel while a pressure transducer (purple icon) was placed in a socket welded into the top dome. Both the temperature probe and pressure transducer logged data to a temperature and pressure data logger (orange icon). Temperature and pressure data were obtained for each experimental run and were downloaded to an external computer for further processing.

After initial commissioning experimental runs were performed, it was found that there is heat loss through the pressure vessel walls. To minimize the heat loss through the pressure vessel walls the whole vessel was enclosed with glass wool and covered with foil backed insulation paper. It was found that the wax solidified in the bottom dome during the initial experiments. This is due to the bottom dome being in direct contact with the atmosphere (no insulation). To minimize the heat loss through the bottom dome and to assist with the heating capabilities, trace heating was installed. The trace heating consisted of a controller, a trace heating cable and a temperature probe [Pt100]. The trace heating cable and the temperature probe were installed onto the bottom dome by means of thermal foil tape. To further prevent heat loss through the bottom dome of the pressure vessel, the dome was then covered with glass wool and foil backed insulation paper. The controller [Gefran©] maintained the temperature of the trace heating cable at the set point. To prevent heat loss through the Teflon tubing supplying the hot water to the pressure vessel, tubing insulation was installed on all the tubing running from the hot water tank to the pressure vessel. This ensured that the water temperature was kept between 90 – 100°C.

The frequency inverters of **M-101** and **M-102**, *Frequency Inverter 1* and *Frequency Inverter 2* respectively (blue icons), were connected to each other with a Dead Stop. This was for safety purposes in case something went wrong inside of the pressure vessel with the stirrer or high shear homogenizer during an experimental run. If the dead stop was pressed, both **M-101** and **M-102** would completely cut out stopping both the stirrer and high shear homogenizer. In addition, the frequency inverters have a built in failsafe in case the motors experience any excessive strain. Another safety feature installed onto the pilot plant was a pressure relief valve (red icon **V-8**) connected to the top dome of the pressure vessel. The pressure relief valve opened at 4 bar (abs) preventing any possible pressure runaways. To protect the operator during an experimental run, safety covers (PlexiGlass©) were installed covering the top dome of the pressure vessel. Additionally, a stainless steel cover was manufactured to cover the fan-belt driving the high shear homogenizer's axle via its pulley. The cover prevented any possible injury due to the fan-belt jumping of the pulleys. Additional information and calibrations of the equipment can be viewed in **Appendix B**.

4.3 Control of Process Variables

In this chapter the pilot plant's design and setup were discussed in detail. Various decisions were made on the grounds of the experimental runs that had to be performed. In this sub-section the control systems of a few process variables that will be focussed on during the course of the experimental runs, will briefly be discussed. The process variables will be discussed in more detail in **Chapter 6**. The process variables are as follow:

- **Temperature:**

The temperature inside the pressure vessel was controlled by means of the heating oil that was pumped through the heating coil situated inside the vessel. The temperature of the oil was controlled by means of the circulator [HAAKE©] [E-103]. In addition, the temperature of the trace heating could be set to contribute to the heating capabilities of the pressure vessel. The heating capabilities of the pressure vessel had a temperature range of 0 – 140°C.

The temperature inside the pressure vessel was monitored and logged by means of a temperature probe (PT100) situated inside of the bottom dome of the pressure vessel [accuracy of $\pm 1^\circ\text{C}$]. The PT100 was connected to a data logger which logged the temperature during the course of the experimental runs.

- **Pressure:**

The pressure inside the vessel is dependent on the temperature of the vessel and the nature of the emulsion inside the vessel while the vessel is sealed. A pressure transducer was placed in a socket welded into the top dome of the pressure vessel [range = 0 – 10 bar, accuracy $\leq 1\%$]. The pressure transducer was connected to a data logger which logged the pressure during the course of the experimental runs. This made it possible to see the inversion point (as discussed in **Section 2.4.2 – The Inversion Point**) during the experimental runs. The pressure vessel has a pressure relief valve that prevents it from reaching a pressure above 4 bar (*abs*).

- **Stirring- and High Shear Homogenization Speed**

The speed of both the stirrer and the high shear homogenizer was controlled by means of the variable speed drives. **M-101** and **M-102** were both equipped with a variable speed controllers (frequency inverter) [Yaskawa©] to ensure a constant stirring rate, independent of the viscosity of the emulsion. A significant change in the viscosity was expected, especially when the phase inversion point was approached, as stated by Bouchama et al. (Bouchama et

al. 2003). The variable speed drives were calibrated and were set according to the required axle rotation speed (rpm).

- **Inverting Phase Addition Rate**

In the experimental runs performed during this study the inverting phase was water. The inverting phase addition rate was controlled by means of a stroke rate controller [F.M.I©] that was installed on the hot water positive displacement pump [F.M.I©] [E-102]. The stroke rate controller was calibrated according to the hot water flow rate. The stroke rate controller had a flow rate range of 0.1 – 4.2 l/h and could withstand pressures up to 6 bar (abs).

- **Cooling Rate**

The pressure vessel was cooled by means of cooling water. Due to the cooling water being tap water, the temperature of the water fluctuated according to the ambient temperature at the time of usage. In addition, the water pressure also varied over the course of the experimental runs. As a result, the cooling rate was divided up into three settings according to the valve opening of cooling water inlet. Setting –1 indicated no cooling water was used and the emulsion cooled by means of the ambient air. Setting 0 indicated that the cooling water valve was set at 1/2 Open. And finally, Setting 1 indicated that the cooling water valve was fully open during cooling.

Chapter 5: Materials and Methods

Edible wax emulsions have been studied by various authors (Baker, Hagenmaier 1997, Hagenmaier 1998, McClements 2010, Chen, Nussinovitch 2001, Bosquez-Molina, Guerrero-Legarreta & Vernon-Carter 2003, Chiumarelli, Hubinger 2012, Mannheim, Soffer 1996). All of these authors focussed on the development and characterisation of the emulsions with very little emphasis on the optimisation of the process and/or the final product. In order to optimize the process and/or the final product it is essential that the responses be measured quantitatively. This will allow statistical analysis to be performed on the data generated through the required analytical techniques.

5.1 Materials

The formulations that will be used in this study (as presented in **Section 2.3.4**) will be discussed in more detail in **Chapter 6**. A brief discussion of each component (raw materials) used in this study follows.

Carnauba Wax

Carnauba wax is a yellow to light brown vegetable wax produced by the leaves of the Brazilian palm tree, as mentioned in **Section 2.3.4**. It consists of 75 – 85% aliphatic and aromatic (cinnamic acid base) mono- and di-esters, 3 – 6% free wax acids, 10 – 15% free wax alcohols, 2 – 3% lactides, 1 – 2% hydrocarbons and 4 – 6% resins (Endlein E. 2011). Carnauba wax has a melting point of 80 – 86°C and a liquid surface tension of 0.032 N/m @100°C. The Carnauba wax flakes that were used in this study were acquired from Croda® Chemicals South Africa (Pty). The safety data sheet for Carnauba wax is presented in **Appendix C**.

Oleic Acid

Oleic acid is a fatty acid that naturally occurs in various animal and vegetable fats and oils (Hagenmaier 1998). It is an odourless light yellow coloured oil. Oleic acid has a molecular weight of 282.46 g/mol and its chemical formula is $C_{18}H_{34}O_2$. The Oleic acid used in this study was Priolene® 6940 acquired from Croda® Chemicals South Africa (Pty). The safety data sheet for Oleic acid is presented in **Appendix C**.

Potassium Hydroxide Solution

A 45% Potassium hydroxide solution was acquired from Protea Chemicals Cape (Pty). Potassium hydroxide has a chemical formula KOH and a molecular weight of 56.11 g/mol . It is classified as a category *1A* for skin corrosion and a category *4* for acute toxicity – oral. Precautions were taken when working with this substance. Potassium oleate has an HLB value of 20 which is a clear indication of it being a solubilizing agent (O/W). The safety data sheet for Potassium hydroxide solution is presented in **Appendix C**.

Ammonium Hydroxide Solution

A 25% Ammonium hydroxide solution was also acquired from Protea Chemicals Cape (Pty). Ammonium hydroxide has a chemical formula NH_4OH and a molecular weight of 35.05 g/mol . It is classified as a category *1B* for skin corrosion, category *3* for specific target organ toxicity – single exposure and category *1* for acute aquatic toxicity. Precautions were taken when working with this substance. The safety data sheet for Ammonium hydroxide solution is presented in **Appendix C**.

5.2 Experimental Procedure

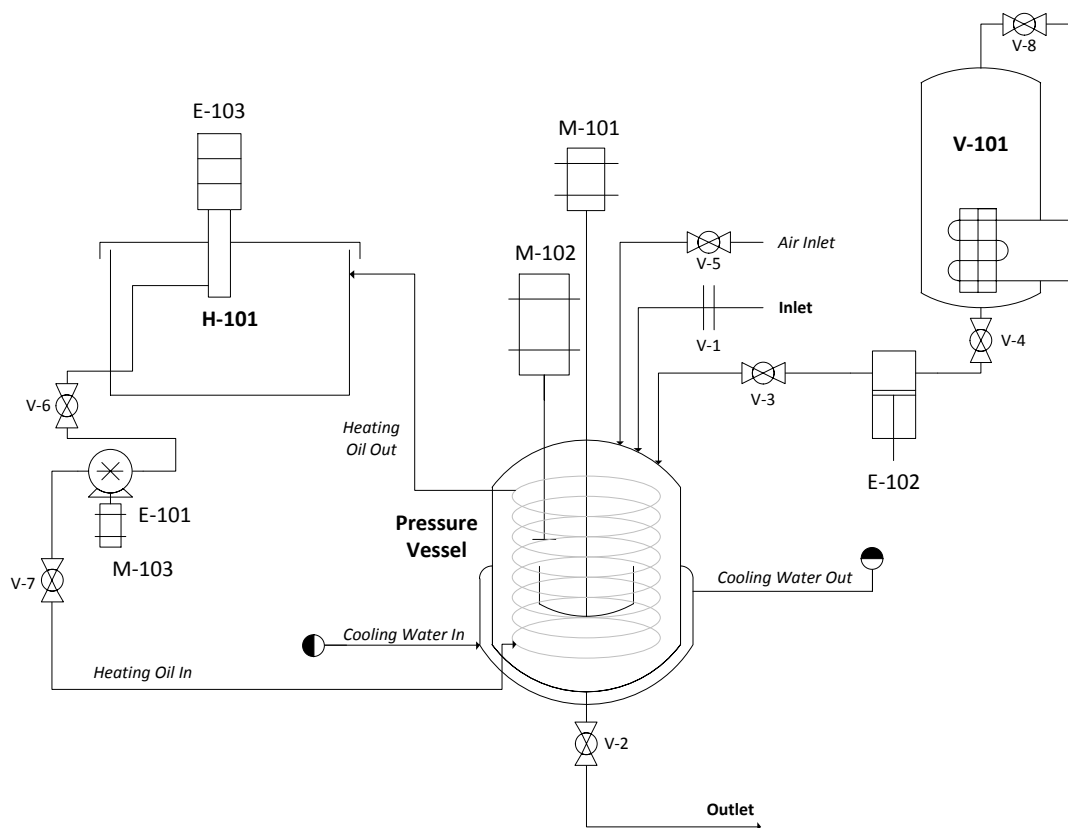


Figure 32 - Pilot Plant Setup

Figure 32 will be used as reference throughout the experimental procedure.

Stage 1: Heating-Up

1. Set the emulsification temperature on the heating recirculator **E-103** and the trace heating control panel.
2. Switch on the heating recirculator **E-103** to heat up the oil to the appropriate temperature. **NB! Ensure there that there is enough oil in the oil recirculating system**
3. Ensure that valves **V-6**, **V-7** and **V-8** are open for the heating oil to be pumped through the heating coil and steam to exit the hot water tank.
4. Ensure that valves **V-2**, **V-3** and **V-4** are closed.
5. Fill the pressure vessel with water until it covers the heating coil.
6. Switch on the mechanical seal water to prevent the mechanical seals from running dry.
7. Switch on the oil pump **E-101** to circulate the heating oil through the heating coil.
8. Switch on the additional fans for the motors **M-101** and **M-102**.

9. Set motor **M-101** at a low speed of 20 Hz/660 rpm to circulate the water inside the pressure vessel.
10. While the system is heating up, ensure that the PT100 temperature probe socket is tightened and that there are no leaks.
11. Fill the hot water tank **V-101** to about 3 cm from the top, to allow the water to expand and boil.
12. Allow the system (PT100 reading) to reach the correct temperature of 95°C.

Stage 2: Water-in-Wax

1. Once the system has reached the correct temperature, open valve **V-2** and empty the pressure vessel into a bucket.
2. Immediately close valve **V-2**.
3. Add the required *Initial Water* (boiled water weighed with a calibrated scale) through inlet **V-1**.
4. Once the *Initial Water* has been added, immediately start adding the *Carnauba wax* in small amounts, allowing the *Carnauba wax* to melt before adding the next increment. Ensure the correct amount of *Carnauba wax* is weighed (with a calibrated scale) beforehand.
5. As soon as the last *Carnauba wax* has been added add the correct amount (weighed with a calibrated scale) of *Potassium hydroxide* and close inlet **V-1**.

At this point the pressure vessel should be completely sealed

Stage 3: Inversion Point – Wax-in-Water

1. Ensure that the hot water tank's (**V-101**) thermostat is set to 95 – 100°C.
2. Start motor **M-102** and set its frequency at the required speed. Adjust the frequency of motor **M-101** to the required speed.
3. Place the **V-4** connector in the measured (with a calibrated scale) amount of *Ammonium hydroxide*. Ensure that there is no left over water in the tube.
4. Open valve **V-3** and inject the *Ammonium hydroxide*.
5. Immediately connect the **V-4** connector to the hot water valve **V-4** and open valve **V-4**.
6. Allow the correct amount of boiling water (95 – 100°C) for the first *Hot water injection*.
7. Close valve **V-3**.

8. Allow the required time to homogenize (*High Shear Time Interval*).
9. Once the *High Shear Time Interval* has passed, inject the next *Hot water injection*, ensuring that the cold water remaining in the tube is discarded beforehand.
10. Repeat steps **8** and **9** until all the *Hot water injections* have been injected.

Stage 4: Cooling-Down

1. Once the final *Hot water injection* has been injected and the *High Shear Time Interval* has passed, switch off the trace heating and stop the circulation of hot oil through the heating coil (switch off oil pump **E-101** and heating recirculator **E-103**).
2. Open the cooling water valve (at the required setting) to allow the pressure vessel to cool down.
3. ***NB! Do not open any valves or unscrew any sockets until the vessel has reached atmospheric pressure***
4. Once the pressure vessel has reached atmospheric pressure, disconnect the **V-3** connector and open valve **V-3**, allowing the pressure vessel to remain at atmospheric pressure and not end in a below atmospheric pressure state (vacuum).
5. Allow the emulsion to cool to below 30°C.
6. Switch off motor **M-102** and decrease the speed of motor **M-101** to 20 Hz.

Stage 5: Sampling

1. Once the emulsion has cooled down to below 30°C, close valve **V-3**.
2. Open valve **V-2** and ensure that the sampling jar is placed below the opening of valve **V-2**.
3. Slowly open the air inlet valve **V-5**, forcing the emulsion out of the pressure vessel into the sampling jar.
4. Close valve **V-5** once sampling is completed.
5. Switch off motor **M-101**.
6. Once the appropriate number of samples has been drawn, allow the rest of the excess emulsion to exit the pressure vessel into a bucket.
7. Close the cooling water valve.
8. Open the inlet **V-1** and rinse the pressure vessel's inside, taking into account that hot water will have to be used to rinse out all of the excess wax emulsion.

5.3 Analytical Techniques

5.3.1 Particle Size Analysis

The droplet size distributions of the Carnauba wax emulsions were determined by means of laser diffraction using a Saturn DigiSizer 5200 Particle Sizer (Micrometrics, UK) with a measuring range of 0.1 – 1000 μm . Data from the laser diffraction and polarization intensity differential scattering (PIDS) were combined to calculate the particle size distribution with the Micrometrics© Saturn DigiSizer 5200 V1.10 software. Samples were diluted and measured in distilled water.

Laser diffraction was chosen as method for analysis due to it being a widely used particle sizing technique for materials ranging from hundreds of nanometres up to several millimetres in size (Saturn DigiSizer 5200 2000). One of the main reasons for the success of laser diffraction is the large number of particles it is able to sample in each measurement (Saturn DigiSizer 5200 2000). This ensures that analysis' repeatability is significant and more accurate than counting-based techniques such as image analysis. Laser diffraction reports the volume of material of a given size, since the light energy reported by the detector system is proportional to the volume of material present (Saturn DigiSizer 5200 2000). Small particle scatter light at a large angles relative to the laser beam while large particles scatter light at small angles, as illustrated in **Figure 33** (Saturn DigiSizer 5200 2000).

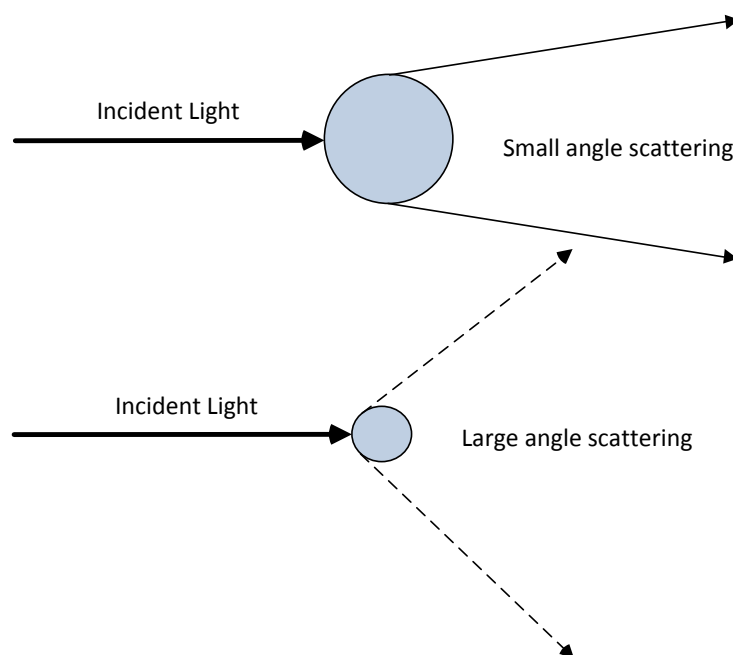


Figure 33 - Scattering of light from small and large particles – Laser Diffraction

The Mie theory of light scattering is used to analyse the angular scattering intensity data (Saturn DigiSizer 5200 2000). The particle size is reported as a volume equivalent sphere diameter (Saturn DigiSizer 5200 2000).

5.3.1.1 Volume, Area and Number Distribution

The median in statistics and probability theory is defined as the number separating the higher half of a data sample (population or probability distribution) from the lower half, thus it is the middle point of a collection of numbers (*D50*) (Stat-Ease 2010). The mean is defined as the sum of a collection of numbers (data sample, population or probability distribution) divided by the number of numbers in the collection (Stat-Ease 2010).

There is a significant difference between the particle sizes recorded by means of the volume of the particles (volume distribution), as it travels through the laser while it is analysed, and the particle size converted to the number- and area (surface area) distribution, by means of mathematical models. When comparing volume-, area- and number distributions, it is important to remember that there are different relationships between the volume, area and size of a particle respectively.

In comparing volume and number distributions, there is a cubic relationship between the volume of a particle and its size. For example if a wax emulsion sample containing one 500 μm particle and one million 5 μm particles was analysed using a volume-based technique (as in the case of laser diffraction), the contribution of these particle sizes to the overall distribution will be equivalent (Saturn DigiSizer 5200 2000). Therefore, volume distributions are very sensitive to the presence of a few large particles due to their large volume. Conversely, number distributions are very sensitive to the appearance of fine particles. It is possible to convert between volume distributions and number distribution and vice versa. That said, it should be emphasised that the errors involved in each of these techniques are cubed [x^3] (Saturn DigiSizer 5200 2000).

The defining equations for that the volume, area and number mathematical equations are based on the equations presented below:

Volume Mean Diameter:

$$d_{mm} = \frac{\sum nd^4}{\sum nd^3}$$

(Saturn DigiSizer 5200 2000)

Area Mean Diameter:

$$d_{sm} = \frac{\sum nd^3}{\sum nd^2}$$

(Saturn DigiSizer 5200 2000)

Number Mean Diameter:

$$d_{sm} = \frac{\sum nd^2}{\sum nd}$$

(Saturn DigiSizer 5200 2000)

5.3.2 Roughness

The roughness (Ra) of the dried edible Carnauba wax layers was measured with a portable Time© Roughness tester TR110 (Time©) that was acquired from BAMR© South Africa. The TR110 has an accuracy of $\pm 15\%$ and a repeatability better than 12%. The TR110 was calibrated with the roughness test plate supplied with the instrument and set at an evaluation length of 5 mm (the longest length). The following procedure was followed to measure the roughness of the Carnauba wax emulsions:

1. The Carnauba wax emulsion was placed on a plexiglass© test plate (3 mm × 50 mm × 120 mm) by means of a pipet.
2. A 0.5 mm gauge was used to ensure a 0.5 mm wet film thickness was left on the test plate.
3. The test plate was then placed in a vacuum chamber for 2 hours to ensure that the wax layer has completely dried.
4. The TR110 was used to measure the roughness (Ra) of the dried wax layer.
5. A total of 10 randomized measurements were recorded for each sample.

5.3.3 Gloss

The gloss (GU) of the dried edible Carnauba wax layers were measured with a portable GT60 Gloss tester that was acquired from BAMR© South Africa. The GT60 gloss tester measures the gloss at an angle of 60°. It has an accuracy of $\pm 1.5 GU$ and a repeatability better than $\pm 0.4 GU$. The GT60

was calibrated with the standard test plate supplied with the instrument. The following procedure was followed to measure the gloss of the Carnauba wax emulsions:

1. The Carnauba wax emulsion was placed on a plexiglass[®] test plate (3 mm × 50 mm × 120 mm) by means of a pipet.
2. A 0.5 mm gauge was used to ensure a 0.5 mm wet film thickness was left on the test plate.
3. The test plate was then placed in a vacuum chamber for 2 hours to ensure that the wax layer has completely dried.
4. The GT60 was used to measure the gloss (*GU*) of the dried wax layer.
5. A total of 10 randomized measurements were recorded for each sample.

5.3.4 Dynamic Viscosity

The viscosity of the Carnauba wax emulsions manufactured throughout this study was measured with a MCR 501 Rheometer (Anton Paar[®]). It has a wide range of cone and plate tools (Φ25 and 50 mm and angles 1, 2 and 4°) available. Standard operating procedures were followed to perform viscosity measurements on the Carnauba wax emulsion samples. Basic instructions on how to operate a MCR 501 Rheometer can be viewed in **Appendix D** (Anton Paar[®]).

5.3.5 pH

A digital pH-meter, which compensates for effect of temperature, was used in accordance with an EC620131 glass-body, open pore, for polymer gel applications, pH electrode (Eutech Instruments[®]) to measure the pH of the Carnauba wax emulsion samples. An average of three pH measurements was taken for each sample. The following procedure was followed to measure the pH of the Carnauba wax emulsions:

1. The Carnauba wax emulsion sample was poured into a glass beaker.
2. The pH electrode was placed inside the Carnauba wax emulsion sample.
3. Time was allowed for the pH-meter to reach a stable pH value.
4. The pH reading was noted and removed from the Carnauba wax emulsion sample.
5. The electrode was placed in distilled water.
6. The electrode was then DABBED dry with a clean paper towel. Dabbing prevents electrostatic energy from damaging the pH electrode.
7. A total of 3 readings were taken for each sample.

5.3.6 Density

The density of the Carnauba wax emulsion samples were measured with a calibrated density flask with a fixed volume of 24.873 ml. A thermometer ensured that the readings were measured at a temperature of 20°C. The following procedure was followed to measure the density of the Carnauba wax emulsions:

1. The density flask (volume = 24.873 ml) was weighed on a calibrated scale (to an accuracy of 3 decimals).
2. The Carnauba wax emulsion was injected into the density flask by means of a pipet.
3. The thermometer cap was inserted into the filled density flask. It was crucial not to cause any bubbles to be trapped inside the density flask, to prevent deviations in the recorded measurements.
4. The density flask was placed in a water bath set at 20°C.
5. Once the density flask's thermometer indicated that the contents were at a temperature of 20°C, the density flask was weighed on a calibrated scale (to an accuracy of 3 decimals).
6. The content was emptied and the density flask rinsed with Acetone.
7. The density flask was allowed to completely dry and the process was repeated.
8. A total of 10 measurements were recorded for each sample.

The dynamic viscosity, pH and density was measured during the confirmation runs and final optimized run to confirm whether or not the measurements fall within ranges stated in literature and material data sheets of commercial wax coatings (**Appendix A**).

Chapter 6: Design of Experiments

Various authors have studied edible wax coatings for the post-harvest food industry (Baker, Hagenmaier 1997, Hagenmaier 1998, Hagenmaier 2004, Hagenmaier 2000, Bosquez-Molina, Guerrero-Legarreta & Vernon-Carter 2003, Chiumarelli, Hubinger 2012, Robert D. 2000, Baldwin 1994, Brasil et al. 2012). Most of these authors focussed on the properties of the food products and how they are affected by the applied edible wax coatings, with very little emphasis on the formulation, manufacturing process and optimisation of the manufacturing process and/or of the edible wax coating itself. This is due to edible wax coatings formulations and manufacturing processes being trade secrets and not openly available in literature. That said, by using the correct optimisation techniques, there is the possibility of significantly improving the manufacturing process and product quality of edible wax coatings, especially for natural edible wax coatings that comply with the EU and USA food regulations.

J. M. Guitierrez et al. (2008) stated in her study on nano-emulsions, that the properties of these emulsions depend on both composition variables and preparation variables (process variables) e.g. the emulsifying path, agitation or emulsification time (Gutiérrez et al. 2008). Thus, optimization studies are required to achieve the best properties before these emulsions can be applied in the industry (Gutiérrez et al. 2008). Due to the large number of variables that can influence the final product quality of nano-emulsions, Guitierrez et al. (2008) proposed that optimization be carried out by means of experimental designs (Gutiérrez et al. 2008). In addition optimization can also be carried out by selective variation of one variable (Gutiérrez et al. 2008).

Design of experiments (DOE) is a set of tools and methods that offer a powerful means to reach breakthrough improvements in product quality and process efficiency by extracting the maximum valuable information from a minimum set of experiments (Anderson, Kraber 1999, Clarke 2012). For this reason, DOE will be used to determine which process- and raw material (formulation) factors affect the key properties of the final product. In order to set up an appropriate DOE, the key characteristics of edible Carnauba wax coatings need to be defined. Once the main process- and raw material factors have been identified, the formulation and process can be optimized to produce a final product that contains these key characteristics.

Models will be fitted to the data obtained through the DOEs by means of the analysis of variance (ANOVA). It is important to state and understand the major assumptions that need to be satisfied when using ANOVA. These major assumptions are as follow:

1. ***The data points are independent***
2. ***The response is normally distributed***
3. ***Variance is similar within different groups (homogenous)***

These three major assumptions are discussed in more detail in ***Appendix E: Validation of ANOVA Assumptions***.

In this section the various experimental designs will be discussed and validated. This section also contains a discussion on some of the major factors and responses that will be investigated during the experimental phase. Any assumptions that had to be made during the experimental phase will be stated and validations will be included. Each of the experimental designs will be presented including the various settings of both the formulation and process variables.

6.1 Assumptions

Various assumptions were made in order to perform the required experimentation. These assumptions were as follows:

- 1) The *wt%* surfactant referred to during the experimental designs consist of the sum of the *wt%* oleic acid, *wt%* ammonium hydroxide and *wt%* potassium hydroxide.
- 2) The temperature process parameter mentioned during the experimental stages, refers to the temperature of the heating oil and trace heating settings.
- 3) From the commissioning experimental runs that were performed, before the Screening experimental stage, it was determined that the total maximum weight of product produced during one experimental run is 3500 *g*. This is due to the size of the pressure vessel and the average amount of foam formed during the process. With a maximum weight of 3500 *g* there is still visibility through the sight glass at the top of the pressure vessel.
- 4) For the Screening experimental stage, it was assumed that the weight of initial water will be 90% of the weight of the wax added during the run. Hagenmaier et al. used a percentage of between 70 – 110% during his experiments with Carnauba wax using the pressure method (Hagenmaier 1998). Thus, for the screening experiments, an average of 70 – 110% was assumed, hence 90%.
- 5) In order to determine the ratio of Oleic acid to Ammonium hydroxide to Potassium hydroxide, the formulation stated by Robert D. Hagenmaier was used as reference. An average of ***Formulation 1, 2 and 4*** was assumed for the Screening experimental

stage. This is due to all three of these formulations consisting of Carnauba wax, Oleic acid, Ammonium hydroxide and Potassium hydroxide (Hagenmaier, Baker 1994, Baker, Hagenmaier 1997, Hagenmaier, Baker 1997, Hagenmaier 1998). It was calculated that the ratio of Oleic acid to Ammonium hydroxide to Potassium hydroxide should be 4.7: 2.2: 1. It was also assumed that this ratio is kept constant during the Screening experimental stage.

- 6) It was assumed that the addition rate of the Ammonium hydroxide, during all of the experimental runs, was that of the addition rate of the inverting phase (water). Thus the flow of liquid into the pressure vessel was kept constant throughout each experimental run.
- 7) The high shear time interval was based on the time of stirring and homogenizing inbetween the inverting phase increments' addition times.
- 8) Li et al. (2010) varied the surfactant between 3 – 8 wt%. They found that emulsions containing 5 – 10 wt% surfactant were all quite stable (Li et al. 2010). For this reason the surfactant was varied between 5 – 8 wt% during the Screening experimental stage, which is the overlapped range stated by Li et al. (2010) (Li et al. 2010). However, for the Mixture experimental design the range was widened to 5 – 10 wt%.
- 9) It assumed that the ambient temperature did not have an effect on the emulsification temperature and overall emulsification process. Thus, the heat loss of the pilot plant was constant throughout all the experimental runs.
- 10) All of the emulsions were cooled at the slowest possible stirring rate (20 Hz/ 660 rpm) with the high shear homogenizer off, to room temperature. Lashmar et al. validates this assumption with their findings on slow agitation cooling (Lashmar, Richardson & Erbod 1995). They found that emulsions deteriorated the least and showed better long-term stability when they were cooled at the slowest agitation rate to room temperature (Lashmar, Richardson & Erbod 1995).
- 11) The inverting phase (water) increments that were added during the experimental runs were as follow:
 - 10 wt% of total mass of product
 - 10 wt% of total mass of product
 - 51 wt% of total mass of product
 - Final increment consisted of the left over inverting phase (water)

This distribution of increments is stated by Robert D. Hagenmaier and assumed to be the appropriate amount of inverting phase (water) to be added (Hagenmaier, Baker 1997). This is also the only openly available literature source that states the amount of inverting phase (water) to be added during experimental runs with Carnauba wax.

- 12) In order to perform particle size analyses (laser diffraction) on the Carnauba wax emulsions, it was assumed that the emulsion particles (dispersed phase) were composed solely of Carnauba wax. This assumption is supported by Gusman in his study on Carnauba wax emulsions (Gusman 1947).
- 13) In addition to **Assumption 12** it was assumed that the particles were homogeneous spheres with a refractive index of 1.45. This assumption is validated by McClements in his research on edible nano-emulsions (McClements 2010). McClements states that the mathematical models used by analyses instruments (e.g. Malvern Particle Size Analyser - laser diffraction) to calculate the particle sizes and distributions, assume that the particles are homogenous spheres with well-defined properties (McClements 2010).

6.2 Experimental Designs

The main focus of DOE is to extract the maximum amount of valuable information from a minimum set of experiments (Gutiérrez et al. 2008, Clarke 2012). To do so, the minimum number of factors needs to be investigated. This will minimize the number of experiments and in return reduce the experimental expenses. Due to there being a large number of factors that can influence the key characteristics of the final edible Carnauba wax coating, some sort of sifting process was required to minimize the number of factors that were investigated. Initially the number of factors was sifted by making assumptions supported by literature. Once the final factors were determined, screening experiments were performed to determine the key factors influencing the final product.

For the edible Carnauba wax coating manufacturing process, the following potential factors and responses were identified (**Table 17**):

Table 17 - Possible factors and responses

| No. | Factors | Responses |
|-----|--|-----------------------------------|
| 1 | Type of Wax | Particle size |
| 2 | Mass of Carnauba wax | Particle size distribution |
| 3 | Type of Fatty acid | pH |
| 4 | Mass of Oleic acid | Density |
| 5 | Initial temperature the reactor | Viscosity |
| 6 | Heating rate | Turbidity |
| 7 | Mass of initial water | Gloss of dried coating |
| 8 | Ammonium Hydroxide concentration | Roughness of dried coating |
| 9 | Mass of Ammonium Hydroxide | Stability |
| 10 | Potassium Hydroxide concentration | Contrast Ratio |
| 11 | Mass of Potassium Hydroxide | Spreading rate of coating |
| 12 | Temperature of water added during process | Zeta potential |
| 13 | Temperature of water added at the end of the process (final water) | Interfacial Tension |
| 14 | Cooling rate | Rheology flow curve |
| 15 | Final temperature of the reactor | Non-Volatile content |
| 16 | Mixer speed | Volatile content |
| 17 | Mixer time | Clarity |
| 18 | High shear homogenizer speed | Colour |
| 19 | Mixer blade spacing | |
| 20 | Mixer blade configuration | |
| 21 | Emulsification time | |
| 22 | Cooling time | |
| 23 | Heating time | |
| 24 | Water addition time | |

| No. | Factors | Responses |
|-----|---------------------------------------|-----------|
| 25 | Water addition rate | |
| 26 | Oleic acid addition time | |
| 27 | Ammonium Hydroxide addition time | |
| 28 | Ammonium Hydroxide addition rate | |
| 29 | Heating oil (coil) temperature | |
| 30 | Trace heating temperature | |

* Bold printed factors and responses are considered relevant for this study

The justification for the relevant factors and responses are as follow:

Factors:

1. **Type of wax:**

Various natural waxes exist which can be used as coatings on non-processed fruit. This study was limited by the availability of the wax, the cost associated with the wax and the accessibility of formulations containing the relevant waxes. It was found that Carnauba wax was the best choice of wax since it is currently used in the post-harvest industry as an edible wax coating for fruit, it complies with the EU and USA food regulations, there are formulations containing Carnauba wax available in literature and it is more cost effective than most of the other natural waxes available for edible wax coatings. The type of wax was kept constant and not viewed as a variable in this study.

2. **Mass of Carnauba wax:**

Since the final dried coating consists solely of wax, the mass of wax in the emulsion will have a significant effect on the final product quality. However, most of the edible Carnauba wax coating formulations obtained from literature require the mass of wax to make up about 20% of the emulsion (Hagenmaier, Baker 1994, Hagenmaier, Baker 1997, Hagenmaier 1998, Hagenmaier 2004). For this reason the amount of wax-to-water was varied during the Screening- and Mixture Experimental stages in order to determine the optimum wax content. In addition, the amount of wax-to-surfactant ratio also had a significant effect on the final product quality as stated by various authors (Fernandez et al. 2004, Danghui, Fengyan & Tianbo 2012, Salager et al. 2002, Pérez et al. 2002a). Therefore the wax-to-surfactant ratio was also varied during the Screening- and Mixture Experimental stages.

3. **Type of Fatty Acid and Base (cation) [Surfactant]:**

Hagenmaier (2004) concluded in his study of fruit coatings that both the identity of the cation and the fatty acid determines the emulsification properties of the surfactant (Hagenmaier 2004). The use of palmitic- and stearic acid in edible wax micro-emulsion

coatings for fruit resulted in unfavourable wettability (only 70% of the fruit is coated) once applied to fruit (Hagenmaier, Baker 1994). In the case of Oleic acid, only 2% of the coated surface was affected (Hagenmaier, Baker 1994). In his study, Hagenmaier (2004) studied Oleic-, Myristic- and Lauric acid, separate and in combination in his Carnauba wax emulsions (Hagenmaier 2004).

The choice of base was between Morpholine and Ammonium hydroxide. According to Hagenmaier (1898) wax emulsions made with aqueous ammonia are generally more acceptable in the food industry, due to it being approved by the FDA (FDA, 21CFR.172.235) (Hagenmaier 1998). He also stated that a small amount of Potassium hydroxide improved the gloss of Carnauba wax coatings (Hagenmaier 1998). For this reason Oleic acid, Ammonium hydroxide and potassium hydroxide was used to form the surfactant.

4. ***Mass of Oleic acid, Ammonium Hydroxide and Potassium Hydroxide:***

It was concluded in Hagenmaier's study on wax micro-emulsions and emulsion as citrus coatings, that the weight loss of the fruit coated with oxidized Polyethylene or Carnauba wax were affected by the type and amount of fatty acid in the formulation (Hagenmaier, Baker 1994). Thus the fatty acid content was investigated. For the Screening experimental stage, the ratio of Oleic acid : Ammonium hydroxide : Potassium hydroxide was kept constant. This ratio was based on the available Carnauba wax formulations from Hagenmaier et al. Pey et al. concluded that there is an optimum surfactant mixing ratio (Pey et al. 2006). During the Mixture experimental stage the ratio of Oleic acid : Ammonium hydroxide : Potassium hydroxide was varied in order to establish the optimal formulation.

5. ***Cooling Rate:***

Robert D. Hagenmaier (1998) concluded in his study on wax micro-emulsion formulations used as fruit coatings, that both Carnauba- and Candelilla wax coatings in general had higher gloss if the micro-emulsions were rapidly cooled (Hagenmaier 1998). Lashmar et al. on the other hand concluded in his study on the correlation of physical parameters of an oil in water emulsion with manufacturing procedures and stability, that the slow cooling of the emulsion appeared to be beneficial to its stability (Lashmar, Richardson & Erbod 1995). In addition, he also concluded that the speed of agitation during cooling seemed to have little or no effect on the stability of the emulsion (Lashmar, Richardson & Erbod 1995). In light of the above mentioned conclusions, the cooling rate was varied during the Screening experimental stage to determine whether it had a significant effect on the final product quality. However the cooling rate was set at the maximum cooling rate for the Mixture- and Composite experimental stages, due to the results of the Screening experimental stage.

6. Mixer Speed & High Shear Homogenizer Speed:

Various authors have studied the effect of mixing rate on emulsions (Gutiérrez et al. 2008, Gutiérrez et al. 2008, Li et al. 2010, Pey et al. 2006, Lashmar, Richardson & Erbod 1995, Danghui, Fengyan & Tianbo 2012, Myers et al. 1999, Ee et al. 2008, Klein, Lowry 1996). Even though these authors did not work with Carnauba wax emulsions, there is evidence enough that both the mixer and high shear homogenizing speed should be varied during the Screening Experimental stage to determine whether these two factors have a significant effect on the final product quality or not. Li et al. investigated the effect of both the stirring rate and the homogenizing rate during their study, by varying the rates between 100 – 1000 *rpm* and 2000 – 8000 *rpm* respectively (Li et al. 2010). As a result, both the stirrer and high shear homogenizer's speed was varied during both the Screening- and Composite experimental stages.

7. Emulsification Time:

Numerous authors who studied the effect of manufacturing procedures of emulsification processes investigated the effect of emulsification time on the final emulsion quality (Gutiérrez et al. 2008, Lashmar, Richardson & Erbod 1995, Lashmar, Beesley 1993, Danghui, Fengyan & Tianbo 2012, Adler-Nissen, Mason & Jacobsen 2004, Milanovic et al. 2011, Windhab et al. 2005). Lashmar et al. found that extending the emulsification time improved the stability of the emulsions (Lashmar, Richardson & Erbod 1995, Lashmar, Beesley 1993). Adler-Nissen et al. concluded that enough time is required for a stable interface to form around the drop in order to form a stable emulsion (Adler-Nissen, Mason & Jacobsen 2004). Danghui et al. on the other hand stated that the emulsification time should not be too long or too short (Danghui, Fengyan & Tianbo 2012). From the authors mentioned above it is clear that the emulsification time will likely have a significant effect on the final emulsion product. To have established an optimum emulsification time, the emulsion time was varied during the Screening- and Composite experimental stages.

8. Water Addition Rate:

Gutierrez et al. investigated various authors' studies on the addition rate of the inverting phase (usually water) during emulsification processes (Gutiérrez et al. 2008, Pey et al. 2006, Wang et al. 2007, Uson, Garcia & Solans 2004). They concluded that by slowly adding the inverting phase, nano-emulsions can be obtained, while emulsions with larger particle sizes are obtained by rapidly adding the inverting phase (Gutiérrez et al. 2008). Lashmar et al. also investigated the findings of other author's studies on the addition rate of the inverting phase during emulsion processes (Lashmar, Richardson & Erbod 1995, Lin 1978). Their findings are

in agreement with those of Gutierrez et al. (Gutiérrez et al. 2008, Pey et al. 2006, Wang et al. 2007, Lashmar, Richardson & Erbod 1995, Uson, Garcia & Solans 2004). Conversely, Lin et al. found that the addition rate of the inverting phase had no effect on the final emulsion product quality (Lin 1978). As a result of this controversy, the inverting phase addition rate was varied during both the Screening- and Composite experimental stages.

9. **Temperature:**

Emulsification temperature is a process parameter that many authors have investigated (Han, Aristippos 2005, Li et al. 2010, Lashmar, Richardson & Erbod 1995, Danghui, Fengyan & Tianbo 2012, Adler-Nissen, Mason & Jacobsen 2004). Lashmar et al. investigated the findings of Bornfriend (Bornfriend 1978)(Bornfriend 1978)(Bornfriend, 1978) and Jass on the effect of temperature on emulsification processes (Lashmar, Richardson & Erbod 1995, Jass 1967, Bornfriend 1978). Both of these authors found that the emulsification temperature had a significant effect on the particle size (quality) of the final emulsion product (Jass 1967, Bornfriend 1978). Li et al.'s findings were in agreement with Jass and Bornfriend's in that the emulsion properties were improved when the emulsification temperature was increased, during their study on the formation of wax emulsions (Li et al. 2010). The emulsification temperature was varied during the Screening- and the Composite experimental designs.

Responses:

1. **Particle Size and Distribution:**

Various authors have stated in their study on emulsions that the physicochemical properties of emulsions, e.g. optical properties, stability, rheology etc., are mainly determined by the characteristics of the particles (Griffin 1945, Lashmar, Richardson & Erbod 1995, Danghui, Fengyan & Tianbo 2012, McClements 2010, Milanovic et al. 2011, Karbowiak, Debeaufort & Voilley 2007, Pérez et al. 2002b). Perez et al. stated that the understanding of the factors (both formulation and composition orientated) influencing the particle size of emulsions are without a doubt of great relevance (Pérez et al. 2002b). Therefore, the particle size and distribution of the emulsions manufactured during the experimental stages were viewed as the main response in this study.

2. **Roughness of Dried Coating:**

As mentioned above, the particle size and distribution of emulsions has a significant influence on its physicochemical properties, including its optical properties (Griffin 1945, Lashmar, Richardson & Erbod 1995, Danghui, Fengyan & Tianbo 2012, McClements 2010, Milanovic et al. 2011, Karbowiak, Debeaufort & Voilley 2007, Pérez et al. 2002b). That said it

is important to keep in mind that the Carnauba wax coatings manufactured in this study will be used on fresh fruit. Thus appearance is the most important quality attribute, with the main focus being on uniformity, gloss and colour (Lin, Zhao 2007). Chen et al. tested the roughness of various wax-hydrocolloid coatings (including commercial wax coatings) in his study to get an impression of any possible changes in fruit surface uniformity after coating (Chen, Nussinovitch 2001). In Trezza and Krochta's study on the specular reflection, gloss, roughness and surface heterogeneity of biopolymer coatings, they found that small average particles size and narrow particle size distributions promoted more homogenous surfaces (low roughness) with high gloss (Trezza, Krochta 2001). With this in mind the roughness of each of the dried coatings manufactured during the experimental stages was analysed.

3. ***Gloss of Dried Coating:***

High gloss is considered to be aesthetically essential in the post-harvest industry, thus making high gloss very favourable for edible wax coatings (Bai, Baldwin & Hagenmaier 2002). Similarly to the roughness response discussed above, the gloss of a wax emulsion coating is also mainly determined by the particles size (Bai, Baldwin & Hagenmaier 2002, Trezza, Krochta 2001, Vargas et al. 2009, Trezza, Krochta 2000, Lin, Zhao 2007). Due to the gloss being an important property of edible wax coatings, the gloss of each of the dried coatings manufactured during the experimental stages was analysed.

4. ***pH:***

Manufacturers provide various physical properties in order to characterise their various coatings for the market. These physical properties include emulsifier charge, solids type, percentage non-volatiles, viscosity and pH. For the purpose of this study three additional physical properties were included as responses, to be able to compare the physical properties with those supplied by the commercial manufacturers. These three properties are pH, viscosity and density. Vargas et al. characterized the film-forming dispersions (emulsions) in their study by, for one, measuring the pH (Vargas et al. 2009). Michelman® and Citrosol®, edible Carnauba wax coatings manufacturers, both provide the pH on their information sheets of all their wax coating products. For this reason, the pH of all the coatings manufactured during the Screening experimental stage and for confirmation during the Composite experimental stage was analysed.

5. ***Viscosity (Rheological Behaviour):***

Vargas et al. also analysed the rheological behaviour of the film forming dispersions investigated during their study on composite films (Vargas et al. 2009). Apparent viscosities were calculated at a certain time step while the rheological curves were obtained by means

of a rotational rheometer (Vargas et al. 2009). Michelman® also provides the viscosity on their information sheets of all their wax coating products. To contribute to the characterisation of the coatings manufactured during the Screening experimental stage and confirmation runs during the Mixture- and Composite stages, the viscosity was analysed.

6. *Density:*

Density analyses were included in the characterization studies performed on the film forming dispersions investigated during Vargas et al.'s study (Vargas et al. 2009). Both Michelman® and Citrosol® provide the density of their Carnauba wax coatings on their information sheets. The density of the coatings manufactured during the Screening experimental stage as well as confirmation runs during the Mixture- and Composite stages were analysed.

A discussion on each of the experimental stages performed during this study follows.

6.2.1 Commissioning Experimental Runs

Commissioning experiments were performed in order to determine whether the pilot plant (heating- and cooling capabilities, data logging, sealing etc.) was functioning correctly and to determine the limits of the pilot plant and emulsification process. Initially the pilot plant was run with only water to prevent wasting any raw materials (e.g. Carnauba wax). The temperature and pressure were recorded and is presented in **Figure 34**. **Figure 34** confirms that the pilot plant is operable in the expected pressure range of 0.5 – 1.2 *bar (abs)*.

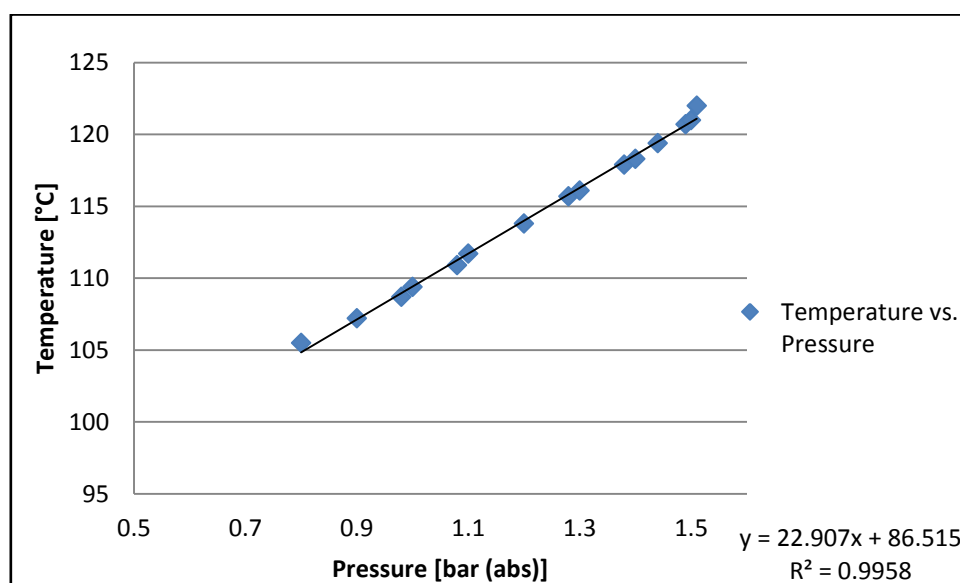


Figure 34 – Commissioning Experiment - Temperature vs. Pressure

Once the pilot plant was modified and the functionality confirmed, experimental runs were performed with the identified components (Carnauba wax, Oleic acid, Ammonium hydroxide and Potassium hydroxide). Due to the availability of formulations in literature being limited, the initial experiments were performed on a trial and error basis. Fifteen test experiments were performed. The first five experiments were performed before the trace heating was installed on the bottom dome. The commissioning experiments' configurations and formulations are presented in **Table 18**.

Table 18 - Commissioning Experimental Runs Configurations and Formulations

| Experiment | Stirrer Speed [rpm] | HSH Speed [rpm]* | Water [wt%] | Wax [wt%] | Oleic Acid [wt%] | Ammonium Hydroxide [wt%] | Potassium Hydroxide [wt%] | Wax : Surfactant Ratio | Temperature [°C] |
|-------------|---------------------|------------------|-------------|-----------|------------------|--------------------------|---------------------------|------------------------|------------------|
| Test Run 1 | 1090 | 2915 | 67.35% | 22.33% | 7.26% | 1.86% | 1.21% | 2.16 | 185 |
| Test Run 2 | 1500 | 4060 | 81.49% | 20.47% | 6.53% | 2.18% | 1.12% | 2.27 | 185 |
| Test Run 3 | 660 | 4060 | 72.00% | 21.77% | 5.95% | 2.05% | 0.93% | 2.08 | 185 |
| Test Run 4 | 660 | 4060 | 72.00% | 21.77% | 5.95% | 2.05% | 0.93% | 2.44 | 120 |
| Test Run 5 | 660 | 4320 | 52.09% | 16.74% | 3.35% | 2.23% | 0.00% | 2.44 | 185 |
| Test Run 6 | 660 | 0 | 52.09% | 16.74% | 3.35% | 2.23% | 0.00% | 3.00 | 100 |
| Test Run 7 | 660 | 0 | 48.37% | 14.88% | 3.35% | 2.23% | 0.00% | 3.00 | 120 |
| Test Run 8 | 660 | 1450 | 72.56% | 18.60% | 5.95% | 2.05% | 0.93% | 2.67 | 120 |
| Test Run 9 | 660 | 1450 | 72.56% | 18.60% | 5.95% | 2.05% | 0.93% | 2.62 | 140 |
| Test Run 10 | 660 | 1450 | 72.56% | 18.60% | 5.58% | 2.23% | 0.74% | 2.08 | 120 |
| Test Run 11 | 800 | 4320 | 72.56% | 18.60% | 7.14% | 2.46% | 1.12% | 2.08 | 110 |
| Test Run 12 | 800 | 4320 | 58.44% | 9.30% | 1.86% | 1.25% | 0.43% | 2.17 | 110 |
| Test Run 13 | 800 | 4320 | 58.44% | 9.30% | 2.79% | 0.93% | 0.43% | 1.74 | 110 |
| Test Run 14 | 800 | 4320 | 67.35% | 22.33% | 7.26% | 1.86% | 1.21% | 2.63 | 100 |
| Test Run 15 | 800 | 4320 | 81.49% | 20.47% | 6.53% | 2.18% | 1.12% | 2.24 | 100 |

* HSH – High Shear Homogenizing

A constant inverting phase addition rate of 3.6 l/h was set for each of the commissioning experimental runs. In addition, the commissioning runs were also cooled down to room temperature at a constant maximum cooling rate. It was difficult to estimate the amount of emulsion the pressure vessel could hold, due to the varying amount of foam that forms during the experimental runs being dependant on the stirring- and high shear homogenizing speed. This was noted during the first five test experiments. The formulation was adapted to prevent the pressure vessel from being filled past the point where the visibility through the sight glass was hampered.

One of the main process factors that were varied over the largest range was the temperature. Initially the temperature was set at 185°C and it was quickly noted that the emulsion was burning at the heating coils' surface resulting in an emulsion with a very dark brown/black colour. The

formulation was adapted to see if the burning was caused as a result of one of the components. However, a heating test was performed with the Carnauba wax and it was determined that the wax's colour darkens (burns) at a temperature of 120°C. The emulsification temperature was set at a maximum of 120°C. For the purpose of commissioning experiments, the high shear time interval was ignored.

Multiple Linear Regression was performed on the data collected to obtain the correlation between the volume particle size and the process- and formulation parameters. The following regression results were obtained (**Table 19**):

Table 19 - Regression statistics - Commissioning Experiments

| Regression Statistics | |
|-----------------------|-------|
| Multiple R | 0.995 |
| R Square | 0.99 |
| Adjusted R Square | 0.969 |

The regression coefficients were plotted in order to compare the effect of each term. This gives an indication of what the significant process- or formulation parameters could be. **Figure 35** illustrates the relative importance of the process- and formulation parameters on the volume mean particle size.

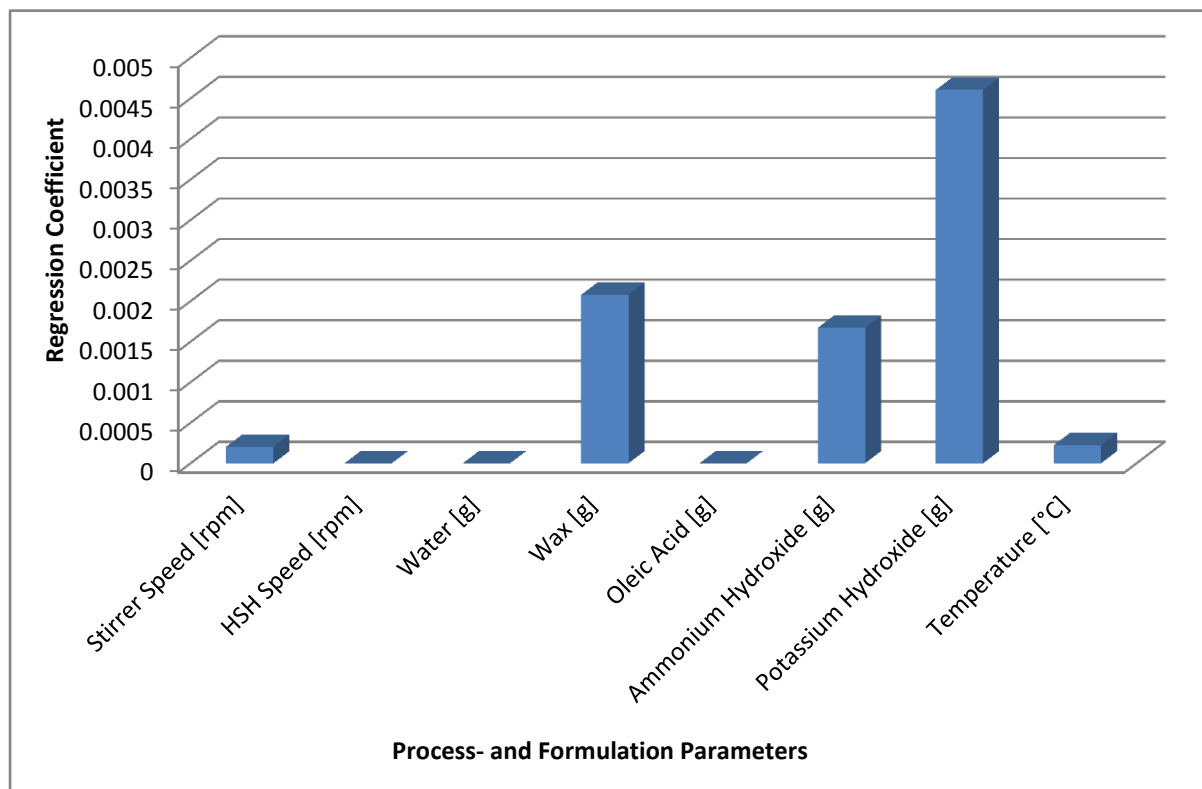


Figure 35 - Relative contribution of the process- and formulation parameters to the volume mean particle size

Figure 35 indicates that the Stirrer Speed [rpm], Temperature [°C] and the complete formulation could possibly have a significant effect on the particle size. This will be further investigated by means of the experimental designs.

Once the limits of pilot plant and the emulsification process were determined for safe and repeatable operations, the Screening experiments could commence.

6.2.2 Screening Experimental Design

A type of sifting process was required to minimize the number of experiments while testing the large number of factors that were identified (**Table 17**). The sifting was performed by means of screening experiments. Screening experiments is a DOE used to sift through a large number of factors with the fewest number of experiments (Clarke 2012). Due to there being both formulation- and process variables, a mixture design was chosen for the screening experiments to evaluate all the factors simultaneously. Guitterez et al. evaluated the effects of both the composition variables and preparation variables by means of a Mixture design, in their study on Nano-emulsions (Gutiérrez et al. 2008).

A fixed ratio of oleic acid : Ammonium hydroxide : Potassium hydroxide was assumed for the Screening experimental design. This ratio was published by Hagenmaier (Hagenmaier 2004) as 4.7:2.2:1. The ranges of each component for the mixture part of the Screening experimental design were as follow (based on findings by Hagenmaier) (**Table 20**):

Table 20 - Screening Experimental Design - Formulation Parameters Ranges

| Component | Minimum [wt%] | Maximum [wt%] |
|------------|---------------|---------------|
| Water | 80 | 85 |
| Wax | 10 | 15 |
| Surfactant | 5 | 8 |

A D-Optimal Combined design was selected for the screening experiments. A Point Exchange selection, with only the vertices and the overall centroid as design points, were selected. Three additional centre points, two replicates and two additional points to estimate lack of fit were included. **Figure 36** shows the formulation blends as points on triangles, repeated at each of the eight corners of a cube which represents the process.

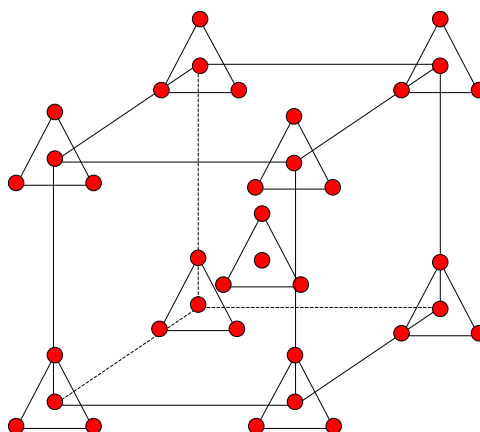


Figure 36 - Screening experimental design: Five formulation blends at nine process combinations

The D-Optimal design is much more efficient than the User Defined design (Stat-Ease 2010). This is due to Design Expert© setting up the DOE in the most effective way as compared to the User defined design where the user can specify which mixture blends and which process points to run (Stat-Ease 2010). The design was based on a linear model for both the mixture and process variables. This is acceptable since the centre points will indicate if curvature is present or not. If curvature is present, the model would be modified accordingly. The final Screening experimental design is presented in **Table 21**.

Table 21 - Screening Experimental Design

| Experiment | Surfactant [wt%] *** | Wax [wt%] | Water [wt%] | Stirrer Speed [rpm] | HSH Speed [rpm] | HS Time Interval [min] | Cooling Rate [coded] ** | Inverting Phase AR* [l/h] | Temp [°C] |
|------------|----------------------|-----------|-------------|---------------------|-----------------|------------------------|-------------------------|---------------------------|-----------|
| 1 | 5 | 10 | 85 | 1500 | 6800 | 10 | 1 | 3 | 100 |
| 2 | 5 | 10 | 85 | 1500 | 4300 | 40 | 1 | 4 | 100 |
| 3 | 5 | 15 | 80 | 800 | 4300 | 10 | -1 | 3 | 120 |
| 4 | 5 | 15 | 80 | 1500 | 4300 | 40 | 1 | 4 | 120 |
| 5 | 5 | 15 | 80 | 800 | 4300 | 10 | 1 | 4 | 100 |
| 6 | 5 | 15 | 80 | 1500 | 4300 | 10 | 1 | 3 | 100 |
| 7 | 5 | 10 | 85 | 800 | 6800 | 10 | 1 | 4 | 100 |
| 8 | 5 | 15 | 80 | 800 | 6800 | 40 | 1 | 3 | 120 |
| 9 | 5 | 10 | 85 | 800 | 6800 | 40 | 1 | 3 | 120 |
| 10 | 5 | 15 | 80 | 1500 | 6800 | 40 | -1 | 4 | 100 |
| 11 | 5 | 15 | 80 | 1500 | 6800 | 10 | 1 | 4 | 120 |
| 12 | 5 | 10 | 85 | 1500 | 4300 | 10 | -1 | 4 | 120 |
| 13 | 5 | 10 | 85 | 1500 | 6800 | 40 | -1 | 4 | 100 |
| 14 | 8 | 10 | 82 | 1500 | 4300 | 40 | -1 | 4 | 100 |
| 15 | 8 | 12 | 80 | 1500 | 4300 | 40 | 1 | 3 | 120 |
| 16 | 8 | 10 | 82 | 800 | 4300 | 10 | -1 | 3 | 120 |
| 17 | 8 | 12 | 80 | 800 | 6800 | 40 | 1 | 3 | 100 |

| Experiment | Surfactant [wt%] *** | Wax [wt%] | Water [wt%] | Stirrer Speed [rpm] | HSH Speed [rpm] | HS Time Interval [min] | Cooling Rate [coded] ** | Inverting Phase AR* [l/h] | Temp [°C] |
|------------|----------------------|-----------|-------------|---------------------|-----------------|------------------------|-------------------------|---------------------------|-----------|
| 18 | 8 | 12 | 80 | 800 | 6800 | 40 | -1 | 4 | 120 |
| 19 | 8 | 12 | 80 | 1500 | 6800 | 10 | -1 | 3 | 100 |
| 20 | 8 | 10 | 82 | 1500 | 6800 | 10 | 1 | 4 | 120 |
| 21 | 5 | 10 | 85 | 800 | 4300 | 10 | -1 | 3 | 100 |
| 22 | 8 | 10 | 82 | 1500 | 6800 | 40 | -1 | 3 | 120 |
| 23 | 6.5 | 11.75 | 81.75 | 1150 | 5550 | 25 | 0 | 3.5 | 110 |
| 24 | 6.5 | 11.75 | 81.75 | 1150 | 5550 | 25 | 0 | 3.5 | 110 |
| 25 | 6.5 | 11.75 | 81.75 | 1150 | 5550 | 25 | 0 | 3.5 | 110 |
| 26 | 6.5 | 11.75 | 81.75 | 1150 | 5550 | 25 | 0 | 3.5 | 110 |
| 27 | 5 | 15 | 80 | 800 | 6800 | 40 | 1 | 3 | 120 |
| 28 | 5 | 15 | 80 | 1500 | 4300 | 10 | 1 | 3 | 100 |

* AR – Addition Rate

** A cooling rate of 1 indicates that the cooling water was at its maximum flow rate while a cooling rate of –1 indicates that the cooling water’s flow rate was 0 l/h. A cooling rate of 0 indicates that the cooling water’s valve was set to 1/2 open

*** %Surfactant is the total weight percentage of the amount of oleic acid, ammonium hydroxide and potassium hydroxide

Once all the screening experiments were completed, analyses were performed on the final products. The results that were obtained through the analyses were entered into the screening experimental design in Design Expert®. Once the data were entered, models were fit to each data set. The models were optimized to yield a favourable final product based on quality factors obtained in literature. The optimization was based on the minimizing of the particle size, the maximizing of the gloss of the dried coatings and the minimizing of the roughness of the dried coatings. When only the process factors were examined, it was found that the main significant factors were likely to be the temperature, high shear time interval, the stirring speed and the high shear homogenizing speed.

6.2.3 Mixture Experimental Design

To establish an optimal formulation a D-optimal Mixture design was set up which tested the ranges of the water, wax, oleic acid, ammonium hydroxide and potassium hydroxide to yield the optimal formulation. Three additional replicates, three additional points to estimate lack of fit and two additional centre points were included in the design. The candidate points that were selected include the vertices, axial check blends and an overall centroid. The Mixture design is represented in **Figure 37**.

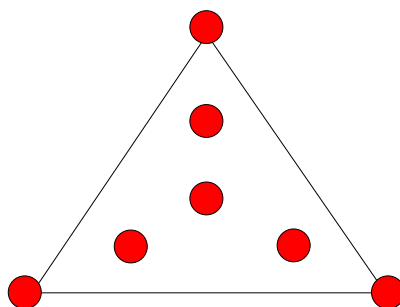


Figure 37 - Mixture experimental design: Seven blends

The ranges of each component were altered from the screening experiments and were as follow (**Table 22**):

Table 22 - Mixture Experimental Design - Formulation Parameters Ranges

| Component | Minimum [wt%] | Maximum [wt%] |
|---------------------|---------------|---------------|
| Water | 75 | 79.9 |
| Wax | 15 | 19.9 |
| Oleic Acid | 3 | 6.96 |
| Ammonium Hydroxide | 1.6 | 3 |
| Potassium Hydroxide | 0.5 | 1.3 |

The ranges of each of the components were determined from literature and observations made during the experimental runs that were performed. To ensure that the correct ranges and combinations were tested, the following constraints were placed over the ranges:

1. $0 \leq \%Oleic\ acid - \%Ammonium\ hydroxide$
2. $\%Oleic\ acid - 4 * Ammonium\ hydroxide \leq 0$

These constraints were obtained from the information acquired from literature and the experimental data obtained. Thus the correct ratio range of Oleic acid : Ammonium hydroxide was ensured. The ratios of Oleic acid : Ammonium hydroxide published in literature for Carnauba wax coatings range

from 1.32 to 1.67 (Hagenmaier, Baker 1994, Hagenmaier, Baker 1997, Hagenmaier 1998). During the commissioning experiments it was found that an Oleic acid : Ammonium hydroxide ratio of ± 2.9 yielded a favourable inverted emulsion. Lower ratios resulted in uninverted emulsions. The ratio of Oleic acid : Ammonium hydroxide determines the amount of oleates (cationic surfactant) that will form. To cover a wide Oleic acid : Ammonium hydroxide range and to ensure that the optimum falls within the range, the ratio range was set to 1 – 4. The final Mixture experimental design is presented in **Table 23**.

Table 23 - Mixture Experimental Design

| Experiment | Water [%] | Wax [%] | Oleic Acid [%] | Potassium Hydroxide [%] | Ammonium Hydroxide [%] |
|------------|-----------|---------|----------------|-------------------------|------------------------|
| 1 | 78.50 | 15.00 | 3.00 | 0.50 | 3.00 |
| 2 | 76.82 | 15.47 | 4.07 | 1.08 | 2.56 |
| 3 | 75.47 | 16.22 | 5.77 | 0.68 | 1.86 |
| 4 | 75.47 | 17.92 | 4.07 | 0.68 | 1.86 |
| 5 | 75.00 | 15.00 | 6.50 | 0.50 | 3.00 |
| 6 | 75.00 | 17.70 | 3.00 | 1.30 | 3.00 |
| 7 | 75.94 | 15.94 | 5.14 | 0.86 | 2.12 |
| 8 | 79.10 | 15.00 | 3.00 | 1.30 | 1.60 |
| 9 | 75.00 | 19.90 | 3.00 | 0.50 | 1.60 |
| 10 | 75.00 | 15.00 | 6.50 | 0.50 | 3.00 |
| 11 | 75.00 | 19.90 | 3.00 | 0.50 | 1.60 |
| 12 | 75.94 | 15.94 | 5.14 | 0.86 | 2.12 |
| 13 | 79.90 | 15.00 | 3.00 | 0.50 | 1.60 |
| 14 | 75.00 | 15.00 | 6.96 | 1.30 | 1.74 |
| 15 | 75.00 | 17.70 | 3.00 | 1.30 | 3.00 |

6.2.4 Composite Experimental Design

A standard multifactor response surface methodology (RSM) design, called a Central Composite Design (CCD), was used to set up the final experiments. Composite DOEs are well suited for fitting a quadratic surface, which makes it favourable for process optimization (Stat-Ease 2010). In a composite design each numeric factor is varied over five levels. These five levels consist of a centre point, plus and minus α (axial points represented by the star icons in **Figure 38**) and plus and minus one. Two additional replicates were included as well as six centre points. **Figure 38** represents the CCD for a three factor design.

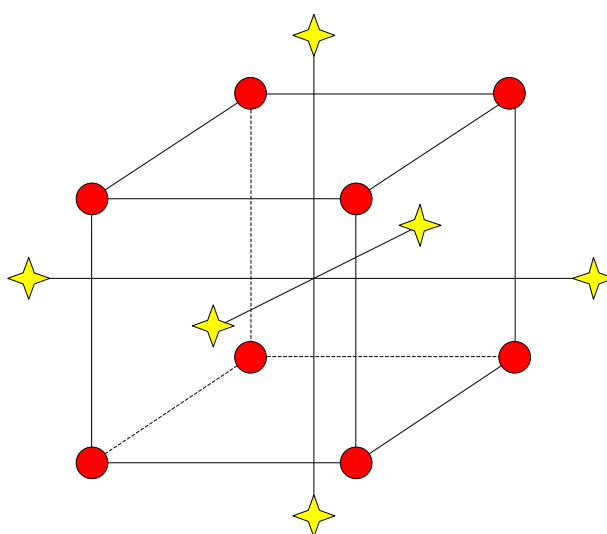


Figure 38 - Central Composite Design for three factors

The range of each process parameter is presented in **Table 24**.

Table 24 - Composite Experimental Design - Process Parameters' Ranges

| Factor | Minimum | Maximum |
|------------------------------------|---------|---------|
| Temperature (°C) | 100 | 140 |
| High Shear Time Interval (min) | 0 | 55 |
| Stirrer Speed (rpm) | 450 | 1850 |
| High Shear Homogenizer Speed (rpm) | 3050 | 8050 |

The value of α , for the purpose of this study, was set at two (recommended by Design Expert©) (Stat-Ease 2010). An α value of two ensures rotatability and it establishes new extremes for the low and high settings for all factors (Stat-Ease 2010). The final Composite experimental design is presented in **Table 25**.

Table 25 - Composite Experimental Design

| Run | Temperature [°C] | High Shear Time Interval [min] | High Shear Speed [rpm] | Stirring Speed [rpm] |
|-----|------------------|--------------------------------|------------------------|----------------------|
| 1 | 110 | 10 | 4300 | 800 |
| 2 | 110 | 40 | 6800 | 800 |
| 3 | 120 | 25 | 8050 | 1150 |
| 4 | 120 | 25 | 5550 | 450 |
| 5 | 120 | 25 | 5550 | 1150 |
| 6 | 110 | 40 | 6800 | 1500 |
| 7 | 100 | 25 | 5550 | 1150 |
| 8 | 110 | 40 | 4300 | 800 |
| 9 | 120 | 25 | 5550 | 1150 |
| 10 | 140 | 25 | 5550 | 1150 |
| 11 | 120 | 25 | 5550 | 1150 |
| 12 | 120 | 25 | 5550 | 1150 |
| 13 | 130 | 40 | 6800 | 800 |
| 14 | 130 | 10 | 6800 | 800 |
| 15 | 120 | 25 | 5550 | 1850 |
| 16 | 120 | 55 | 5550 | 1150 |
| 17 | 130 | 40 | 6800 | 1500 |
| 18 | 120 | 25 | 5550 | 1150 |
| 19 | 110 | 10 | 6800 | 800 |
| 20 | 130 | 40 | 4300 | 1500 |
| 21 | 120 | -5 | 5550 | 1150 |
| 22 | 130 | 10 | 4300 | 1500 |
| 23 | 120 | 25 | 3050 | 1150 |
| 24 | 130 | 10 | 6800 | 1500 |
| 25 | 130 | 40 | 4300 | 800 |
| 26 | 110 | 10 | 6800 | 1500 |
| 27 | 110 | 40 | 4300 | 1500 |
| 28 | 130 | 10 | 4300 | 800 |
| 29 | 120 | 25 | 5550 | 1150 |
| 30 | 110 | 10 | 4300 | 1500 |

Chapter 7: Results and Discussion

In this section the results that were obtained from the experimental runs are discussed. The data that were gathered during analyses is compared to literature data in order to verify the results that were obtained. The repeatability of the pilot plant data are presented by considering identical experimental runs during each of the main experimental designs. Statistical models are discussed and validated by means of confirmation experimental runs.

7.1 Screening Experimental Phase

Once all the screening experiments were completed the results were entered into the Screening experimental design in Design Expert®. The Screening experimental design was originally set up as a linear model for both the mixture- and process variables. Additional centre points were included to indicate any curvature. A p-value of less than 0.05 indicate a significant model term, while values greater than 0.1 indicate that the model terms are not significant (Stat-Ease 2010). The responses were analysed and the following results were obtained.

7.1.1 Particle Size

The average particle size and particle size distribution of the edible Carnauba wax emulsions were measured with a Saturn DigiSizer 5200 Particle Sizer (Micrometrics, UK) and recorded. As previously mentioned in **Section 5.3.1.1 – Volume, Area and Number Distribution** there was a significant difference between the particle sizes recorded as volume, area (surface area) and number respectively. The mean volume-, area- and number particles sizes that were obtained during the Screening experimental phase for each experimental run are as follow (**Table 26**):

Table 26 – Mean Particle Sizes (Comparing the Volume-, Area- and Number Distributions) for the Screening Experimental Design

| Experiment | Mean Particle Diameter (Volume Distribution) [µm] | Mean Particle Diameter (Area Distribution) [µm] | Mean Particle Diameter (Number Distribution) [µm] |
|------------|---|---|---|
| EXP S1 | 26.84 | 4.747 | 0.643 |
| EXP S2 | 15.28 | 2.775 | 0.661 |
| EXP S3 | 12.95 | 2.51 | 0.641 |
| EXP S4 | 8.612 | 1.533 | 0.757 |
| EXP S5 | 21.15 | 2.217 | 0.668 |
| EXP S6 | 10.07 | 2.144 | 0.638 |
| EXP S7 | 14.78 | 2.571 | 0.613 |

| Experiment | Mean Particle Diameter (Volume Distribution) [μm] | Mean Particle Diameter (Area Distribution) [μm] | Mean Particle Diameter (Number Distribution) [μm] |
|------------|--|---|--|
| EXP S8 | 19.73 | 2.346 | 0.664 |
| EXP S9 | 21.78 | 2.394 | 0.63 |
| EXP S10 | 10.38 | 2.705 | 0.698 |
| EXP S11 | 11.63 | 1.602 | 0.605 |
| EXP S12 | 14.39 | 2.422 | 0.683 |
| EXP S13 | 19.16 | 4.398 | 0.756 |
| EXP S14 | 41.89 | 5.991 | 0.63 |
| EXP S15 | 18.86 | 2.013 | 0.647 |
| EXP S16 | 16.61 | 3.609 | 0.636 |
| EXP S17 | 32.85 | 4.603 | 0.668 |
| EXP S18 | 20.96 | 3.42 | 0.603 |
| EXP S19 | 23.23 | 3.271 | 0.608 |
| EXP S20 | 44.32 | 5.094 | 0.654 |
| EXP S21 | 16.65 | 4.414 | 0.692 |
| EXP S22 | 16.72 | 3.953 | 0.645 |
| EXP S23 | 21.37 | 3.165 | 0.683 |
| EXP S24 | 10.61 | 2.054 | 0.625 |
| EXP S25 | 17.85 | 2.859 | 0.614 |
| EXP S26 | 14.57 | 2.323 | 0.625 |
| EXP S27 | 5.828 | 1.457 | 0.614 |
| EXP S28 | 10.46 | 2.246 | 0.639 |

When examining the cumulative particle size distributions of Screening Experiment 1 (*EXP S1*), represented in **Figure 39**, it is possible to see that there is a significant difference in the volume-, area- and number particle size distributions.

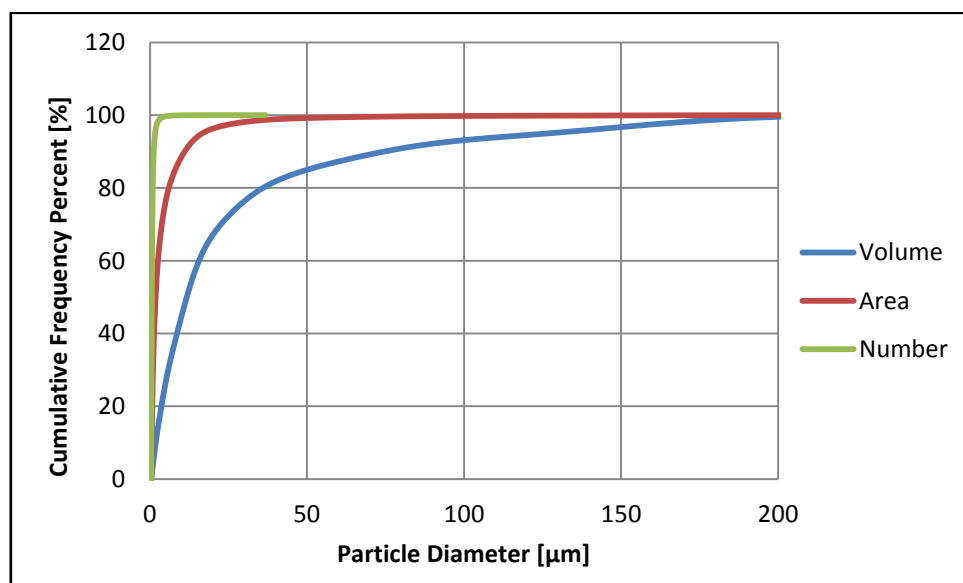


Figure 39 - EXP S1: Volume, Area and Number Cumulative Frequency vs. Particle Diameter

Due to the number distribution being very sensitive to the presence of fine particles within a sample, the main peaks of the particle size frequency for the number distribution will be in the range of $\pm 0 - 5 \mu\text{m}$, as seen in **Figure 40**.

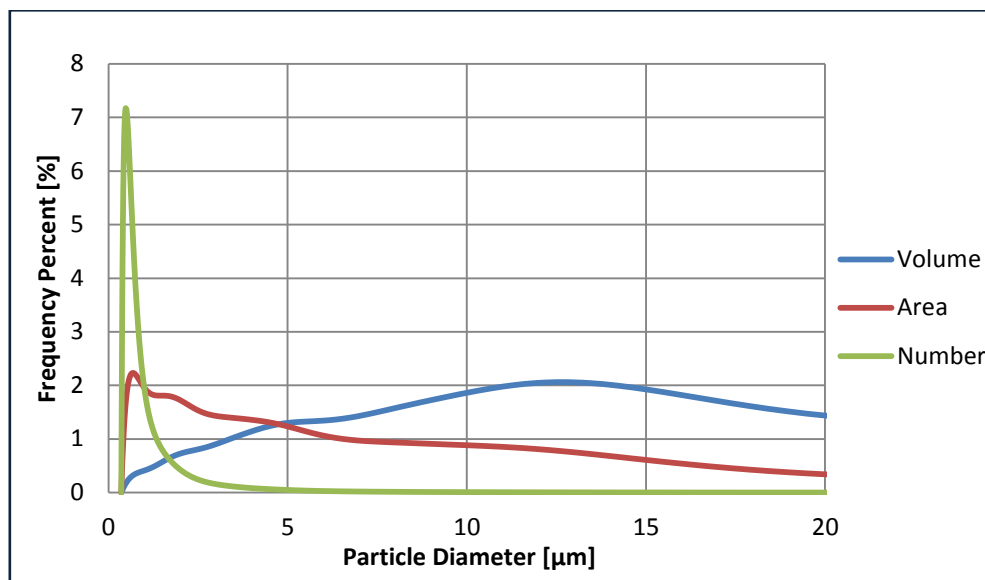


Figure 40 - EXP S1: Volume, Area and Number Frequency vs. Particle Diameter (0 – 20 μm)

When examining **Figure 39**, it is clear from the volume distribution curve (between 50 – 225 μm) that there were large particles present in sample *EXP S1*. From both **Figure 39** and **Figure 40** it is possible to see that the area distribution is less sensitive to large particles than the volume distribution, but more sensitive than the number distribution. Furthermore, the area distribution is less sensitive to fine particles than the number distribution, but more sensitive to fine particles than the volume distribution. This is expected since there is cubic relationship between the number distribution and the volume distribution, while there is a quadratic relationship between number distribution and the area distribution, and the volume distribution and area distribution (Saturn DigiSizer 5200 2000, Stat-Ease 2010).

For the purpose of screening the volume, area and number particle sizes were analysed and will be discussed. In addition both the mean and median particle sizes were analysed for the volume, area and number distributions.

7.1.1.1 Volume Distribution

A sample from each run in the Screening experimental design was analysed by means of laser diffraction using a Saturn DigiSizer 5200 Particle Sizer (Micrometrics, UK). The volume particle size data were collected for further processing.

Volume Mean Particle Size

Volume Mean Particle Size Model V1 (Screening Experimental Design)

Once the volume mean particle size data were analysed with Design Expert®, it was noted that the linear model was not statistically significant ($p > 0.05$), as seen in the ANOVA **Table 27** (validation for the ANOVA assumptions is presented in **Appendix E**).

Table 27 - Volume Mean Particle Size (Linear Model) ANOVA

| Analysis of Variance Table – Volume Mean Particle Size (Linear Model) | | | | | | |
|---|---------|----|--------|-------|----------|-----------------|
| | Sum of | | Mean | F | p-value | |
| Source | Squares | df | Square | Value | Prob > F | |
| Model | 1711.33 | 20 | 85.57 | 1.194 | 0.430 | not significant |
| Linear Mixture | 91.44 | 2 | 45.72 | 0.638 | 0.557 | |
| Residual | 501.72 | 7 | 71.67 | | | |
| Lack of Fit | 40.90 | 2 | 20.45 | 0.222 | 0.809 | not significant |
| Pure Error | 460.82 | 5 | 92.16 | | | |
| Cor Total | 2213.05 | 27 | | | | |
| Adeq Precision | 4.78 | | | | | |

A quadratic model was fitted to the particle size data for both the mixture- and process variables. As a result there were various insignificant terms included in the new model. This is due to the mixture and process models being crossed which creates many unnecessary high-order terms (Stat-Ease 2010). A model reduction was performed to eliminate the insignificant terms. The ANOVA for the reduced quadratic model is presented in **Table 28**.

Table 28 - Volume Mean Particle Size (Reduced Quadratic Model) ANOVA

| Analysis of Variance Table - Volume Mean Particle Size (Reduced Quadratic Model) | | | | | | |
|--|---------|----|--------|-------|----------|-----------------|
| | Sum of | | Mean | F | p-value | |
| Source | Squares | df | Square | Value | Prob > F | |
| Model | 1289.96 | 6 | 214.99 | 4.891 | 0.0028 | significant |
| <i>%Wax * HS Time</i> | 289.94 | 1 | 289.94 | 6.596 | 0.0179 | |
| <i>%Wax * Cooling Rate</i> | 385.10 | 1 | 385.10 | 8.761 | 0.0075 | |
| <i>%Water * Stirring Speed</i> | 425.76 | 1 | 425.76 | 9.686 | 0.0053 | |
| <i>%Water * Inverting Phase AR</i> | 349.47 | 1 | 349.47 | 7.950 | 0.0103 | |
| Residual | 923.09 | 21 | 43.96 | | | |
| Lack of Fit | 462.28 | 16 | 28.89 | 0.313 | 0.9653 | not significant |
| Pure Error | 460.82 | 5 | 92.16 | | | |
| Cor Total | 2213.05 | 27 | | | | |
| Adeq Precision | 9.61 | | | | | |

By examining **Table 28** it is possible to see that the reduced quadratic model is statistically significant ($p < 0.05$). There is only a 0.28% chance that a Model F-Value this large (4.89) could occur due random noise. From **Table 28** it is possible to see that all four of the model terms (printed in red) provided in the ANOVA are significant ($p < 0.05$). They are; *%Wax*HS Time*, *%Wax*Cooling Rate*, *%Water*Stirring Speed* and *%Water*Inverting Phase AR*. *Adeq Precision* (Adequate Precision) measures the signal to noise ratio and a ratio greater than 4 is desirable. A value of 9.607 indicates an adequate signal and shows that the model can be used to navigate the design space (Stat-Ease 2010). The *Pred R-Squared* (Predicted R-squared) is a measure of how good the model predicts a response value (Stat-Ease 2010). The *Adj R-Squared* (Adjusted R-squared) on the other hand is the R-squared adjusted for the number of parameters in the model relative to the number of points in the design (Stat-Ease 2010). In other words it is a measure of the amount of variation about the mean explained by the model (Stat-Ease 2010). The adjusted R-squared and predicted R-squared values should be within approximately 0.2 of each other to be in “reasonable agreement” (Stat-Ease 2010). The R-squared values for the **Volume Mean Particle Size Model V1 (Screening)** are as follow (**Table 29**):

Table 29 - Volume Mean Particle Size Model V1 (Screening) - R-Squared Values

| Model | R-Squared | Adj R-Squared | Pred R-Squared |
|------------------------------------|-----------|---------------|----------------|
| Volume Mean Particle Size Model V1 | 0.5829 | 0.4637 | 0.1374 |

From the R-squared values it is possible to see that the predicted R-squared value is not as close to the adjusted R-squared value as one might normally expect. This may indicate that there are outlier points in the data set. It should be noted that fractional factorials (the screening experimental design) is favourable for screening experimental purposes, but suffers from aliasing the factor effects which can be problematic for low resolution designs (Clarke 2012). In low resolution designs the important effects and their interactions can be aliased resulting in the influential factors not being determined (Clarke 2012). Thus the Screening experimental design is purely to identify and project the significant system parameters onto a smaller design space and to create a stronger design model by means of a response surface statistical design (Clarke 2012). The final **Volume Mean Particle Size Model V1 (Screening)** equation in terms of the actual components and actual factors are as follow:

$$\begin{aligned}
 \text{Particle Size } [\mu\text{m}] = & +3.73268 \times \% \text{Surfactant} \\
 & +2.22508 \times \% \text{Wax} \\
 & -0.55150 \times \% \text{Water} \\
 & +3.83250 \times 10^{-3} \times \% \text{Surfactant} \times \text{Stirring Speed} \\
 & -7.37627 \times 10^{-3} \times \% \text{Surfactant} \times \text{HS Time} \\
 & -0.14820 \times \% \text{Surfactant} \times \text{Cooling Rate} \\
 & -2.41283 \times \% \text{Surfactant} \times \text{Inverting Phase AR} \\
 & +3.83250 \times 10^{-3} \times \% \text{Wax} \times \text{Stirring Speed} \\
 & +0.066386 \times \% \text{Wax} \times \text{HS Time} \\
 & +1.33384 \times \% \text{Wax} \times \text{Cooling Rate} \\
 & -2.41283 \times \% \text{Wax} \times \text{Inverting Phase AR} \\
 & -9.58126 \times 10^{-4} \times \% \text{Water} \times \text{Stirring Speed} \\
 & -7.37627 \times 10^{-3} \times \% \text{Water} \times \text{HS Time} \\
 & -0.24820 \times \% \text{Water} \times \text{Cooling Rate} \\
 & +0.60321 \times \% \text{Water} \times \text{Inverting Phase AR}
 \end{aligned}$$

From the final model equation (**Volume Mean Particle Size Model V1 (Screening)**), one can see that the mixture (composition) variables have a significant influence on the particle size. This is expected since the amount of surfactant determines the total interfacial area and thus the particle size and emulsions stability (Li et al. 2010). In **Figure 41** the **Volume Mean Particle Size Model V1 (Screening)** is represented by a plot of the particle size versus the wax-to-surfactant ratio versus the stirring speed.

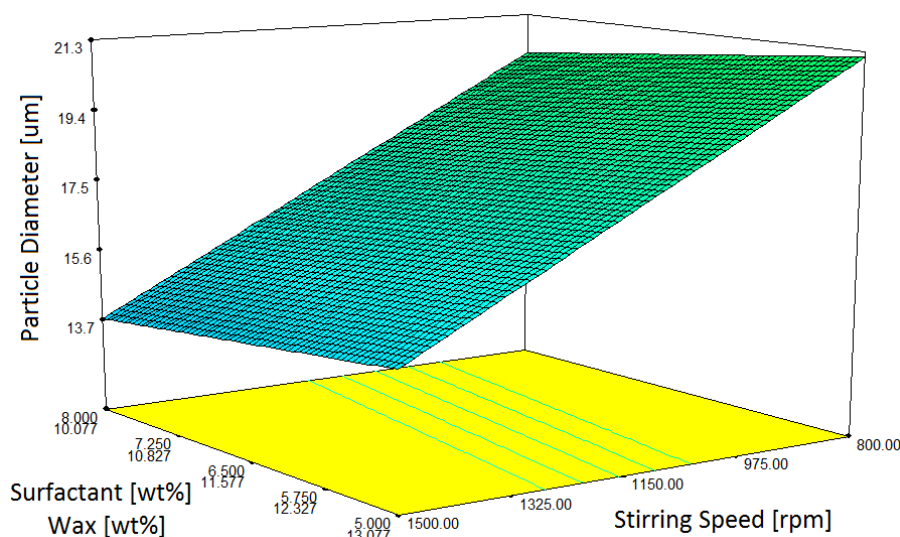


Figure 41 - Volume Mean Particle Size Model V1 (Screening Experimental Design) – Particle Size vs. Wax-to-Surfactant Ratio vs. Stirring Speed

When examining **Figure 41**, it is possible to see that the stirring speed has a significant effect on the mean particle diameter. An increase in the stirring speed resulted in the volume mean particle diameter decreasing. McClements (2010) supports this finding with his conclusion that an increase in the intensity or duration of the energy input (stirring speed or high shear homogenizing speed) of an emulsification system results in a decrease in particle size (McClements 2010). Chen et al. also found that more efficient agitation gives better emulsions (Chen, Tao 2005). **Figure 42** shows the effect of the wax-to-surfactant ratio on the particle size in more detail (Process Conditions: Stirring Speed = 1150 rpm, High Shear Homogenizing Speed = 5550 rpm, HS Time Interval = 25 mins, Cooling Rate = 0, Inverting Phase AR = 3.5 l/h, Temperature = 110°C).

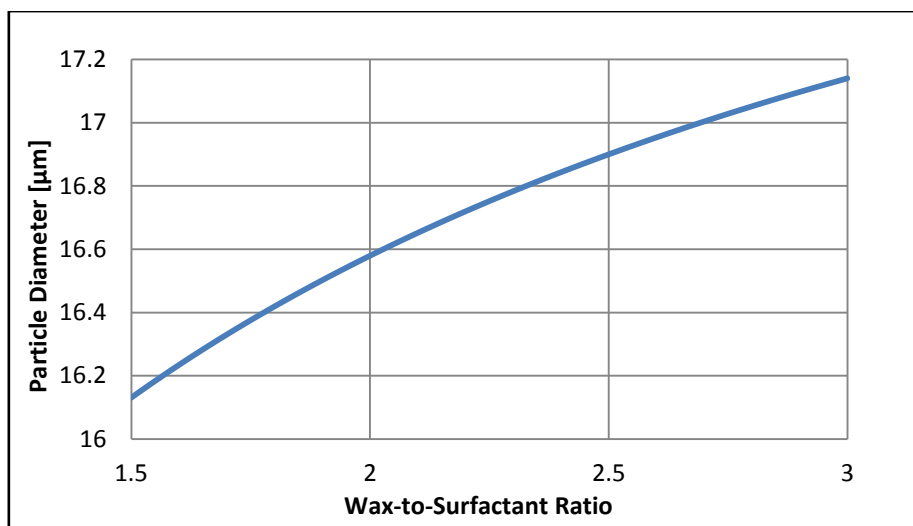


Figure 42 - Volume Mean Particle Size Model V1 (Screening Experimental Design) – Particle Size vs. Wax-to-Surfactant Ratio

By examining **Figure 42** it is possible to see that the volume mean particle diameter increases with an increase in the wax-to-surfactant ratio. Gusman, Liu et al., Pey et al. and Sadurni et al. confirm this trend of the average particle size increasing with an increase in the wax-to-surfactant ratio (Pey et al. 2006, Liu et al. 2006, Gusman 1947, Sadurní et al. 2005). McClements also states that by increasing the concentration (of the emulsifier in the system) will decrease the particle size, supporting the trend that is presented in **Figure 42** (McClements 2010). Danghui et al. supports McClements finding that a decrease in emulsifier resulted in an increase in particle size and a wider particle size distribution (Danghui, Fengyan & Tianbo 2012). A wider particle size distribution was obtained with an increase in surfactant during the screening experimental runs, as seen in **Figure 43**.

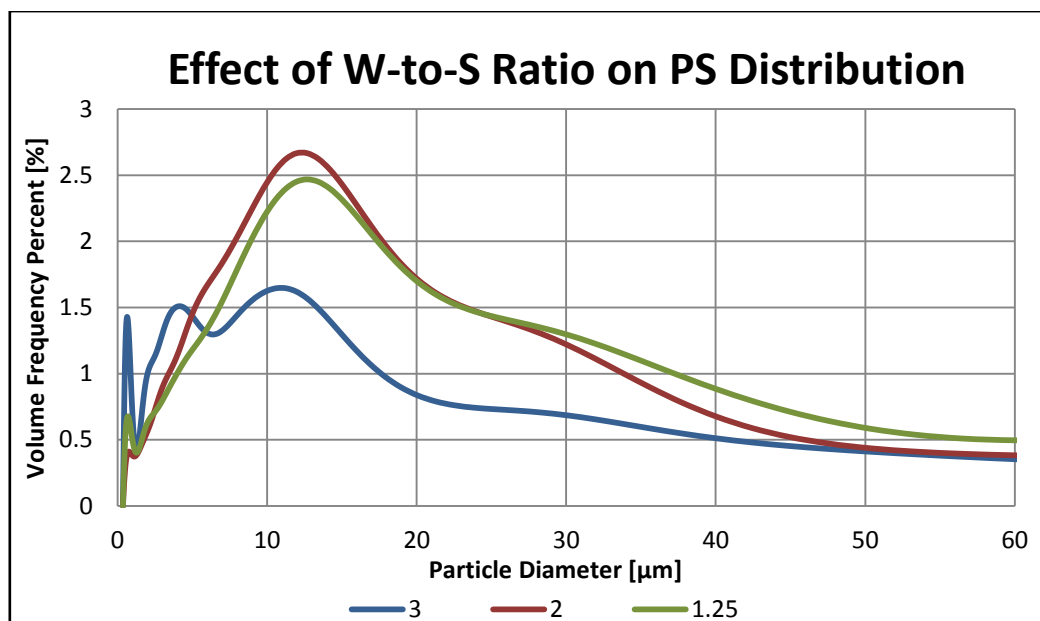


Figure 43 - The effect of Wax-to-Surfactant Ratio on the Particle Size Distribution (Screening Experimental Design)

The particle size distribution produced with wax-to-surfactant ratios of 1.25 and 2 respectively, have a more concentrated distribution than the distribution produced with a wax-to-surfactant ratio of 3 (Figure 43). This trend is supported by Danghui et al.’s findings (Danghui, Fengyan & Tianbo 2012).

Other significant process factors that are included in the *Volume Mean Particle Size Model V1 (Screening)* are the high shear (HS) time interval, the cooling rate and the inverting phase addition rate (AR). Figure 44 shows the effect of varying the high shear time interval on the particle size.

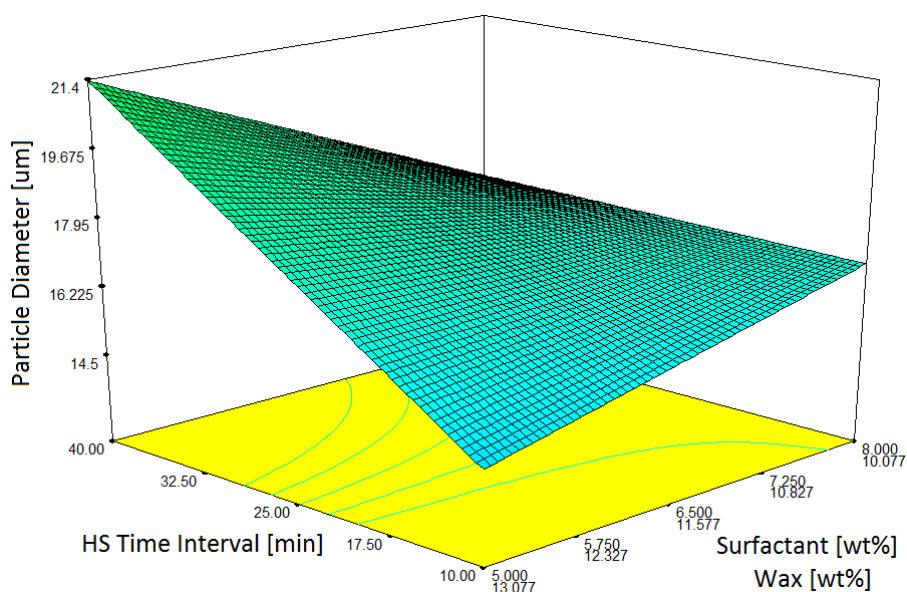


Figure 44 - Volume Mean Particle Size Model V1 (Screening Experimental Design) – Particle Size vs. Wax-to-Surfactant Ratio vs. HS Time Interval - 1

From **Figure 44** it is seen that the particle size decreases with a decrease in the high shear time interval. McClements stated in his study on nano-emulsions that the particle size can be reduced by increasing the intensity or duration of homogenization (McClements 2010). Adler-Nissen et al. agreed with McClements conclusion in that there must be enough time given for a stable interface to form around the drops during the emulsification processes (Adler-Nissen, Mason & Jacobsen 2004). Lashma et al. supports both McClements and Adler-Nissen et al.'s findings (Lashmar, Beesley 1993). The trend in **Figure 44** is clearly contradicting to what McClements, Adler-Nissen et al. and Lashmaer et al. obtained during their studies.

A possible explanation could be that that at long high shear time intervals coalescence (Ostwald ripening) is occurring while only breaking is occurring during the shorter high shear time intervals. This is supported by Guitierrez et al. who states in his study on nano-emulsions, that an optimum shear or shearing time can exist if breaking and coalescence are competing phenomena during the emulsification process (Gutiérrez et al. 2008). Chen et al. states in his study on oil-water emulsions that the emulsifier becomes more effective with increased mixing time (Chen, Tao 2005). In addition he also adds that if the mixing time is too long that the effectiveness of the emulsifier will decrease due to the intense stirring causing the emulsifier to drop out from the oil-water interface (Chen, Tao 2005). This supports Guitierrez et al.'s findings. Another possible explanation could be due to outlier points affecting the accuracy of the model.

That said, when examining the effect of varying high shear time interval on the particle size at the favourable low wax-to-surfactant ratio (1.25), it is possible to see that the high shear time interval has no effect on the particle size, as seen in **Figure 45**.

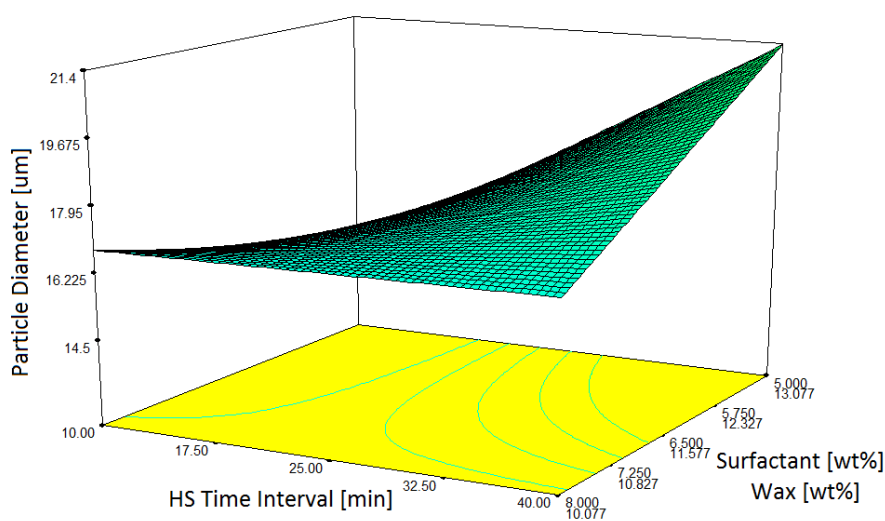


Figure 45 - Volume Mean Particle Size Model V1 (Screening Experimental Design) - Particle Size vs. Wax-to-Surfactant Ratio vs. HS Time Interval - 2

This could be due to breaking and coalescence not being competing phenomena at a wax-to-surfactant ratio of 1.25 (Gutiérrez et al. 2008). Another possibility could be that the emulsion has not inverted at higher wax-to-surfactant ratios resulting in a water-in-wax emulsion instead of wax-in-water emulsion (Fernandez et al. 2004). The effect of varying the cooling rate on the particle size is presented in **Figure 46**.

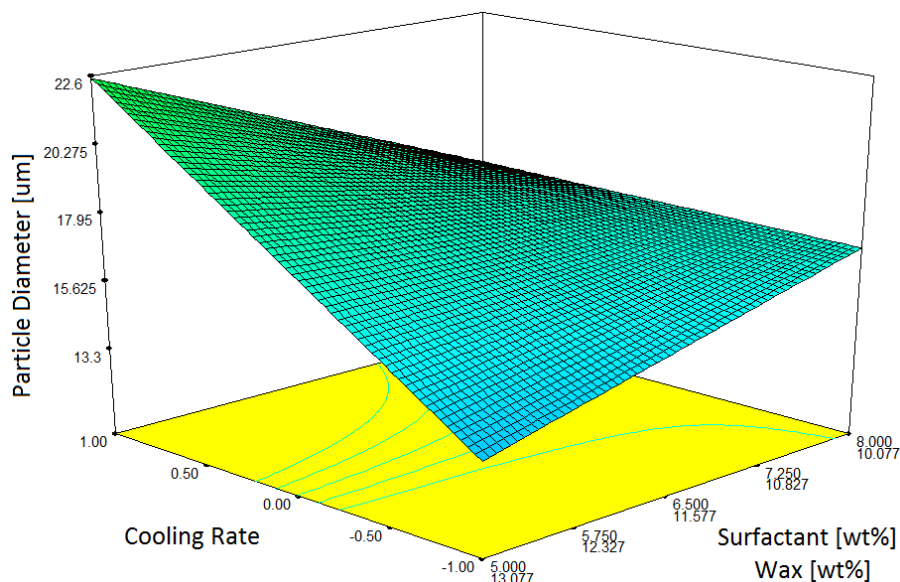


Figure 46 - Volume Mean Particle Size Model V1 (Screening Experimental Design) – Particle Size vs. Wax-to-Surfactant Ratio vs. Cooling Rate - 1

From **Figure 46** it can be seen that the particle size decreases with a decrease in the cooling rate. Lashmar et al. stated in his study on the correlation of physical parameters of an oil in water emulsion with manufacturing procedures and stability, that the slow cooling rate of the emulsion appears to be beneficial to its stability (Lashmar, Richardson & Erbod 1995). Li et al. on the other hand concluded in his study on the formation of paraffin wax emulsions, that by increasing the emulsification temperature and cooling rate improves emulsion properties, i.e. results in a smaller particle size (Li et al. 2010). The cooling rate trend in **Figure 46** is contradicting to the findings of Li et al. (Li et al. 2010). Once again this could be due to outlier points affecting the accuracy of the model.

When examining the effect of varying the cooling rate on the particle size at a favourable low wax-to-surfactant ratio it is possible to see that the cooling rate had no effect on the particle size, as seen in **Figure 47**.

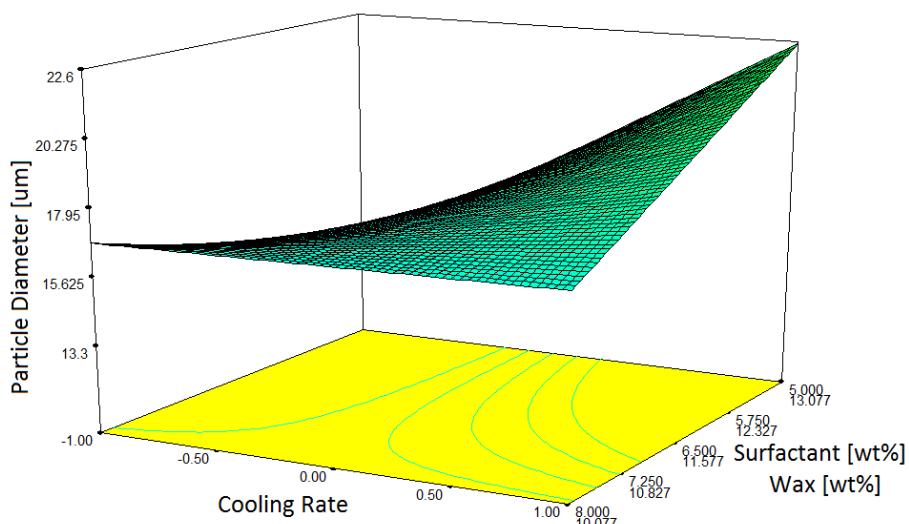


Figure 47 - Volume Mean Particle Size Model V1 (Screening Experimental Design) - Particle Size vs. Wax-to-Surfactant Ratio vs. Cooling Rate - 2

However, the trend of varying the wax-to-surfactant ratio on the particle size at a high cooling rate is in agreement with Li et al. (Li et al. 2010). The final significant process factor that is present in the **Volume Mean Particle Size Model V1 (Screening)** is the inverting phase addition rate. The effect of varying the inverting phase addition rate on the particle size is shown in **Figure 48**.

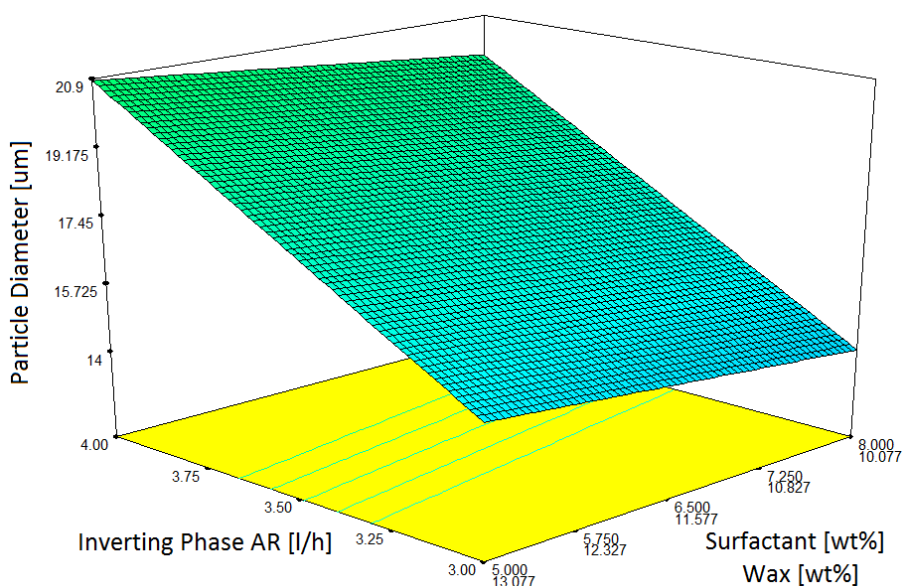


Figure 48 - Volume Mean Particle Size Model V1 (Screening Experimental Design) - Particle Size vs. Wax-to-Surfactant Ratio vs. Inverting Phase Addition Rate

By examining **Figure 48**, it is seen that the particle size decreases with a decrease in the inverting phase addition rate. This trend is in agreement with Gutierrez et al., Pey et al., Wang et al. and Lashmar e al.'s findings. Gutierrez et al. investigated various authors' studies on the addition rate of the inverting phase (usually water) during emulsification processes (Gutiérrez et al. 2008, Pey

et al. 2006, Wang et al. 2007, Uson, Garcia & Solans 2004). They concluded that by slowly adding the inverting phase nano-emulsions can be obtained, while emulsions with larger particle sizes are obtained by rapidly adding the inverting phase (Gutiérrez et al. 2008). Lashmar et al. also investigated the findings of other author’s studies on the addition rate of the inverting phase during emulsion processes (Lashmar, Richardson & Erbod 1995, Lin 1978). Their findings are in agreement with those of Gutierrez et al.’s and the trend presented in **Figure 48** (Gutiérrez et al. 2008, Pey et al. 2006, Wang et al. 2007, Lashmar, Richardson & Erbod 1995, Uson, Garcia & Solans 2004).

To show how accurate the **Volume Mean Particle Size Model V1 (Screening)** is, the predicted values are compared to the actual value, as seen in **Figure 49**.

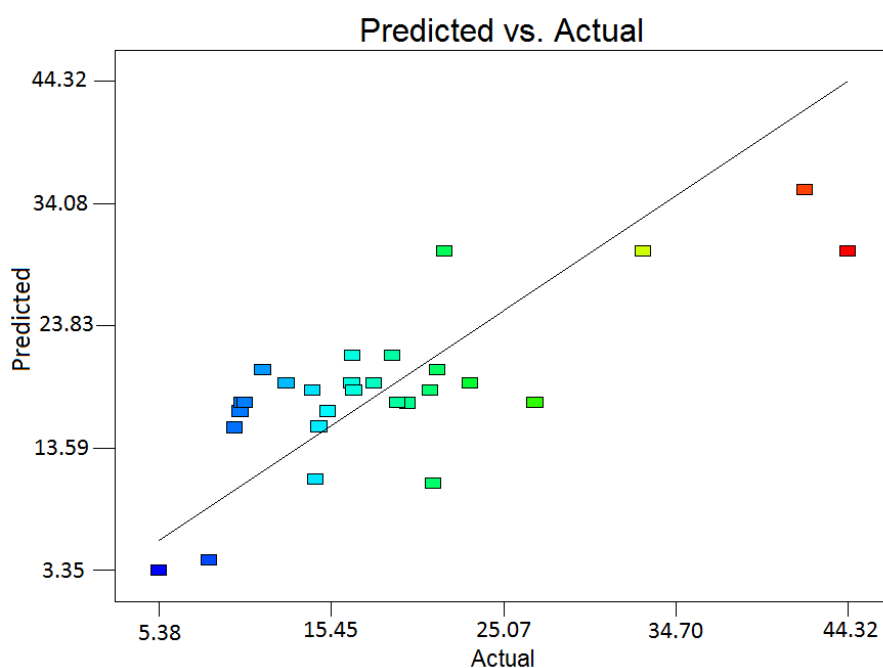


Figure 49 - Volume Mean Particle Size Model V1 (Screening Experimental Design) - Predicted vs. Actual

Color Key:

Color points by value of Particle Size:



It should be kept in mind that the screening experimental design is purely to minimize the large amount of variables associated with the emulsification process. In addition it should also be noted

that the emulsification process is very sensitive to the ambient temperature. It was observed during experimental runs performed during cool temperatures that the wax had a tendency to start to solidify during the *Ammonium hydroxide injection*. This could have resulted in a larger particle size. Any variation in the volume particle size data could be due to the varying ambient conditions during the experimental runs. By examining **Figure 49** one can see that the model is not a hundred percent accurate, yet for the purpose of screening it is sufficient enough ($p < 0.5$, adequate precision value of 9.607). That said it is also possible to see that there are two outlier points (red markers) that could be causing the model to be more inaccurate than what it could be. The two outlier points are **Std #7 Run #14** and **Std #27 Run #20**. During these two experimental runs the time during which the wax was added to the pressure vessel/reactor, was shorter than recorded throughout the rest of the screening experiments. In the event of wax added too quickly to the reactor, unmelted clumps of wax could form. This could possibly explain the large particle sizes. The two outlier points were excluded from the volume mean particle size data set and the model was refitted to the data.

Volume Mean Particle Size Model V2 (Screening Experimental Design)

The two outlier points (**EXP S7** and **EXP S27**) were excluded and a reduced quadratic model was refitted to the rearranged data and is presented in the ANOVA **Table 30** (validation for the ANOVA assumptions is presented in **Appendix E**).

Table 30 - Volume Mean Particle Size (Reduced Quadratic Model) ANOVA

| Analysis of Variance Table – Volume Mean Particle Size (Reduced Quadratic Model) | | | | | | |
|---|----------------|-----------|---------------|--------------|--------------------|-----------------|
| | Sum of | | Mean | F | p-value | |
| Source | Squares | df | Square | Value | Prob > F | |
| Model | 900.17 | 5 | 180.03 | 5.027 | 0.0038 | significant |
| %Wax * HS Time | 313.82 | 1 | 313.82 | 8.762 | 0.0077 | |
| %Wax * Cooling Rate | 321.97 | 1 | 321.97 | 8.990 | 0.0071 | |
| %Water * Cooling Rate | 128.56 | 1 | 128.56 | 3.590 | 0.0727 | |
| Residual | 716.31 | 20 | 35.82 | | | |
| Lack of Fit | 277.40 | 16 | 17.34 | 0.158 | 0.9970 | not significant |
| Pure Error | 438.90 | 4 | 109.73 | | | |
| Cor Total | 1616.48 | 25 | | | | |
| Adeq Precision | 9.02 | | | | | |

From **Table 30** it is possible to see that that the effect of excluding the two outlier points were not that significant. The **Volume Mean Particle Size Model V1 (Screening)** has a p-value of 0.0028 while the newly fitted **Volume Mean Particle Size Model V2 (Screening)** has a p-value of 0.0038 indicating that it is less statistically significant than the original model. It is also possible to

see that the cooling rate is one of the process factors that are present in the main model terms, indicating that it has a significant effect on the particle size. The R-squared values for the **Volume Mean Particle Size Model V2 (Screening)** are as follow (**Table 31**):

Table 31 - Volume Mean Particle Size Model V2 (Screening) - R-Squared Values

| Model | R-Squared | Adj R-Squared | Pred R-Squared |
|---|-----------|---------------|----------------|
| Volume Mean Particle Size Model V2 | 0.5569 | 0.4461 | 0.1712 |

From the R-squared values it is possible to see that the predicted R-squared value is larger for the newly fitted model without the two outlier points than the previous model. For this reason the model will be investigated. The final **Volume Mean Particle Size Model V2 (Screening)** equation in terms of the actual components and actual factors are as follow:

$$\begin{aligned}
 \text{Particle Size } [\mu\text{m}] = & +0.25182 \times \% \text{Surfactant} \\
 & -1.35927 \times \% \text{Wax} \\
 & +0.32716 \times \% \text{Water} \\
 & -8.07792 \times 10^{-3} \times \% \text{Surfactant} \times \text{HS Time} \\
 & +0.57025 \times \% \text{Surfactant} \times \text{Cooling Rate} \\
 & +0.072701 \times \% \text{Wax} \times \text{HS Time} \\
 & +1.95085 \times \% \text{Wax} \times \text{Cooling Rate} \\
 & -0.87792 \times 10^{-3} \times \% \text{Water} \times \text{HS Time} \\
 & -0.31514 \times \% \text{Water} \times \text{Cooling Rate}
 \end{aligned}$$

Figure 50 illustrates the actual measured response value for this observation against the response value predicted by the model for this set of experimental conditions. Whilst in **Figure 50** the model does not predict the actual values hundred percent accurate, it is of little concern particularly since this is only the screening phase model and should help obtain an understanding of the process system as a whole. This is not the final response surface model.



Figure 50 - Actual measured response vs. model predicted value

The relative effect of each factor is presented in **Figure 51**. The blue line indicates the lower bound of the 95% confidence interval that surrounds the coefficient estimate for the specific factor while the red line indicates the upper bound of the 95% confidence interval (Stat-Ease 2010).

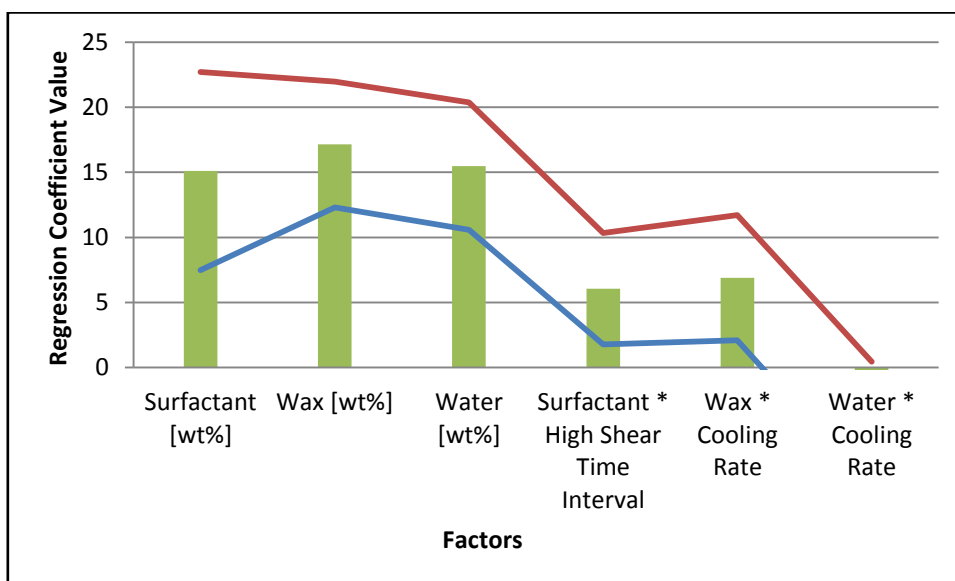


Figure 51 - Relative contribution of the volume mean particle size model factors to the volume mean particle size

From **Figure 51** it is noted that the formulation has a significant effect on the volume mean particle size. In addition the high shear time interval and cooling rate is identified as statistically significant factors to the particle size ($p < 0.05$). Keeping in mind the low R-squared value of the model, the factors identified above is an indication of what parameters should be investigated next.

The effect of varying the high shear time interval on the particle size is presented in **Figure 52**.

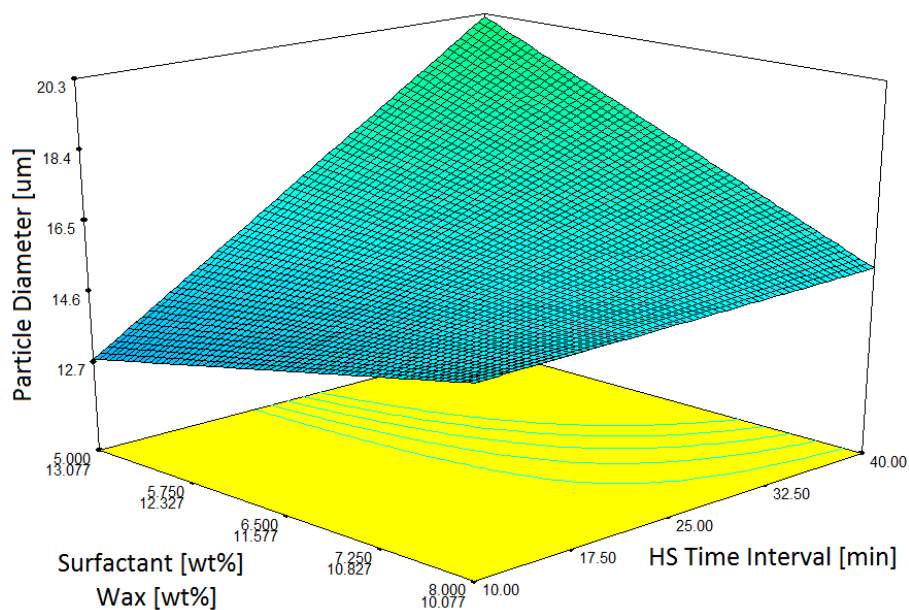


Figure 52 - Volume Mean Particle Size Model V2 (Screening Experimental Design) - Particle Size vs. Wax-to-Surfactant Ratio vs. HS Time Interval

An identical trend to the one obtained with the **Volume Mean Particle Size Model V1 (Screening)** was obtained with the **Volume Mean Particle Size Model V2 (Screening)**, as seen in **Figure 52**. This finding indicates that the outlier points did not affect the effect of varying the high shear time interval has on the particle size. The accuracy of the **Volume Mean Particle Size Model V2 (Screening)** is represented by the actual values versus the predicted values seen in **Figure 53**.

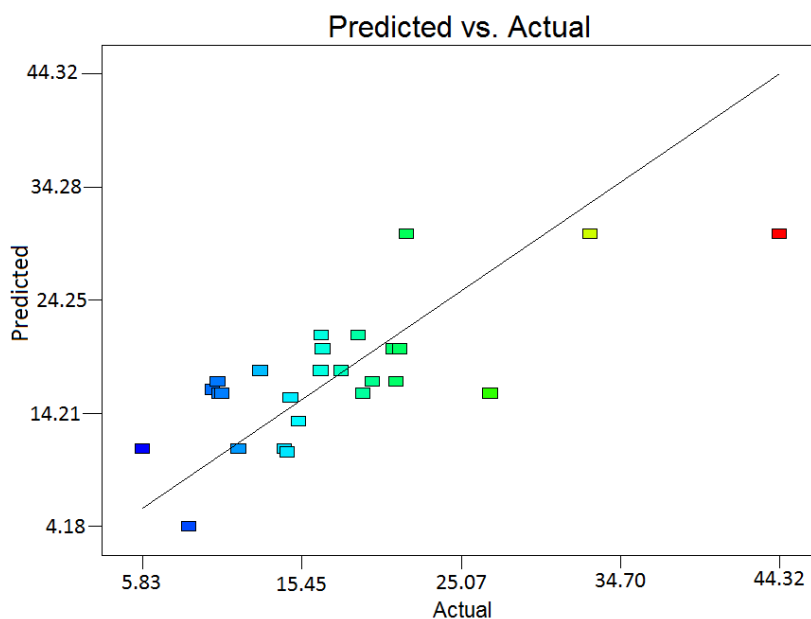


Figure 53 - Volume Mean Particle Size Model V2 (Screening Experimental Design) - Predicted vs. Actual

When comparing **Figure 49** with **Figure 53** it is possible to see that **Figure 53** is more concentrated around the predicted vs. actual line. It should be kept in mind that the p-value of the **Volume Mean Particle Size Model V2 (Screening)** (0.0038) is more than that of the **Volume Mean Particle Size Model V1 (Screening)** (0.0028).

A similar approach that was followed during the 'Screening Experimental Design Volume Mean Particle Size' subsection was followed for the volume median, area mean, area median, number mean and number median's data analysis and results discussion. All the data and discussion can be viewed in Appendix F: Screening Experimental Design Particle Size Results & Discussion.

7.1.1.2 Final Remarks on the Screening Experimental Design - Particle Size Data

In terms of the volume particle size data it was clearly noted that a few large particles had a larger influence on the mean- than on the median particle sizes. This occurrence is due to the median particle size being less affected by outlier particle sizes i.e. a small number of large particles (Lund, Lund 2013, Lund, Lund 2013). The refitted **Volume Mean Particle Size Model V2 (Screening)** which excluded two outlier points is not statistically more significant than the **Volume Mean Particle Size Model V1 (Screening)**. Likewise the **Volume Median Particle Size Model V1 (Screening)** is statistically more significant than the refitted **Volume Median Particle Size Model V2 (Screening)**, which also excluded two outlier points. When comparing the **Volume Mean Particle Size Model V1 (Screening)** with the **Volume Median Particle Size Model V1 (Screening)** it was found that the high shear time interval is not a significant process variable in the **Volume Median Particle Size Model V1 (Screening)**. This could be due to the mean particle size being affected by a small number of large particles which have a tendency to coalesce instead of breaking as time progresses (Fernandez et al. 2004, McClements 2010).

It was clearly noted that the area mean particle size data were less affected by the few large particles that were present in the Screening experimental samples. This was expected as described in **Section 5.3.1.1 – Volume, Area and Number Distribution**. It was noted that the **Area Mean Particle Size Model V1 (Screening)** contains the cooling rate, the stirring speed and the inverting phase addition rate as the significant process variables. An outlier point was removed from the area mean particle size and a quadratic model was refitted to the modified data set. However, the refitted **Area Mean Particle Size Model V2 (Screening)** is not statistically significant ($p > 0.05$). In the case of the area median particle size data, **Area Median Particle Size Model V1 (Screening)** is

not statistically significant ($p > 0.05$). Two outlier points were excluded from the area median data set and a quadratic model was refitted. The **Area Median Particle Size Model V2 (Screening)** is not only statistically significant ($p < 0.05$), but the adjusted- and predicted R-squared values are in reasonable agreement (within 0.2) with each other, which indicates that the model can be used to navigate the design space. **All the data and discussions can be viewed in Appendix F: Screening Experimental Design Particle Size Results & Discussion.**

Finally, in terms of the number particle size data it was evident that the data were only marginally affected by the few large particles present in the Screening experimental samples. Once again this was expected as explained in **Section 5.3.1.1 – Volume, Area and Number Distribution**. The initial reduced quadratic model (**Number Mean Particle Size Model V1 (Screening)**) that was fitted to the number mean particle size data included the cooling rate, the high shear homogenising speed and the temperature as the main process variables that affects the average particle size. However it was noted that there are two outlier points in the number mean particle size data set. A reduced quadratic model was refitted to the modified data set excluding the two outlier points. The **Number Mean Particle Size Model V2 (Screening)** has a higher statistical significance than the previous model. In addition the adjusted- and predicted R-squared values are in reasonable agreement (within 0.2) with each other which indicates that the model can be used to navigate the design space. **All the data and discussion can be viewed in Appendix F: Screening Experimental Design Particle Size Results & Discussion.**

With the number median particle size data it was not possible to fit a reduced quadratic model or any model to the data set. It was noted that there are two outlier points in the number median particle size data set. A reduced quadratic model was fitted to the modified number median data set excluding the two outlier points. The **Number Median Particle Size Model V2 (Screening)** is statistical significant ($p < 0.05$). It was clear that the **Number Median Particle Size Model V2 (Screening)** is very similar to the **Number Mean Particle Size Model V2 (Screening)**. Identical trends were obtained with the **Number Mean Particle Size Model V2 (Screening)** for all of the mixture- and process variables. A summary of the significant process- and formulation (mixture) variables for all the models obtained during the Screening Experimental analysis is presented in **Table 32**.

Table 32 - Comparison of Models' Process- and Formulation Variables

| Model | HS Time Interval [min] | Cooling Rate | Stirring Speed [rpm] | HSH Speed [rpm] | Inverting Phase Addition Rate [l/h] | Temperature [°C] | Surfactant: Wax Ratio |
|--------------------------------|------------------------|--------------|----------------------|-----------------|-------------------------------------|------------------|-----------------------|
| Volume Mean Particle Size V1 | X | X | X | | X | | X |
| Volume Mean Particle Size V2 | X | X | | | | | X |
| Volume Median Particle Size V1 | | X | X | | X | | X |
| Volume Median Particle Size V2 | | X | | | | | X |
| Area Mean Particle Size V1 | | X | X | | X | | X |
| Area Mean Particle Size V2 | | | | | | | |
| Area Median Particle Size V1 | | | X | X | X | | X |
| Area Median Particle Size V2 | X | X | X | X | X | X | X |
| Number Mean Particle Size V1 | | X | | X | | X | X |
| Number Mean Particle Size V2 | X | X | X | X | X | X | X |
| Number Median Particle Size V1 | | | | | | | |
| Number Median Particle Size V2 | X | X | X | X | X | X | X |

Comparisons of the area-, number- and volume mean particle size data and the area-, number- and volume median particle size data are presented in *Figure 54* and *Figure 55*, respectively.

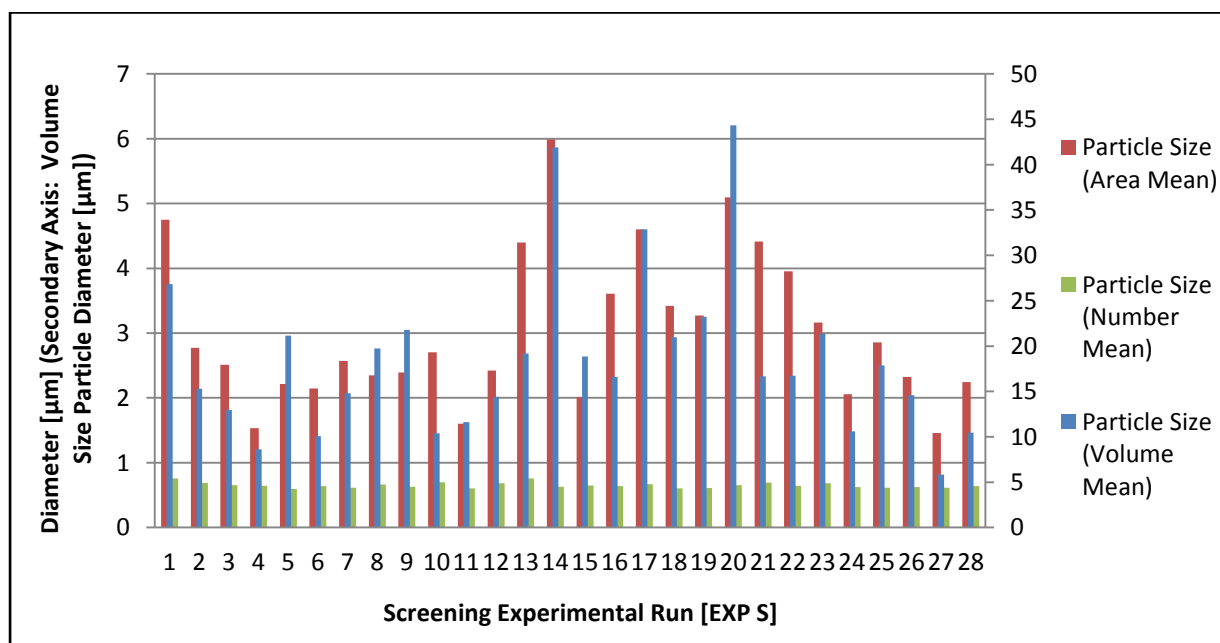


Figure 54 - Area- vs. Number- vs. Volume Mean Particle Size Data Comparison

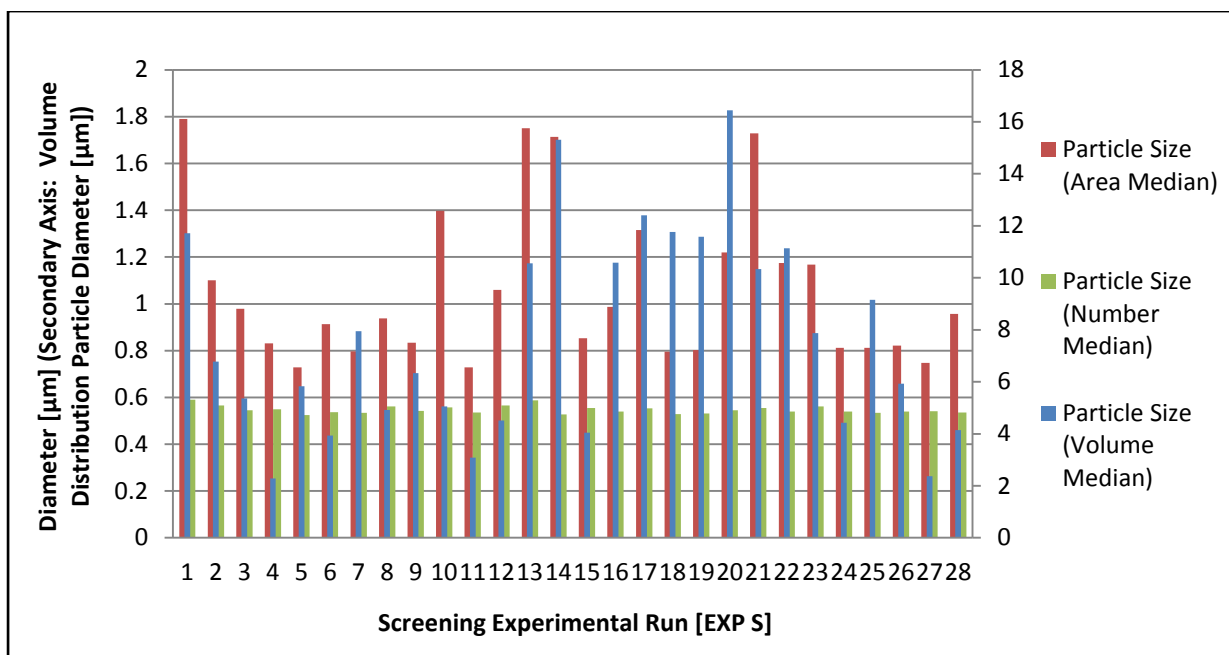


Figure 55 - Area- vs. Number- vs. Volume Median Particle Size Data Comparison

When examining these two figures it noted that the number particle size is the smallest in both the mean- and median particle size data sets. This could indicate that the amount of random large particles differ for each screening experimental run. **EXP S4** had the least amount of large particles present while **EXP S20** had the most, as seen in **Figure 56**.

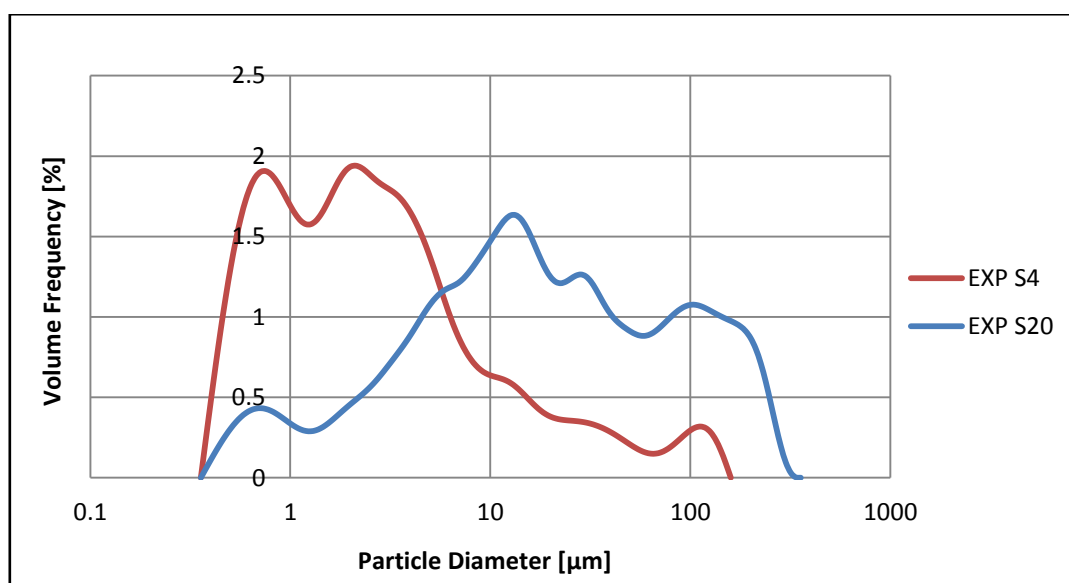


Figure 56 - Comparison of EXP S4 vs. EXP S20

It is also noted that there are no clear trends between the area-, number- and volume particle data sets (both the mean and median) (**Figure 54** and **Figure 55**).

The median in statistics and probability theory is defined as the number separating the higher half of a data sample (population or probability distribution) from the lower half, thus it is the middle point of a number set (*D50*) (Stat-Ease 2010). The mean is defined as the sum of a collection of numbers (data sample, population or probability distribution) divided by the number of numbers in the collection (Stat-Ease 2010).

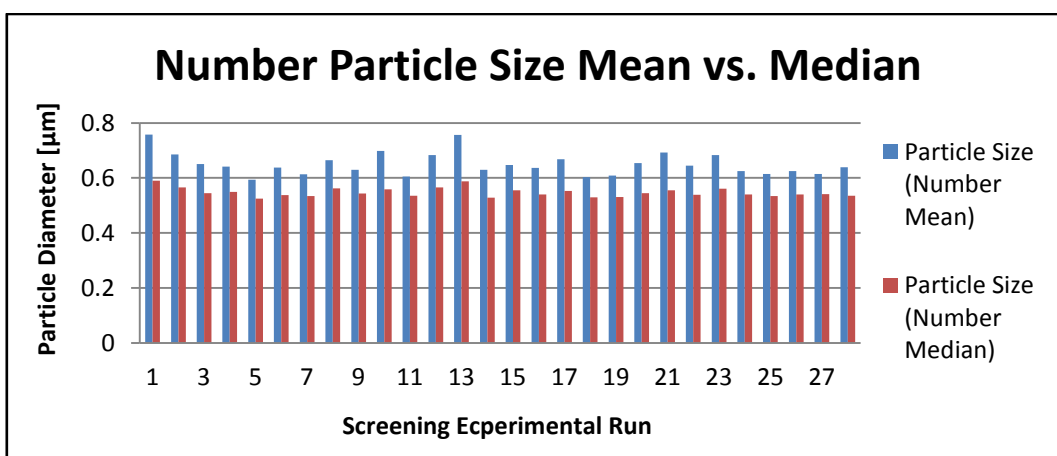
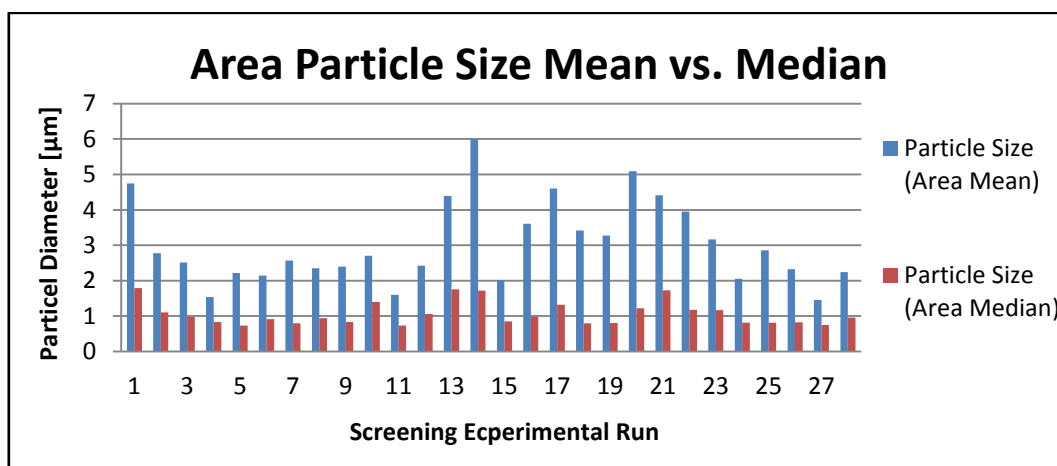
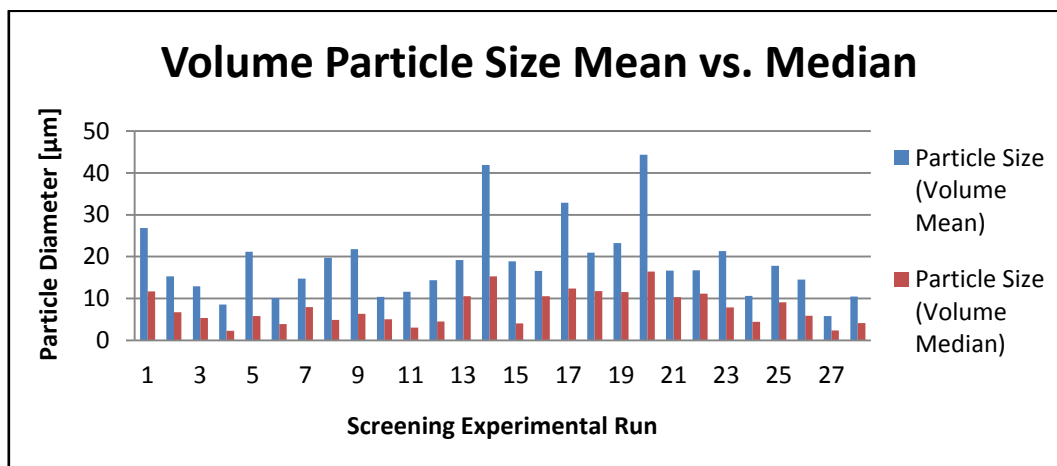


Figure 57 - Mean vs. Median Comparison for the Volume-, Area and Number Particle Size Distributions

Figure 57 is a comparison of the mean and the median for each of the particle size data sets (volume, area and number). It is noted that the difference between the mean and median values of the number particle size data set is the smallest. The difference for the volume particle size data set is the largest. This confirms that the volume mean particle data set takes into account the larger particles and is a more accurate and true representation of the average particle size and – distribution of the emulsions obtained during the screening experiments. The volume-, area- and number particle size data sets for **EXP S4** are compared in **Figure 58** to show the significant difference in the particle size distributions.

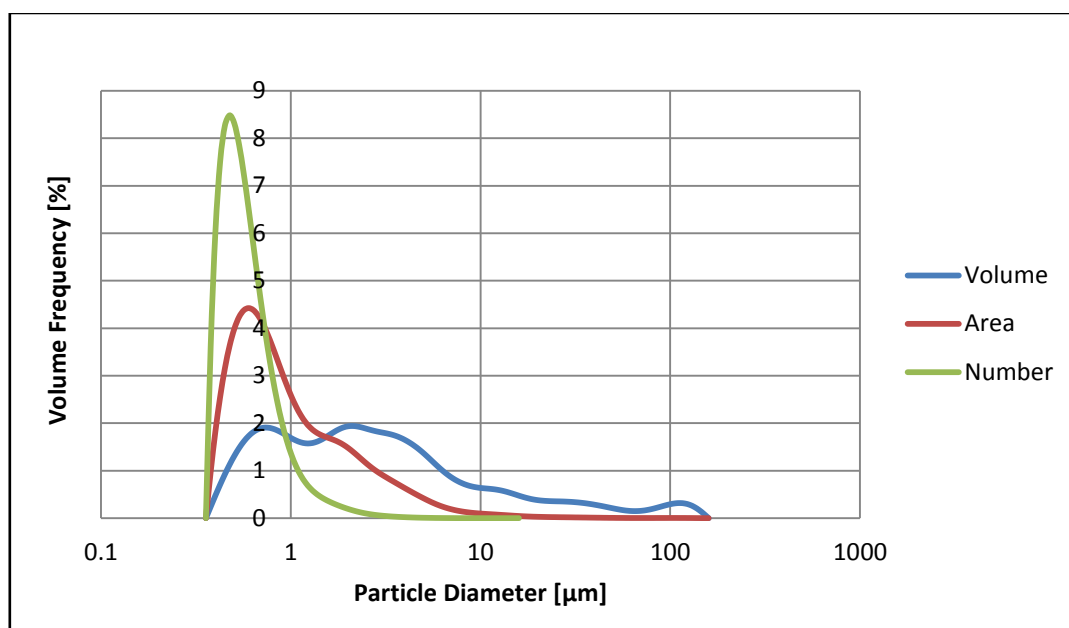


Figure 58 - EXP S4 Volume-, Area- and Number Particle Size Data Sets Comparison

From the results obtained during the particle size data analysis, it is concluded that the **Volume Mean Particle Size Model V2 (Screening)** is the most appropriate model to use for further investigation. This is supported by the fact that large particles are taken into account with the **Volume Mean Particle Size Model V2 (Screening)** and that the trends obtained are supported by literature. Thus, the **Volume Mean Particle Size Model V2 (Screening)** will be used for screening optimization purposes (the yellow highlighted model in **Table 32**). It is kept in mind that the Screening experimental design suffers from aliasing of the factor effect. However, the Screening experimental phase was performed to obtain the best understanding of the process system as a whole.

7.1.2 Roughness

Both the roughness and gloss was included as responses during this study as to not lose critical information of the system, even though they are both directly influenced by the particle size. The *Ra* readings obtained during the screening experimental runs are presented in **Table 33**.

Table 33 - Roughness [Ra] Readings for the Screening Experimental Design

| Experiment | Average [Ra] | STD DEV [Ra] | Significantly Cracked |
|------------|--------------|--------------|-----------------------|
| EXP S1 | 1.847 | 3.689 | Yes |
| EXP S2 | 0.682 | 0.658 | Yes |
| EXP S3 | 0.423 | 0.357 | No |
| EXP S4 | 0.494 | 0.722 | No |
| EXP S5 | 1.266 | 1.375 | Yes |
| EXP S6 | 0.284 | 0.172 | No |
| EXP S7 | 1.477 | 3.418 | Yes |
| EXP S8 | 0.321 | 0.199 | No |
| EXP S9 | 0.414 | 0.279 | Yes |
| EXP S10 | 0.327 | 0.187 | No |
| EXP S11 | 0.291 | 0.258 | No |
| EXP S12 | 0.417 | 0.411 | No |
| EXP S13 | 0.654 | 0.677 | No |
| EXP S14 | 6.244 | 6.075 | Yes |
| EXP S15 | 11.201 | 3.904 | Yes |
| EXP S16 | 11.927 | 3.997 | Yes |
| EXP S17 | 3.678 | 3.994 | Yes |
| EXP S18 | 4.201 | 5.533 | Yes |
| EXP S19 | 5.295 | 6.278 | Yes |
| EXP S20 | 4.332 | 6.080 | Yes |
| EXP S21 | 0.374 | 0.151 | No |
| EXP S22 | 6.043 | 5.952 | Yes |
| EXP S23 | 0.569 | 0.987 | Yes |
| EXP S24 | 0.828 | 1.494 | Yes |
| EXP S25 | 1.64 | 2.311 | Yes |
| EXP S26 | 0.707 | 0.590 | Yes |
| EXP S27 | 0.484 | 0.487 | No |
| EXP S28 | 0.249 | 0.128 | No |
| Control* | | 0.07 | |

* Control – The roughness of the Plexiglas® test plate

From **Table 33** it is clear that a wide range of Ra values were recorded during the analysis of some of the experimental runs e.g. **EXP S15** and **EXP S16**. These values are justified when examining the images of the test samples for both **EXP S15** and **EXP S16** presented in **Figure 59**.



Figure 59 - Roughness Specimens for EXP S15 and S16 (top and bottom, respectively)

These large Ra values are as a result of cracking that occurred during the drying process as presented in **Figure 59**. A possible explanation for the cracking could be as a result of formulation- and process parameter combinations falling outside the operating window (e.g. a low wax content resulting in the final dried coating being dried brittle surfactant that cracks).

When comparing the Ra values obtained in **Table 33** with the values obtained by Chen and Nussinovitch (2001), **Table 34**, it is noted that some of the Ra values recorded with the screening experimental formulations fall within the range of values obtained by Chen and Nussinovitch (Chen, Nussinovitch 2001).

Table 34 - Roughness [Ra] measurements of various wax-hydrocolloid coatings (Chen et al., 2001)

| Coating | Ra |
|----------------------------------|------------------|
| Wax coating* with Xanthan | 0.86 ± 0.07 |
| Wax coating* with Guar | 0.82 ± 0.13 |
| Wax coating* with Locus Bean Gum | 0.89 ± 0.21 |
| Wax coating | 0.84 ± 0.035 |
| Commercial | 0.78 ± 0.035 |
| Control | 0.7 |

In terms of the standard deviations (*STD DEV*) calculated during the roughness analysis (**Table 33**), **EXP S28** (*STD DEV* = 0.128 *Ra*) is the only experimental run that has a *STD DEV* that falls within the ranges published by Chen et al. (2001). However, none of the *STD DEV* recorded for the dried coatings obtained during the screening experimental design fall within the *STD DEV* range recorded by Chen et al. (2001) for pure wax coatings.

The roughness data were entered into the Screening experimental design (**Volume Mean Particle Size Model V2 (Screening)**) in Design Expert© for further processing. Once the screening roughness data were analysed with Design Expert© it was noted that the linear model was not statistically significant ($p > 0.05$), as seen in the ANOVA **Table 35** (validation for the ANOVA assumptions is presented in **Appendix E**).

Table 35 - Roughness (Linear Model) ANOVA

| Analysis of Variance Table – Roughness (Linear Model) | | | | | | |
|---|---------|----|--------|-------|----------|-----------------|
| | Sum of | | Mean | F | p-value | |
| Source | Squares | df | Square | Value | Prob > F | |
| Model | 237.11 | 20 | 11.86 | 4.22 | 0.0584 | not significant |
| Linear Mixture | 9.81 | 2 | 4.91 | 1.75 | 0.2659 | |
| Residual | 14.04 | 5 | 2.81 | | | |
| Lack of Fit | 4.98 | 1 | 4.98 | 2.20 | 0.2124 | not significant |
| Pure Error | 9.06 | 4 | 2.27 | | | |
| Cor Total | 251.15 | 25 | | | | |
| Adeq Precision | 7.92 | | | | | |

A quadratic model was fitted to the roughness data for both the mixture- and process variables. As a result there were various insignificant terms included in the new model. A model reduction was performed to eliminate these insignificant terms. The ANOVA for the reduced quadratic model is presented in **Table 36**.

Table 36 - Roughness (Reduced Quadratic Model) ANOVA

| Analysis of Variance Table – Roughness (Reduced Quadratic Model) | | | | | | |
|--|---------|----|--------|-------|----------|-----------------|
| | Sum of | | Mean | F | p-value | |
| Source | Squares | df | Square | Value | Prob > F | |
| Model | 238.86 | 16 | 14.93 | 10.93 | 0.0005 | significant |
| Residual | 12.29 | 9 | 1.37 | | | |
| Lack of Fit | 3.23 | 5 | 0.64 | 0.28 | 0.8996 | not significant |
| Pure Error | 9.06 | 4 | 2.27 | | | |
| Cor Total | 251.15 | 25 | | | | |
| Adeq Precision | | | | | | |

From **Table 36** it is clear that the reduced quadratic model is statistically significant ($p < 0.05$) to the roughness data. The particle size of the wax emulsions will be classified as the main property. This is supported by the limited research on roughness of edible wax coatings. The R-squared values for the **Roughness Model** are presented in **Table 37**.

Table 37 - Roughness Model - R-Squared Values

| Model | R-Squared | Adj R-Squared | Pred R-Squared |
|------------------------|-----------|---------------|----------------|
| Roughness Model | 0.951 | 0.864 | 0.369 |

The R-squared values for the **Roughness Model** is a clear indication that the model fits well and can be used to navigate the design space. **Figure 60** illustrates the actual measured response value for this observation against the response value predicted by the model for this set of experimental conditions.



Figure 60 - Actual measured response vs. model predicted value

The model and actual values compare fairly well and is expected with an R-squared value of 0.951 and an adjusted R-squared value of 0.864. The relative effect of each factor on the roughness is presented in **Figure 61**. The blue line indicates the lower bound of the 95% confidence interval that surrounds the coefficient estimate for the specific factor while the red line indicates the upper bound of the 95% confidence interval (Stat-Ease 2010).

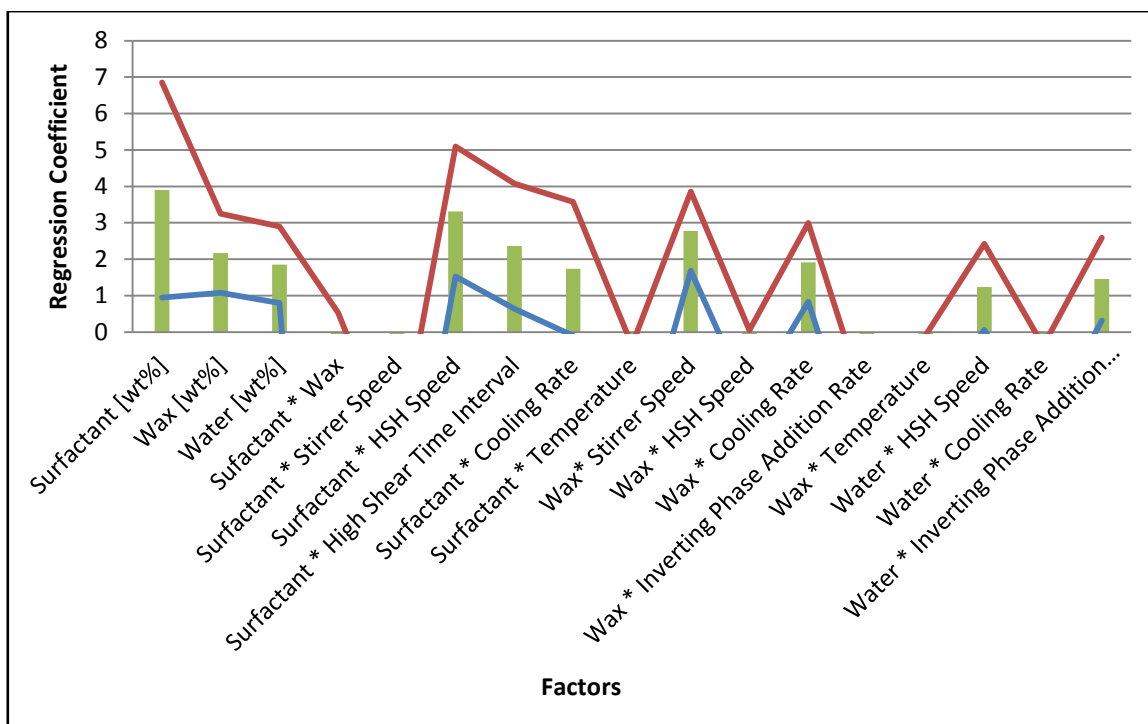


Figure 61 - Relative contribution of factors to the roughness

Figure 61 indicates that the formulation has the biggest influence on the roughness. The high shear homogenizing speed and stirrer speed has the second and third largest effect on the roughness, respectively. The effect of varying the wax-to-surfactant ratio and the temperature on the roughness of the dried edible wax layers is presented in Figure 62.

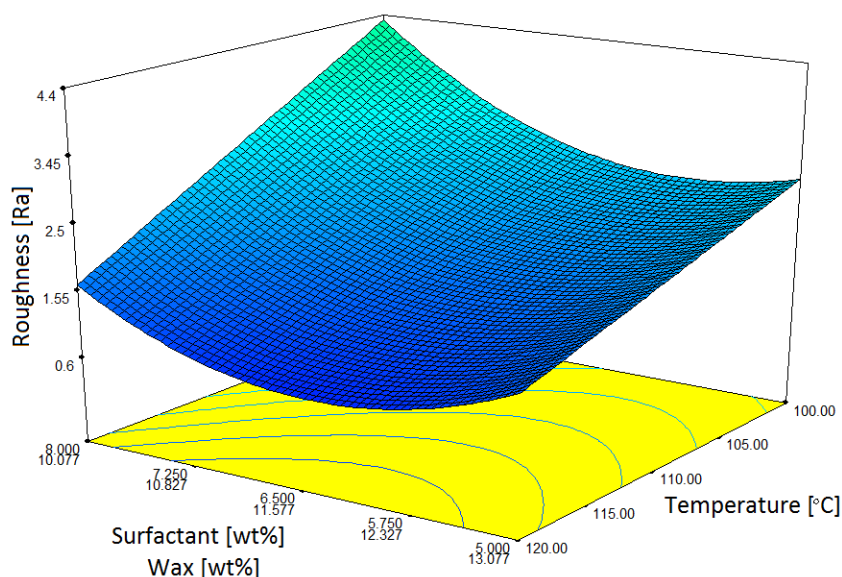


Figure 62 - Volume Mean Particle Size Model V2 (Screening Experimental Design) - Roughness vs. Wax-to-Surfactant Ratio vs. Temperature

From **Figure 62** it is seen that the roughness decreases with an increase in the emulsification temperature. This is expected since an increase in the emulsification temperature results in a decrease in the particle size of the emulsion (Li et al. 2010, Bornfreund 1978). It is also noted that there is an optimum wax-to-surfactant ratio required to achieve a favourable minimum roughness. This optimum wax-to-surfactant ratio is confirmed during the Composite experimental design's results discussion (to follow). The effect of varying the wax-to-surfactant ratio and the stirring speed on the roughness of the dried edible wax layers is presented in **Figure 63**.

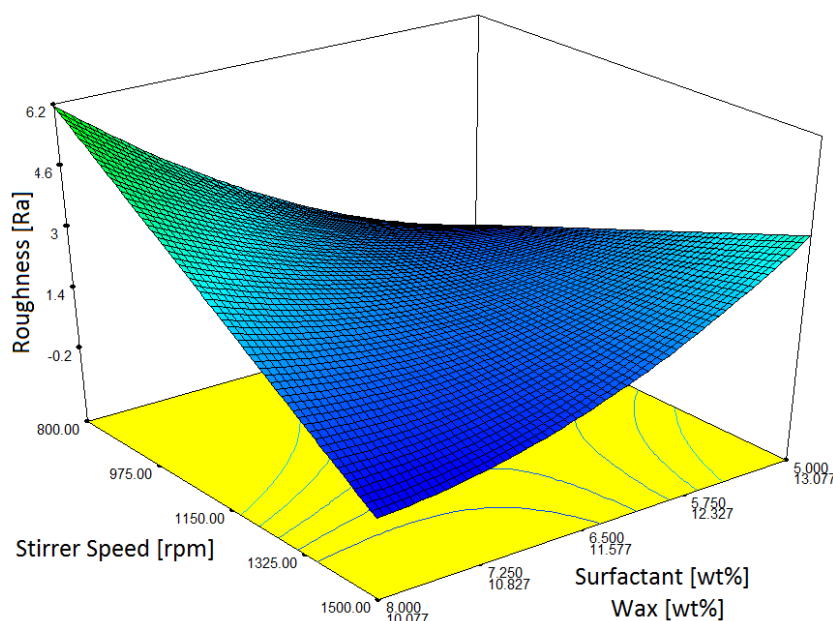


Figure 63 - Volume Mean Particle Size Model V2 (Screening Experimental Design) - Roughness vs. Wax-to-Surfactant Ratio vs. Stirring Speed

It is noted that **Figure 63** is a saddle point. The trends were investigated to obtain more information about the system and not for predictive purposes. At a favourable low wax-to-surfactant ratio, an increase in the stirring speed results in a decrease in the roughness, as seen in **Figure 63**. This finding is indirectly supported by McClements who concluded that an increase in the intensity or duration of the energy input (stirring speed or high shear homogenizing speed) of an emulsification system results in a decrease in particle size, which indirectly will result in a decrease in the roughness (McClements 2010). At an unfavourable high wax-to-surfactant ratio the opposite is observed (**Figure 63**). A possible explanation could be that the emulsion has not inverted at the higher wax-to-surfactant ratio resulting in a water-in-wax emulsion instead of wax-in-water emulsion (Fernandez et al. 2004).

Figure 64 represents a comparison of the roughness data and the volume distribution particle size data. By examining **Figure 64** it is noted that there are no visible trends between the roughness [*Ra*] and the volume particle diameter.

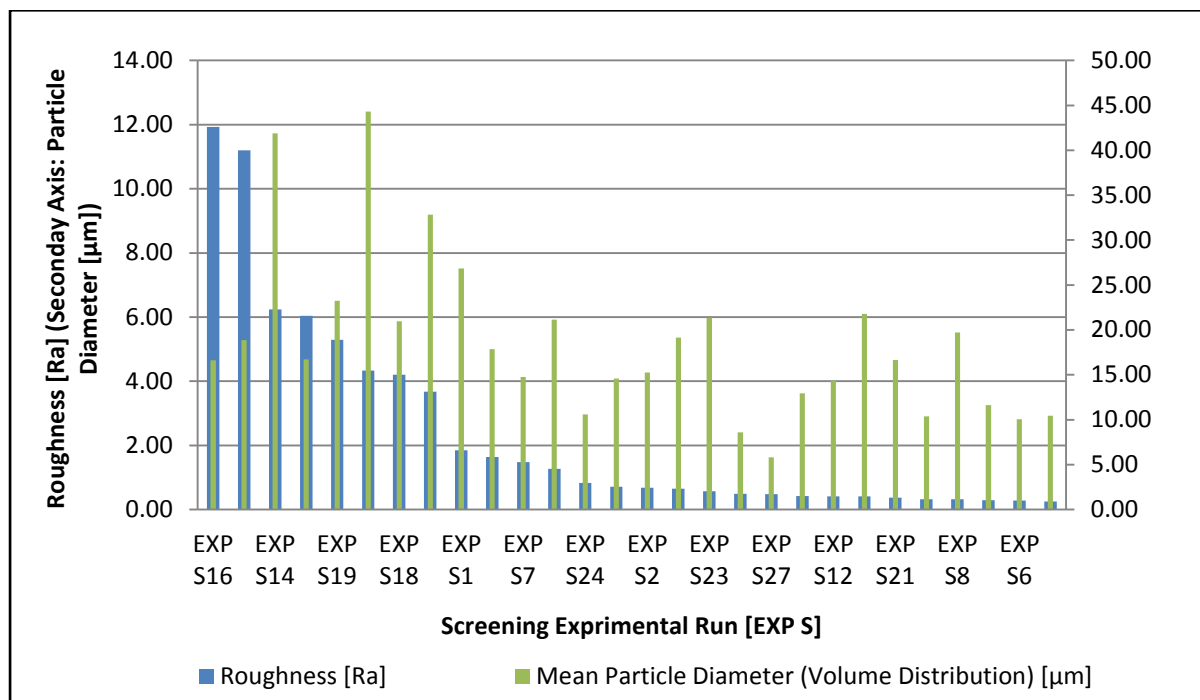


Figure 64 - Roughness Data vs. Volume Distribution Particle Size Data Comparison

7.1.3 Gloss

According to Hagenmaier (1998), experience has shown that a necessary condition for having a good wax coating is that the wax must be prepared as a micro-emulsion, so that when the water evaporated, the emulsion will have a smooth surface (Hagenmaier 1998). The *GU* readings obtained during the screening experimental runs are presented in **Table 38**.

Table 38 - Gloss [GU] Readings for the Screening Experimental Design

| Experiment | Average [GU] | STD DEV [GU] | Significantly Cracked |
|------------|--------------|--------------|-----------------------|
| EXP S1 | 61.540 | 10.761 | Yes |
| EXP S2 | 92.250 | 35.189 | Yes |
| EXP S3 | 67.180 | 38.068 | No |
| EXP S4 | 89.640 | 37.690 | No |
| EXP S5 | 49.400 | 12.982 | Yes |
| EXP S6 | 63.560 | 35.642 | No |
| EXP S7 | 73.220 | 17.905 | Yes |
| EXP S8 | 64.690 | 29.677 | No |
| EXP S9 | 100.340 | 10.084 | Yes |

| Experiment | Average [GU] | STD DEV [GU] | Significantly Cracked |
|------------|--------------|--------------|-----------------------|
| EXP S10 | 33.140 | 15.071 | No |
| EXP S11 | 53.850 | 32.963 | No |
| EXP S12 | 38.470 | 3.490 | No |
| EXP S13 | 30.930 | 15.703 | No |
| EXP S14 | 58.280 | 30.724 | Yes |
| EXP S15 | 75.480 | 38.102 | Yes |
| EXP S16 | 54.220 | 31.717 | Yes |
| EXP S17 | 70.220 | 12.475 | Yes |
| EXP S18 | 65.560 | 32.400 | Yes |
| EXP S19 | 36.590 | 25.642 | Yes |
| EXP S20 | 63.170 | 40.896 | Yes |
| EXP S21 | 43.850 | 29.345 | No |
| EXP S22 | 21.580 | 14.349 | Yes |
| EXP S23 | 83.390 | 21.884 | Yes |
| EXP S24 | 93.220 | 22.969 | Yes |
| EXP S25 | 77.660 | 25.851 | Yes |
| EXP S26 | 61.960 | 18.358 | Yes |
| EXP S27 | 58.440 | 22.883 | No |
| EXP S28 | 48.420 | 19.345 | No |
| Control* | 135 | | |

*** Control – The gloss of the Plexiglas® test plate**

When comparing the gloss measurements obtained during the screening experimental design (**Table 38**) to the values obtained by both Trezza and Krochta (2000) and Bosquez-Molina et al. (2003) (measured at different coating thicknesses), **Table 39** and **Table 40**, it was noted that the gloss readings that were obtained, fall within the range of the published data (Trezza, Krochta 2000, Bosquez-Molina, Guerrero-Legarreta & Vernon-Carter 2003).

Table 39 - The effect of lipid content and storage time on the gloss of lipid containing edible biopolymer coatings (Trezza and Krochta, 2000)

| Coating | Number of Samples | Mean Gloss [GU] |
|-------------------------------|-------------------|-----------------|
| Shellac | 9 | 93 |
| Zein | 3 | 92 |
| Whey Protein Isolate | 13 | 91 |
| Dextrin | 4 | 84 |
| Hydroxypropyl methylcellulose | 4 | 64 |

Table 40 - Gloss of Mesquite based coatings (Bosquez-Molina et al., 2003)

| Coating | Gloss [GU] |
|---------------------------------|------------|
| Mesquite-Candelilla:Mineral oil | 52.1 |
| | 51.6 |
| | 52.2 |
| | 54.3 |
| | 45.7 |
| Mesquite-Candelilla | 43.5 |
| | 41.6 |
| | 45.7 |
| | 22.1 |
| Mesquite-Candelilla:Oleic acid | 31.6 |
| | 32.2 |
| | 22.3 |
| | 38.9 |
| Mesquite-Candelilla:Beeswax | 44.4 |
| | 43.3 |
| | 43.8 |

A possible explanation for the high *GU* values recorded for **EXP S9** and **EXP S24** (the highest recorded *GU* values for the screening experimental design) could be due to a low wax content in both of the emulsions [**EXP S9** = 10 %*Wax*, **EXP S24** = 11.75 %*Wax*) . With a low wax content the surfactant and water content is higher resulting in a more brittle (both **EXP S9** and **EXP S24** were cracked) coating due to the lack of wax. In addition to the lack of wax, the *GU* measurements are not all recorded on a 100% wax layer but dried Oleic acid as well (surfactant is more reflective than wax, thus a higher average *GU* value is recorded). As mentioned in the Roughness Analysis [**Section 7.1.2**], it is clear that there are formulation- and process parameter combinations that fall outside the operating window. The correlations between the volume mean particle size, roughness and gloss are listed in **Table 41**. A correlation value of 1 indicates a 100% positive correlation while a value of -1 indicate a 100% negative correlation and 0 no correlation (Clarke 2012). An effect size of ± 0.5 is considered as **large**, ± 0.3 as **medium** and ± 0.1 as **small**.

Table 41 - Correlations for the screening experimental responses

| | Roughness [Ra] | Gloss [GU] | Particle Size (Volume Mean) [μm] |
|---|----------------|------------|---|
| Roughness [Ra] | 1 | | |
| Gloss [GU] | -0.088 | 1 | |
| Particle Size (Volume Mean) [μm] | 0.372 | 0.007 | 1 |

It is noted that the roughness correlate with the volume mean particle size of the Carnauba wax coatings. The gloss does not correlate well with the volume mean particle size.

The gloss data were entered into the Screening experimental design (**Volume Mean Particle Size Model V2 (Screening)**) in Design Expert© for further processing. Once the screening gloss data were analysed with Design Expert© it was noted that the linear model was not statistically significant ($p > 0.05$), as seen in **Table 42** (validation for the ANOVA assumptions is presented in **Appendix E**).

Table 42 - Gloss (Linear Model) ANOVA

| Analysis of Variance Table - Gloss (Linear Model) | | | | | | |
|---|----------|----|--------|-------|----------|-----------------|
| | Sum of | | Mean | F | p-value | |
| Source | Squares | df | Square | Value | Prob > F | |
| Model | 4331.59 | 6 | 721.93 | 2.407 | 0.0669 | not significant |
| Lack of Fit | 2930.43 | 15 | 195.36 | 0.282 | 0.9683 | not significant |
| Pure Error | 2767.23 | 4 | 691.81 | | | |
| Cor Total | 10029.25 | 25 | | | | |
| Adeq Precision | 5.01 | | | | | |

A quadratic model was fitted to the gloss data for both the mixture- and process variables. In addition a model reduction was also performed to eliminate insignificant terms. The revised model for the gloss data is presented in **Table 43**.

Table 43 - Gloss (Reduced Quadratic Model) ANOVA

| Analysis of Variance Table – Gloss (Reduced Quadratic Model) | | | | | | |
|--|----------|----|--------|-------|----------|-----------------|
| | Sum of | | Mean | F | p-value | |
| Source | Squares | df | Square | Value | Prob > F | |
| Model | 5972.73 | 6 | 995.46 | 4.663 | 0.0045 | significant |
| Residual | 4056.52 | 19 | 213.50 | | | |
| Lack of Fit | 1289.28 | 15 | 85.95 | 0.124 | 0.9989 | not significant |
| Pure Error | 2767.23 | 4 | 691.81 | | | |
| Cor Total | 10029.25 | 25 | | | | |
| Adeq Precision | 7.75 | | | | | |

Examining **Table 43** it is noted that the revised reduced quadratic model is statistically significant ($p < 0.05$) to the gloss data. Once again it should be emphasised that the particle size and – distribution of the edible wax emulsions are considered the main physical characteristic. This is supported by the fact that most of the physical characteristics (including the gloss, roughness, density etc.) are dependent on the particle size and –distribution (Bosquez-Molina, Guerrero-Legarreta & Vernon-Carter 2003, Lin, Zhao 2007). As with the roughness data, there is also limited research on the gloss of edible wax coatings, thus the particle size of the wax emulsions will be classified as the main property.

The R-squared values for the **Gloss Model** are presented in **Table 44**.

Table 44 - Gloss Model - R-Squared Values

| Model | R-Squared | Adj R-Squared | Pred R-Squared |
|-------------|-----------|---------------|----------------|
| Gloss Model | 0.596 | 0.468 | 0.414 |

From the R-squared values it is noted that the R-squared value is not as high as what an accurate model should be. That said, the R-squared and predicted R-squared is relatively close to each other (within < 0.2 of each other) indicating that the model can be used to navigate the design space. Figure 65 illustrates the actual measured response value for this observation against the response value predicted by the model for this set of experimental conditions. Whilst in **Figure 65** the model does not predict the actual values hundred percent accurate, it is of little concern particularly since this is only the screening phase model and should help obtain an understanding of the process system as a whole. This is not the final response surface model.

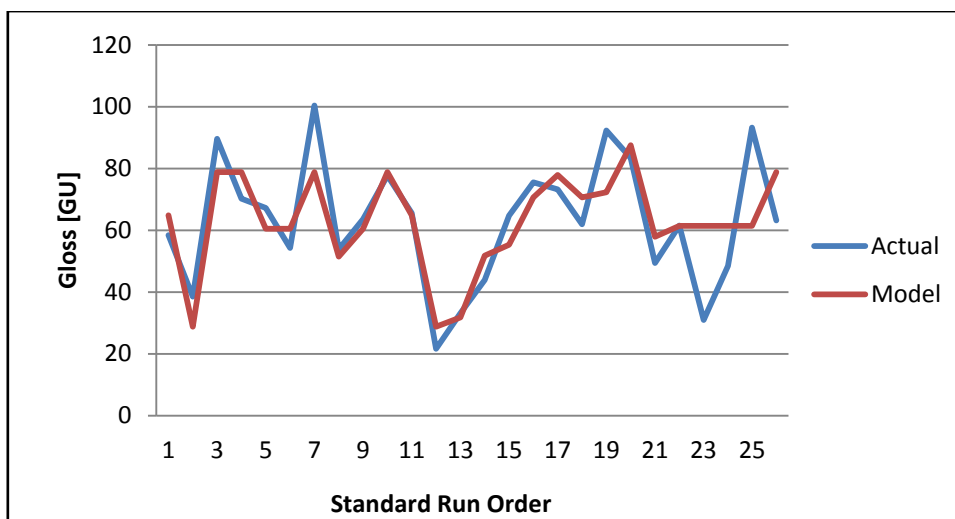


Figure 65 - Actual measured response vs. model predicted value

The relative effect of each factor to the gloss is presented in **Figure 66**. The blue line indicates the lower bound of the 95% confidence interval that surrounds the coefficient estimate for the specific factor while the red line indicates the upper bound of the 95% confidence interval (Stat-Ease 2010).

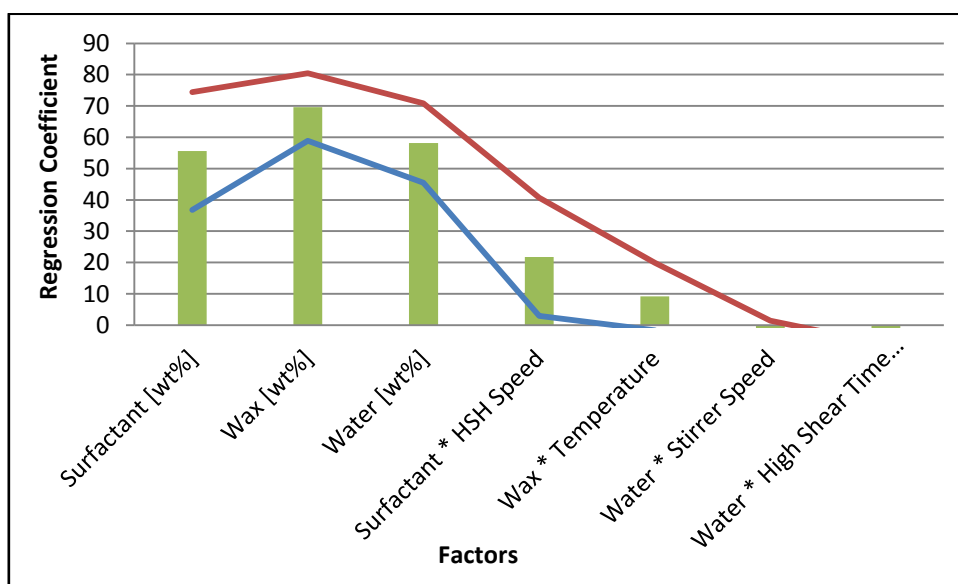


Figure 66 - Relative contribution of the factors to the gloss

The formulation has the biggest influence on the gloss value, followed by the high shear homogenizing speed and temperature. The effect of varying the wax-to-surfactant ratio and the high shear homogenizing speed on the gloss of the dried edible wax layers is presented in **Figure 67**.

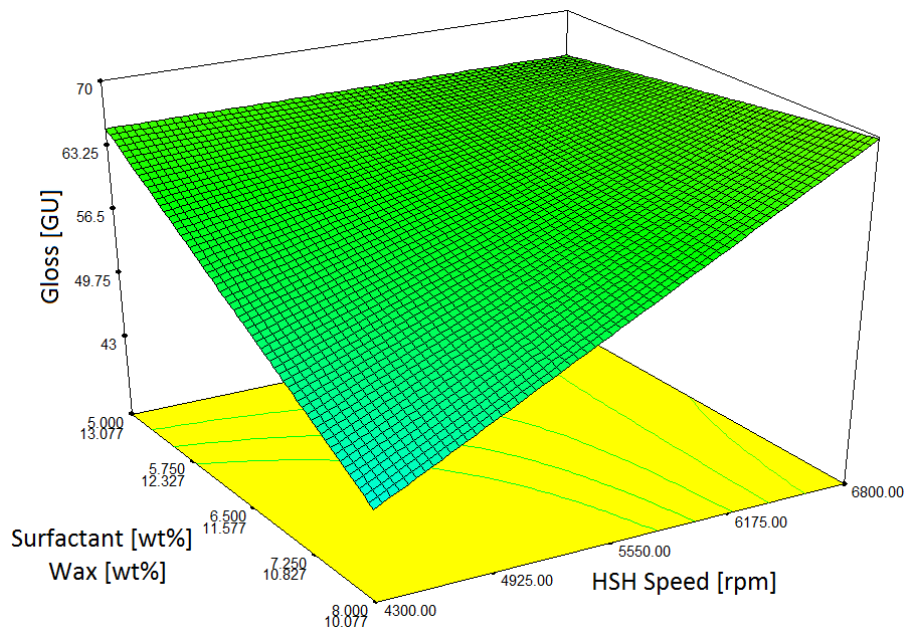


Figure 67 - Volume Mean Particle Size Model V2 (Screening Experimental Design) - Gloss vs. Wax-to-Surfactant Ratio vs. High Shear Homogenizing Speed

By examining **Figure 67** it is clear that at a favourable low wax-to-surfactant ratio, the gloss increases with an increase in the high shear homogenizing speed. This is expected since an increase in the energy input (stirring speed or high shear homogenizing speed) results in a decrease in the particle size, which in return lowers the turbidity of the emulsion and will result in a clearer and more glossier (reflective) dried coating (Gusman 1947, McClements 2010, Sadurní et al. 2005, Chen, Nussinovitch 2001). It is also noted that at a high high sheer homogenizing speed [6800 rpm] the gloss decreases with an increase in wax-to-surfactant ratio. A possible explanation could be due to the higher amount of surfactant resulting in the gloss measurements being taken on dried surfactant (higher reflectivity) instead of dried wax.

The effect of varying the high shear time interval on the gloss of the dried coatings is presented in **Figure 68**.

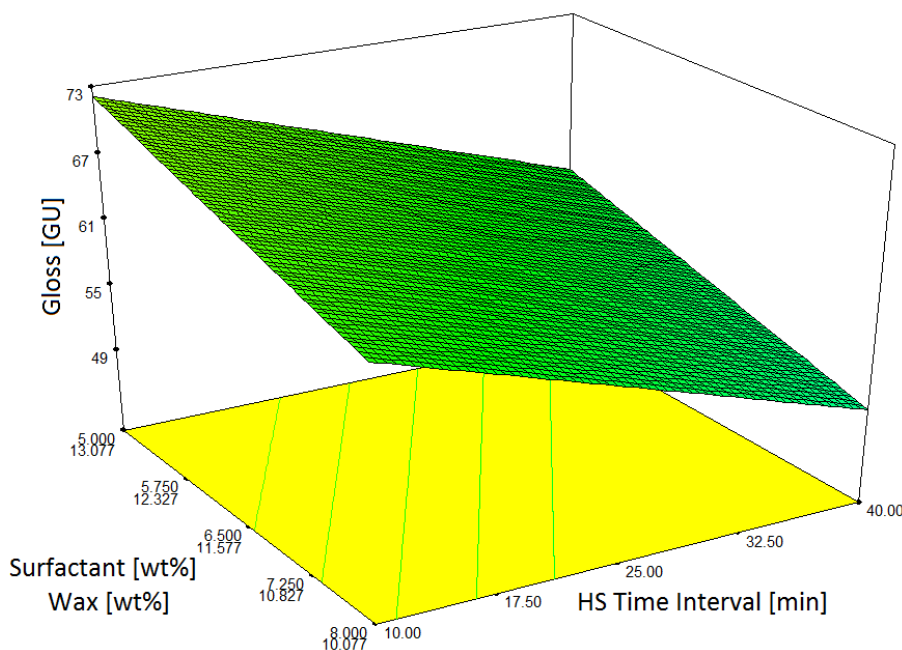


Figure 68 - Volume Mean Particle Size Model V2 (Screening Experimental Design) 0 Gloss vs. Wax-to-Surfactant Ratio vs HS Time Interval

From **Figure 68** it is noted that an increase in the high shear time interval decreases the gloss of the dried coatings. This could possibly be due to the wax being burnt as a result of being exposed to heating for a longer period of time. The burnt wax forms a more turbid emulsion and a less glossy dried coating. **Figure 69** represents a comparison of the gloss- [GU] and the volume mean particle size data sets. There are no visible trends between these two data sets, as seen in **Figure 69**.

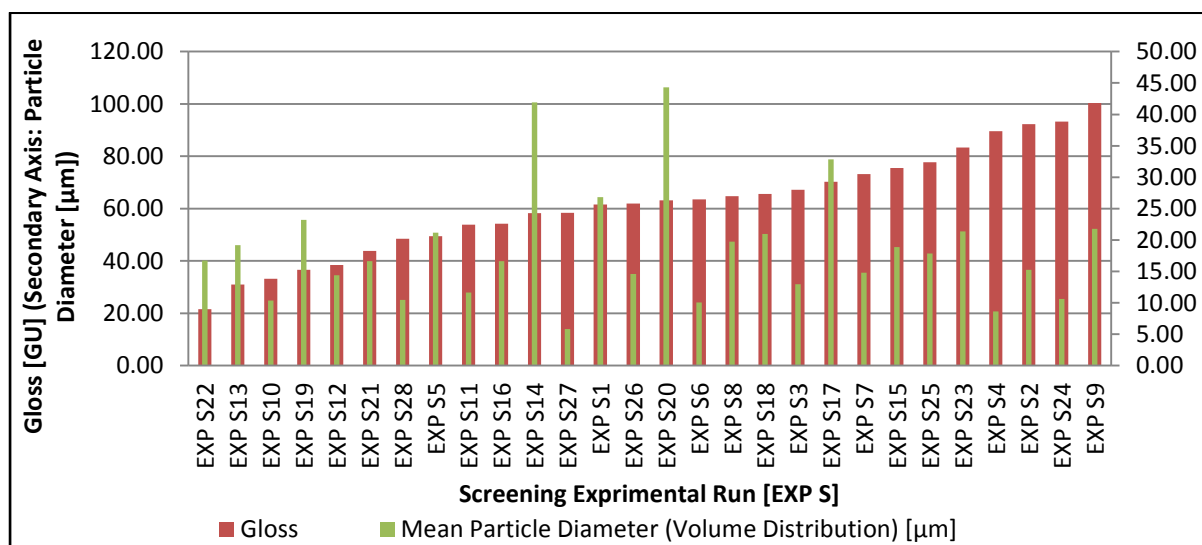


Figure 69 - Gloss Data vs. Volume Distribution Particle Size Data Comparison

A comparison of the gloss- and the roughness data sets is presented in **Figure 70**.

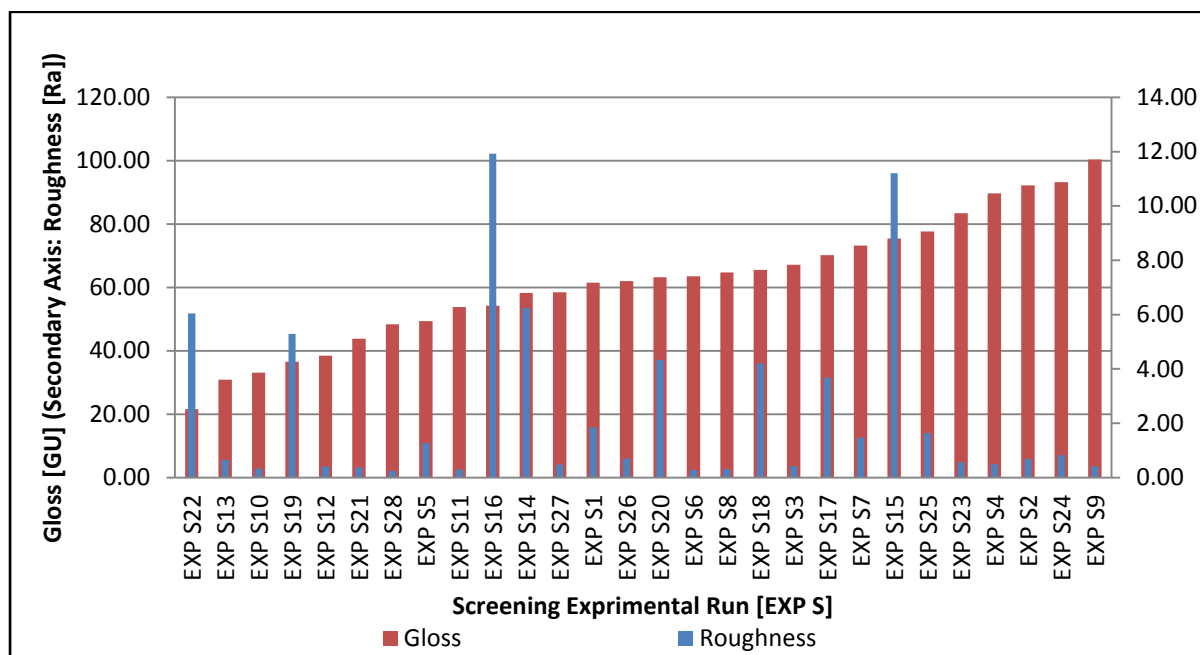


Figure 70 - Gloss Data vs. Roughness Data Comparison

From **Figure 70** it is noted that there are no visible trends between the gloss- and roughness data sets that were recorded during the screening experimental design analysis. It should be kept in mind that the screening experimental design experiments are purely for screening purposes. From the Particle Size discussion [**Section 7.1.1**] it was already noted that there are formulation- and process parameter combinations that fall outside the operating window. This could explain the lack of trends between the various responses.

7.1.4 Viscosity, pH and Density

The dynamic viscosity, pH and density were measured for each of the edible coating formulations. The viscosity was measured with a MCR 501 Rheometer (Anton Paar©). A digital pH-meter, which compensates for effect of temperature, was used in accordance with an *EC620131* glass-body, open pore, for polymer gel applications, pH electrode (Eutech Instruments©). Three pH measurements were recorded for each formulation. The density was measured with a calibrated density flask with a fixed volume of *24.873 ml*. Ten measurements were recorded for each formulation at a temperature of 20°C. The viscosity, pH and density readings for the screening experimental runs are presented in **Table 45**.

Table 45 - Viscosity, pH and Density Readings for the Screening Experimental Design

| Experiment | Viscosity [mPa.s] | pH | Density [kg/m^3] |
|------------|-------------------|-------|----------------------|
| EXP S1 | 3.636 | 10.20 | 996.516 |
| EXP S2 | 3.761 | 10.21 | 996.632 |
| EXP S3 | 5.904 | 10.08 | 996.938 |
| EXP S4 | 5.224 | 10.17 | 996.713 |
| EXP S5 | 5.296 | 10.11 | 997.158 |
| EXP S6 | 6.435 | 10.18 | 996.702 |
| EXP S7 | 3.967 | 10.17 | 995.848 |
| EXP S8 | 6.068 | 10.05 | 996.524 |
| EXP S9 | 3.392 | 10.17 | 996.273 |
| EXP S10 | 5.958 | 10.14 | 996.805 |
| EXP S11 | 6.174 | 10.08 | 996.667 |
| EXP S12 | 4.053 | 10.26 | 996.776 |
| EXP S13 | 3.853 | 10.35 | 996.580 |
| EXP S14 | 5.979 | 10.29 | 995.109 |
| EXP S15 | 6.747 | 10.21 | 996.222 |
| EXP S16 | 5.670 | 10.31 | 995.331 |
| EXP S17 | 5.556 | 10.36 | 995.433 |
| EXP S18 | 8.18 | 10.26 | 995.324 |
| EXP S19 | 7.885 | 10.38 | 994.739 |
| EXP S20 | 6.552 | 10.27 | 995.036 |
| EXP S21 | 4.026 | 10.27 | 996.882 |
| EXP S22 | 5.652 | 10.33 | 995.541 |
| EXP S23 | 6.544 | 10.14 | 996.165 |
| EXP S24 | 6.383 | 10.23 | 995.582 |
| EXP S25 | 6.331 | 10.11 | 996.060 |
| EXP S26 | 6.125 | 10.22 | 995.421 |
| EXP S27 | 5.833 | 10.24 | 996.246 |
| EXP S28 | 6.417 | 10.22 | 996.220 |

When comparing the pH and density values obtained during the screening experimental design (**Table 45**) to the values published by Hagenmaier (1995) and the specifications of the commercial Citrosol® and DECC Citrashine® Carnauba wax emulsions, it is possible to see that the values obtained during the screening experimental runs fall within their ranges. Citrosol® has a pH of 9.9 – 10.9 and a density of 995 – 1010 kg/m^3 while DECC Citrashine® has a pH of 9 – 11. An alternative product from Citrosol® containing polyethylene wax has a pH of 8.5 – 10.1 and a density of 1000 – 1014 kg/m^3 (Documentation can be viewed in **Appendix A**). Hagenmaier (1998) stated in his study on micro-emulsion formulations that the pH of Carnauba wax emulsions manufactured with the pressure cell method should be between 9.2 – 10.6 (Hagenmaier 1998).

Thus, the pH values obtained during the Screening experimental design fall within the range stated by Hagenmaier.

The viscosity, pH and density data were entered into the Screening experimental design in Design Expert® for further processing. Once the data were analysed for each product characteristic with Design Expert®, it was noted that the linear model was not statistically significant ($p > 0.05$), as seen in **Table 46**.

Table 46 - Viscosity, pH and Density (linear Model) ANOVA

| Analysis of Variance Table – Dynamic Viscosity (Linear Model) | | | | | | |
|---|---------|----|--------|-------|----------|-----------------|
| | Sum of | | Mean | F | p-value | |
| Source | Squares | df | Square | Value | Prob > F | |
| Model | 1.575 | 2 | 0.788 | 0.443 | 0.6477 | not significant |
| Residual | 40.925 | 23 | 1.780 | | | |
| Lack of Fit | 28.365 | 19 | 1.493 | 0.475 | 0.8797 | not significant |
| Pure Error | 12.560 | 4 | 3.140 | | | |
| Cor Total | 42.500 | 25 | | | | |
| Adeq Precision | 1.594 | | | | | |

| Analysis of Variance Table – pH (Linear Model) | | | | | | |
|--|---------|----|--------|-------|----------|-----------------|
| | Sum of | | Mean | F | p-value | |
| Source | Squares | df | Square | Value | Prob > F | |
| Model | 0.076 | 6 | 0.013 | 1.387 | 0.2703 | not significant |
| Residual | 0.175 | 19 | 0.009 | | | |
| Lack of Fit | 0.145 | 15 | 0.010 | 1.325 | 0.4297 | not significant |
| Pure Error | 0.029 | 4 | 0.007 | | | |
| Cor Total | 0.251 | 25 | | | | |
| Adeq Precision | 4.345 | | | | | |

| Analysis of Variance Table – Density (Linear Model) | | | | | | |
|---|---------|----|--------|-------|----------|-----------------|
| | Sum of | | Mean | F | p-value | |
| Source | Squares | df | Square | Value | Prob > F | |
| Model | 0.530 | 2 | 0.265 | 0.741 | 0.4875 | not significant |
| Residual | 8.224 | 23 | 0.358 | | | |
| Lack of Fit | 6.387 | 19 | 0.336 | 0.732 | 0.7171 | not significant |
| Pure Error | 1.837 | 4 | 0.459 | | | |
| Cor Total | 8.754 | 25 | | | | |
| Adeq Precision | 1.935 | | | | | |

A reduced quadratic model was fitted to the viscosity, pH and density data for both the mixture- and process variables. The revised models are presented in **Table 47**.

Table 47 - Viscosity, pH and Density (Reduced Quadratic Model)

| Analysis of Variance Table – Viscosity (Reduced Quadratic Model) | | | | | | |
|--|---------|----|--------|-------|----------|-----------------|
| | Sum of | | Mean | F | p-value | |
| Source | Squares | df | Square | Value | Prob > F | |
| Model | 7.436 | 3 | 2.479 | 1.555 | 0.2285 | not significant |
| Pure Error | 12.560 | 4 | 3.140 | | | |
| Cor Total | 42.500 | 25 | | | | |
| Adeq Precision | 4.087 | | | | | |

| Analysis of Variance Table – pH (Reduced Quadratic Model) | | | | | | |
|---|---------|----|--------|-------|----------|-----------------|
| | Sum of | | Mean | F | p-value | |
| Source | Squares | df | Square | Value | Prob > F | |
| Model | 0.222 | 21 | 0.011 | 1.444 | 0.3945 | not significant |
| Pure Error | 0.029 | 4 | 0.007 | | | |
| Cor Total | 0.251 | 25 | | | | |
| Adeq Precision | 4.788 | | | | | |

| Analysis of Variance Table – Density (Reduced Quadratic Model) | | | | | | |
|--|---------|----|--------|-------|----------|-----------------|
| | Sum of | | Mean | F | p-value | |
| Source | Squares | df | Square | Value | Prob > F | |
| Model | 0.530 | 2 | 0.265 | 0.741 | 0.4875 | not significant |
| Pure Error | 1.837 | 4 | 0.459 | | | |
| Cor Total | 8.754 | 25 | | | | |
| Adeq Precision | 1.935 | | | | | |

Examining **Table 47** one can see that the revised reduced quadratic models are also not statistically significant ($p > 0.05$) to the viscosity, pH and density data. For the purpose of this study the viscosity, pH and density will be used to determine whether it falls in range of the commercial coatings and the values published by Hagenmaier on Carnauba wax coatings. It will not be used for optimization purposes.

7.1.5 Temperature and Pressure

During the literature study on edible wax coatings it was stated by various authors that a pressure drop occurs at the phase inversion point (Hagenmaier, Baker 1994, Baciú, Moşescu & Nan 2008). Hagenmaier (1994) stated that as the continuous phase (water) is added to the wax and surfactant mixture during the Pressure method, the viscosity gradually increases and then decreases as the inversion point is passed (Hagenmaier, Baker 1994). Baciú (2008) confirms this finding by stating that at the phase inversion point in any case, both liquids must be at intimate contact and the pressure drop peak (associated with phase inversion) can be evaluated with emulsion viscosity models (Baciú, Moşescu & Nan 2008). It is also stated that near the phase inversion, the rheological characteristics of the dispersion and the associated pressure drop changes abruptly and significantly (Baciú, Moşescu & Nan 2008). It was noted during the Screening experimental design experiments that a pressure drop occurred during the emulsion inversion point, as seen in **Figure 71** (pressure is presented as bar guage).

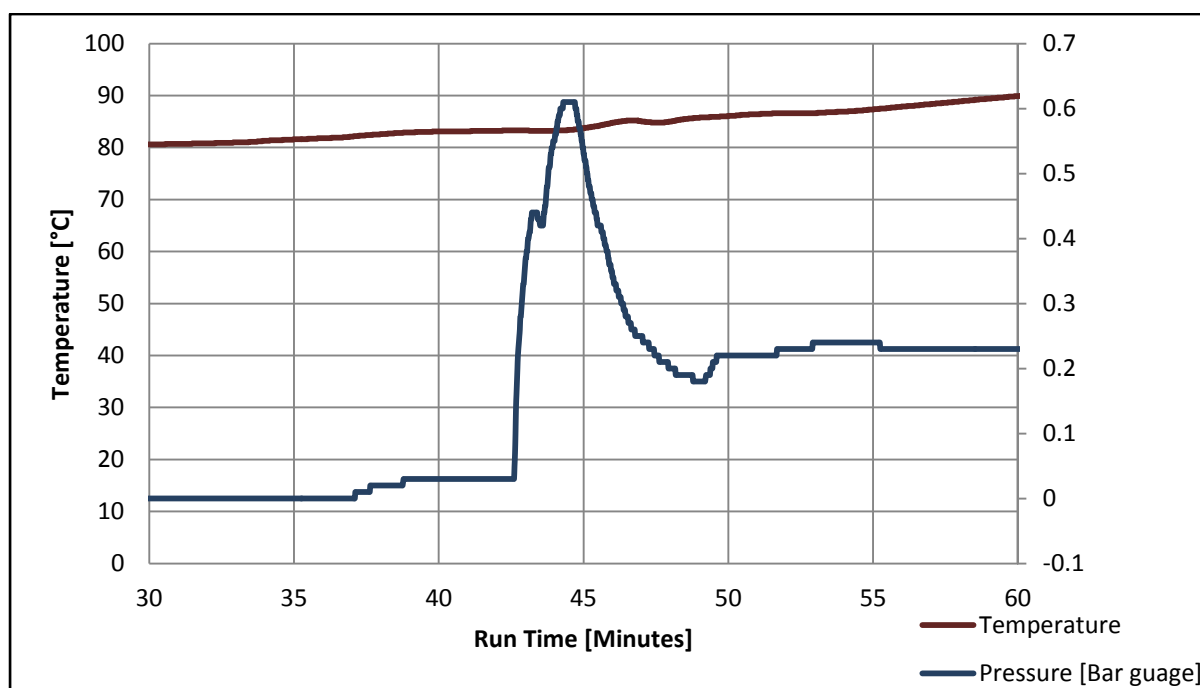


Figure 71 - Temperature and Pressure Curve - EXP S27

At a run time of 45 mins there is a clear pressure peak visible in **Figure 71**. At this pressure peak the Carnuba wax emulsion was inverted from a water-in-wax emulsion to a wax-in-water emulsion. Due to this inversion, the rheology of the emulsion changes abruptly and the pressure drops significantly [e.g. at 48 mins] (Hagenmaier, Baker 1994, Baciú, Moşescu & Nan 2008).

7.1.6 Optimization

The Screening experimental design (**Volume Mean Particle Size Model V2 (Screening)**) was optimized in terms of the particle size, roughness and gloss. The viscosity, pH and density were excluded since their models were not statistically significant. The particle size was set as the most significant factor, the gloss as the second most significant- and the roughness as the third most significant factor. This is in accordance with Guitierrez (2008) who stated that, in general, optimization is directed to obtain minimum droplet size and/or minimum polydispersity (Gutiérrez et al. 2008). In addition, Berkman and Egloff (1941) and Griddin (1945) states that that the stability of an emulsion is indicated, among other factors, by the presence of small globules and that the larger the particle size, the greater is the tendency to coalescence and increase in particle size (Griffin 1945)(Berkman, Egloff 1941).

The idea of optimization is to find the best set of trade-offs to satisfy the goals that are set (Stat-Ease 2010). For the purpose of this study the main goals will be to minimize the particle size, maximize the gloss and minimize the roughness of the Carnuba wax emulsion. Desirability is based on how well the specified goals are met and the closer the goals are met, the higher the desirability number will be. The desirability objective function is as follow:

$$D = (d_1 \times d_2 \times \dots \times d_n)^{\frac{1}{n}} = \left(\prod_{i=1}^n d_i \right)^{\frac{1}{n}}$$

(Stat-Ease 2010)

The reliability of the results from the optimization depends on the validity of the predictive models. It is assumed that the predictive models are valid and that the optimized process variables are useable to predict the optimum mixture during the Mixture experimental design. The system was optimized according to three different particle size (main response) output goals. These outputs are the target-, minimizing- and step response outputs. The outputs are presented in **Figure 72**, **Figure 73** and **Figure 74**, respectively.

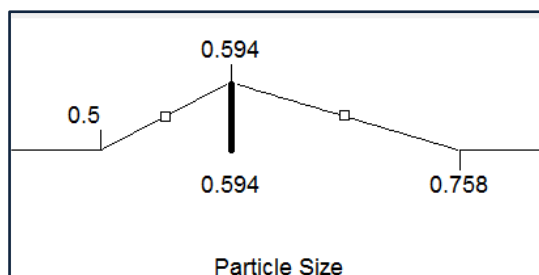


Figure 72 - Target Response Output

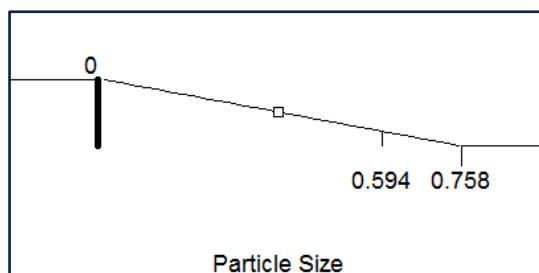


Figure 73 - Minimizing Response Output

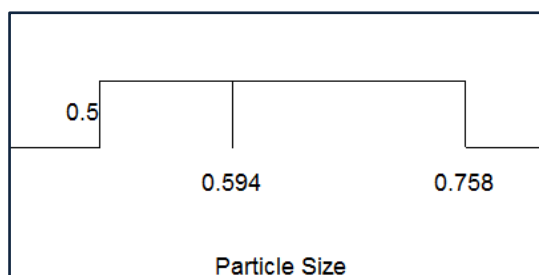


Figure 74 - Step Response Output

It should be emphasised at this point that the Screening experimental design was performed and optimized to obtain an understanding of the process system as a whole in the shortest time and the most economical way. Once the screening experimental data were optimized, it was noted that the optimum mixture was not included in the mixture design ranges (results can be viewed in **Appendix G**). In order to determine the optimum mixture, the process parameters were optimized so that mixture design experiments could be performed, while keeping the process parameters constant at their optimum settings thus far. With the purpose of having to optimize the process parameters it was assumed that there are no interactions between the process- and the mixture variables. The process parameters' optimization results from the three response outputs are presented in **Table 48**.

Table 48 - Optimization Results - Screening Experimental Design

| Stirrer Speed [rpm] | HSH Speed [rpm] | HS Time [min] | Cooling Rate | Inverting Phase AR [l/hr] | Temperature [°C] | Desirability |
|---------------------|-----------------|---------------|--------------|---------------------------|------------------|--------------|
| 808.22 | 6799.94 | 10.00 | 0.448 | 3.025 | 120.000 | 0.649 |
| 800.63 | 6799.91 | 10.27 | -1.000 | 3.023 | 119.773 | 0.865 |
| 800.01 | 6799.97 | 10.00 | -0.676 | 3.010 | 120.000 | 0.547 |
| 800.01 | 6693.57 | 10.00 | -0.271 | 3.019 | 120.000 | 0.929 |
| 812.11 | 6799.97 | 10.29 | 0.303 | 3.000 | 119.982 | 0.510 |
| 800.49 | 6799.81 | 10.44 | -0.159 | 3.000 | 120.000 | 0.760 |
| 801.82 | 6799.92 | 10.00 | 0.146 | 3.000 | 120.000 | 0.761 |
| 800.00 | 6799.90 | 10.00 | -0.960 | 3.013 | 120.000 | 0.858 |
| 800.63 | 6799.91 | 10.27 | -1.000 | 3.023 | 119.773 | 0.904 |
| 816.63 | 6799.99 | 10.00 | 0.384 | 3.020 | 120.000 | 0.802 |
| 800.00 | 6799.80 | 10.01 | -0.072 | 3.020 | 119.994 | 0.916 |
| 800.00 | 6798.90 | 10.00 | -0.025 | 3.004 | 120.000 | 0.929 |
| 800.00 | 6800.00 | 10.00 | 0.871 | 3.105 | 119.995 | 0.678 |
| 800.63 | 6799.91 | 10.27 | -1.000 | 3.023 | 119.773 | 0.865 |
| 823.62 | 6799.99 | 10.94 | -1.000 | 3.000 | 120.000 | 0.509 |
| 800.63 | 6799.91 | 10.27 | -1.000 | 3.023 | 119.773 | 0.648 |
| 800.04 | 6800.00 | 10.00 | -0.753 | 3.012 | 120.000 | 0.570 |
| 800.00 | 6710.65 | 10.00 | -0.802 | 3.068 | 120.000 | 0.929 |
| 800.00 | 6799.99 | 10.32 | 0.591 | 3.023 | 120.000 | 0.822 |

The three response outputs yielded similar results with the exception being the cooling rate, as seen in **Table 48**. The variation in the cooling rate could be due to it not being a significant process factor. For the purpose of optimizing the process parameters to perform formulation experiments, the cooling rate was kept at 1 (cooling water full). This decreased the experimental run time making it possible to perform a full mixture design. The optimized process parameters that were used to perform the formulation experiments are as follow (**Table 49**):

Table 49 - Screening Experimental Design - Optimized Process Parameters

| Process Parameter | Setting |
|--------------------------|---------|
| Stirrer Speed [rpm] | 800 |
| HSH Speed [rpm] | 6800 |
| HS Time Interval [min] | 10 |
| Cooling Rate [-1/0/1] | 1 |
| Inverting Phase AR [l/h] | 3 |
| Temperature [°C] | 120 |

The optimized formulation parameters that were obtained through the optimization of the screening experimental data are as follow (**Table 50**):

Table 50 - Screening Experimental Design - Optimized Formulation Parameters

| Formulation Parameter | Setting |
|------------------------------|----------------|
| Wax Content [wt%] | 10 |
| Water Content [wt%] | 85 |
| Surfactant Content [wt%] | 5 |

Due to the wax-, water- and surfactant content falling at the limits of the experimental ranges (wax content = 10 – 15%, water content = 80 – 85% and surfactant content = 5 – 8%) it is an indication that the optimum mixture do not fall within the ranges specified for the Screening experimental design. Since the optimum mixture was not included in the mixture ranges of the Screening experimental design, no further optimization was performed on the Screening experimental design results.

Additional assumptions were made during the experimental phase. They are as follow:

- It was assumed that the predictive models were valid and that the optimized process variables (obtained during the Screening experimental design) were statistically significant enough to predict the optimum mixture during the Mixture experimental design.
- It was assumed that there are no significant interactions between the composition- and process variables during the Screening Experimental Design optimization.

A similar approach that was followed with the Screening Experimental Design was followed with the Mixture Experimental Design and the Composite Experimental Design.

7.2 Formulation Experimental Phase

7.2.1 Mixture Experimental Design

Once the data from the screening experiments were entered into Design Expert®, it was found that the ranges of the components (%water, %wax and %surfactant), did not include the optimal formulation. This was as a result of the oleic acid, ammonium hydroxide and potassium hydroxide being fixed at a certain ratio obtained from literature, which was not necessarily the optimal ratio for the experimental setup (bench scale pilot plant) being used. However, in terms of the process variables, it was clear which variables had a significant impact and which ones could be set at a fixed setting for the experimental runs that would follow. The ranges were determined from literature and observations made during the experimental runs that were performed thus far. To ensure that the correct ranges and combinations were tested, the following constraints were enforced on the ranges:

1. $0 \leq \%Oleic\ acid - \%Ammonium\ hydroxide$
2. $\%Oleic\ acid - 4 * Ammonium\ hydroxide \leq 0$

These constraints were obtained from the information acquired from literature and the experimental data obtained thus far. Due to the focus being on the surfactant composition (%Oleic acid : %Ammonium hydroxide : %Potassium hydroxide), the ratio of Oleic acid to Ammonium hydroxide was examined for all the formulations obtained from literature and those tested during the commissioning- and screening runs. The ratio of Oleic acid : Ammonium hydroxide determines the amount of oleates formed, thus determining whether or not the emulsion is inverted or not. The recorded Oleic acid : Ammonium hydroxide ratios are presented in **Table 51**.

Table 51 - Oleic Acid : Ammonium Hydroxide Ratios

| Formulation | Oleic Acid : Ammonium Hydroxide Ratio |
|---------------------------------|---------------------------------------|
| Hagenmaier et al. Formulation 1 | 1.67 |
| Hagenmaier et al. Formulation 2 | 1.5 |
| Hagenmaier et al. Formulation 3 | 1.32 |
| Commissioning Experiments | 2.9 |
| Screening Experiments | 2.13 |

An Oleic acid-to-Ammonium hydroxide ratio range of 1 – 4 was tested during the Mixture design experiments. It was assumed that the optimal formulation would lie in between these two limits. The final Mixture experimental design is presented in **Table 52**.

Table 52 - Mixture Experimental Design

| Experiment | Water [wt%] | Wax [wt%] | Oleic Acid [wt%] | Potassium Hydroxide [wt%] | Ammonium Hydroxide [wt%] |
|------------|-------------|-----------|------------------|---------------------------|--------------------------|
| 1 | 78.50 | 15.00 | 3.00 | 0.50 | 3.00 |
| 2 | 76.82 | 15.47 | 4.07 | 1.08 | 2.56 |
| 3 | 75.47 | 16.22 | 5.77 | 0.68 | 1.86 |
| 4 | 75.47 | 17.92 | 4.07 | 0.68 | 1.86 |
| 5 | 75.00 | 15.00 | 6.50 | 0.50 | 3.00 |
| 6 | 75.00 | 17.70 | 3.00 | 1.30 | 3.00 |
| 7 | 75.94 | 15.94 | 5.14 | 0.86 | 2.12 |
| 8 | 79.10 | 15.00 | 3.00 | 1.30 | 1.60 |
| 9 | 75.00 | 19.90 | 3.00 | 0.50 | 1.60 |
| 10 | 75.00 | 15.00 | 6.50 | 0.50 | 3.00 |
| 11 | 75.00 | 19.90 | 3.00 | 0.50 | 1.60 |
| 12 | 75.94 | 15.94 | 5.14 | 0.86 | 2.12 |
| 13 | 79.90 | 15.00 | 3.00 | 0.50 | 1.60 |
| 14 | 75.00 | 15.00 | 6.96 | 1.30 | 1.74 |
| 15 | 75.00 | 17.70 | 3.00 | 1.30 | 3.00 |

For the Mixture experiments only the particle size, gloss of the dried coatings and roughness of the dried coatings were analysed. This was due to the remaining quality factors (pH, viscosity and density) being relatively stable over the ranges that were previously tested. Because of the nature of the models, the only quality factor that was taken into consideration during the optimization was the particle size. This is justified due to the gloss and roughness being directly dependent on the particle size and the particle size distribution (Gutiérrez et al. 2008, Danghui, Fengyan & Tianbo 2012, Hagenmaier 2004). Once the optimal formulation was obtained, a confirmation experimental run was performed to confirm if the optimization was successful and accurate.

7.2.2 Experiments

The ranges that were set for each component for the Mixture experimental phase are presented in **Table 53**.

Table 53 - Mixture Experimental Design - Formulation Parameter Ranges

| Component | Minimum [wt%] | Maximum [wt%] |
|---------------------|---------------|---------------|
| Water | 75 | 79.9 |
| Wax | 15 | 19.9 |
| Oleic Acid | 3 | 6.96 |
| Ammonium Hydroxide | 1.6 | 3 |
| Potassium Hydroxide | 0.5 | 1.3 |

As with the Screening experimental design, the Mixture design was also set up as a linear model with two additional centre points which will indicate any curvature and in addition confirm repeatability with the additional three replicate points. The process parameters were set at the following settings (**Table 54**):

Table 54 - Formulation Experimental Design - Process Parameter Settings

| Process Parameter | Setting |
|--------------------------|---------|
| Stirrer Speed [rpm] | 800 |
| HSH Speed [rpm] | 6800 |
| HS Time Interval [min] | 10 |
| Cooling Rate [-1/0/1] | 1 |
| Inverting Phase AR [l/h] | 3 |
| Temperature [°C] | 120 |

The responses were analysed and the following results were obtained.

7.2.3 Particle Size

During the Screening experimental design it was noted that there were small amounts of large particles affecting the mean particle size. As a result the median was also investigated during the Mixture experimental design. Outlier sized particles do not carry such a significant weight on the median value as with the mean value. The mean and median particle sizes obtained during the Mixture experimental design are as follow (**Table 55**):

Table 55 - Mean- and Median Particle Sizes for the Mixture Experimental Design

| Experiment | Particle Size (Volume Mean) [μm] | Particle Size (Volume Median) [μm] | Particle Size (Area Mean) [μm] | Particle Size (Area Median) [μm] | Particle Size (Number Mean) [μm] | Particle Size (Number Median) [μm] |
|------------|---|---|---|---|---|---|
| EXP M1 | 22.51 | 2.682 | 1.523 | 0.694 | 0.595 | 0.531 |
| EXP M2 | 7.601 | 1.477 | 1.185 | 0.679 | 0.591 | 0.533 |
| EXP M3 | 11.21 | 6.17 | 2.113 | 0.646 | 0.558 | 0.507 |
| EXP M4 | 35.18 | 9.33 | 4.325 | 1.891 | 0.668 | 0.533 |
| EXP M5 | 48.08 | 25.22 | 5.013 | 0.745 | 0.582 | 0.516 |
| EXP M6 | 28.56 | 1.652 | 1.353 | 0.694 | 0.602 | 0.544 |
| EXP M7 | 38.79 | 14.72 | 3.963 | 1.044 | 0.654 | 0.548 |
| EXP M8 | 34.7 | 4.846 | 1.718 | 0.697 | 0.598 | 0.536 |
| EXP M9 | 25.42 | 4.623 | 2.143 | 0.762 | 0.606 | 0.526 |
| EXP M10 | 68.15 | 25.94 | 6.316 | 1.327 | 0.658 | 0.546 |
| EXP M11 | 4.672 | 2.146 | 1.349 | 0.71 | 0.598 | 0.528 |
| EXP M12 | 11.52 | 3.494 | 1.821 | 0.81 | 0.628 | 0.541 |
| EXP M13 | 9.235 | 2.92 | 1.717 | 0.859 | 0.646 | 0.552 |
| EXP M14 | 35.81 | 13.44 | 2.552 | 0.658 | 0.57 | 0.518 |
| EXP M15 | 65.94 | 19.46 | 1.876 | 0.635 | 0.569 | 0.523 |

When examining the particle size distribution of Mixture Experiment 11 (**EXP M11**), represented in **Figure 75**, it is noted that there is a significant improvement in the volume-, area- and number particle size distributions in comparing to the Screening experimental design particle size results (**Figure 39** and **Figure 40**).

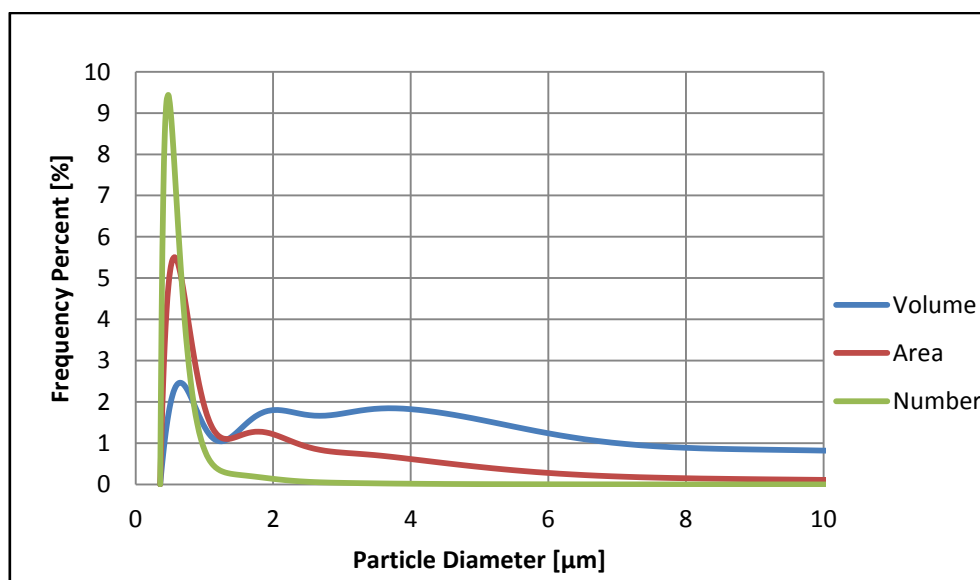


Figure 75 - EXP M11: Volume, Area and Number Frequency vs. Particle Diameter

By examining **Figure 75** one can see that the volume-, area- and number particle size distributions peak at a similar particle size. This indicates that the particles are more uniform in size

and that there are less large particles present in the Carnuba wax emulsion samples (Saturn DigiSizer 5200 2000). That said, the volume particle size distribution curve (blue curve in **Figure 75**) still indicates the presence of large particles. This however is not a negative quality for Carnuba wax emulsions, since a small variation in particle size promotes gas exchange after drying, which is favourable for post-harvest fruit applications (Hagenmaier, Baker 1994, Hagenmaier 2004, Hagenmaier, Shaw 2002, Hagenmaier 2005, Robert D. 2000).

Once all the particle size data were entered into the Mixture experimental design in Design Expert© it was found that the linear models were not statistically significant ($p > 0.05$) for the volume-, area- and number particle size data sets. This applied to both the mean and median particle size data sets. As a result, reduced quadratic models were fitted to all six particle size data sets. The results indicated that the reduced quadratic model (backwards variable selection) of the Area Median particle size data set was the only model that was statistically significant ($p < 0.05$) (All the mixture particle size data analysis can be viewed in **Appendix H**), as seen in the ANOVA **Table 56**.

Table 56 - Area Median Particle Size (Reduce Quadratic Model) ANOVA

| Analysis of Variance Table - Area Median Particle Size (Reduced Quadratic Model) | | | | | | |
|--|---------|----|--------|----------|----------|-----------------|
| | Sum of | | Mean | F | p-value | |
| Source | Squares | df | Square | Value | Prob > F | |
| Model | 1.285 | 6 | 0.214 | 5.200813 | 0.0182 | significant |
| %Water * %Wax | 1.080 | 1 | 1.080 | 26.2299 | 0.0009 | |
| %Water * %Oleic Acid | 0.599 | 1 | 0.599 | 14.54459 | 0.0051 | |
| Residual | 0.329 | 8 | 0.041 | | | |
| Lack of Fit | 0.130 | 4 | 0.032 | 0.648362 | 0.6576 | not significant |
| Pure Error | 0.200 | 4 | 0.050 | | | |
| Cor Total | 1.614 | 14 | | | | |
| Adeq Precision | 9.132 | | | | | |

From **Table 56** it is clear that the model is statistically significant ($p < 0.05$). An *Adeq Precision* value of 9.132 indicates an adequate signal which confirms that the model can be used to navigate the design space. The R-squared values for the **Area Median Particle Size Model (Mixture)** are presented in **Table 57**.

Table 57 - Area Median Particle Size Model (Mixture) - R-Squared Values

| Model | R-squared | Adj R-squared |
|--|-----------|---------------|
| Area Median Particle Size Model | 0.796 | 0.643 |

An R-squared value of 0.796 is relatively good and provides support to the validity of the model. The **Area Median Particle Size Model (Mixture)** equation in terms of the actual components and actual factors are as follow:

$$\begin{aligned}
 \text{Particle Size } [\mu\text{m}] = & -3.33224 \times \% \text{Water} \\
 & -63.01100 \times \% \text{Wax} \\
 & +41.07138 \times \% \text{Oleic Acid} \\
 & +9.82122 \times \% \text{Potassium Hydroxide} \\
 & +10.07629 \times \% \text{Ammonium Hydroxide} \\
 & +0.97377 \times \% \text{Water} \times \% \text{Wax} \\
 & -0.41344 \times \% \text{Water} \times \% \text{Oleic Acid}
 \end{aligned}$$

Figure 76 illustrates the actual measured response value for this observation against the response value predicted by the model for this set of experimental conditions.



Figure 76 - Actual measured response vs. model predicted value

Due to the relatively high R-squared value of the **Area Median Particle Size Model (Mixture)** the model is more accurate than what was achieved in the Screening experimental phase. The relative effect of each factor is presented in **Figure 77**.

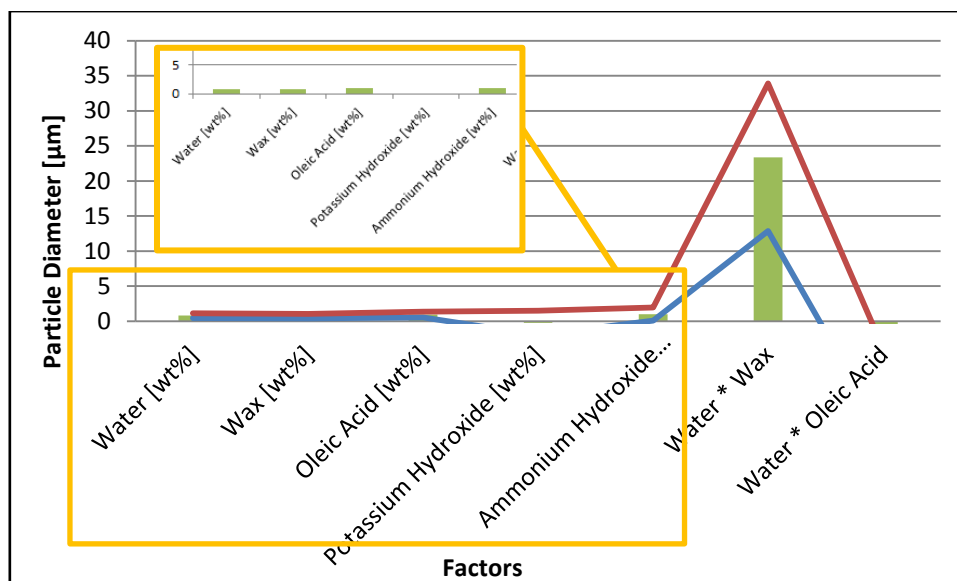


Figure 77 - Relative contribution of the area median particle size model factors to the area median particle size

The water, wax, Oleic acid and Ammonium hydroxide content have the most significant effect on the area median particle size. Both **Figure 76** and **Figure 77** is an indication that the model can be used to navigate the design space. The effect of varying the water-, wax- and Oleic acid content on the particle size is represented in **Figure 78**.

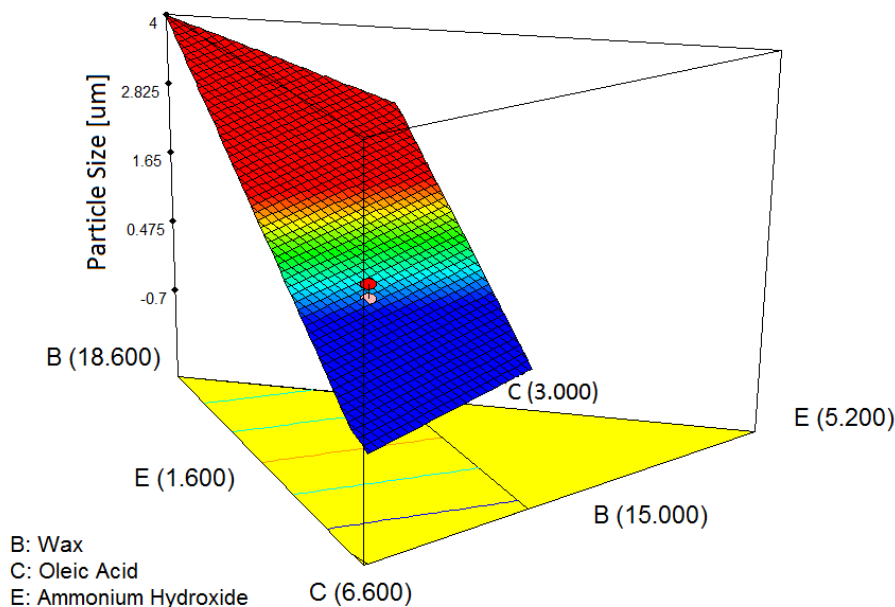


Figure 78 - Area Median Particle Size Model (Mixture Experimental Design) - Particle Size vs. %Wax vs. %Oleic Acid vs. %Ammonium Hydroxide

When examining **Figure 78** it is noted that there is a clear increase in the particle size as the Oleic acid content decreases. This is expected since the Oleic acid forms part of the surfactant. Thus

a decrease in the surfactant content results in an increase in the particle size as supported by Danghui, McClements, Gusman, Liu et al., Pey et al. and Sadurni et al. (Pey et al. 2006, Danghui, Fengyan & Tianbo 2012, Liu et al. 2006, Gusman 1947, McClements 2010, Sadurní et al. 2005).

The **Area Median Particle Size Model (Mixture)** is presented in **Figure 79** as a function of particle size and wax-to-surfactant ratio. It also presents actual values obtained during the formulation experiments (Water [wt%] kept constant at 75%).

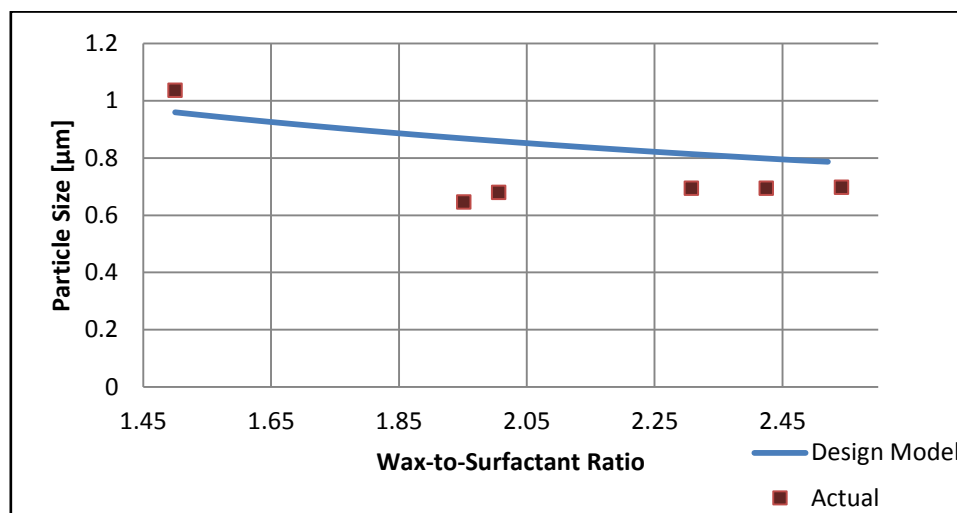


Figure 79 - Area Median Particle Size Model (Mixture Experimental Design) - Particle Size vs. Wax-to-Surfactant Ratio

The **Area Median Particle Size Model (Mixture)** design model contradicts the findings of Danghui, McClements, Gusman, Liu et al., Pey et al. and Sadurni et al. (Pey et al. 2006, Danghui, Fengyan & Tianbo 2012, Liu et al. 2006, Gusman 1947, McClements 2010, Sadurní et al. 2005). A possible explanation could be the accuracy of the model affecting the trend at a water content of 75%. Thus all the factors are not taken into account at once in **Figure 79**. It should be noted that the model is not for prediction purposes, but to indicate where in the design space the optimum is situated, while taking all the factors into account. The accuracy of the **Area Median Particle Size Model (Mixture)** is represented by the actual values versus the predicted values seen in **Figure 80**.

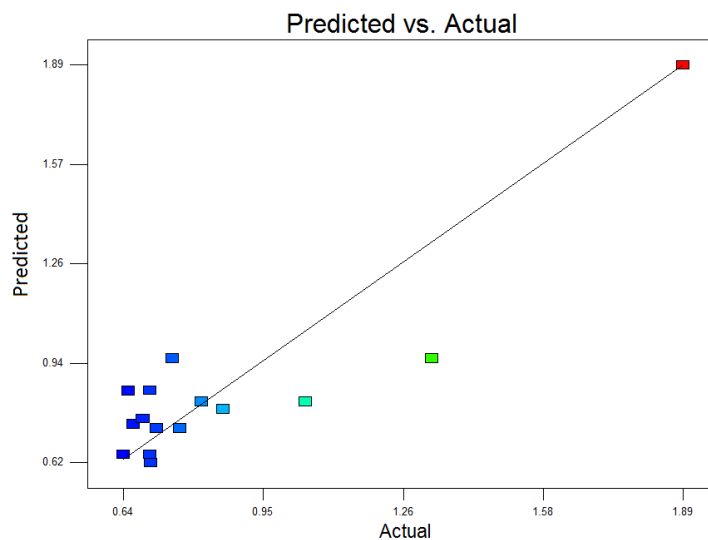


Figure 80 - Area Median Particle Size Model (Mixture Experimental Design) - Predicted vs. Actual

From **Figure 80** it is clearly visible that the **Area Median Particle Size Model (Mixture)** predicts the particle size relatively accurate for high or low values but seems to deviate for sizes that fall in between ($1 - 1.7 \mu\text{m}$). This could explain the contradicting trend to the literature, seen in **Figure 79**.

That said, the **Area Median Particle Size Model (Mixture)** is the only model that is statistically significant for the particle size data. In addition, the model is a good prediction of the experimental setup, as seen in **Figure 79**. Thus, the **Area Median Particle Size Model (Mixture)** will be used to optimize the formulation in terms of the particle size.

7.2.4 Roughness

The roughness (Ra) values obtained during the formulation experimental runs are presented in **Table 58**.

Table 58 - Roughness [Ra] Readings for the Mixture Experimental Design

| Experiment | Average [Ra] | STD DEV [Ra] |
|------------|--------------|--------------|
| EXP M1 | 0.711 | 0.673 |
| EXP M2 | 0.158 | 0.047 |
| EXP M3 | 0.119 | 0.029 |
| EXP M4 | 0.379 | 0.477 |
| EXP M5 | 0.325 | 0.319 |
| EXP M6 | 0.354 | 0.271 |
| EXP M7 | 0.956 | 2.070 |
| EXP M8 | 1.356 | 3.744 |
| EXP M9 | 3.208 | 4.695 |
| EXP M10 | 0.301 | 0.243 |
| EXP M11 | 0.184 | 0.203 |
| EXP M12 | 1.978 | 3.276 |
| EXP M13 | 0.579 | 1.003 |
| EXP M14 | 0.301 | 0.229 |
| EXP M15 | 1.495 | 2.850 |
| Control | 0.07 | |

*** Control – The roughness of the Plexiglas® test plate**

The roughness readings obtained during the Mixture experimental design (**Table 58**) are on average much lower than those obtained during the Screening experimental design. The average Ra value obtained during the Screening experimental design is 2.381 Ra (STD DEV = 3.199) while the average for the Mixture experimental design is 0.827 Ra (STD DEV = 0.862). The large Ra values (**EXP M8**, **EXP M12** and **EXP M15**) present in **Table 58** are as a result of cracking that occurred during the drying process, as seen in **Figure 81**.

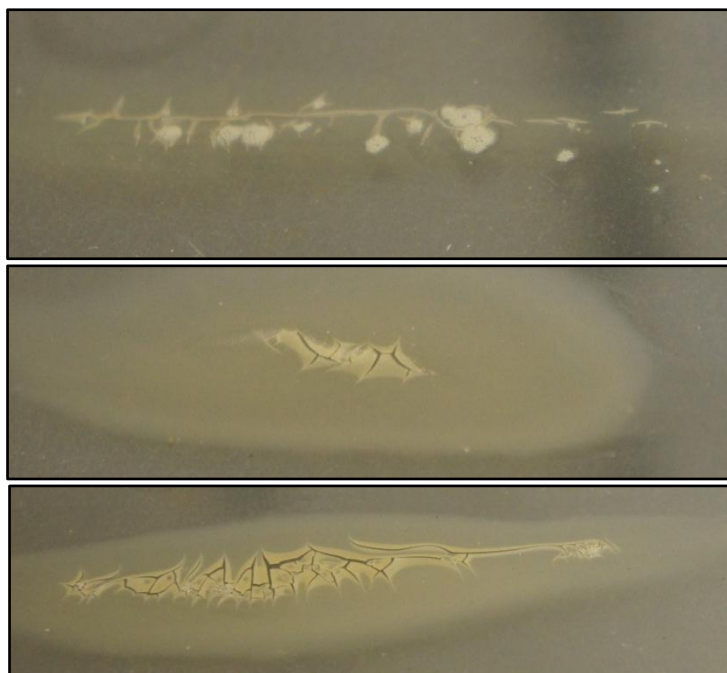


Figure 81 - Cracked dried Carnauba wax coating (EXP M8, EXP M12 and EXP M15)

The low Ra values (e.g. **EXP M3**) clearly indicates a uniform Carnauba wax layer was achieved, as confirmed in **Figure 82**.



Figure 82 - Uniform dried Carnauba wax coating (EXP M3)

Just by examining the dried coatings obtained from the formulation experiments it is clear that an optimum Carnauba wax emulsion formulation falls within the ranges set for the Mixture experimental design. The significant high $STD DEV$ calculated in **Table 58 (EXP M7, EXP M8, EXP M9, EXP M12, EXP M13 and EXP M15)** can be attributed to the cracks and blisters that formed during the drying process (as seen in **Appendix O**). Note that these experiments are independent of

the process parameters, thus the process parameters will still have to be optimized to achieve an overall optimum.

The roughness data were entered into the Mixture experimental design in Design Expert© for further processing. Once the mixture roughness data were analysed with Design Expert© it was noted that the linear model was not statistically significant ($p > 0.05$). A reduced quadratic model was fitted to the data and the results indicated that it was also not statistically significant ($p > 0.05$) (All the mixture roughness data analysis can be viewed in **Appendix I**). Due to the roughness data models not being statistically significant ($p > 0.05$) the roughness model will not be taken into account during the optimization of the Mixture experimental design.

7.2.5 Gloss

The gloss (GU) values obtained during the formulation experimental runs are presented in **Table 59**.

Table 59 - Gloss [GU] Readings for the Mixture Experimental Design

| Experiment | Average [GU] | STD DEV [GU] |
|------------|--------------|--------------|
| EXP M1 | 52.77 | 6.801 |
| EXP M2 | 56.89 | 14.407 |
| EXP M3 | 49.45 | 7.190 |
| EXP M4 | 51.40 | 24.285 |
| EXP M5 | 33.00 | 9.380 |
| EXP M6 | 17.17 | 4.282 |
| EXP M7 | 51.79 | 7.162 |
| EXP M8 | 37.50 | 15.040 |
| EXP M9 | 49.15 | 6.989 |
| EXP M10 | 67.39 | 13.542 |
| EXP M11 | 74.54 | 10.189 |
| EXP M12 | 80.77 | 14.029 |
| EXP M13 | 70.41 | 8.529 |
| EXP M14 | 82.76 | 10.665 |
| EXP M15 | 20.27 | 7.544 |
| Control | 135 | |

*** Control – The gloss of the Plexiglas© test plate**

When examining the gloss readings obtained during the Mixture experimental design (**Table 59**) it is clear that there is a wide spectrum of values, ranging from 17.17 GU (**EXP M6**) to 82.76 GU (**EXP M14**). The gloss values are on average lower for the Mixture experimental design than the

Screening experimental design (Screening experimental design: Average = 61.795 *GU*, STD DEV = 19.915 ; Mixture experimental design: Average = 53.017 *GU*, STD DEV = 20.13). This could be an indication that the process parameters will influence the gloss more than the formulation. This is expected since the gloss is greatly affected by the emulsification temperature, due to the temperature directly affecting the extent of melting of the Carnauba wax. That said, the gloss values obtained during the formulation experiments still fall within the range of gloss readings published by Bosquez-Molina et al. (2003) (

Table 40) (Bosquez-Molina, Guerrero-Legarreta & Vernon-Carter 2003).

The gloss data were entered into the Mixture experimental design in Design Expert© for further processing. It was noted that both the linear- and reduced quadratic model was not statistically significant ($p > 0.05$) (All the mixture gloss data analysis can be viewed in **Appendix J**). Due to the gloss data models not being statistically significant ($p > 0.05$) the gloss model will not be taken into account during the optimization of the Mixture experimental design.

7.2.6 Temperature and Pressure

The pressure drop (**Section 7.1.6: Temperature and Pressure**) was also noticed during the Formulation experimental design, as seen in **Figure 83** (pressure is presented as bar guage).

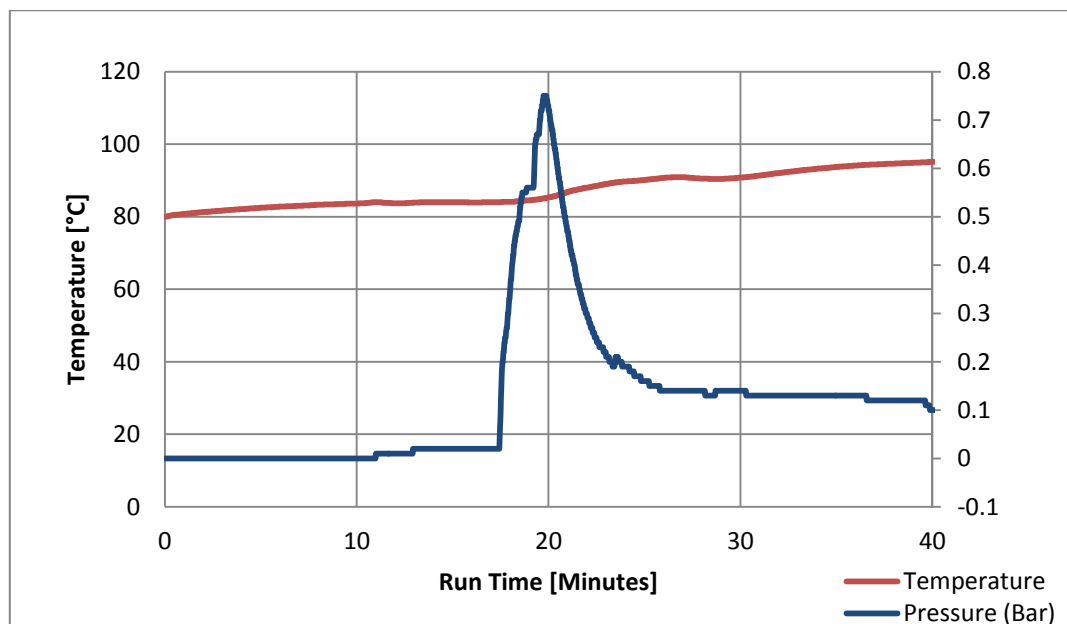


Figure 83 - Temperature and Pressure Curve - EXP M11

At a run time of 20 mins a clear pressure peak is noticed in **Figure 83**. As noticed with the Screening experimental (**EXP S27**), at this pressure peak the Carnuba wax emulsion was inverted from a water-in-wax emulsion to a wax-in-water emulsion. Due to this inversion, the rheology of the emulsion changes abruptly and the pressure drops significantly (Hagenmaier, Baker 1994, Baci, Moşescu & Nan 2008). This pressure drop occurrence was recorded by various authors studying emulsion rheology and manufacturing methods (Hagenmaier, Baker 1994, Fernandez et al. 2004, Baci, Moşescu & Nan 2008, Izquierdo et al. 2004).

7.2.7 Optimization

The Mixture experimental design (**Area Median Particle Size Model (Mixture)**) was optimized in terms of only the particle size, since the roughness and gloss models were not statistically significant. The same three particle size outputs (target-, minimizing- and step response outputs) used during the Screening experimental design optimization were used for the Mixture experimental design optimization. The mixture design optimization averages of the results from the three response outputs are presented in **Table 60** (the full set of optimization results can be viewed in **Appendix K**).

Table 60 - Optimization Results - Mixture Experimental Design

| %Water | %Wax | %Oleic Acid | %Potassium Hydroxide | %Ammonium Hydroxide | Desirability |
|--------|--------|-------------|----------------------|---------------------|--------------|
| 75.298 | 15.829 | 6.254 | 0.599 | 2.020 | 0.903 |

The three response outputs yielded similar results, as seen in **Appendix K**. A confirmation run was performed to confirm the optimized formulation. The results of the confirmation run are presented in **Table 61**.

Table 61 - Confirmation Run Results

| Area Median Particle Size [μm] | Roughness [Ra] | Gloss [GU] |
|---|----------------|------------|
| 0.576 | 0.11 | 109.8 |
| STD DEV | 0.021 | 0.789 |

It is clear that the particle size of the confirmation run, achieved with the optimized formulation, is the smallest that have been attained so far. The roughness is also the lowest and the gloss the highest values obtained thus far. The **Area Median Particle Size Model (Mixture)** is presented in

Figure 84 as a function of particle size and wax-to-surfactant ratio including the actual values and the optimized value (Water% kept constant at 75%).

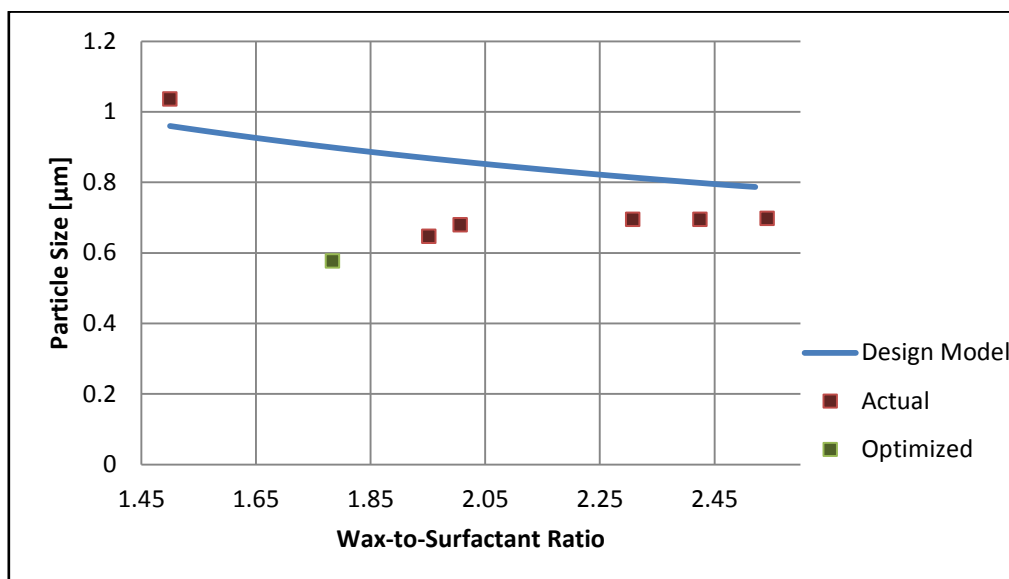


Figure 84 - Area Median Particle Size Model (Mixture Experimental Design) - Particle Size vs. Wax-to-Surfactant Ratio

From **Figure 84** it is clearly visible that the formulation was optimized since the particle size obtained during the optimization confirmation experiment (green marker) is the lowest yet. The optimized formulation obtained during the Mixture experimental design optimization will be set as the formulation for the Composite experimental design. Again it should be emphasized that the design model was used to indicate where in the design space the optimum lies. **Figure 84** does not take into account the effect of the Water% since it was kept constant at 75%. Thus the variance in the model could be due to not all the model factors being taken into account. That said an optimum was achieved.

7.3 Composite Experimental Phase

7.3.1 Composite Experimental Design

With the optimal formulation established, the final experimental design was based on the four process parameters that were identified as process parameters that should be investigated further, during the screening experimental phase. The final Composite design consisted of thirty experimental runs which included six centre points, as seen in **Table 62**.

Table 62 - Composite Experimental Design

| Experiment | Temperature (°C) | High Shear Time Interval (min) | High Shear Speed (rpm) | Stirring Speed (rpm) |
|------------|------------------|--------------------------------|------------------------|----------------------|
| 1 | 110 | 10 | 4300 | 800 |
| 2 | 110 | 40 | 6800 | 800 |
| 3 | 120 | 25 | 8050 | 1150 |
| 4 | 120 | 25 | 5550 | 450 |
| 5 | 120 | 25 | 5550 | 1150 |
| 6 | 110 | 40 | 6800 | 1500 |
| 7 | 100 | 25 | 5550 | 1150 |
| 8 | 110 | 40 | 4300 | 800 |
| 9 | 120 | 25 | 5550 | 1150 |
| 10 | 140 | 25 | 5550 | 1150 |
| 11 | 120 | 25 | 5550 | 1150 |
| 12 | 120 | 25 | 5550 | 1150 |
| 13 | 130 | 40 | 6800 | 800 |
| 14 | 130 | 10 | 6800 | 800 |
| 15 | 120 | 25 | 5550 | 1850 |
| 16 | 120 | 55 | 5550 | 1150 |
| 17 | 130 | 40 | 6800 | 1500 |
| 18 | 120 | 25 | 5550 | 1150 |
| 19 | 110 | 10 | 6800 | 800 |
| 20 | 130 | 40 | 4300 | 1500 |
| 21 | 120 | 0 | 5550 | 1150 |
| 22 | 130 | 10 | 4300 | 1500 |
| 23 | 120 | 25 | 3050 | 1150 |
| 24 | 130 | 10 | 6800 | 1500 |
| 25 | 130 | 40 | 4300 | 800 |
| 26 | 110 | 10 | 6800 | 1500 |
| 27 | 110 | 40 | 4300 | 1500 |
| 28 | 130 | 10 | 4300 | 800 |
| 29 | 120 | 25 | 5550 | 1150 |
| 30 | 110 | 10 | 4300 | 1500 |

Analyses were performed and the data from the composite design experiments were collected. Once again only the particle size and gloss- and roughness of the dried coatings were analysed. The data were entered into the Composite experimental design in Design Expert®. Statistical models were fitted to the data and optimized according to particle size. Only the particle size was taken into account during the optimization, due to the nature of the models that were fitted. Five additional experiments were performed to confirm that the optimization was successful. Only five experiments could be performed due to the limited amount of Carnauba wax.

7.3.2 Experimentation

The final experimental design, the Composite experimental design, was performed to obtain the optimum process parameter combination. A complete composite design was set up and the experiments were performed. Once all the composite experiments were performed and all the required data recorded, the results were entered into the Composite experimental design in Design Expert®. The Composite design contains six centre points and an alpha value set at two, as previously discussed. The process parameters' ranges for the Composite experimental design are presented **Table 63**.

Table 63 - Composite Experimental Design - Process Parameters' Ranges

| Factor | Minimum | Maximum |
|------------------------------------|---------|---------|
| Temperature (°C) | 100 | 140 |
| High Shear Time Interval (min) | 0 | 55 |
| Stirrer Speed (rpm) | 450 | 1850 |
| High Shear Homogenizer Speed (rpm) | 3050 | 8050 |

Once again additional centre points were included to indicate any curvature and in addition to confirm repeatability. The formulation was set at the optimized formulation obtained during the Mixture experimental design. The formulation is presented in **Table 64**.

Table 64 - Composite Experimental Design - Formulation Settings

| Component | wt% |
|---------------------|------|
| Water | 75.3 |
| Wax | 15.8 |
| Oleic Acid | 6.3 |
| Potassium Hydroxide | 0.6 |
| Ammonium Hydroxide | 2 |

The responses were analysed and the following results were obtained.

7.3.3 Particle Size

Once again both the mean- and median particle sizes were investigated during the Composite experimental design. The mean and median particle sizes that were obtained are as follow (**Table 65**):

Table 65 - Mean- and Median Particle Sizes for the Composite Experimental Design

| Experiment | Particle Size (Volume Mean) [μm] | Particle Size (Volume Median) [μm] | Particle Size (Area Mean) [μm] | Particle Size (Area Median) [μm] | Particle Size (Number Mean) [μm] | Particle Size (Number Median) [μm] |
|------------|---|---|---|---|---|---|
| EXP F1 | 8.943 | 5.451 | 1.941 | 0.628 | 0.551 | 0.503 |
| EXP F2 | 9.012 | 2.87 | 1.238 | 0.534 | 0.534 | 0.5 |
| EXP F3 | 15.98 | 3.544 | 1.255 | 0.561 | 0.524 | 0.495 |
| EXP F4 | 14.95 | 3.336 | 1.321 | 0.58 | 0.536 | 0.501 |
| EXP F5 | 71.6 | 47.09 | 3.075 | 0.567 | 0.524 | 0.494 |
| EXP F6 | 81.68 | 56.32 | 3.277 | 0.561 | 0.521 | 0.493 |
| EXP F7 | 73.46 | 38.05 | 4.132 | 0.624 | 0.549 | 0.507 |
| EXP F8 | 68.38 | 32.27 | 4.254 | 0.643 | 0.554 | 0.505 |
| EXP F9 | 76.9 | 43.59 | 3.532 | 0.589 | 0.535 | 0.499 |
| EXP F10 | 69.79 | 42.35 | 3.221 | 0.587 | 0.536 | 0.501 |
| EXP F11 | 66.28 | 36.34 | 2.969 | 0.567 | 0.524 | 0.493 |
| EXP F12 | 1.657 | 0.58 | 0.679 | 0.515 | 0.495 | 0.476 |
| EXP F13 | 4.718 | 0.741 | 0.916 | 0.546 | 0.516 | 0.49 |
| EXP F14 | 15.1 | 4.13 | 1.379 | 0.575 | 0.532 | 0.498 |
| EXP F15 | 2.235 | 0.573 | 0.67 | 0.512 | 0.493 | 0.476 |
| EXP F16 | 4.156 | 0.642 | 0.808 | 0.524 | 0.502 | 0.481 |
| EXP F17 | 1.114 | 0.557 | 0.607 | 0.515 | 0.496 | 0.478 |
| EXP F18 | 7.996 | 0.867 | 1.004 | 0.541 | 0.512 | 0.488 |
| EXP F19 | 20.27 | 6.703 | 1.663 | 0.565 | 0.523 | 0.492 |
| EXP F20 | 7.328 | 0.789 | 0.97 | 0.537 | 0.509 | 0.486 |
| EXP F21 | 1.856 | 0.66 | 0.773 | 0.549 | 0.519 | 0.492 |
| EXP F22 | 17.39 | 3.476 | 1.209 | 0.594 | 0.517 | 0.491 |
| EXP F23 | 34.62 | 10.5 | 1.893 | 0.571 | 0.527 | 0.495 |
| EXP F24 | 19.37 | 4.484 | 1.244 | 0.545 | 0.514 | 0.489 |
| EXP F25 | 8.481 | 0.805 | 0.985 | 0.543 | 0.514 | 0.49 |
| EXP F26 | 44.89 | 14.46 | 1.775 | 0.538 | 0.508 | 0.485 |
| EXP F27 | 35.32 | 10.51 | 1.754 | 0.544 | 0.511 | 0.485 |
| EXP F28 | 16.02 | 3.78 | 1.205 | 0.545 | 0.514 | 0.489 |
| EXP F29 | 14.16 | 3.723 | 1.273 | 0.554 | 0.519 | 0.491 |
| EXP F30 | 32.13 | 9.564 | 1.396 | 0.519 | 0.496 | 0.477 |

When examining the particle size distribution of Composite Design Experiment 17 (**EXP F17**), represented in **Figure 85**, it is clearly visible that there is a significant improvement in the volume-, area- and number particle size distributions in comparison to the Screening- and Formulation experimental design particle size results (**Figure 39**, **Figure 40** and **Figure 75**).

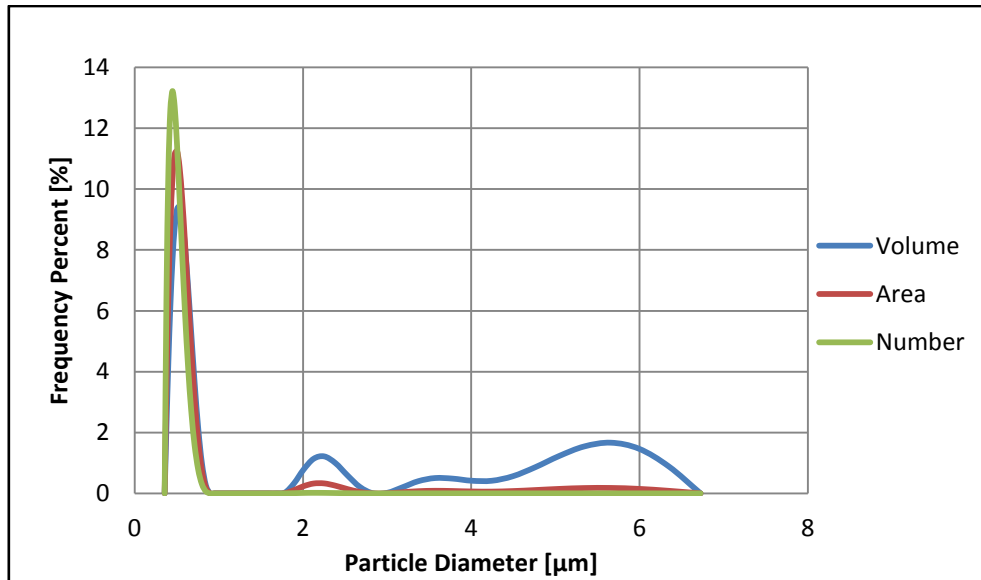


Figure 85 - EXP F17: Volume, Area and Number Frequency vs. Particle Diameter

The difference in particle size distribution is highlighted in the volume particle size distribution graphs (**Figure 86** and **Figure 87**) comparing the best results obtained during the Screening-, Mixture- and Composite experimental design (ED) results, respectively.

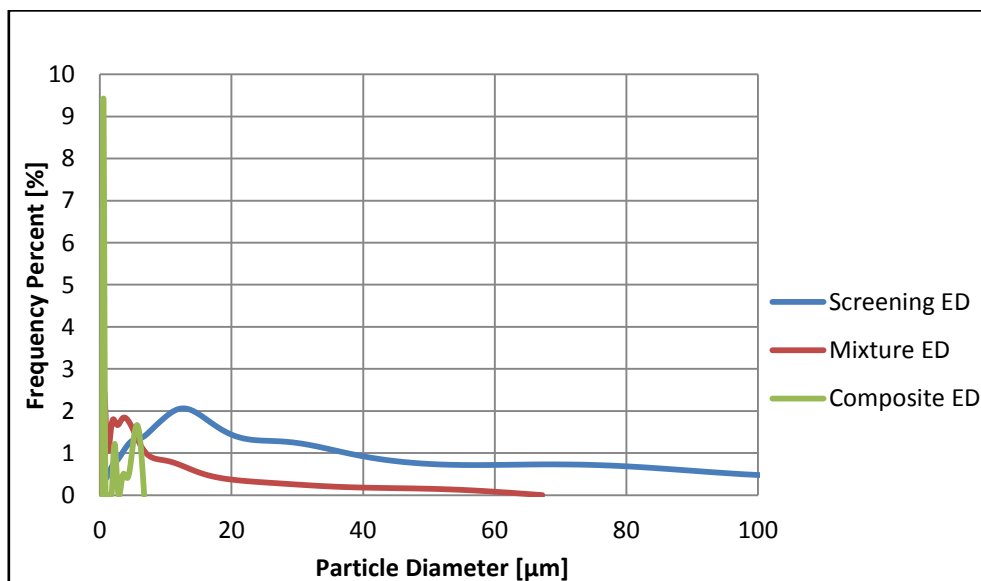


Figure 86 - Comparison of Screening-, Mixture and Composite Experimental Design Volume Particle Size Distribution [Range=0-100 µm]

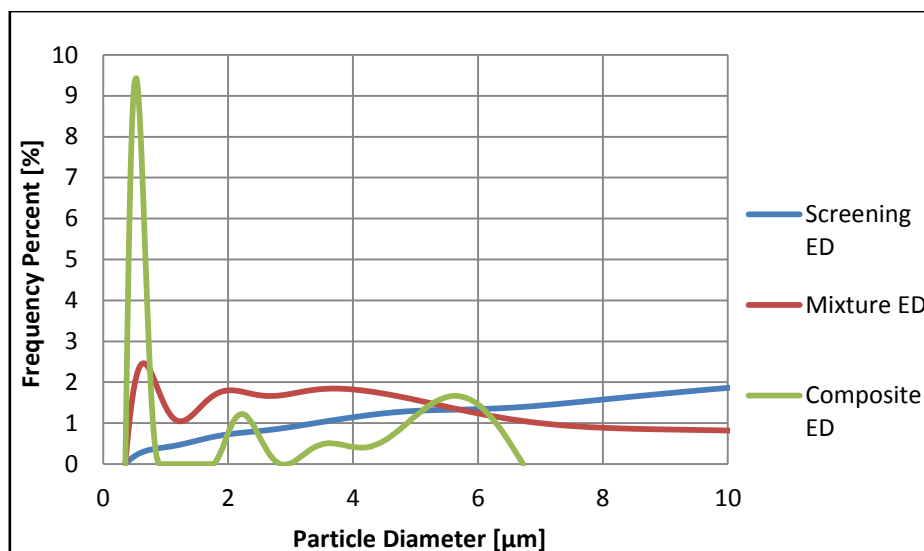


Figure 87 - Comparison of Screening-, Mixture and Composite Experimental Design Volume Particle Size Distribution [Range=0-10 μm]

From both **Figure 86** and **Figure 87** it is noted that a significantly smaller mean particle size and particle size distribution were obtained during the Composite experimental design. A smaller mean particle size indicates more favourable product characteristics as supported by McClements (2010), Milanovic (2011), Griffin (1945), Karbowski (2007), Lashmar (1995), Danghui (1995) and Perez (2002) (Griffin 1945, Lashmar, Richardson & Erbod 1995, Danghui, Fengyan & Tianbo 2012, McClements 2010, Milanovic et al. 2011, Karbowski, Debeaufort & Voilley 2007, Pérez et al. 2002b). This clearly indicates a significant improvement in the process parameter combination that developed from the Screening experimental design through to the Composite experimental design.

Also visible in **Figure 86** and **Figure 87** is the presence of a small amount of large particles in the Composite experimental design's volume particle size distribution too. This is an advantage for Carnuba wax emulsions since a small variation in particle size promotes gas exchange after drying, which is favourable for post-harvest fruit applications (Hagenmaier, Baker 1994, Hagenmaier 2004, Hagenmaier, Shaw 2002, Hagenmaier 2005, Robert D. 2000). Thus looking at the volume particle size distribution obtained during **EXP F17**, an overall small mean particle size was achieved with the additional advantage of a small amount of larger particles.

Once all the particle size data were entered into the Composite experimental design in Design Expert© it was found that the linear models were not statistically significant ($p > 0.05$) for the area- and volume particle size data sets (both mean- and median particle size data sets), but it was for the number particle size data sets (both the mean- and median particle size data sets). In order to increase the accuracy of the number mean- and median particle size linear models, a reduced

quadratic model (backwards variable selection) was fitted to the number particle size data sets to determine whether it will be more accurate or not.

7.3.3.1 Number Mean Particle Size

The R-squared values for the number mean particle size models are presented in **Table 66**.

Table 66 - Number Mean Particle Size Models (Composite) - R-Squared Values

| Model | R-Squared | Adj R-Squared | Pred -Squared |
|---------------------------------------|-----------|---------------|---------------|
| Number Mean (Linear Model) | 0.432 | 0.342 | 0.175 |
| Number Mean (Reduced Quadratic Model) | 0.676 | 0.591 | 0.481 |

From the R-squared values presented above, it is clear that the reduced quadratic model is more significant for the data and is a more accurate representation of the design space. The number mean particle size ANOVA for the reduced quadratic model can be seen in **Table 67** (validation for the ANOVA assumptions is presented in **Appendix E**).

Table 67 - Number Mean Particle Size (Reduced Quadratic Model) ANOVA

| Analysis of Variance Table – Number Mean Particle Size (Reduced Quadratic Model) | | | | | | |
|--|----------------|----|-------------|---------|------------------|-----------------|
| Source | Sum of Squares | df | Mean Square | F Value | p-value Prob > F | |
| Model | 5.077E-03 | 6 | 8.461E-04 | 7.978 | < 0.0001 | significant |
| A-Temperature | 5.227E-04 | 1 | 5.227E-04 | 4.928 | 0.0366 | |
| B-High Shear Time | 4.817E-05 | 1 | 4.817E-05 | 0.454 | 0.5071 | |
| D-Stirrer Speed | 2.646E-03 | 1 | 2.646E-03 | 24.949 | < 0.0001 | |
| AB | 4.410E-04 | 1 | 4.410E-04 | 4.158 | 0.0531 | |
| AD | 4.623E-04 | 1 | 4.623E-04 | 4.359 | 0.0481 | |
| A^2 | 9.568E-04 | 1 | 9.568E-04 | 9.022 | 0.0063 | |
| Residual | 2.439E-03 | 23 | 1.061E-04 | | | |
| Lack of Fit | 1.512E-03 | 18 | 8.402E-05 | 0.453 | 0.9013 | not significant |
| Pure Error | 9.268E-04 | 5 | 1.854E-04 | | | |
| Cor Total | 7.516E-03 | 29 | | | | |
| Adeq Precision | 10.732 | | | | | |

From **Table 67** it is noted that the number mean particle size quadratic model is statistically significant ($p < 0.05$). An *Adeq Precision* value of 10.732 indicates an adequate signal which confirms that the model can be used to navigate the design space.

The **Number Mean Particle Size Model (Composite)** equation in terms of the actual factors is as follows:

$$\begin{aligned}
 \text{Particle Size } [\mu\text{m}] = & +1.545 \\
 & -0.015 \times \text{Temperature} \\
 & +4.106 \times 10^{-3} \times \text{High Shear Time} \\
 & -2.143 \times 10^{-4} \times \text{Stirrer Speed} \\
 & -3.5 \times 10^{-5} \times \text{Temperature} \times \text{High Shear Time} \\
 & +1.536 \times 10^{-6} \times \text{Temperature} \times \text{Stirrer Speed} \\
 & +5.764 \times 10^{-5} \times \text{Temperature}^2
 \end{aligned}$$

Figure 88 illustrates the actual measured response value for this observation against the response value predicted by the model for this set of experimental conditions.

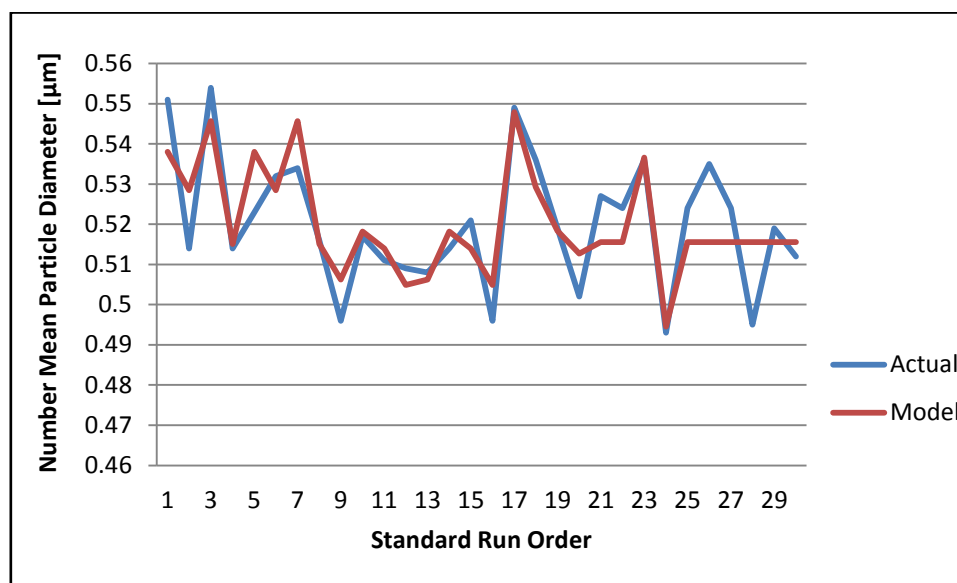


Figure 88 - Actual measured response vs. model predicted value

From **Figure 88** it is noted that the model fits the number mean particle size more accurately than any of the other particle size models obtained thus far. The relative effect of each factor is presented in **Figure 89**. The blue line indicates the lower bound of the 95% confidence interval that surrounds the coefficient estimate for the specific factor while the red line indicates the upper bound of the 95% confidence interval (Stat-Ease 2010).

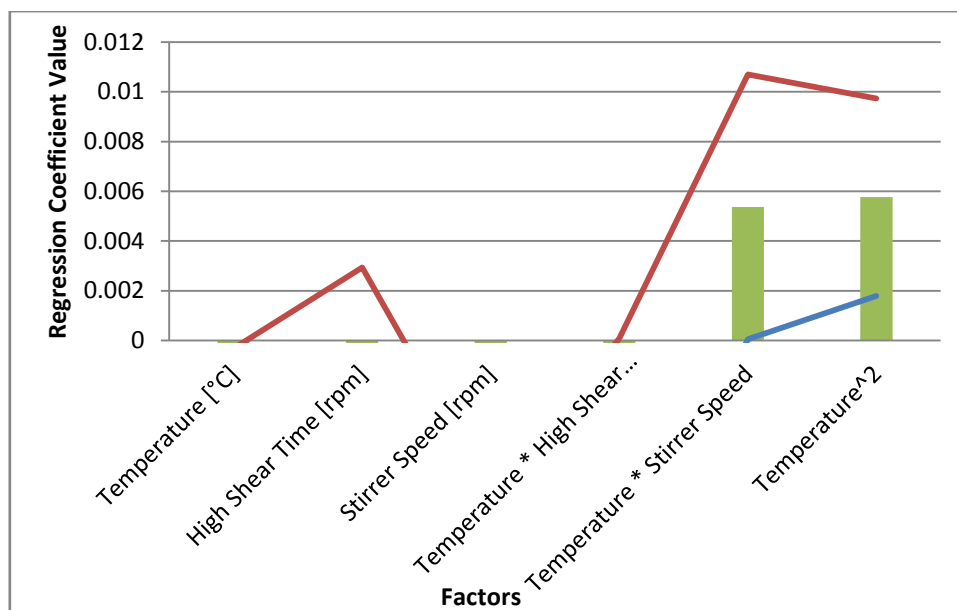


Figure 89 - Relative contribution of the Number Mean Particle Size Model factors to the number mean particle size

It is noted that the temperature and stirrer speed has the most significant effect on the number mean particle size. The effect of varying the temperature and stirring speed on the particle size is presented in **Figure 90**.

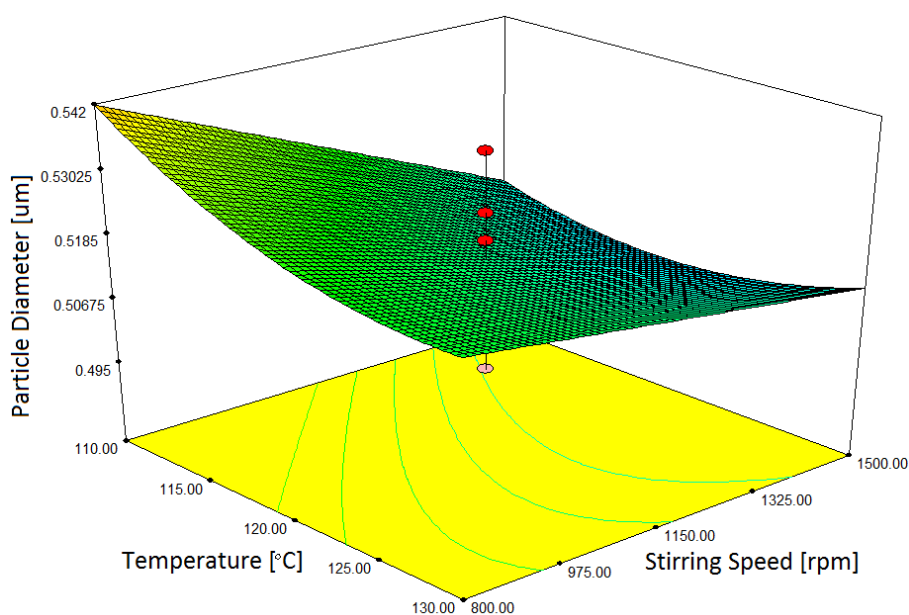


Figure 90 - Number Mean Particle Size Model (Composite Experimental Design) - Particle Size vs. Temperature vs. Stirring Speed

When examining **Figure 90**, one can clearly see that an increase in the stirring speed resulted in a decrease in the particle size. This is supported by McClements (2010) who found that an increase in the intensity or duration of the energy input (stirring speed or high shear homogenizing speed) of an emulsification system results in a decrease in particle size (McClements

2010). This finding is also supported by Chen et al. (2005) who found that more efficient agitation results in a superior emulsion with a smaller particle size (Chen, Tao 2005). It is also noted from **Figure 90** that an increase in the temperature results in a decrease in the particle size. This trend is in agreement with the findings of Lashmar et al., Li et al., Bornfriend and Jass (Li et al. 2010, Lashmar, Richardson & Erbod 1995, Jass 1967, Bornfriend 1978). They concluded that the particle size decreases with an increase in the emulsification temperature (Li et al. 2010, Lashmar, Richardson & Erbod 1995, Jass 1967, Bornfriend 1978). That said, it is also noted that there is a minimum particle size that is achieved in between the highest and lowest emulsification temperature. A possible explanation could be that at the higher emulsification temperature the Carnauba wax is burning, resulting in larger particles. Similarly, at the lower emulsification temperature the Carnauba wax is not completely melted, thus also resulting in larger particles. **Figure 91** shows the effect of varying the temperature and high shear time interval on the particle size.

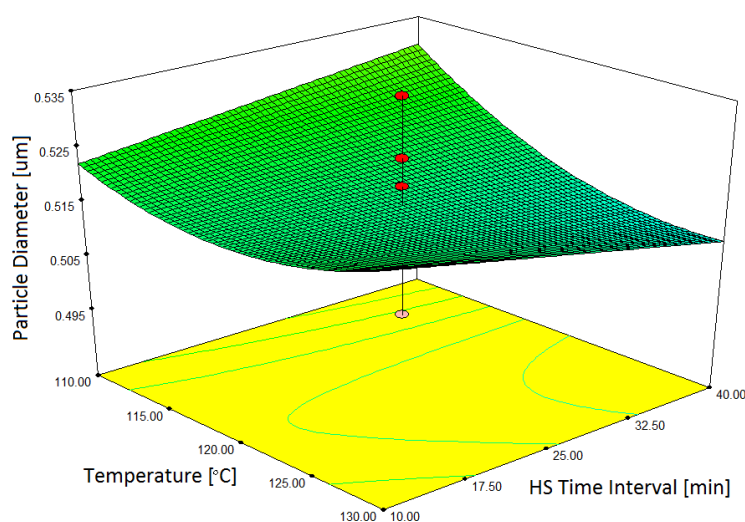


Figure 91 - Number Mean Particle Size Model (Composite Experimental Design) - Particle Size vs. Temperature vs. HS Time Interval

From **Figure 91** one can see that the particle size decreases with an increase in the high shear time interval at a high emulsification temperature, while the particle size decreases with a decrease in the high shear time interval at a low emulsification temperature. McClements stated in his study on nano-emulsions that the particle size can be reduced by increasing the intensity or duration of homogenization (McClements 2010). Adler-Nissen et al. agreed with McClements conclusion that there must be enough time given for a stable interface to form around the drop during emulsification processes (Adler-Nissen, Mason & Jacobsen 2004). These findings are contradicting to the trend obtained at a low emulsification temperature. A possible explanation could be that at a

low emulsification temperature the Carnauba wax is not completely melted resulting in larger particles, as mentioned above.

7.3.3.2 Number Median Particle Size

A reduced quadratic model (backwards variable selection) was fit to the number median particle size data set. The number median particle size models' R-squared values are presented in **Table 68**.

Table 68 - Number Median Particle Size Models - R-Squared Values

| Model | R-Squared | Adj R-Squared | Pred -Squared |
|---|-----------|---------------|---------------|
| Number Median (Linear Model) | 0.397 | 0.301 | 0.134 |
| Number Median (Reduced Quadratic Model) | 0.609 | 0.528 | 0.433 |

Similarly as with the number mean particle size models the quadratic model has an improved fit. The number median particle size ANOVA for the reduced quadratic model is presented in **Table 69** (validation for the ANOVA assumptions is presented in **Appendix E**).

Table 69 - Number Median Particle Size (Reduced Quadratic Model) ANOVA

| Analysis of Variance Table – Number Median Particle Size (Reduced Quadratic Model) | | | | | | |
|--|----------------|----|-------------|---------|------------------|-----------------|
| Source | Sum of Squares | df | Mean Square | F Value | p-value Prob > F | |
| Model | 1.260E-03 | 5 | 2.519E-04 | 7.475 | 0.0002 | significant |
| A-Temperature | 7.004E-05 | 1 | 7.004E-05 | 2.078 | 0.1624 | |
| B-High Shear Time | 1.504E-05 | 1 | 1.504E-05 | 0.446 | 0.5105 | |
| D-Stirrer Speed | 7.370E-04 | 1 | 7.370E-04 | 21.867 | < 0.0001 | |
| AB | 1.501E-04 | 1 | 1.501E-04 | 4.452 | 0.0455 | |
| A^2 | 2.875E-04 | 1 | 2.875E-04 | 8.531 | 0.0075 | |
| Residual | 8.089E-04 | 24 | 3.371E-05 | | | |
| Lack of Fit | 5.021E-04 | 19 | 2.643E-05 | 0.431 | 0.9167 | not significant |
| Pure Error | 3.068E-04 | 5 | 6.137E-05 | | | |
| Cor Total | 2.069E-03 | 29 | | | | |
| Adeq Precision | 10.453 | | | | | |

Table 69 clearly indicates that the number median quadratic model is also statistically significant ($p < 0.05$).

The **Number Median Particle Size Model (Composite)** equation in terms of the actual factors is as follow:

$$\text{Particle Size } [\mu\text{m}] = +0.923$$

$$-7.244 \times 10^{-3} \times \text{Temperature}$$

$$+2.397 \times 10^{-3} \times \text{High Shear Time}$$

$$-1.583 \times 10^{-5} \times \text{Stirrer Speed}$$

$$-2.042 \times 10^{-5} \times \text{Temperature} \times \text{High Shear Time}$$

$$+3.16 \times 10^{-5} \times \text{Temperature}^2$$

Figure 92 shows the actual measured response value for this observation against the response value predicted by the model for this set of experimental conditions.

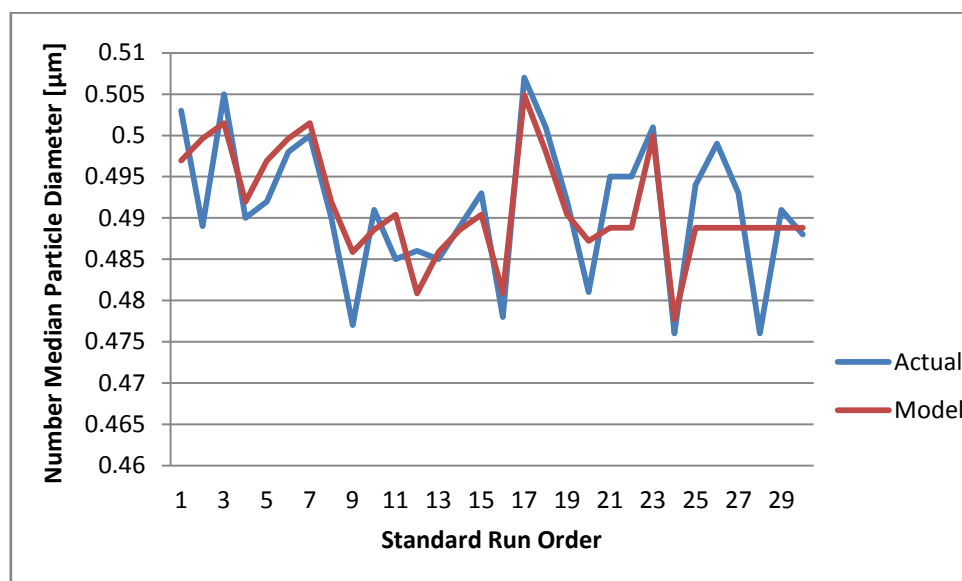


Figure 92 - Actual measured response vs. model predicted value

From **Figure 92** it is noted that the model predicts the actual values with a similar accuracy as the **Number Mean Particle Size Model**. The relative effect of each factor is presented in **Figure 93**. The blue line indicates the lower bound of the 95% confidence interval that surrounds the coefficient estimate for the specific factor while the red line indicates the upper bound of the 95% confidence interval (Stat-Ease 2010).

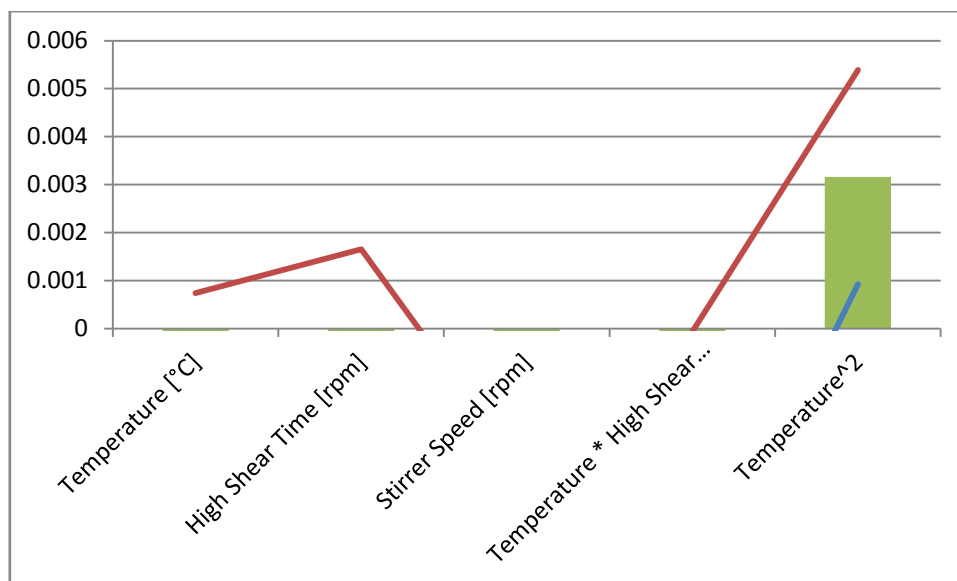


Figure 93 - Relative contribution of the Number Median Particle Size Model factors to the number median particle size

The temperature has the most significant effect on the number median particle size. Identical trends obtained with the *Number Mean Particle Size Model (Composite)* were obtained with the *Number Median Particle Size Model (Composite)*.

7.3.3.3 Area Median Particle Size

Further investigation indicated that the area median particle size reduced quadratic model (backwards variable selection was performed on the area median particle size data set) is statistically significant, as indicated in **Table 70**.

Table 70 - Area Median Particle Size (Reduced Quadratic Model) ANOVA

| Analysis of Variance Table – Area Median Particle Size (Reduced Quadratic Model) | | | | | | |
|--|----------------|----|-------------|---------|------------------|-----------------|
| Source | Sum of Squares | df | Mean Square | F Value | p-value Prob > F | |
| Model | 1.392E-02 | 4 | 3.481E-03 | 4.839 | 0.0050 | significant |
| A-Temperature | 1.768E-03 | 1 | 1.768E-03 | 2.458 | 0.1295 | |
| D-Stirrer Speed | 5.460E-03 | 1 | 5.460E-03 | 7.590 | 0.0108 | |
| AD | 2.256E-03 | 1 | 2.256E-03 | 3.136 | 0.0888 | |
| A² | 4.440E-03 | 1 | 4.440E-03 | 6.172 | 0.0200 | |
| Residual | 1.799E-02 | 25 | 7.194E-04 | | | |
| Lack of Fit | 1.475E-02 | 20 | 7.373E-04 | 1.138 | 0.4869 | not significant |
| Pure Error | 3.240E-03 | 5 | 6.479E-04 | | | |
| Cor Total | 3.191E-02 | 29 | | | | |

The R-squared values for the area median particle size reduced quadratic model are presented in **Table 71**.

Table 71 - Area Median Particle Size Model (Composite) - R-Squared Values

| Model | R-Squared | Adj R-Squared | Pred -Squared |
|---------------------------------------|-----------|---------------|---------------|
| Area Median (Reduced Quadratic Model) | 0.436 | 0.346 | 0.205 |

From the R-squared values presented above it is clear that both the number mean- and number median reduced quadratic models are more significant to the particle size data. The **Area Median Particle Size Model (Composite)** equation in terms of the actual factors is as follow:

$$\begin{aligned}
 \text{Particle Size } [\mu\text{m}] = & +2.978 \\
 & -0.035 \times \text{Temperature} \\
 & -4.502 \times 10^{-4} \times \text{Stirrer Speed} \\
 & +3.393 \times 10^{-6} \times \text{Temperature} \times \text{Stirrer Speed} \\
 & +1.232 \times 10^{-6} \times \text{Temperature}^2
 \end{aligned}$$

Figure 94 illustrates the actual measured response value for this observation against the response value predicted by the model for this set of experimental conditions.



Figure 94 - Actual measured response vs. model predicted value

The model predictions are not as accurate as those predicted with the **Number Mean-** and **Number Median Particle Size Models**. This is due to the R-squared value being lower for the **Area Median Particel Size Model (Number Mean Particle Size Model $R^2 = 0.676$, Number Median Particle Size Model $R^2 = 0.609$, Area Median Particle Size Model $R^2 = 0.436$)**. Similar trends that were obtained with the **Number Mean Particle Size Model (Composite)** and the **Number Median Particle Size Model (Composite)** were obtained with the **Area Median Particle Size Model (Composite)**.

Additional information on the **Number Mean Particle Size Model (Composite)**, **Number Median Particle Size Model (Composite)** and the **Area Median Particle Size Model (Composite)** can be viewed in **Appendix L**.

7.3.4 Roughness

The roughness (Ra) values obtained during the final composite experimental runs are presented in **Table 72**.

Table 72 - Roughness [Ra] Readings for the Composite Experimental Design

| Experiment | Roughness | |
|------------|-----------|---------|
| | Average | STD DEV |
| EXP F1 | 0.202 | 0.092 |
| EXP F2 | 0.215 | 0.107 |
| EXP F3 | 0.123 | 0.031 |
| EXP F4 | 0.266 | 0.126 |
| EXP F5 | 0.218 | 0.058 |
| EXP F6 | 0.168 | 0.073 |
| EXP F7 | 0.248 | 0.172 |
| EXP F8 | 0.248 | 0.274 |
| EXP F9 | 0.268 | 0.082 |
| EXP F10 | 0.214 | 0.126 |
| EXP F11 | 0.262 | 0.059 |
| EXP F12 | 0.233 | 0.226 |
| EXP F13 | 0.227 | 0.129 |
| EXP F14 | 0.265 | 0.033 |
| EXP F15 | 0.283 | 0.047 |
| EXP F16 | 0.368 | 0.065 |
| EXP F17 | 0.433 | 0.188 |
| EXP F18 | 0.293 | 0.040 |
| EXP F19 | 0.343 | 0.107 |
| EXP F20 | 0.240 | 0.024 |
| EXP F21 | 0.231 | 0.131 |
| EXP F22 | 0.207 | 0.043 |

| Experiment | Roughness | |
|------------|-----------|---------|
| | Average | STD DEV |
| EXP F23 | 0.193 | 0.088 |
| EXP F24 | 0.243 | 0.102 |
| EXP F25 | 0.135 | 0.050 |
| EXP F26 | 0.241 | 0.144 |
| EXP F27 | 0.177 | 0.072 |
| EXP F28 | 0.210 | 0.074 |
| EXP F29 | 0.252 | 0.213 |
| EXP F30 | 0.313 | 0.138 |
| Control | 0.07 | |

*** Control – The roughness of the Plexiglas® test plate**

The significantly high *STD DEV* recorded for **EXP F8** is as a result of air bubbles being entrapped in the emulsion during the wet application process, as seen in **Figure 95**.



Figure 95 - EXP F8: Dried Coating

This is purely an anomaly and should not be seen as the norm, as proven in **Table 72**. **Table 73** is a comparison of the average roughness obtained during the screening-, formulation- and composite experimental designs.

Table 73 - Comparison of the Average Roughness (Screening-, Formulation- and Composite Experimental Designs)

| Experimental Design | Average Roughness [Ra] | STD DEV [Ra] |
|---------------------|------------------------|--------------|
| Screening | 2.381 | 3.199 |
| Formulation | 0.827 | 0.862 |
| Composite | 0.244 | 0.064 |

From the data presented above it is clear that the lowest average roughness was obtained during the final composite experimental design. This indicates that both the formulation- and process parameters have been optimized. By examining **Table 72** it is noted that there are no large roughness readings. This is due to there being no cracking on any of the composite experimental

samples. All of the composite samples produced smooth uniform Carnauba wax layers (with the exception being **EXP F8** having entrapped air bubbles) once dried, as seen in **Figure 96**.



Figure 96 - Uniform dried Carnauba wax coating (EXP F1)

This is an indication that the design space was narrowed down to a feasible operating window throughout the Design of Experiments. In addition, the narrowed down design space also contains the optimum system (formulation- and process parameter combination) for the specific experimental setup and components.

The roughness data were entered into the Composite design experimental design in Design Expert© for further processing. Once the composite roughness data were analysed with Design Expert© it was found that neither the linear nor the reduced quadratic model was statistically significant ($p > 0.05$) (ANOVA tables can be viewed in **Appendix L**). Due to the roughness data model not being statistically significant ($p > 0.05$), it will not be taken into account during the optimization of the Composite experimental design.

7.3.5 Gloss

The gloss (*GU*) values obtained during the final composite experimental runs are presented in **Table 74**.

Table 74 - Gloss [GU] Readings for the Composite Experimental Design

| Experiment | Gloss | |
|------------|---------|---------|
| | Average | STD DEV |
| EXP F1 | 49.68 | 7.353 |
| EXP F2 | 46.28 | 2.557 |
| EXP F3 | 70.86 | 5.226 |
| EXP F4 | 45.76 | 3.810 |
| EXP F5 | 85.82 | 3.546 |
| EXP F6 | 53 | 1.113 |
| EXP F7 | 28.46 | 5.665 |
| EXP F8 | 104 | 5.448 |
| EXP F9 | 79.75 | 4.497 |
| EXP F10 | 47.86 | 2.804 |
| EXP F11 | 80.85 | 11.705 |
| EXP F12 | 42.89 | 6.148 |
| EXP F13 | 41.34 | 6.357 |
| EXP F14 | 60.06 | 1.960 |
| EXP F15 | 75.27 | 4.814 |
| EXP F16 | 47.33 | 0.838 |
| EXP F17 | 70.34 | 2.839 |
| EXP F18 | 47.16 | 6.161 |
| EXP F19 | 31.07 | 3.847 |
| EXP F20 | 91.75 | 3.975 |
| EXP F21 | 70.47 | 3.988 |
| EXP F22 | 62.86 | 10.149 |
| EXP F23 | 45.89 | 2.157 |
| EXP F24 | 59.11 | 4.229 |
| EXP F25 | 56.84 | 2.927 |
| EXP F26 | 33.32 | 1.415 |
| EXP F27 | 38.26 | 3.396 |
| EXP F28 | 73.74 | 4.154 |
| EXP F29 | 80.11 | 4.701 |
| EXP F30 | 50.72 | 3.542 |
| Control | 135 | |

*** Control – The gloss of the Plexiglas® test plate**

When examining the gloss readings obtained during the composite experimental runs (**Table 74**) it was clear that a wide range of gloss values were once again achieved (28.46 – 104 *GU*). As mentioned in the discussion on the Mixture experimental design it was expected that the process parameters had a greater influence on the gloss as proven by the results obtained (**Table 74**). The gloss values all fall within the range of gloss readings published by Bosquez-Molina et al. (2003) (**Table 40**) (Bosquez-Molina, Guerrero-Legarreta & Vernon-Carter 2003).

The gloss data were entered into the Composite experimental design in Design Expert® for further processing. It was noted that the linear model was not statistically significant ($p > 0.05$). A reduced quadratic model was fitted to the composite experimental gloss data. The revised model for the gloss data are presented in **Table 75**.

Table 75 - Gloss (Reduced Quadratic Model) ANOVA - Composite Experimental Design

| Analysis of Variance Table – Gloss (Reduced Quadratic Model) | | | | | | |
|--|----------|----|----------|-------|----------|-----------------|
| | Sum of | | Mean | F | p-value | |
| Source | Squares | df | Square | Value | Prob > F | |
| Model | 2159.674 | 2 | 1079.837 | 3.475 | 0.045 | significant |
| A-Temperature | 918.968 | 1 | 918.968 | 2.958 | 0.097 | |
| A ² | 1240.706 | 1 | 1240.706 | 3.993 | 0.055 | |
| Residual | 8388.949 | 27 | 310.702 | | | |
| Lack of Fit | 6569.011 | 22 | 298.591 | 0.820 | 0.667 | not significant |
| Pure Error | 1819.938 | 5 | 363.988 | | | |
| Cor Total | 10548.62 | 29 | | | | |
| Adeq Precision | 6.930 | | | | | |

The reduced quadratic model that was fitted to the gloss data was statistically significant ($p < 0.05$), as seen in **Table 75**. That said, when examining the R-squared values it is noted that the model is not a good representation of the design space. The R-squared values for the reduced quadratic gloss model is presented in **Table 76**.

Table 76 - Gloss Model (Composite) - R-Squared Values

| Model | R-Squared | Adj R-Squared | Pred –Squared |
|---------------------------------|-----------|---------------|---------------|
| Gloss (Reduced Quadratic Model) | 0.205 | 0.146 | 0.078 |

Due to the gloss model not being a good representation of the design space and to prevent a decrease in desirability, the gloss model will not be taken into account during the optimization of the Composite experimental design.

7.3.6 Temperature and Pressure

A similar pressure drop, noticed during the Screening- and Formulation Experimental Designs, was recorded at the inversion points of the Composite Experimental Design experiments, as seen in **Figure 97** (pressure is presented as bar guage).

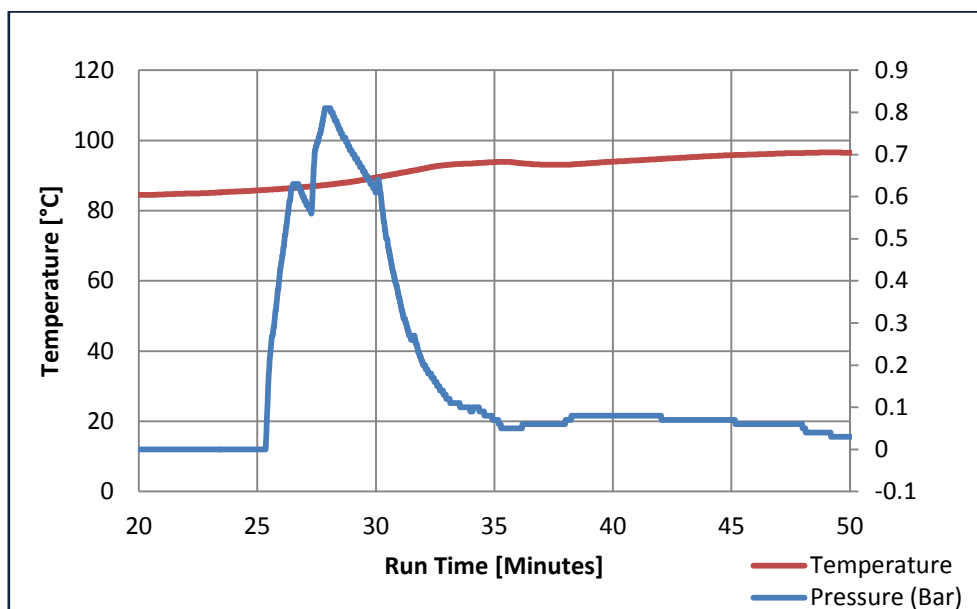


Figure 97 - Temperature and Pressure Curve - EXP F1

At a run time of 28 mins a clear pressure peak was noticed in **Figure 97**. During this pressure peak the Carnauba wax emulsion was inverted from a water-in-wax emulsion to a wax-in-water emulsion. This inversion caused the rheology of the emulsion to change abruptly resulting in the significant pressure drop (Hagenmaier, Baker 1994, Fernandez et al. 2004, Baciú, Moşescu & Nan 2008, Izquierdo et al. 2004). The clear pressure drop indicated that the Carnauba wax emulsion was inverted and that the final product was a wax-in-water emulsion.

7.3.7 Optimization

Once it was determined that the roughness model was not statistically significant and that the gloss model was not a good enough representation of the design space, the particle size was set as the main response for optimization purposes. Each of the three particle size models that were identified during the Composite experimental design discussion was optimized. The optimization results are presented in **Table 77** (the complete set of results generated from the optimization can be viewed in **Appendix M**).

Table 77 - Composite Experimental Design Optimization Results

| Model | Temperature [°C] | High Shear Time [min] | High Shear Speed [rpm] | Stirrer Speed [rpm] | Particle Size [µm] | Desirability |
|----------------------------|------------------|-----------------------|------------------------|---------------------|--------------------|--------------|
| Number Mean Model | 123.969 | 39.992 | 5613.645 | 1499.925 | 0.503 | 0.840 |
| Number Median Model | 127.569 | 39.999 | 5631.903 | 1499.997 | 0.481 | 0.849 |
| Area Median Model | 118.898 | 10.954 | 5714.154 | 1499.988 | 0.533 | 0.832 |

From **Table 77** it was noted that the highest desirability was obtained with the **Number Median Particle Size Model (Composite)**. Due to all three models' desirability being relatively close to each other, confirmation experiments were performed with all three optimized models. As a result of limited components there was only enough material left for five experimental runs. It was decided that two runs will be performed with the **Number Median Particle Size Model (Composite)** and the **Area Median Particle Size Model (Composite)** while only one confirmation experimental run will be performed with the **Number Mean Particle Size Model (Composite)**. The following results were obtained with the confirmation experimental runs **Table 78**.

Table 78 - Composite Experimental Design - Confirmation Runs Results

| Model | Particle Size [µm] | Gloss [GU] | Gloss [STD DEV] | Roughness [Ra] | Roughness [STD DEV] |
|----------------------------|--------------------|------------|-----------------|----------------|---------------------|
| Number Median Model | 0.472 | 101.95 | 1.921 | 0.202 | 0.132 |
| Number Median Model | 0.476 | 90.64 | 31.509 | 0.201 | 0.061 |
| Number Mean Model | 0.491 | 103.7 | 0.823 | 0.168 | 0.076 |
| Area Median Model | 0.595 | 96.25 | 6.105 | 0.158 | 0.032 |
| Area Median Model | 0.52 | 122.8 | 3.910 | 0.193 | 0.145 |

It is clear that the particle size of the confirmation runs performed with the **Number Median Particle Size Model (Composite)** are the smallest that have been achieved so far in this study. The

correlations between the relevant particle size distributions, roughness, gloss, stirrer speed and high shear homogenizing speed are listed in **Table 79**. A correlation value of 1 indicates a 100% positive correlation while a value of -1 indicate a 100% negative correlation and 0 no correlation (Clarke 2012). An effect size of ± 0.5 is considered as **large**, ± 0.3 as **medium** and ± 0.1 as **small**.

Table 79 - Correlations for the composite experimental data

| | Stirring Speed [rpm] | High Shear Speed [rpm] | Number (Mean) [μm] | Number (Median) [μm] | Area (Median) [μm] | Gloss [GU] | Roughness [Ra] |
|-----------------------------------|----------------------|------------------------|---------------------------------|-----------------------------------|---------------------------------|------------|----------------|
| Stirring Speed [rpm] | 1 | | | | | | |
| High Shear Speed [rpm] | 0.000 | 1 | | | | | |
| Number (Mean) [μm] | -0.593 | -0.066 | 1 | | | | |
| Number (Median) [μm] | -0.597 | -0.004 | 0.983 | 1 | | | |
| Area (Median) [μm] | -0.414 | -0.222 | 0.913 | 0.870 | 1 | | |
| Gloss [GU] | 0.110 | -0.166 | 0.051 | 0.034 | 0.114 | 1 | |
| Roughness [Ra] | 0.125 | 0.156 | -0.318 | -0.369 | -0.271 | -0.011 | 1 |

The stirring speed has a large effect on the particle size while just a small effect on the gloss and roughness. It is also noted that the particle size has a medium effect on the roughness. This is expected since a small particle size produces a smooth surface with low roughness. The high shear speed has a small effect on the gloss as well. Each of the particle size models (the **Number Mean Particle Size Model (Composite)**, **Number Median Particle Size Model (Composite)** and the **Area Median Particle Size Model (Composite)**) were plotted with the actual values obtained from the confirmation- and additional runs. The effect of temperature on the particle size for the **Number Mean Particle Size Model (Composite)** is presented in **Figure 98**.

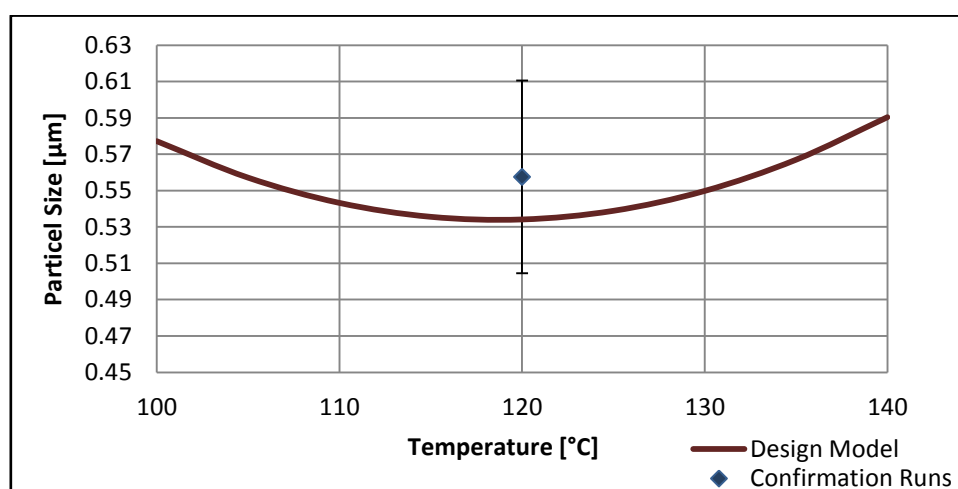


Figure 98 - Number Mean Particle Size Model (Composite Experimental Design) - Particle Size vs. Temperature

The **Number Median Particle Size Model (Composite)** plot is presented in **Figure 99**.

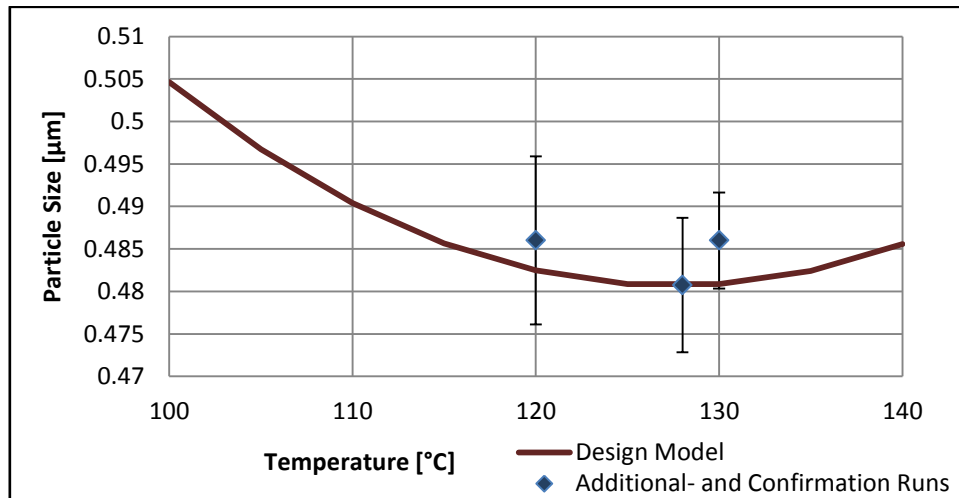


Figure 99 - Number Median Particle Size Model (Composite Experimental Design) - Particle Size vs. Temperature

Finally the **Area Median Particle Size Model (Composite)** plot is presented in **Figure 100**.

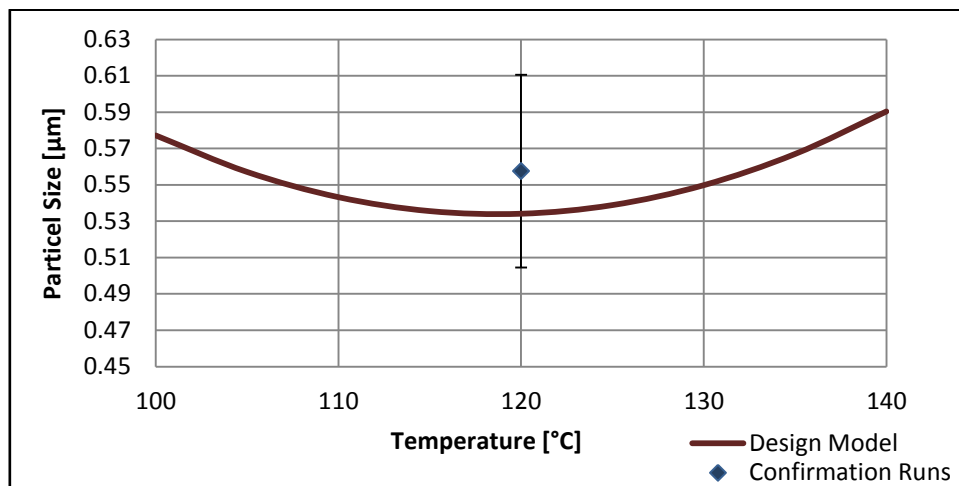


Figure 100 - Area Median Particle Size Model (Composite Experimental Design) - Particle Size vs. Temperature

From the three plots presented above (**Figure 98**, **Figure 99** and **Figure 100**) it is clear that the **Number Median Particle Size Model (Composite)** is the most significant model, resulting in the smallest average particle size. The full range of particle sizes for three of the five confirmation runs are presented in **Figure 101**.

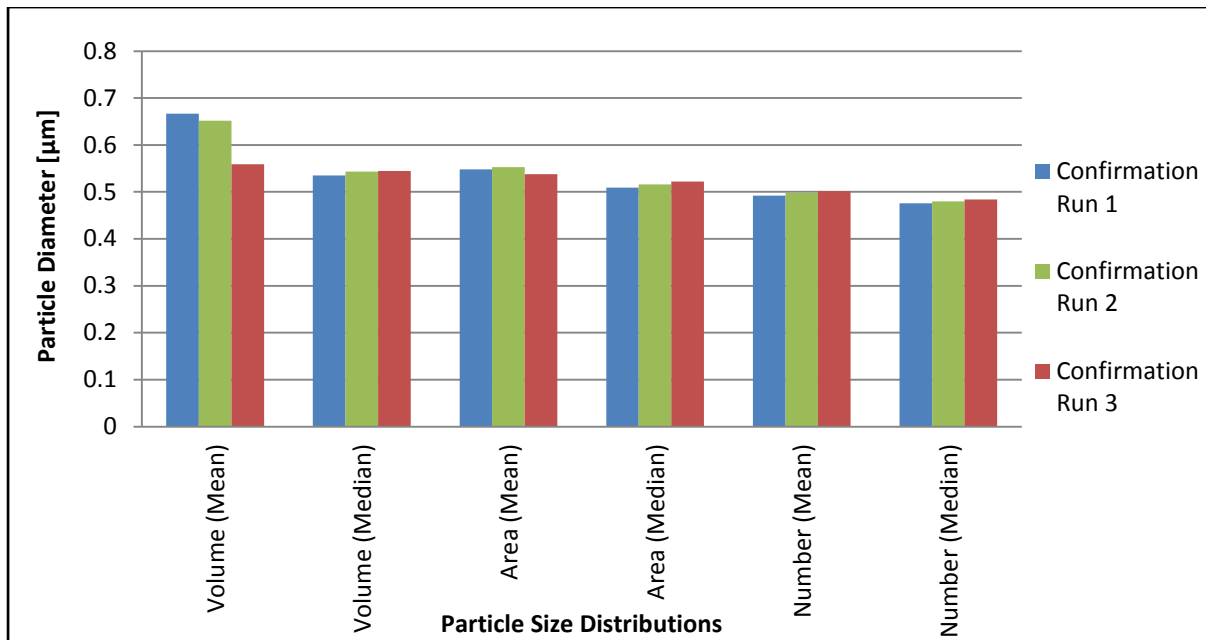


Figure 101 - Number Median Model - Mean- and Median Particle Sizes

It is clearly visible in **Figure 101** that the particle sizes (volume-, area- and number particle size distributions) are the same order of magnitude and more comparable to each other. This indicates that there is an insignificant amount of random large particles which barely influences the volume particle size distribution (sensitive to large particles).

The **Number Median Particle Size Model (Composite)** [**Number Median Model (Composite)**] is the final optimized model that will be used to compare to commercial waxes currently being used in the industry.

7.3.7.1 Viscosity, pH and Density

To ensure that the final optimized Carnauba wax emulsion fall within the ranges published by Hagenmaier (1995) and the specifications of the commercial Citrosol© and DECC Citrashine© Carnauba wax emulsions, the viscosity, pH and density were measured and recorded. The viscosity was excluded since there is no published data to compare the results to. The pH and density readings for the composite optimization experimental runs are presented in **Table 80**.

Table 80 - pH and Density Readings for the Composite Experimental Design

| Experiment | pH | Density [kg/m ³] |
|------------|-------|------------------------------|
| EXP O1 | 10.05 | 992.00 |
| EXP O2 | 10.05 | 992.78 |
| EXP O3 | 9.93 | 992.58 |
| EXP O4 | 9.96 | 992.47 |
| EXP O5 | 9.98 | 992.62 |

When comparing the pH and density values obtained during the composite optimization experimental runs (**Table 80**) to the values published by Hagenmaier (1995) and the specifications of the commercial Citrosol© and DECC Citrashine© Carnauba wax emulsions, it is noted that the values obtained fall within their ranges. This confirms that the **Number Median Model (Composite)** can be used to manufacture Carnauba wax emulsions.

7.3.7.2 Final Carnauba Wax Emulsion Formulation

The final Carnauba wax emulsion formulation- and process parameter setup that was obtained through this study is presented in **Table 81**.

Table 81 - Final Optimized Formulation- and Process Parameter Settings

| Process Parameter/Formulation Parameter | | Range [Min-Max] |
|---|----------|---------------------------------|
| Temperature [°C] | 127.6 | 100 - 140°C |
| High Shear Time [min] | 40 | 0 - 55 min |
| High Shear Speed [rpm] | 5630 | 3050 - 8050 rpm |
| Stirrer Speed [rpm] | 1500 | 460 - 1850 rpm |
| Cooling Rate | 1 (Full) | Fixed (Screening Experiments) |
| Inverting Phase Addition Rate [l/h] | 3 | Fixed (Screening Experiments) |
| %Water [wt%] | 75.3 | Fixed (Formulation Experiments) |
| %Wax [wt%] | 15.8 | Fixed (Formulation Experiments) |
| %Oleic Acid [wt%] | 6.3 | Fixed (Formulation Experiments) |
| %Potassium Hydroxide [wt%] | 0.6 | Fixed (Formulation Experiments) |
| %Ammonium Hydroxide [wt%] | 2 | Fixed (Formulation Experiments) |

When examining the ranges of the process parameters that were optimized (**Table 81**), it is clearly noted that the settings lie within in the ranges, indicating that they are true optimums.

7.3.8 Scaling up to Commercial Scale

Similar scaling criteria's used to downscale the plant scale reactor, can be used to scale up the optimized final Carnauba wax emulsion formulation- and process parameter setup to commercial scale. The equal power input per unit mass and geometrical similarity scaling criterion of McCabe, Smith & Harriot (presented below), can be used to scale the agitator impeller rotational speed (McCabe, Smith & Harriott 1985).

$$N_i/N_1 = (D_{a1}/D_{ai})^{2/3}$$

(McCabe, Smith & Harriott 1985)

N – Impeller rotation speed (rpm)

D – Impeller diameter (meter)

For the high shear homogenizer, the constant Froude number rule can be used to scale up the impeller rotational speed to commercial scale with the Rahmanian et al. criterion, as presented below (Rahmanian et al. 2008).

The three scaling rules on the mechanical strength of granules (Rahmanian et al. 2008):

- Constant tip speed ($n = 1$)
- Constant shear stress ($n = 0.8$)
- Constant Froude number ($n = 0.5$)

These three scaling rules can be summarized by **Equation 12** below (Rahmanian et al. 2008):

$$N_x/N_y = \left(D_y/D_x \right)^n$$

(Rahmanian et al. 2008)

N – Impeller rotational speed (rpm)

D – Blade diameter (m)

x, y – Different scales of high – shear mixers

n – Constant depending on the rule

As mentioned by Hu in a study he conducted on the scaling-up and scaling-down of bioreactors, it is crucial to keep the most important variable(s) constant or at least above the critical value (Hu 2004). Thus for scaling up the Carnauba wax emulsion formulation- and process parameter setup to commercial scale, the *Temperature*, *Stirrer Speed* and *High Shear Time Interval* will have to be kept constant or just above their respective critical values.

Chapter 8: Comparisons with Commercial Coatings

The **Number Median Model (Composite)** formulated throughout this study yielded an optimum formulation that was used to produce an optimum final coating that was compared to various commercial waxes currently being used in the post-harvest industry. All the waxes that are included in this comparison are Carnuba wax emulsions. Commercial waxes from four different commercial wax companies were obtained and analysed. The comparison of the **Number Median Model (Composite)** coating with the commercial waxes obtained from three of the four companies is presented in **Figure 102**.

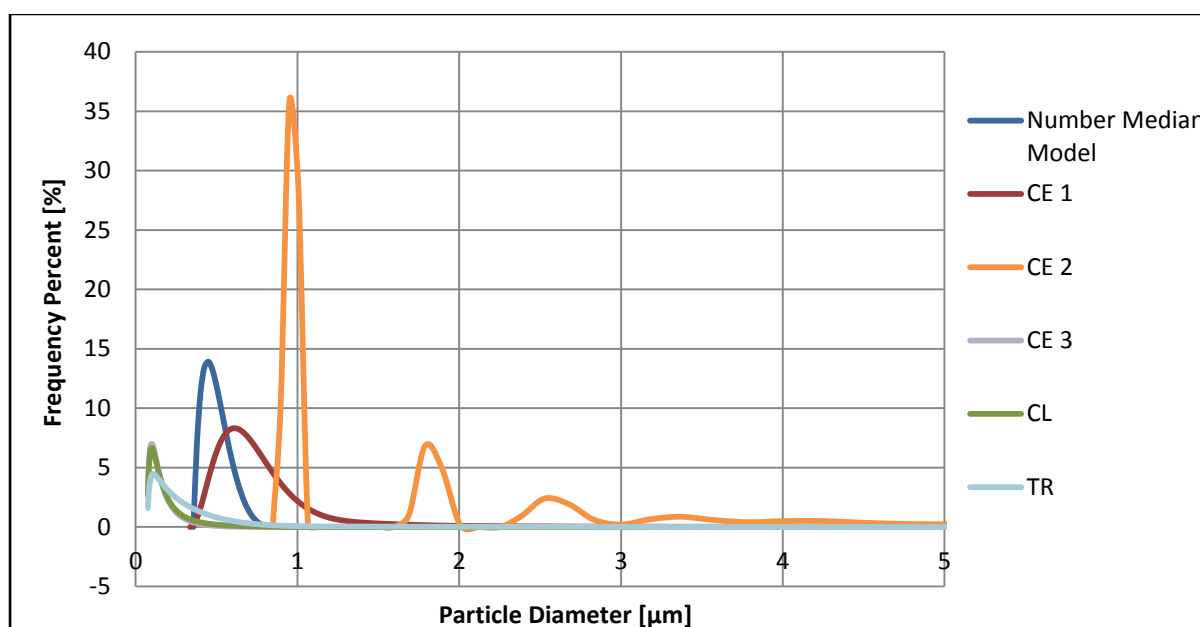


Figure 102 – Comparison of Number Median Model (Composite) and Commercial Waxes

When examining **Figure 102** it is clearly visible that the particle size distribution obtained with the **Number Median Model (Composite)** falls within the average particle size and –distribution ranges of the five commercial Carnuba wax emulsions CE1, CE2, CE3, CL and TR. It is noted that the CE3, CL and TR coatings have a smaller average particle size while the CE1 and CE2 coatings have a larger average particle size than the **Number Median Model (Composite)** coating. A possible explanation for the CE3, CL and TR coatings having a smaller average particle size and –distribution could be the method of manufacturing and the difference in process setup. In addition to the setup and formulation, the scale of production will also make a difference. That said, the **Number Median**

Model (Composite) coating compares well with the commercial Carnauba wax emulsions CE1, CE2, CE3, CL and TR, in terms of average particle size and –distribution.

Figure 102 was re-plotted with a logarithmic scale X-axis to present clearer representations of the average particle sizes and –distributions (number, volume and area), as seen in **Figure 103**, **Figure 104** and **Figure 105**.

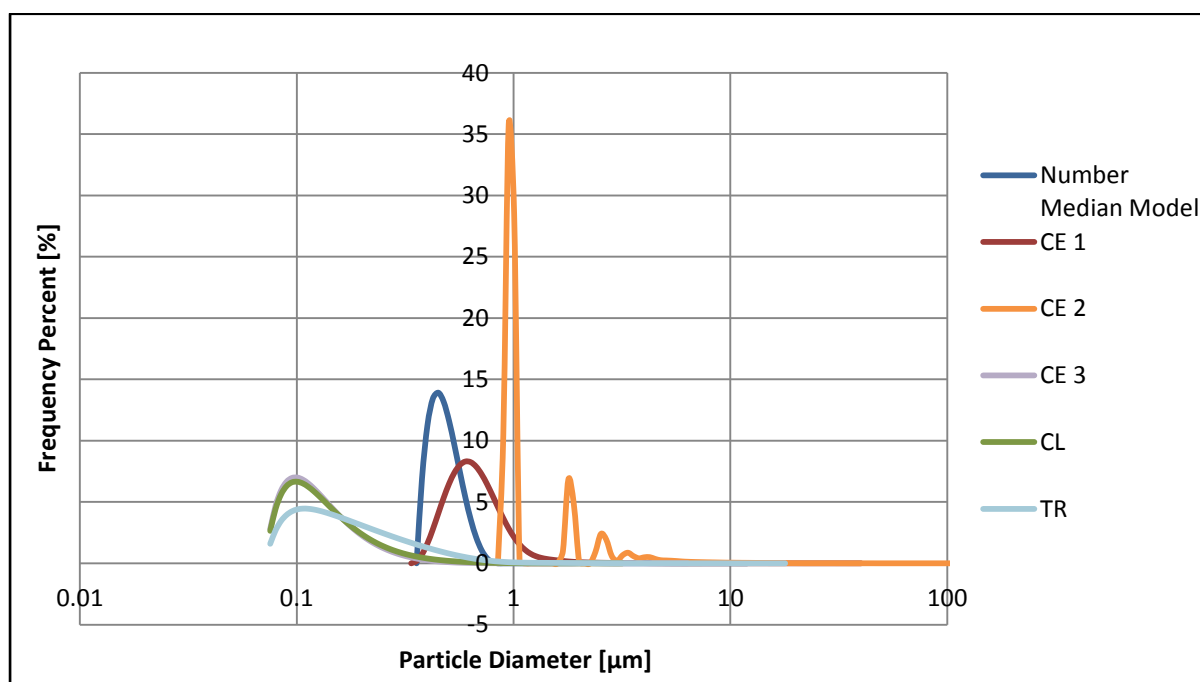


Figure 103 – Comparison of Number Median Model (Composite) and Commercial Waxes – Number Distribution (logarithmic scale)

Figure 103 presents the number particle size distribution data for the **Number Median Model (Composite)** coating, CE1, CE2, CE3, CL and TR coatings. As with **Figure 102**, it is clear that the CE3, CL and TR coatings have a smaller average particle size while the CE1 and CE2 coatings have a larger average particle size than the **Number Median Model (Composite)** coating. **Figure 104** represents the volume particle size distribution data for the **Number Median Model (Composite)** coating, CE1, CE2, CE3, CL and TR coatings.

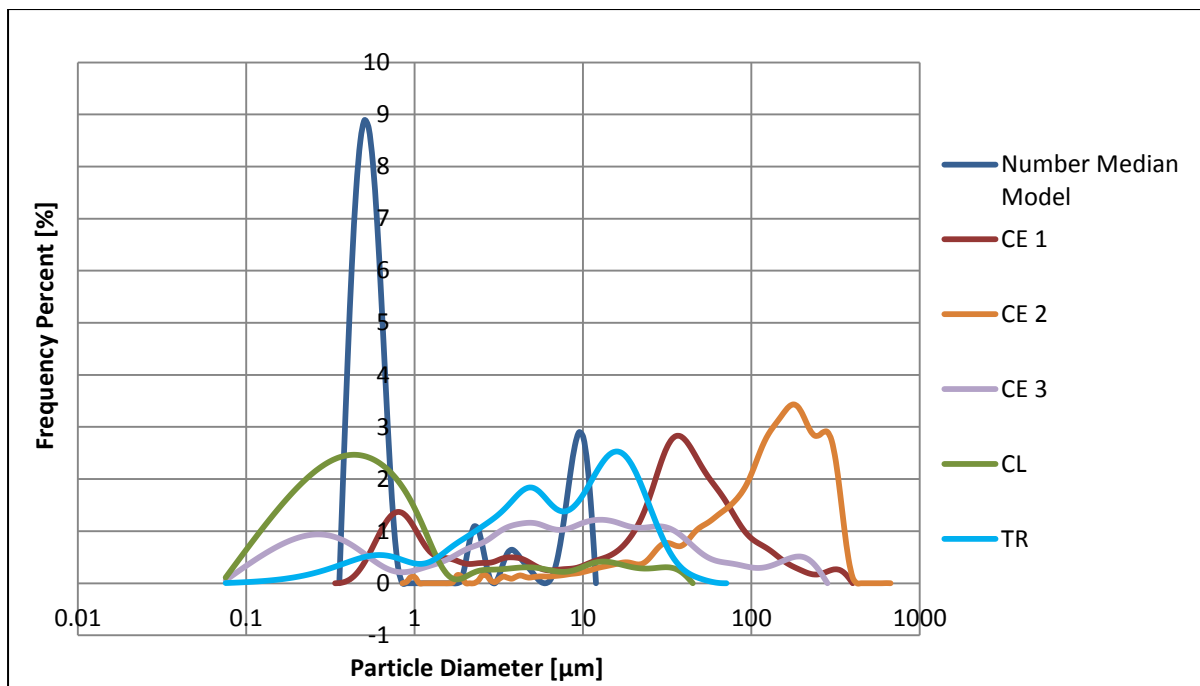


Figure 104 – Comparison of Number Median Model (Composite) and Commercial Waxes – Volume Distribution (logarithmic scale)

Examining **Figure 104**, it is noted that CE2 has a significant amount of large particles when comparing it to the number particle size distribution (**Figure 103**). Also, it is clear that the **Number Median Model (Composite)** coating has a small amount of large particles, as seen in **Figure 104**.

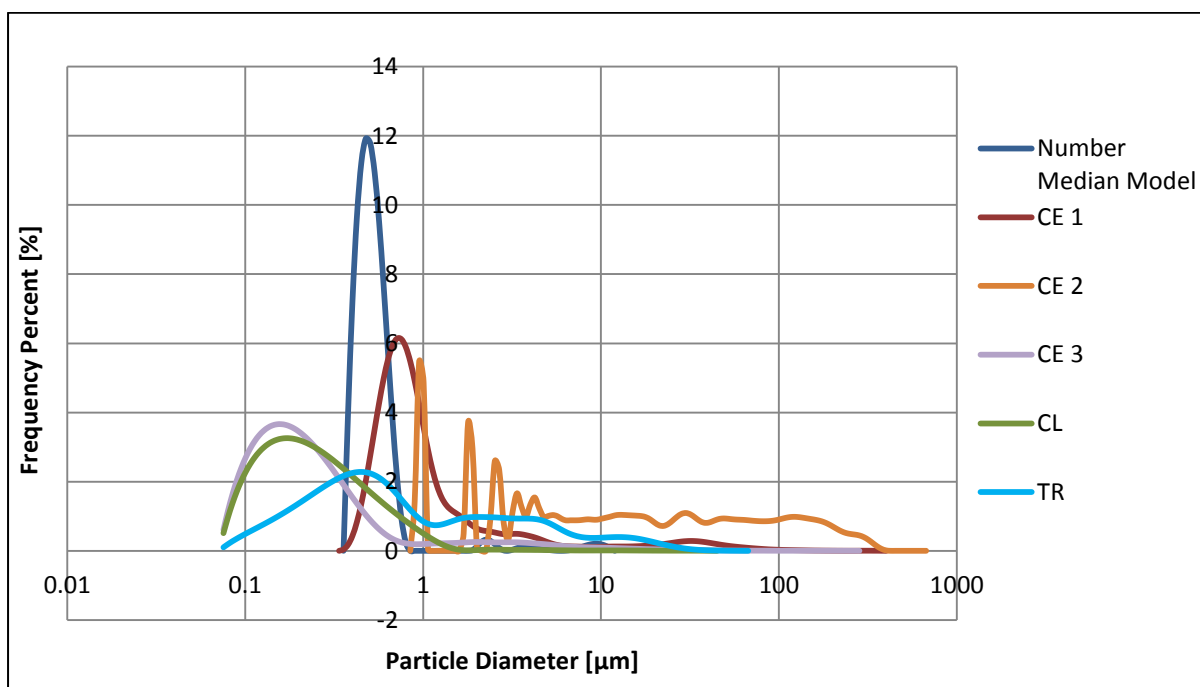


Figure 105 – Comparison of Number Median Model (Composite) and Commercial Waxes - Area Distribution (logarithmic scale)

Figure 105 is a representation of the area particle size distribution data of the coatings. From all three figures (**Figure 102**, **Figure 103** and **Figure 104**) it is clear that the **Number Median Model (Composite)** coating has a small amount of large particles and a significant amount of small particles.

To show the significant amount of large particles in the TR coating, a comparison of the volume-, area- and number particle size distributions are presented in **Figure 106**, while **Figure 107** is a representation of the **Number Median Model (Composite)** coating's volume-, area- and number particle size distribution data.

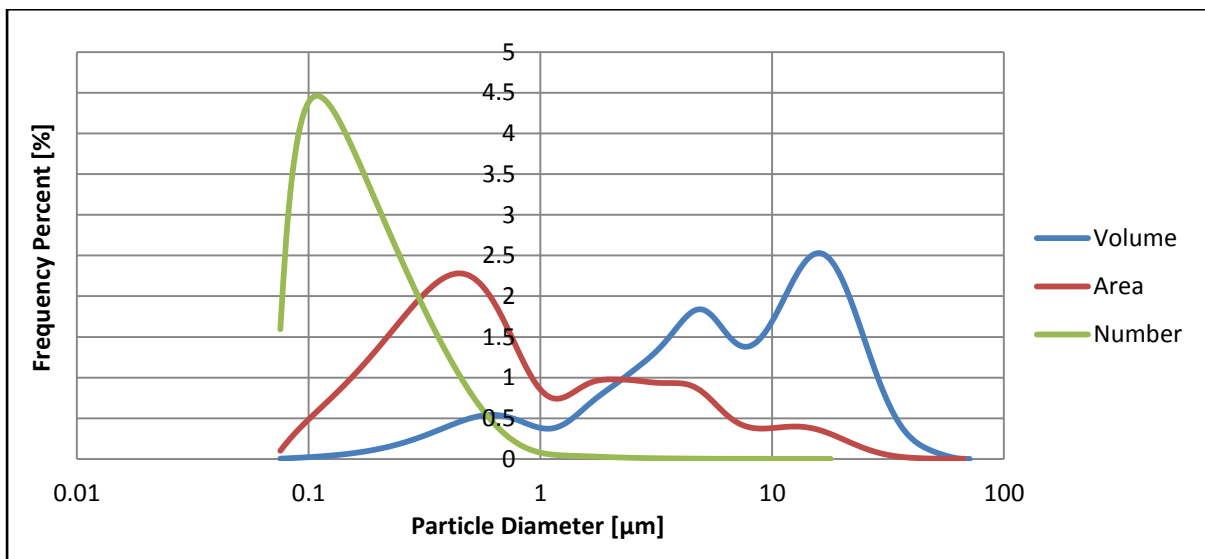


Figure 106 – Volume-, Area- and Number Particle Size Data – TR Coating

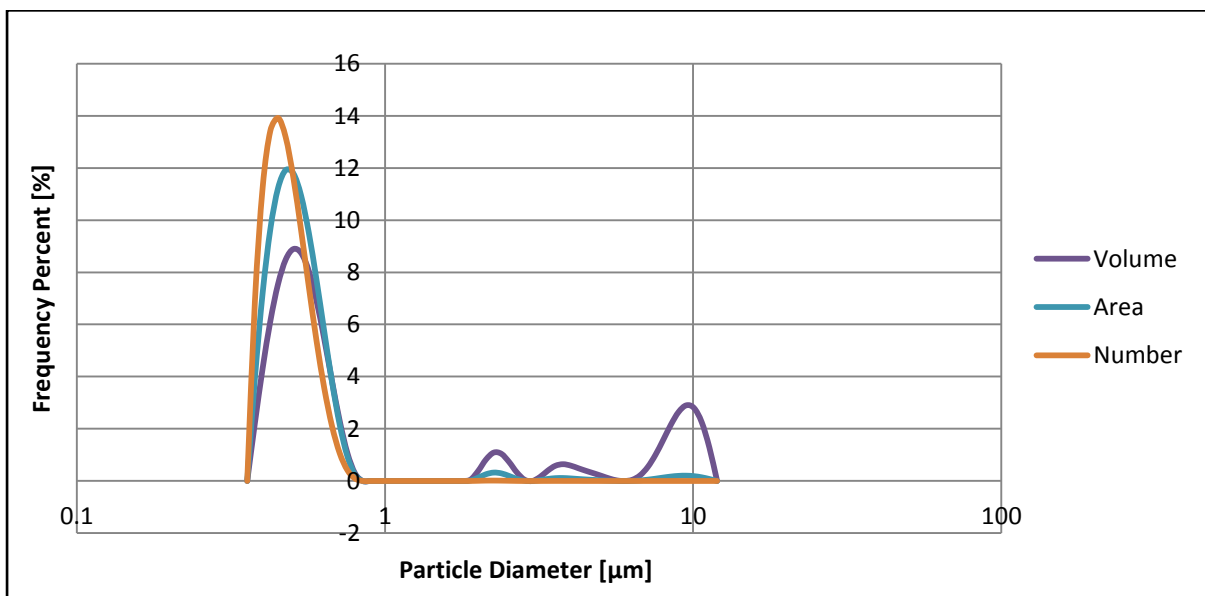


Figure 107 – Volume-, Area- and Number Particle Size Data - Number Median Model (Composite)

From **Figure 106** it is noted that even though the TR coating has a smaller average particle size compared to the **Number Median Model (Composite)** coating, it contains a significant amount of large particles that is clearly evident when examining the volume-, area- and number particle size data. The **Number Median Model (Composite)** coating on the other hand has fewer large particles affecting the number- and area particle size distributions, as seen in **Figure 107**. Additional visual comparisons of the **Number Median Model (Composite)** coating with the commercial waxes (CE, CL and TR) can be viewed in **Appendix N**.

Six additional commercial waxes, which were obtained from a fourth commercial wax company, were compared to the **Number Median Model (Composite)** coating. These six Carnauba wax emulsions are compared with the **Number Median Model (Composite)** coating in **Figure 108**.

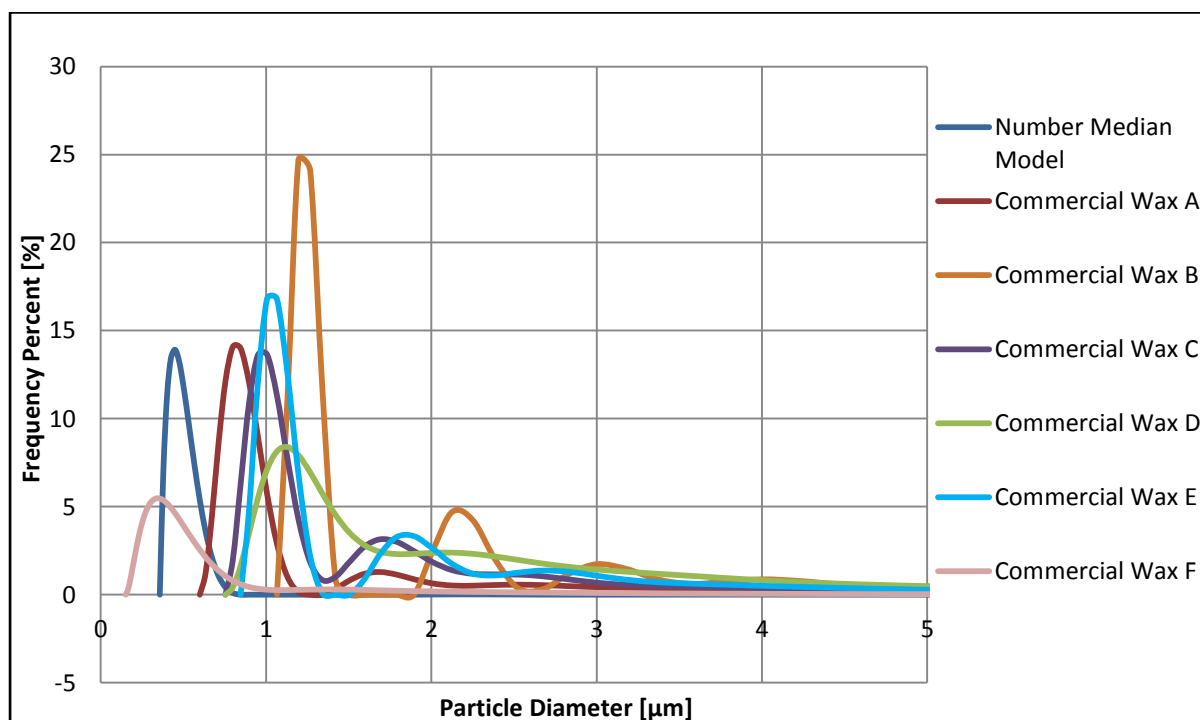


Figure 108 - Comparison of Number Median Model (Composite) and Commercial Waxes

Figure 108 clearly indicates that, on the basis of average particle size and –distribution, the **Number Median Model (Composite)** coating compares very well to the commercial waxes obtained from the fourth commercial wax company. As mentioned above with the Carnauba wax emulsions obtained from CE, CL and TR, the formulation, setup and scale of production is not known and therefore could contribute to the difference in average particle size and –distribution. The same counts for the commercial waxes obtained from the fourth commercial wax company.

The data in **Figure 108** was re-plotted with a logarithmic X-axis to represent the data more visually accurate, as seen in **Figure 109**.

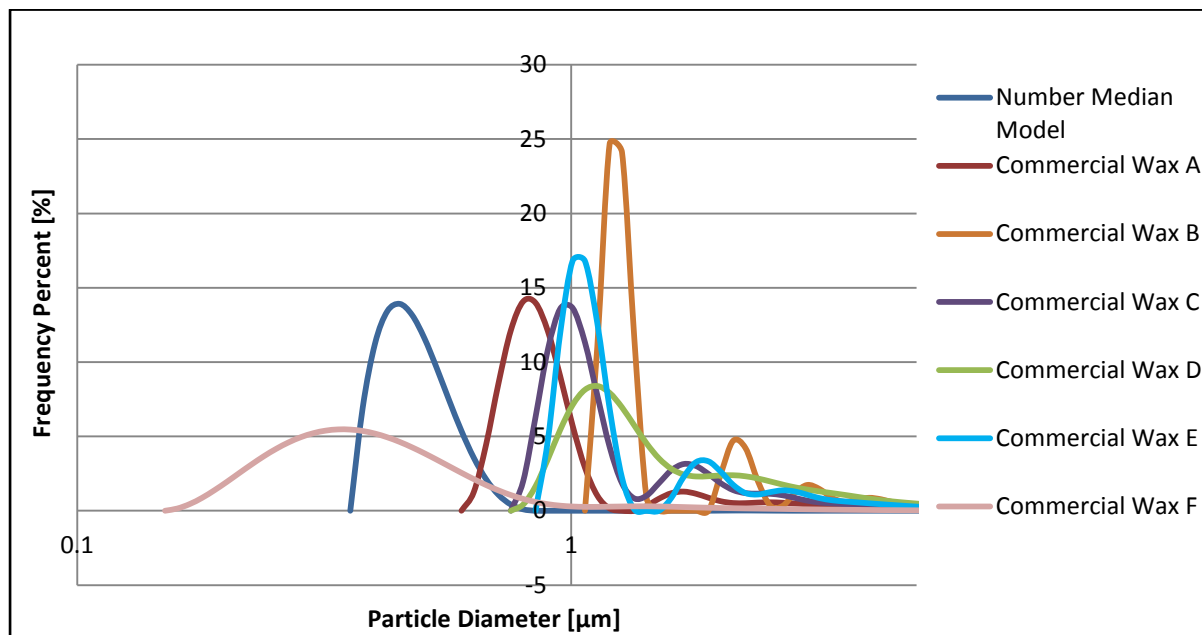


Figure 109 - Comparison of Number Median Model (Composite) and Commercial Waxes – Number Distribution (logarithmic scale)

Of the six additional commercial waxes from fourth commercial wax company, only Commercial Wax F had a smaller average particle size (number distribution) than what was obtained with the **Number Median Model (Composite)**.

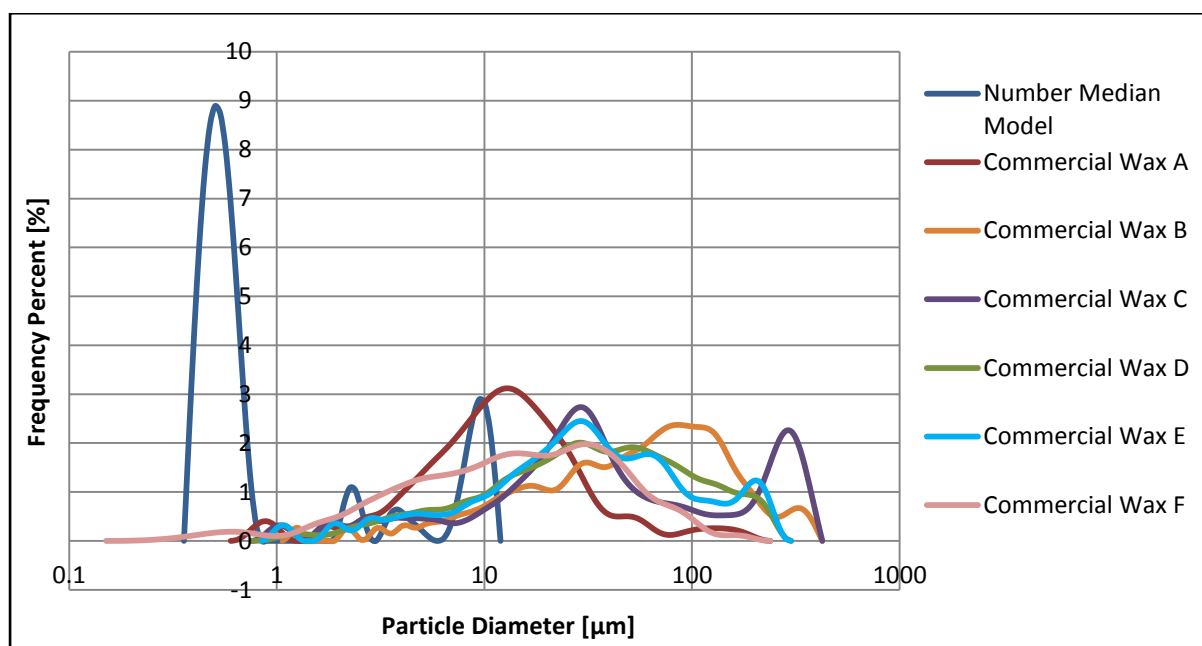


Figure 110 – Comparison of Number Median Model (Composite) and Commercial Waxes - Volume Distribution (logarithmic scale)

Figure 110 is a comparison of the volume particle size distribution data of the **Number Median Model (Composite)** coating with the additional commercial waxes from the fourth commercial wax company. From **Figure 110** it is clearly noted that all six additional commercial waxes contain a significant amount of large particles, since the **Number Median Model (Composite)** coating has the smallest average particle size (volume distribution). A similar occurrence appears in **Figure 111** which is a comparison of the area particle size data.

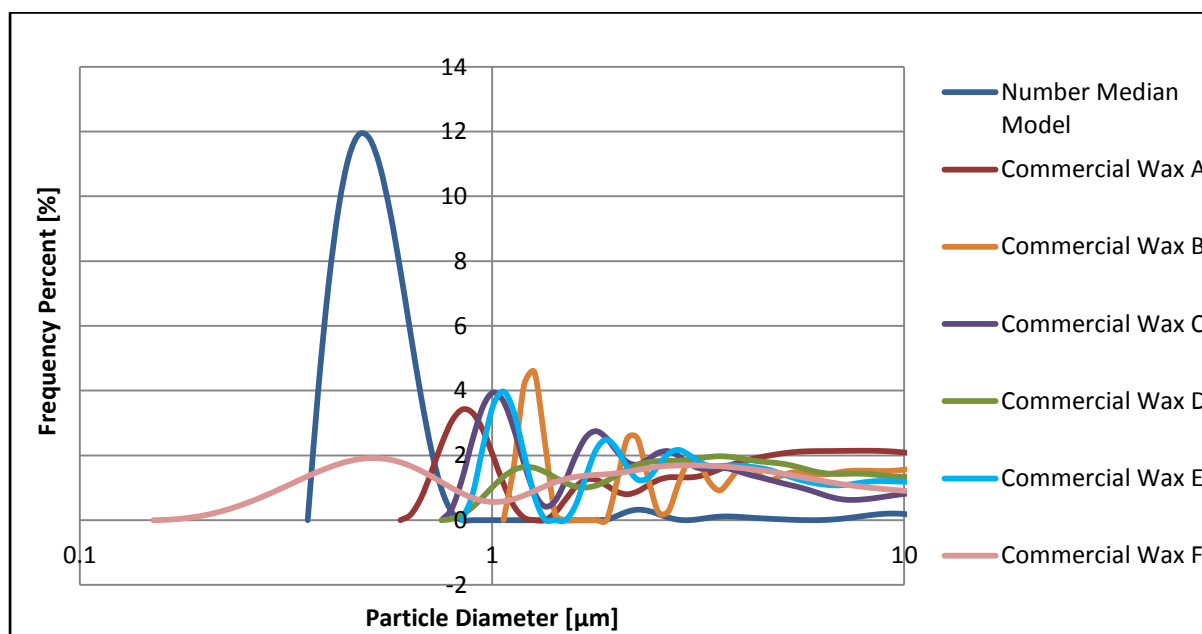


Figure 111 – Comparison of Number Median Model (Composite) and Commercial Waxes - Area Distribution (logarithmic scale)

Commercial Wax F coating’s volume-, area- and number particle size data are presented in **Figure 112**.

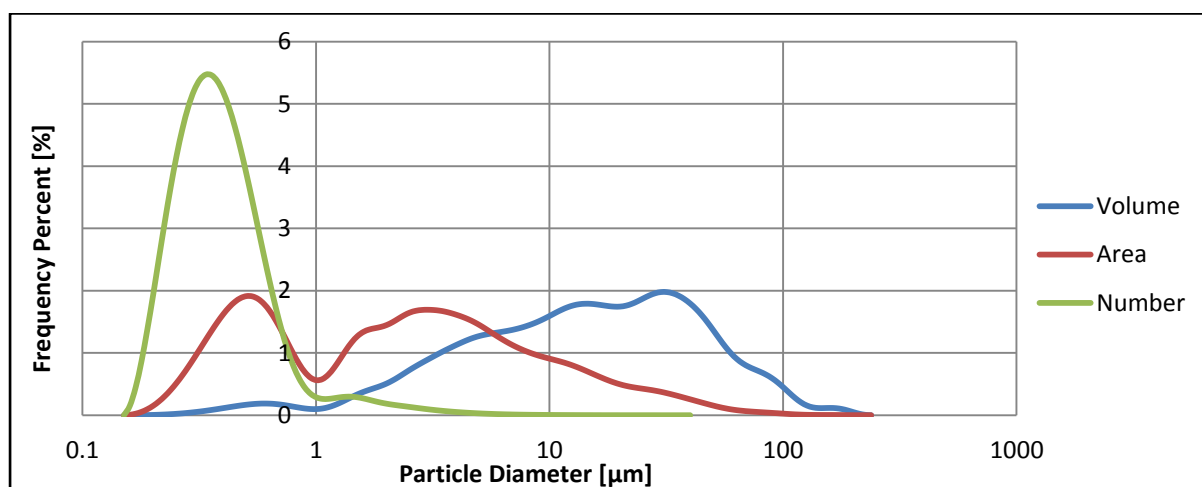


Figure 112 - Volume-, Area- and Number Particle Size Data - Commercial Wax F

When comparing the **Number Median Model (Composite)** coating results (**Figure 107**) with the Commercial Wax F coating (**Figure 112**) it is evident that the **Number Median Model (Composite)** achieves a smaller average- and a more consistent particle size than the Commercial Wax F coating and essentially all of the additional commercial coatings from the fourth commercial wax company. Additional visual comparisons of the **Number Median Model (Composite)** coating with the commercial waxes from the fourth commercial wax company can be viewed in **Appendix N**.

Overall, when comparing the **Number Median Model (Composite)** coating with all of the above mentioned commercial coatings, the **Number Median Model (Composite)** coating contains fewer large particles affecting the number- and area particle size distributions and a more consistent particle size distribution and average particle size. This is favourable characteristics for edible wax coatings, as mentioned by McClements (2010), Milanovic (2011), Griffin (1945), Karbowski (2007), Lashmar (1995), Danghui (1995) and Perez (2002) (Griffin 1945, Lashmar, Richardson & Erbod 1995, Danghui, Fengyan & Tianbo 2012, McClements 2010, Milanovic et al. 2011, Karbowski, Debeaufort & Voilley 2007, Pérez et al. 2002b).

Chapter 9: Conclusions & Recommendations

The conclusions of this study are divided into two sections. The first section focusses on the bench scale pilot plant design, construction and commissioning while the second section focusses on the experimentation, statistical modelling and optimization. Finally, recommendations for future studies are given regarding the overall study.

9.1 Designing, Building and Commissioning of a Bench Scale Pilot Plant

An existing commercial size pressure vessel of 6000 l, which is currently operational, was down-scaled to a 6 l bench scale semi-batch pressure vessel. The pressure vessel includes a high shear homogenizer and stirrer, amongst other things. Customized seal housings were designed and manufactured to maintain the pressure inside the pressure vessel while the two axles (stirrer and high shear homogenizer) rotated at their required speeds. The 6 l pressure vessel was incorporated into a complete bench scale pilot plant.

Data logging, temperature control and additional safety features were installed to aid in establishing a proper operating procedure and design of experiments. Data logging capabilities were set up to record pressure transmitter- and temperature probe (PT100) data for experimental analysis purposes. A heating coil (oil), heat tracing and double vessel wall configuration (water) were installed for temperature control purposes. Safety interlocks and dead switches were also set up for safe operation of the bench scale pilot plant.

The bench scale pilot plant was commissioned by running the process with water while ensuring that there were no leaks in the system. The wet-run also confirmed that the heating and cooling capabilities of the pressure vessel are sufficient. Once the bench scale pilot plant was fully operational, commissioning experiments were performed with basic formulations obtained from literature. These formulations served as a baseline in establishing the final natural wax edible coating formulation.

9.2 Experimentation, Statistical Modelling and Optimization

The primary focus of the experiments was to establish an optimum edible wax micro-emulsion coating with favourable properties evaluated according to literature. The commissioning experiments were used to establish a baseline formulation. A preliminary investigation in the form of screening experiments (including both process- and formulation parameters), were performed to identify the main process parameters. The process parameters that were investigated (according to literature) were the *Temperature* [°C], *High Shear Time Interval* [min], *Stirrer Speed* [rpm], *High Shear Homogenizer Speed* [rpm], *Cooling Rate* [-1,0,1] and *Inverting Phase Addition Rate* [l/min]. Once the screening experiments were completed, particle size-, roughness-, gloss-, viscosity-, pH- and density analyses were performed and the measurements were entered into statistical analysis software for further processing. In terms of the particle size it was concluded that the **Volume Mean Particle Size Model V2 (Screening)** was the most appropriate model to use for optimization purposes. The Screening experimental design was optimized in terms of the particle size (to decrease), roughness (to decrease) and gloss (to increase). The viscosity, pH and density were excluded since the models were statistically insignificant. Once the screening experimental data were optimized the significant process parameters were identified as the *Temperature* [°C], the *High Shear Time Interval* [min], the *Stirrer Speed* [rpm] and the *High Shear Homogenizer Speed* [rpm]. In terms of the mixture, it was established that the optimum formulation was not included in the initial mixture design ranges.

Formulation experiments were performed to obtain the optimum formulation. A D-Optimal Mixture design was set up which tested the ranges of the water, wax, oleic acid, ammonium hydroxide and potassium hydroxide to yield the optimal formulation. Three additional replicates, three additional points to estimate lack of fit and two additional centre points were included in the design. Once the formulation experiments were completed, particle size-, roughness and gloss analyses were performed and the measurements were entered into statistical analysis software for further processing. The viscosity-, pH- and density analyses were used purely as confirmation measurements. In terms of the particle size it was concluded that the **Area Median Particle Size Model (Mixture)** was the only model that is statistically significant. The **Area Median Particle Size Model (Mixture)** was optimized in terms of the particle size only, since the roughness- and gloss models were statistically insignificant. An optimized formulation was obtained by taking an average of the response outputs. The formulation is as follow: %Water [75.3 %], %Carnauba Wax [15.8 %], %Oleic Acid [6.3 %], %Potassium Hydroxide [0.6 %], %Ammonium Hydroxide [2 %]. A confirmation run was performed that confirmed the optimized formulation.

The final experimental design, the Composite experimental design, was performed to obtain the optimum process parameter combination. A standard multifactor response surface methodology design, Central Composite Design, was used to set up the experiments. Each factor was varied over five levels. Once the composite experiments were completed with the formula obtained during the formulation experiments, particle size-, roughness- and gloss analyses were performed and the measurements were entered into statistical analysis software for further processing. The viscosity-, pH- and density analyses were used purely as confirmation measurements. It was determined that the roughness model was not statistically significant while the gloss model was not a good enough representation for the design space (*Predicted vs. Actual*). As a result the particle size was set as the main response for optimization purposes.

Three particle size models (***Number Mean Model (Composite)***, ***Number Median Model (Composite)***) and the ***Area Median Model (Composite)*** were identified as statistically significant. All three of the models were optimized in terms of the particles size. Optimum process parameter combinations were obtained for each model. Confirmation runs were performed for each model to confirm and identify the optimum process parameter settings. The ***Number Median Model (Composite)*** obtained the smallest average particle size and particle size distribution. Throughout the three experimental designs, the design space was decreased to a feasible operating window. The ***Number Median Model (Composite)*** is as follow:

$$\begin{aligned}
 \text{Particle Size } [\mu\text{m}] = & +0.923 \\
 & -7.244 \times 10^{-3} \times \text{Temperature } [^{\circ}\text{C}] \\
 & +2.397 \times 10^{-3} \times \text{High Shear Time } [\text{min}] \\
 & -1.583 \times 10^{-5} \times \text{Stirrer Speed } [\text{rpm}] \\
 & -2.042 \times 10^{-5} \times \text{Temperature } [^{\circ}\text{C}] \times \text{High Shear Time} [\text{min}] \\
 & +3.16 \times 10^{-5} \times \text{Temperature } [^{\circ}\text{C}]^2
 \end{aligned}$$

When comparing the models obtained during the Screening-, Mixture- and Composite Experimental Designs, it is clearly noted that the most significant models in each of the designs were based on the volume distribution, area distribution and the number distribution, respectively. This is due to the initial experiments (Screening Experimental Design) containing a significant amount of large particles, thus making the volume distribution model a more accurate representation of the design space (model takes into account the presence of large particles). Similarly, during the final

Composite Experimental Design, there were minimal large particles present in the coatings which resulted in the number distribution model being the most accurate representation of the design space (model takes into account the lack of large particles).

The **Number Median Model (Composite)** yielded an optimum formulation that was used to produce an optimum final coating that was compared to commercial waxes currently being used in the industry. The final formulation- and process parameter setup that was obtained with the **Number Median Model (Composite)** is as follow: *Temperature* [127°C], *High Shear Time* [40 min], *High Shear Speed* [5630 rpm], *Stirrer Speed* [1500 rpm], *Cooling Rate* [1], *Inverting Phase Addition Rate* [3 l/h], %*Water* [75.3 %], %*Carnauba Wax* [15.8 %], %*Oleic Acid* [6.3 %], %*Potassium Hydroxide* [0.6 %], %*Ammonium Hydroxide* [2 %]. Eleven commercial waxes obtained from four different commercial wax companies were compared with the final product obtained with the **Number Median Model (Composite)**. It was found that the **Number Median Model (Composite)** coating contains fewer large particles affecting the number- and area particle size distributions and a more consistent particle size distribution and average particle size. These are favourable characteristics for edible wax coatings as stated by various literature sources. All of the commercial waxes had a significant amount of large particles affecting the volume particle size distributions, while the **Number Median Model (Composite)** coating stayed relatively constant across the number-, area- and volume particle size distributions.

The main conclusion of this study is that a bench scale pilot plant facility for the manufacturing of edible wax coatings has been established which aided in optimizing a specific natural edible Carnauba wax micro-emulsion coating formulation. The final optimized formulation and process parameter settings resulted in a final product with superior qualities when compared to commercial waxes currently being used in the post-harvest industry.

9.3 Recommendations for Future Work

Due to the limited literature on edible Carnauba wax emulsion coatings and their process parameters, only the main process parameters identified in literature were varied in this study. This included the *Temperature* [°C], *High Shear Time Interval* [min], *Stirrer Speed* [rpm], *High Shear Homogenizer Speed* [rpm], *Cooling Rate* [rating] and *Inverting Phase Addition Rate* [l/min]. The current bench scale pilot plant can be used to perform a complete parametric study on edible wax emulsion coatings. Some of the additional variables include: type of wax, type of surfactant (surfactant composition), heating times (wax melting sequence etc.), addition rate and -sequence, stirrer- and homogenizer configuration, pressure etc. The bench scale pilot plant can also be

modified to accommodate high speed stirrer- and high shear homogenising configurations. Performing these parametric studies will allow for in depth literature data to be available for system modelling and scale-up studies (Podgórska, Baldyga 2001, Klein, Lowry 1996, Beaudette 2001, Rahmanian et al. 2008, Hu 2004, Khang, Levenspiel 1976, Sánchez et al.). Commercial scale experimental runs can then be performed to confirm the scale-up findings, thus establishing scaling factors for the manufacturing of edible wax emulsion coatings. Additional modelling for example neural nets and fuzzy logic can be included in future works.

A complete study on various edible waxes, including Carnauba-, Shellac-, Candelilla- and Montan wax, on a single bench scale pilot plant will give great insight into what effects the various waxes have on the characteristics of the final product. These experimental studies could include gaseous exchange analyses performed on fruit coated with the various coatings and placed in identical environments. Gaseous exchange (mass transfer) studies can be performed by means of mass spectrometry analyses performed with syringed liquid samples from the coated fruit over a certain period as described by Hagenmaier and Bai (Hagenmaier, Shaw 1991, Bai, Baldwin & Hagenmaier 2002, Bosquez-Molina, Guerrero-Legarreta & Vernon-Carter 2003, Hagenmaier 2005, Chiumarelli, Hubinger 2012), while fluid studies can be performed with simple weighing techniques. Additional studies could include rheological behaviour of the emulsions, light-scattering-, stability-, physical parameter- and formation studies (Lashmar, Richardson & Erbod 1995, Lashmar, Beesley 1993, Kamienski 1986, Bornfriend 1978, Chen, Tao 2005, Cazabat, Langevin & Pouchelon 1980, Peña, Salager 2001, Bourtoom 2008).

There is a large market for extending perishable food's shelf life without changing its consistency or composition. Once additional studies on different edible waxes have been performed, experimental application tests can be performed on other fruits, vegetables and other food groups e.g. soft fruit, candies, chocolates, meats etc. (Debeaufort, Quezada-Gallo & Voilley 1998, McClements 2010). These studies could include shelf life-, coating breakdown-, additive- and sensory studies. Feasibility studies could be included when entering new opportunities in competitive fields. In addition new-product development can originate from the above mentioned studies.

Finally, scaling studies can be performed to scale up the existing setup to commercial scale and to validate the results (models) obtained on bench scale throughout this study. Due to the nature of edible wax coatings, the possibilities for future applications in the food industry are endless.

References

- Measures of Central Tendencies* 2013, [Homepage of Aerd Statistics], [Online]. Available: <https://statistics.laerd.com/statistical-guides/measures-central-tendency-mean-mode-median.php> December 2013].
- Carnauba Wax Background Paper* 2011, January 2011-last update [Homepage of Ethical Consumer], [Online]. Available: <http://www.ethicalconsumer.org/> [2013, 23 July 2013].
- Saturn DigiSizer 5200 Operator's Manual V1.04* 2000, Operator's Manual edn, Micromeritics Instrument Corporation, United States of America.
- Available: <http://www.inkline.gr/inkjet/newtech/tech/dispersion/#electrostatic>.
- Adams, R.E. 1975, *Homogenizer-mixer*, Grant, US 3889931 A.
- Adler-Nissen, J., Mason, S. & Jacobsen, C. 2004, "Apparatus for emulsion production in small scale and under controlled shear conditions", *Food and Bioproducts Processing*, vol. 82, no. 4, pp. 311-319.
- Akay, G. 1998, "Flow-induced phase inversion in the intensive processing of concentrated emulsions", *Chemical Engineering Science*, vol. 53, no. 2, pp. 203-223.
- Allende, A., Tomás-Barberán, F.A. & Gil, M.I. 2006, "Minimal processing for healthy traditional foods", *Trends in Food Science & Technology*, vol. 17, no. 9, pp. 513-519.
- Anderson, M.J. & Kraber, S.L. 1999, "Keys to successful designed experiments", *Conference of Quality Management Division of American Society for Quality*.
- Anton, N., Benoit, J. & Saulnier, P. 2008, "Design and production of nanoparticles formulated from nano-emulsion templates—A review", *Journal of Controlled Release*, vol. 128, no. 3, pp. 185-199.
- Arshady, R. 1992, "Suspension, emulsion, and dispersion polymerization: A methodological survey", *Colloid & Polymer Science*, vol. 270, no. 8, pp. 717-732.
- Averbach, B.L. 1992, "Natural and synthetic edible moisture barrier", Grant, US 5130151 A.
- Baciu, A., Moşescu, N. & Nan, G. "Example for Determination of the Phase Inversion Point", University Petrol-Gaze din Ploiesti.
- Bai, J., Baldwin, E.A. & Hagenmaier, R.H. 2002, "Alternatives to shellac coatings provide comparable gloss, internal gas modification, and quality for 'Delicious' apple fruit", *HortScience*, vol. 37, no. 3, pp. 559-563.
- Baker, R.A. & Hagenmaier, R.D. 1997, "Reduction of fluid loss from grapefruit segments with wax microemulsion coatings", *Journal of Food Science*, vol. 62, no. 4, pp. 789-792.
- Baldwin, E.A. 1994, "Edible coatings for fresh fruits and vegetables: past, present, and future", *Edible coatings and films to improve food quality*, vol. 1, pp. 25.
- Beaudette, L. 2001, *Successful Scale-Up of High shear Batch and In-line Mixers*, Admix Inc., Manchester.

- Bengsten, P. 2011, January 2011-last update, *Carnauba Wax Background Paper* [Homepage of Ethical Consumer], [Online]. Available: <http://www.ethicalconsumer.org/> [2013, 23 July 2013].
- Bennett, H. 1975, *Industrial waxes*, Chemical Pub. Co., 2 v. (413 p., 323 p.).
- Berkman, S. & Egloff, G. 1941, "EMULSIONS AND FOAMS", Reinhold Publishing Corporation.
- Bornfriend, R. 1978, "Effect of processing on the rheological behaviour of emulsions", *Cosmet.Toiletries*, vol. 93, pp. 61-69.
- Borsinger, G.G. & Hassan, A. 2007, *Wax emulsion coating applications*, Grant, US 7267743.
- Bosquez-Molina, E., Guerrero-Legarreta, I. & Vernon-Carter, E. 2003, "Moisture barrier properties and morphology of mesquite gum-candelilla wax based edible emulsion coatings", *Food Research International*, vol. 36, no. 9-10, pp. 885-893.
- Bouchama, F., van Aken, G.A., Autin, A.J.E. & Koper, G.J.M. 2003, "On the mechanism of catastrophic phase inversion in emulsions", *Colloids and Surfaces A: Physicochemical and Engineering Aspects*, vol. 231, no. 1-3, pp. 11-17.
- Bourtoom, T. 2008, "Edible films and coatings: characteristics and properties.", *International Food Research Journal*, vol. 15, no. 3.
- Brasil, I., Gomes, C., Puerta-Gomez, A., Castell-Perez, M. & Moreira, R. 2012, "Polysaccharide-based multilayered antimicrobial edible coating enhances quality of fresh-cut papaya", *LWT-Food Science and Technology*.
- Brooks, B.W. & Richmond, H.N. 1994, "Phase inversion in non-ionic surfactant—oil—water systems—I. The effect of transitional inversion on emulsion drop sizes", *Chemical Engineering Science*, vol. 49, no. 7, pp. 1053-1064.
- Cazabat, A., Langevin, D., Meunier, J. & Pouchelon, A. 1982, "Critical behavior in microemulsions", *Advances in Colloid and Interface Science*, vol. 16, no. 1, pp. 175-199.
- Cazabat, A., Langevin, D. & Pouchelon, A. 1980, "Light--scattering study of water-oil microemulsions", *Journal of colloid and interface science*, vol. 73, no. 1, pp. 1-12.
- Chen, G. & Tao, D. 2005, "An experimental study of stability of oil-water emulsion", *Fuel Processing Technology*, vol. 86, no. 5, pp. 499-508.
- Chen, S. & Nussinovitch, A. 2001, "Permeability and roughness determinations of wax-hydrocolloid coatings, and their limitations in determining citrus fruit overall quality", *Food Hydrocolloids*, vol. 15, no. 2, pp. 127-137.
- Chen, Z., Pruss, J. & Warnecke, H.J. 1998, "A population balance model for disperse systems: : Drop size distribution in emulsion", *Chemical engineering science*, vol. 53, no. 5, pp. 1059-1066.
- Chiumarelli, M. & Hubinger, M.D. 2012, "Stability, solubility, mechanical and barrier properties of cassava starch – Carnauba wax edible coatings to preserve fresh-cut apples", *Food Hydrocolloids*, vol. 28, no. 1, pp. 59-67.
- Cisneros-Zevallos, L. & Krochta, J.M. 2003, "Dependence of Coating Thickness on Viscosity of Coating Solution Applied to Fruits and Vegetables by Dipping Method", *Journal of Food Science*, vol. 68, no. 2, pp. 503-510.
- Clarke, S.A. 2012, *Modeling & optimisation of coarse multi-vesiculated particles*, MScEng, Stellenbosch University.

- Clayton, W. 1943, *The theory of emulsions and their technical treatment*, The Blakiston co.
- Colla, E., do Amaral Sobral, P.J. & Menegalli, F.C. 2006, "Amaranthus cruentus flour edible films: influence of stearic acid addition, plasticizer concentration, and emulsion stirring speed on water vapor permeability and mechanical properties", *Journal of Agricultural and Food Chemistry*, vol. 54, no. 18, pp. 6645-6653.
- Daglas, D. & Stamatoudis, M. 2000, "Effect of impeller vertical position on drop sizes in agitated dispersions", *Chemical Engineering & Technology*, vol. 23, no. 5, pp. 437-440.
- Danghui, D., Fengyan, L. & Tianbo, Z. 2012, "Effects of Preparation Parameters on Paraffin Wax Microemulsion", *中国炼油与石油化工 (英文版)*, vol. 1, pp. 004.
- De Gennes, P. & Taupin, C. 1982, "Microemulsions and the flexibility of oil/water interfaces", *The Journal of physical chemistry*, vol. 86, no. 13, pp. 2294-2304.
- Dean, R.B. 1948, *Modern colloids*, Van Nostrand.
- Debeaufort, F., Quezada-Gallo, J.A. & Voilley, A. 1998, "Edible films and coatings: tomorrow's packagings: a review", *Critical Reviews in Food Science*, vol. 38, no. 4, pp. 299-313.
- Dickinson, E. & Patino, J.M.R. 1999, *Food emulsions and foams: interfaces, interactions and stability*, Royal Society of Chemistry.
- Djaković, L., Dokić, P., Radivojević, P., Šefer, I. & Sovilj, V. 1987, "Action of emulsifiers during homogenization of o/w emulsions", *Colloid & Polymer Science*, vol. 265, no. 11, pp. 993-1000.
- Donati, G. & Paludetto, R. 1997, "Scale up of chemical reactors", *Catalysis today*, vol. 34, no. 3, pp. 483-534.
- Ee, S.L., Duan, X., Liew, J. & Nguyen, Q.D. 2008, "Droplet size and stability of nano-emulsions produced by the temperature phase inversion method", *Chemical Engineering Journal*, vol. 140, no. 1, pp. 626-631.
- Fernandez, P., André, V., Rieger, J. & Kühnle, A. 2004, "Nano-emulsion formation by emulsion phase inversion", *Colloids and Surfaces A: Physicochemical and Engineering Aspects*, vol. 251, no. 1, pp. 53-58.
- Flint, G.W. & Sharp, T.E. 1942, *Polish*.
- Florence, A. & Whitehill, D. 1982, "The formulation and stability of multiple emulsions", *Int.J.Pharm*, vol. 11, no. 4, pp. 277-308.
- Forgiarini, A., Esquena, J., Gonzalez, C. & Solans, C. 2001, "Formation of nano-emulsions by low-energy emulsification methods at constant temperature", *Langmuir*, vol. 17, no. 7, pp. 2076-2083.
- Gassner, S.A. 1969, *POLYETHYLENE-NATURAL WAX EMULSIONS FOR THE COATING OF FRUITS AND VEGETABLES*.
- Gennadios, A. & Weller, C.L. 1990, "Edible films and coatings from wheat and corn proteins", *Food Technology*, vol. 44, no. 10.
- Gibson, J.W., Holl, R.J. & Tipton, A.J. 2001, *Emulsion-based processes for making microparticles*.

- Gingras, J.P., Fradette, L., Tanguy, P. & Jorda, E. 2007, "Concentrated bitumen-in-water emulsification in coaxial mixers", *Industrial & Engineering Chemistry Research*, vol. 46, no. 6, pp. 1818-1825.
- Goodwin, J.W. & Wiley, J. 2004, *Colloids and interfaces with surfactants and polymers: an introduction*, J. Wiley.
- Griffin, W.C. 1945, *Emulsions*, Atlas Powder Co, Grant, US 2380166 A.
- Guilbert, S., Cuq, B. & Gontard, N. 1997, "Recent innovations in edible and/or biodegradable packaging materials", *Food additives and contaminants*, vol. 14, no. 6-7, pp. 741-751.
- Guilbert, S., Gontard, N. & Gorris, L.G.M. 1996, "Prolongation of the Shelf-life of Perishable Food Products using Biodegradable Films and Coatings", *LWT - Food Science and Technology*, vol. 29, no. 1-2, pp. 10-17.
- Gusman, S. 1947, *A study of carnauba wax emulsions*, Massachusetts Institute of Technology.
- Gutiérrez, J.M., González, C., Maestro, A., Solè, I., Pey, C.M. & Nolla, J. 2008, "Nano-emulsions: New applications and optimization of their preparation", *Current Opinion in Colloid & Interface Science*, vol. 13, no. 4, pp. 245-251.
- Hagenmaier, R.D. 2004, "Fruit coatings containing ammonia instead of morpholine", U.S. Citrus and Subtropical Products Laboratory.
- Hagenmaier, R.D. 2000, "Evaluation of a polyethylene-candelilla coating for 'Valencia' oranges", *Postharvest Biology and Technology*, vol. 19, no. 2, pp. 147-154.
- Hagenmaier, R.D. 1998, "Wax microemulsion formulations used as fruit coatings", *PROCEEDINGS-FLORIDA STATE HORTICULTURAL SOCIETY* FLORIDA STATE HORTICULTURAL SOCIETY, pp. 251.
- Hagenmaier, R.D. & Baker, R.A. 1997, "Edible coatings from morpholine-free wax microemulsions", *Journal of Agricultural and Food Chemistry*, vol. 45, no. 2, pp. 349-352.
- Hagenmaier, R.D. & Baker, R.A. 1994, "Wax microemulsions and emulsions as citrus coatings", *Journal of Agricultural and Food Chemistry*, vol. 42, no. 4, pp. 899-902.
- Hagenmaier, R.D. & Shaw, P.E. 1991, "Permeability of coatings made with emulsified polyethylene wax", *Journal of Agricultural and Food Chemistry*, vol. 39, no. 10, pp. 1705-1708.
- Hagenmaier, R. & Shaw, P. 2002, "Changes in volatile components of stored tangerines and other specialty citrus fruits with different coatings", *Journal of Food Science*, vol. 67, no. 5, pp. 1742-1745.
- Hagenmaier, R.D. 2005, "A comparison of ethane, ethylene and CO₂ peel permeance for fruit with different coatings", *Postharvest Biology and Technology*, vol. 37, no. 1, pp. 56-64.
- Hamdy, M.M. & White, H.S. 1969, "Edible coating compositions and method for coating food", Acher Daniels Midland Co, Grant, US 3471303.
- Han, J.H. & Aristippos, G. 2005, "15 - Edible films and coatings: A review" in *Innovations in Food Packaging*, ed. Jung H. Han, Academic Press, London, pp. 239-262.
- Hautala, J. "Scale-up of high-shear mixers-", Pharmtech, Helsinki.
- Hu, W. 2004, "Scale-up and Scale-down of Cell Culture Bioreactors".

- Huber, K.C. *Edible Films and Coatings for Food Applications*, Springer New York.
- Hunter, R.J. 1981, *Zeta potential in colloid science: principles and applications*, Academic press London.
- Hyman, D. 1962, "Mixing and agitation", *Advances in Chemical Engineering*, vol. 3, pp. 119-202.
- Hyun Jin, P. 1999, "Development of advanced edible coatings for fruits", *Trends in Food Science & Technology*, vol. 10, no. 8, pp. 254-260.
- Izquierdo, P., Esquena, J., Tadros, T.F., Dederen, J.C., Feng, J., Garcia-Celma, M.J., Azemar, N. & Solans, C. 2004, "Phase behavior and nano-emulsion formation by the phase inversion temperature method", *Langmuir*, vol. 20, no. 16, pp. 6594-6598.
- Jass, H. 1967, "Effect of process variables on the stability of some specific emulsions", *J.Soc.Cosmet.Chem*, vol. 18, pp. 561-598.
- Kabalnov, A.S. & Shchukin, E.D. 1992, "Ostwald ripening theory: applications to fluorocarbon emulsion stability", *Advances in Colloid and Interface Science*, vol. 38, pp. 69-97.
- Kamel, A., Hurckes, L.C. & Morelli, M.M. 1990, *Wax encapsulated actives and emulsion process for their production*.
- Kamienski, J. 1986, "Mixing power of turbine-type impellers with divided, inclined blades", vol. 30, no. 3.
- Karbowiak, T., Debeaufort, F. & Voilley, A. 2007, "Influence of thermal process on structure and functional properties of emulsion-based edible films", *Food Hydrocolloids*, vol. 21, no. 5-6, pp. 879-888.
- Kawashimà, Y., Hino, T., Takeuchi, H., Niwa, T. & Horibe, K. 1991, "Rheological study of w/o/w emulsion by a cone-and-plate viscometer: Negative thixotropy and shear-induced phase inversion", *International journal of pharmaceuticals*, vol. 72, no. 1, pp. 65-77.
- Khang, S.J. & Levenspiel, O. 1976, "New scale-up and design method for stirrer agitated batch mixing vessels", *Chemical Engineering Science*, vol. 31, no. 7, pp. 569-577.
- Khang, S.J. & Levenspiel, O. 1976, "New scale-up and design method for stirrer agitated batch mixing vessels", *Chemical Engineering Science*, vol. 31, no. 7, pp. 569-577.
- Kiebler, M. 1945, "High Speed Agitator for Pressure Vessels.", *Industrial & Engineering Chemistry*, vol. 37, no. 6, pp. 538-540.
- Kielhorn, J. & Rosner, G. 1996, *Morpholine*, World health organization.
- Klahn, J.K., Janssen, J.J.M., Vaessen, G.E.J., de Swart, R. & Agterof, W.G.M. 2002, "On the escape process during phase inversion of an emulsion", *Colloids and Surfaces A: Physicochemical and Engineering Aspects*, vol. 210, no. 2-3, pp. 167-181.
- Klein, A. & Lowry, V. "Some mixing Scale-Up considerations for emulsion Polymerization" in *Emulsion Polymers* Institute Lehigh University.
- Klein, K. 2008, "Liquid Crystals and Emulsions: A Wonderful Marriage", Cosmetech Laboratories, Fairfield, New Jersey, USA.
- Langevin, D. 1988, "Microemulsions", *Accounts of Chemical Research*, vol. 21, no. 7, pp. 255-260.

- Lashmar, U. & Beesley, J. 1993, "Correlation of rheological properties of an oil in water emulsion with manufacturing procedures and stability", *International journal of pharmaceuticals*, vol. 91, no. 1, pp. 59-67.
- Lashmar, U., Richardson, J. & Erbod, A. 1995, "Correlation of physical parameters of an oil in water emulsion with manufacturing procedures and stability", *International journal of pharmaceuticals*, vol. 125, no. 2, pp. 315-325.
- Lemaire, B., Bothorel, P. & Roux, D. 1983, "Micellar interactions in water-in-oil microemulsions. 1. Calculated interaction potential", *The Journal of physical chemistry*, vol. 87, no. 6, pp. 1023-1028.
- Li, C., Mei, Z., Liu, Q., Wang, J., Xu, J. & Sun, D. 2010, "Formation and properties of paraffin wax submicron emulsions prepared by the emulsion inversion point method", *Colloids and Surfaces A: Physicochemical and Engineering Aspects*, vol. 356, no. 1, pp. 71-77.
- Lin, D. & Zhao, Y. 2007, "Innovations in the development and application of edible coatings for fresh and minimally processed fruits and vegetables", *Comprehensive Reviews in Food Science and Food Safety*, vol. 6, no. 3, pp. 60-75.
- Lin, T. 1978, "Low-surfactant emulsification", *J.Soc.Cosmet.Chem*, vol. 28, pp. 273-295.
- Lin, T., Kurihara, H. & Ohta, H. 1975, "Effects of phase inversion and surfactant location on the formation of O/W emulsions", *J.Soc.Cosmet.Chem*, vol. 26, pp. 121-139.
- Liu, W., Sun, D., Li, C., Liu, Q. & Xu, J. 2006, "Formation and stability of paraffin oil-in-water nano-emulsions prepared by the emulsion inversion point method", *Journal of colloid and interface science*, vol. 303, no. 2, pp. 557-563.
- Liu, Y., Carter, E.L., Gordon, G.V., Feng, Q.J. & Friberg, S.E. "An investigation into the relationship between catastrophic inversion and emulsion phase behaviors", *Colloids and Surfaces A: Physicochemical and Engineering Aspects*.
- Lund, A. & Lund, M. 2013, , *Measures of Central Tendencies* [Homepage of Aerd Statistics], [Online]. Available: <https://statistics.laerd.com/statistical-guides/measures-central-tendency-mean-mode-median.php> [December 2013].
- Maa, Y.F. & Hsu, C. 1996, "Liquid-liquid emulsification by rotor/stator homogenization", *Journal of Controlled Release*, vol. 38, no. 2-3, pp. 219-228.
- Mannheim, C.H. & Soffer, T. 1996, "Permeability of different wax coatings and their effect on citrus fruit quality", *Journal of Agricultural and Food Chemistry*, vol. 44, no. 3, pp. 919-923.
- Marszall, L. 1985, "Emulsion inversion point and properties of the oil phase", *Journal of colloid and interface science*, vol. 107, no. 2, pp. 572-573.
- Marszall, L. 1977, "Cloud point and emulsion inversion point in the presence of additives", *Journal of colloid and interface science*, vol. 59, no. 2, pp. 376-377.
- McCabe, W.L., Smith, J.C. & Harriott, P. 1985, "Unit operations of chemical engineering", Scilab.
- McClements, D.J. 2010, "Edible nanoemulsions: fabrication, properties, and functional performance", *Soft Matter*.
- Mehyar, G.F., Al-Ismail, K., Han, J.H. & Chee, G.W. 2012, "Characterization of Edible Coatings Consisting of Pea Starch, Whey Protein Isolate, and Carnauba Wax and their Effects on Oil Rancidity and Sensory Properties of Walnuts and Pine Nuts", *Journal of Food Science*.

- Mei, Z., Xu, J. & Sun, D. 2011, "O/W nano-emulsions with tunable PIT induced by inorganic salts", *Colloids and Surfaces A: Physicochemical and Engineering Aspects*, vol. 375, no. 1-3, pp. 102-108.
- Meinders, M.B., Kloek, W. & van Vliet, T. 2001, "Effect of surface elasticity on Ostwald ripening in emulsions", *Langmuir*, vol. 17, no. 13, pp. 3923-3929.
- Milanovic, J., Levic, S., Manojlovic, V., Nedovic, V. & Bugarski, B. 2011, "Carnauba wax microparticles produced by melt dispersion technique", *Chemical Papers*, vol. 65, no. 2, pp. 213-220.
- Miller, D.N. 1971, "Scale-Up of agitated vessels. Mass transfer from suspended solute particles", *Industrial & Engineering Chemistry Process Design and Development*, vol. 10, no. 3, pp. 365-375.
- Miller, D.J., Henning, T. & Grünbein, W. 2001, "Phase inversion of W/O emulsions by adding hydrophilic surfactant — a technique for making cosmetics products", *Colloids and Surfaces A: Physicochemical and Engineering Aspects*, vol. 183-185, no. 0, pp. 681-688.
- Milner, S.T. & Safran, S. 1987, "Dynamical fluctuations of droplet microemulsions and vesicles", *Physical Review A*, vol. 36, no. 9, pp. 4371.
- Morrison, I.D. & Ross, S. 2002, *Colloidal dispersions: suspensions, emulsions, and foams*, Wiley-Interscience New York.
- Myers, K.J., Reeder, M.F., Ryan, D. & Daly, G. 1999, "Get a fix on high-shear mixing", *Chemical Engineering Progress*, vol. 95, no. 11, pp. 33-42.
- Olivas, G. & Barbosa-Cánovas, G. 2005, "Edible coatings for fresh-cut fruits", *Critical reviews in food science and nutrition*, vol. 45, no. 7-8, pp. 657-670.
- Olivieri, L., Seiller, M., Bromberg, L., Ron, E., Couvreur, P. & Grossiord, J.L. 2001, "Study of the breakup under shear of a new thermally reversible water-in-oil-in-water (W/O/W) multiple emulsion", *Pharmaceutical research*, vol. 18, no. 5, pp. 689-693.
- Olson, J.M. 1943, *Liquid wax polish*.
- Paul, S., Bisal, S. & Moulik, S.P. 1992, "Physicochemical studies on microemulsions: test of the theories of percolation", *The Journal of physical chemistry*, vol. 96, no. 2, pp. 896-901.
- Peña, A. & Salager, J. 2001, "Effect of stirring energy upon the dynamic inversion hysteresis of emulsions", *Colloids and Surfaces A: Physicochemical and Engineering Aspects*, vol. 181, no. 1-3, pp. 319-323.
- Pérez, M., Zambrano, N., Ramirez, M., Tyrode, E. & Salager, J.L. 2002, "Surfactant-oil-water systems near the affinity inversion. XII. Emulsion drop size versus formulation and composition", *Journal of Dispersion Science and Technology*, vol. 23, no. 1-3, pp. 55-63.
- Pérez, M., Zambrano, N., Ramirez, M., Tyrode, E. & Salager, J. 2002, "Surfactant-oil-water systems near the affinity inversion. XII. Emulsion drop size versus formulation and composition", *Journal of Dispersion Science and Technology*, vol. 23, no. 1-3, pp. 55-63.
- Pey, C., Maestro, A., Solé, I., González, C., Solans, C. & Gutiérrez, J.M. 2006, "Optimization of nano-emulsions prepared by low-energy emulsification methods at constant temperature using a factorial design study", *Colloids and Surfaces A: Physicochemical and Engineering Aspects*, vol. 288, no. 1, pp. 144-150.

- Pizzino, A., Rodriguez, M.P., Xuereb, C., Catté, M., Van Hecke, E., Aubry, J.M. & Salager, J.L. 2007, "Light backscattering as an indirect method for detecting emulsion inversion", *Langmuir*, vol. 23, no. 10, pp. 5286-5288.
- Podgórska, W. & Baldyga, J. 2001, "Scale-up effects on the drop size distribution of liquid-liquid dispersions in agitated vessels", *Chemical engineering science*, vol. 56, no. 3, pp. 741-746.
- Porter, S.C. & Woznicki, E.J. 1985, *Dry edible film coating composition, method and coating form*.
- Rahmanian, N., Ng, B., Hassanpour, A., Ghadiri, M., Ding, Y., Jia, X. & Antony, J. 2008, "Scale-up of high shear mixer granulators".
- Rhe America 2014, *Rhe America Engineering Firm*. Available: <http://www.rhe-america.com/index.html> [2015].
- Rinaudo, M., Milas, M. & Dung, P.L. 1993, "Characterization of chitosan. Influence of ionic strength and degree of acetylation on chain expansion", *International journal of biological macromolecules*, vol. 15, no. 5, pp. 281-285.
- Robert D., H. 2000, "Evaluation of a polyethylene-candelilla coating for 'Valencia' oranges", *Postharvest Biology and Technology*, vol. 19, no. 2, pp. 147-154.
- Rojas-Graü, M.A., Soliva-Fortuny, R. & Martín-Belloso, O. 2009, "Edible coatings to incorporate active ingredients to fresh-cut fruits: a review", *Trends in Food Science & Technology*, vol. 20, no. 10, pp. 438-447.
- Rojas-Grau, M., Tapia, M., Rodríguez, F., Carmona, A. & Martín-Belloso, O. 2007, "Alginate and gellan-based edible coatings as carriers of antibrowning agents applied on fresh-cut Fuji apples", *Food Hydrocolloids*, vol. 21, no. 1, pp. 118-127.
- Rojas-Graü, M.A., Soliva-Fortuny, R. & Martín-Belloso, O. 2009, "Edible coatings to incorporate active ingredients to fresh-cut fruits: a review", *Trends in Food Science & Technology*, vol. 20, no. 10, pp. 438-447.
- Rosano, H.L. 1979, *Method for preparing microemulsions*, Grant, US 4146499 A.
- Ruckenstein, E. & Chi, J. 1975, "Stability of microemulsions", *J.Chem.Soc., Faraday Trans.2*, vol. 71, no. 0, pp. 1690-1707.
- Sadurní, N., Solans, C., Azemar, N. & García-Celma, M.J. 2005, "Studies on the formation of O/W nano-emulsions, by low-energy emulsification methods, suitable for pharmaceutical applications", *European Journal of Pharmaceutical Sciences*, vol. 26, no. 5, pp. 438-445.
- Sajjadi, S. 2006, "Nanoemulsion formation by phase inversion emulsification: on the nature of inversion", *Langmuir*, vol. 22, no. 13, pp. 5597-5603.
- Salager, J.L., Perez-Sanchez, M. & Garcia, Y. 1996, "Physicochemical parameters influencing the emulsion drop size", *Colloid & Polymer Science*, vol. 274, no. 1, pp. 81-84.
- Salager, J., Moreno, N., Antón, R. & Marfisi, S. 2002, "Apparent equilibration time required for a surfactant-oil-water system to emulsify into the morphology imposed by the formulation", *Langmuir*, vol. 18, no. 3, pp. 607-611.
- Salager, J. 1988, "Phase transformation and emulsion inversion on the basis of catastrophe theory", *Encyclopedia of emulsion technology*, vol. 3, pp. 79-134.
- Salager, J., Loaiza-Maldonado, I., Minana-Perez, M. & Silva, F. 1982, "Surfactant-oil-water systems near the affinity inversion Part I: Relationship between equilibrium phase behavior

- and emulsion type and stability", *JOURNAL OF DISPERSION SCIENCE AND TECHNOLOGY*, vol. 3, no. 3, pp. 279-292.
- Sánchez, L., Sánchez, P., Carmona, M., de Lucas, A. & Rodríguez, J.F. 2008, "Influence of operation conditions on the microencapsulation of PCMs by means of suspension-like polymerization", *Colloid & Polymer Science*, vol. 286, no. 8, pp. 1019-1027.
- Sánchez, M., Sánchez, P., Carmona, M., Borreguero, A. & Rodríguez, J. "SCALE UP OF THE ENCAPSULATION PROCESS TO OBTAIN MICROCAPSULES CONTAINING PHASE CHANGE MATERIALS".
- Saturn DigiSizer 5200 2000, *Saturn DigiSizer 5200 Operator's Manual V1.04*, Operator's Manual edn, Micromeritics Instrument Corporation, United States of America.
- Schade, J.A. 1934, *WAX EMULSION COATING*, Willbur White Chemical Company, Grant, US 1943468 A.
- Schalper, K., Harnisch, S., Müller, R.H. & Hildebrand, G.E. 2005, "Preparation of microparticles by micromixers: Characterization of Oil/Water process and prediction of particle size", *Pharmaceutical research*, vol. 22, no. 2, pp. 276-284.
- Schulman, J.H., Stoeckenius, W. & Prince, L.M. 1959, "Mechanism of formation and structure of micro emulsions by electron microscopy", *The Journal of physical chemistry*, vol. 63, no. 10, pp. 1677-1680.
- Seaborne, J. & Egberg, D.C. 1987, *Edible coating composition and method of preparation*.
- Sherman, P. 1968, *Emulsion science*, Academic Press New York.
- Shinnar, R. & Church, J. 1960, "Statistical theories of turbulence in predicting particle size in agitated dispersions", *Industrial & Engineering Chemistry*, vol. 52, no. 3, pp. 253-256.
- Silva, F., Peña, A., Miñana-Pérez, M. & Salager, J.L. 1998, "Dynamic inversion hysteresis of emulsions containing anionic surfactants", *Colloids and Surfaces A: Physicochemical and Engineering Aspects*, vol. 132, no. 2-3, pp. 221-227.
- Sjoblom, J. 2005, *Emulsions and Emulsion Stability: Surfactant Science Series/61*, CRC.
- Solans, C., Izquierdo, P., Nolla, J., Azemar, N. & Garcia-Celma, M.J. 2005, "Nano-emulsions", *Current Opinion in Colloid & Interface Science*, vol. 10, no. 3-4, pp. 102-110.
- Stat-Ease 2010, "User Guide to Design-Expert Version 8 Software".
- Štěpina, V. & Veselý, V. 1992, *Lubricants and special fluids*, Elsevier Science.
- Suslick, K.S. 1998, "Kirk-Othmer encyclopedia of chemical technology", *John Wiley and Sons, Inc., New York*.
- Tadros, T., Izquierdo, P., Esquena, J. & Solans, C. 2004, "Formation and stability of nano-emulsions", *Advances in Colloid and Interface Science*, vol. 108, pp. 303-318.
- Tanaka, M., Okada, F., Oba, T., Oohashi, H. & Tanaka, T. 1989, *Process for preparing organopolysiloxane emulsion*.
- Tardos, G.I., Hapgood, K.P., Ipadeola, O.O. & Michaels, J.N. 2004, "Stress measurements in high-shear granulators using calibrated "test" particles: application to scale-up", *Powder Technology*, vol. 140, no. 3, pp. 217-227.

- Tardos, G.I., Khan, M.I. & Mort, P.R. 1997, "Critical parameters and limiting conditions in binder granulation of fine powders", *Powder Technology*, vol. 94, no. 3, pp. 245-258.
- Taylor, P. 1998, "Ostwald ripening in emulsions", *Advances in Colloid and Interface Science*, vol. 75, no. 2, pp. 107-163.
- Tolosa, L.I., Forgiarini, A., Moreno, P. & Salager, J.L. 2006, "Combined effects of formulation and stirring on emulsion drop size in the vicinity of three-phase behavior of surfactant-oil water systems", *Industrial & Engineering Chemistry Research*, vol. 45, no. 11, pp. 3810-3814.
- Trezza, T. & Krochta, J. 2001, "Specular reflection, gloss, roughness and surface heterogeneity of biopolymer coatings", *Journal of Applied Polymer Science*, vol. 79, no. 12, pp. 2221-2229.
- Trezza, T. & Krochta, J. 2000, "The gloss of edible coatings as affected by surfactants, lipids, relative humidity, and time", *Journal of Food Science*, vol. 65, no. 4, pp. 658-662.
- Uson, N., Garcia, M.J. & Solans, C. 2004, "Formation of water-in-oil (W/O) nano-emulsions in a water/mixed non-ionic surfactant/oil systems prepared by a low-energy emulsification method", *Colloids and Surfaces A: Physicochemical and Engineering Aspects*, vol. 250, no. 1, pp. 415-421.
- Vaessen, G.E.J. & Stein, H.N. 1995, "The Applicability of Catastrophe Theory to Emulsion Phase Inversion", *Journal of colloid and interface science*, vol. 176, no. 2, pp. 378-387.
- Vargas, M., Albors, A., Chiralt, A. & González-Martínez, C. 2009, "Characterization of chitosan-oleic acid composite films", *Food Hydrocolloids*, vol. 23, no. 2, pp. 536-547.
- Vitale, S.A. & Katz, J.L. 2003, "Liquid droplet dispersions formed by homogeneous liquid-liquid nucleation: "The ouzo effect"", *Langmuir*, vol. 19, no. 10, pp. 4105-4110.
- Vold, R. & Vold, M. 1983, "Colloid and Interfacial Chemistry", *Addison-Wiley*, NY.
- Wagner, C. 1976, "Contribution to the thermodynamics of emulsions", *Colloid & Polymer Science*, vol. 254, no. 4, pp. 400-408.
- Wang, L., Li, X., Zhang, G., Dong, J. & Eastoe, J. 2007, "Oil-in-water nanoemulsions for pesticide formulations", *Journal of colloid and interface science*, vol. 314, no. 1, pp. 230-235.
- Wasser, R.B. 1998, *Sizing emulsion*, Cytec Technology Corp., Grant, US 5759249.
- Weiser, H.B. 1950, "Colloid chemistry", *Annual Review of Physical Chemistry*, vol. 1, no. 1, pp. 347-356.
- Weissenborn, P.K. & Motiejauskaite, A. 2000, "Emulsification, drying and film formation of alkyd emulsions", *Progress in Organic Coatings*, vol. 40, no. 1-4, pp. 253-266.
- Western Asphalt Products, L. 2013, *What is Emulsion*. Available: <http://westernasphalt.ca/what-is-emulsion/> [2013, May].
- Wiley, R.M. 1966, *Water-in-oil emulsion polymerization process for polymerizing water-soluble monomers*, Dow Chemical Co, Grant, US 3284393 A.
- Windhab, E., Dressler, M., Feigl, K., Fischer, P. & Megias-Alguacil, D. 2005, "Emulsion processing—from single-drop deformation to design of complex processes and products", *Chemical Engineering Science*, vol. 60, no. 8, pp. 2101-2113.

- Yang, Z., Xu, Y., Zhao, D. & Xu, M. 2000, "Preparation of waterborne dispersions of epoxy resin by the phase-inversion emulsification technique. 1. Experimental study on the phase-inversion process", *Colloid & Polymer Science*, vol. 278, no. 12, pp. 1164-1171.
- Yang, F., Li, C., Xu, C. & Song, M. 2012, "Studies on the normal-to-abnormal emulsion inversion of waxy crude oil-in-water emulsion induced by continuous stirring", *Journal of Petroleum Science and Engineering*, vol. 81, no. 0, pp. 64-69.
- Zambaux, M.F., Bonneaux, F., Gref, R., Maincent, P., Dellacherie, E., Alonso, M.J., Labrude, P. & Vigneron, C. 1998, "Influence of experimental parameters on the characteristics of poly(lactic acid) nanoparticles prepared by a double emulsion method", *Journal of Controlled Release*, vol. 50, no. 1-3, pp. 31-40.

Appendix A: Commercial Waxes Data Sheets



FICHA TÉCNICA

CITROSOL A S EXTRA UE

RECUBRIMIENTOS CÉREOS POST-COSECHA

QUE ES CITROSOL A S EXTRA UE

Es una cera de recubrimiento para el tratamiento post-cosecha de frutos cítricos.

Proporciona un excelente brillo y un buen control de pérdida de peso, retrasando el envejecimiento de la fruta por reducción de la transpiración y la respiración.

Las excelentes propiedades de secado de esta cera, reducen la temperatura necesaria a aplicar en el túnel de secado. Con lo cual se consigue un ahorro de energía y una menor emisión de gases contaminantes.

DOSIS Y MODO DE EMPLEO

Se aplica por pulverización sobre la rulada de la máquina aplicadora por la que se deslizan los agrios mientras los cepillos distribuyen la cera.

Dosis: 1 litro de CITROSOL A S EXTRA UE para 1000 kilos de fruta, proporciona un encerado de grado alto. Vigilar la homogeneidad entre el gasto del producto y el paso de la fruta.

Agitar bien el producto 5 minutos antes de su aplicación y mantener en agitación lenta durante su aplicación, mediante dispositivos adecuados a tal efecto. Los frutos deben estar perfectamente secos en el momento de la aplicación del tratamiento céreo. Revisar frecuentemente que las boquillas no sufran embozamientos para que se aplique el tratamiento adecuado. Observar que se forma una película uniforme sin heterogeneidad de la aplicación. Controlar la temperatura del túnel de secado para optimizar la reducción de la temperatura al utilizar CITROSOL A S EXTRA UE (Secado Rápido).

Aplicación bajo Asesoramiento Técnico.

PRESENTACION

Bidón conteniendo 200 Kg.
Contenedores de 1000 Kg.

REGISTRO SANITARIO

39.02553V

CARACTERISTICAS TECNICAS

Emulsión cera/agua

pH: 8,5-10,1

Densidad: 1,000 -1,014 g/cc.

Composición:

Poliétileno y goma laca.....18 % p/v.

La composición de las ceras comercializadas por Productos Citrosol, S. A. en España está exenta de morfina y cumplen estrictamente la legislación europea de aditivos alimentarios (Directiva 95/2 CE y Reglamento (CE) 1333/2008).

PRECAUCIONES

Xi



Irritante

- Irrita los ojos, la piel y vías respiratorias.
- Manténgase fuera del alcance de los niños.
- Manténgase lejos de alimentos bebidas y piensos.
- Evítese el contacto con los ojos y la piel.
- Úsense guantes adecuados.
- EN CASO DE ACCIDENTE O MALESTAR ACÚDASE INMEDIATAMENTE AL MÉDICO (a ser posible muéstrele la etiqueta).

NOTA

La información aquí contenida es, según nuestro criterio correcta. No obstante, como las condiciones en las que se usan estos productos caen fuera de nuestro control, no podemos responsabilizarnos de las consecuencias de su utilización.

(Versión 02)



FICHA TÉCNICA

CITROSOL A K ORGÁNICA UE

RECUBRIMIENTOS CÉREOS POST-COSECHA

QUE ES CITROSOL A K ORGÁNICA UE

Es una cera vegetal de recubrimiento para el tratamiento post-cosecha de frutos cítricos.

Proporciona un buen brillo y un buen control de pérdida de peso, retrasando el envejecimiento de la fruta por reducción de la transpiración y la respiración.

DOSIS Y MODO DE EMPLEO

Se aplica por pulverización sobre la rulada de la máquina aplicadora por la que se deslizan los agrios mientras los cepillos distribuyen la cera.

Dosis: 1 litro de CITROSOL-A K ORGÁNICA UE para 1000 kilos de fruta, proporciona un encerado de grado medio. Vigilar la homogeneidad entre el gasto del producto y el paso de la fruta.

Agitar bien el producto 5 minutos antes de su aplicación y mantener en agitación lenta durante su aplicación, mediante dispositivos adecuados a tal efecto. Los frutos deben estar perfectamente secos en el momento de la aplicación del tratamiento céreo. Revisar frecuentemente que las boquillas no sufran embozamientos para que se aplique el tratamiento adecuado. Observar que se forma una película uniforme sin heterogeneidad de la aplicación. Controlar la temperatura del túnel de secado para optimizar el coste/eficacia del proceso.

Aplicación bajo Asesoramiento Técnico.

PRESENTACION

Bidón conteniendo 200 Kg.
Contenedores de 1000 Kg.

REGISTRO SANITARIO

39.02553/V

CARACTERISTICAS TECNICAS

Emulsión cera/agua

pH: 9,9 – 10,9.

Densidad: 0.995 – 1.010 g/cc.

Composición:

Carnauba18% p/v.

La composición de las ceras comercializadas por Productos Citrosol, S. A. en España está exenta de morfina y cumplen estrictamente la legislación europea de aditivos alimentarios (Directiva 95/2/CE y Reglamento (CE) 1333/2008).

PRECAUCIONES

Xi



Irritante

- Irrita los ojos, la piel y vías respiratorias.
- Manténgase fuera del alcance de los niños.
- Manténgase lejos de alimentos bebidas y piensos.
- Evítese el contacto con los ojos y la piel.
- Úsense guantes adecuados.
- EN CASO DE ACCIDENTE O MALESTAR, ACÚDASE INMEDIATAMENTE AL MÉDICO (a ser posible muéstrole la etiqueta).

NOTA

La información aquí contenida es, según nuestro criterio correcta. No obstante, como las condiciones en las que se usan estos productos caen fuera de nuestro control, no podemos responsabilizarnos de las consecuencias de su utilización.

(Versión 01)



Technical Data Sheet

■ Michem® Lube 160

USAGE Michem® Lube 160 provides superior slip and mar resistance on a variety of substrates such as metal, wood, film and paper. It can also be used in thermal transfer release coatings to give release when used in combination with a thermally active binder. Anti-block properties and broad FDA compliance complete the Michem® Lube 160 package.

DESCRIPTION Anionic carnauba wax emulsion

PHYSICAL PROPERTIES

The following properties are typical but should not be considered specifications:

| | |
|--------------------------------|------------------------------|
| Appearance: | Cream colored, opaque liquid |
| Emulsifier Charge: | Anionic |
| Solids Type: | Carnauba |
| Non-Volatile (%): | 24.5 - 25.5 |
| Brookfield Viscosity (cps): | < 15 |
| Spindle Number: | 1 |
| RPM: | 60 |
| pH: | 4.5 - 6.0 |
| Recommended pH of your system: | 1.0 - 12.0 |

SITE OF MANUFACTURE (and PRODUCT CODE)

USA (ML160), Singapore (ML160.S)

Revised 25 September 2002

The following information for this product, specific to each site of manufacture, is available upon request:

- **Material Safety Data Sheets** in various formats and languages (includes global chemical inventory listing)
- **Food Contact Declaration of Compliance**



Technical Data Sheet

■ Michem® Lube 160F

USAGE Michem® Lube 160F provides superior slip and mar resistance on a variety of substrates such as metal, wood, film and paper. Anti-block properties and broader FDA clearances add to the advantages of Michem® Lube 160F.

DESCRIPTION Anionic carnauba wax emulsion

PHYSICAL PROPERTIES The following properties are typical but should not be considered specifications:

| | |
|--------------------------------|------------------------------|
| Appearance: | Cream colored, opaque liquid |
| Emulsifier Charge: | Anionic |
| Solids Type: | Carnauba |
| Non-Volatile (%): | 24.5 - 25.5 |
| Brookfield Viscosity (cps): | < 15 |
| Spindle Number: | 1 |
| RPM: | 60 |
| pH: | 3.5 - 6.0 |
| Recommended pH of your system: | 1.0 - 12.0 |

SITE OF MANUFACTURE (and PRODUCT CODE) USA (ML160F), Belgium (ML160F.E), Singapore (ML160F.S)

Revised 12 August 2010

The following information for this product, specific to each site of manufacture, is available upon request:

- ▶ **Material Safety Data Sheets** in various formats and languages (includes global chemical inventory listing)
- ▶ **Food Contact Declaration of Compliance**



Technical Data Sheet

■ Michem® Lube 160PF

USAGE Michem® Lube 160PF is an APEO-free additive which imparts slip, abrasion resistance and anti-block properties, in a variety of coatings and varnishes.

DESCRIPTION Anionic carnauba wax emulsion

PHYSICAL PROPERTIES The following properties are typical but should not be considered specifications:

| | |
|--------------------------------|------------------------------|
| Appearance: | Cream colored, opaque liquid |
| Emulsifier Charge: | Anionic |
| Solids Type: | Carnauba |
| Non-Volatile (%): | 24.5 - 25.5 |
| Brookfield Viscosity (cps): | < 15 |
| Spindle Number: | 1 |
| RPM: | 60 |
| pH: | 4.5 - 7.0 |
| Recommended pH of your system: | 1.0 - 12.0 |

SITE OF MANUFACTURE (and PRODUCT CODE) USA (ML160PF), Belgium (ML160PF.E), Singapore (ML160PF.S)

Revised 01 November 2010

The following information for this product, specific to each site of manufacture, is available upon request:

- **Material Safety Data Sheets** in various formats and languages (includes global chemical inventory listing)
- **Food Contact Declaration of Compliance**



Technical Data Sheet

■ Michem® Lube 160PFP

USAGE Michem® Lube 160PFP is a phenol-free, anionic, slip and anti-block additive for OPP films and various other coating formulations.

DESCRIPTION Anionic carnauba wax emulsion

PHYSICAL PROPERTIES The following properties are typical but should not be considered specifications:

| | |
|--------------------------------|------------------------------|
| Appearance: | Cream colored, opaque liquid |
| Emulsifier Charge: | Anionic |
| Solids Type: | Carnauba |
| Non-Volatile (%): | 24.5 - 25.5 |
| Brookfield Viscosity (cps): | < 15 |
| Spindle Number: | 1 |
| RPM: | 60 |
| pH: | 4.0 - 7.0 |
| Recommended pH of your system: | < 7.0 |

SITE OF MANUFACTURE (and PRODUCT CODE) USA (ML160PFP), Belgium (ML160PFP.E)

Revised 02 August 2010

The following information for this product, specific to each site of manufacture, is available upon request:

- ▶ **Material Safety Data Sheets** in various formats and languages (includes global chemical inventory listing)
- ▶ **Food Contact Declaration of Compliance**

Appendix B: Pilot Plant Additional Information and Calibrations

Additional Information and Images

Both the safety glass and the fan-belt cover can be seen in **Figure 113**.

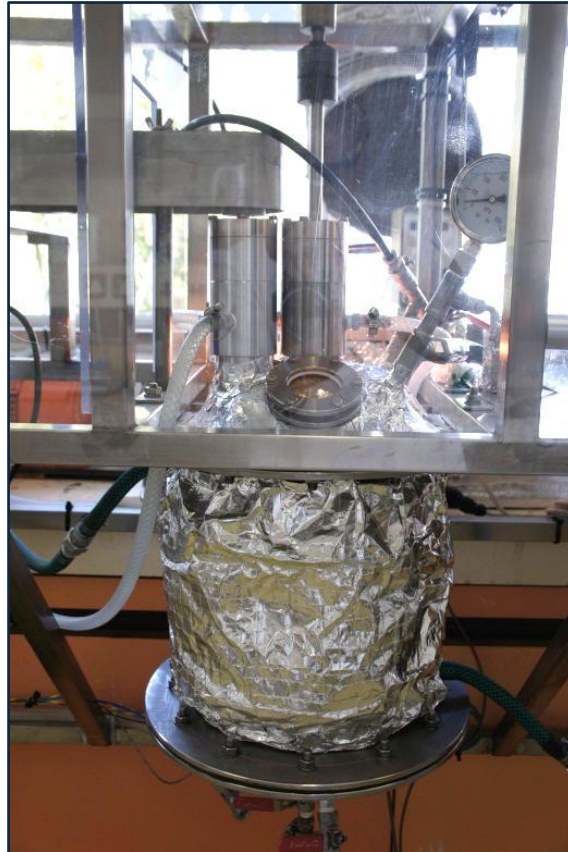


Figure 113 - Top dome area showing the safety glass and fan-belt cover

Pilot Plant Frame

A pilot plant frame was designed to accommodate all the process equipment. The frame had to be compact yet have enough space to keep the pilot plant safe for the operator. A basic frame was designed that could be bolted to a working surface in an existing lab. The basic design of the frame is presented in **Figure 114**.

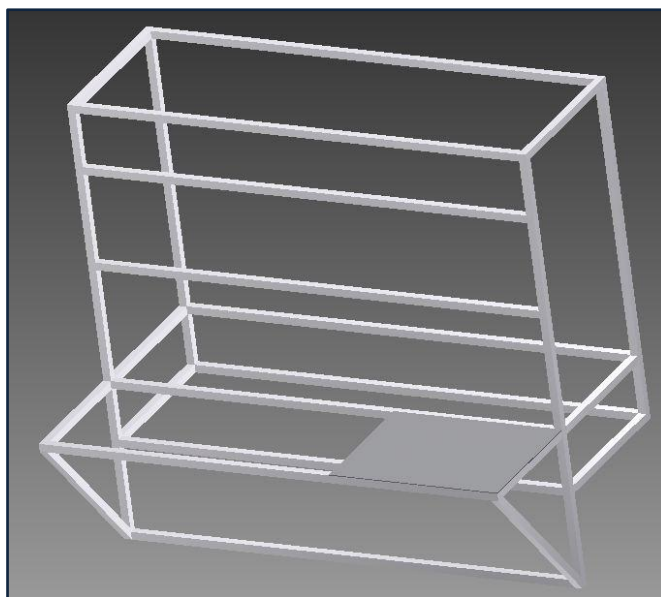


Figure 114 - Schematic of the pilot plant frame

The frame was constructed from 25 mm 316 stainless steel square tubing. The tubing was cut and welded together. The working surface (the dark shaded surface **Figure 114**) was cut from a 3 mm 316 stainless steel sheet and welded to the frame. Minor modifications were made to the frame in order to install the process equipment. These modifications included: drilling holes, welding stands and brackets to the frame and attaching cables to the frame by means of cable ties. The completed pilot plant with all the process units installed is presented in **Figure 115**.

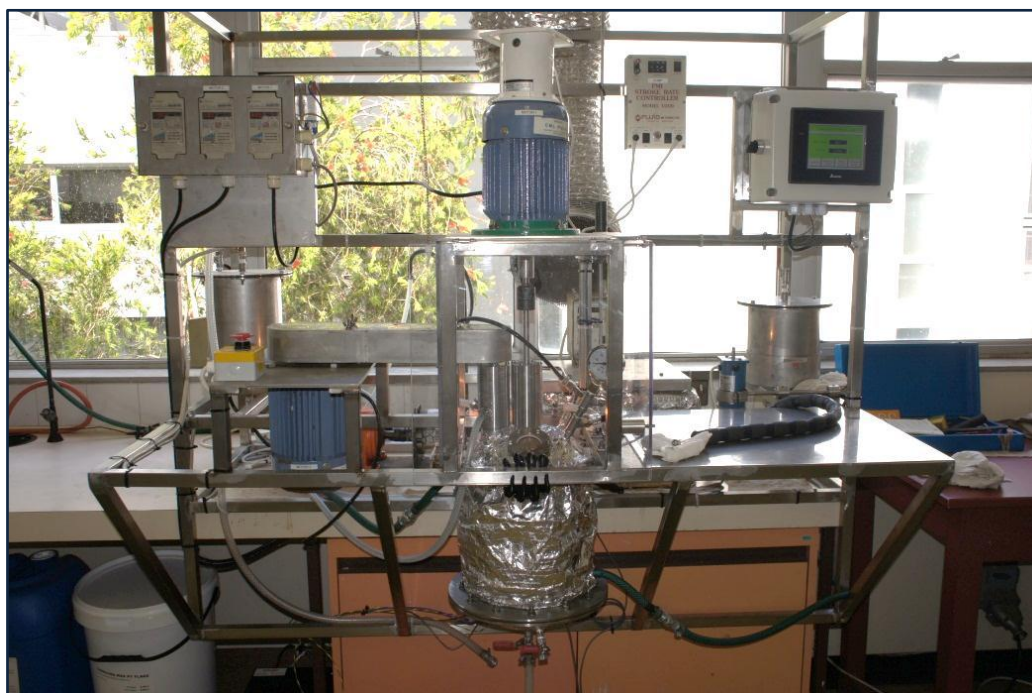


Figure 115 - Completed Pilot Plant

Equipment Calibrations

Hot Water Pump [E-102] Calibration

The positive displacement pump [F.M.I©] [E-102] was calibrated by measuring a known amount of water at various pump settings and plotting the pump setting against the flow rate. An average of four readings was taken at each point. The calibration was performed with a water temperature of 90 – 95°C. A graph representing the data collected during the calibration is presented in **Figure 116**.

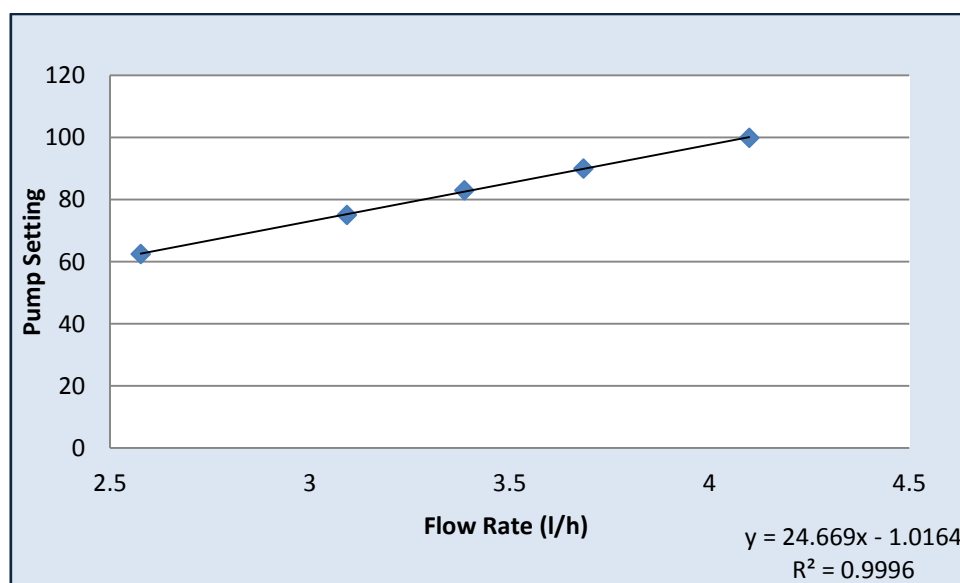


Figure 116 – Hot Water Pump [E-102] Calibration

A trend line was fitted to the data in order to obtain a relationship between the pump setting and the flow rate. This relationship is as follow:

$$y = 24.667x - 1.0164$$

This relationship has a R^2 value of 0.9996 which is an indication that it can be used with confidence to control the hot water flow rate accurately. y represents the hot water flow rate (l/h) while x represents the stroke rate controller's [F.M.I©] setting.

Motor [M-101 & M-102] Calibrations

The variable speed drives' (frequency inverters) settings were calibrated for both the stirrer and high shear homogenizer's rotation speeds. A Tachometer was used to measure the rotational speed of the axes (rpm) at certain frequency settings (Hz). The rotation speeds were plotted against the frequencies and the results for the stirrer's motor [M-101] and for the high shear homogenizer's motor [M-102] can be seen in **Figure 117** and **Figure 118** respectively.

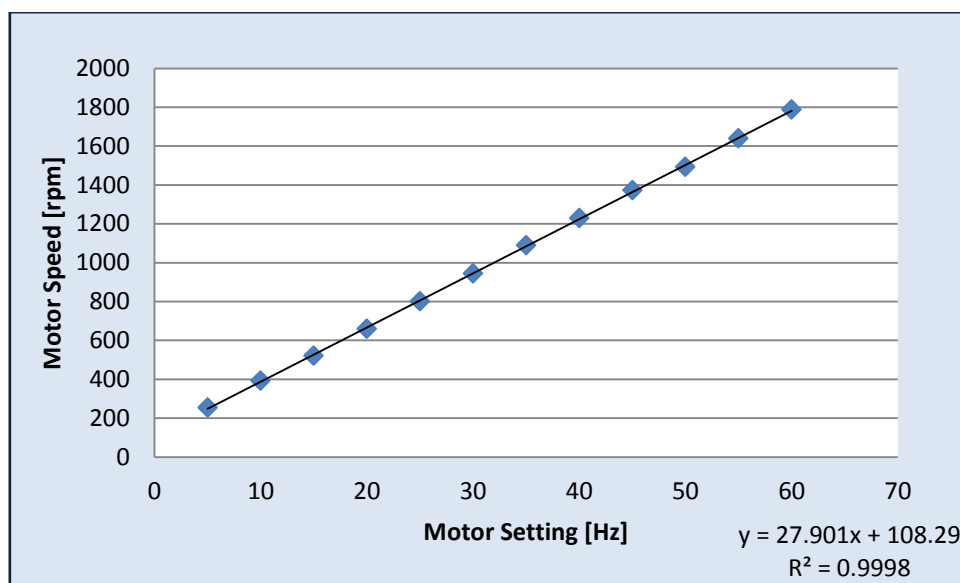


Figure 117 - Stirrer motor [M-101] calibration

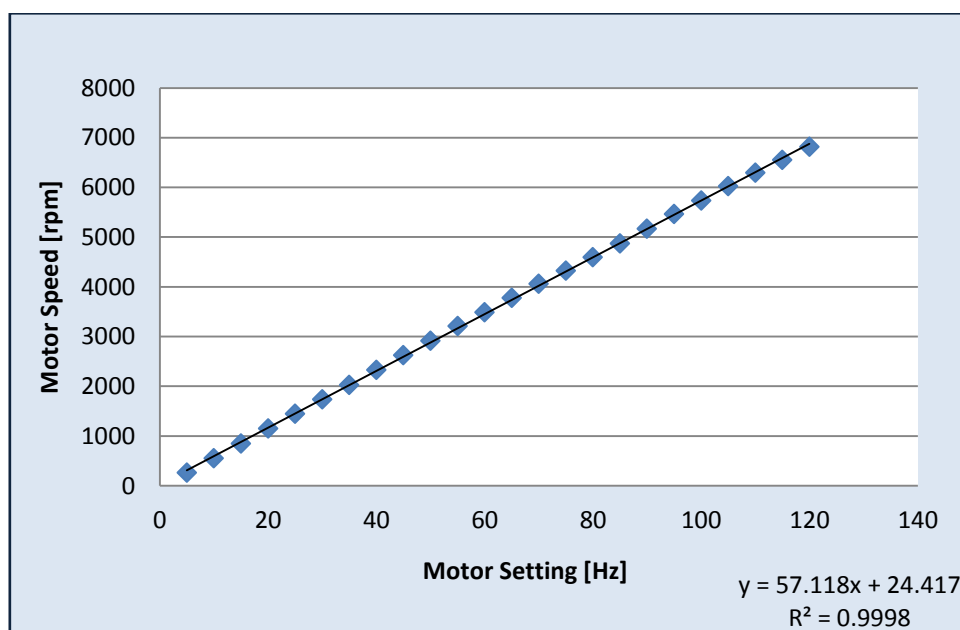


Figure 118 - High shear homogenizer motor [M-102] calibration

A trend line was fitted to both sets of data in order to obtain a relationship between the frequency setting of the variable speed controllers installed on the motors and the rotational speeds of the axles. The relationships are as follow:

M-101

$$y = 27.901x + 108.29$$

M-102

$$y = 57.118x + 24.417$$

Both these relationships have a R^2 value of 0.9998 which indicates that they can be used with confidence to accurately control the speed of both the stirrer's and high shear homogenizer's axles. y represents the variable speed drive setting (Hz) while x represents the rotational speed (rpm).

Appendix C: Material Safety Data Sheets

SIGMA-ALDRICH

sigma-aldrich.com

SAFETY DATA SHEET

according to Regulation (EC) No. 1907/2006

Version 5.0 Revision Date 31.10.2012

Print Date 26.11.2012

GENERIC EU MSDS - NO COUNTRY SPECIFIC DATA - NO OEL DATA

1. IDENTIFICATION OF THE SUBSTANCE/MIXTURE AND OF THE COMPANY/UNDERTAKING

1.1 Product identifiers

Product name : Camauba wax No. 1 yellow

Product Number : 243213
Brand : Aldrich
CAS-No. : 8015-86-9

1.2 Relevant identified uses of the substance or mixture and uses advised against

Identified uses : Laboratory chemicals, Manufacture of substances

1.3 Details of the supplier of the safety data sheet

Company : Sigma-Aldrich (Pty.) Ltd.
17 Pomona Street
Aviation Park, Unit 4
KEMPTON PARK
1619 SOUTH AFRICA

Telephone : +27 11 979 1188
Fax : +27 11 979 1119

1.4 Emergency telephone number

Emergency Phone # :

2. HAZARDS IDENTIFICATION

2.1 Classification of the substance or mixture

Not a hazardous substance or mixture according to Regulation (EC) No. 1272/2008.
This substance is not classified as dangerous according to Directive 67/548/EEC.

2.2 Label elements

The product does not need to be labelled in accordance with EC directives or respective national laws.

2.3 Other hazards - none

3. COMPOSITION/INFORMATION ON INGREDIENTS

3.1 Substances

Synonyms : Brazil wax

4. FIRST AID MEASURES

4.1 Description of first aid measures

If inhaled

If breathed in, move person into fresh air. If not breathing, give artificial respiration.

In case of skin contact

Wash off with soap and plenty of water.

In case of eye contact

Flush eyes with water as a precaution.



CERTIFICATE OF ANALYSIS

BUXUS PRODUCTS AND SERVICES P/L
 UNIT 26, WILD FIG BUSINESS PARK
 1494 CRANBERRY STREET
 HONEYDEW 2170
 JOHANNESBURG, SOUTH AFRICA

| | | |
|---------------------|---|--------------|
| INVOICE NO. | : | 152281 |
| SALES REFERENCE NO. | : | 20622/ |
| EXTERNAL REFERENCE | : | SYM87 |
| CONTAINER NO | : | PCIU 2144028 |
| DATE OF MANUFACTURE | : | 19/08/2011 |
| NEW DATE OF EXPIRY | : | 18/02/2013 |

We hereby certify the following batch number analysis is of the product supplied

SYM-OL 6910
 BATCH NO. 1230F37 X 80 DRUMS

| | Results |
|--|-----------|
| Iodine Value (gmI ₂ /100gm) | 88.3 |
| Acid Value (mgKOH/gm) | 201 |
| Sap Value (mgKOH/gm) | 202 |
| Cloud Point (°C) | 6.0 |
| Colour (51/4" Lovibond) | 3.8Y/0.2R |

FATTY ACID COMPOSITION

| | |
|----------|--------|
| C12 | : 0.1 |
| C14 | : 3.8 |
| C15GROUP | : 1.3 |
| C16 | : 4.1 |
| C16.1 | : 4.8 |
| C17GROUP | : 3.1 |
| C18 | : 1.3 |
| C18.1 | : 71.7 |
| C18.2 | : 6.2 |
| C18.3 | : 1.7 |
| C20 | : 1.3 |
| OTHER | : 0.6 |



SAVANNAH FINE CHEMICALS (PTY) LTD

++27 11 856 4500 + +27 21 551 5353+
 ++27 31 202 0794+

Mary Kapetanias
 LABORATORY MANAGER

SYMEX HOLDINGS LIMITED

14 WOODRUFF STREET PORT MELBOURNE VIC 3207 AUSTRALIA
 TELEPHONE +61 3 9261 2311 FACSIMILE +61 3 9645 2001
www.symex.com.au

ACN 081 252 262 ABN 28 081 058 380



Quality
 ISO 9001

SIGMA-ALDRICH

SAFETY DATA SHEET

according to Regulation (EC) No. 1907/2006

Version 4.4 Revision Date 15.01.2012

Print Date 26.11.2012

GENERIC EU MSDS - NO COUNTRY SPECIFIC DATA - NO OEL DATA

1. IDENTIFICATION OF THE SUBSTANCE/MIXTURE AND OF THE COMPANY/UNDERTAKING

1.1 Product identifiers

Product name : Oleic acid

Product Number : W281506

Brand : Aldrich

CAS-No. : 112-80-1

1.2 Relevant identified uses of the substance or mixture and uses advised against

Identified uses : Laboratory chemicals, Manufacture of substances

1.3 Details of the supplier of the safety data sheet

Company : Sigma-Aldrich (Pty.) Ltd.
17 Pomona Street
Aviation Park, Unit 4
KEMPTON PARK
1619 SOUTH AFRICA

Telephone : +27 11 979 1188

Fax : +27 11 979 1119

1.4 Emergency telephone number

Emergency Phone # :

2. HAZARDS IDENTIFICATION

2.1 Classification of the substance or mixture

Classification according to Regulation (EC) No 1272/2008 [EU-GHS/CLP]

Skin irritation (Category 2)

Classification according to EU Directives 67/548/EEC or 1999/45/EC

Irritating to skin.

2.2 Label elements

Labelling according Regulation (EC) No 1272/2008 [CLP]

Pictogram



Signal word : Warning

Hazard statement(s)

H315 : Causes skin irritation.

Precautionary statement(s) : none

Supplemental Hazard Statements : none

According to European Directive 67/548/EEC as amended.

Hazard symbol(s)



R-phrase(s)

R38 : Irritating to skin.

S-phrase(s) : none

SIGMA-ALDRICHsigma-aldrich.com**SAFETY DATA SHEET**

according to Regulation (EC) No. 1907/2006

Version 5.0 Revision Date 22.11.2012

Print Date 26.11.2012

GENERIC EU MSDS - NO COUNTRY SPECIFIC DATA - NO OEL DATA

1. IDENTIFICATION OF THE SUBSTANCE/MIXTURE AND OF THE COMPANY/UNDERTAKING**1.1 Product identifiers**

Product name : Ammonium hydroxide solution

Product Number : 05002

Brand : Sigma-Aldrich

1.2 Relevant identified uses of the substance or mixture and uses advised against

Identified uses : Laboratory chemicals, Manufacture of substances

1.3 Details of the supplier of the safety data sheetCompany : Sigma-Aldrich (Pty.) Ltd.
17 Pomona Street
Aviation Park, Unit 4
KEMPTON PARK
1619 SOUTH AFRICA

Telephone : +27 11 979 1188

Fax : +27 11 979 1119

1.4 Emergency telephone number

Emergency Phone # :

2. HAZARDS IDENTIFICATION**2.1 Classification of the substance or mixture**

Classification according to Regulation (EC) No 1272/2008 [EU-GHS/CLP]

Skin corrosion (Category 1B)

Specific target organ toxicity - single exposure (Category 3)

Acute aquatic toxicity (Category 1)

Classification according to EU Directives 67/548/EEC or 1999/45/EC

Causes burns. Very toxic to aquatic organisms.

2.2 Label elements

Labelling according Regulation (EC) No 1272/2008 [CLP]

Pictogram



Signal word : Danger

Hazard statement(s)

H314 : Causes severe skin burns and eye damage.

H335 : May cause respiratory irritation.

H400 : Very toxic to aquatic life.

Precautionary statement(s)

P281 : Avoid breathing vapours.

P273 : Avoid release to the environment.

P280 : Wear protective gloves/ protective clothing/ eye protection/ face protection.

P305 + P351 + P338 : IF IN EYES: Rinse cautiously with water for several minutes. Remove contact lenses, if present and easy to do. Continue rinsing.

SIGMA-ALDRICHsigma-aldrich.com**SAFETY DATA SHEET**

according to Regulation (EC) No. 1907/2006

Version 3.5 Revision Date 12.04.2012

Print Date 26.11.2012

GENERIC EU MSDS - NO COUNTRY SPECIFIC DATA - NO OEL DATA

1. IDENTIFICATION OF THE SUBSTANCE/MIXTURE AND OF THE COMPANY/UNDERTAKING**1.1 Product identifiers**

Product name : Potassium hydroxide solution

Product Number : 417681
Brand : Sigma-Aldrich
Index-No. : 019-002-00-8**1.2 Relevant identified uses of the substance or mixture and uses advised against**

Identified uses : Laboratory chemicals, Manufacture of substances

1.3 Details of the supplier of the safety data sheetCompany : Sigma-Aldrich (Pty.) Ltd.
17 Pomona Street
Aviation Park, Unit 4
KEMPTON PARK
1819 SOUTH AFRICATelephone : +27 11 979 1188
Fax : +27 11 979 1119**1.4 Emergency telephone number**

Emergency Phone # :

2. HAZARDS IDENTIFICATION**2.1 Classification of the substance or mixture**

Classification according to Regulation (EC) No 1272/2008 [EU-GHS/CLP]

Skin corrosion (Category 1A)

Acute toxicity, Oral (Category 4)

Classification according to EU Directives 67/548/EEC or 1999/45/EC

Causes severe burns. Harmful if swallowed.

2.2 Label elements

Labelling according Regulation (EC) No 1272/2008 [CLP]

Pictogram



Signal word : Danger

Hazard statement(s)

H302

Harmful if swallowed.

H314

Causes severe skin burns and eye damage.

Precautionary statement(s)

P280

Wear protective gloves/ protective clothing/ eye protection/ face protection.

P305 + P351 + P338

IF IN EYES: Rinse cautiously with water for several minutes. Remove contact lenses, if present and easy to do. Continue rinsing.

P310

Immediately call a POISON CENTER or doctor/ physician.

Supplemental Hazard Statements

none

Appendix D: Anton Paar Viscometer Procedure

Anton Paar® MCR 501 Stress-controlled Rheometer

Here the basic instructions on how to work with the Anton Paar MCR 501 Stress-controlled Rheometer. For more information you can refer to the instrument and software manuals available in the laboratory, or contact either Zahra Fahimi (Z.Fahimi@tue.nl) or Hans Wyss (H.M.Wyss@tue.nl).

1. Turn on the Rheometer (The on/off button is at the left side of the instrument) Check if the status on the display of instrument is “OK”

Caution: In case a warning on low air pressure is displayed do not touch the spindle or the instrument may get damaged.

2. Turn on the thermostat water bath. The setpoint should be between 20°C to 30°C. (The bath is used only as a thermal reservoir for the Peltier system.)

3. If the computer is off, turn it on with login: Rheometer, password: Correl@tor

4. Start the Rheoplus program on the computer

5. In the toolbar, press icon “device”, which is a symbol of a Rheometer

6. In the control panel tab in the new window, press “Initialize” to start

7. Put your desired tool

There is a line at the end of your tool that should be aligned with a corresponding line on the spindle. The instrument should automatically recognize your tool; a dialog box should be displayed.

8. In the control panel tab, press “Set zero gap”

9. In the control panel tab, set to measuring position (or at least 0.5mm the minimum recommended distance for performing a motor adjustment for CP geometry and 1.0mm for PP geometry.)

10. Go to service tab

11. In the service tab, press “Motor adjustment”

12. Set it as “Default adjustment”

13. Press “Start” to begin the adjustment

Do not touch the device and the table during the adjustment (it takes 2:58 minutes)

Appendix E: Validation of ANOVA Assumptions

To prove that the data points of the particle size data are independent, a plot of the residual versus the experimental run order is presented in **Figure 119**.

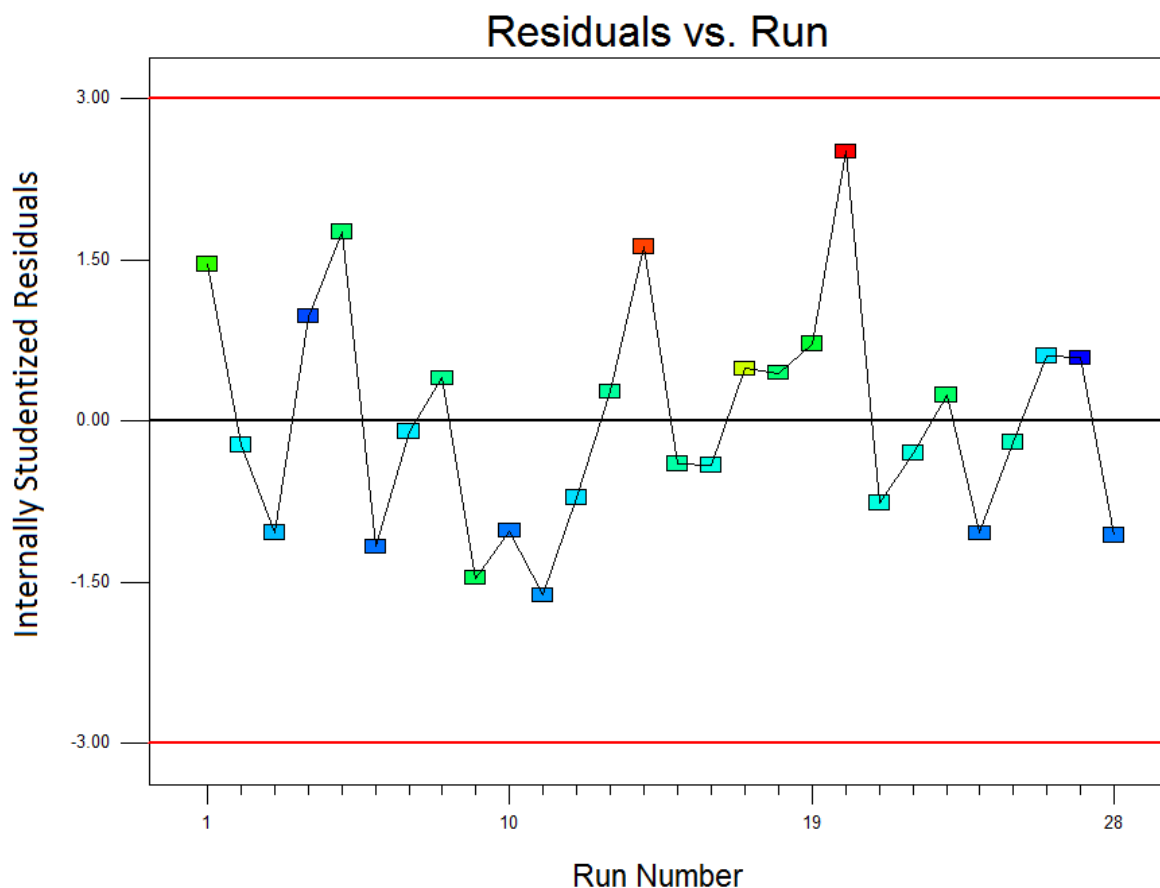


Figure 119 – Screening Experimental Design Particle Size Data - Residuals vs. Run

To validate the assumption of *independent data points*, the plot should show random scatter. From **Figure 119** it is clear that the data points are independent. There are no visible trends which are expected since the Screening-, Mixture- and Composite experimental designs were randomized which is insurance against trends ruining the analysis (Stat-Ease 2010).

The second assumption that needs to be satisfied is that the response is normally distributed. This assumption is presented in **Figure 120**.

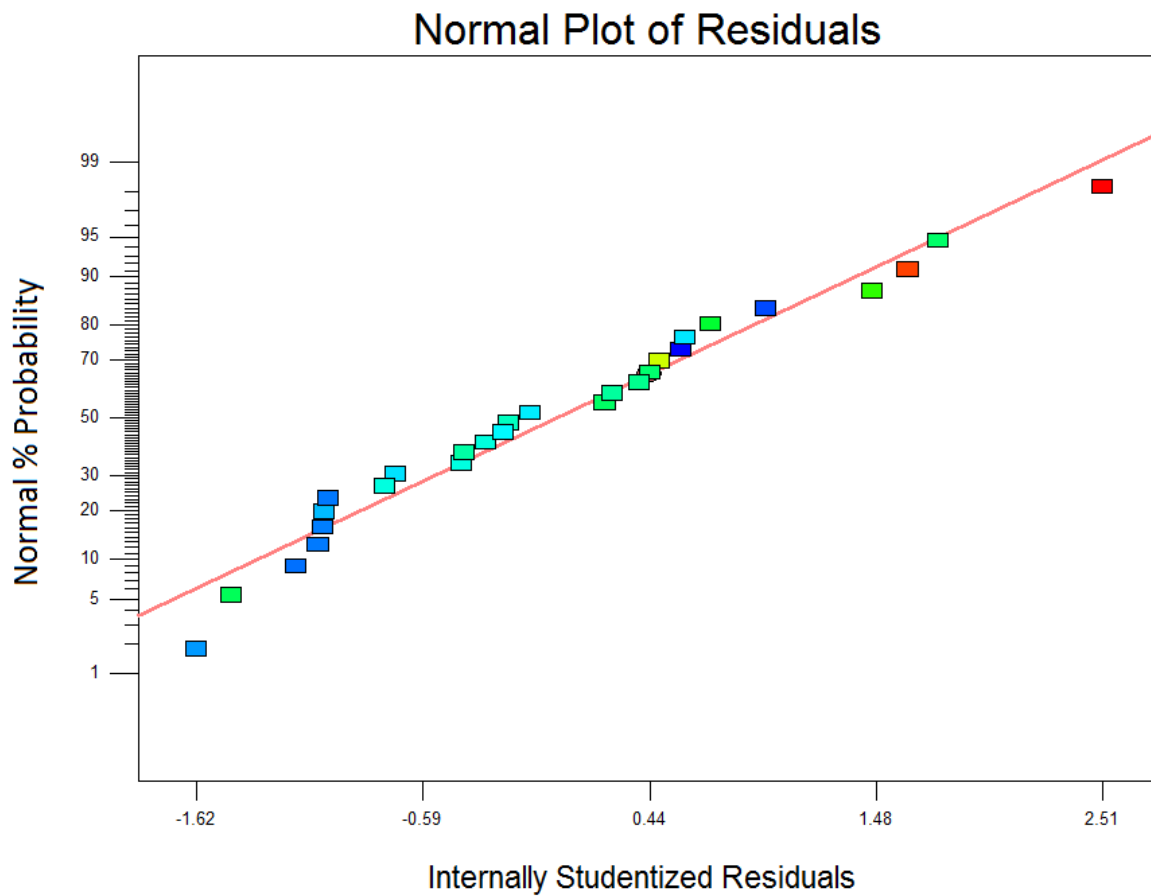


Figure 120 - Screening Experimental Design Particle Size Data - Normal Plot of Residuals

From **Figure 120** it is clear that the response is normally distributed. The residuals are situated on the normal line as presented in **Figure 120**.

Finally, the third assumption that needs to be satisfied is that the variance is similar within different groups (homogenous) [homoscedasticity] (Stat-Ease 2010). The final assumption is proven with **Figure 121**.

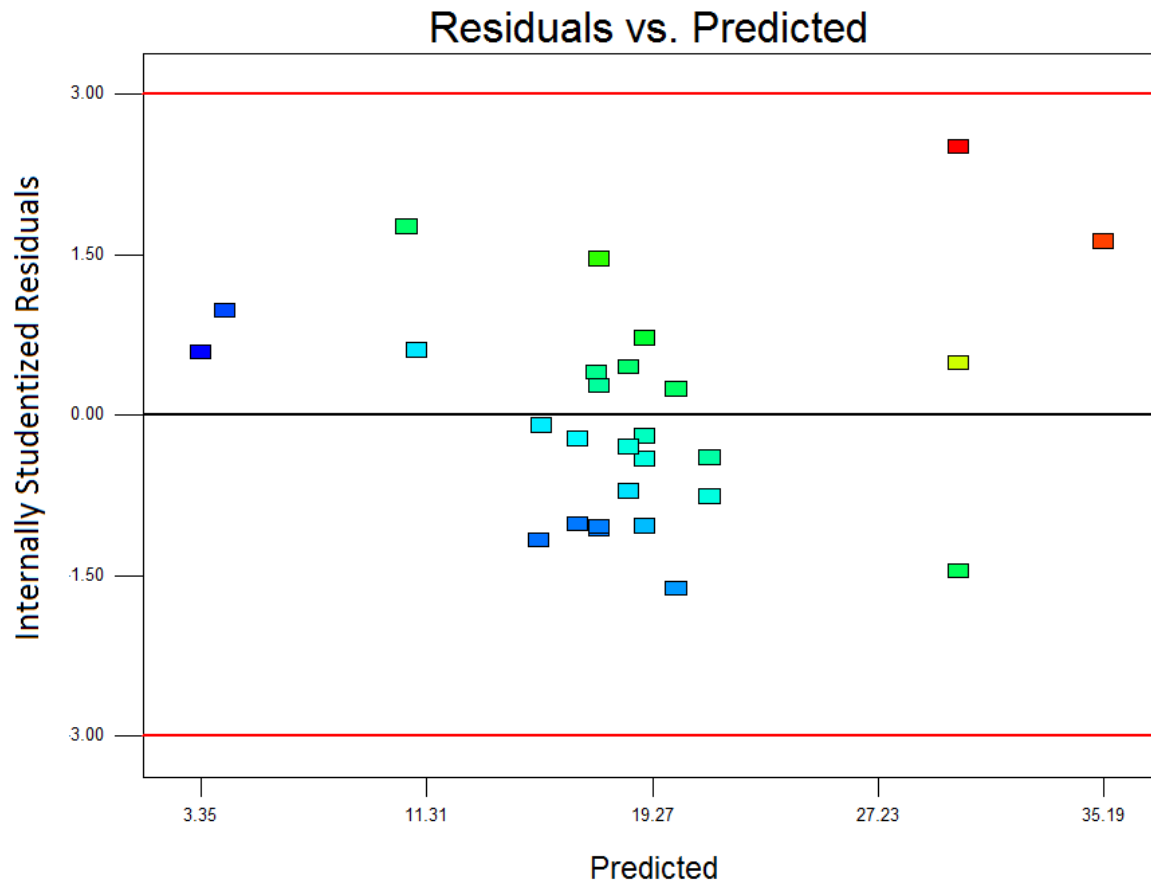


Figure 121 - Screening Experimental Design Particle Size Data - Residuals vs. Predicted

If the third and final assumption is satisfied, the residuals should vary randomly around zero and the spread of the residuals should be about the same throughout the plot (no systematic patterns). From **Figure 121** it is clear that the residuals vary randomly around zero. However, the spread is not the same throughout the plot. That said, with the residuals randomly varied around zero, the final assumption is satisfied.

By satisfying all three assumptions it is proven that ANOVA analysis can be used during the Screening-, Mixture- and Composite experimental designs' statistical analysis.

Appendix F: Screening Experimental Design Particle Size

Results and Discussion

Volume Distribution

Volume Median Particle Size

Volume Median Particle Size Model V1 (Screening Experimental Design)

The volume median particle size data were analysed by Design Expert© and a statistical model was fitted to the data. The Screening experimental design was originally set up as a linear model for both the mixture and process variables. Again it was noted that the linear model was not statistically significant ($p > 0.05$), as seen in the ANOVA **Table 82** (validation for the ANOVA assumptions is presented in **Appendix E**).

Table 82 - Volume Median Particle Size (Linear Model) ANOVA

| Analysis of Variance Table – Volume Median Particle Size (Linear Model) | | | | | | |
|---|----------------|----|-------------|---------|------------------|-----------------|
| Source | Sum of Squares | df | Mean Square | F Value | p-value Prob > F | |
| Model | 24.77 | 2 | 12.38 | 0.8007 | 0.4602 | not significant |
| Linear Mixture | 24.77 | 2 | 12.38 | 0.8007 | 0.4602 | |
| Residual | 386.65 | 25 | 15.47 | | | |
| Lack of Fit | 287.40 | 20 | 14.37 | 0.7239 | 0.7268 | not significant |
| Pure Error | 99.25 | 5 | 19.85 | | | |
| Cor Total | 411.41 | 27 | | | | |
| Adeq Precision | 1.98 | | | | | |

A reduced quadratic model was fitted to the volume median particle size data and is presented in **Table 83**.

Table 83 - Volume Median Particle Size (Reduced Quadratic Model) ANOVA

| Analysis of Variance Table – Volume Median Particle Size (Reduced Quadratic Model) | | | | | | |
|--|----------------|----|-------------|---------|------------------|-----------------|
| Source | Sum of Squares | df | Mean Square | F Value | p-value Prob > F | |
| Model | 188.45 | 5 | 37.69 | 3.719 | 0.0137 | significant |
| <i>%Wax * Cooling Rate</i> | 69.33 | 1 | 69.33 | 6.841 | 0.0158 | |
| <i>%Water * Stirring Speed</i> | 31.84 | 1 | 31.84 | 3.142 | 0.0902 | |
| <i>%Water * Inverting Phase AR</i> | 93.04 | 1 | 93.04 | 9.180 | 0.0062 | |
| Residual | 222.96 | 22 | 10.13 | | | |
| Lack of Fit | 123.71 | 17 | 7.28 | 0.367 | 0.9451 | not significant |
| Pure Error | 99.25 | 5 | 19.85 | | | |
| Cor Total | 411.41 | 27 | | | | |
| Adeq Precision | 8.39 | | | | | |

From **Table 83** it is possible to see that the reduced quadratic model is statistically significant ($p < 0.05$). There is only a 1.37% chance that a Model F-Value this large (3.71895) could occur due to noise. The statistically significant ($p < 0.05$) model terms are *%Wax*Cooling Rate*, *%Water*Stirring Speed* and *%Water*Inverting Phase AR*. An adequate precision value of 8.391 indicates an adequate signal and shows that the model can be used to navigate the design space (Stat-Ease 2010). The R-squared values for the **Volume Median Particle Size Model V1 (Screening)** are as follow:

| Model | R-Squared | Adj R-Squared | Pred R-Squared |
|---|-----------|---------------|----------------|
| Volume Median Particle Size Model V1 | 0.4581 | 0.3349 | 0.1746 |

From the R-squared values it is possible to see that the predicted R-squared value is not as close to the adjusted R-squared value as one might normally expect, yet it is still within the 0.2 “reasonable agreement” range, indicating that the model can be used to navigate the design space (Stat-Ease 2010). The final **Volume Median Particle Size Model V1 (Screening)** equation in terms of the actual components and actual factors are as follow:

$$\begin{aligned}
 \text{Particle Size } [\mu\text{m}] = & +2.96834 \times \% \text{Surfactant} \\
 & +3.13103 \times \% \text{Wax} \\
 & -0.68379 \times \% \text{Water}
 \end{aligned}$$

$$+1.04804 \times 10^{-3} \times \%Surfactant \times Stirring\ Speed$$

$$-0.062863 \times \%Surfactant \times Cooling\ Rate$$

$$-1.24495 \times \%Surfactant \times Inverting\ Phase\ AR$$

$$+1.04804 \times 10^{-3} \times \%Wax \times Stirring\ Speed$$

$$+0.56577 \times \%Wax \times Cooling\ Rate$$

$$-1.24495 \times \%Wax \times Inverting\ Phase\ AR$$

$$-2.62011 \times 10^{-4} \times \%Water \times Stirring\ Speed$$

$$-0.062863 \times \%Water \times Cooling\ Rate$$

$$+0.31124 \times \%Water \times Inverting\ Phase\ AR$$

From the final model equation it is again noted that the mixture (composition) variables have a significant influence on the particle size. The effect of varying the wax-to-surfactant ratio and stirring speed on the particle size is presented in **Figure 122**.

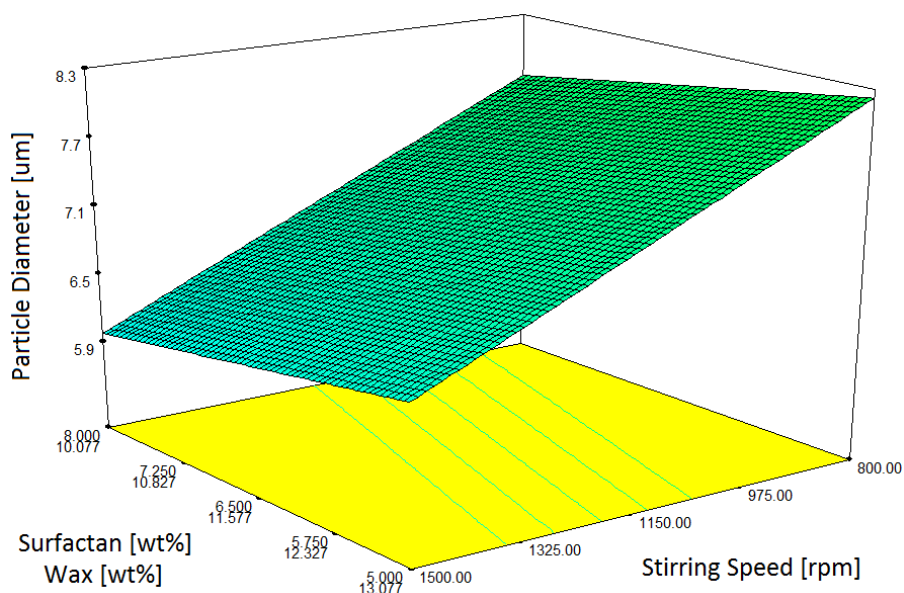


Figure 122 - Volume Median Particle Size Model V1 (Screening Experimental Design) - Particle Size vs. Wax-to-Surfactant Ratio vs. Stirring Speed

It is possible to see from **Figure 122** that a similar trend was obtained for both the wax-to-surfactant ratio and the stirring speed, as obtained with the **Volume Mean Particle Size Model V1 (Screening)**. The particle size decreases with a decrease in the wax-to-surfactant ratio. In terms of the stirring

speed, the particle size decreases with an increase in the stirring speed. As stated in the **Volume Mean Particle Size Section** these trends are supported by McClements, Chen et al., Gusman and Sadurni et al. (Gusman 1947, McClements 2010, Sadurní et al. 2005, Chen, Tao 2005). **Figure 123** shows the effect of varying the wax-to-surfactant ratio on the particle size in more detail (Processing Conditions: Stirring Speed = 1150 rpm, High Shear Homogenizing Speed = 5550 rpm, HS Time Interval = 25 mins, Cooling Rate = 0, Inverting Phase AR = 3.5 l/h, Temperature = 110°C).

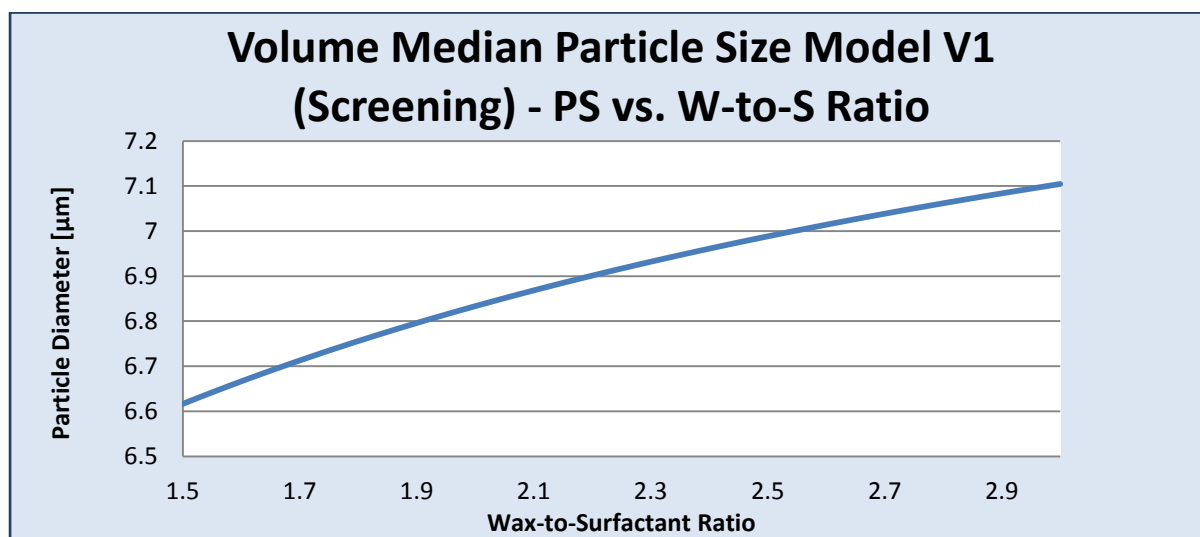


Figure 123 - Volume Median Particle Size Model V1 (Screening Experimental Design) - Particle Size vs. Wax-to-Surfactant Ratio

The trend seen in **Figure 122** is confirmed in **Figure 123**. It is noted that the particle size range is between 6.5 – 7.2 µm whereas the volume mean particle size range was between 16 – 17.2 µm. This is due to the median not being as influenced by outliers as the mean (Lund, Lund 2013, Lund, Lund 2013). Thus the median is not as influenced by random large particles as with the mean (Lund, Lund 2013, Lund, Lund 2013). **Figure 124** shows the effect of varying the cooling rate on the particle size.

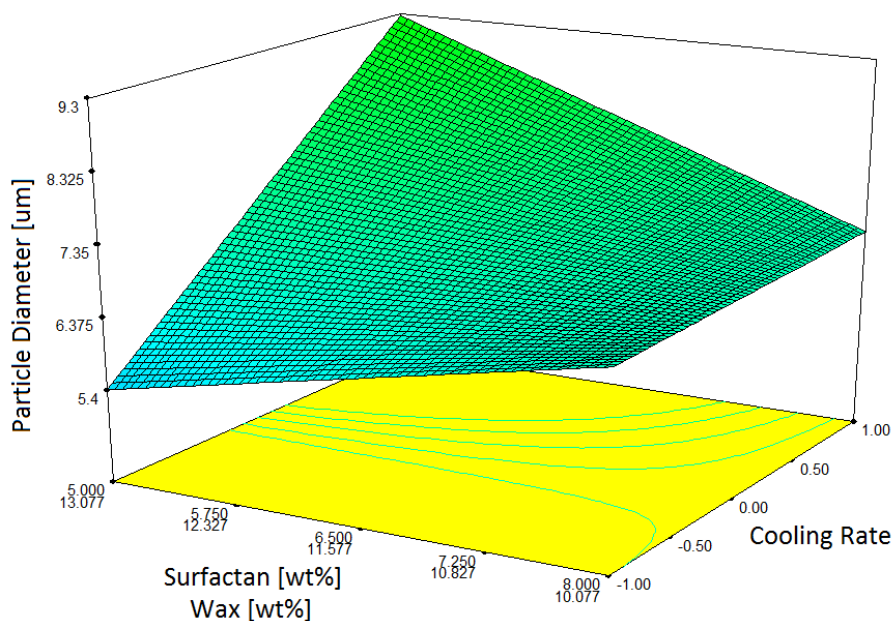


Figure 124 - Volume Median Particle Size Model V1 (Screening Experimental Design) - Particle Size vs. Wax-to-Surfactant Ratio vs. Cooling Rate

Once again it is possible to see that at a low wax-to-surfactant ratio the cooling rate has little or no effect on the particle size. However, at high a wax-to-surfactant ratio the cooling rate has a significant effect on the particle size. These findings were similar to the trends obtained with the **Volume Mean Particle Size Model V1 (Screening)**. At a wax-to-surfactant ratio of 2.6 it is noted that the particle size increases with an increase in the cooling rate. This trend is in agreement with Lashmar et al.'s findings, but not with Li et al.'s (Li et al. 2010, Lashmar, Richardson & Erbod 1995). However, the trend of varying the wax-to-surfactant ratio on the particle size at a high cooling rate is in agreement with Li et al. (Li et al. 2010).

The final significant process variable in the **Volume Median Particle Size Model V1 (Screening)** is the inverting phase addition rate. The effect of varying inverting phase addition rate on the particle size is presented in **Figure 125**.

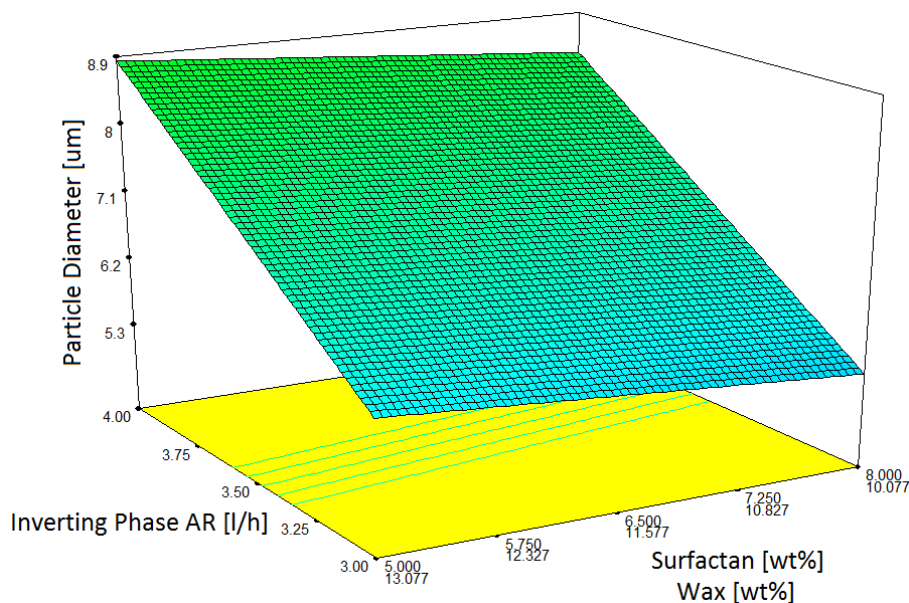


Figure 125 - Volume Median Particle Size Model V1 (Screening Experimental Design) - Particle Size vs. Wax-to-Surfactant Ratio vs. Inverting Phase Addition Rate

By examining **Figure 125** one can see that the particle size decreases with a decrease in the inverting phase addition rate. As with the **Volume Mean Particle Size Model V1 (Screening)**, this trend is in agreement with Gutierrez et al., Pey et al., Wang et al. and Lashmar et al.'s findings. They concluded that by slowly adding the inverting phase nano-emulsions can be obtained, while emulsions with larger particle sizes are obtained by rapidly adding the inverting phase (Gutiérrez et al. 2008, Pey et al. 2006, Wang et al. 2007, Lashmar, Richardson & Erbod 1995, Uson, Garcia & Solans 2004).

The predicted values calculated by means of the **Volume Median Particle Size Model V1 (Screening)** is plotted against the actual values obtained during the screening experimental runs, in **Figure 126**.

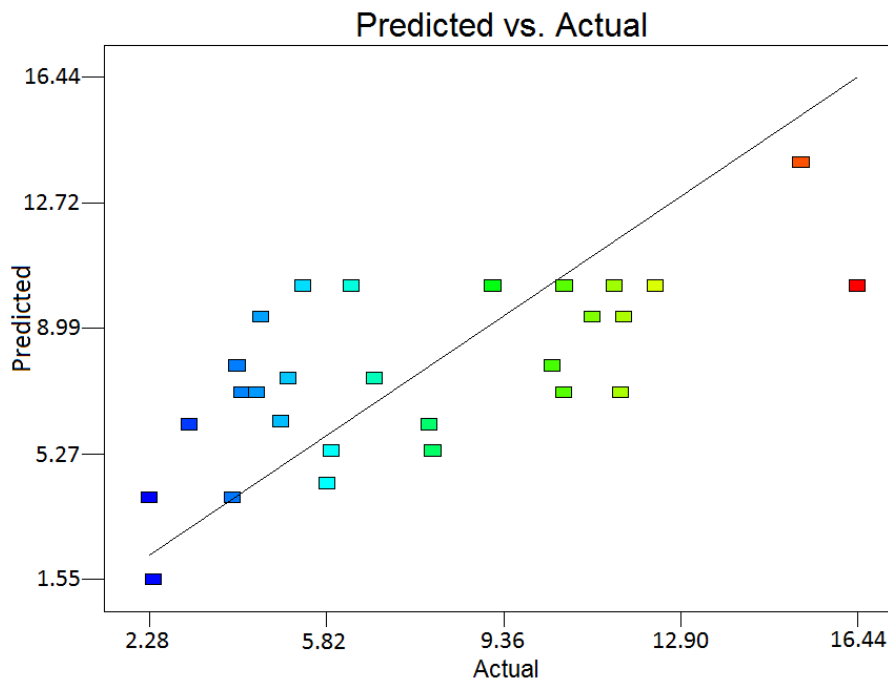
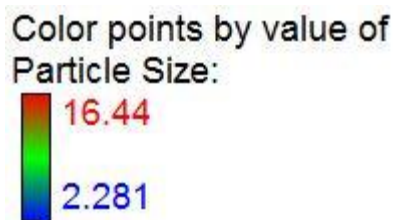


Figure 126 - Volume Median Particle Size Model V1 (Screening Experimental Design) - Predicted vs. Actual

Color Key:



Once again it should be kept in mind that any variation in the volume particle size data could be due to the varying ambient conditions during the experimental runs. By examining **Figure 126** it is clear that the model is not a hundred percent accurate, yet for the purpose of screening it is sufficient enough ($p < 0.05$, adequate precision value of 8.391). That said, it is noted that there are two outlier points (red markers) in **Figure 126**. These outlier points could be causing the model to be more inaccurate than what it could be.

Volume Median Particle Size Model V2 (Screening Experimental Design)

The outlier points (*EXP S7* and *EXP S27*) were excluded from the data set and a reduced quadratic model was refitted to the rearranged data and is presented in the ANOVA **Table 84** (validation for the ANOVA assumptions is presented in **Appendix E**).

Table 84 - Volume Median Particle Size (Reduced Quadratic Model) ANOVA

| Analysis of Variance Table – Volume Median Particle Size (Reduced Quadratic Model) | | | | | | |
|---|----------------|-----------|---------------|--------------|--------------------|-----------------|
| | Sum of | | Mean | F | p-value | |
| Source | Squares | df | Square | Value | Prob > F | |
| Model | 135.98 | 4 | 33.99 | 3.614 | 0.0216 | significant |
| <i>%Wax * Cooling Rate</i> | 59.73 | 1 | 59.73 | 6.350 | 0.0199 | |
| <i>%Water * Cooling Rate</i> | 56.19 | 1 | 56.20 | 5.974 | 0.0234 | |
| Residual | 197.55 | 21 | 9.41 | | | |
| Lack of Fit | 98.80 | 17 | 5.81 | 0.235 | 0.9855 | not significant |
| Pure Error | 98.75 | 4 | 24.69 | | | |
| Cor Total | 333.52 | 25 | | | | |
| Adeq Precision | 4.70 | | | | | |

From **Table 30** it is possible to see that the p-value for the newly fitted **Volume Median Particle Size Model V2 (Screening)** (0.0216) is more than the p-value of the **Volume Median Particle Size Model V1 (Screening)** (0.0137). The R-squared values for the **Volume Mean Particle Size Model V2 (Screening)** are as follow:

| Model | R-Squared | Adj R-Squared | Pred R-Squared |
|---|------------------|----------------------|-----------------------|
| Volume Median Particle Size Model V2 | 0.4077 | 0.2949 | 0.1760 |

From the R-squared values it is possible to see that the predicted R-squared value is more for the newly fitted **Volume Median Particle Size Model V2 (Screening)** (0.1760) without the two outlier points than the previous model (1.746). It is also noted that the predicted R-squared value falls within the 0.2 range, which indicates that this model can be used to navigate the design space (Stat-Ease 2010). The final **Volume Median Particle Size Model V2 (Screening)** equation in terms of the actual components and actual factors are as follow:

$$\begin{aligned}
 \text{Particle Size } [\mu\text{m}] = & -0.092106 \times \% \text{Surfactant} \\
 & +0.15032 \times \% \text{Wax} \\
 & +0.066845 \times \% \text{Water} \\
 & +0.40885 \times \% \text{Surfactant} \times \text{Cooling Rate} \\
 & +1.00313 \times \% \text{Wax} \times \text{Cooling Rate} \\
 & -0.17650 \times \% \text{Water} \times \text{Cooling Rate}
 \end{aligned}$$

It is noted from the **Volume Median Particle Size Model V2 (Screening)** that the cooling rate is the main process variable. The effect of varying the cooling rate on the particle size is presented in **Figure 127**.

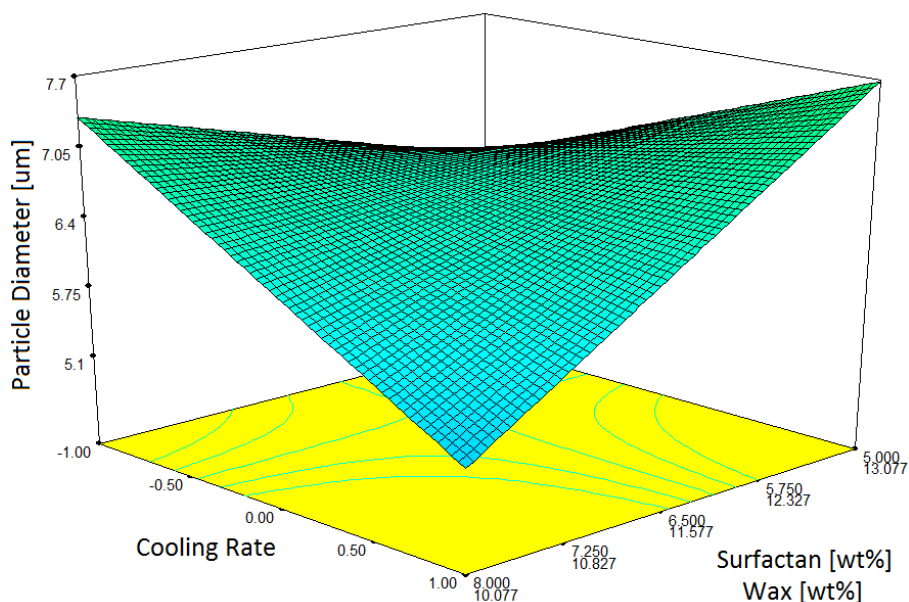


Figure 127 - Volume Median Particle Size Model V2 (Screening Experimental Design) - Particle Size vs. Wax-to-Surfactant Ratio vs. Cooling Rate

By examining **Figure 127** one can see that at a favourable low wax-to-surfactant ratio, the particle size decreases with an increase in the cooling rate. This is identical to the trend that was obtained with the **Volume Mean Particle Size Model V2 (Screening)** and is in agreement with Li et al. who concluded in his study on the formation of paraffin wax emulsions, that by increasing the emulsification temperature and cooling rate improves emulsion properties, i.e. results in a smaller particle size (Li et al. 2010). The accuracy of the **Volume Median Particle Size Model V2 (Screening)** is represented by the actual values versus the predicted values seen in **Figure 128**.

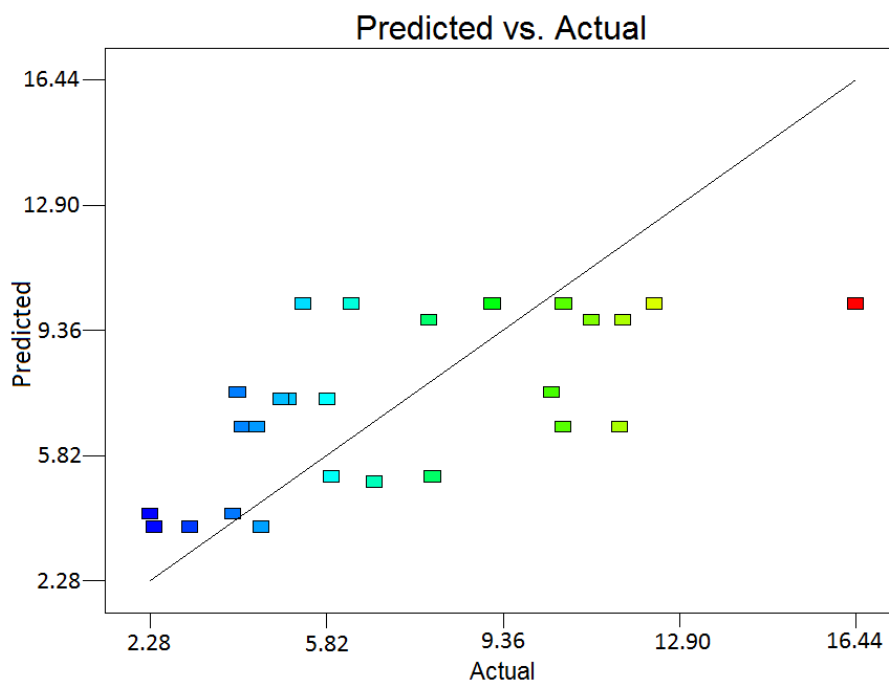


Figure 128 - Volume Median Particle Size Model V2 (Screening Experimental Design) - Predicted vs. Actual

When comparing **Figure 126** with **Figure 128** one can see that **Figure 128** is more concentrated around the predicted vs. actual line, with the exception of the one outlier point (red marker). It should be kept in mind that the p-value for the newly fitted **Volume Median Particle Size Model V2 (Screening)** (0.0216) is more than the p-value of the **Volume Median Particle Size Model V1 (Screening)** (0.0137).

Area Distribution

The area particle size data were calculated from the observed scattering of the laser through the sample medium by means of mathematical models (**Section 5.3.1.1**). The area particle size data were collected from the Saturn DigiSizer 5200 Particle Sizer (Micrometrics, UK) for further processing.

Area Mean Particle Size

Area Mean Particle Size Model V1 (Screening Experimental Design)

Once the area mean particle size data were analysed with Design Expert©, it was noted that the linear model was not statistically significant ($p > 0.05$), as seen in the ANOVA **Table 85** (validation for the ANOVA assumptions is presented in **Appendix E**).

Table 85 - Area Mean Particle Size (Linear Model) ANOVA

| Analysis of Variance Table – Area Mean Particle Size (Linear Model) | | | | | | |
|---|----------------|----|-------------|---------|---------|-----------------|
| Source | Sum of Squares | df | Mean Square | F Value | p-value | |
| Model | 0.903 | 2 | 0.452 | 0.314 | 0.734 | not significant |
| Linear Mixture | 0.903 | 2 | 0.452 | 0.314 | 0.734 | |
| Residual | 35.974 | 25 | 1.439 | | | |
| Lack of Fit | 26.324 | 20 | 1.316 | 0.682 | 0.756 | not significant |
| Pure Error | 9.650 | 5 | 1.930 | | | |
| Cor Total | 36.877 | 27 | | | | |
| Adeq Precision | 1.070 | | | | | |

A reduced quadratic model was fitted to the area mean particle size data and the revised ANOVA can be seen in **Table 86**.

Table 86 - Area Mean Particle Size (Reduced Quadratic Model) ANOVA

| Analysis of Variance Table – Area Mean Particle Size (Reduced Quadratic Model) | | | | | | |
|--|----------------|----|-------------|---------|---------|-------------|
| Source | Sum of Squares | df | Mean Square | F Value | p-value | |
| Model | 16.415 | 5 | 3.283 | 3.530 | 0.0171 | significant |
| <i>%Wax * Cooling Rate</i> | 4.243 | 1 | 4.243 | 4.562 | 0.0441 | |
| <i>%Water * Stirring Speed</i> | 5.322 | 1 | 5.322 | 5.722 | 0.0257 | |
| <i>%Water * Inverting Phase AR</i> | 10.353 | 1 | 10.353 | 11.131 | 0.0030 | |
| Residual | 20.462 | 22 | 0.930 | | | |
| Lack of Fit | 10.812 | 17 | 0.636 | 0.330 | 0.9612 | not |

| | | | | |
|----------------|--------|----|-------|-------------|
| | | | | significant |
| Pure Error | 9.650 | 5 | 1.930 | |
| Cor Total | 36.877 | 27 | | |
| Adeq Precision | 10.013 | | | |

From **Table 86** one can see that the reduced quadratic model is statistically significant ($p < 0.05$). There is only a 171. % chance that a Model F-Value this large (3.529876) could occur due to noise. The statistically significant ($p < 0.05$) model terms are *%Wax*Cooling Rate*, *%Water*Stirring Speed* and *%Water*Inverting Phase AR*. An adequate precision value of 10.013 indicates an adequate signal and shows that the model can be used to navigate the design space (Stat-Ease 2010). The R-squared values for the **Area Mean Particle Size Model V1 (Screening)** are as follow:

| Model | R-Squared | Adj R-Squared | Pred R-Squared |
|----------------------------------|-----------|---------------|----------------|
| Area Mean Particle Size Model V1 | 0.4451 | 0.319 | 0.1199 |

The final **Area Mean Particle Size Model V1 (Screening)** equation in terms of the actual components and actual factors are as follow:

$$\begin{aligned}
 \text{Particle Size } [\mu\text{m}] = & +0.94424 \times \% \text{Surfactant} \\
 & +0.92848 \times \% \text{Wax} \\
 & -0.19865 \times \% \text{Water} \\
 & +4.28455 \times 10^{-4} \times \% \text{Surfactant} \times \text{Stirring Speed} \\
 & -0.015551 \times \% \text{Surfactant} \times \text{Cooling Rate} \\
 & -0.41529 \times \% \text{Surfactant} \times \text{Inverting Phase AR} \\
 & +4.28455 \times 10^{-4} \times \% \text{Wax} \times \text{Stirring Speed} \\
 & +0.13996 \times \% \text{Wax} \times \text{Cooling Rate} \\
 & -0.41529 \times \% \text{Wax} \times \text{Inverting Phase AR} \\
 & -1.07114 \times 10^{-4} \times \% \text{Water} \times \text{Stirring Speed}
 \end{aligned}$$

$$-0.015551 \times \%Water \times Cooling Rate$$

$$+0.10382 \times \%Water \times Inverting Phase AR$$

Once again it is noted that the mixture (composition) variables have a significant influence on the particle size. **Figure 129** shows the effect of varying the stirring speed on the particle size.

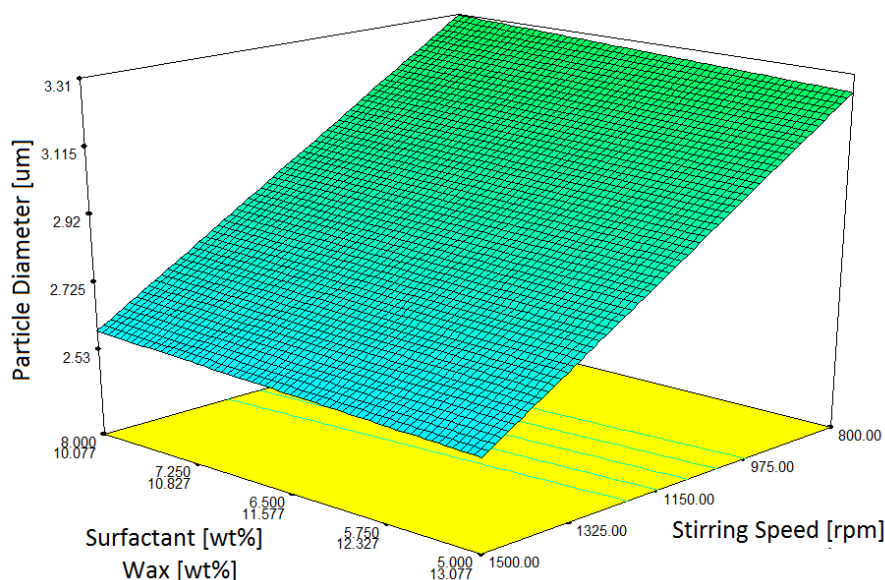


Figure 129 - Area Mean Particle Size Model V1 (Screening Experimental Design) - Particle Size vs. Wax-to-Surfactant Ratio vs. Stirring Speed

From **Figure 129** it is possible to see that an increase in the stirring speed results in a decrease in the particle size. This is similar to the findings of McClements, Chen et al., Gusman and Sadurni et al. (Gusman 1947, McClements 2010, Sadurni et al. 2005, Chen, Tao 2005). In addition it is also similar to the trends obtained with both the **Volume Mean Particle Size Model V1 (Screening)** and the **Volume Median Particle Size Model V1 (Screening)**. Looking at the wax-to-surfactant ratio one can see that there is a very small change in the particle size as the wax-to-surfactant ratio varies. **Figure 130** shows the effect of varying the wax-to-surfactant ratio on the particle size in more detail (Process Conditions: Stirring Speed = 1150 rpm, High Shear Homogenizing Speed = 5550 rpm, HS Time Interval = 25 mins, Cooling Rate = 0, Inverting Phase AR = 3.5 l/h, Temperature = 110°C).

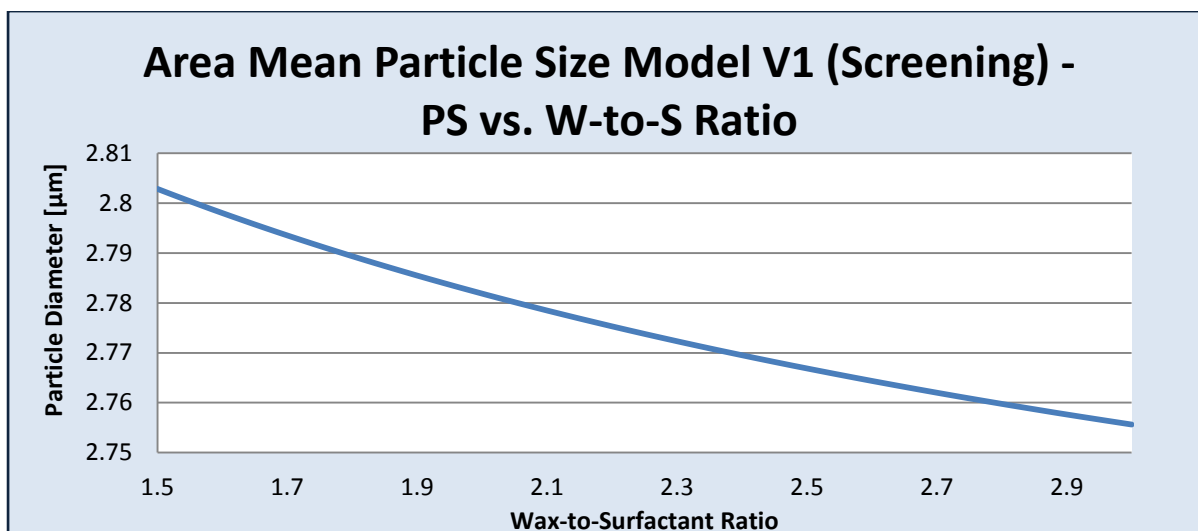


Figure 130 - Area Mean Particle Size Model V1 (Screening Experimental Design) - Particle Size vs. Wax-to-Surfactant Ratio

The trend in **Figure 130** contradicts the findings obtained with the **Volume Mean Particle Size Model V1 (Screening)** and the **Volume Median Particle Size Model V1 (Screening)** which were in agreement with the findings of Gusman, Liu et al., Pey et al. and Sadurni et al. (Pey et al. 2006, Liu et al. 2006, Gusman 1947, Sadurni et al. 2005). However, when examining **Figure 129** more closely it is possible to see that at a high stirring speed (1500 rpm), the wax-to-surfactant ratio does not have any effect on the particle size. This could possibly be due to the stirring speed having a more significant effect on the particle size than that of the wax-to-surfactant ratio. At this point it should be emphasised that the ratio of Oleic acid : Ammonium hydroxide : Potassium hydroxide was fixed for the Screening experimental design.

The effect of varying the cooling rate on the particle size is presented in **Figure 131**.

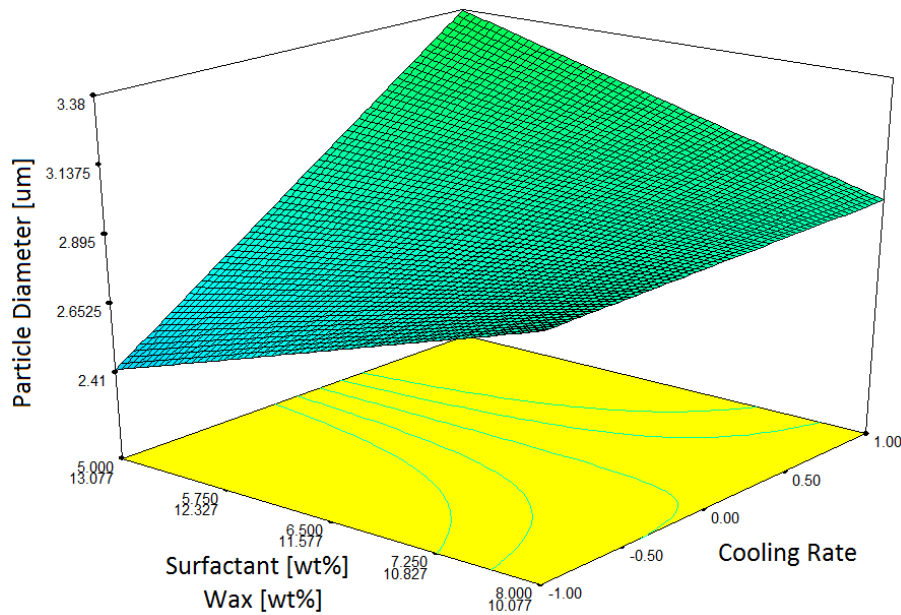


Figure 131 - Area Mean Particle Size Model V1 (Screening Experimental Design) - Particle Size vs. Wax-to-Surfactant Ratio vs. Cooling Rate

As with the volume mean- and volume median particle size data sets it is possible to see that at a favourable low wax-to-surfactant ratio the cooling rate has little or no effect on the particle size. However, at a high wax-to-surfactant ratio the particle size decreases with a decrease in the cooling rate. This trend is in agreement with Lashmar et al.'s findings, but not with Li et al.'s (Li et al. 2010, Lashmar, Richardson & Erbod 1995). However, the trend of varying the wax-to-surfactant ratio on the particle size at a high cooling rate is in agreement with Li et al. (Li et al. 2010). The last significant process variable in the **Area Mean Particle Size Model V1 (Screening)** is the inverting phase addition rate.

Figure 132 shows the effect of varying the inverting phase addition rate on the particle size.

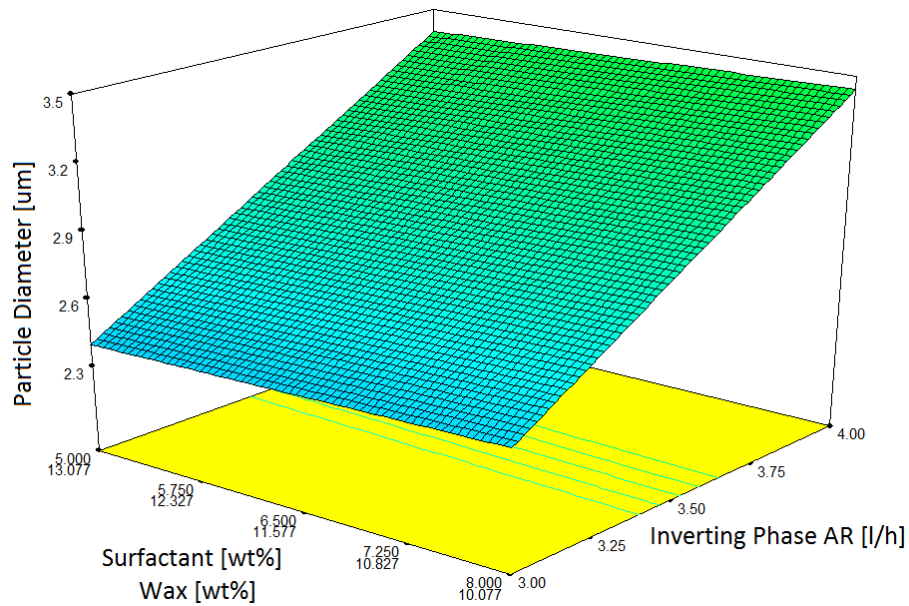


Figure 132 - Area Mean Particle Size Model V1 (Screening Experimental Design) - Particle Size vs. Wax-to-Surfactant Ratio vs. Inverting Phase Addition Rate

From **Figure 132** one can see that the particle size decreases with a decrease in the inverting phase addition rate. This trend is in agreement with Gutierrez et al., Pey et al., Wang et al. and Lashmar et al.'s findings. They concluded that by slowly adding the inverting phase nano-emulsions can be obtained, while emulsions with larger particle sizes are obtained by rapidly adding the inverting phase (Gutiérrez et al. 2008, Pey et al. 2006, Wang et al. 2007, Lashmar, Richardson & Erbod 1995, Uson, Garcia & Solans 2004).

Area Mean Particle Size Model V2 (Screening Experimental Design)

The outlier point (EXP 57) was excluded and a reduced quadratic model was refitted to the rearranged data and is presented in the ANOVA **Table 87** (validation for the ANOVA assumptions is presented in **Appendix E**).

Table 87 - Area Mean Particle Size (Reduced Quadratic Model) ANOVA

| Analysis of Variance Table – Area Mean Particle Size (Reduced Quadratic Model) | | | | | | |
|---|-----------------------|-----------|--------------------|----------------|----------------------------|-----------------|
| Source | Sum of Squares | df | Mean Square | F Value | p-value Prob > F | |
| Model | 8.381 | 4 | 2.095 | 2.376 | 0.0832 | not significant |
| <i>%Wax * Cooling Rate</i> | 4.006 | 1 | 4.006 | 4.542 | 0.0445 | |
| <i>%Water * Cooling Rate</i> | 3.240 | 1 | 3.240 | 3.674 | 0.0684 | |
| Residual | 19.403 | 22 | 0.882 | | | |
| Lack of Fit | 9.753 | 17 | 0.574 | 0.297 | 0.9729 | not significant |
| Pure Error | 9.650 | 5 | 1.930 | | | |
| Cor Total | 27.784 | 26 | | | | |
| Adeq Precision | 3.817 | | | | | |

It is visible in **Table 87** that the refitted quadratic model is not statistically significant ($p > 0.05$). The R-squared values for the **Area Mean Particle Size Model V2 (Screening)** are as follow:

| Model | R-Squared | Adj R-Squared | Pred R-Squared |
|---|------------------|----------------------|-----------------------|
| Area Mean Particle Size Model V2 | 0.3017 | 0.1747 | 0.0841 |

From the R-squared values it can be seen that all the R-squared values have decreased from the previous **Area Mean Particle Size Model V1 (Screening)**. Due to the p-value being less than 0.05 and the R-squared values less than the **Area Mean Particle Size Model V1 (Screening)**, the **Area Mean Particle Size Model V2 (Screening)** will not be studied further.

Area Median Particle Size**Area Median Particle Size Model V1 (Screening Experimental Design)**

The area median particle size data were analysed by Design Expert© and a statistical model was fitted. Again it was noted that the linear model of the original Screening design setup was not statistically significant ($p > 0.05$) to the area median particle size data, as seen in **Table 88** (validation for the ANOVA assumptions is presented in **Appendix E**).

Table 88 - Area Median Particle Size (Linear Model) ANOVA

| Analysis of Variance Table – Area Median Particle Size (Linear Model) | | | | | | |
|---|----------------|----|-------------|---------|---------|-----------------|
| Source | Sum of Squares | df | Mean Square | F Value | p-value | Prob > F |
| Model | 0.062 | 2 | 0.031 | 0.260 | 0.7734 | not significant |
| Linear Mixture | 0.062 | 2 | 0.031 | 0.260 | 0.7734 | |
| Residual | 2.962 | 25 | 0.118 | | | |
| Lack of Fit | 2.074 | 20 | 0.104 | 0.584 | 0.8222 | not significant |
| Pure Error | 0.888 | 5 | 0.178 | | | |
| Cor Total | 3.023 | 27 | | | | |
| Adeq Precision | 1.138 | | | | | |

A reduced quadratic model was fitted to the area median particle size data and is presented in **Table 89**.

Table 89 - Area Median Particle Size (Reduced Quadratic Model) ANOVA

| Analysis of Variance Table – Volume Median Particle Size (Reduced Quadratic Model) | | | | | | |
|--|----------------|----|-------------|---------|---------|-----------------|
| Source | Sum of Squares | df | Mean Square | F Value | p-value | Prob > F |
| Model | 1.094 | 5 | 0.219 | 2.495 | 0.0619 | not significant |
| <i>%Surfactant *</i> | 0.432 | 1 | 0.432 | 4.929 | 0.0370 | |
| <i>HSH Speed</i> | | | | | | |
| <i>%Water * Stirring Speed</i> | 0.281 | 1 | 0.281 | 3.206 | 0.0872 | |
| <i>%Water *</i> | 0.457 | 1 | 0.458 | 5.217 | 0.0324 | |
| <i>Inverting Phase AR</i> | | | | | | |
| Residual | 1.929 | 22 | 0.088 | | | |
| Lack of Fit | 1.041 | 17 | 0.061 | 0.345 | 0.9548 | not significant |
| Pure Error | 0.888 | 5 | 0.178 | | | |
| Cor Total | 3.023 | 27 | | | | |
| Adeq Precision | 7.141 | | | | | |

By examining **Table 89** one can see that the reduced quadratic model is also not statistically significant ($p > 0.05$). That said, it is possible to see that there are three relevant model terms of which two of them are statistically significant ($p < 0.05$). These two model terms are the %Surfactant*HSH Speed- and the %Water*Inverting Phase AR term. Apart from the fact that the **Area Median Particle Size Model V1 (Screening)** is not statistically significant, the trends of the model will be briefly examined. The R-squared values for the **Area Median Particle Size Model V1 (Screening)** are as follow:

| Model | R-Squared | Adj R-Squared | Pred R-Squared |
|------------------------------------|-----------|---------------|----------------|
| Area Median Particle Size Model V1 | 0.3619 | 0.2168 | -0.0293 |

From the R-squared values it is noted that the predicted R-squared value is negative. This indicates that the overall mean is a better predictor of the response than the current model (Stat-Ease 2010). **Figure 134** shows the effect of varying the high shear homogenizing speed and the wax-to-surfactant ratio on the particle size.

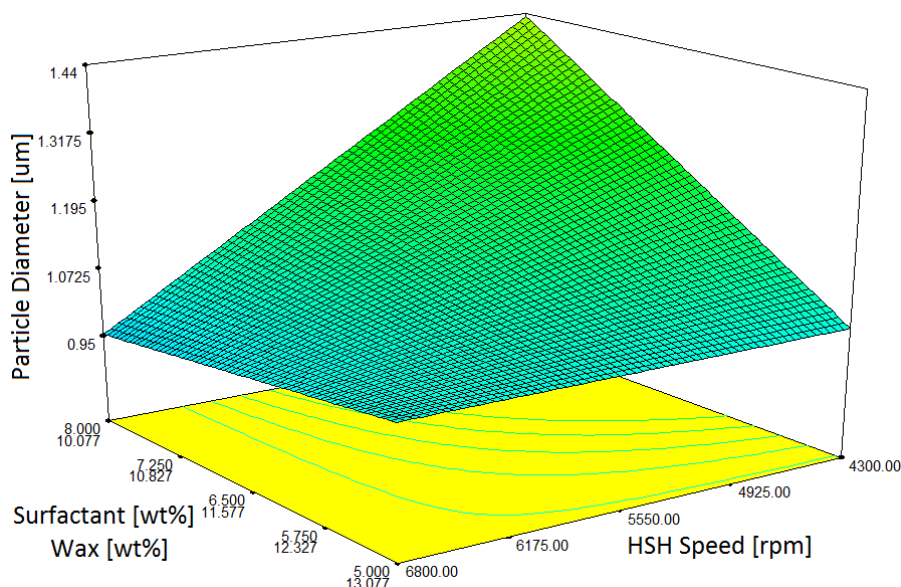


Figure 134 - Area Median Particle Size Model V1 (Screening Experimental Design) - Particle Size vs. Wax-to-Surfactant Ratio vs. High Shear Homogenizing Speed

One can see from **Figure 134** that at a favourable low wax-to-surfactant ratio the particle size decreases with an increase in the high shear homogenizing speed. This trend is in agreement with the findings of McClements, who concluded that an increase in the intensity or duration of the energy input (stirring speed or high shear homogenizing speed) of an emulsification system results in a decrease in particle size (McClements 2010). It is also noted that the high shear homogenizing

speed has no effect on the particle size at a high wax-to-surfactant ratio. This could possibly be due to the emulsions not inverting at high wax-to-surfactant ratios. Thus, being a water-in-wax emulsion, the speed of the high shear homogenizer will not have an effect on the particle size. **Figure 135** shows the effect of varying the wax-to-surfactant ratio on the particle size in more detail (Process Conditions: Stirring Speed = 1150 rpm, High Shear Homogenizing Speed = 5550 rpm, HS Time Interval = 25 mins, Cooling Rate = 0, Inverting Phase AR = 3.5 l/h, Temperature = 110°C).

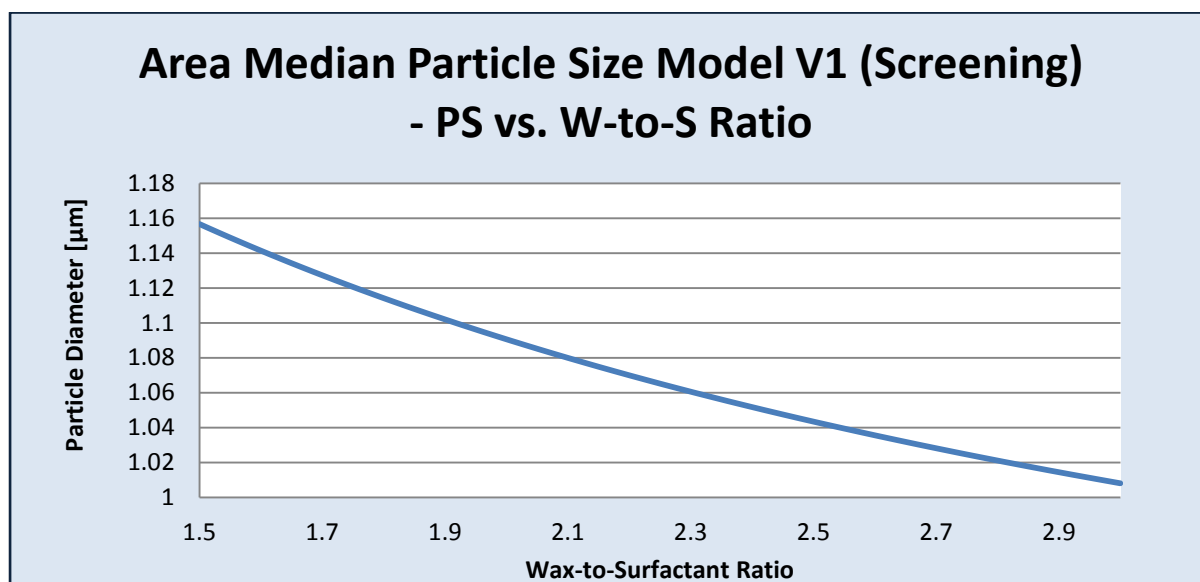


Figure 135 - Area Median Particle Size Model V1 (Screening Experimental Design) - Particle Size vs. Wax-to-Surfactant Ratio

The trend in **Figure 135** is contradicting to findings obtained with the **Volume Mean Particle Size Model V1 (Screening)** and the **Volume Median Particle Size Model V1 (Screening)** which were in agreement with the findings of Gusman, Liu et al., Pey et al. and Sadurni et al. (Pey et al. 2006, Liu et al. 2006, Gusman 1947, Sadurni et al. 2005). However, it is similar to the trend obtained with the **Area Mean Particle Size Model V1 (Screening)**, which was also contradicting to the findings of Gusman, Liu et al., Pey et al. and Sadurni et al. (Pey et al. 2006, Liu et al. 2006, Gusman 1947, Sadurni et al. 2005). A possible explanation could be that the model contains outlier points affecting its accuracy. The effect of varying the inverting phase addition rate on the particle size is presented in **Figure 136**.

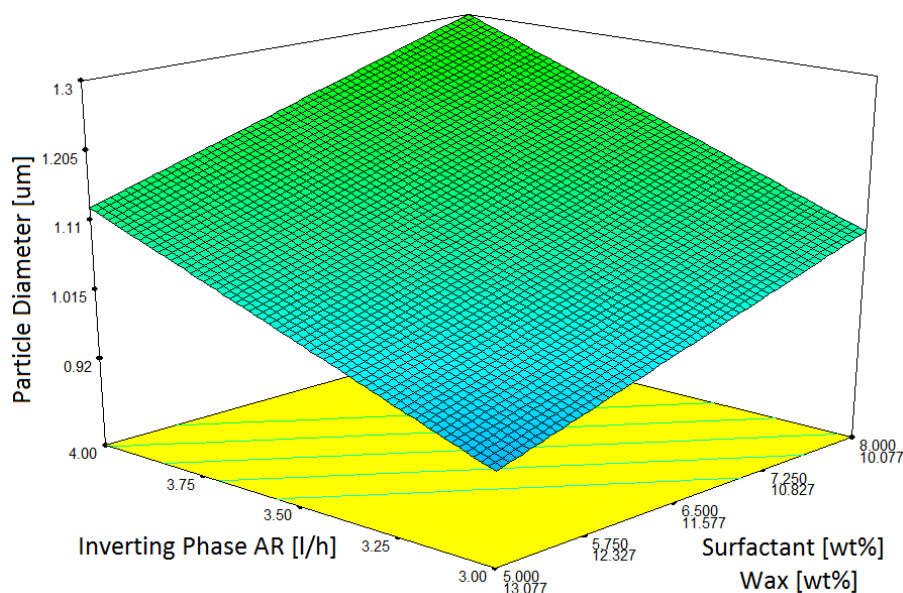


Figure 136 - Area Median Particle Size Model V1 (Screening Experimental Design) - Particle Size vs. Wax-to-Surfactant Ratio vs. Inverting Phase Addition Rate

From **Figure 136** one can see that the particle size decreases with a decrease in the inverting phase addition rate. This trend is in agreement with Gutierrez et al., Pey et al., Wang et al. and Lashmar et al.'s findings (Gutiérrez et al. 2008, Pey et al. 2006, Wang et al. 2007, Lashmar, Richardson & Erbod 1995). One can also see that the particle size decreases with an increase in the wax-to-surfactant ratio. This is contradicting to the findings of Gusman, Liu et al., Pey et al. and Sadurni et al. (Pey et al. 2006, Liu et al. 2006, Gusman 1947, Sadurní et al. 2005). That said, it should be kept in mind that the **Area Median Particle Size Model V1 (Screening)** is not statistically significant ($p > 0.05$) and all the findings should be interpreted with caution. The actual versus the predicted values of the **Area Median Particle Size Model V1 (Screening)** is presented in **Figure 137**.

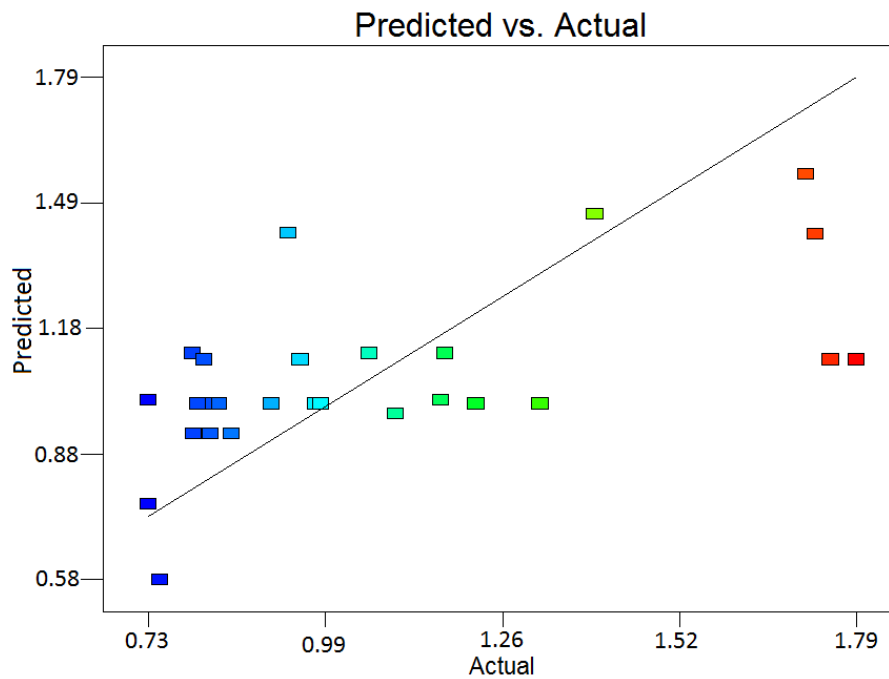


Figure 137 - Area Median Particle Size Model V1 (Screening Experimental Design) - Predicted vs. Actual

From **Figure 137** it is clear that the **Area Median Particle Size Model V1 (Screening)** does not predict the particle size values very accurately. This is expected since the model is not statistically significant ($p > 0.05$). As a result, the **Area Median Particle Size Model V1 (Screening)** will not be considered for optimization purposes. When examining **Figure 137** it is noted that there are two distinct outlier points (red markers). It is possible that these two outlier points could be causing the model to be statistically insignificant.

Area Median Particle Size Model V2 (Screening Experimental Design)

The two outlier points (*EXP S23* and *EXP S24*) were excluded from the data set and a reduced quadratic model was refitted to the rearranged data and is presented in the ANOVA **Table 90** (validation for the ANOVA assumptions is presented in **Appendix E**).

Table 90 - Area Median Particle Size (Reduced Quadratic Model)

| Analysis of Variance Table – Area Median Particle Size (Reduced Quadratic Model) | | | | | | |
|--|----------------|----|-------------|---------|----------|-----------------|
| Source | Sum of Squares | df | Mean Square | F Value | p-value | |
| Model | 1.710 | 10 | 0.171 | 11.012 | < 0.0001 | significant |
| <i>%Surfactant * Stirring Speed</i> | 0.168 | 1 | 0.168 | 10.838 | 0.0049 | |
| <i>%Surfactant * HSH Speed</i> | 0.219 | 1 | 0.219 | 14.099 | 0.0019 | |
| <i>%Surfactant * Cooling Rate</i> | 0.066 | 1 | 0.066 | 4.232 | 0.0575 | |
| <i>%Wax * HSH Speed</i> | 0.084 | 1 | 0.084 | 5.381 | 0.0349 | |
| <i>%Wax * HS Time</i> | 0.180 | 1 | 0.180 | 11.577 | 0.0039 | |
| <i>%Water * Stirring Speed</i> | 0.340 | 1 | 0.340 | 21.860 | 0.0003 | |
| <i>%Water * Inverting Phase</i> | 0.334 | 1 | 0.334 | 21.515 | 0.0003 | |
| <i>AR</i> | | | | | | |
| <i>%Water * Temperature</i> | 0.273 | 1 | 0.273 | 17.591 | 0.0008 | |
| Residual | 0.233 | 15 | 0.016 | | | |
| Lack of Fit | 0.131 | 12 | 0.011 | 0.321 | 0.9333 | not significant |
| Pure Error | 0.102 | 3 | 0.034 | | | |
| Cor Total | 1.943 | 25 | | | | |
| Adeq Precision | 11.794 | | | | | |

Removing the two outlier points from the area median particle size data set had a significant effect on the quadratic model that was fitted, as seen in **Table 90**. The p-value of the **Area Median Particle Size Model V2 (Screening)** (0.0001) is significantly less than the p-value of the **Area Median Particle Size Model V1 (Screening)** (0.0619) which was not statistically significant. The R-squared values for the **Area Median Particle Size Model V2 (Screening)** are as follow:

| Model | R-Squared | Adj R-Squared | Pred R-Squared |
|---|-----------|---------------|----------------|
| Area Median Particle Size Model V2 | 0.8801 | 0.8002 | 0.6688 |

From the R-squared values it is possible to see that the predicted R-squared value is much larger for the newly fitted model without the two outlier points than the previous model. The predicted R-squared value is within the 0.2 “reasonable agreement” range and can be used to

navigate the design space. For this reason the model will be investigated. The final **Area Median Particle Size Model V2 (Screening)** equation in terms of the actual components and actual factors are as follow:

$$\begin{aligned}
 \text{Particle Size } [\mu\text{m}] = & -0.091338 \times \% \text{Surfactant} \\
 & -0.18362 \times \% \text{Wax} \\
 & +0.055067 \times \% \text{Water} \\
 & +2.50507 \times 10^{-4} \times \% \text{Surfactant} \times \text{Stirring Speed} \\
 & -4.31746 \times 10^{-5} \times \% \text{Surfactant} \times \text{HSH Speed} \\
 & -2.20371 \times 10^{-4} \times \% \text{Surfactant} \times \text{HS Time} \\
 & +0.030677 \times \% \text{Surfactant} \times \text{Cooling Rate} \\
 & -0.075578 \times \% \text{Surfactant} \times \text{Inverting Phase AR} \\
 & +3.33546 \times 10^{-3} \times \% \text{Surfactant} \times \text{Temperature} \\
 & +1.03109 \times 10^{-4} \times \% \text{Wax} \times \text{Stirring Speed} \\
 & -1.39796 \times 10^{-5} \times \% \text{Wax} \times \text{HSH Speed} \\
 & +1.98334 \times 10^{-3} \% \text{Wax} \times \text{HS Time} \\
 & -1.6146 \times 10^{-3} \times \% \text{Wax} \times \text{Cooling Rate} \\
 & -0.075578 \times \% \text{Wax} \times \text{Inverting Phase AR} \\
 & +3.33546 \times 10^{-3} \times \% \text{Wax} \times \text{Temperature} \\
 & -3.49897 \times 10^{-5} \times \% \text{Water} \times \text{Stirring Speed} \\
 & +4.18434 \times 10^{-6} \times \% \text{Water} \times \text{HSH Speed} \\
 & -2.20371 \times 10^{-4} \times \% \text{Water} \times \text{HS Time} \\
 & -1.6146 \times 10^{-3} \times \% \text{Water} \times \text{Cooling Rate} \\
 & +0.018894 \times \% \text{Water} \times \text{Inverting Phase AR}
 \end{aligned}$$

$$-8.33864 \times 10^{-4} \times \%Water \times Temperature$$

It is noted that the refitted **Area Median Particle Size Model V2 (Screening)** includes all of the mixture- and process variables. The statistically significant model terms will be briefly discussed.

Figure 138 shows the effect of varying the stirring speed on the particle size.

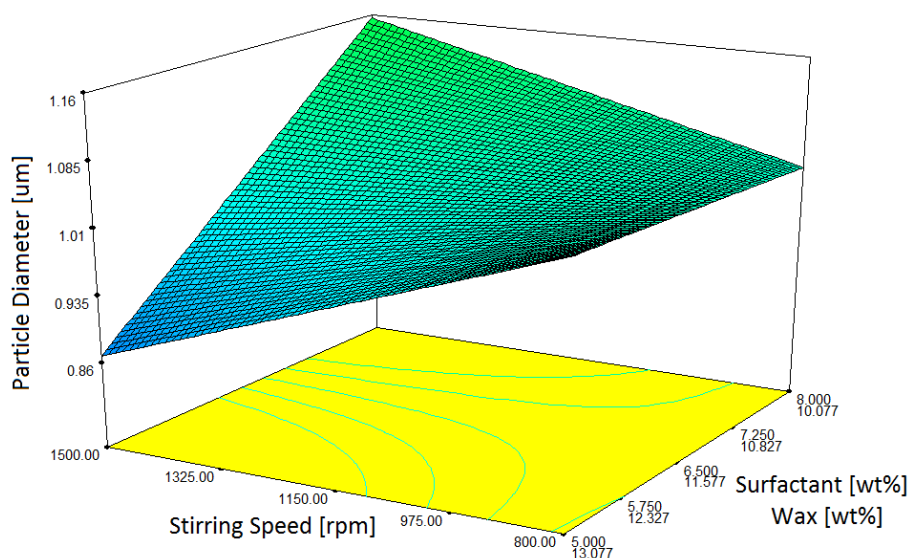


Figure 138 - Area Median Particle Size Model V2 (Screening Experimental Design) - Particle Size vs. Wax-to-Surfactant Ratio vs. HS Time Interval

From **Figure 138** it is noted that that at a high wax-to-surfactant ratio the particle size decreases with an increase in the stirring speed. This trend is in agreement with the findings of McClements, Chen et al., Gusman and Sadurni et al. (Gusman 1947, McClements 2010, Sadurní et al. 2005, Chen, Tao 2005). However at a favourable low wax-to-surfactant ratio the particle size increases with an increase in the stirring speed. This is contradicting to the trend obtained at a high wax-to-surfactant ratio. The effect of varying the high shear homogenizing speed on the particle size is presented in **Figure 139**.

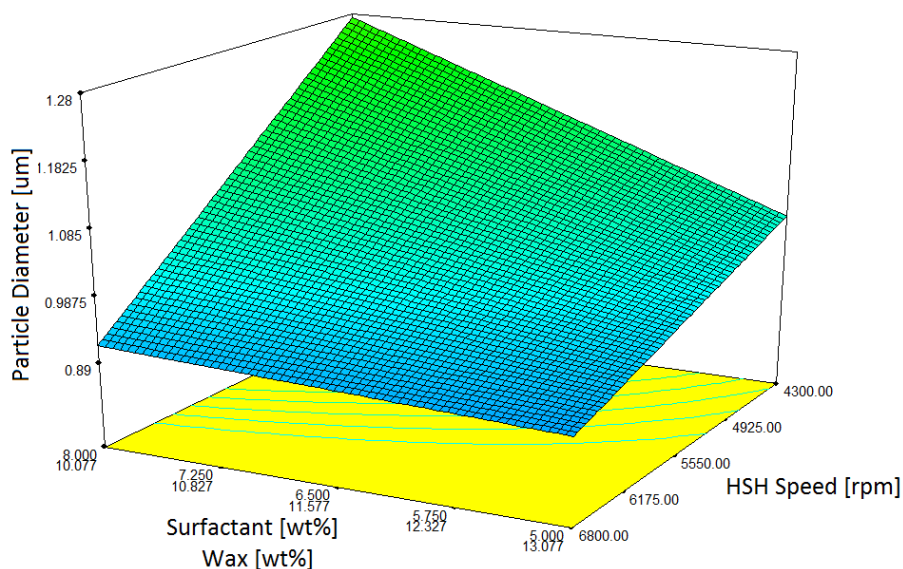


Figure 139 - Area Median Particle Size Model V2 (Screening Experimental Design) - Particle Size vs. Wax-to-Surfactant Ratio vs. High Shear Homogenizing Speed

By examining **Figure 139** one can clearly see that the particle size decreases with an increase in the high shear homogenizing speed, irrespectively of the wax-to-surfactant ratio. This is expected since an increase in the high shear homogenising speed is an increase in the energy input which should result in an increase in droplet breakup. McClements supports this finding with his conclusion that an increase in the intensity or duration of the energy input (stirring speed or high shear homogenizing speed) of an emulsification system results in a decrease in particle size (McClements 2010). Chen et al. also found that more efficient agitation gives better emulsions, i.e. a decrease in the average particle size (Chen, Tao 2005). **Figure 140** shows the change in particle size with varying high shear time interval.

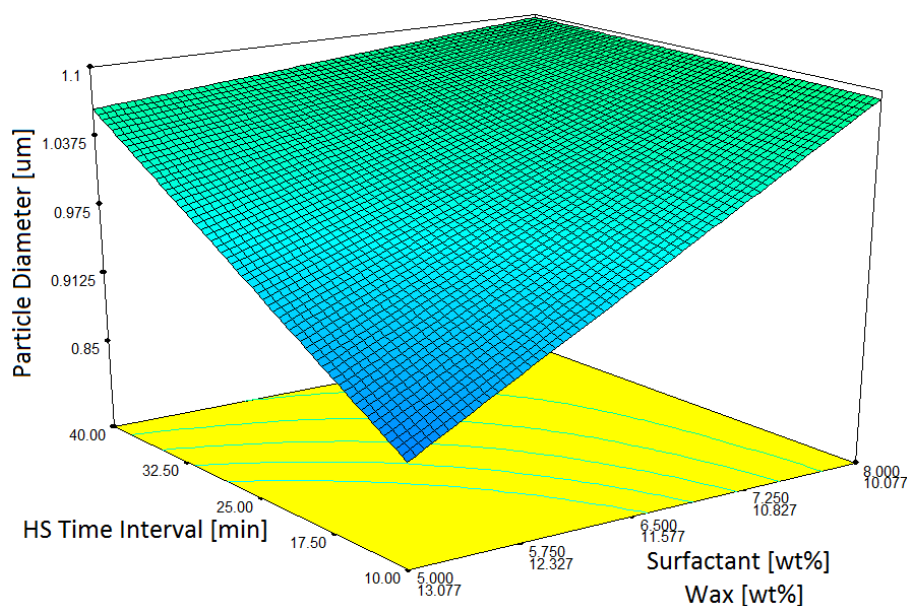


Figure 140 - Area Median Particle Size Model V2 (Screening Experimental Design) - Particle Size vs. Wax-to-Surfactant Ratio vs. HS Time Interval

From **Figure 140** one can see that the particle size decreases with a decrease in the high shear time interval, regardless of the wax-to-surfactant ratio. McClements stated in his study on nano-emulsions that the particle size could be reduced by increasing the intensity or duration of homogenization (McClements 2010). Adler-Nissen et al. agreed with McClement's conclusion in that there must be enough time given for a stable interface to form around the drop during emulsification processes (Adler-Nissen, Mason & Jacobsen 2004). Lashma et al. supported both McClements and Adler-Nissen et al.'s findings (Lashmar, Beesley 1993). However, the trend in **Figure 140** is clearly contradicting to what McClements, Adler-Nissen et al. and Lashmaer et al. obtained during their studies.

A possible explanation could be that at long high shear time intervals coalescence is occurring while only breaking is occurring during the shorter high shear time intervals. This is supported by Guitierrez et al. who states in their study on nano-emulsions, that an optimum shear or shearing time can exist if breaking and coalescence are competing phenomena during the emulsification process (Gutiérrez et al. 2008). Chen et al. states in their study on oil-water emulsions that the emulsifier becomes more effective with increased mixing time (Chen, Tao 2005). In addition they also add that if the mixing time is too long that the effectiveness of the emulsifier will decrease due to the intense stirring causing the emulsifier to drop out from the oil-water interface (Chen, Tao 2005). This supports Guitierrez et al.'s findings. However at a favourable low wax-to-surfactant ratio the high shear time interval seems to have a marginal effect on the particle size. The effect of varying the inverting phase addition rate on the particle size is presented in **Figure 141**.

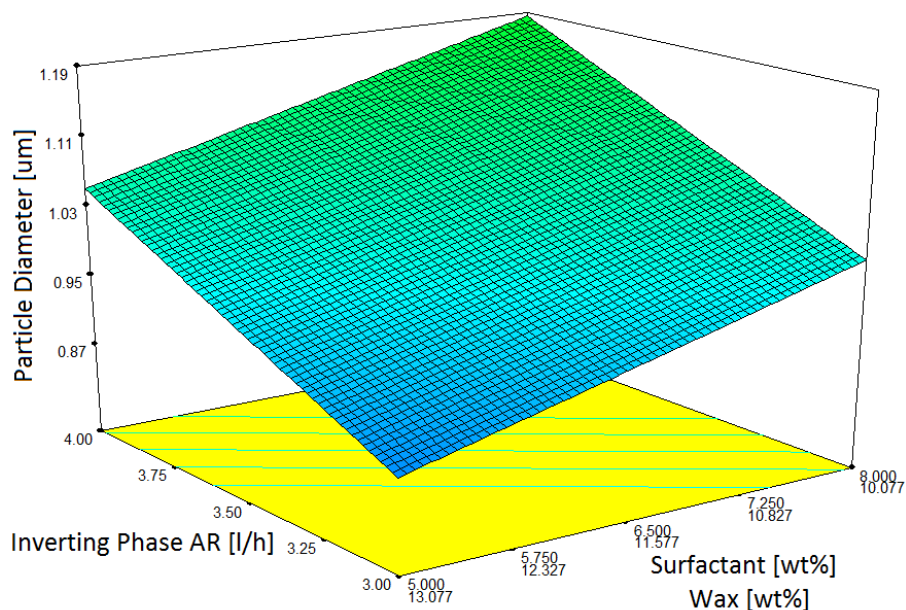


Figure 141 - Area Median Particle Size Model V2 (Screening Experimental Design) - Particle Size vs. Wax-to-Surfactant Ratio vs. Inverting Phase Addition Rate

By examining **Figure 141** one can see that the particle size decreases with a decrease in the inverting phase addition rate, irrespective of the wax-to-surfactant ratio. This trend is in agreement with Gutierrez et al., Pey et al., Wang et al. and Lashmar et al.'s findings. Gutierrez et al. investigated various authors' studies on the addition rate of the inverting phase (usually water) during emulsification processes (Gutiérrez et al. 2008, Pey et al. 2006, Wang et al. 2007, Uson, Garcia & Solans 2004).

Figure 142 shows the effect of varying the temperature on the particle size.

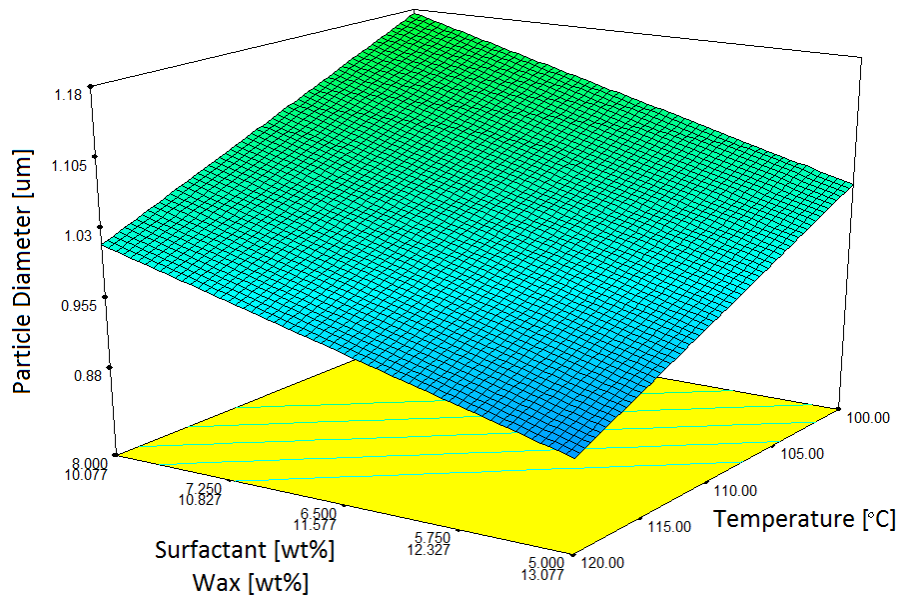


Figure 142 - Area Median Particle Size Model V2 (Screening Experimental Design) - Particle Size vs. Wax-to-Surfactant Ratio vs. Temperature

From **Figure 142** one can see that the particle size decreases with an increase in the emulsification temperature, regardless of the wax-to-surfactant ratio. This trend is in agreement with the findings of Lashmar et al., Li et al., Bornfriend and Jass (Li et al. 2010, Lashmar, Richardson & Erbod 1995, Jass 1967, Bornfriend 1978). They concluded that the particle size decreases with an increase in the emulsification temperature (Li et al. 2010, Lashmar, Richardson & Erbod 1995, Jass 1967, Bornfriend 1978).

The accuracy of the **Area Median Particle Size Model V2 (Screening)** is represented by the actual values versus the predicted values presented in **Figure 143**.

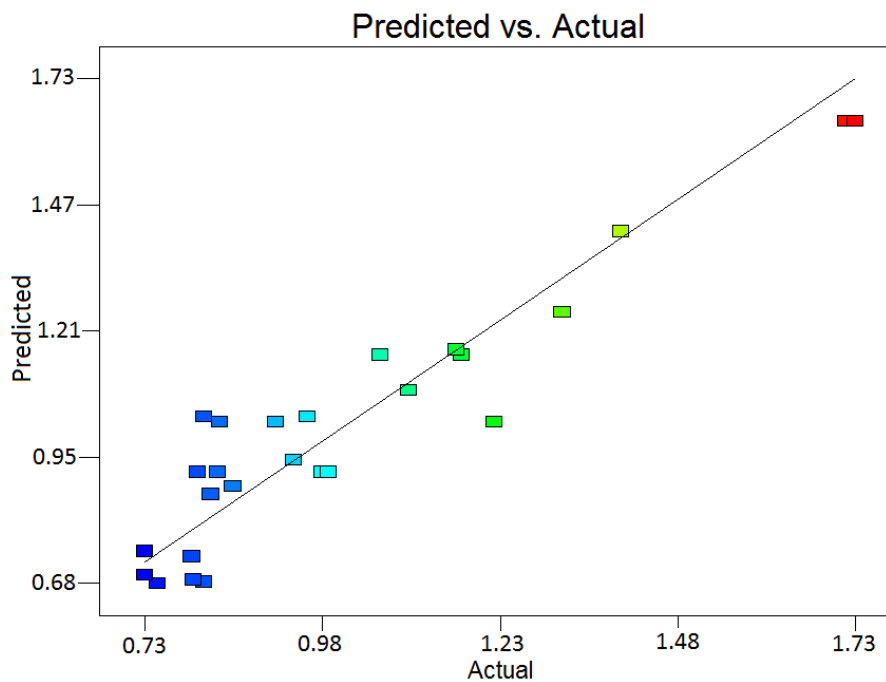


Figure 143 - Area Median Particle Size Model V2 (Screening Experimental Design) - Predicted vs. Actual

When comparing **Figure 137** with **Figure 143** it is seen that the actual values in **Figure 143** are much more concentrated around the model line. This clearly indicates and proves that the **Area Median Particle Size Model V2 (Screening)** is a more accurate representation of the area median particle size data than the **Area Median Particle Size Model V1 (Screening)**.

Number Distribution

The number particle size data, as with the area particle size data, were calculated from the observed scattering of the laser through the sample medium by means of mathematical models (**Section 5.3.1.1**). The number particle size data were collected from the Saturn DigiSizer 5200 Particle Sizer (Micrometrics, UK) for further processing.

Number Mean Particle Size

Number Mean Particle Size Model V1 (Screening Experimental Design)

The number mean particle sizes are within the order of magnitude (0.4 – 0.7 μm) recorded by Gusman et al. in their study on Carnauba wax emulsions, as seen in the visual representation in **Figure 144**.

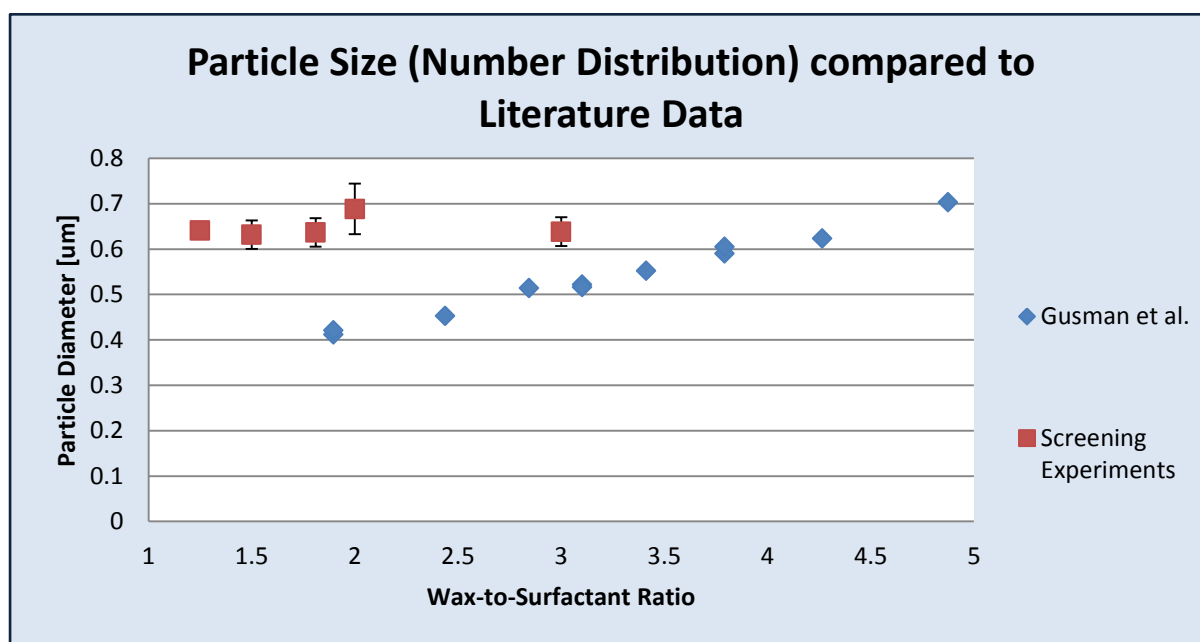


Figure 144 - Particle Size compared to Literature Data

The Screening experimental design was originally set up as a linear model for the both the mixture and process variables. An additional three centre points were added to the experimental design to ensure that any curvature will be identified if the models are not linear. Once the data were analysed with Design Expert®, it was noted that a linear model was not statistically significant ($p > 0.05$) to the number mean particle size data, as seen in the ANOVA **Table 91** (validation for the ANOVA assumptions is presented in **Appendix E**).

Table 91 - Number Mean Particle Size (Linear Model) ANOVA

| Analysis of Variance Table - Number Mean Particle Size (Linear Model) | | | | | | |
|---|----------------|----|-------------|---------|---------|-----------------|
| Source | Sum of Squares | df | Mean Square | F Value | p-value | |
| Model | 0.0022 | 2 | 0.0011 | 0.6238 | 0.5441 | not significant |
| Linear Mixture | 0.0022 | 2 | 0.0011 | 0.6238 | 0.5441 | |
| Residual | 0.0445 | 25 | 0.0018 | | | |
| Lack of Fit | 0.0281 | 20 | 0.0014 | 0.4278 | 0.9203 | not significant |
| Pure Error | 0.0164 | 5 | 0.0033 | | | |
| Cor Total | 0.0467 | 27 | | | | |
| Adeq Precision | 1.628 | | | | | |

A reduced quadratic model was fitted to the particle size data. In addition a model reduction was performed to eliminate the insignificant terms. The ANOVA table for the reduced quadratic model can be seen in **Table 92**.

Table 92 - Number Mean Particle Size (Reduced Quadratic Model) ANOVA

| Analysis of Variance Table – Number Mean Particle Size (Reduced Quadratic Model) | | | | | | |
|--|----------------|----|-------------|---------|---------|-----------------|
| Source | Sum of Squares | df | Mean Square | F Value | p-value | |
| Model | 0.0230 | 7 | 0.0033 | 2.780 | 0.0343 | significant |
| <i>%Surfactant * %Wax</i> | 0.0049 | 1 | 0.0049 | 4.149 | 0.0551 | |
| <i>%Surfactant * %Water</i> | 0.0092 | 1 | 0.0092 | 7.791 | 0.0113 | |
| <i>%Surfactant * Cooling Rate</i> | 0.0047 | 1 | 0.0047 | 3.940 | 0.0610 | |
| <i>%Water * HSH Speed</i> | 0.0040 | 1 | 0.0040 | 3.345 | 0.0824 | |
| <i>%Water * Temperature</i> | 0.0052 | 1 | 0.0052 | 4.420 | 0.0484 | |
| Residual | 0.0237 | 20 | 0.0012 | | | |
| Lack of Fit | 0.0073 | 15 | 0.0005 | 0.148 | 0.9983 | not significant |
| Pure Error | 0.0164 | 5 | 0.0033 | | | |
| Cor Total | 0.0467 | 27 | | | | |
| Adeq Precision | 6.438 | | | | | |

When examining **Table 92**, it is possible to see that the new reduced quadratic model is statistically significant ($p < 0.05$) and thus a better model than the linear model. There is only a 3.43 % chance that a Model F-Value this large (2.78) could occur due to noise. For the **Number Particle Size Model V1 (Screening) (Table 92)** *%Surfactant*%Water* and *%Water*Temperature* are significant model terms. That said *%Surfactant*%Wax*, *%Surfactant*Cooling Rate* and *%Water*HSH Speed* will also be included in the model, due to their P-values being less than 0.1. An adequate

precision value of 6.438 indicates an acceptable signal. This also indicates that the model can be used to navigate the design space (Stat-Ease 2010). The final **Number Mean Particle Size Model V1 (Screening)** equation in terms of the actual components and actual factors are as follow:

$$\begin{aligned}
 \text{Particle Size } [\mu\text{m}] = & -1.91 \times \% \text{Surfactant} \\
 & +8.928 \times 10^{-3} \times \% \text{Wax} \\
 & -2.935 \times 10^{-3} \times \% \text{Water} \\
 & +0.0195 \times \% \text{Surfactant} \times \% \text{Wax} \\
 & +0.0224 \times \% \text{Surfactant} \times \% \text{Water} \\
 & +1.585 \times 10^{-3} \times \% \text{Surfactant} \times \text{Cooling Rate} \\
 & -1.411 \times 10^{-7} \times \% \text{Water} \times \text{HSH Speed} \\
 & -6.993 \times 10^{-6} \times \% \text{Water} \times \text{Temperature}
 \end{aligned}$$

From the final equation it is noted that the composition variables have a significant influence on the particle size. This is expected since the amount of surfactant determines the total interfacial area and thus the particle size and emulsion stability (Li et al. 2010). The R-squared values for the **Number Mean Particle Size Model V1 (Screening)** are as follow:

| Model | R-Squared | Adj R-Squared | Pred R-Squared |
|------------------------------------|-----------|---------------|----------------|
| Number Mean Particle Size Model V1 | 0.4931 | 0.3157 | -0.0352 |

From the R-squared values it is noted that the predicted R-squared value is negative. This indicates that the overall mean is a better predictor of the response than the current model (Stat-Ease 2010). The effect of varying the temperature on the particle size is presented in **Figure 145**.

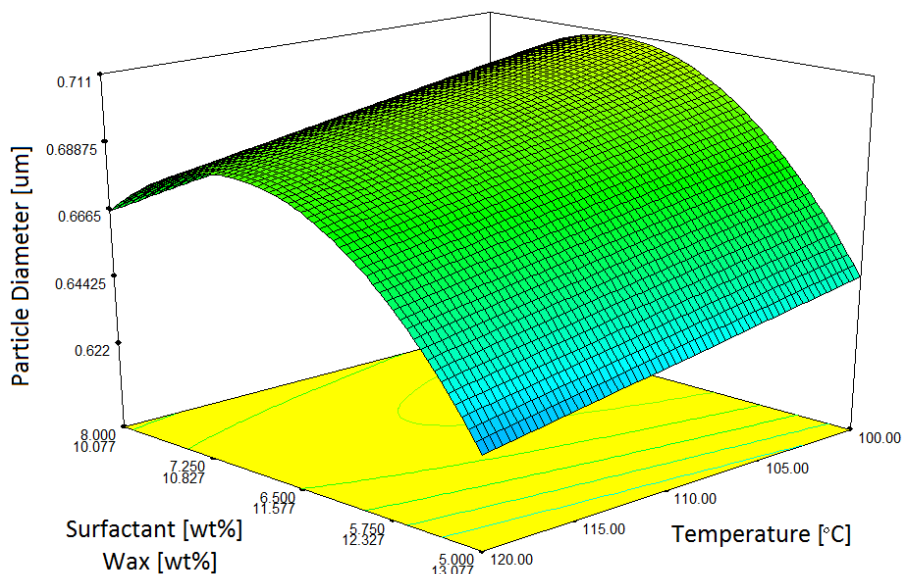


Figure 145 - Number Mean Particle Size Model V1 (Screening Experimental Design) - Particle Size vs. Wax-to-Surfactant Ratio vs. Temperature

From **Figure 145** it is possible to see that the particle size decreases with an increase in the emulsification temperature. This trend is in agreement with the findings of Lashmar et al., Li et al., Bornfreund and Jass (Li et al. 2010, Lashmar, Richardson & Erbod 1995, Jass 1967, Bornfreund 1978). They concluded that the particle size decreases with an increase in the temperature (Li et al. 2010, Lashmar, Richardson & Erbod 1995, Jass 1967, Bornfreund 1978). **Figure 146** shows the effect of varying the wax-to-surfactant ratio on the particle size in more detail (Process Conditions: Stirring Speed = 1150 rpm, High Shear Homogenizing Speed = 5550 rpm, HS Time Interval = 25 mins, Cooling Rate = 0, Inverting Phase AR = 3.5 l/h, Temperature = 110°C).

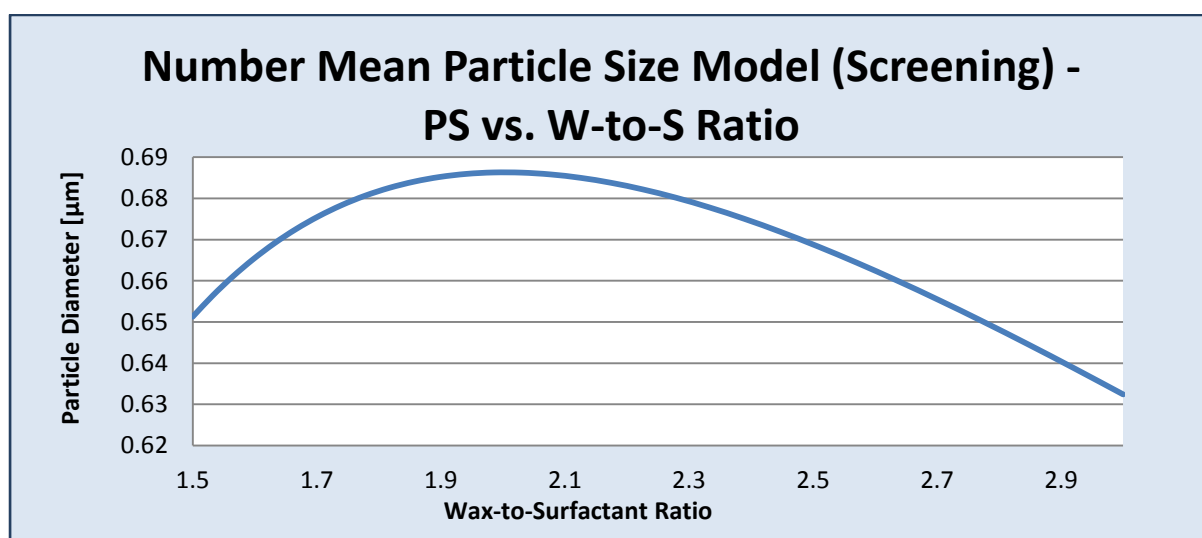


Figure 146 - Number Mean Particle Size Model V1 (Screening Experimental Design) - Particle Size vs. Wax-to-Surfactant Ratio

The trend observed in **Figure 146** deviates from the previously observed trends. It is noted that the particle size increases from a wax-to-surfactant ratio of 1.5 – 2 and decreases from a wax-to-surfactant ratio of 2 – 3. Thus, the favourable low wax-to-surfactant ratio range of 1.5 – 2 is in agreement with the findings of Gusman, Liu et al., Pey et al. and Sadurni et al. who found that the average particle size increases with an increase in the wax-to-surfactant ratio (Pey et al. 2006, Liu et al. 2006, Gusman 1947, Sadurní et al. 2005). However, the trend obtained with a wax-to-surfactant ratio of between 2 – 3 is contradicting to the findings of Gusman, Liu et al., Pey et al., Sadurni et al., McClements and Chen et al. (Pey et al. 2006, Liu et al. 2006, Gusman 1947, McClements 2010, Sadurní et al. 2005, Chen, Tao 2005). This contradicting trend could be as a result of outlier points affecting the accuracy of the model. The accuracy of the **Number Mean Particle Size Model V1 (Screening)** is represented by a plot of the actual values versus the predicted values, as seen in **Figure 147**.

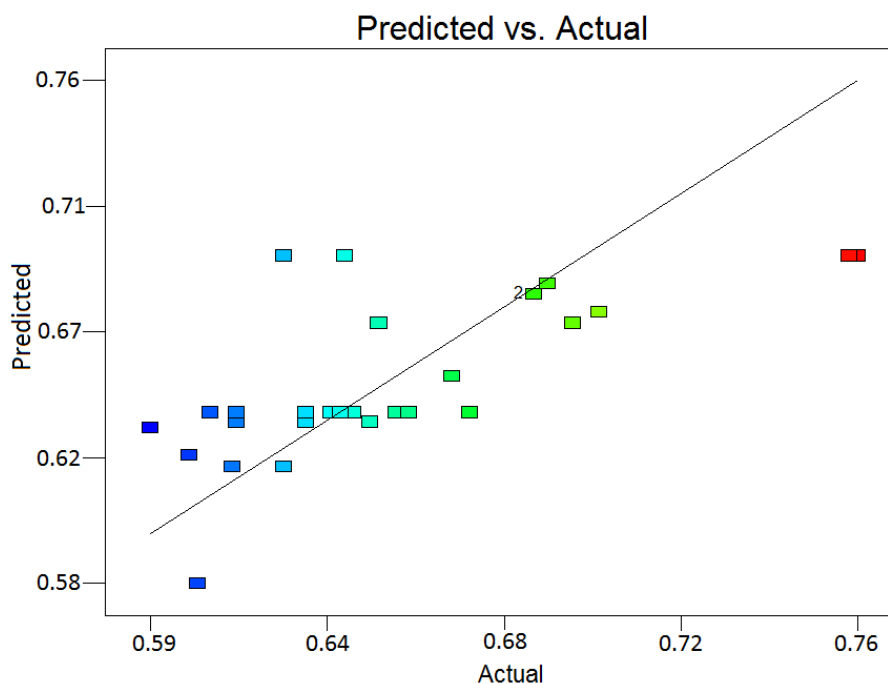


Figure 147 - Number Mean Particle Size Model V1 (Screening Experimental Design) – Predicted vs. Actual

By examining **Figure 147** it is clearly noted that there are two outlier points (red markers) in the **Number Mean Particle Size Model V1 (Screening)** that could be affecting the accuracy of the model. The two outlier points were excluded from the number particle size data set and the model was refitted.

Number Mean Particle Size Model V2 (Screening Experimental Design)

The two outlier points (*EXP S23* and *EXP S24*) were excluded and a reduced quadratic model was refitted to the rearranged data set and is presented in the ANOVA **Table 93**.

Table 93 - Number Mean Particle Size (Reduced Quadratic Model) ANOVA

| Analysis of Variance Table – Number Mean Particle Size (Reduced Quadratic Model) | | | | | | |
|--|----------------|----|-------------|---------|---------|-----------------|
| Source | Sum of Squares | df | Mean Square | F Value | p-value | |
| Model | 0.0203 | 14 | 0.0015 | 9.170 | 0.0004 | significant |
| <i>%Surfactant * %Wax</i> | 0.0011 | 1 | 0.0011 | 7.058 | 0.0223 | |
| <i>%Surfactant * %Water</i> | 0.0006 | 1 | 0.0006 | 3.657 | 0.0822 | |
| <i>%Surfactant * HSH Speed</i> | 0.0016 | 1 | 0.0016 | 10.411 | 0.0081 | |
| <i>%Surfactant * HS Time</i> | 0.0014 | 1 | 0.0014 | 9.143 | 0.0116 | |
| <i>%Surfactant * Cooling Rate</i> | 0.0041 | 1 | 0.0041 | 25.780 | 0.0004 | |
| <i>%Surfactant * Inverting Phase AR</i> | 0.0008 | 1 | 0.0008 | 5.207 | 0.0434 | |
| <i>%Wax * HSH Speed</i> | 0.0008 | 1 | 0.0008 | 5.198 | 0.0435 | |
| <i>%Wax * HS Time</i> | 0.0013 | 1 | 0.0013 | 8.250 | 0.0152 | |
| <i>%Water * Stirring Speed</i> | 0.0006 | 1 | 0.0006 | 3.485 | 0.0888 | |
| <i>%Water * HSH Speed</i> | 0.0033 | 1 | 0.0033 | 21.170 | 0.0008 | |
| <i>%Water * HS Time</i> | 0.0014 | 1 | 0.0014 | 8.610 | 0.0136 | |
| <i>%Water * Temperature</i> | 0.0049 | 1 | 0.0049 | 30.697 | 0.0002 | |
| Residual | 0.0017 | 11 | 0.0002 | | | |
| Lack of Fit | 0.0010 | 8 | 0.0001 | 0.463 | 0.8290 | not significant |
| Pure Error | 0.0008 | 3 | 0.0002 | | | |
| Cor Total | 0.0220 | 25 | | | | |
| Adeq Precision | 10.227 | | | | | |

From **Table 93** it is noted that by excluding the two outlier points resulted in a significant effect on the model. The **Number Mean Particle Size Model V1 (Screening)** has a p-value of 0.0343 while the newly fitted **Number Mean Particle Size Model V2 (Screening)** has a p-value of 0.0004, indicating that the newly fitted model is statistically more significant than the previous one. The R-squared values for the **Number Mean Particle Size Model V2 (Screening)** are as follow:

| Model | R-Squared | Adj R-Squared | Pred R-Squared |
|------------------------------------|-----------|---------------|----------------|
| Number Mean Particle Size Model V2 | 0.9211 | 0.8206 | 0.6625 |

From the R-squared values it is noted that the predicted R-squared value is much larger for the newly fitted model without the two outlier points than the previous model. The predicted R-squared value is in the 0.2 “reasonable agreement” range from the adjusted R-squared value which indicates that the model can be used to navigate the design space (Stat-Ease 2010). The final **Number Mean Particle Size Model V2 (Screening)** equation in terms of the actual components and actual factors are as follow:

$$\begin{aligned}
 \text{Particle Size } [\mu\text{m}] = & +0.71317 \times \% \text{Surfactant} \\
 & -0.040577 \times \% \text{Wax} \\
 & +0.023399 \times \% \text{Water} \\
 & -0.011278 \times \% \text{Surfactant} \times \% \text{Wax} \\
 & -8.29653 \times 10^{-3} \times \% \text{Surfactant} \times \% \text{Water} \\
 & +4.22927 \times 10^{-6} \times \% \text{Surfactant} \times \text{Stirring Speed} \\
 & -1.17845 \times 10^{-6} \times \% \text{Surfactant} \times \text{HSH Speed} \\
 & -5.01617 \times 10^{-4} \times \% \text{Surfactant} \times \text{HS Time} \\
 & +7.99039 \times 10^{-3} \times \% \text{Surfactant} \times \text{Cooling Rate} \\
 & +7.12546 \times 10^{-3} \times \% \text{Surfactant} \times \text{Inverting Phase AR} \\
 & +4.66088 \times 10^{-4} \times \% \text{Surfactant} \times \text{Temperature} \\
 & +4.22927 \times 10^{-6} \times \% \text{Wax} \times \text{Stirring Speed} \\
 & +1.49496 \times 10^{-6} \times \% \text{Wax} \times \text{HSH Speed} \\
 & +3.36197 \times 10^{-5} \times \% \text{Wax} \times \text{HS Time} \\
 & -4.20547 \times 10^{-4} \times \% \text{Wax} \times \text{Cooling Rate} \\
 & -3.75024 \times 10^{-4} \times \% \text{Wax} \times \text{Inverting Phase AR} \\
 & +4.66088 \times 10^{-4} \times \% \text{Wax} \times \text{Temperature} \\
 & -1.05732 \times 10^{-6} \times \% \text{Water} \times \text{Stirring Speed}
 \end{aligned}$$

$$-3.20213 \times 10^{-7} \times \%Water \times HSH \text{ Speed}$$

$$+3.69714 \times 10^{-5} \times \%Water \times HS \text{ Time}$$

$$-4.20547 \times 10^{-4} \times \%Water \times Cooling \text{ Rate}$$

$$-3.75024 \times 10^{-4} \times \%Water \times Inverting \text{ Phase AR}$$

$$-1.16522 \times 10^{-4} \times \%Water \times Temperature$$

As with the **Area Median Particle Size Model V2 (Screening)** the refitted **Number Mean Particle Size Model V2 (Screening)** also includes all of the mixture- and process variables. Once again only the statistically significant terms will be briefly discussed. The effect of varying the high shear homogenizing speed on the particle size is presented in **Figure 148**.

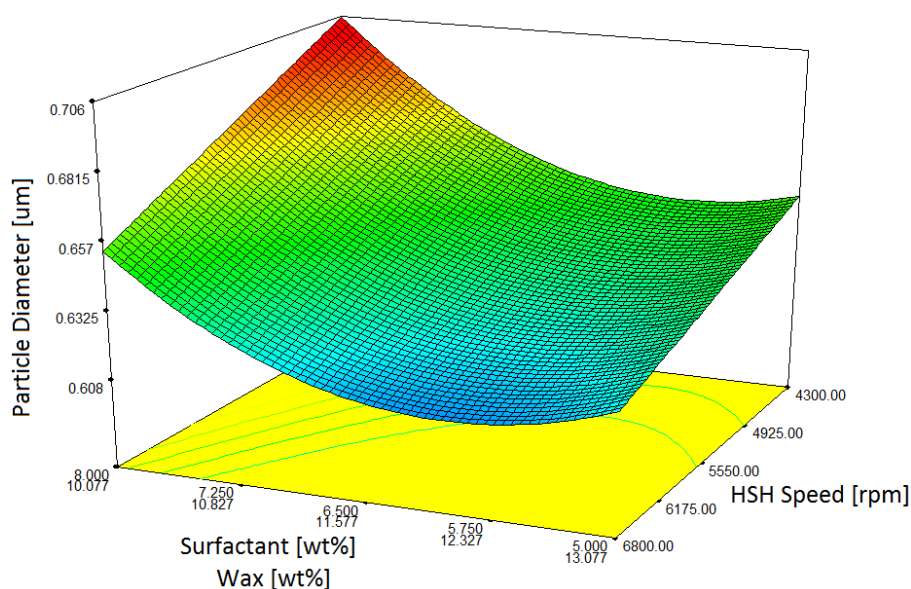


Figure 148 - Number Mean Particle Size Model V2 (Screening Experimental Design) - Particle Size vs. Wax-to-Surfactant Ratio vs. High Shear Homogenizing Speed

From **Figure 148** it is noted that the particle size decreases with an increase in the high shear homogenising speed, irrespective of the wax-to-surfactant ratio. This trend is confirmed by McClements and Chen et al. (McClements 2010, Chen, Tao 2005). Both these authors found that an increase in the energy input in emulsification systems results in a decrease in the average particle size (McClements 2010, Chen, Tao 2005). **Figure 149** shows the effect of varying the cooling rate on the average particle size.

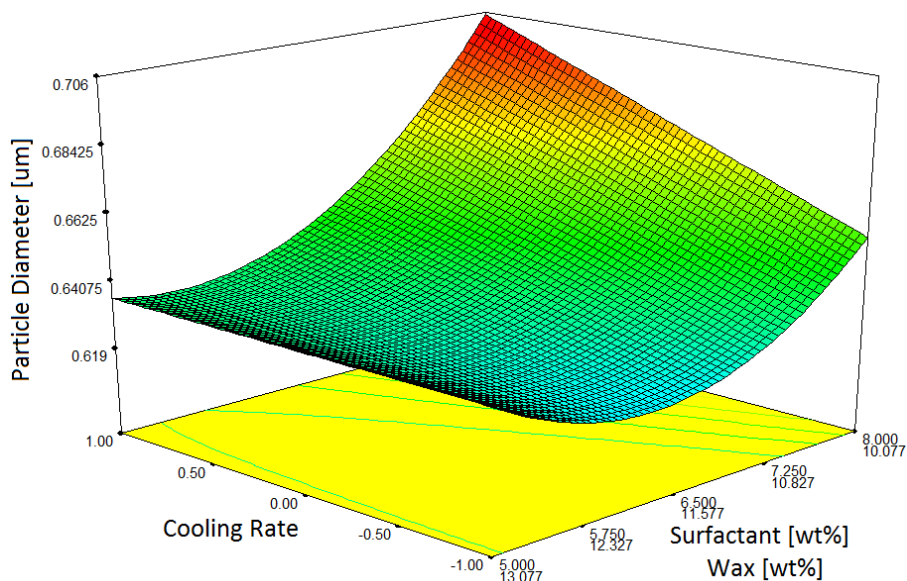


Figure 149 - Number Mean Particle Size Model V2 (Screening Experimental Design) - Particle Size vs. Wax-to-Surfactant Ratio vs. Cooling Rate

From **Figure 149** one can see that at a favourable low wax-to-surfactant ratio the particle size decreases with a decrease in the cooling rate. This trend is in contradiction to the findings of Lashmar et al. who concluded in their study on the correlation of physical parameters of an oil in water emulsion with manufacturing procedures and stability, that the slow cooling of the emulsion appeared to be beneficial to its stability, i.e. reduced the average droplet size (Lashmar, Richardson & Erbod 1995). It is also noted in **Figure 149** that at a high wax-to-surfactant ratio the cooling rate has no effect on the particle size. **Figure 150** shows the effect of varying the high shear time interval on the particle size.

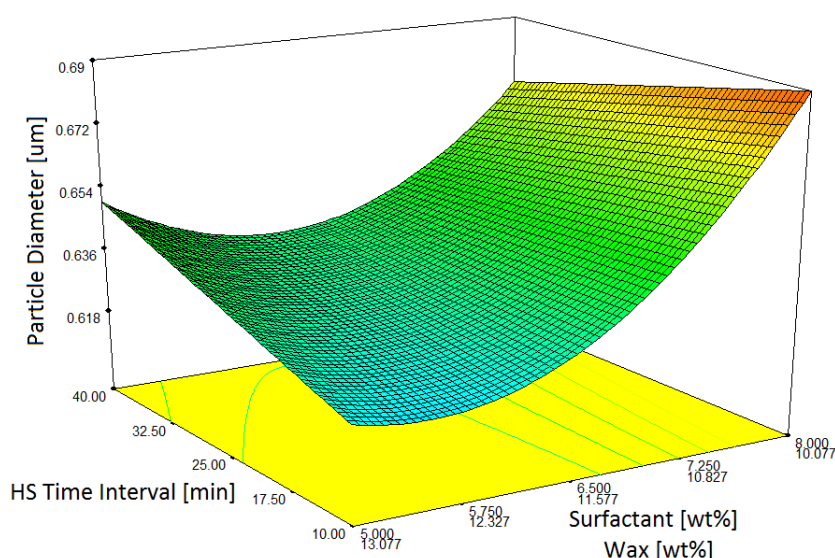


Figure 150 - Number Mean Particle Size Model V2 (Screening Experimental Design) - Particle Size vs. Wax-to-Surfactant Ratio vs. HS Time Interval

At a favourable low wax-to-surfactant ratio the particle size decreases with an increase in the high shear time interval, as seen in **Figure 150**. This trend is in agreement with McClements, Adler-Nissen et al. and Lashmar et al. who found that the particle size of an emulsion can be reduced by increasing the intensity or duration of homogenization (Lashmar, Richardson & Erbod 1995, McClements 2010, Adler-Nissen, Mason & Jacobsen 2004). However, at a high wax-to-surfactant ratio the trend is clearly contradicting to what McClements, Adler-Nissen et al. and Lashmaer et al. obtained during their studies. This could be as a result of the mixing time being too long which causes the effectiveness of the emulsifier to decrease due to the intense stirring causing the emulsifier to drop out from the wax-water interface (Chen, Tao 2005). This finding is also supported by Guitierrez et al. (Gutiérrez et al. 2008). The effect of varying the inverting phase addition rate on the particle size is presented in **Figure 151**.

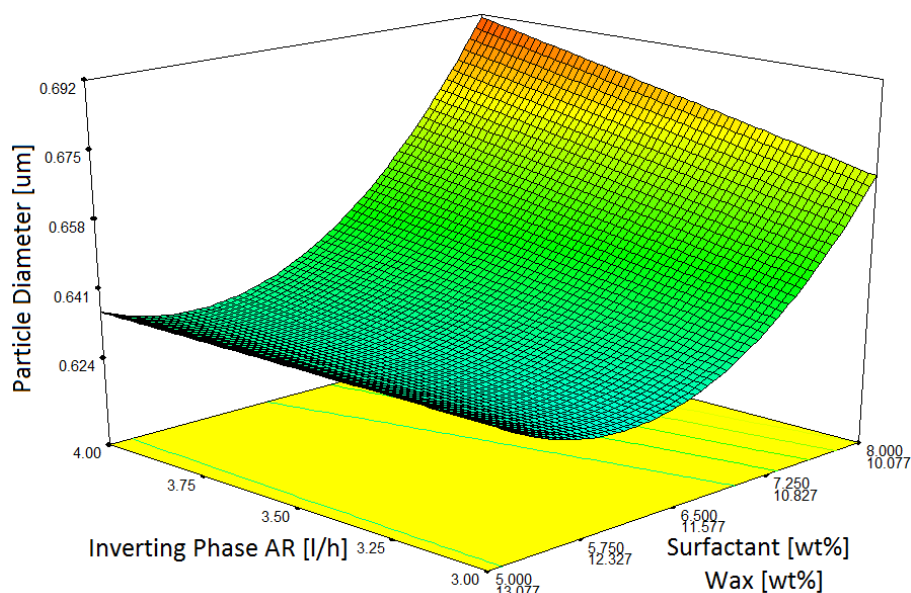


Figure 151 - Number Mean Particle Size Model V2 (Screening Experimental Design) - Particle Size vs. Wax-to-Surfactant Ratio vs. Inverting Phase Addition Rate

From **Figure 151** one can see that at a favourable low wax-to-surfactant ratio the particle size decreases with a decrease in the inverting phase addition rate. This trend is in agreement with Gutierrez et al., Pey et al., Wang et al. and Lashmar et al.'s findings. Gutierrez et al. investigated various authors' studies on the addition rate of the inverting phase (usually water) during emulsification processes (Gutiérrez et al. 2008, Pey et al. 2006, Wang et al. 2007, Uson, Garcia & Solans 2004).

Figure 152 shows the effect of varying the temperature on the particle size.

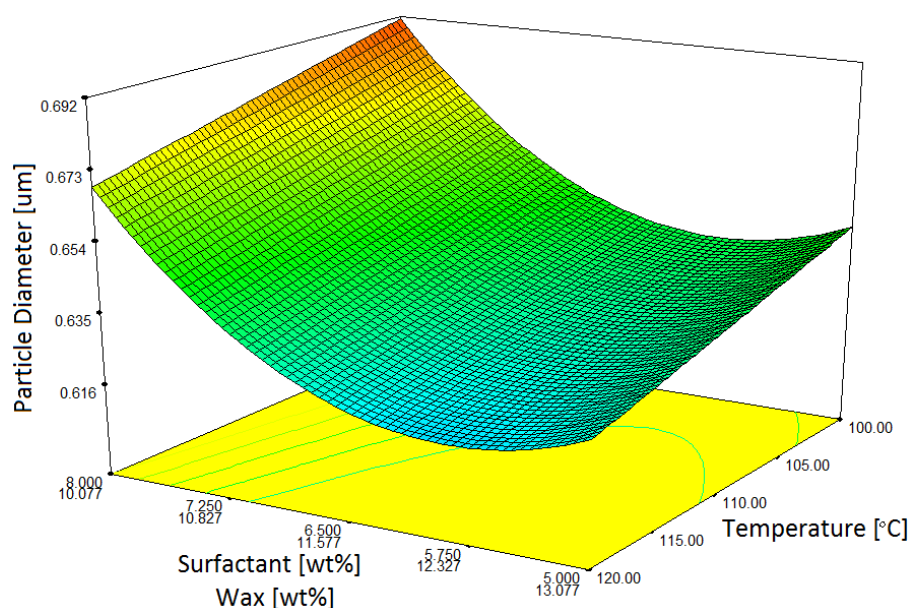


Figure 152 - Number Mean Particle Size (Screening Experimental Design) - Particle Size vs. Wax-to-Surfactant Ratio vs. Temperature

From **Figure 152** it is seen that the particle size decreases with an increase in the emulsification temperature, regardless of the wax-to-surfactant ratio. This trend is in agreement with the findings of Lashmar et al., Li et al., Bornfriend and Jass (Li et al. 2010, Lashmar, Richardson & Erbod 1995, Jass 1967, Bornfriend 1978). They concluded that the particle size decreases with an increase in the emulsification temperature (Li et al. 2010, Lashmar, Richardson & Erbod 1995, Jass 1967, Bornfriend 1978).

The accuracy of the **Number Mean Particle Size Model V2 (Screening)** is represented by the actual values versus the predicted values presented in **Figure 153**.

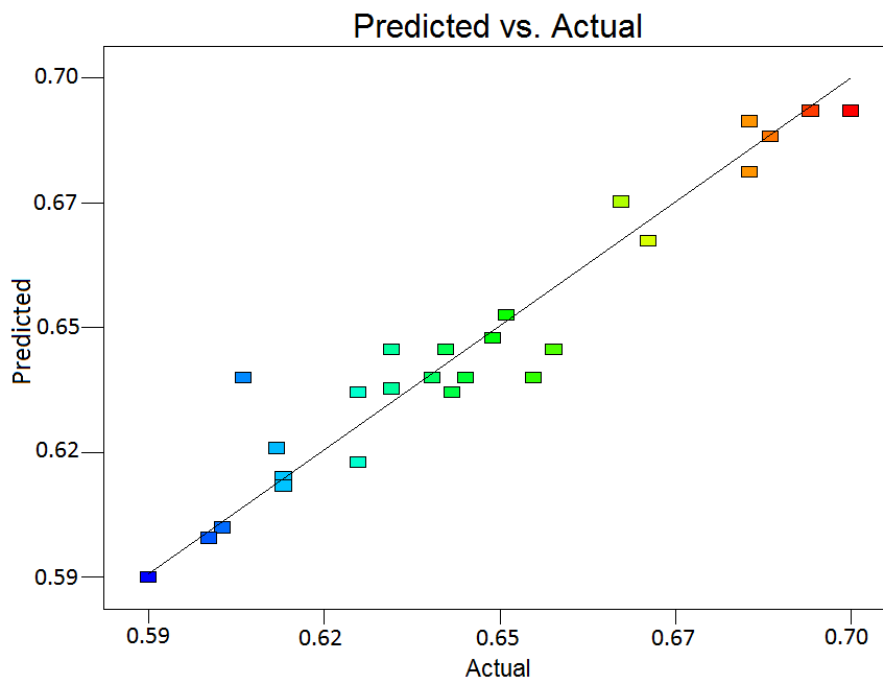


Figure 153 - Number Mean Particle Size Model V2 (Screening Experimental Design) - Predicted vs. Actual

When comparing the previous **Number Mean Particle Size Model V1 (Screening)** (**Figure 147**) with the newly fitted model represented in **Figure 153** it is clear that the actual values are considerably more concentrated around the predicted line. This clearly indicates and proves that the **Number Mean Particle Size Model V2 (Screening)** is a more accurate representation of the area median particle size data than the **Number Mean Particle Size Model V1 (Screening)**.

Number Median Particle Size**Number Median Particle Size Model V1 (Screening Experimental Design)**

The final set of data for the particle size analysis of the Screening experimental stage is the number median particle size data. The data set were analysed by Design Expert© and a statistical model was fitted. From the ANOVA **Table 94** it is clear that the linear model of the original Screening design setup is not statistically significant ($p > 0.05$) to the number median particle size data (validation for the ANOVA assumptions is presented in **Appendix E**).

Table 94 - Number Median Particle Size (Linear Model) ANOVA

| Analysis of Variance Table – Number Median Particle Size (Linear Model) | | | | | | |
|---|----------------|----|-------------|---------|---------|-----------------|
| Source | Sum of Squares | df | Mean Square | F Value | p-value | |
| Model | 0.0005 | 2 | 0.0002 | 0.8456 | 0.4412 | not significant |
| Linear Mixture | 0.0005 | 2 | 0.0002 | 0.8456 | 0.4412 | |
| Residual | 0.0069 | 25 | 0.0003 | | | |
| Lack of Fit | 0.0042 | 20 | 0.0002 | 0.3848 | 0.9426 | not significant |
| Pure Error | 0.0027 | 5 | 0.0005 | | | |
| Cor Total | 0.0073 | 27 | | | | |
| Adeq Precision | 1.934 | | | | | |

With an adequate precision value of 1.934 it indicates that the model should not be used to navigate the design space (Stat-Ease 2010). A reduced quadratic model was fitted to the number median particle size data and is presented in **Table 95**.

Table 95 - Number Median Particle Size (Reduced Quadratic Model) ANOVA

| Analysis of variance table [Partial sum of squares - Type III] | | | | | | |
|--|----------------|----|-------------|---------|---------|-----------------|
| Source | Sum of Squares | df | Mean Square | F Value | p-value | |
| Model | 0.0005 | 2 | 0.0002 | 0.8456 | 0.4412 | not significant |
| Residual | 0.0069 | 25 | 0.0003 | | | |
| Lack of Fit | 0.0042 | 20 | 0.0002 | 0.3848 | 0.9426 | not significant |
| Pure Error | 0.0027 | 5 | 0.0005 | | | |
| Cor Total | 0.0073 | 27 | | | | |
| Adeq Precision | 1.934 | | | | | |

From **Table 95** it is clear that the reduced quadratic model is not statistically significant. The R-squared values for the **Number Median Particle Size Model V1 (Screening)** are as follow:

| Model | R-Squared | Adj R-Squared | Pred R-Squared |
|---|-----------|---------------|----------------|
| Number Median Particle Size Model V1 | 0.0634 | -0.0116 | -0.1153 |

The negative predicted R-squared value implies that the overall mean is a better predictor of the particle size response than the **Number Median Particle Size Model V1 (Screening)**. When examining the predicted values versus the actual values plot in **Figure 154** one can see that the actual values are concentrated in a horizontal line while the model line is at an angle.

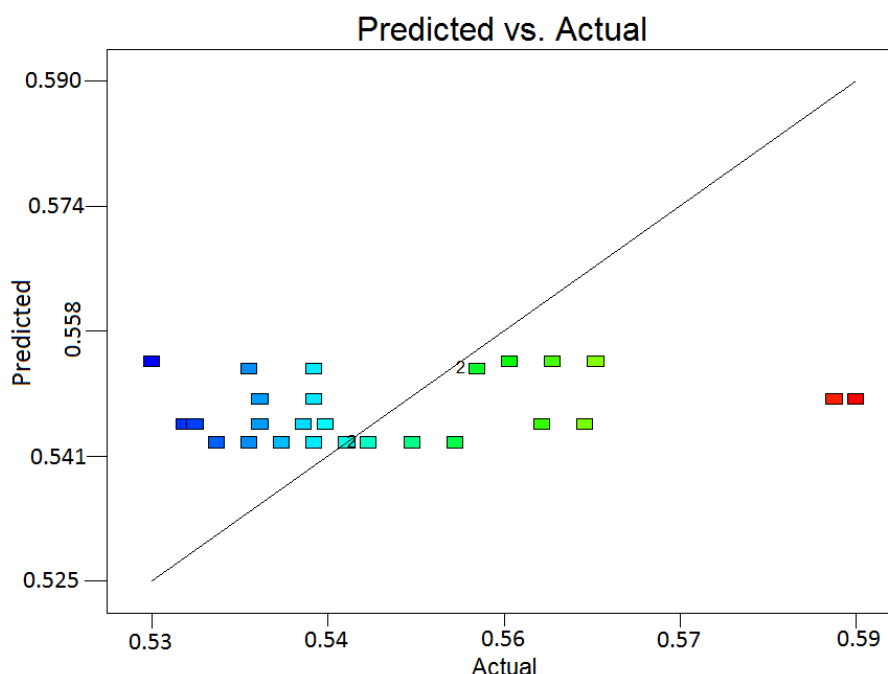


Figure 154 - Number Median Particle Size Model V1 (Screening Experimental Design) - Predicted vs. Actual

A reduced quadratic model could not be fitted to the number mean particle size model. A possible explanation could be due to the abnormal particle size distribution, as seen in **Figure 154**. That said, it is noted that there are two outlier points (red markers) in **Figure 154**. These two outlier points could be preventing a reduced quadratic model from fitting to the number median particle size data.

Number Median Particle Size Model V2 (Screening Experimental Design)

The outlier points (*EXP S23* and *EXP S24*) were excluded from the number median particle size data and a reduced quadratic model was refitted to the rearranged data and is presented in the ANOVA **Table 96**.

Table 96 - Number Mean Particle Size (Reduced Quadratic Model) ANOVA

| Analysis of Variance Table – Number Median Particle Size (Reduced Quadratic Model) | | | | | | |
|--|----------------|----|-------------|---------|----------|-----------------|
| Source | Sum of Squares | df | Mean Square | F Value | p-value | |
| Model | 0.0034 | 17 | 0.0002 | 11.685 | 0.0007 | significant |
| <i>%Surfactant * %Wax</i> | 0.0004 | 1 | 0.0004 | 21.314 | 0.0017 | |
| <i>%Surfactant * %Water</i> | 0.0002 | 1 | 0.0002 | 12.254 | 0.0081 | |
| <i>%Surfactant * Stirring Speed</i> | 8.04E-05 | 1 | 8.04E-05 | 4.627 | 0.0637 | |
| <i>%Surfactant * HSH Speed</i> | 6.87E-05 | 1 | 6.87E-05 | 3.953 | 0.0820 | |
| <i>%Surfactant * HS Time</i> | 0.0006 | 1 | 0.0006 | 33.801 | 0.0004 | |
| <i>%Surfactant * Cooling Rate</i> | 0.0009 | 1 | 0.0009 | 52.541 | < 0.0001 | |
| <i>%Surfactant * Inverting Phase AR</i> | 8.8E-05 | 1 | 8.8E-05 | 5.067 | 0.0545 | |
| <i>%Surfactant * Temperature</i> | 7.29E-05 | 1 | 7.29E-05 | 4.197 | 0.0747 | |
| <i>%Wax * HSH Speed</i> | 0.0002 | 1 | 0.0002 | 10.231 | 0.0126 | |
| <i>%Wax * HS Time</i> | 9.68E-05 | 1 | 9.68E-05 | 5.575 | 0.0459 | |
| <i>%Wax * Temperature</i> | 0.0001 | 1 | 0.0001 | 6.143 | 0.0382 | |
| <i>%Water * HSH Speed</i> | 0.0008 | 1 | 0.0008 | 44.154 | 0.0002 | |
| <i>%Water * HS Time</i> | 0.0003 | 1 | 0.0003 | 17.965 | 0.0028 | |
| <i>%Water * Inverting Phase AR</i> | 0.0003 | 1 | 0.0003 | 15.505 | 0.0043 | |
| <i>%Water * Temperature</i> | 0.0005 | 1 | 0.0005 | 30.809 | 0.0005 | |
| Residual | 0.0001 | 8 | 1.74E-05 | | | |
| Lack of Fit | 8.39E-05 | 5 | 1.68E-05 | 0.916 | 0.5669 | not significant |
| Pure Error | 0.0001 | 3 | 1.83E-05 | | | |
| Cor Total | 0.0036 | 25 | | | | |
| Adeq Precision | | | | | | |

The two outlier points had a significant effect on the **Number Median Particle Size Model V1 (Screening)**. The newly fitted **Number Median Particle Size Model V2 (Screening)** is statistically significant ($p < 0.05$). The p-value of the **Number Median Particle Size Model V2 (Screening)** (0.0007) is significantly less than the p-value of the **Number Median Particle Size Model V1 (Screening)** (0.4412) which was not statistically significant.

The R-squared values for the **Number Median Particle Size Model V2 (Screening)** are as follow:

| Model | R-Squared | Adj R-Squared | Pred R-Squared |
|---|-----------|---------------|----------------|
| Number Median Particle Size Model V2 | 0.9613 | 0.879 | N/A |

The predicted R-squared value is not applicable in this case due to there being a leverage value/s of 1. Leverage is the potential for a design point to influence the fit of the model coefficients (Stat-Ease 2010). This influence is based on the position of the design point in the design space (Stat-Ease 2010). It is noted that the R-squared values of the newly fitted **Number Median Particle Size Model V2 (Screening)** is much larger than the previous model's values. For this reason the model will be investigated. The final **Number Median Particle Size Model V2 (Screening)** equation in terms of the actual components and actual factors are as follow:

$$\begin{aligned}
 \text{Particle Size } [\mu\text{m}] = & +0.39687 \times \% \text{Surfactant} \\
 & -0.013848 \times \% \text{Wax} \\
 & +0.011983 \times \% \text{Water} \\
 & -5.4358 \times 10^{-3} \times \% \text{Surfactant} \times \% \text{Wax} \\
 & -4.45701 \times 10^{-3} \times \% \text{Surfactant} \times \% \text{Water} \\
 & -1.00026 \times 10^{-6} \times \% \text{Surfactant} \times \text{Stirring Speed} \\
 & +7.55206 \times 10^{-7} \times \% \text{Surfactant} \times \text{HSH Speed} \\
 & -2.59976 \times 10^{-4} \times \% \text{Surfactant} \times \text{HS Time} \\
 & +8.50248 \times 10^{-4} \times \% \text{Surfactant} \times \text{Cooling Rate} \\
 & +2.70105 \times 10^{-3} \times \% \text{Surfactant} \times \text{Inverting Phase AR} \\
 & +6.83533 \times 10^{-5} \times \% \text{Surfactant} \times \text{Temperature} \\
 & +7.05584 \times 10^{-7} \times \% \text{Wax} \times \text{HSH Speed} \\
 & +1.59603 \times 10^{-5} \times \% \text{Wax} \times \text{HS Time} \\
 & +1.86147 \times 10^{-4} \times \% \text{Wax} \times \text{Temperature}
 \end{aligned}$$

$$-2.36601 \times 10^{-7} \times \%Water \times HSH \text{ Speed}$$

$$+1.76031 \times 10^{-5} \times \%Water \times HS \text{ Time}$$

$$-2.00430 \times 10^{-4} \times \%Water \times Inverting \text{ Phase AR}$$

$$-3.62486 \times 10^{-5} \times \%Water \times Temperature$$

The **Number Median Particle Size Model V2 (Screening)** is very similar to the **Number Mean Particle Size Model V2 (Screening)**. Identical trends were obtained with the **Number Mean Particle Size Model V2 (Screening)** for all of the mixture- and process variables. The effect of varying the high shear homogenizing speed on the particle size is presented in **Figure 155**.

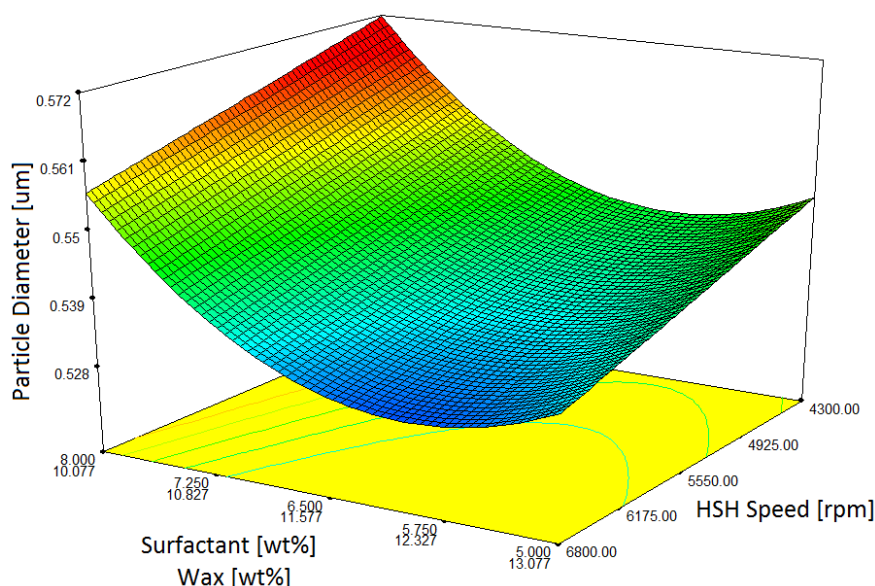


Figure 155 - Number Median Particle Size Model V2 (Screening Experimental Design) - Particle Size vs. Wax-to-Surfactant Ratio vs. High Shear Homogenizing Speed

From **Figure 155** it is noted that the particle size decreases with an increase in the high shear homogenising speed, irrespective of the wax-to-surfactant ratio. This trend is confirmed by McClements and Chen et al. (McClements 2010, Chen, Tao 2005). Both these authors found that an increase in the energy input in emulsification systems results in a decrease in the average particle size (McClements 2010, Chen, Tao 2005). **Figure 156** shows the effect of varying the cooling rate on the average particle size.

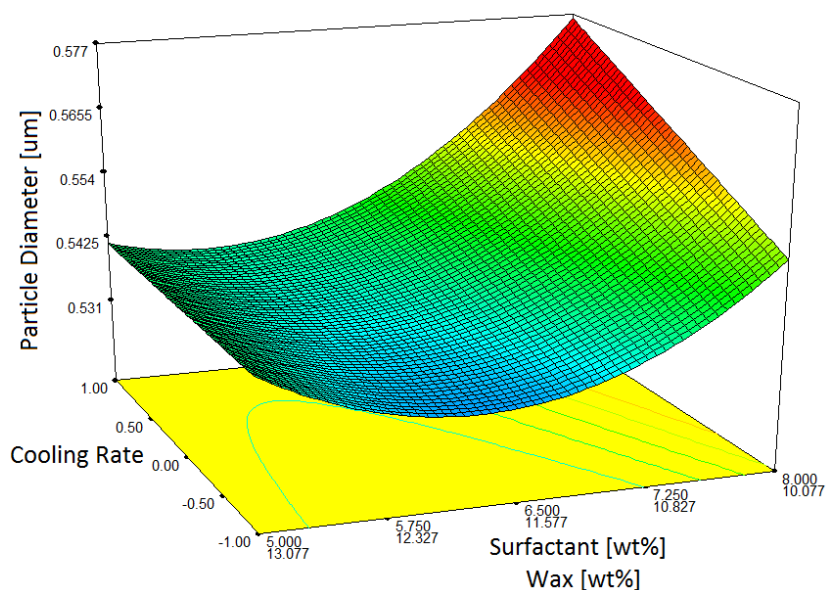


Figure 156 - Number Median Particle Size Model V2 (Screening Experimental Design) - Particle Size vs. Wax-to-Surfactant Ratio vs. Cooling Rate

From **Figure 156** one can see that at a favourable low wax-to-surfactant ratio it is noted that the particle size decreases with a decrease in the cooling rate. This trend is in contradicting to the findings of Lashmar et al. who concluded in his study on the correlation of physical parameters of an oil in water emulsion with manufacturing procedures and stability, that the slow cooling of the emulsion appeared to be beneficial to its stability, i.e. reduced the average droplet size (Lashmar, Richardson & Erbod 1995). It is also noted in **Figure 156** that at a high wax-to-surfactant ratio the cooling rate has no effect on the particle size. **Figure 157** shows the effect of varying the high shear time interval on the particle size.

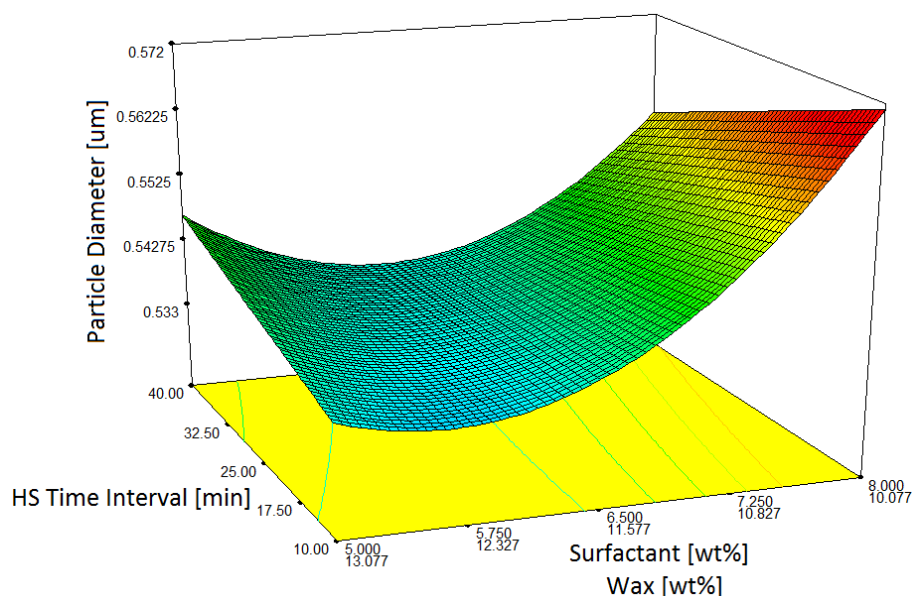


Figure 157 - Number Median Particle Size Model V2 (Screening Experimental Design) - Particle Size vs. Wax-to-Surfactant Ratio vs. HS Time Interval

At a favourable low wax-to-surfactant ratio the particle size decreases with an increase in the high shear time interval, as seen in **Figure 157**. This trend is in agreement with McClements, Adler-Nissen et al. and Lashmar et al. who found that the particle size of an emulsion can be reduced by increasing the intensity or duration of homogenization (Lashmar, Richardson & Erbod 1995, McClements 2010, Adler-Nissen, Mason & Jacobsen 2004). However, at a high wax-to-surfactant ratio the trend is clearly contradicting to what McClements, Adler-Nissen et al. and Lashmar et al. obtained during their studies. This could be due to mixing time being too long which causes the effectiveness of the emulsifier to decrease due to the intense stirring causing the emulsifier to drop out from the oil-water interface (Chen, Tao 2005). This finding is also supported by Guitierrez et al. (Gutiérrez et al. 2008). The effect of varying the inverting phase addition rate on the particle size is presented in **Figure 158**.

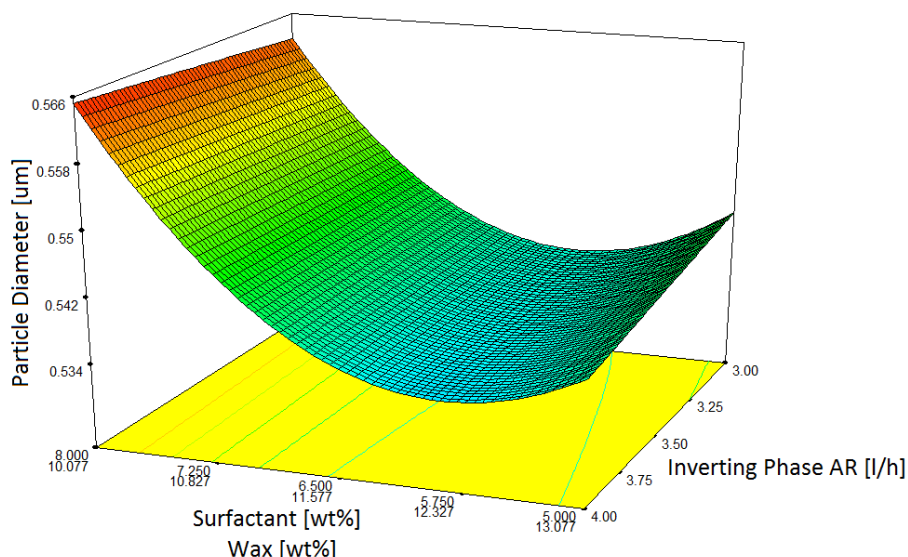


Figure 158 - Number Median Particle Size Model V2 (Screening Experimental Design) - Particle Size vs. Wax-to-Surfactant Ratio vs. Inverting Phase Addition Rate

From **Figure 158** one can see that at a favourable low wax-to-surfactant ratio the particle size decreases with a decrease in the inverting phase addition rate. This trend is in agreement with Gutierrez et al., Pey et al., Wang et al. and Lashmar e al.'s findings. Gutierrez et al. investigated various authors' studies on the addition rate of the inverting phase (usually water) during emulsification processes (Gutiérrez et al. 2008, Pey et al. 2006, Wang et al. 2007, Uson, Garcia & Solans 2004). **Figure 159** shows the effect of varying the temperature on the particle size.

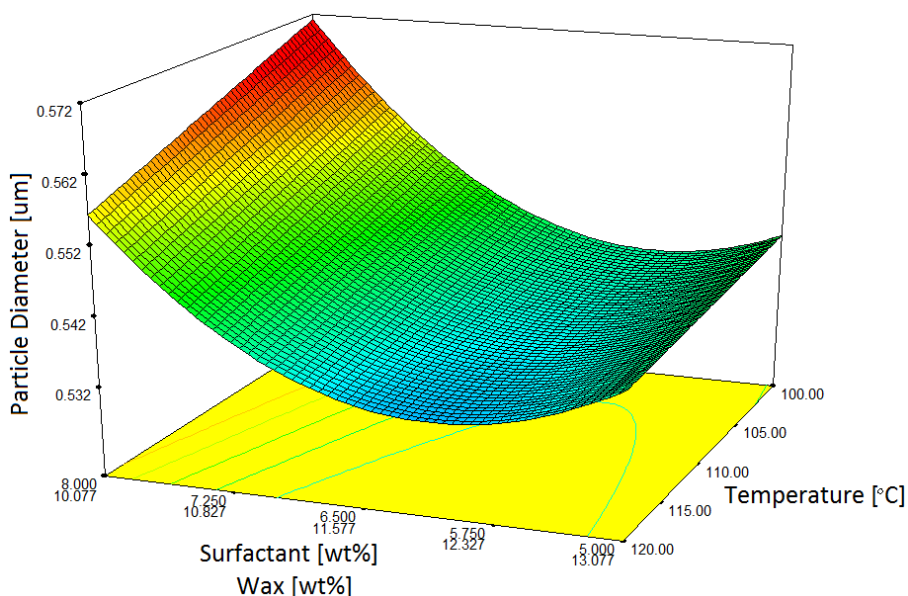


Figure 159 - Number Median Particle Size Model V2 (Screening Experimental Design) - Particle Size vs. Wax-to-Surfactant Ratio vs. Temperature

From **Figure 159** it is possible to see that the particle size decreases with an increase in the emulsification temperature, regardless of the wax-to-surfactant ratio. This trend is in agreement with the findings of Lashmar et al., Li et al., Bornfriend and Jass (Li et al. 2010, Lashmar, Richardson & Erbod 1995, Jass 1967, Bornfriend 1978). They concluded that the particle size decreases with an increase in the emulsification temperature (Li et al. 2010, Lashmar, Richardson & Erbod 1995, Jass 1967, Bornfriend 1978). The accuracy of the **Number Median Particle Size Model V2 (Screening)** is represented by the actual values versus the predicted values plot presented in **Figure 160**.

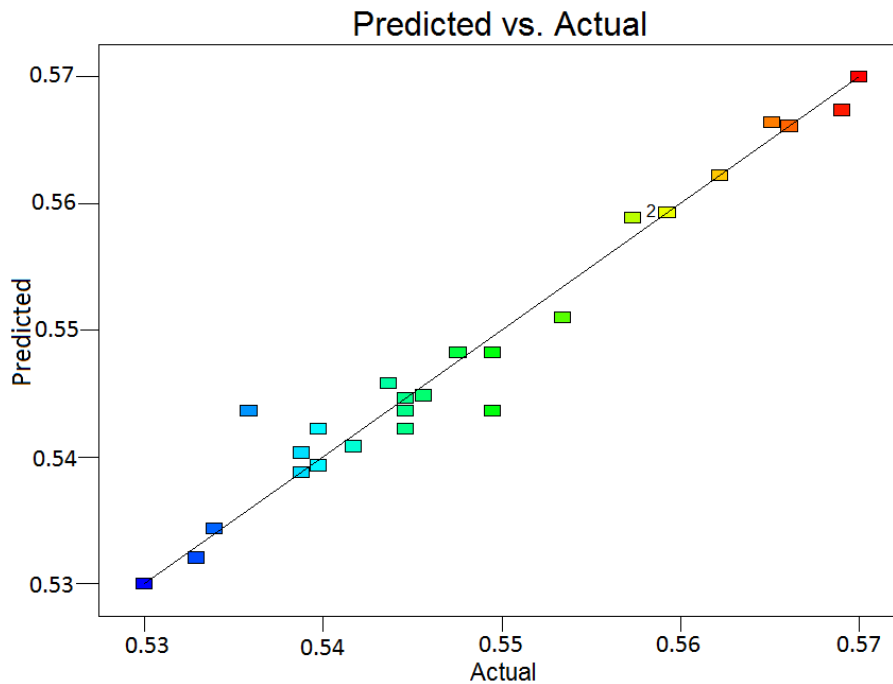


Figure 160 - Number Median Particle Size Model V2 (Screening Experimental Design) - Predicted vs. Actual

From **Figure 160** it is clear that the newly fitted **Number Median Particle Size Model V2 (Screening)** is a more accurate representation of the number median particle size data than the **Number Median Particle Size Model V1 (Screening)**.

Appendix G: Screening Experimental Design Optimization

Data

| <i>Surfactant</i> | <i>Wax</i> | <i>Water</i> |
|-------------------|------------|--------------|
| 5.00 | 10.00 | 85.00 |
| 5.00 | 10.00 | 85.00 |
| 5.00 | 10.00 | 85.00 |
| 5.00 | 10.00 | 85.00 |
| 5.00 | 10.00 | 85.00 |
| 5.00 | 10.00 | 85.00 |
| 5.00 | 10.00 | 85.00 |
| 5.00 | 10.00 | 85.00 |
| 5.00 | 10.00 | 85.00 |
| 5.00 | 10.00 | 85.00 |
| 5.00 | 10.00 | 85.00 |
| 5.00 | 10.00 | 85.00 |
| 5.00 | 10.00 | 85.00 |
| 5.00 | 10.19 | 84.81 |
| 5.00 | 10.00 | 85.00 |
| 5.00 | 10.00 | 85.00 |
| 5.00 | 10.00 | 85.00 |
| 5.00 | 10.00 | 85.00 |
| 5.00 | 10.00 | 85.00 |
| 5.00 | 11.34 | 83.66 |
| 5.00 | 10.00 | 85.00 |

Appendix H: Mixture Experimental Design Particle Size Data Analysis

| Analysis of Variance Table – Area Median Particle Size (Linear Model) | | | | | | |
|---|----------------|----|-------------|---------|------------------|-----------------|
| Source | Sum of Squares | df | Mean Square | F Value | p-value Prob > F | |
| Model | 0.2017 | 4 | 0.050 | 0.357 | 0.834 | not significant |
| Linear Mixture | 0.2017 | 4 | 0.050 | 0.357 | 0.834 | |
| Residual | 1.413 | 10 | 0.141 | | | |
| Lack of Fit | 1.212 | 6 | 0.202 | 4.046 | 0.099 | not significant |
| Pure Error | 0.200 | 4 | 0.050 | | | |
| Cor Total | 1.614 | 14 | | | | |

| Analysis of Variance Table – Area Median Particle Size (Reduced Quadratic Model) | | | | | | |
|--|----------------|----|-------------|---------|------------------|-----------------|
| Source | Sum of Squares | df | Mean Square | F Value | p-value Prob > F | |
| Model | 1.285 | 6 | 0.214 | 5.200 | 0.018 | significant |
| AB | 1.080 | 1 | 1.080 | 26.230 | 0.001 | |
| AC | 0.599 | 1 | 0.599 | 14.545 | 0.005 | |
| Residual | 0.329 | 8 | 0.041 | | | |
| Lack of Fit | 0.130 | 4 | 0.032 | 0.648 | 0.658 | not significant |
| Pure Error | 0.200 | 4 | 0.050 | | | |
| Cor Total | 1.614 | 14 | | | | |

| Analysis of Variance Table – Area Mean Particle Size (Linear Model) | | | | | | |
|---|----------------|----|-------------|---------|------------------|-----------------|
| Source | Sum of Squares | df | Mean Square | F Value | p-value Prob > F | |
| Model | 19.650 | 4 | 4.913 | 3.451 | 0.051 | not significant |
| Linear Mixture | 19.650 | 4 | 4.913 | 3.451 | 0.051 | |
| Residual | 14.233 | 10 | 1.423 | | | |
| Lack of Fit | 10.638 | 6 | 1.773 | 1.973 | 0.266 | not significant |
| Pure Error | 3.595 | 4 | 0.899 | | | |
| Cor Total | 33.883 | 14 | | | | |

Analysis of Variance Table – Area Mean Particle Size (Reduced Quadratic Model)

| Source | Sum of Squares | df | Mean Square | F Value | p-value Prob > F | |
|-------------|----------------|----|-------------|---------|------------------|-----------------|
| Model | 19.650 | 4 | 4.913 | 3.451 | 0.051 | not significant |
| Residual | 14.233 | 10 | 1.423 | | | |
| Lack of Fit | 10.638 | 6 | 1.773 | 1.973 | 0.266 | not significant |
| Pure Error | 3.595 | 4 | 0.899 | | | |
| Cor Total | 33.884 | 14 | | | | |

Analysis of Variance Table – Number Median Particle Size (Linear Model)

| Source | Sum of Squares | df | Mean Square | F Value | p-value Prob > F | |
|----------------|----------------|----|-------------|---------|------------------|-----------------|
| Model | 0.00047 | 4 | 0.00012 | 0.635 | 0.649 | not significant |
| Linear Mixture | 0.00047 | 4 | 0.00012 | 0.635 | 0.649 | |
| Residual | 0.00184 | 10 | 0.00018 | | | |
| Lack of Fit | 0.00114 | 6 | 0.00019 | 1.092 | 0.488 | not significant |
| Pure Error | 0.00070 | 4 | 0.00017 | | | |
| Cor Total | 0.00231 | 14 | | | | |

Analysis of Variance Table – Number Median Particle Size (Reduced Quadratic Model)

| Source | Sum of Squares | df | Mean Square | F Value | p-value Prob > F | |
|-------------|----------------|----|-------------|---------|------------------|-----------------|
| Model | 0.00047 | 4 | 0.00012 | 0.635 | 0.649 | not significant |
| Residual | 0.00184 | 10 | 0.00018 | | | |
| Lack of Fit | 0.00114 | 6 | 0.00019 | 1.092 | 0.488 | not significant |
| Pure Error | 0.00070 | 4 | 0.00017 | | | |
| Cor Total | 0.00231 | 14 | | | | |

| Analysis of Variance Table – Number Mean Particle Size (Linear Model) | | | | | | |
|---|----------------|----|-------------|---------|---------|-----------------|
| Source | Sum of Squares | df | Mean Square | F Value | p-value | Prob > F |
| Model | 0.0026 | 4 | 0.00064 | 0.450 | 0.771 | not significant |
| Linear Mixture | 0.0026 | 4 | 0.00064 | 0.450 | 0.771 | |
| Residual | 0.0143 | 10 | 0.00143 | | | |
| Lack of Fit | 0.0105 | 6 | 0.00175 | 1.844 | 0.288 | not significant |
| Pure Error | 0.0038 | 4 | 0.00095 | | | |
| Cor Total | 0.0169 | 14 | | | | |

| Analysis of Variance Table – Number Mean Particle Size (Reduced Quadratic Model) | | | | | | |
|--|----------------|----|-------------|---------|---------|-----------------|
| Source | Sum of Squares | df | Mean Square | F Value | p-value | Prob > F |
| Model | 0.0026 | 4 | 0.00064 | 0.450 | 0.771 | not significant |
| Residual | 0.0143 | 10 | 0.00143 | | | |
| Lack of Fit | 0.0105 | 6 | 0.00175 | 1.844 | 0.288 | not significant |
| Pure Error | 0.0038 | 4 | 0.00095 | | | |
| Cor Total | 0.0169 | 14 | | | | |

| Analysis of Variance Table – Volume Median Particle Size (Linear Model) | | | | | | |
|---|----------------|----|-------------|---------|---------|-----------------|
| Source | Sum of Squares | df | Mean Square | F Value | p-value | Prob > F |
| Model | 567.643 | 4 | 141.91 | 3.133 | 0.065 | not significant |
| Linear Mixture | 567.643 | 4 | 141.91 | 3.133 | 0.065 | |
| Residual | 452.901 | 10 | 45.29 | | | |
| Lack of Fit | 227.999 | 6 | 38.00 | 0.676 | 0.682 | not significant |
| Pure Error | 224.901 | 4 | 56.23 | | | |
| Cor Total | 1020.544 | 14 | | | | |

Analysis of Variance Table – Volume Median Particle Size (Reduced Quadratic Model)

| Source | Sum of Squares | df | Mean Square | F Value | p-value Prob > F | |
|-------------|----------------|----|-------------|---------|------------------|-----------------|
| Model | 567.643 | 4 | 141.911 | 3.133 | 0.065 | not significant |
| Residual | 452.901 | 10 | 45.291 | | | |
| Lack of Fit | 227.999 | 6 | 38.000 | 0.676 | 0.682 | not significant |
| Pure Error | 224.901 | 4 | 56.225 | | | |
| Cor Total | 1020.543 | 14 | | | | |

Analysis of Variance Table – Volume Mean Particle Size (Linear Model)

| Source | Sum of Squares | df | Mean Square | F Value | p-value Prob > F | |
|----------------|----------------|----|-------------|---------|------------------|-----------------|
| Model | 2120.68 | 4 | 530.17 | 1.532 | 0.266 | not significant |
| Linear Mixture | 2120.68 | 4 | 530.17 | 1.532 | 0.266 | |
| Residual | 3460.93 | 10 | 346.09 | | | |
| Lack of Fit | 1973.82 | 6 | 328.97 | 0.885 | 0.575 | not significant |
| Pure Error | 1487.10 | 4 | 371.78 | | | |
| Cor Total | 5581.61 | 14 | | | | |

Analysis of Variance Table – Volume Mean Particle Size (Reduced Quadratic Model)

| Source | Sum of Squares | df | Mean Square | F Value | p-value Prob > F | |
|-------------|----------------|----|-------------|---------|------------------|-----------------|
| Model | 2120.68 | 4 | 530.17 | 1.532 | 0.266 | not significant |
| Residual | 3460.93 | 10 | 346.09 | | | |
| Lack of Fit | 1973.82 | 6 | 328.97 | 0.885 | 0.575 | not significant |
| Pure Error | 1487.10 | 4 | 371.78 | | | |
| Cor Total | 5581.61 | 14 | | | | |

Appendix I: Mixture Experimental Design Roughness Data

| Analysis of Variance Table – Area Roughness (Reduced Quadratic Model) | | | | | | |
|---|----------------|----|-------------|---------|------------------|-----------------|
| Source | Sum of Squares | df | Mean Square | F Value | p-value Prob > F | |
| Model | 1.930 | 4 | 0.483 | 0.570 | 0.691 | not significant |
| Residual | 8.473 | 10 | 0.847 | | | |
| Lack of Fit | 2.728 | 6 | 0.455 | 0.316 | 0.899 | not significant |
| Pure Error | 5.746 | 4 | 1.436 | | | |
| Cor Total | 10.404 | 14 | | | | |

| Analysis of Variance Table – Number Roughness (Reduced Quadratic Model) | | | | | | |
|---|----------------|----|-------------|---------|------------------|-----------------|
| Source | Sum of Squares | df | Mean Square | F Value | p-value Prob > F | |
| Model | 1.930 | 4 | 0.483 | 0.570 | 0.691 | not significant |
| Residual | 8.473 | 10 | 0.847 | | | |
| Lack of Fit | 2.728 | 6 | 0.455 | 0.316 | 0.899 | not significant |
| Pure Error | 5.746 | 4 | 1.436 | | | |
| Cor Total | 10.403 | 14 | | | | |

| Analysis of Variance Table – Volume Roughness (Reduced Quadratic Model) | | | | | | |
|---|----------------|----|-------------|---------|------------------|-----------------|
| Source | Sum of Squares | df | Mean Square | F Value | p-value Prob > F | |
| Model | 1.930 | 4 | 0.483 | 0.570 | 0.691 | not significant |
| Residual | 8.473 | 10 | 0.847 | | | |
| Lack of Fit | 2.728 | 6 | 0.455 | 0.316 | 0.899 | not significant |
| Pure Error | 5.746 | 4 | 1.436 | | | |
| Cor Total | 10.404 | 14 | | | | |

Appendix J: Mixture Experimental Design Gloss Data

| Analysis of Variance Table – Area Gloss (Reduced Quadratic Model) | | | | | | |
|---|----------------|----|-------------|---------|------------------|-----------------|
| Source | Sum of Squares | df | Mean Square | F Value | p-value Prob > F | |
| Model | 2864.65 | 4 | 716.16 | 2.550 | 0.105 | not significant |
| Residual | 2808.25 | 10 | 280.82 | | | |
| Lack of Fit | 1469.86 | 6 | 244.98 | 0.732 | 0.652 | not significant |
| Pure Error | 1338.39 | 4 | 334.60 | | | |
| Cor Total | 5672.90 | 14 | | | | |

| Analysis of Variance Table – Number Gloss (Reduced Quadratic Model) | | | | | | |
|---|----------------|----|-------------|---------|------------------|-----------------|
| Source | Sum of Squares | df | Mean Square | F Value | p-value Prob > F | |
| Model | 2864.65 | 4 | 716.16 | 2.550 | 0.105 | not significant |
| Residual | 2808.25 | 10 | 280.82 | | | |
| Lack of Fit | 1469.86 | 6 | 244.98 | 0.732 | 0.652 | not significant |
| Pure Error | 1338.39 | 4 | 334.60 | | | |
| Cor Total | 5672.90 | 14 | | | | |

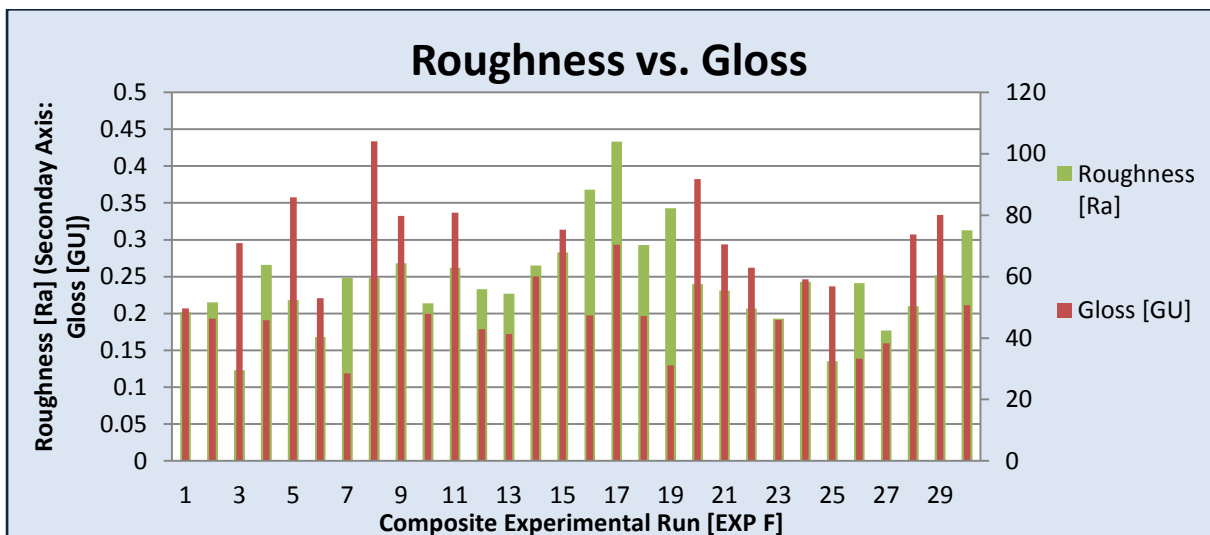
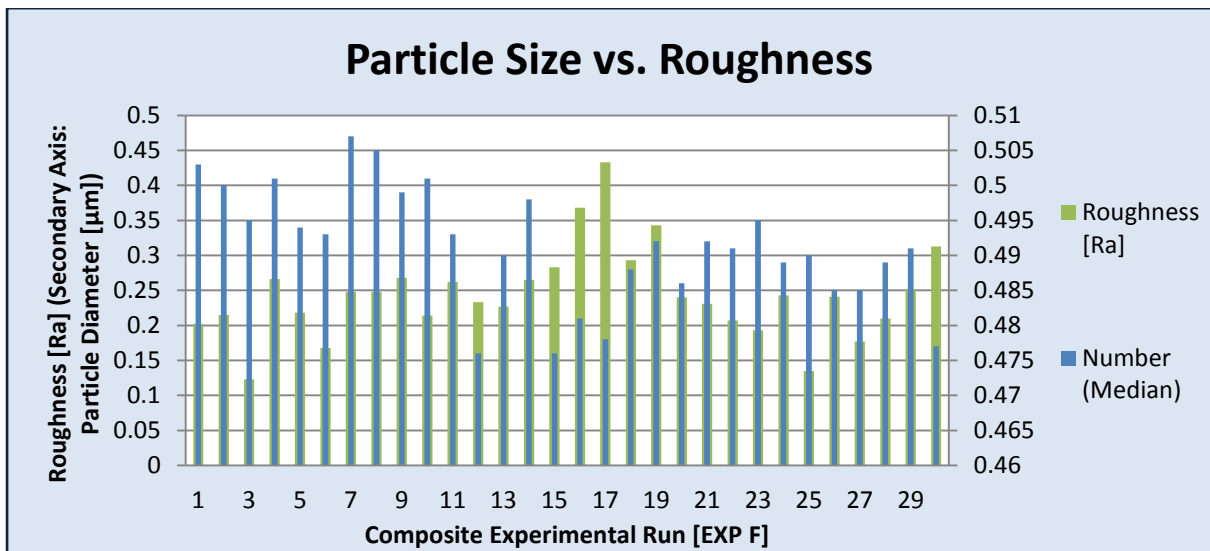
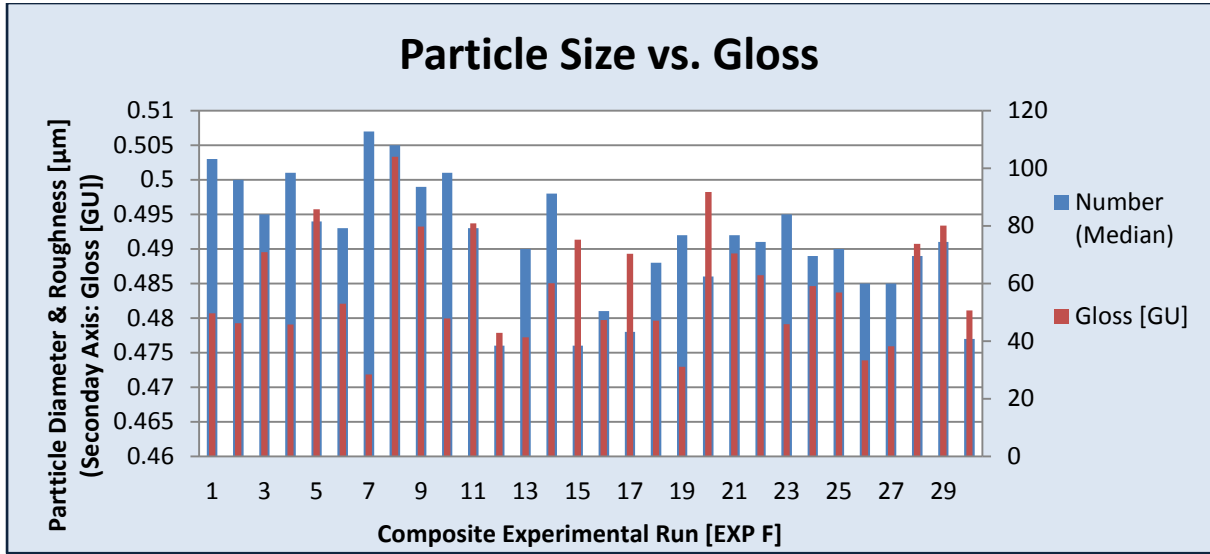
| Analysis of Variance Table – Volume Gloss (Reduced Quadratic Model) | | | | | | |
|---|----------------|----|-------------|---------|------------------|-----------------|
| Source | Sum of Squares | df | Mean Square | F Value | p-value Prob > F | |
| Model | 2864.65 | 4 | 716.16 | 2.550 | 0.105 | not significant |
| Residual | 2808.25 | 10 | 280.82 | | | |
| Lack of Fit | 1469.86 | 6 | 244.98 | 0.732 | 0.652 | not significant |
| Pure Error | 1338.39 | 4 | 334.60 | | | |
| Cor Total | 5672.90 | 14 | | | | |

Appendix K: Mixture Experimental Design Optimization

Data

| <i>%Water</i> | <i>%Wax</i> | <i>%Oleic Acid</i> | <i>%Potassium Hydroxide</i> | <i>%Ammonium Hydroxide</i> | <i>Desirability</i> |
|---------------|-------------|--------------------|-----------------------------|----------------------------|---------------------|
| 75.291 | 16.214 | 6.368 | 0.527 | 1.600 | 0.903 |
| 75.355 | 15.704 | 6.121 | 0.633 | 2.186 | 0.902 |
| 75.320 | 15.815 | 6.208 | 0.582 | 2.075 | 0.901 |
| 75.292 | 16.208 | 6.400 | 0.500 | 1.600 | 0.905 |
| 75.315 | 15.617 | 6.153 | 0.729 | 2.187 | 0.902 |
| 75.367 | 15.550 | 6.149 | 0.500 | 2.434 | 0.906 |
| 75.230 | 15.991 | 6.411 | 0.545 | 1.823 | 0.904 |
| 75.306 | 15.592 | 6.172 | 0.719 | 2.211 | 0.902 |
| 75.322 | 15.437 | 6.197 | 0.500 | 2.544 | 0.902 |
| 75.270 | 15.503 | 6.231 | 0.726 | 2.271 | 0.901 |
| 75.337 | 15.713 | 6.107 | 0.721 | 2.121 | 0.900 |
| 75.164 | 16.140 | 6.400 | 0.696 | 1.600 | 0.899 |
| 75.315 | 15.000 | 6.391 | 1.300 | 1.994 | 0.885 |
| 75.449 | 15.666 | 6.036 | 0.500 | 2.348 | 0.906 |
| 75.372 | 15.718 | 6.161 | 0.500 | 2.249 | 0.905 |
| 75.350 | 15.608 | 6.137 | 0.624 | 2.281 | 0.904 |
| 75.185 | 16.154 | 6.400 | 0.661 | 1.600 | 0.900 |
| 75.385 | 15.647 | 6.091 | 0.602 | 2.275 | 0.904 |
| 75.293 | 16.207 | 6.400 | 0.500 | 1.600 | 0.904 |
| 75.332 | 15.790 | 6.182 | 0.588 | 2.108 | 0.902 |
| 75.145 | 16.104 | 6.472 | 0.660 | 1.618 | 0.901 |
| 75.292 | 16.208 | 6.400 | 0.500 | 1.600 | 0.905 |
| 75.325 | 15.790 | 6.246 | 0.500 | 2.139 | 0.904 |
| 75.251 | 15.937 | 6.373 | 0.534 | 1.905 | 0.903 |
| 75.223 | 16.176 | 6.400 | 0.602 | 1.600 | 0.902 |
| 75.405 | 15.585 | 6.055 | 0.627 | 2.328 | 0.899 |
| 75.307 | 15.493 | 6.204 | 0.603 | 2.392 | 0.902 |
| 75.312 | 15.831 | 6.222 | 0.582 | 2.054 | 0.901 |
| 75.257 | 15.567 | 6.215 | 0.830 | 2.131 | 0.900 |
| 75.298 | 15.829 | 6.254 | 0.599 | 2.020 | 0.903 |

Appendix L: Composite Experimental Design Data



Appendix M: Composite Experimental Design Optimization Data

| <u>Area Median O1,O2 Optimization</u> | | | | | | |
|---------------------------------------|--------------------|------------------------|-------------------------|----------------------|----------------------|---------------------|
| Number | Temperature | High Shear Time | High Shear Speed | Stirrer Speed | Particle Size | Desirability |
| 1 | 118.68 | 10.15 | 6448.03 | 1500.00 | 0.53 | 0.83 |
| 2 | 118.67 | 12.49 | 4895.87 | 1500.00 | 0.53 | 0.83 |
| 3 | 118.66 | 12.24 | 4614.11 | 1500.00 | 0.53 | 0.83 |
| 4 | 118.66 | 12.24 | 6485.89 | 1500.00 | 0.53 | 0.83 |
| 5 | 118.68 | 11.08 | 6071.64 | 1500.00 | 0.53 | 0.83 |
| 6 | 118.68 | 10.51 | 6589.91 | 1500.00 | 0.53 | 0.83 |
| 7 | 118.69 | 10.39 | 4333.74 | 1500.00 | 0.53 | 0.83 |
| 8 | 118.68 | 11.43 | 6675.35 | 1500.00 | 0.53 | 0.83 |
| 9 | 119.06 | 10.00 | 6799.89 | 1499.84 | 0.53 | 0.83 |
| 10 | 118.69 | 10.05 | 4697.93 | 1500.00 | 0.53 | 0.83 |
| 11 | 118.65 | 11.52 | 4562.78 | 1500.00 | 0.53 | 0.83 |
| 12 | 118.65 | 11.52 | 6537.22 | 1500.00 | 0.53 | 0.83 |
| 13 | 118.68 | 10.00 | 4773.61 | 1500.00 | 0.53 | 0.82 |
| 14 | 118.69 | 10.03 | 4788.40 | 1500.00 | 0.53 | 0.83 |
| 15 | 118.67 | 11.81 | 6429.60 | 1500.00 | 0.53 | 0.83 |
| 16 | 118.65 | 11.52 | 4562.78 | 1500.00 | 0.53 | 0.83 |
| 17 | 118.65 | 11.52 | 6537.22 | 1500.00 | 0.53 | 0.83 |
| 18 | 118.69 | 10.58 | 6618.88 | 1500.00 | 0.53 | 0.83 |
| 19 | 120.49 | 10.00 | 6799.87 | 1499.94 | 0.53 | 0.83 |
| 20 | 120.98 | 10.00 | 5060.37 | 1500.00 | 0.53 | 0.83 |
| Average | 118.90 | 10.95 | 5714.15 | 1499.99 | 0.53 | 0.83 |

Number Mean 03
Optimization

| Number | Temperature | High Shear Time | High Shear Speed | Stirrer Speed | Particle Size | Desirability |
|----------------|--------------------|------------------------|-------------------------|----------------------|----------------------|---------------------|
| 1 | 123.95 | 40.00 | 4948.85 | 1500.00 | 0.50 | 0.84 |
| 2 | 123.94 | 40.00 | 4831.10 | 1500.00 | 0.50 | 0.84 |
| 3 | 123.95 | 40.00 | 5158.45 | 1500.00 | 0.50 | 0.84 |
| 4 | 123.95 | 40.00 | 5941.55 | 1500.00 | 0.50 | 0.84 |
| 5 | 123.96 | 40.00 | 6389.04 | 1500.00 | 0.50 | 0.84 |
| 6 | 123.96 | 40.00 | 4710.96 | 1500.00 | 0.50 | 0.84 |
| 7 | 123.96 | 40.00 | 5690.94 | 1500.00 | 0.50 | 0.84 |
| 8 | 123.95 | 40.00 | 6718.90 | 1500.00 | 0.50 | 0.84 |
| 9 | 123.96 | 40.00 | 6657.30 | 1500.00 | 0.50 | 0.84 |
| 10 | 123.96 | 40.00 | 4782.33 | 1500.00 | 0.50 | 0.84 |
| 11 | 123.93 | 40.00 | 6798.74 | 1499.96 | 0.50 | 0.84 |
| 12 | 123.93 | 40.00 | 4301.26 | 1499.96 | 0.50 | 0.84 |
| 13 | 123.91 | 39.99 | 5993.22 | 1500.00 | 0.50 | 0.84 |
| 14 | 123.92 | 39.99 | 6497.48 | 1500.00 | 0.50 | 0.84 |
| 15 | 123.73 | 40.00 | 5663.33 | 1500.00 | 0.50 | 0.84 |
| 16 | 123.97 | 40.00 | 5827.10 | 1499.89 | 0.50 | 0.84 |
| 17 | 123.95 | 40.00 | 5092.60 | 1499.54 | 0.50 | 0.84 |
| 18 | 124.47 | 40.00 | 4354.87 | 1500.00 | 0.50 | 0.84 |
| 19 | 123.99 | 40.00 | 6199.63 | 1499.16 | 0.50 | 0.84 |
| 20 | 124.04 | 39.85 | 5715.26 | 1500.00 | 0.50 | 0.84 |
| Average | 123.97 | 39.99 | 5613.65 | 1499.92 | 0.50 | 0.84 |

| <u>Number</u> 04,05 | | | | | | |
|---------------------------------|--------------------|------------------------|-------------------------|----------------------|----------------------|---------------------|
| <u>Median</u> | | | | | | |
| <u>Optimization</u> | | | | | | |
| Number | Temperature | High Shear Time | High Shear Speed | Stirrer Speed | Particle Size | Desirability |
| 1 | 127.54 | 40.00 | 5786.25 | 1500.00 | 0.48 | 0.85 |
| 2 | 127.54 | 40.00 | 5313.75 | 1500.00 | 0.48 | 0.85 |
| 3 | 127.54 | 40.00 | 5053.50 | 1500.00 | 0.48 | 0.85 |
| 4 | 127.54 | 40.00 | 5274.63 | 1500.00 | 0.48 | 0.85 |
| 5 | 127.55 | 40.00 | 5760.13 | 1500.00 | 0.48 | 0.85 |
| 6 | 127.53 | 40.00 | 4982.45 | 1500.00 | 0.48 | 0.85 |
| 7 | 127.57 | 40.00 | 5733.43 | 1500.00 | 0.48 | 0.85 |
| 8 | 127.55 | 40.00 | 6727.45 | 1500.00 | 0.48 | 0.85 |
| 9 | 127.54 | 40.00 | 5000.61 | 1500.00 | 0.48 | 0.85 |
| 10 | 127.58 | 40.00 | 6161.44 | 1500.00 | 0.48 | 0.85 |
| 11 | 127.58 | 40.00 | 4938.56 | 1500.00 | 0.48 | 0.85 |
| 12 | 127.55 | 40.00 | 5724.39 | 1500.00 | 0.48 | 0.85 |
| 13 | 127.50 | 40.00 | 6579.61 | 1500.00 | 0.48 | 0.85 |
| 14 | 127.58 | 40.00 | 4379.83 | 1500.00 | 0.48 | 0.85 |
| 15 | 127.53 | 40.00 | 5104.83 | 1500.00 | 0.48 | 0.85 |
| 16 | 127.57 | 40.00 | 6115.19 | 1500.00 | 0.48 | 0.85 |
| 17 | 127.72 | 40.00 | 5952.73 | 1500.00 | 0.48 | 0.85 |
| 18 | 127.49 | 40.00 | 5563.02 | 1499.95 | 0.48 | 0.85 |
| 19 | 127.78 | 40.00 | 6599.50 | 1500.00 | 0.48 | 0.85 |
| 20 | 127.60 | 39.99 | 5886.75 | 1500.00 | 0.48 | 0.85 |
| Average | 127.57 | 40.00 | 5631.90 | 1500.00 | 0.48 | 0.85 |

A comparison of the particle diameter with the roughness and gloss data recorded during the Composite experimental design is presented in **Figure 161**.

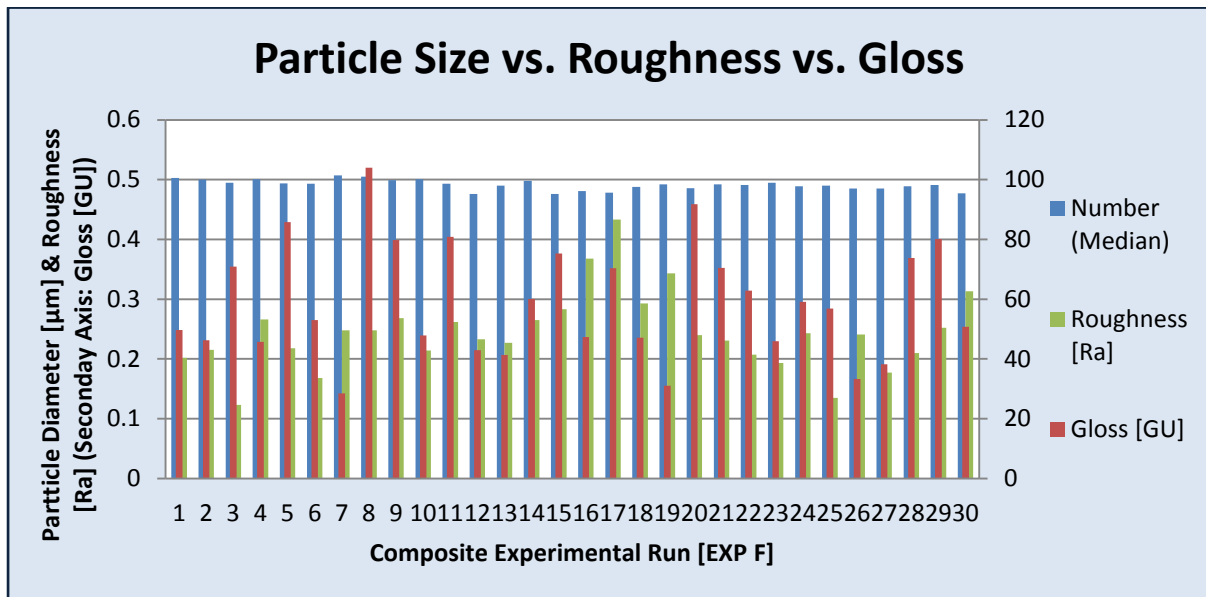


Figure 161 – Number Median Particle Size Distribution Data vs. Roughness- and Gloss Data Comparison

From **Figure 161** it is noted that there are no clear trends visible between the particle size-, roughness- and gloss data sets (detailed graphs can be viewed in **Appendix L**). A possible explanation for the lack of trends could be the fact that the roughness data were not statistically significant and that the gloss data are not a good representation of the design space. The particle size- and gloss data are compared in **Figure 162**.

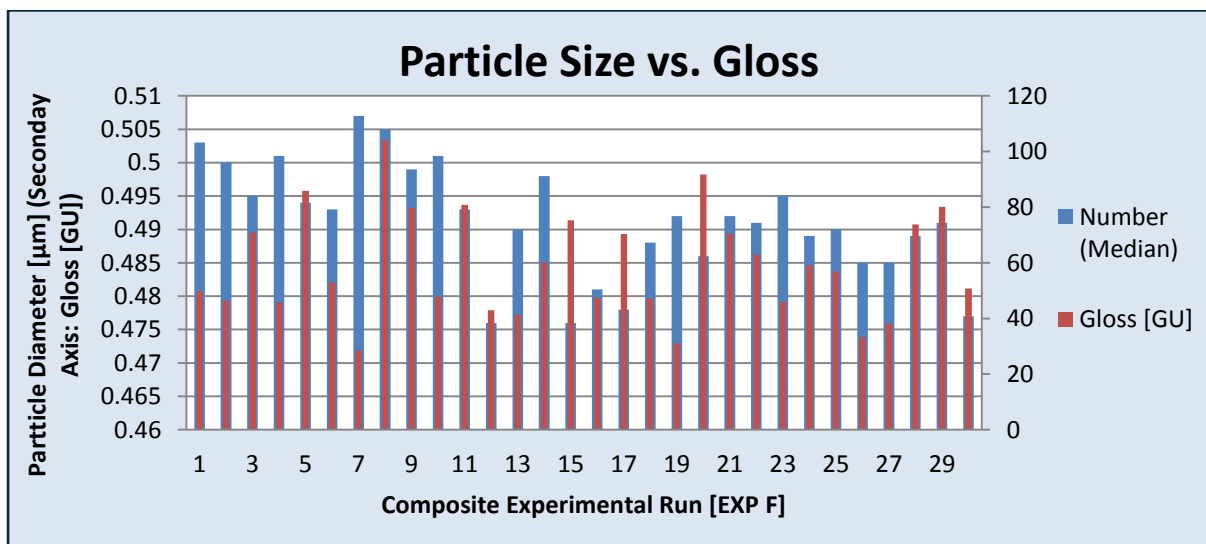
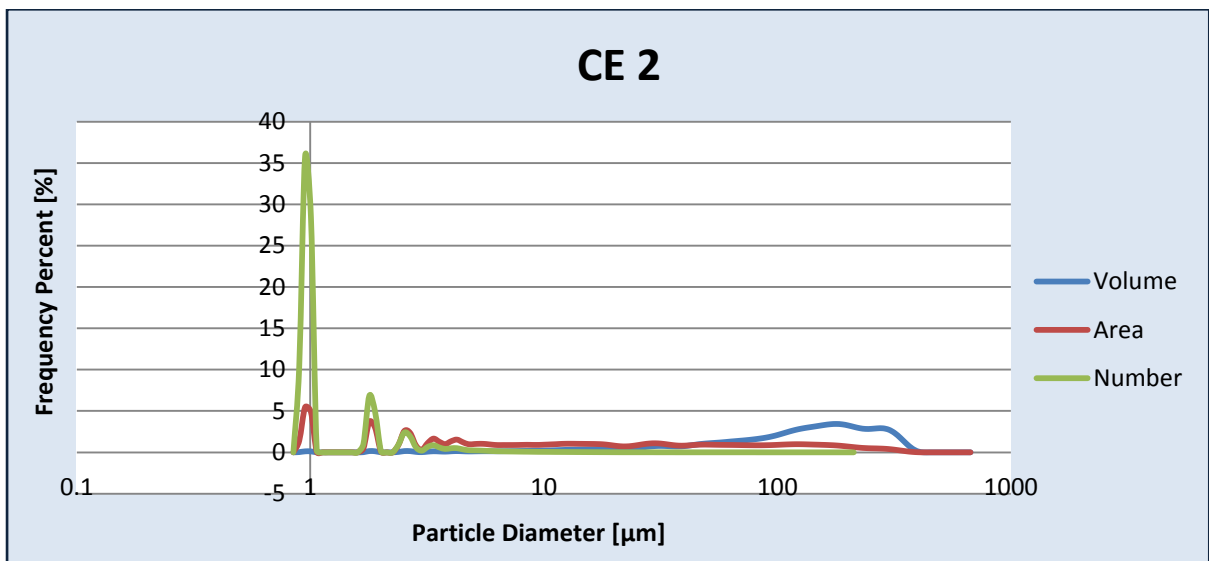
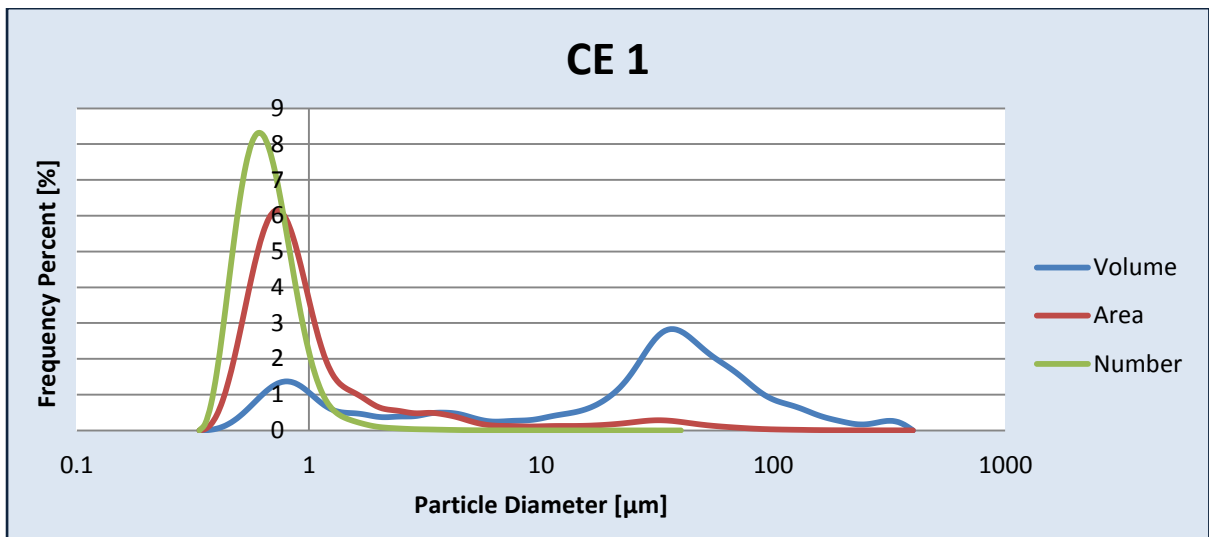
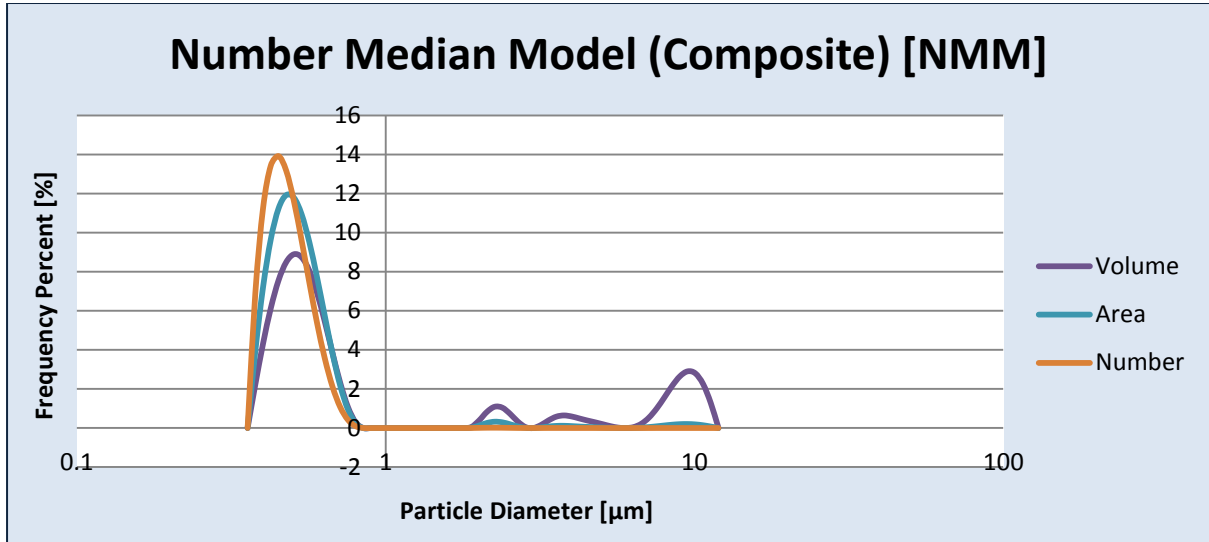
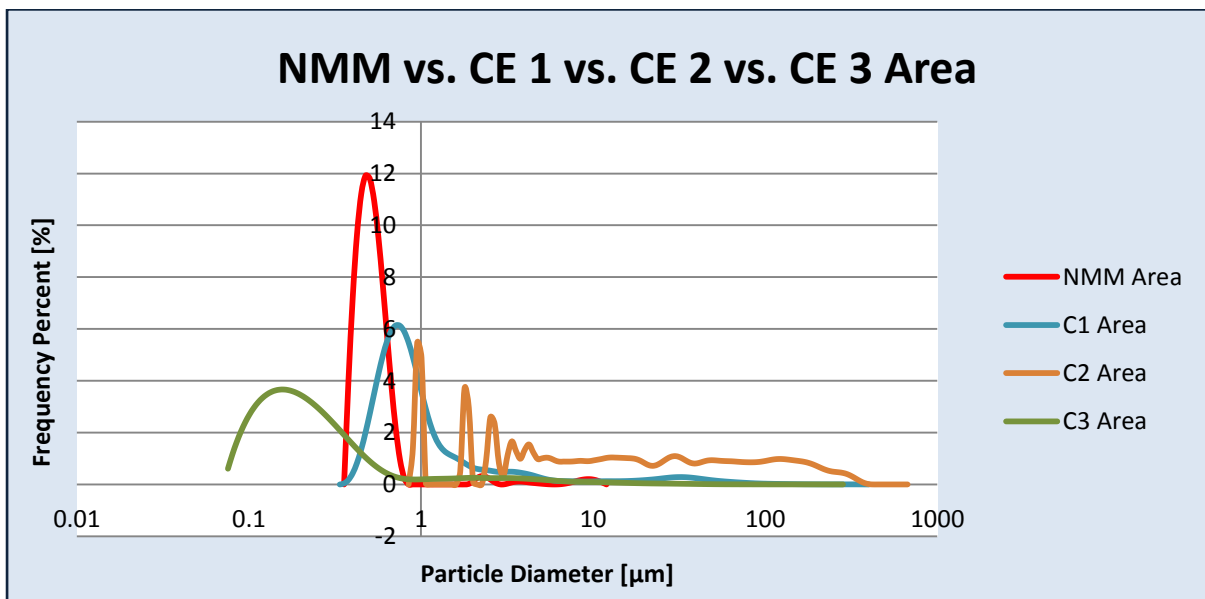
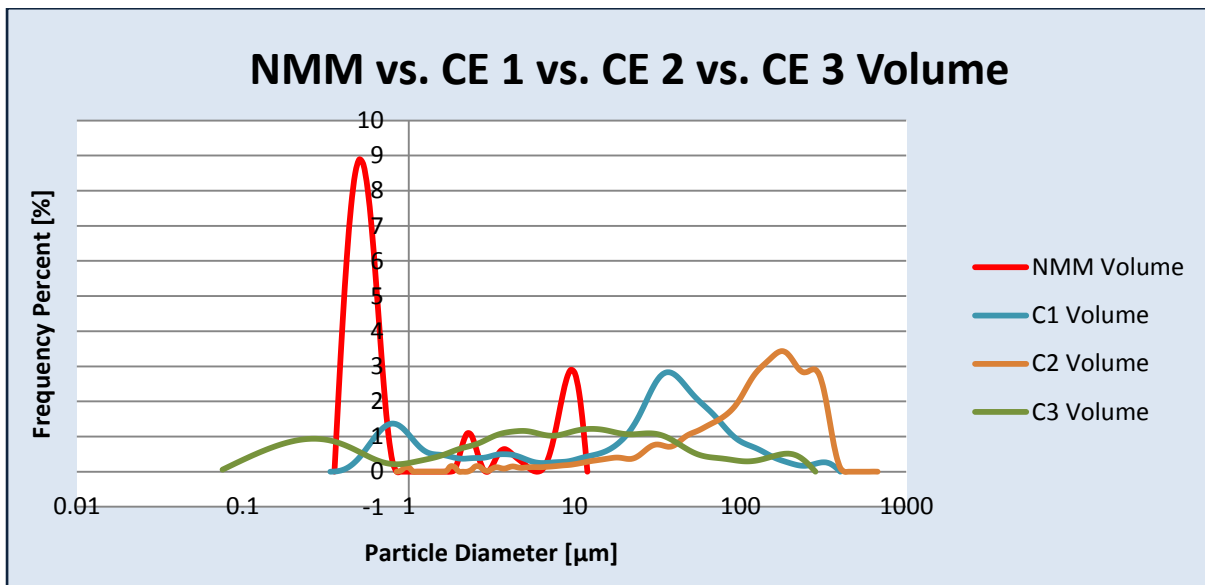
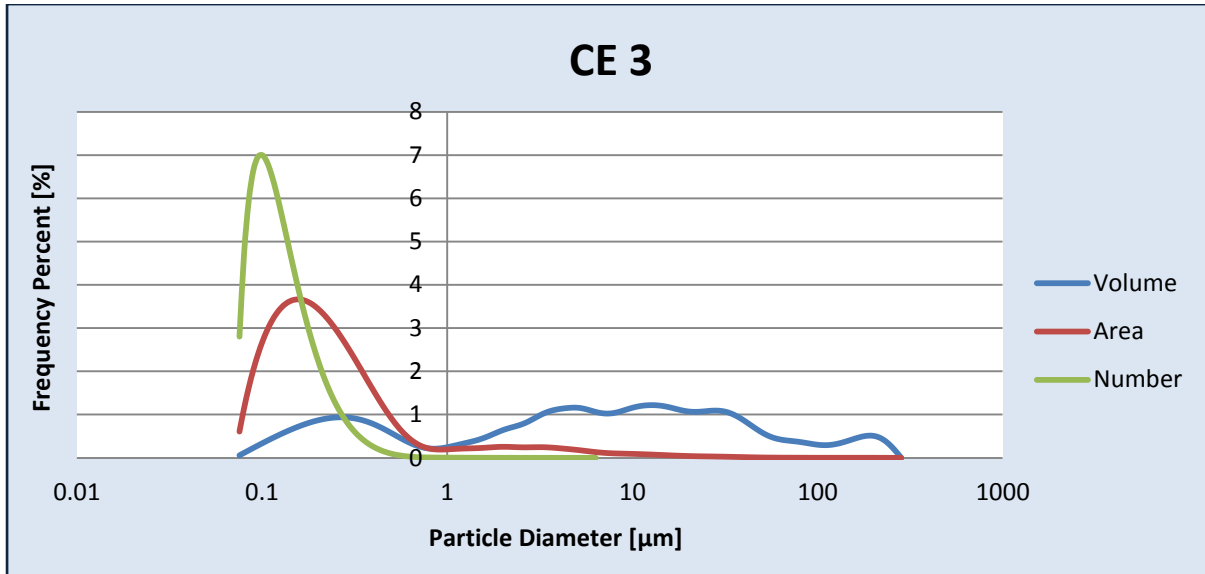
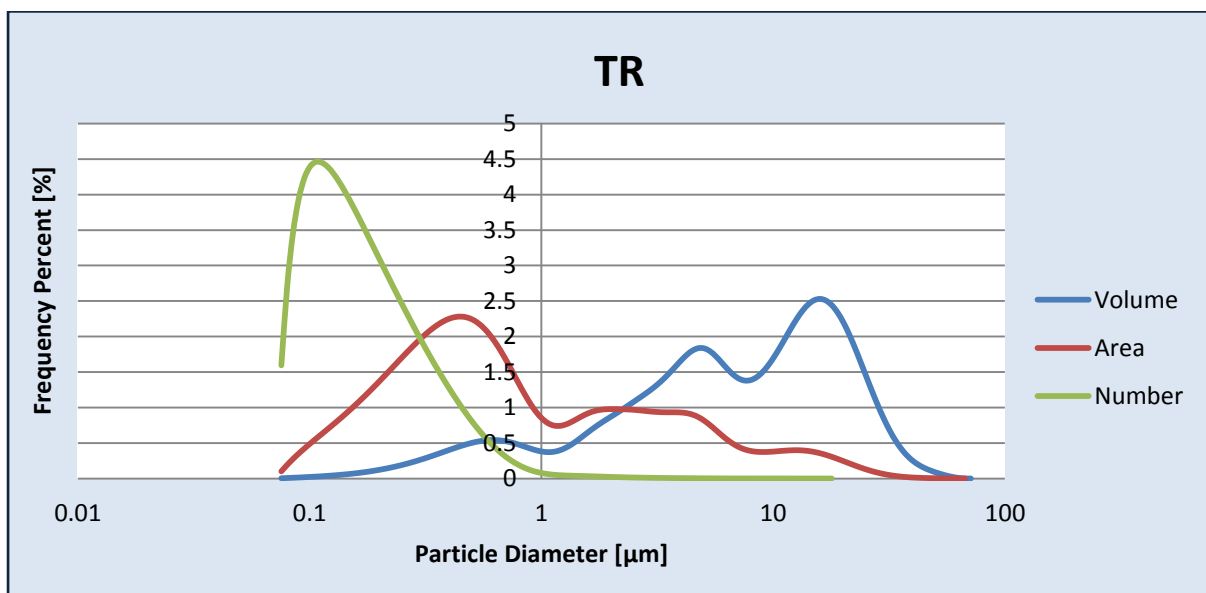
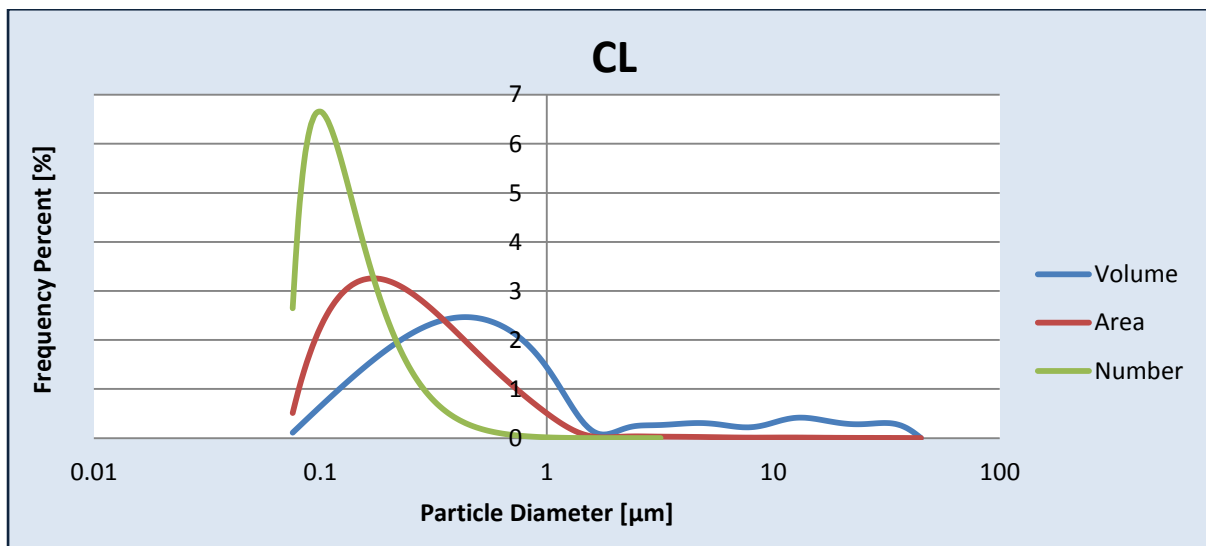
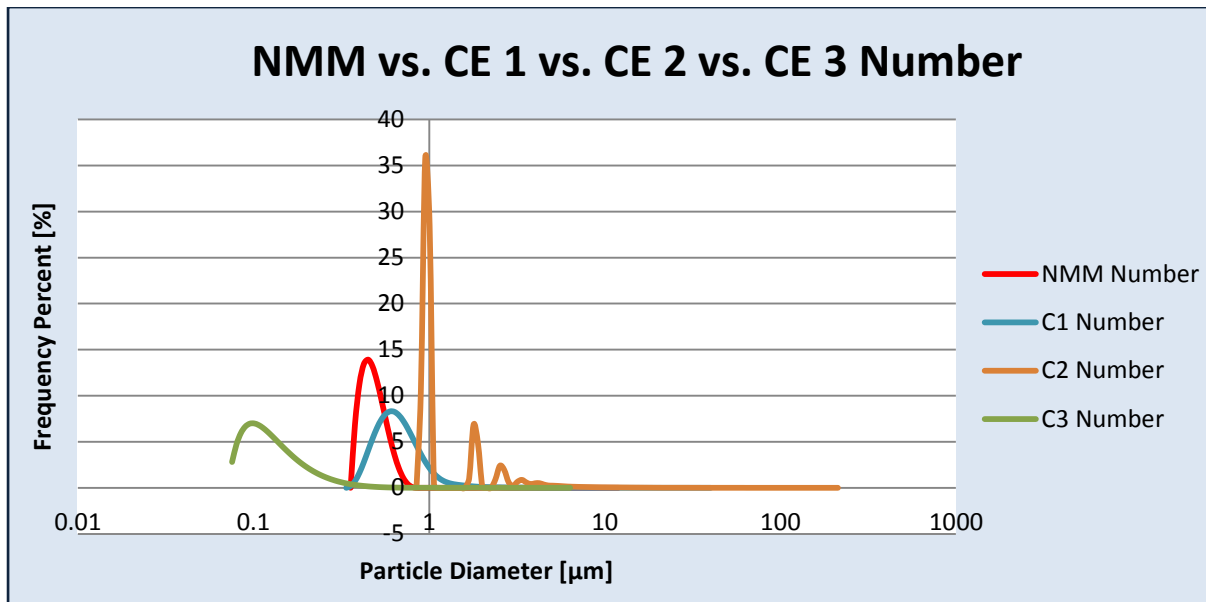


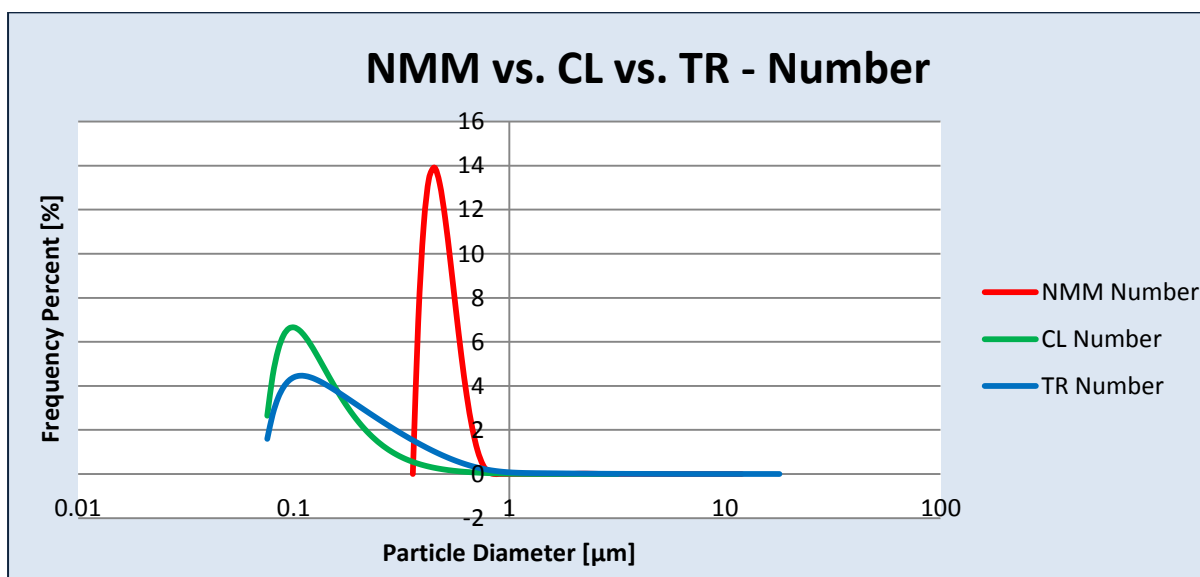
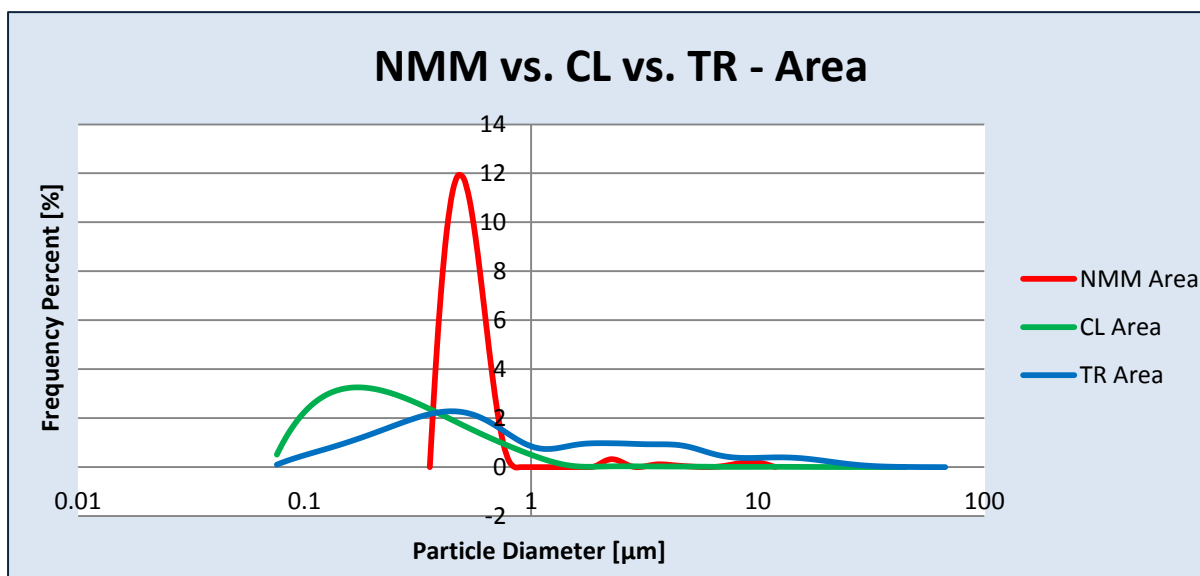
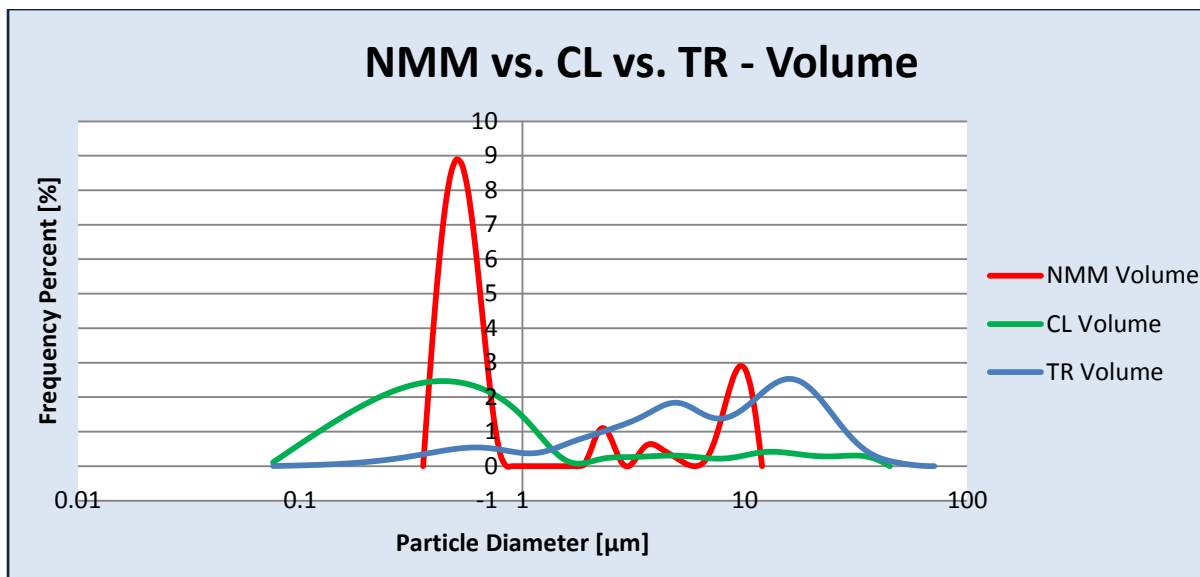
Figure 162 – Number Median Particle Size Distribution Data vs. Gloss Data Comparison

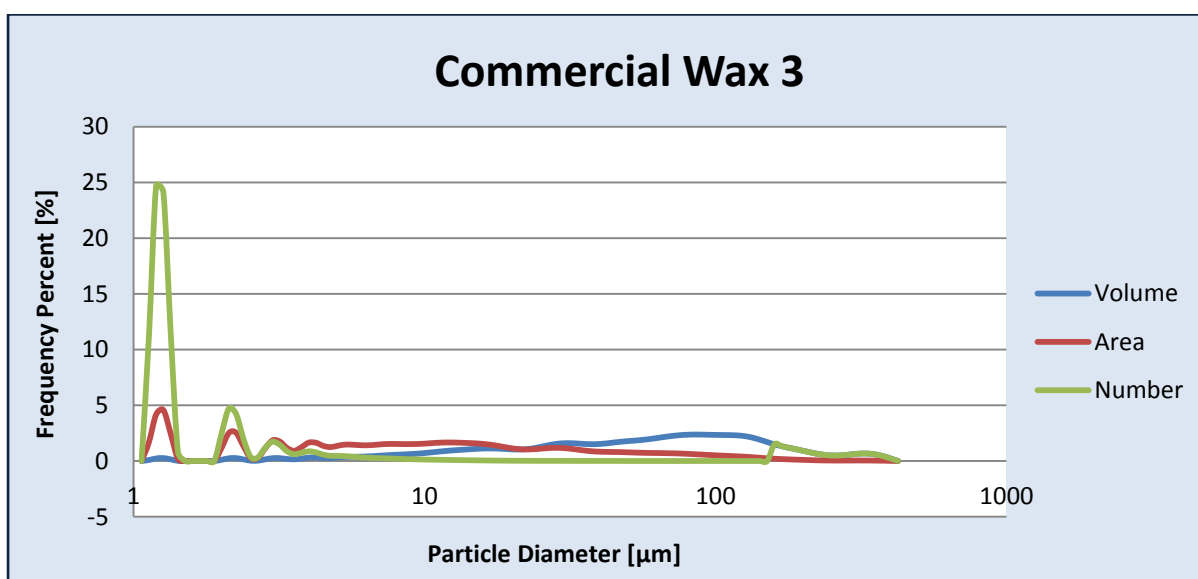
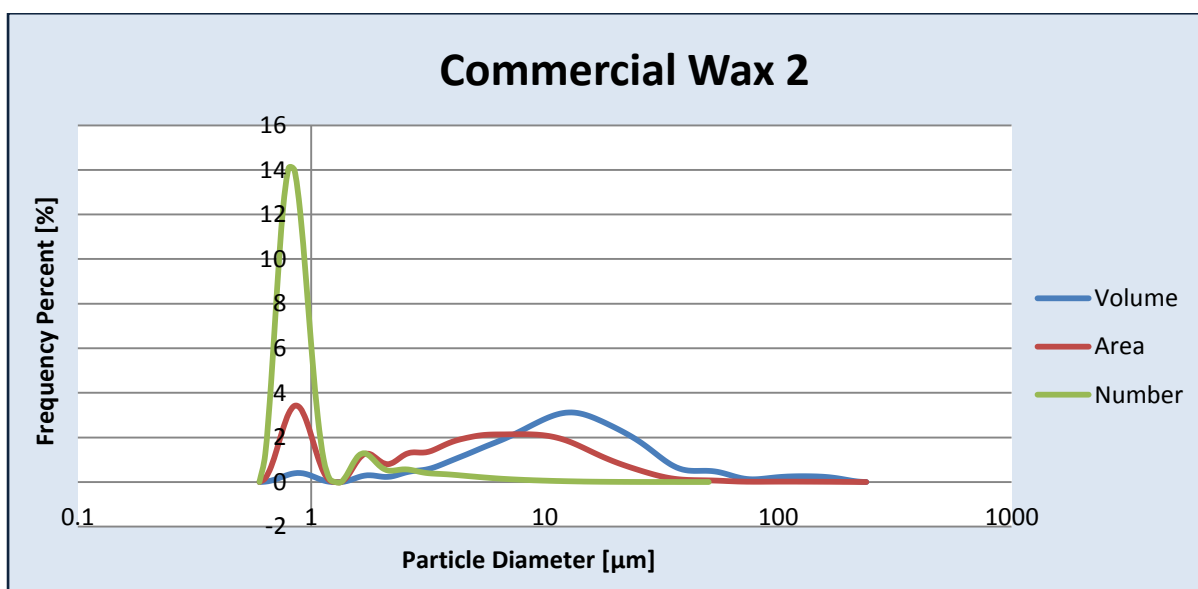
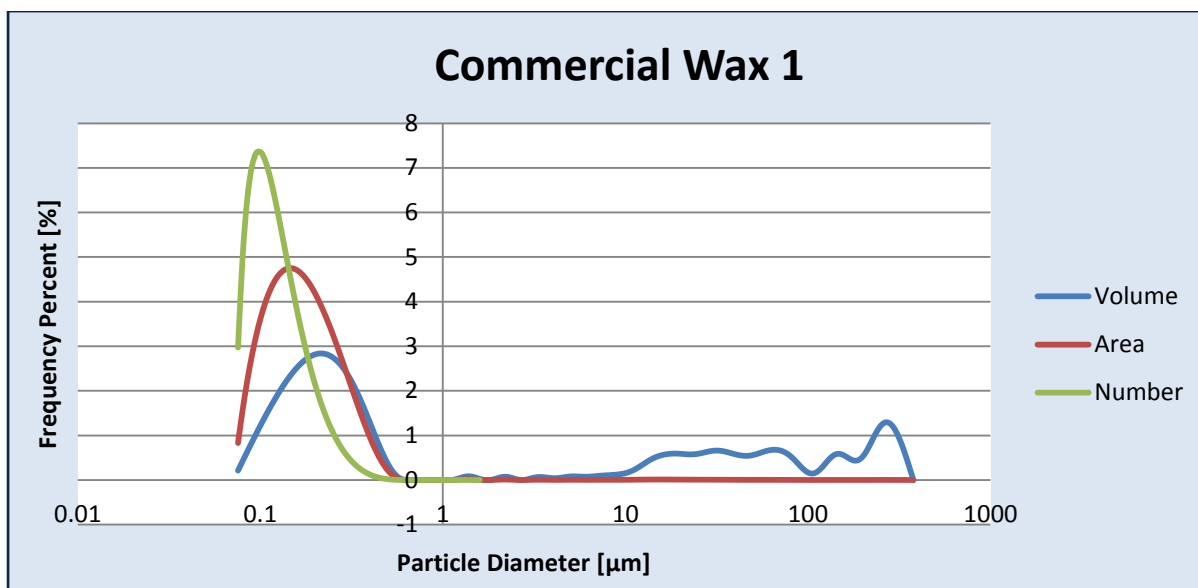
Appendix N: Comparison with Commercial Coatings

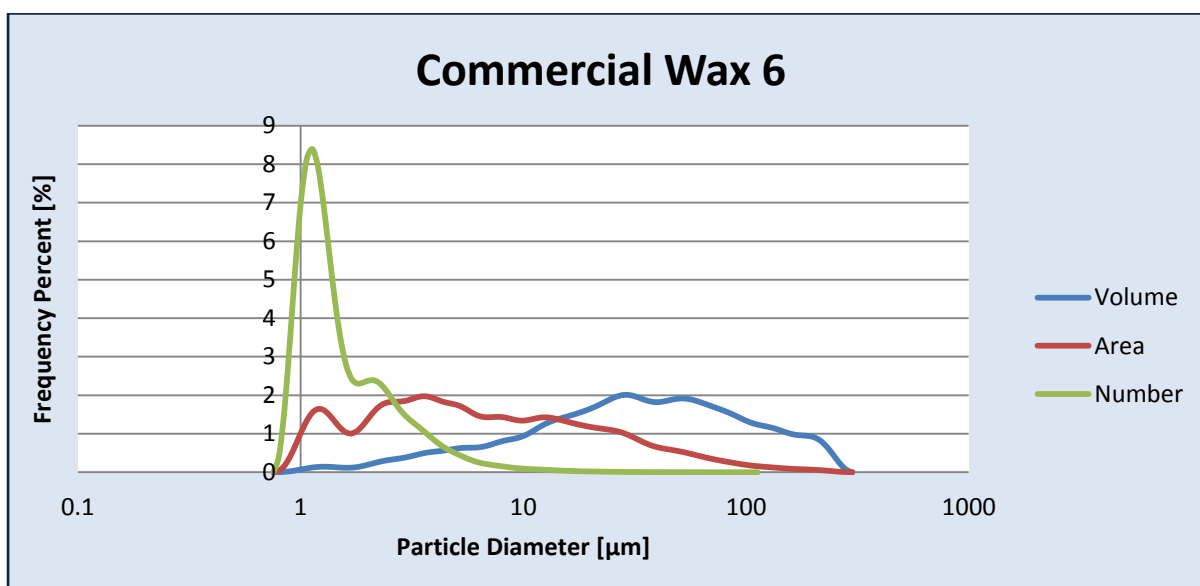
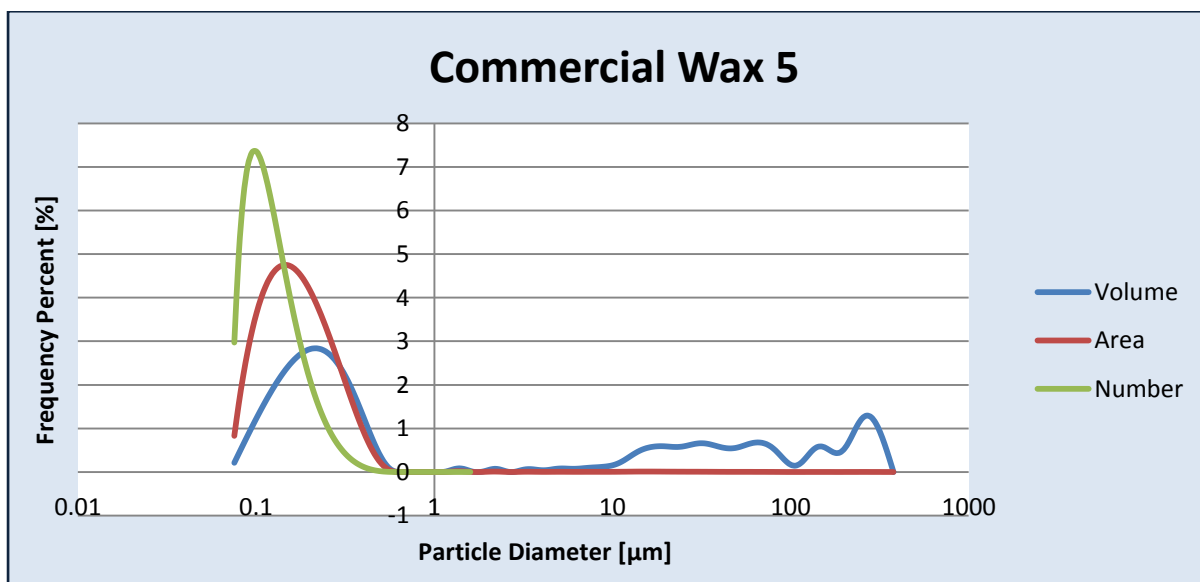
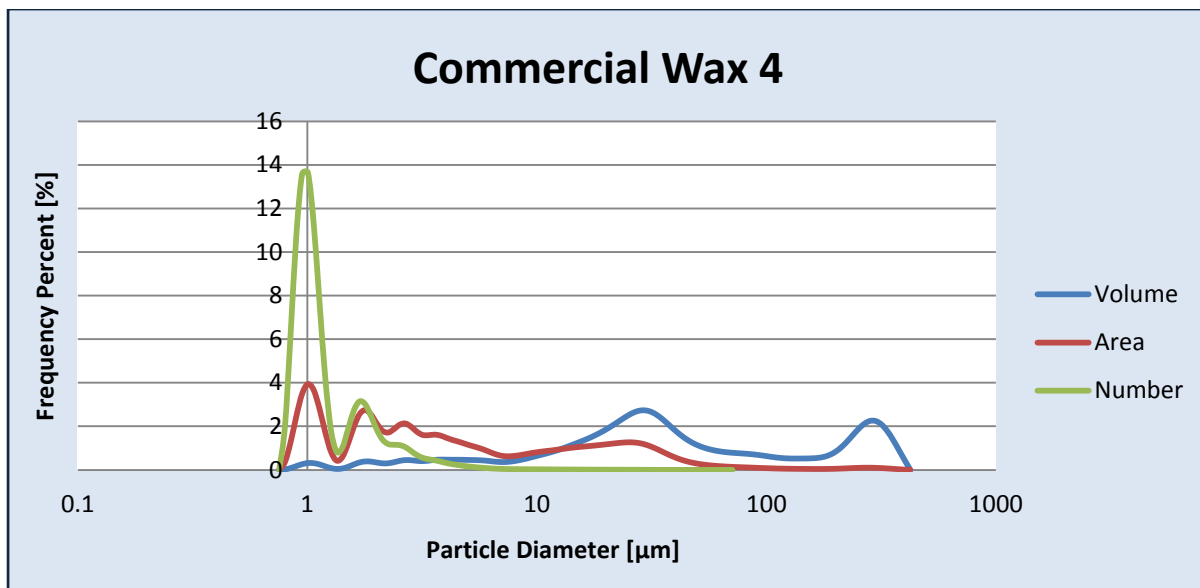


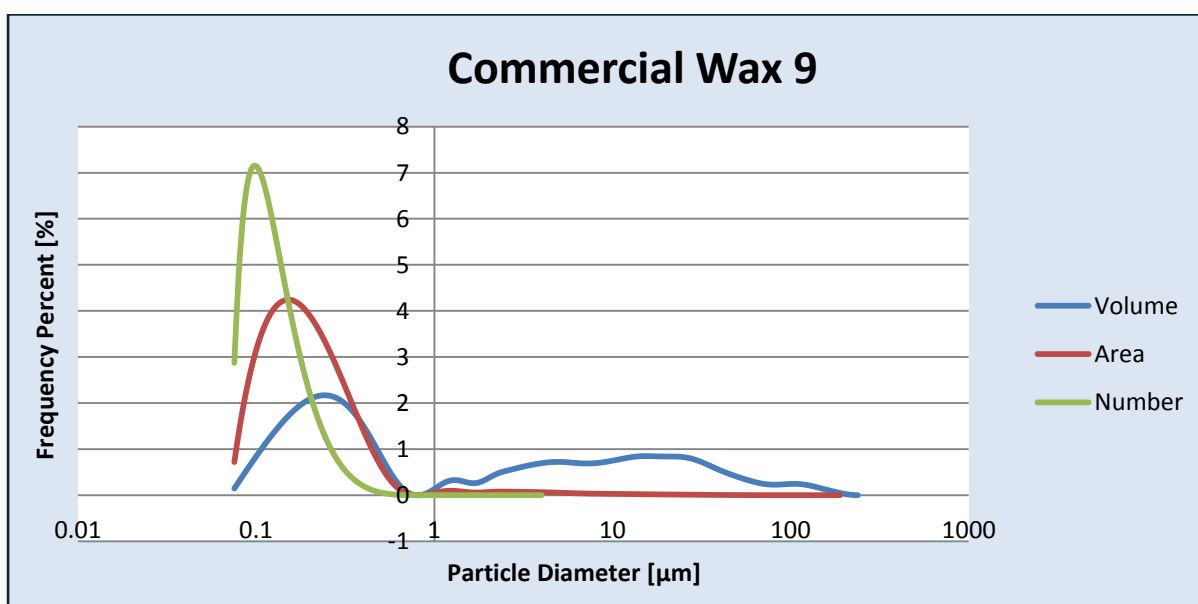
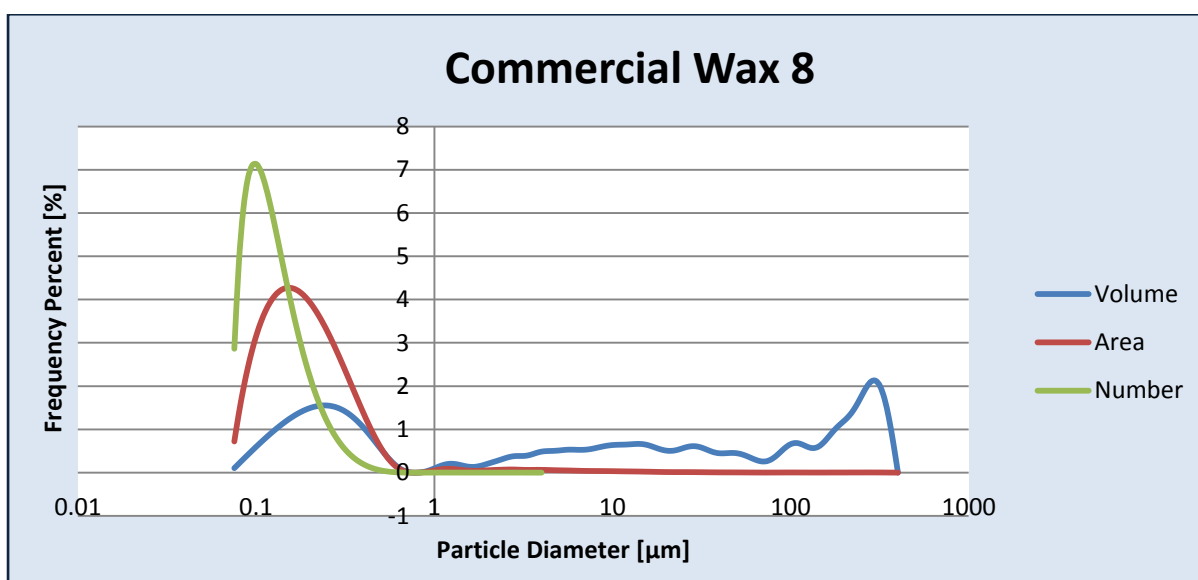
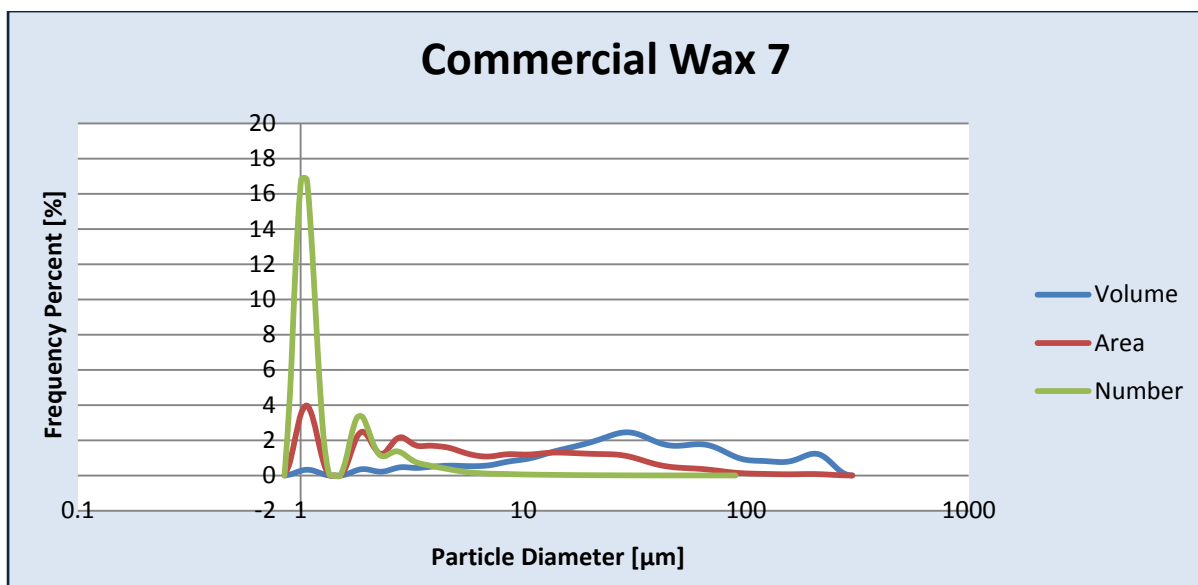


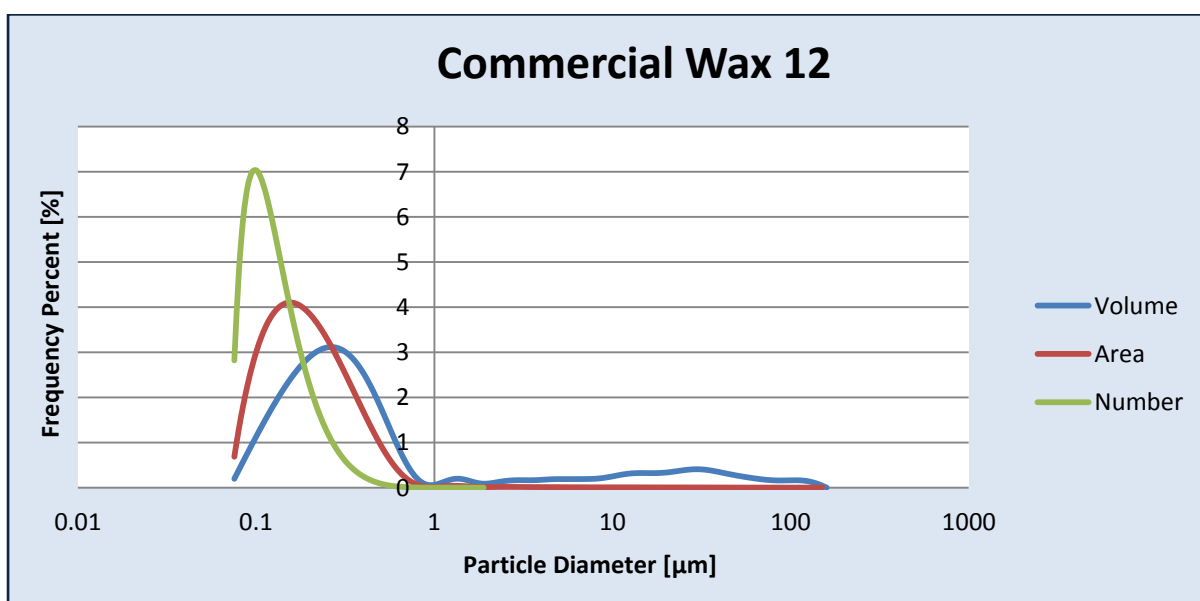
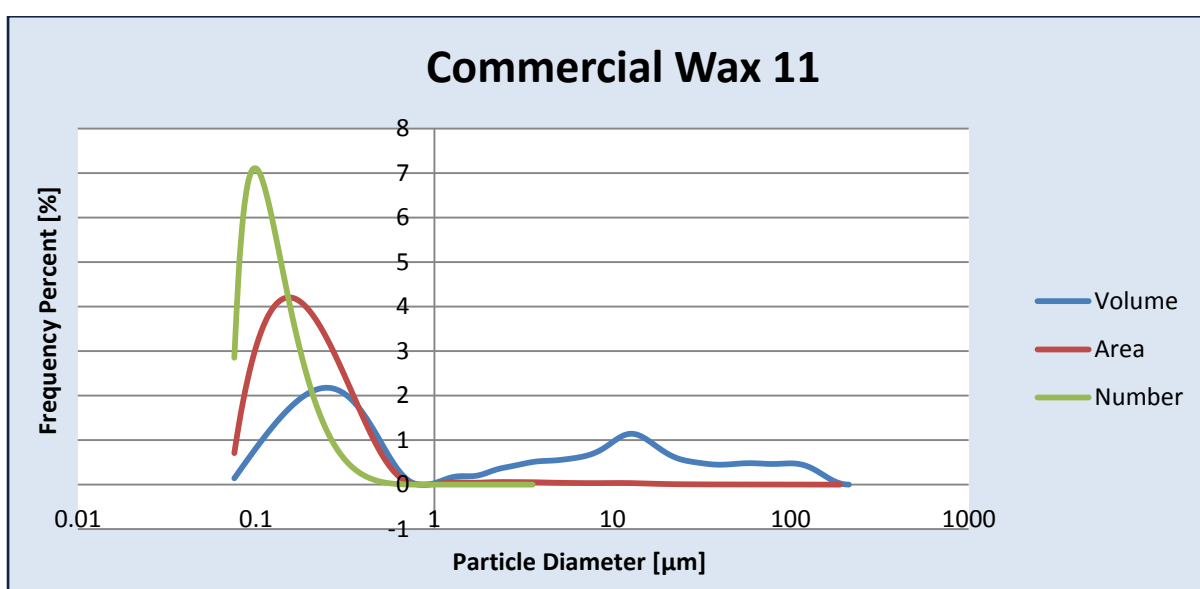
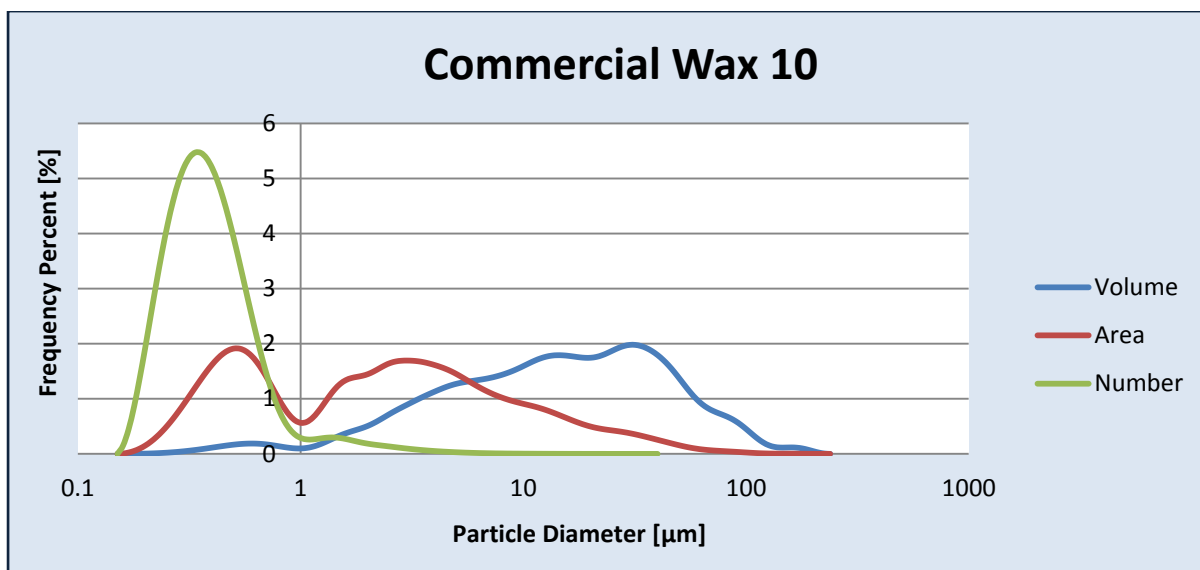




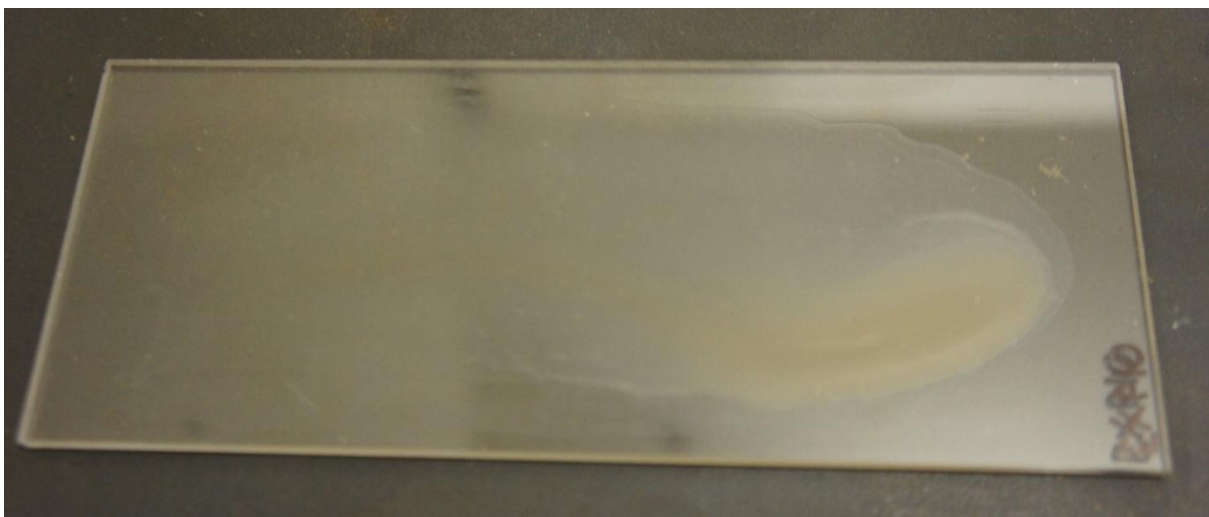






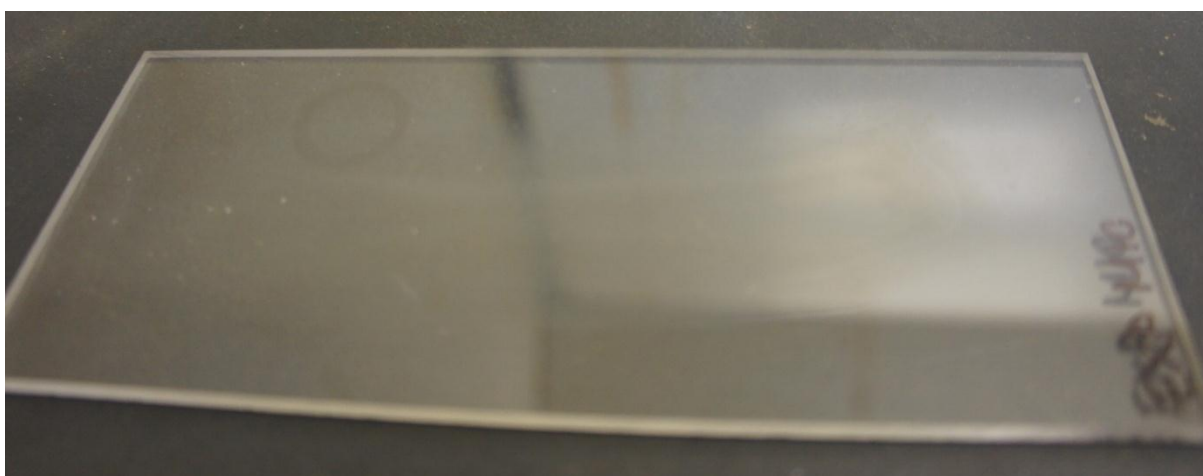
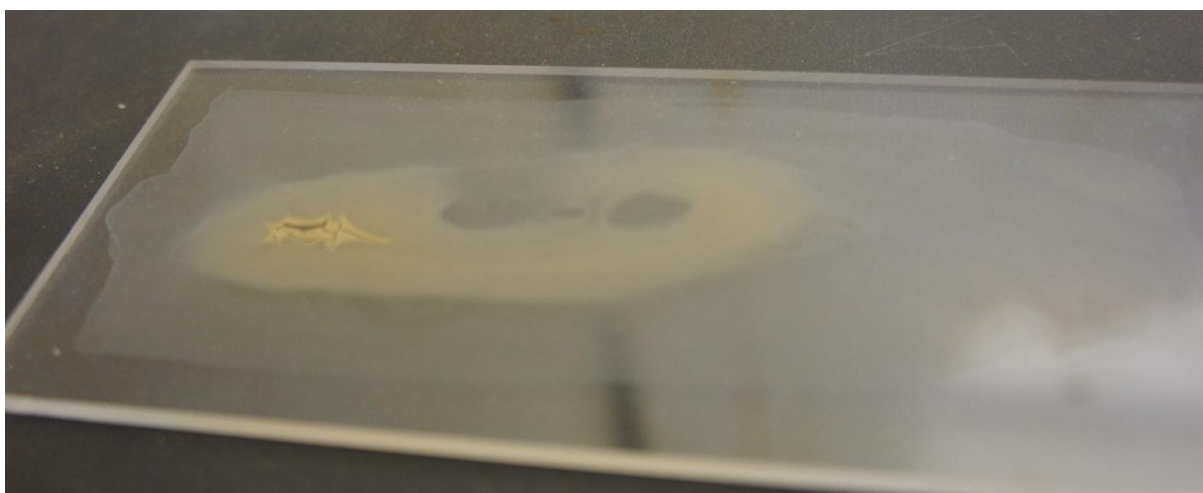
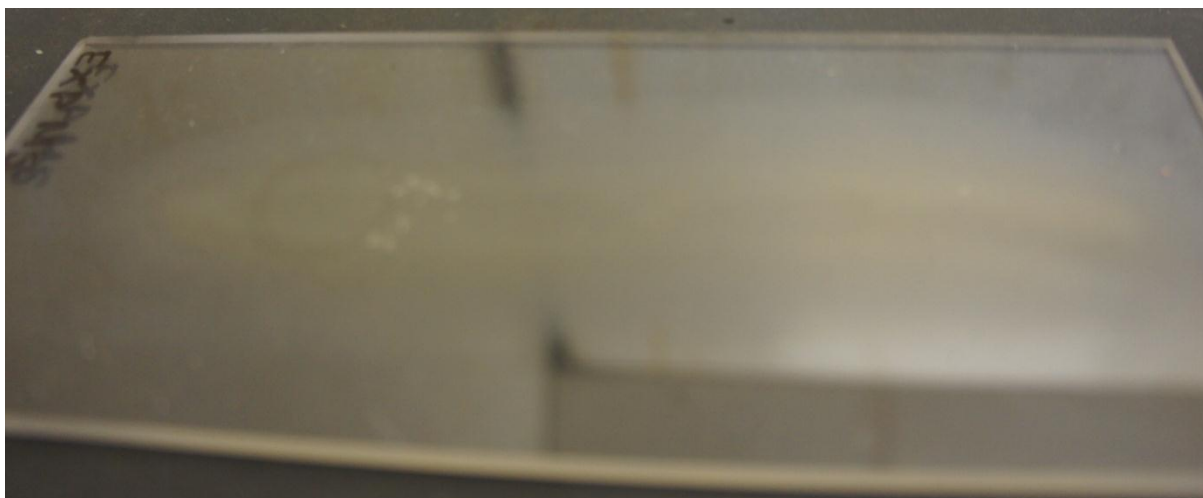


Appendix O: Screening Experimental Images



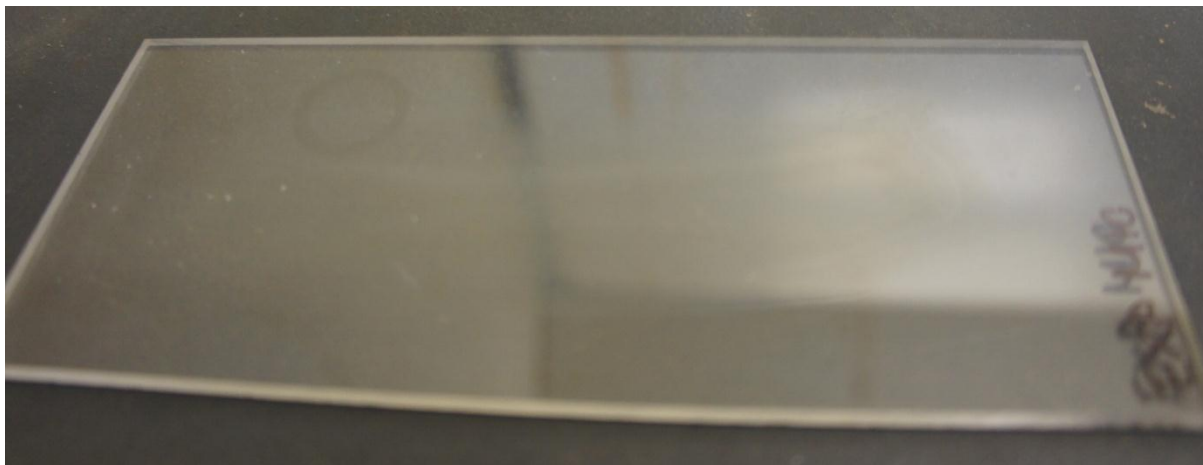
Several cracked and uneven coatings.

Appendix P: Mixture Experimental Images



Minimal cracked coatings.

Appendix Q: Composite Experimental Images



No cracked coatings.

Appendix R: Operational Images



**Image of the Initial Water and Carnauba
Wax during the melting process**



**Image of the Carnauba wax emulsion
before the inversion point is reached**